

Session III

Abundances of Li, Be and B:

Observations



Livia Schnyder, Elisa Delgado Mena, Jonay Gonzalez Hernandez



Martin Asplund & Karin Lind

The light elements in the light of 3D and non-LTE effects

Martin Asplund¹ and Karin Lind²

¹Max-Planck-Institut für Astrophysik, Postfach 1317, D-85741 Garching, Germany
email: asplund@mpa-garching.mpg.de

²European Southern Observatory, Karl-Schwarzschild-Strasse 2, D-85748 Garching, Germany
email: klind@eso.org

Abstract. In this review we discuss possible systematic errors inherent in classical 1D LTE abundance analyses of late-type stars for the light elements (here: H, He, Li, Be and B). The advent of realistic 3D hydrodynamical model atmospheres and the availability of non-LTE line formation codes place the stellar analyses on a much firmer footing and indeed drastically modify the astrophysical interpretations in many cases, especially at low metallicities. For the T_{eff} -sensitive hydrogen lines both stellar granulation and non-LTE are likely important but the combination of the two has not yet been fully explored. A fortuitous near-cancellation of significant but opposite 3D and non-LTE effects leaves the derived ^7Li abundances largely unaffected but new atomic collisional data should be taken into account. We also discuss the impact on 3D non-LTE line formation on the estimated lithium isotopic abundances in halo stars in light of recent claims that convective line asymmetries can mimic the presence of ^6Li . While Be only have relatively minor non-LTE abundance corrections, B is sensitive even if the latest calculations imply smaller non-LTE effects than previously thought.

Keywords. convection, line: formation, radiative transfer, Sun: abundances, Sun: atmosphere, stars: abundances, stars: atmospheres, stars: Population II, Galaxy: abundances

1. Stellar model atmospheres and spectral line formation

Stellar chemical compositions are not observed: to decipher the spectral fingerprints in terms of abundances requires realistic models for the stellar atmospheres and the line formation processes. Traditionally abundance analyses of late-type stars have been carried out relying on 1D, time-independent, hydrostatic model atmospheres, which treat convection with the rudimentary mixing length theory. All of these are dubious approximations as even a casual glance at the solar atmosphere will immediately reveal. The solar atmosphere, as for other late-type stars, is dominated by granulation, which is the observational manifestation of convection: an evolving pattern of broad, warm upflows in the midst of narrow cool downdrafts. Because of the great temperature sensitivity of the opacity, the temperature drops precipitously as the ascending gas nears the optical surface before it overturns and is accelerated downwards. The temperature contrast is therefore very pronounced in the photospheric layers, amounting to $> 1000\text{ K}$ at the optical surface for the Sun (even when averaged over surfaces of equal optical depths these rms-differences amount to $\approx 400\text{ K}$). In addition to ignoring such atmospheric inhomogeneities, 1D model atmospheres can not be expected to have the correct mean temperature stratification because of the simplified convection treatment and the neglect of convective overshoot. Even small temperature differences can propagate to very large changes in the emergent stellar spectrum because of the non-linearities in the radiative transfer and the extreme opacity variations.

Over the past decade or so, 3D, time-dependent, hydrodynamical model atmospheres for a range of stellar parameters have started to be developed and applied to stellar abundance work (e.g. Asplund 2005, and references therein). Such 3D models solve the standard hydrodynamical conservation equations coupled with a simultaneous solution of the 3D radiative transfer equation and therefore self-consistently predict the convective and radiative energy transport (see e.g. Nordlund et al. 2009, for further details). To make the 3D modelling computationally tractable, the radiative transfer is not solved for the many thousands of wavelength points as routinely done in 1D model atmosphere codes. Instead the frequencies are sorted in opacity and more recently also in wavelength space for $\approx 4 - 20$ bins for which the radiative transfer is solved. The resulting total radiative heating/cooling as a function of atmospheric depth is surprisingly well reproduced. The 3D models are based on similarly realistic microphysics (equation-of-state and continuous/line opacities) as employed in standard 1D model atmospheres. Currently there are mainly four different codes being used to develop 3D models – STAGGER (e.g. Nordlund et al. 2009), CO5BOLD (e.g. Ludwig et al. 2009b), MURAM (e.g. Vögler et al. 2005) and ANTARES (e.g. Muthsam et al. 2009) – although essentially all abundance related work to date has been performed within the first two collaborations.

Being more sophisticated in the modelling does not automatically translate to being more realistic. Over the past few years, substantial effort has therefore been dedicated to verify the suitability of the 3D models for quantitative stellar spectroscopy using an arsenal of observational diagnostics. Some of the striking successes are that the 3D models accurately predict the detailed solar granulation properties (e.g. Nordlund et al. 2009) as well as spectral line profiles, including their asymmetries and shifts (e.g. Asplund et al. 2000), which strongly suggests that the 3D modelling captures the essence of the real atmospheric structure and macroscopic gas motions. Another crucial test is the continuum center-to-limb variation, which is an excellent probe of the mean temperature stratification in the solar atmosphere. As shown in Fig. 1, the latest generation of 3D models computed with the STAGGER code reproduces the observations extremely well (Pereira et al. 2010); the CO5BOLD solar model does a similarly good job (H.-G. Ludwig, private communication). This is a remarkable achievement. The 3D solar model not only outperforms all tested theoretical 1D model atmospheres like the Kurucz, MARCS and PHOENIX flavours in this respect, it also does noticeably better than the Holweber & Müller (1974) semi-empirical model, which was constructed largely to fulfill this observational constraint. The 3D solar model also performs very well when confronted with other tests, such as the spectral energy distribution, H lines (Pereira et al. 2010) and spatially resolved line profiles (Pereira et al. 2009a,b). In all aspects the most recent 3D solar models are clearly highly realistic and can therefore safely be trusted for abundance analysis purposes (Asplund et al. 2009).

The success in the solar case gives some credence to the 3D modelling being similarly realistic also for other stars for which far fewer indisputable observational tests are available. 3D models now exist for a sizable portion of the HR-diagram covering essentially spectral types A, F, G, K, M and even later (e.g. Collet et al. 2007; Ludwig et al. 2009b). Both dwarfs, subgiants, giants and even some supergiants have been simulated and for a wide range of metallicities. Qualitatively the granulation behaves similarly to the Sun for most of these stars but typically the convection becomes more vigorous towards higher T_{eff} and lower $\log g$. Perhaps the most marked difference compared with 1D models are apparent at low $[\text{Fe}/\text{H}]$, where 3D models have much cooler temperatures in the optically thin regime (Asplund et al. 1999). This is a natural consequence of the dominance of adiabatic heating over radiative heating in absence of a heavy line-blanketing at low metallicities. The low temperatures are bound to affect especially minority species, low

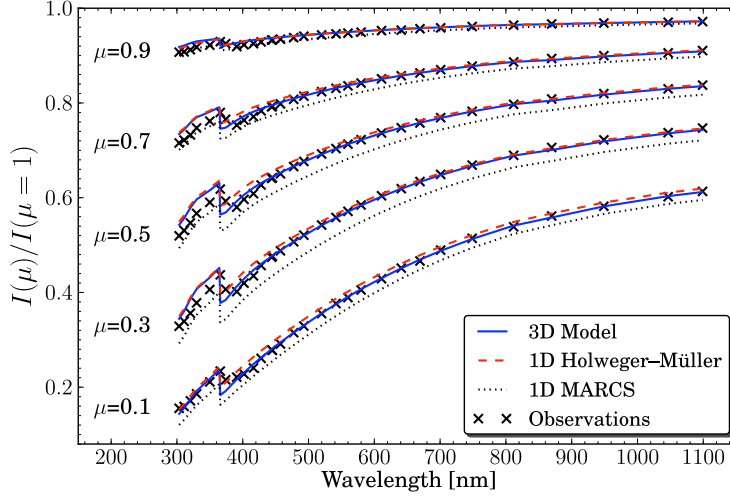


Figure 1. Comparison of the observed continuum center-to-limb variation as a function of wavelength (Neckel & Labs 1994) against the predictions for different solar model atmospheres. The 3D solar model employed by Asplund et al. (2009) outperforms the 1D theoretical MARCS model and even the 1D semi-empirical Holweger & Müller (1974) model atmosphere.

excitation lines and molecules, with 3D LTE abundance corrections often amounting to $> +0.5$ dex (e.g. Asplund 2005). One should be aware though that the steep temperature gradients may significantly enhance the non-LTE effects compared to the 1D case.

With a stellar model atmosphere it is possible to compute the emergent spectrum, which normally for late-type stars is done within the LTE approximation and in 1D. It should not come as a surprise that this approach often leads to severe systematic errors. In recent years, efforts towards rectifying these shortcomings have mainly focused on 1D non-LTE investigations and 3D LTE calculations, but the combination of 3D and non-LTE is still largely unexplored (e.g. Asplund 2005, and references therein). When solving the non-LTE problem one must solve the rate equations for all relevant levels involving both radiative and collisional transitions coupled with a simultaneous solution of the radiative transfer equation for all necessary frequencies. Needless to say, it rapidly becomes far more cumbersome than in LTE with a great deal of additional atomic data that must be considered. While the radiative processes like transition probabilities and photo-ionization cross-sections are now in reasonably good shape – especially for the non-complicated cases like the light elements – the main uncertainty in non-LTE calculations often stems from the poorly known collisional excitation and ionization due to electrons and H as well as charge transfer reactions. Especially the inelastic H collisions are a major problem in stellar abundance analyses. Mostly simple but likely erroneous classical recipes like the Drawin (1968) formula are applied, often with an additional ad-hoc scaling factor. For a few elements, Li being a notable case in point, detailed quantum mechanical or laboratory measurements exist (e.g. Belyaev & Barklem 2003), which reveal that the Drawin (1968) formula typically overestimates the real cross-sections by several orders of magnitude. An alternative approach is to attempt to calibrate the unknown collisional rates using various observations, such as obtaining consistent results from different lines or using center-to-limb variations. Not surprisingly, such empirical procedures suggest a range of scaling factors, from ≤ 0.1 for Mn (Bergemann & Gehren 2008), to ≈ 1 for O

(Pereira et al. 2009a) or even > 1 for Fe (Korn et al. 2003). Whether these are realistic values, or merely artificial results due to too simplified modelling (e.g. 1D) remains to be seen. It is also worth remembering that a common scaling factor for all transitions within the same species, let alone between different elements, is highly unlikely. In spite of the remaining uncertainties introduced by our still poor handle on all atomic data, the alternative of relying on the LTE approximation will most often lead to even more severe systematic errors.

2. The light elements

2.1. *Hydrogen*

As the most abundant element and the main provider of continuous opacity, it is not possible to derive the stellar H abundance spectroscopically. The H lines are still of great use in stellar physics as a probe of the atmospheric conditions. In late-type stars the wings of the Balmer lines reflect the effective temperature and the temperature gradient near the continuum forming layers with only a relatively small gravity dependence. The great temperature sensitivity arises from the high excitation potential of the lower level ($\chi_{\text{exc}} = 10.2\text{eV}$) of the Balmer lines. Fortunately, both the Stark broadening and self-broadening are now well established (e.g. Barklem et al. 2000; Allard et al. 2008); the new broadening results in significantly lower T_{eff} , especially at low $[\text{Fe}/\text{H}]$.

The H lines are however sensitive to the convection treatment, which in 1D normally is estimated by the mixing length theory (MLT) and its inherent four free parameters. Before comparing the best-fitting α_{MLT} and T_{eff} between different studies it is therefore important to bear in mind the various flavours of MLT existing in different 1D model atmospheres. Given the rudimentary nature of MLT to describe the correct convective energy transport and overshoot near/in the optical surface, 1D-based T_{eff} -scales from H lines will always be uncertain in an absolute sense even if highly accurate relative values can be obtained (e.g. Asplund et al. 2006). As explained above, 3D hydrodynamical models do provide an attractive alternative through their self-consistent computation of the convection without the need to invoke free parameters. Ludwig et al. (2009a) have investigated the 3D LTE formation of $\text{H}\alpha$, $\text{H}\beta$ and $\text{H}\gamma$ lines for six different 3D models, including the Sun and metal-poor dwarfs/subgiants and compared with 1D models computed with identical microphysics but with different MLT implementations; see also Sbordone et al. (2010) for further discussions. Ludwig et al. (2009a) found a very complex dependence on the 3D corrections to the 1D-based estimates of T_{eff} with differences amounting to $\pm 300\text{K}$ depending on the line in consideration and the T_{eff} , $[\text{Fe}/\text{H}]$ and α_{MLT} of the 1D model. An extra complication arises from the different line shapes in 3D and 1D, which can not be directly translated to a T_{eff} difference without specifying exactly which wavelength regions have been used for the comparison. The prospect for using pre-tabulated 3D corrections to 1D-based T_{eff} estimates is therefore not encouraging. It would be advantageous to directly compare observations with 3D predictions, which should be possible in the near future with the advent of grids of 3D models.

Until recently it has always been argued that the wings of the H Balmer wings are formed in LTE. Barklem (2007) has investigated whether this is indeed correct and found that it is not necessarily so. In particular he found that electron collisions are not sufficient to establish LTE. In terms of T_{eff} , the non-LTE calculations would imply $\geq 100\text{K}$ higher values than in LTE. This however depends crucially on the still uncertain inelastic H collisions – improved atomic physics calculations are clearly needed to resolve this issue. It would also be necessary to perform 3D non-LTE H line computations, especially at

low metallicity. Such calculations have recently been performed in the solar case with encouraging results (Pereira et al. 2010).

2.2. Helium

While in hot stars the very highly excited transitions of He I enable a determination of the He abundance (see Kaufer, these proceedings), in late-type stars the corresponding atomic levels are not sufficiently populated at typical photospheric temperatures. Instead the He I lines (e.g. 1083.0 nm) have a chromospheric origin and can neither probe the He abundance nor the photospheric temperature structure.

2.3. Lithium

Stellar Li abundance are usually determined only from the resonance line at 670.7 nm but in exceptional cases also from the weaker subordinate line at 610.4 nm. Contrary to most elements, the simplicity of the Li atom has enabled quantum mechanical calculations of all atomic data necessary for non-LTE investigations, especially of cross-sections for collisional excitation and charge transfer with neutral hydrogen (Barklem et al. 2003). The widely used study of Carlsson et al. (1994) mapped out the non-LTE effects in late-type stars and their detailed variation with metallicity, effective temperature, surface gravity, and lithium line strength. Recently, Lind et al. (2009a) revisited the 1D non-LTE line formation with improved collisional data and treatment of line-blocking (see Fig 2). The investigations have shown that two competing effects govern the population levels of Li. Over-ionization from the first excited level of Li I is prominent at low effective temperatures due to a strong $J_\nu - B_\nu$ excess bluewards of the photo-ionization threshold at 350 nm. When the Li line is weak, the balance between UV over-ionization from the first excited state and over-recombination to higher excited levels determines the population levels of Li I. The resulting non-LTE corrections are typically minor, smaller than ± 0.1 dex, but increasing up to $+0.5$ dex in red giants. However, when the line is close to saturation, the loss of line photons establishes an efficient recombination and de-excitation ladder, which increases the population of low-excited levels of neutral Li. Furthermore, the scattering-dominated resonance line source function drops far below B_ν . The non-LTE corrections then change sign and reach -0.5 dex in extreme cases. Lind et al. (2009a) have made available convenient routines to interpolate the non-LTE corrections for a wide range of stellar parameters and Li abundances.

In LTE the Li I level populations depend on the local conditions, especially the gas temperature. The much cooler mean temperature stratifications in 3D models than corresponding 1D models at low metallicity translate to a 3D LTE abundance correction of ≈ -0.3 dex for the Li I 670.8 nm resonance line in metal-poor dwarfs and subgiants (e.g. Asplund et al. 1999). In addition, the presence of atmospheric inhomogeneities typically also increase the line strength. One should be aware however that the steeper temperature gradients in the 3D models are likely to boost the over-ionization. Spatially resolved observations of the solar surface show how the line actually is weaker in the bright, granular upflows, despite the drastic drop in temperature that they undergo. This can be understood since the intense UV radiation field in the granules produces pronounced over-ionization (Kiselman 1997).

Asplund et al. (2003) performed full 3D non-LTE computations for the Sun and two metal-poor stars using a 21-level Li model atom. They concluded that the line strengthening due to the cooler temperatures in the upper atmospheric layers on the one hand and line weakening from increased over-ionization on the other hand largely cancel each other. Barklem et al. (2003) updated these results in light of new collisional data, especially charge transfer reactions and reached similar conclusions. The 3D non-LTE calculations

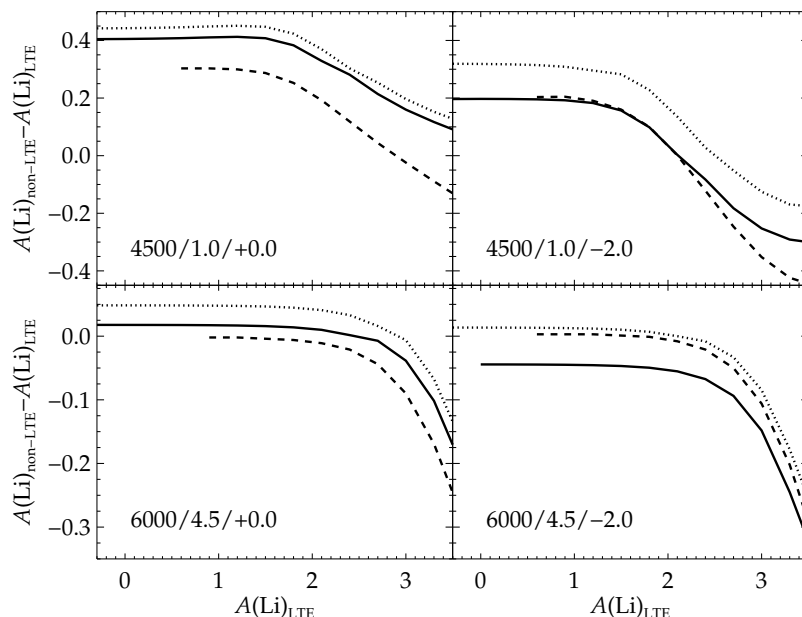


Figure 2. The 1D non-LTE abundance corrections for a selection of stellar parameters (labelled with $T_{\text{eff}}/\log g/[\text{Fe}/\text{H}]$) from the study of Lind et al. (2009a). The solid line denotes the case with all transitions considered while the dotted line correspond to the case when the charge transfer reactions of Barklem et al. (2003) are ignored. Also shown as dashed lines are the non-LTE corrections from Carlsson et al. (1994).

thus agree with the 1D non-LTE results to within 0.05–0.1 dex. In fact, even better agreement between the two is seen in the recent study of extremely metal-poor stars by Sbordone et al. (2010) with difference of < 0.03 dex, at least compared with the particular family of 1D model atmospheres they used. Sbordone et al. (2010) used a smaller atom (8 levels) but computed for more 3D models. They also provided a very handy functional relation between the Li abundance and the line strength, which allows direct computation of the 3D non-LTE based abundance without invoking any particular 1D model atmosphere. The Spite & Spite (1982) Li-plateau as inferred from 1D analyses is thus unlikely to be seriously in danger although the exact slope with for example $[\text{Fe}/\text{H}]$ may be affected (e.g. Asplund et al. 2006; Sbordone et al. 2010), which deserves to be studied closer with improved 3D non-LTE calculations.

2.4. ${}^6\text{Li}/{}^7\text{Li}$

The minor isotope ${}^6\text{Li}$ can be detected through the isotopic shift in the Li I 670.8 nm line. The distortion of the line profile is very small and therefore necessitates extremely high-quality spectra ($S/N > 400$, $\lambda/\Delta\lambda > 100,000$ and minimal fringing). At solar metallicity, possible blending lines must also be carefully evaluated (Israelian et al. 2003), a problem which however disappears at low $[\text{Fe}/\text{H}]$. The first positive detection in a halo star was claimed by Smith et al. (1993) for HD 84937. Asplund et al. (2006) boosted the number of $> 2\sigma$ detections to 10 (including HD 84937) using high-quality VLT/UVES spectra

analysed both in 1D and 3D LTE. The derived ${}^6\text{Li}$ abundance at $[\text{Fe}/\text{H}] < -2.5$ can not be easily accommodated with standard Galactic cosmic ray production, which has spurred a number of studies of more speculative production channels, including non-standard Big Bang nucleosynthesis with supersymmetric particles (e.g. Jedamzik & Pospelov 2009).

Several potential problems linger over the published ${}^6\text{Li}/{}^7\text{Li}$ analyses. García Pérez et al. (2009) have suggested that residual fringing in the observed spectra can cause large uncertainties. Their Subaru/HDS spectra are, however, much more inflicted by fringing than the VLT/UVES spectra of Asplund et al. (2006), who furthermore carefully assessed their possible impact on the results. More worrisome is the restriction to 1D or 3D LTE line formation. The atmospheric convective motions typically result in C-shaped line asymmetries (e.g. Asplund et al. 2000), which can thus mimic the presence of ${}^6\text{Li}$. Indeed, Cayrel et al. (2007) have argued based on 3D non-LTE calculations that the Asplund et al. (2006) results must be reevaluated. Steffen et al. (2010) have considered this in more detail and concluded that the derived ${}^6\text{Li}/{}^7\text{Li}$ ratios in a 1D analysis are overestimated by typically 0.015, which if true could explain the tendency for most stars with non-significant detections in the Asplund et al. (2006) sample to cluster around ${}^6\text{Li}/{}^7\text{Li} \approx 0.01$. Furthermore, Steffen et al. (2010) argue that by taking this convective effect into account, only 4 out of 10 stars would remain as $> 2\sigma$ detections.

We argue that the Steffen et al. (2010) results should not be over-interpreted, since there are subtle but crucial differences in the analyses. Steffen et al. (2010) rely only on the Li line itself to determine all parameters: ${}^7\text{Li}$ and ${}^6\text{Li}$ abundances, wavelength shift and intrinsic line broadening (rotation in 3D but in 1D also macro-/microturbulence) while Asplund et al. (2006) rely on a range of Fe, Ca etc lines to first determine the line broadening which is then fixed for the Li profile fitting. Since the other lines are also asymmetric, this is accounted for in the profile fitting through a slightly larger required broadening, which then compensates for the use of symmetric Li lines in 1D. Asplund et al. (2006) also did a 3D LTE analysis for all lines and found very similar results as in 1D but with much improved profile fits. We have also performed 3D non-LTE line calculations for Li similar to Steffen et al. (2010) and can in fact exactly reproduce their results and their claimed 0.015 effect in ${}^6\text{Li}/{}^7\text{Li}$ when only using the Li line and not any other lines. We argue though that this does not make full use of the information encoded in the spectra due to the degeneracy between the four fitting parameters. Indeed, their procedure is akin to determining the D abundance in QSO absorption systems only from the Ly α line without first resolving the intrinsic velocity structure of the H I clouds from other metallic lines. Similarly problematic is to rely on 3D non-LTE for Li but 3D LTE for the other lines, in view of the likely pronounced non-LTE effects. The only way forward to convincingly demonstrate whether or not ${}^6\text{Li}$ is present in detectable amounts in the atmospheres of halo turn-off stars is to perform full 3D non-LTE calculations for all lines considered. We are currently working on this and will report the results elsewhere.

In summary, it is not yet possible to say that ${}^6\text{Li}$ has definitely been detected but it is definitely too early to say that ${}^6\text{Li}$ has not been detected. We also note that even Steffen et al. (2010) agree that ${}^6\text{Li}$ is present in HD 84937 and a few other stars. Since ${}^6\text{Li}$ is always destroyed and more so than ${}^7\text{Li}$, one would still end up with a very significant cosmological ${}^6\text{Li}$ problem when invoking stellar depletion to solve the cosmological ${}^7\text{Li}$ problem (e.g. Asplund et al. 2006; Korn et al. 2006; Lind et al. 2009b).

2.5. Beryllium

In late-type stars the Be abundance can in practice only be derived from the resonance doublet of Be II at 313 nm. In contrast to Li and B, Be is normally present in significant amounts in both neutral and singly ionized form due to its high ionization potential, which

makes Be less prone to over-ionization. The Be II line formation proceeds under non-LTE conditions but because the two dominant non-LTE effects – over-ionization and over-excitation – largely compensate each other the resulting non-LTE abundance corrections are typically minor (García López et al. 1995). Both the lower and upper level of the doublet are over-populated relative to the LTE prediction. Be I tends to be somewhat over-ionized due to a UV radiation excess ($J_\nu/B_\nu > 1$), which simultaneously produce an over-excitation of the upper level of the Be II 313 nm transitions. García Pérez et al. (2010) have investigated the non-LTE line formation of the Be II 313 nm doublet across a wide range of stellar parameters. They found that at solar metallicity the two effects almost perfectly balance each other with the resulting non-LTE abundance corrections amounting to $|\Delta \log \epsilon_{\text{Be}}| \leq 0.05$ dex. At low metallicity the non-LTE corrections are positive ($\Delta \log \epsilon_{\text{Be}} \approx 0.1$ dex) for $T_{\text{eff}} \geq 6000$ K and negative ($\Delta \log \epsilon_{\text{Be}} \approx -0.1$ dex) for lower T_{eff} . While the non-LTE effects will not qualitatively change the conclusions for the metallicity evolution of Be (Primas and Boesgaard, these proceedings), accounting for the new non-LTE calculations will tend to make the slope somewhat shallower.

The 3D line formation of the Be II lines have so far only been investigated for the Sun (Asplund et al. 2009). The Be II lines are not very sensitive to 3D effects at least within the LTE approximation. The 3D non-LTE case has not yet been investigated but given the relatively modest non-LTE effects in 1D one would not expect a great difference in 3D, although this prediction should be verified with detailed calculations.

2.6. Boron

As for Be, both over-ionization and over-excitation are at play in the formation of the B I resonance lines at 249.7 nm and 209.0 nm but because B I is the minority ionization stage for $T_{\text{eff}} \geq 6000$ K the effects on the resulting line profiles are much more dramatic (Kiselman & Carlsson 1996). The over-ionization is largely driven by photo-ionization from the excited B I levels since $J_\nu/B_\nu > 1$ at the relevant wavelengths. It is also assisted by pumping in the B I resonance lines, which produces a sufficient over-population of these upper levels. The same pumping results in a substantial increase in the line source function $S_\nu/B_\nu \approx J_\nu/B_\nu > 1$ for the 249.7 and 209.0 nm lines. Thus, in contrast to the case of Be, for the B I resonance lines the two non-LTE effects work in tandem to decrease the non-LTE line strengths substantially compared with the LTE prediction.

Kiselman & Carlsson (1996) computed non-LTE abundance corrections for the B I lines for a grid of MARCS 1D model atmospheres. The non-LTE effects grow in size towards higher T_{eff} and lower $[\text{Fe}/\text{H}]$. Indeed, they found non-LTE abundance corrections as large as $> +0.5$ for typical turn-off halo stars. As both non-LTE processes feed on the UV radiation field, it is important to include background line opacities both for the calculations of the photo-ionization rates and the resonance lines, which Kiselman & Carlsson (1996) did in a somewhat approximate manner. Recently, Tan et al. (2010) confirmed the importance of over-ionization and pumping but they obtained markedly less severe non-LTE effects, which can be traced to a more complete treatment of the line-blocking. Their estimated non-LTE abundance corrections amount to $\approx +0.3$ dex at the lowest $[\text{Fe}/\text{H}]$, when not including the highly uncertain inelastic H collisions according to Drawin (1968); the corrections would be $\approx +0.1$ dex when this formula would be applied without any further scaling factor. As shown in Fig. 3, the new non-LTE results of Tan et al. (2010) make the resulting evolution of B as a function of metallicity somewhat steeper with a slope of ≈ 1.3 . The reader is referred to Primas (these proceedings) for a discussion of the astrophysical implications of such a correlation.

With the exception of the Sun (Asplund et al. 2009), the 3D line formation of the B I lines has not been investigated, neither in LTE nor in non-LTE. In view of the

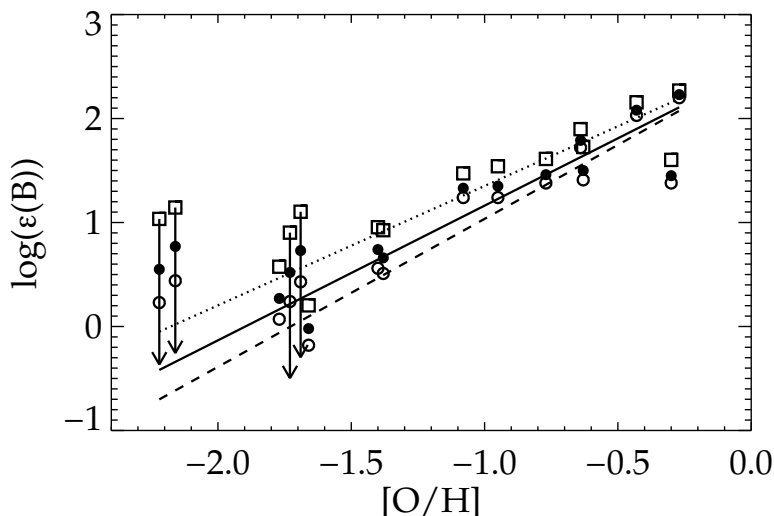


Figure 3. The derived stellar B abundances in halo stars (Tan et al. 2010) as a function of $[O/H]$ for LTE (open circles with dashed line the least square fit) and non-LTE (filled circles and solid line); upper limits are marked with arrows. The O abundances have been corrected for non-LTE effects according to Fabbian et al. (2009). Also shown are the LTE-based B abundances of Tan et al. (2010) but corrected according to the non-LTE calculations of Kiselman & Carlsson (1996) (open squares and dotted line). Inelastic H collisions have not been included for the B non-LTE results but for O according to the Drawin (1968) formula.

prominent non-LTE effects and the general expectation that they would become even more pronounced in 3D due to the atmospheric inhomogeneities, performing detailed 3D non-LTE calculations for B I should have a high priority.

3. Concluding remarks

Important progress has been made over the last decade in terms of improving the abundance analyses of the light elements in late-type stars by accounting for non-LTE as well as 3D effects. The non-LTE line formation of the resonance lines of Li I, Be II, and B I share common properties, but the final non-LTE abundance corrections are always element specific. Especially differences in ionization potential and the extent to which UV radiative transitions contribute to the excitation and ionization balance govern the LTE departures. There are however still several outstanding analysis problems.

Signs are that the new generation of 3D hydrodynamical model atmospheres are indeed highly realistic and thus trustworthy for abundance purposes as they successfully reproduce most, if not all, observational tests they have been exposed to. The key development for the future will be to make such 3D models generally available for a wide range of stellar parameters and actually to get stellar abundance practitioners to start using them routinely. The main obstacle here will likely be to overcome old habits rather than say lack of computational power, since it is now possible to perform a 3D-based solar/stellar abundance analysis for thousands of lines, at least in LTE (Asplund et al. 2009). On the non-LTE side, the challenges are two-fold: improving the necessary atomic

data, especially for collisions, and to couple the non-LTE line formation with 3D model atmospheres, which is still very much uncharted territory. This is now certainly feasible but will require additional (wo)manpower. Only then can we with some degree of confidence argue that our analysis efforts match the investments in obtaining impressive observational data. As outlined above, such modelling efforts will no doubt lead to many reinterpretations of observations with profound implications for our understanding of stellar, galactic and cosmic evolution in general and the light elements in particular.

References

- Allard, N. F., Kielkopf, J. F., Cayrel, R., & van't Veer-Menneret, C. 2008, *A&A*, 480, 581
- Asplund, M. 2005, *ARAA*, 43, 481
- Asplund, M., Carlsson, M., & Botnen, A. V. 2003, *A&A*, 399, L31
- Asplund, M., Grevesse, N., Sauval, A. J., & Scott, P. 2009, *ARAA*, 47, 481
- Asplund, M., Lambert, D. L., Nissen, P. E., Primas, F., & Smith, V. V. 2006, *ApJ*, 644, 229
- Asplund, M., Nordlund, Å., Trampedach, R., et al. 2000, *A&A*, 359, 729
- Asplund, M., Nordlund, Å., Trampedach, R., & Stein, R. F. 1999, *A&A*, 346, L17
- Barklem, P. S. 2007, *A&A*, 466, 327
- Barklem, P. S., Belyaev, A. K., & Asplund, M. 2003, *A&A*, 409, L1
- Barklem, P. S., Piskunov, N., & O'Mara, B. J. 2000, *A&A*, 363, 1091
- Belyaev, A. K. & Barklem, P. S. 2003, *Phys. Rev. A*, 68, 062703
- Bergemann, M. & Gehren, T. 2008, *A&A*, 492, 823
- Carlsson, M., Rutten, R. J., Bruls, J. H. M. J., & Shchukina, N. G. 1994, *A&A*, 288, 860
- Cayrel, R., Steffen, M., Chand, H., et al. 2007, *A&A*, 473, L37
- Collet, R., Asplund, M., & Trampedach, R. 2007, *A&A*, 469, 687
- Drawin, H. 1968, *Zeitschrift für Physik*, 211, 404
- Fabbian, D., Asplund, M., Barklem, P. S., Carlsson, M., & Kiselman, D. 2009, *A&A*, 500, 1221
- García López, R. J., Severino, G., & Gomez, M. T. 1995, *A&A*, 297, 787
- García Pérez, A., Asplund, M., & Kiselman, D. 2010, *A&A*, submitted
- García Pérez, A. E., Aoki, W., Inoue, S., et al. 2009, *A&A*, 504, 213
- Holweger, H. & Müller, E. A. 1974, *Solar Phys.*, 39, 19
- Israelian, G., Santos, N. C., Mayor, M., & Rebolo, R. 2003, *A&A*, 405, 753
- Jedamzik, K. & Pospelov, M. 2009, *New Journal of Physics*, 11, 105028
- Kiselman, D. 1997, *ApJ (Letters)*, 489, L107
- Kiselman, D. & Carlsson, M. 1996, *A&A*, 311, 680
- Korn, A. J., Grundahl, F., Richard, O., et al. 2006, *Nature*, 442, 657
- Korn, A. J., Shi, J., & Gehren, T. 2003, *A&A*, 407, 691
- Lind, K., Asplund, M., & Barklem, P. S. 2009a, *A&A*, 503, 541
- Lind, K., Primas, F., Charbonnel, C., Grundahl, F., & Asplund, M. 2009b, *A&A*, 503, 545
- Ludwig, H., Behara, N. T., Steffen, M., & Bonifacio, P. 2009a, *A&A*, 502, L1
- Ludwig, H., Caffau, E., Steffen, M., et al. 2009b, *MemSAI*, 80, 711
- Muthsam, H. J., Kupka, F., Loew-Baselli, B., et al. 2009, arXiv:0905.0177
- Neckel, H. & Labs, D. 1994, *Solar Phys.*, 153, 91
- Nordlund, Å., Stein, R. F., & Asplund, M. 2009, *Living Reviews in Solar Physics*, 6, 2
- Pereira, T., Asplund, M., Trampedach, R., & Collet, R. 2010, *A&A*, in press
- Pereira, T. M. D., Asplund, M., & Kiselman, D. 2009a, *A&A*, 508, 1403
- Pereira, T. M. D., Kiselman, D., & Asplund, M. 2009b, *A&A*, 507, 417
- Sbordone, L., Bonifacio, P., Caffau, E., et al. 2010, *A&A*, in press
- Smith, V. V., Lambert, D. L., & Nissen, P. E. 1993, *ApJ*, 408, 262
- Spite, F. & Spite, M. 1982, *A&A*, 115, 357
- Steffen, M., Cayrel, R., Bonifacio, P., Ludwig, H., & Caffau, E. 2010, arXiv:1001.3274
- Tan, K., Shi, J., & Zhao, G. 2010, *ApJ*, in press
- Vögler, A., Shelyag, S., Schüssler, M., et al. 2005, *A&A*, 429, 335

Li isotopes in metal-poor halo dwarfs: a more and more complicated story

Monique Spite and François Spite

GEPI, Observatoire de Paris, 92195 Meudon Cedex, CNRS UMR 8111

email: monique.spite@obspm.fr, francois.spite@obspm.fr

Abstract. The nuclei of the lithium isotopes are fragile, easily destroyed, so that, at variance with most of the other elements, they cannot be formed in stars through steady hydrostatic nucleosynthesis.

The ${}^7\text{Li}$ isotope is synthesized during primordial nucleosynthesis in the first minutes after the Big Bang and later by cosmic rays, by novae and in pulsations of AGB stars (possibly also by the ν process). ${}^6\text{Li}$ is mainly formed by cosmic rays. The oldest (most metal-deficient) warm galactic stars should retain the signature of these processes if, (as it had been often expected) lithium is not depleted in these stars. The existence of a "plateau" of the abundance of ${}^7\text{Li}$ (and of its slope) in the warm metal-poor stars is discussed. At very low metallicity ($[\text{Fe}/\text{H}] < -2.7\text{dex}$) the star to star scatter increases significantly towards low Li abundances. The highest value of the lithium abundance in the early stellar matter of the Galaxy ($\log\epsilon(\text{Li}) = A({}^7\text{Li}) = 2.2\text{ dex}^\dagger$) is much lower than the value ($\log\epsilon(\text{Li}) = 2.72$) predicted by the standard Big Bang nucleosynthesis, according to the specifications found by the satellite WMAP. After gathering a homogeneous stellar sample, and analysing its behaviour, possible explanations of the disagreement between Big Bang and stellar abundances are discussed (including early astration and diffusion). On the other hand, possibilities of lower productions of ${}^7\text{Li}$ in the standard and/or non-standard Big Bang nucleosyntheses are briefly evoked.

A surprisingly high value ($A({}^6\text{Li})=0.8\text{ dex}$) of the abundance of the ${}^6\text{Li}$ isotope has been found in a few warm metal-poor stars. Such a high abundance of ${}^6\text{Li}$ independent of the mean metallicity in the early Galaxy cannot be easily explained. But are we really observing ${}^6\text{Li}$?

Keywords. Stars: abundances, Population II – nucleosynthesis – early universe

1. Introduction

1.1. A first view

In the eighties and the nineties, the abundance of ${}^7\text{Li}$ in the warm ($5700 < T_{\text{eff}} < 6500\text{K}$) metal-poor dwarfs was found constant, independent of the temperature and of the metallicity, at least in the interval $-2.8 < [\text{Fe}/\text{H}] < -1.8$: Spite & Spite (1982a, and 1982b) and subsequent papers (e. g. Spite, Spite and Maillard 1984, Hobbs & Thorburn 1991, Molaro, Primas and Bonifacio 1995, Spite et al. 1996, Bonifacio and Molaro 1997, Smith et al. 1998). Later works, published up to 2005, are vividly reviewed in the section 2 of Charbonnel and Primas (2005) : the small differences between authors are discussed.

This "universal" behaviour of lithium suggested that ${}^7\text{Li}$ observed in the old metal poor dwarfs was synthesized during primordial nucleosynthesis (when the Universe was only a few minutes old) and that lithium, although a very fragile element, had survived unaltered in the atmosphere of warm metal-poor dwarfs. In the so called "standard" stellar models (i. e. without diffusion and mixing), the Li depletion is negligible (Deliyannis et al. 1990, Pinsonneault et al. 1992). However, already at that time, several theoreticians of stellar

† In the literature the lithium abundance, is noted indifferently by $\log\epsilon(\text{Li})$ or by $A(\text{Li})$; both notations are in logarithmic scale of number of atoms where $\log\epsilon(\text{H}) = A(\text{H}) = 12$

atmospheres thought that it was difficult to admit that the abundance of lithium in the atmosphere of the old very metal-poor dwarfs had remained unchanged during 13 billions years. Reciprocally, it was also difficult to explain a strictly uniform lithium depletion in the warm metal-poor dwarfs, whatever their temperature, mass and metallicity.

The primordial abundance of ${}^7\text{Li}$ had been then largely identified with the stellar abundance found on the plateau, the value being between $\log\epsilon(\text{Li}) = 2.0$ and $\log\epsilon(\text{Li}) = 2.3$ depending on the temperature scale adopted by the authors. Moreover, taking into account the errors of measurement and the uncertainties of the observed abundances, the simultaneous production of all the light elements (${}^4\text{He}$, ${}^3\text{He}$, D and Li) by the Big Bang, could be explained.

In spite of the obvious difficulty of disentangling the ${}^6\text{Li}$ and ${}^7\text{Li}$ profiles in stellar spectra, attempts were made at finding the abundance of ${}^6\text{Li}$: it was possible only in a handful of metal-poor dwarfs. For the first time Smith, Lambert, & Nissen (1993), claimed a positive detection of ${}^6\text{Li}$ in a metal-poor star: HD84937 ($[\text{Fe}/\text{H}] \approx -2.1$). Later Nissen et al. (1999) observed ${}^6\text{Li}$ in 2 metal-poor stars out of five; see also Cayrel et al. (1999). The existence of ${}^6\text{Li}$ (more fragile than ${}^7\text{Li}$) in some warm metal-poor dwarfs reinforced the idea that ${}^7\text{Li}$ is not depleted in such stars.

1.2. *A second step*

Two astronomical satellites brought new points of view :

- in 1997, Hipparcos has provided accurate parallaxes for numerous stars, improving the determination of the parameters of the stellar atmospheres (and enabling to discriminate dwarfs and subgiants).
- in 2003, WMAP has determined (Bennett et al. 2003) the physical conditions of the Big Bang especially a precise value for the baryons to photons ratio : η , leading to precise values of the abundances of the light elements produced in the standard Big Bang, including lithium. This Li abundance was found much higher than the abundance measured in the warm metal-poor dwarfs and thus the interest for a precise re-determination of the lithium abundance was reactivated.

2. The lithium isotopes in the matter of the early Galaxy

2.1. *Formation of Lithium*

A peculiarity of lithium is that it is very fragile and destroyed at "low" temperatures. Unlike most of the other elements, when it is synthesized inside the stars by hydrostatic nucleosynthesis, it is immediately destroyed. Lithium is formed :

- during the Big Bang (primordial nucleosynthesis) (${}^7\text{Li}$ and negligible amount of ${}^6\text{Li}$).
- by spallation (cosmic rays or in superbubbles: mainly ${}^6\text{Li}$)
- possibly by the " ν " process in type II supernovae (${}^7\text{Li}$)

Pulsations of AGB stars and novae explosions can also enrich the interstellar medium in ${}^7\text{Li}$, but not in the early times of the Galaxy.

2.2. *Primordial abundance of ${}^7\text{Li}$*

The ${}^7\text{Li}$ observed in the atmospheres of the very old galactic stars has been mainly formed by the primordial nucleosynthesis. Cosmic rays and ν process in massive supernovae could produce a small increase of $\epsilon({}^7\text{Li})$ with metallicity (a slope).

In the standard Big-Bang, the production of lithium depends only on the baryons to photons ratio η . This ratio has been deduced, with precision, from the measurements

of the cosmic microwave background radiation by the satellite WMAP : Bennett et al. (2003), Spergel et al. (2007), Cyburt et al. (2008) : $\eta = 6.23 \pm 0.17 \cdot 10^{-10}$.

Then, the primordial lithium abundance is $\log\epsilon(^7\text{Li}) = 2.72 \pm 0.06$ for $\log\epsilon(\text{H}) = 12$ (see also Komatsu et al. 2009, and Iocco et al. 2009, for the discussion of the uncertainties).

2.3. Depletion of lithium in the atmosphere of the stars

It is generally admitted that the abundances measured in the atmospheres of unevolved stars are representative of the abundances in the material from which the star has been originally formed.

However different phenomena are known to affect the superficial abundance of lithium during the life of the star.

Lithium is a very fragile element destroyed as soon as the temperature is higher than $2.5 \cdot 10^6 \text{K}$ for ^7Li and even $2.0 \cdot 10^6 \text{K}$ for ^6Li .

If there is some mixing between the surface of the star and the hot deep layers, little by little lithium is destroyed and disappears from the atmosphere of the star. In giants, Li is strongly diluted after the first dredge-up. Even in dwarfs lithium is often depleted: in the atmosphere of the Sun after 4.5 Gyr, the lithium abundance is only $\log\epsilon(\text{Li}) = 1.03$ (Caffau et al., this volume) although in meteorites $\log\epsilon(\text{Li})$ reaches ≈ 3.25 (a value representative of the abundance of lithium in the material that formed the Sun). However in the warm metal-poor dwarfs/turnoff stars, mixing is not as deep as in solar metallicity stars, and lithium could have been preserved.

Lithium is also supposed to slowly settle down into the stars by diffusion (gravitational settling), but the diffusion can be easily thwarted by turbulent mixing.

3. The behaviour of ^7Li in the most metal poor stars in the Milky Way

The difference between the lithium abundance predicted by BBN + WMAP and the mean value observed in the atmosphere of the old galactic dwarfs, leads to a redetermination of the lithium abundance, with an effort towards better temperature determinations: the determination of lithium abundance is very sensitive to the choice of the temperature of the stellar atmosphere. Moreover, the precise behaviour of $\log\epsilon(\text{Li})$ vs. temperature and metallicity and also the scatter around the mean relations may give a clue about the exact mechanism of lithium depletion.

Since 2005 several papers about the lithium abundance in very metal-poor stars were published. They all try to determine very carefully the temperatures of the stellar atmospheres, using high quality data: it is essential to discriminate between intrinsic scatter and determinations errors.

–Charbonnel & Primas (2005) have determined the temperatures from a very precise photometry (*uvby*) associated with the Alonso et al. (1996) calibration and taking into account very carefully the reddening of the stars. Meléndez et al. (2010 and this symposium) had a similar approach but they used a new implementation of the infrared flux method to determine the temperatures from multiband IR photometry.

–Boesgaard et al. (2005) and Hosford et al. (2009) based their analysis on excitation temperature (the abundances from the Fe I lines must be independent of the excitation potential of the line).

–All the other authors used the wings of the hydrogen lines (mainly $\text{H}\alpha$) to determine the temperatures: Asplund et al. (2006), Bonifacio et al. (2007), González Hernández et al. (2008), García Pérez et al. (2008, 2009), Aoki et al. (2009).

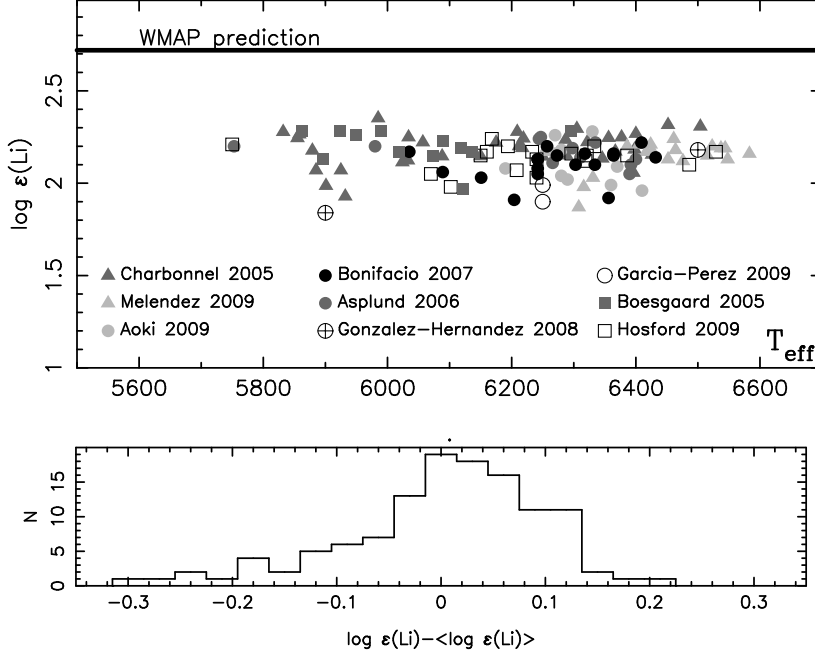


Figure 1. Lithium abundance versus Temperature for metal-poor stars ($[\text{Fe}/\text{H}] < -2$) and (below) histogram. Triangles indicate that the temperature has been determined from photometry, circles from the profile of the hydrogen lines and squares from the excitation temperature. In this interval of temperature and metallicity, the lithium abundance is independent of the temperature but the scatter is rather large. The mean value of the lithium abundance is $\log \epsilon(\text{Li}) \approx 2.15$, more than 0.55 dex below the prediction of standard BB + WMAP (full black line). On the histogram showing the distribution of the distances of each point to the mean value of the lithium abundance it can be seen that the distribution is not gaussian.

In Fig. 1 we present $\log \epsilon(\text{Li})$ versus T_{eff} , for the metal-poor dwarfs and turnoff stars with $[\text{Fe}/\text{H}] < -2.0$, measured in these different works. There is a rather good agreement between the different determinations, (even if some slight systematic differences appear between different authors). No significant trend of $\log \epsilon(\text{Li})$ vs. T_{eff} is apparent. The mean value of the lithium abundance is $\log \epsilon(\text{Li}) \approx 2.15$: about four times less than the abundance formed by the standard Big Bang nucleosynthesis.

This mean value of the lithium abundance measured in the old galactic stars is also very close to the value measured in ω Cen (see Bonifacio et al., this symposium): $\log \epsilon(\text{Li}) \approx 2.19 \pm 0.14$. The cluster ω Cen is now considered as the remnant of a captured dwarf galaxy. As a consequence $\log \epsilon(\text{Li}) = 2.15$ could be a "universal" value of stellar Li abundance at low metallicity.

In Fig. 1 the scatter around the mean value of the lithium abundance is 0.10 dex. This scatter is not symmetric (see the histogram in Fig. 1) and is larger than the measurement errors. It is NOT mainly due to systematic differences between different authors, it exists even for the data of a given author.

What is the cause of this scatter of the lithium abundance when $[\text{Fe}/\text{H}] < -2$?

If we plot $\log \epsilon(\text{Li})$ versus $[\text{Fe}/\text{H}]$ (Fig. 2) a slight decrease of $\epsilon(\text{Li})$ with the metallic-

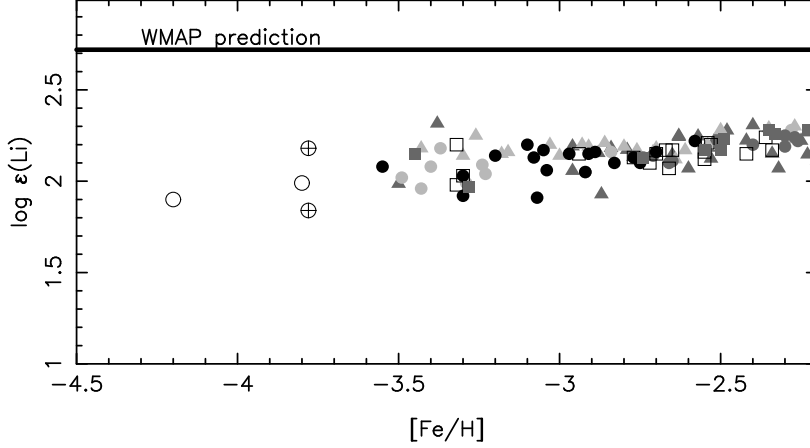


Figure 2. $\log \epsilon(\text{Li})$ vs. $[\text{Fe}/\text{H}]$, for turnoff stars ($T_{\text{eff}} > 5800\text{K}$). The symbols are the same as in Fig. 1. The slight decline of $\log \epsilon(\text{Li})$ when the metallicity decreases appears for $[\text{Fe}/\text{H}] < -3$.

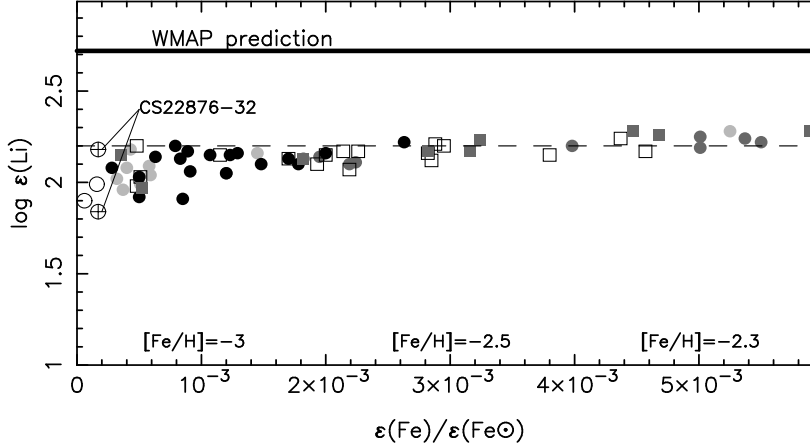


Figure 3. $\log \epsilon(\text{Li})$ vs. the iron abundance $\epsilon(\text{Fe}_*)/\epsilon(\text{Fe}_\odot)$ (linear scale) for turnoff stars ($T_{\text{eff}} > 5800\text{K}$). The symbols are the same as in Fig. 1. To improve the homogeneity, we have kept only the measurements of the lithium abundance based on a temperature determination independent of the reddening (T_{Hydrogen} or T_{exc}). When $\epsilon(\text{Fe}_*)/\epsilon(\text{Fe}_\odot) > 0.001$ ($[\text{Fe}/\text{H}] > -3$), the scatter around the mean curve is very small (0.05 dex) but at a lower metallicity the scatter suddenly increases. The lithium abundances in the two components of the extremely metal-poor binary CS 22876-32 are different by a factor of two. Lithium would sometimes suffers an extra depletion in the atmospheres of the most metal-poor stars. Then, the pristine value of the lithium abundance would correspond to the higher envelope, $\log \epsilon(\text{Li}) \approx 2.2$.

ity appears. As a consequence the scatter observed in Fig 1 should be partly due to a dependence of lithium abundance on metallicity. This decrease suggests that the extrapolated abundance of lithium could be even lower than 2.15 when extrapolating toward zero-metal stars (just after the Big Bang).

In Fig. 3 we have plotted $\log \epsilon(\text{Li})$ versus $\epsilon(\text{Fe}_*)/\epsilon(\text{Fe}_\odot)$ (linear scale), and for a better

homogeneity, we have kept only stars with a temperature determined spectroscopically ($H\alpha$ profiles or excitation temperature) and thus independent of the interstellar reddening. In the interval $2 \times 10^{-3} < \epsilon(\text{Fe})_*/\epsilon(\text{Fe})_\odot < 6 \times 10^{-3}$ the lithium abundance increases steadily and the scatter around the mean curve is extremely small: 0.05 dex.

In the most metal-poor stars ($\epsilon(\text{Fe})_*/\epsilon(\text{Fe})_\odot < 2 \times 10^{-3}$, i. e. $[\text{Fe}/\text{H}] < -2.7$, the mean value of the lithium abundance decreases suddenly to reach $\log\epsilon(\text{Li}) \approx 2.0$ dex at $\epsilon(\text{Fe}) = 0$. (zero-metal stars). Therefore $\log\epsilon(\text{Li}) \approx 2.0$ could be the mean value of the lithium abundance in the early Galaxy. But in this region the scatter at a given metallicity increases strongly (see Sbordone et al. 2010 and this symposium, for confirmation by additional data). This scatter could be interpreted as the result of a variable depletion, decreasing the lithium abundance from a natal value of about $\log\epsilon(\text{Li}) = 2.2$ dex, this value would represent the pristine value of the lithium abundance in the early Galaxy. In both cases the pristine value of the lithium abundance is well below the cosmological value derived from the standard Big Bang (with the WMAP value of the η parameter).

In Fig 3, no stars are found above $\log\epsilon(\text{Li}) = 2.2$ dex for $[\text{Fe}/\text{H}] < -2.7$ and above $\log\epsilon(\text{Li}) = 2.3$ dex for $-2.7 < [\text{Fe}/\text{H}] < -2.2$ defining an upper envelope of the lithium abundance. (A handful of Li-rich halo stars have been found in the literature, but all are several times more metal-rich than the stars considered here.)

Several interpretations can be put forward for explaining the gap between the cosmological and the observed lithium and also the sudden scatter appearing at low metallicity.

3.1. *Astration*

It has been proposed that the "uniform" lithium abundance in halo dwarfs could be due to a general process affecting the whole Milky Way lowering the cosmological Li abundance down to the pristine abundance. Piau et al. (2006) have proposed an early astration in very massive stars Pop III stars (destroying Li). They could have destroyed 3/4 of the primordial lithium, 50% of the mass of the Galactic halo having been processed in these massive stars.

The scatter of the lithium abundance appearing in the most metal-poor stars could then be explained by a still incomplete mixing of the matter in the Galaxy, or by the fact that these most metal-poor stars would have been accreted from different faint dwarf galaxies or satellites (Frebel et al. 2010) with different astration histories. There are objections to a strong initial astration in our Galaxy: the ejecta of the stars destroying Li would have induced (Prantzos 2007) a large early abundance of elements (e. g. C and O) that is not observed. But, in ω Cen, remnant of an accreted dwarf galaxy, the lithium abundance ($\log\epsilon(\text{Li}) \approx 2.19$, Bonifacio et al., this symposium), is very similar to the Galactic value for stars of the same metallicity, although they certainly had different astration histories. Probably, a very early global astration of the matter of the universe, by massive first stars, before the formation of the galaxies, would explain the plateau, but would encounter a similar objection about the early abundances of C and O in the Galaxy. However it could be possible that these massive Pop III stars rotate and thus eject only external layers with hydrogen and helium (Meynet, this symposium).

3.2. *Depletion in the stellar atmospheres*

The gap between the theoretical value of the lithium abundance predicted by the standard Big Bang and the observed value in the atmosphere of the stars, can be also the result of a depletion of lithium, even in the warm metal-poor dwarfs.

The stellar abundance now observed could be due to diffusion (Michaud et al., 1984). Some calculations have been made (e. g. Richard et al., 2005): a depletion such as figured

in Fig. 3, could be matched by a diffusion carefully moderated by some turbulence. The very low scatter of the data around the mean (0.05 dex) in the interval $2 \times 10^{-3} < \epsilon(\text{Fe})_*/\epsilon(\text{Fe})_\odot < 6 \times 10^{-3}$ brings severe constraints to the theoretical computations. Also the sudden downward scatter, at the left part of the Figure 3 needs to be explained.

The computation of lithium depletion by diffusion in a globular cluster (Korn et al, 2007) carefully combined with turbulence, shows that the lithium depletion amounts to about 0.26 dex. If this correction is applied to the most metal-poor field stars the pristine (or natal) Li abundance of these stars should be (in the best case) about 2.46 dex, a value still significantly smaller than the cosmological value. As a consequence the depletion by diffusion moderated by turbulence cannot explain completely the gap. Moreover this depletion by diffusion/turbulence in globular clusters is questioned by González Hernández et al. (this symposium).

We have to remark (Fig. 2 and 3) that the two components of the extremely metal-poor ($[\text{Fe}/\text{H}] \approx -3.8$) binary star CS 22176-32, analyzed by González Hernández et al. (2008) have a lithium abundance different by a factor of two, although their temperature is higher than 5800 K and that, as a consequence, no depletion of lithium is expected in these stars. This difference is above the measurement errors. The two stars were presumably born with the same lithium abundance and thus the only explanation of this large difference is that lithium has been depleted (at least) in CS 22176-32B.

"Extra-scatter" by "extra depletion" in the extremely metal-poor stars? This "extra-depletion" would appear only, and sometimes, at very low metallicity ($[\text{Fe}/\text{H}] < -3$).

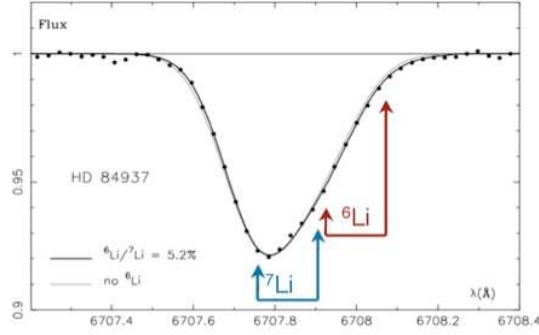


Figure 4. Profile of the doublets of ^7Li and ^6Li in a very metal poor turnoff star HD 84937, compared to a synthetic spectrum computed with no ^6Li and $^6\text{Li}/^7\text{Li}=5\%$

4. Observation of ^6Li in the most metal poor stars in the Milky Way

Since ^6Li is not significantly formed by the standard Big Bang, if ^6Li is observed in very metal-poor stars it is supposed to be formed mainly by cosmic rays.

If ^6Li exists in these stars, its abundance is very small and it is thus very difficult to detect, in particular because the lines (doublets) of ^6Li and ^7Li are overlapping (see Fig. 4). Very high resolution and high S/N spectra are required as also very precise computations of the profiles.

Several groups have recently tried to measure ^6Li in metal-poor halo stars (see in particular Asplund et al. 2006, Asplund & Meléndez 2008, Cayrel et al. 2007, García Pérez et al. 2009).

Asplund et al. (2006, 2008) observed a sample of 27 turnoff stars with $-3.3 < [\text{Fe}/\text{H}] <$

–1.2. In twelve of them, they detected ${}^6\text{Li}$. The abundance of ${}^6\text{Li}$ was constant $\log\epsilon({}^6\text{Li}) \approx 0.8$ dex and the ratio ${}^6\text{Li}/{}^7\text{Li}$ was between 4 and 10%. In all the 27 stars the abundance of lithium or its upper limit is compatible with a plateau with ${}^6\text{Li}/{}^7\text{Li} \approx 5\%$.

This result remains fragile: Cayrel et al. (2007) have shown that, if a classical analysis of a given star would provide a ratio ${}^6\text{Li}/{}^7\text{Li} = 4\%$ the result would be ${}^6\text{Li}/{}^7\text{Li} = 0\%$ if the asymmetry of the lines, due to convection, is taken into account (3D computations).

Recently, García Pérez et al. (2009) have insisted on the fact that the error of the ${}^6\text{Li}$ measurement is generally underestimated due to the uncertainty of the position of the continuum, the residual fringes etc. It is interesting to remark that Asplund & Meléndez (2008) found that the ${}^6\text{Li}/{}^7\text{Li}$ ratio in G64-37 is 11 % while García Pérez et al. (2009) found less than 1%.

4.1. *Have we really observed ${}^6\text{Li}$ in EMP stars ?*

In none of the stars, the ${}^6\text{Li}$ isotope is detected with a precision higher or equal to 3σ (Steffen et al., this symposium). If the error is a little underestimated, and if there is in fact, no ${}^6\text{Li}$ in the old metal-poor stars, the noise would mimic an absorption of ${}^6\text{Li}$ in about half of the stars (detection) and an emission of ${}^6\text{Li}$ in the other half of the stars (no detection). This is not far from what is observed...

More precise computations (NLTE, 3D) about spectra with higher S/N ratios and a better defined continuum are necessary to firmly conclude about the detection and the abundance of ${}^6\text{Li}$ in the most metal-poor stars.

5. Conclusion : Is it possible to explain the behaviour of ${}^6\text{Li}$ and ${}^7\text{Li}$ in the early Galaxy ?

5.1. ${}^6\text{Li}$

The absence of ${}^6\text{Li}$, or at least an abundance below the limit of detection, would be easy to explain since the quantity of ${}^6\text{Li}$ formed by the standard Big Bang and by the cosmic rays is supposed to be very low.

The measurement of the ${}^6\text{Li}$ abundance is difficult. If some ${}^6\text{Li}$ is observed, it should have been formed (before the birth of our old turnoff stars) by Galactic Cosmic Rays or during the explosion of massive supernovae in superbubbles: we should then observe a clear increase of ${}^6\text{Li}$ with $[\text{Fe}/\text{H}]$ like the increase of boron and beryllium (see Boesgaard 2004, Prantzos 2007). At the present time, a large abundance of ${}^6\text{Li}$, more or less constant with $[\text{Fe}/\text{H}]$, such as observed by Asplund et al. (2006, 2008): $\log\epsilon(\text{Li}) = 0.8\text{dex}$, cannot be understood in the frame of the standard theories.

5.2. ${}^7\text{Li}$

Depending on the interpretation of Fig. 3, the pristine stellar abundance of ${}^7\text{Li}$ in our Galaxy is $\log\epsilon(\text{Li}) = 2.0$ or 2.2 dex: in both cases, it is far from the value (2.72 dex) of the ${}^7\text{Li}$ abundance produced by the standard Big Bang nucleosynthesis, according to the WMAP specifications. Some explanations can be proposed none of them completely satisfactory.

- **Early astration** - According to Piau et al. (2006), the primordial ${}^7\text{Li}$, (such as computed by the Big Bang) would have been severely destroyed in the Galaxy before the formation of the old metal-poor stars by astration of the matter in massive Pop III stars, lowering the lithium abundance to the observed pristine abundance. But this theory cannot explain that the same pristine abundance of lithium is observed in the Milky Way and in ωCen (the remnant of an accreted dwarf galaxy) which certainly had different

astration histories (see section 3.1). Moreover in this case a strong excess (not observed) of C and O in the matter of the early Galaxy would be, a priori, expected. However it has been remarked (Meynet, this symposium) that massive rotating Pop III stars would eject only external layers with hydrogen and helium (without excess of C and O).

- **Depletion / Diffusion** - A second hypothesis is that lithium has been depleted in the atmosphere of the observed turnoff stars during their long evolution, by atomic diffusion carefully partially compensated by turbulence (see section 3.2). The data gathered in Fig. 3, which show for $[\text{Fe}/\text{H}] > -3$ a very small scatter (entirely explained by the determination errors) are a challenge to the computations of such an uniform depletion. The downward scatter of the lithium abundance in the extremely metal-poor stars remains to be explained (variable extra-depletion ?), as well as the absence (within our limits of T_{eff} and metallicity) of any (Li-rich) star in the "desert" between the high Big Bang lithium abundance and the plateau. Anyway, if the "depletion correction" computed by Korn et al. (2007) for the globular cluster NGC 6397 is applied to the field metal-poor dwarfs, the resulting value of the pristine lithium abundance (in the best case, about 2.46 dex) is again far from the cosmological predictions.

- **Gravity waves** - The behaviour of lithium should be evaluated taking into account the gravity waves (e. g. Talon & Charbonnel 2004, see also Talon et al., this symposium): the results of this promising theory are eagerly awaited.

- **Uncertainties in the Big Bang theories** - The production of ${}^7\text{Li}$ in the Big Bang could be lower in the standard nucleosynthesis if a resonance level (Cyburt & Pospelov, 2009) is taken into account in the transformation of ${}^7\text{Be}$ into ${}^9\text{B}$.

Moreover, a number of theories have been proposed for various more or less *ad hoc* non-standard Big Bang nucleosyntheses (see e. g. Iocco et al. 2009).

As a conclusion, in addition to progresses in fundamental physics and nucleosynthesis, the use of NLTE, 3D model atmospheres for interpreting high quality spectra, analysing differential observations (comparison dwarfs-subgiants, binaries, delicate trends, small scatters and other such details) should shed some light on the always complex problem of the lithium abundance in the early Galaxy.

6. Acknowledgments

This text benefitted from conversations with P. Bonifacio, L. Sbordone and E. Caffau.

References

- Aoki W., Barklem P.S., Beers T.C., Christlieb N., Inoue S. et al. 2009, *ApJ*, 698, 1803
 Alonso A., Arribas S., Martinez-Roger C. 2009, *A&A*, 313, 873
 Asplund M., Lambert D.L., Nissen P.E., Primas F., Smith V.V. 2006, *ApJ*, 644, 229
 Asplund M. & Meléndez J. 2008, AIP Conf. Proc. FIRST STARS III: First Stars II Conference, Vol 990, p. 342
 Bennett C. L. et al. 2003, *ApJS*, 148, 1
 Boesgaard A.M. 2004, Carnegie Obs. Astrophys. Ser., Vol. 4: Origin and Evolution of the Elements, eds. A. McWilliam and M. Rauch (Cambridge: Cambridge Univ. Press)
 Boesgaard A. M., Stephens A., & Deliyannis C.P. 2005, *ApJ*, 63, 398
 Bonifacio P., Molaro P., Sivarani T., Spite M., Spite F., et al. 2007, *A&A*, 462, 851
 Bonifacio P. & Molaro P. 1997, *MNRAS*, 285, 847
 Cayrel R., Spite M., Spite F., Vangioni-Flam E., Cassé M., & Audouze J. 1999, *A&A*, 343, 923
 Cayrel R., Steffen M., Chand H., Bonifacio P., Spite M., Spite F. et al. 2007, *A&A*, 473, L37
 Charbonnel C., Primas F. 2005, *A&A*, 442, 961

- Cyburt R.H., Fields B. D., & Olive K.A. 2008, *JCAP*, 11, 12
- Cyburt R.H., Pospelov M. 2009, arXiv(0906.4373)
- Deliyannis C. P., Demarque P., & Kawaler S. D. 1990 *ApJS*, 73, 21
- Frebel A., Simon J. D., Geha, M., & Willman B. 2010 *ApJ*, 708, 560
- García Pérez A. E., Aoki W, Inoue S., Ryan S. G., Suzuki T. K., et al. 2009, *A&A*, 504, 213
- García Pérez A.E., Christlieb N., Ryan S.G., Beers T.C. , et al. 2008, *Physica Scripta*, 133, 4036
- González Hernández J. , Bonifacio P., Ludwig H.-G., Caffau E. , Spite M. , Spite F. , et al. 2008, *A&A*, 480, 233
- Hobbs, L. M. & Thorburn, J. A 1991, *ApJ*, 375, 116
- Hosford A., Ryan S.G., García Pérez A.E., Norris J.E., & Olive K.A. 2009, *A&A*, 493, 601
- Iocco F., Mangano G., Miele G., Pisanti O., & Serpico D. 2009, *Phys. Rep.*, 472, 1
- Komatsu E., Dunkley J., Nolte M. R. et al. 2009, *ApJS*, 180, 330
- Korn A. J., Grundahl F., & Richard O. 2007, *ApJ*, 671, 402 (Paper I)
- Meléndez J., Casagrande L., Ramírez I., Asplund M. 2010, Proceedings of the IAU symp. 265
 “Chemical Abundances in the Universe: Connecting First Stars to Planets”, K. Cunha, M. Spite & B. Barbuy, eds., Cambridge University Press, p. 71
- Michaud G., Fontaine G., & Beaudet, G. 1984, *ApJ*, 282, 206
- Molaro P., Primas F. & Bonifacio, P. 1995, *A&A*, 348, 211
- Nissen Poul E., Lambert D. L., Primas F., & Smith V.V. 1999, *A&A*, 295, 47
- Piau L., Beers T. C., Balsara D. S., Sivarani T., Truran J. W., & Ferguson J. W. 2006, *ApJ*, 653, 300
- Pinsonneault M. H., Deliyannis C. P., & Demarque P. 1992, *ApJS*, 78, 179
- Prantzos N. 2007, *Space Sci. Rev.*, 130, 27
- Richard O., Michaud G., & Richer J. 2005, *ApJ*, 619, 538
- Sbordone L., Bonifacio P., Caffau E., Ludwig H.-G., Behara N. et al. 2010, Proceedings IAU Symposium No. 265, “Chemical Abundances in the Universe: Connecting First Stars to Planets”, K. Cunha, M. Spite & B. Barbuy, eds. , Cambridge University Press, p.75
- Smith V.V., Lambert D. L., & Nissen Poul E. 1998, *ApJ*, 408, 262
- Smith V.V., Lambert D. L., Nissen Poul E. 1998, *ApJ*, 506, 405
- Spergel D. N., Bean R., Doré O. et al. 2007, *ApJS*, 170, 377
- Spite M. & Spite F. 1982a, *Nature*, 297, 483
- Spite F. & Spite M. 1982b, *A&A*, 115, 357
- Spite F., Spite M. & Maillard, J. P. 1984, *A&A*, 141, 56
- Spite M., Francois P., Nissen P. E., Spite F. 1996, *A&A*, 307, 172
- Steffen M., Cayrel R., Bonifacio P., Ludwig H.-G., Caffau E. 2010, Proceedings of the IAU symp. 265 “Chemical Abundances in the Universe: Connecting First Stars to Planets”, K. Cunha, M. Spite & B. Barbuy, eds., Cambridge University Press, p. 23
- Talon S. & Charbonnel C. 2004, *A&A*, 418, 1051

Observational signatures for depletion in the Spite plateau: solving the cosmological Li discrepancy?

Jorge Meléndez¹, Luca Casagrande², Iván Ramírez², Martin Asplund² and William J. Schuster³

¹Centro de Astrofísica, Universidade do Porto, Rua das Estrelas, 4150-762 Porto, Portugal
 email: jorge@astro.up.pt

²Max-Planck-Institut für Astrophysik, Karl-Schwarzschild-Str. 1, Postfach 1317, D-85741 Garching, Germany

³Observatorio Astronómico Nacional, UNAM, Apartado Postal 877, Ensenada, BC, CP 22800, Mexico

Abstract. We present Li abundances for 73 stars in the metallicity range $-3.5 < [\text{Fe}/\text{H}] < -1.0$ using improved IRFM temperatures (Casagrande et al. 2010) with precise $E(B-V)$ values obtained mostly from interstellar NaI D lines, and high-quality equivalent widths ($\sigma_{EW} \sim 3\%$). At all metallicities we uncover a fine-structure in the Li abundances of Spite plateau stars, which we trace to Li depletion that depends on both metallicity and mass. Models including atomic diffusion and turbulent mixing seem to reproduce the observed Li depletion assuming a primordial Li abundance $A_{\text{Li}} = 2.64$ dex (MARCS models) or 2.72 (Kurucz overshooting models), in good agreement with current predictions ($A_{\text{Li}} = 2.72$) from standard BBN. We are currently expanding our sample to have a better coverage of different evolutionary stages at the high and low metallicity ends, in order to verify our findings.

Keywords. nucleosynthesis – cosmology: observations – stars: abundances, Population II

1. Introduction

One of the most important discoveries in the study of the chemical composition of stars was made in 1982 by M. and F. Spite, who found an essentially constant Li abundance in warm metal-poor stars (Spite & Spite 1982), a result interpreted as a relic of primordial nucleosynthesis. Due to its cosmological significance, there have been many studies devoted to Li in metal-poor field stars (e.g. Meléndez & Ramírez 2004; Boesgaard et al. 2005; Charbonnel & Primas 2005; Nissen et al. 2005; Asplund et al. 2006; Bonifacio et al. 2007; Shi et al. 2007; Hosford et al. 2009; Aoki et al. 2009), with observed Li abundances at the lowest $[\text{Fe}/\text{H}]$ from as low as $A_{\text{Li}} = 1.94$ to as high as $A_{\text{Li}} = 2.37$.

Using the theory of big bang nucleosynthesis (BBN) and the baryon density obtained from WMAP data, a primordial Li abundance of $A_{\text{Li}} = 2.72^{+0.05}_{-0.06}$ is predicted (Cyburt et al. 2008), which is a factor of 2-6 times higher than the Li abundance inferred from halo stars. There have been many theoretical studies on non-standard BBN trying to explain the cosmological Li discrepancy by exploring the frontiers of new physics (e.g. Coc et al. 2009; Jedamzik & Pospelov 2009; Kohri & Santoso 2009). Alternatively, the Li problem could be explained by a reduction of the original Li stellar abundance due to internal processes (i.e., by stellar depletion). In particular, stellar models including atomic diffusion and mixing can deplete a significant fraction of the initial Li content (e.g., Richard et al. 2005; Korn et al. 2006; Lind et al. 2009).

Due to the uncertainties in the Li abundances and to the limited samples available,

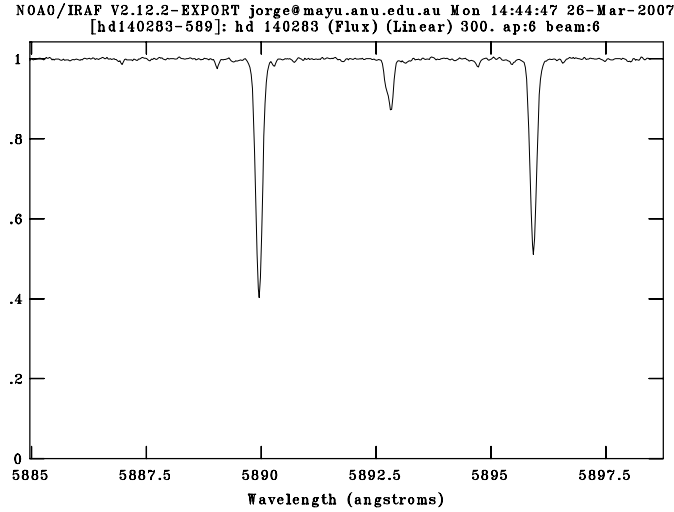


Figure 1. Keck HIRES spectrum around the NaD lines for the nearby (57 pc) metal-poor ($[\text{Fe}/\text{H}] = -2.4$) star HD 140283. The only stellar lines that can be easily seen are NaD (the two strongest features) and a blend of NiI/FeI around 589.3nm. The other features are mostly due to weak telluric water vapor lines. From the absence of IS NaD lines we infer $E(\text{B}-\text{V}) = 0.000$ for this star, although small amounts of reddening (at the level of 0.001 magnitudes) can not be excluded

only limited comparisons of models of Li depletion with stars in a broad range of mass and metallicities have been performed. We are performing such a study (Meléndez et al. 2010), achieving errors in Li abundance lower than 0.035 dex, for a large sample of metal-poor stars ($-3.5 < [\text{Fe}/\text{H}] < -1.0$), for the first time with precisely determined T_{eff} (Casagrande et al. 2010) and masses in a relatively broad mass range ($0.6\text{--}0.9 M_{\odot}$).

Our new temperature scale (Casagrande et al. 2010) is highly accurate, since it has been calibrated using solar twins (Meléndez et al. 2009; Ramírez et al. 2009), and it has also been tested using stellar diameters and absolute flux spectra (Casagrande et al. 2010). Our temperatures are also very precise because for most stars the interstellar (IS) NaI D lines were used in the determination of $E(\text{B}-\text{V})$ (see e.g. Ramírez et al. 2006), implying thus in relatively low errors in our IRFM effective temperatures. An example of a nearby halo star (HD 140283) showing no detectable IS NaD lines ($E(\text{B}-\text{V}) = 0.00$) is presented in Fig. 1.

2. Li depletion in Spite plateau stars

Our work shows that Li is depleted in Spite plateau stars (Fig. 2). The spread of the Spite plateau at any metallicity is much larger than the error bar, as can be clearly seen in Fig. 2. Also, there is a correlation between Li and stellar mass at any probed metallicity (Fig. 3), showing thus that Li has been depleted in Spite plateau stars at any metallicity. In Fig. 3 we confront the stellar evolution predictions of Richard et al. (2005) with our inferred stellar masses and Li abundances. The models include the effects of atomic diffusion, radiative acceleration and gravitational settling but moderated by a parametrized turbulent mixing. The agreement is very good when adopting a turbulent model of T6.25 and an initial $A_{\text{Li}} = 2.64$. The stellar NLTE Li abundances used above

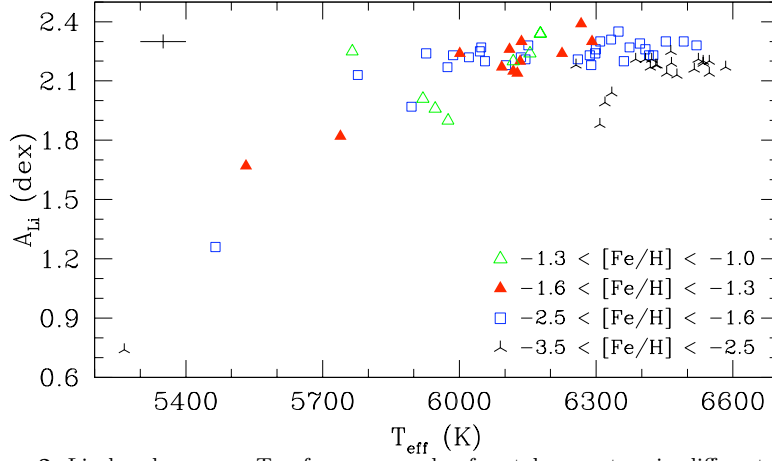


Figure 2. Li abundances vs. T_{eff} for our sample of metal-poor stars in different metallicity ranges. The spread at any given metallicity is much larger than the error bar. Figure taken from Meléndez et al. (2010)

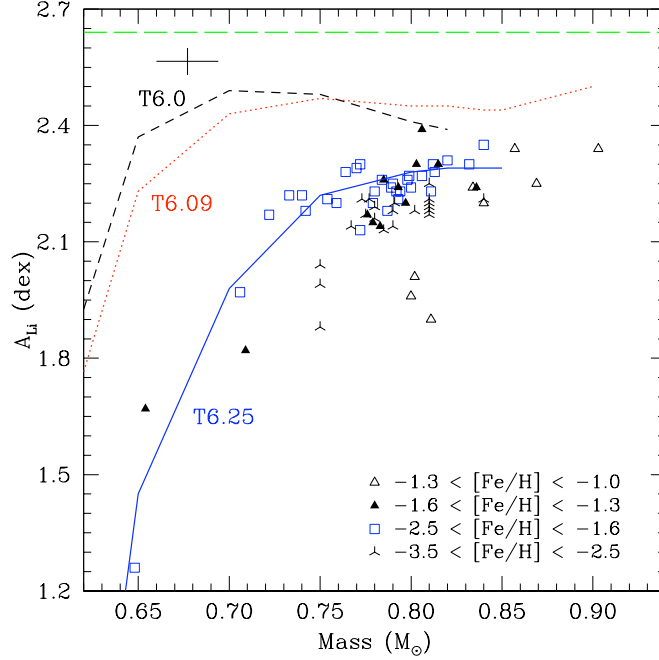


Figure 3. Li abundances as a function of stellar mass in different metallicity ranges. Models at $[\text{Fe}/\text{H}] = -2.3$ including diffusion and T6.0 (short dashed line), T6.09 (dotted line) and T6.25 (solid line) turbulence (Richard et al. 2005) are shown. The models have been rescaled to an initial $A_{\text{Li}}=2.64$ (long dashed line). Figure taken from Meléndez et al. (2010)

were obtained with the latest MARCS models (Gustafsson et al. 2008), but if we use instead the Kurucz convective overshooting models, then the required initial abundance to explain our data would be $A_{\text{Li}} = 2.72$.

Our results imply that the Li abundances observed in Li plateau stars have been depleted from their original values and therefore do not represent the primordial Li abundance (see also Korn et al. 2006 and Lind et al. 2009 for additional signatures of Li depletion in stars of the globular cluster NGC 6397). It appears that the observed Li abundances in metal-poor stars can be reasonably well reconciled with the predictions from standard Big Bang nucleosynthesis (e.g. Cyburt et al. 2008) by means of more realistic stellar evolution models that include Li depletion through diffusion and turbulent mixing (Richard et al. 2005). We caution however, that, although encouraging, our results should not be viewed as proof of the correctness of the Richard et al. models until the free parameters required for the stellar modeling are better understood from basic physical principles. In this context, new physics should not be discarded yet as a solution of the cosmological Li discrepancy, as perhaps the low Li-7 abundances in metal-poor stars might be a signature of supersymmetric particles in the early universe, which could also explain the Li-6 detections in metal-poor stars (e.g. Asplund et al. 2006; Asplund & Meléndez 2008).

We are expanding our sample to have a better coverage of different evolutionary stages at all metallicities. Our expanded sample (Meléndez et al. 2010) will allow us to verify if the Li plateau is indeed depleted at low and high metallicities.

References

- Aoki, W. et al. 2009, *ApJ*, 698, 1803
 Asplund, M., Lambert, D. L., Nissen, P. E., Primas, F., & Smith, V. V. 2006, *ApJ*, 644, 229
 Asplund, M., & Meléndez, J. 2008, *First Stars III*, 990, 342
 Boesgaard, A. M., Stephens, A., & Deliyannis, C. P. 2005, *ApJ*, 633, 398
 Bonifacio, P., et al. 2007, *A&A*, 462, 851
 Casagrande, L., Ramírez, I., Meléndez, J., Bessell, M. & Asplund, M. 2010, *A&A*, submitted
 Charbonnel, C., & Primas, F. 2005, *A&A*, 442, 961
 Coc, A., Olive, K. A., Uzan, J.-P., & Vangioni, E. 2009, *Phys. Rev. D.*, 79, 103512
 Cyburt, R. H., Fields, B. D., & Olive, K. A. 2008, *J. Cosmology & Astro-Particle Phys.*, 11, 12
 Gustafsson, B., Edvardsson, B., Eriksson, K. et al. 2008, *A&A*, 486, 951
 Hosford, A., Ryan, S. G., García Pérez, A. E., Norris, J. E., & Olive, K. A. 2009, *A&A*, 493, 601
 Jedamzik, K., & Pospelov, M. 2009, *New Journal of Physics*, 11, 105028
 Kohri, K., & Santoso, Y. 2009, *Phys. Rev. D.*, 79, 043514
 Korn, A. J., et al. 2006, *Nature*, 442, 657
 Lind, K., Primas, F., Charbonnel, C., Grundahl, F., & Asplund, M. 2009, *A&A*, 503, 545
 Meléndez, J. & Ramírez, I. 2004, *ApJ* (Letters), 615, L33
 Meléndez, J., Asplund, M., Gustafsson, B., & Yong, D. 2009, *ApJ* (Letters), 704, L66
 Meléndez, J., Casagrande, L., Ramírez, I., Asplund, M. 2010, & W. J. Schuster *A&A*, submitted
 Nissen, P. E., Akerman, C., Asplund, M., Fabbian, D., & Pettini, M. 2005, *From Lithium to Uranium: Elemental Tracers of Early Cosmic Evolution*, *IAU Symp.*, 228, 101
 Ramírez, I., Allende Prieto, C., Redfield, S., & Lambert, D. L. 2006, *A&A*, 459, 613
 Ramírez, I., Meléndez, J., & Asplund, M. 2009, *A&A*, 508, L17
 Richard, O., Michaud, G., & Richer, J. 2005, *ApJ*, 619, 538
 Shi, J. R., Gehren, T., Zhang, H. W., Zeng, J. L., & Zhao, G. 2007, *A&A*, 465, 587
 Spite, F., & Spite, M. 1982, *A&A*, 115, 357

Convection and ${}^6\text{Li}$ in the atmospheres of metal-poor halo stars

Matthias Steffen¹, R. Cayrel², P. Bonifacio², H.-G. Ludwig³, and E. Caffau²

¹Astrophysikalisches Institut Potsdam, An der Sternwarte 16, D-14482 Potsdam, Germany
 email: msteffen@aip.de

²GEPI – Observatoire de Paris, Paris, France

³ZAH-Landessternwarte, Königstuhl 12, D-69117 Heidelberg, Germany

Abstract. Based on 3D hydrodynamical model atmospheres computed with the CO⁵BOLD code and 3D non-LTE (NLTE) line formation calculations, we study the effect of the convection-induced line asymmetry on the derived ${}^6\text{Li}$ abundance for a range in effective temperature, gravity, and metallicity covering the stars of the Asplund et al. (2006) sample. When the asymmetry effect is taken into account for this sample of stars, the resulting ${}^6\text{Li}/{}^7\text{Li}$ ratios are reduced by about 1.5% on average with respect to the isotopic ratios determined by Asplund et al. (2006). This purely theoretical correction diminishes the number of significant ${}^6\text{Li}$ detections from 9 to 4 (2σ criterion), or from 5 to 2 (3σ criterion). In view of this result the existence of a ${}^6\text{Li}$ plateau appears questionable. A careful reanalysis of individual objects by fitting the observed lithium 6707 Å doublet both with 3D NLTE and 1D LTE synthetic line profiles confirms that the inferred ${}^6\text{Li}$ abundance is systematically lower when using 3D NLTE instead of 1D LTE line fitting. Nevertheless, halo stars with unquestionable ${}^6\text{Li}$ detection do exist even if analyzed in 3D-NLTE, the most prominent example being HD 84937.

Keywords. stars: abundances, atmospheres – hydrodynamics – convection, radiative transfer – line: formation, profiles – stars: individual (G271-162, HD 74000, HD 84937)

1. Introduction

The spectroscopic signature of the presence of ${}^6\text{Li}$ in the atmospheres of metal-poor halo stars is a subtle extra depression in the red wing of the ${}^7\text{Li}$ doublet, which can only be detected in spectra of the highest quality. Based on high-resolution, high signal-to-noise VLT/UVES spectra of 24 bright metal-poor stars, Asplund et al. (2006) report the detection of ${}^6\text{Li}$ in nine of these objects. The average ${}^6\text{Li}/{}^7\text{Li}$ isotopic ratio in the nine stars in which ${}^6\text{Li}$ has been detected is about 4% and is very similar in each of these stars, defining a ${}^6\text{Li}$ plateau at approximately $\log n({}^6\text{Li}) = 0.85$ (on the scale $\log n(\text{H}) = 12$). A convincing theoretical explanation of this new ${}^6\text{Li}$ plateau turned out to be problematic: the high abundances of ${}^6\text{Li}$ at the lowest metallicities cannot be explained by current models of galactic cosmic-ray production, even if the depletion of ${}^6\text{Li}$ during the pre-main-sequence phase is ignored (see reviews by e.g. Christlieb 2008, Cayrel et al. 2008, Prantzos 2010 [this volume] and references therein).

A possible solution of the so-called ‘second Lithium problem’ was proposed by Cayrel et al. (2007), who point out that the intrinsic line asymmetry caused by convection in the photospheres of metal-poor turn-off stars is almost indistinguishable from the asymmetry produced by a weak ${}^6\text{Li}$ blend on a presumed symmetric ${}^7\text{Li}$ profile. As a consequence, the derived ${}^6\text{Li}$ abundance should be significantly reduced when the intrinsic line asymmetry in properly taken into account. Using 3D NLTE line formation calculations based on 3D

hydrodynamical model atmospheres computed with the CO⁵BOLD code (Freytag et al. 2002, Wedemeyer et al. 2004, see also http://www.astro.uu.se/~bf/co5bold_main.html), we quantify the theoretical effect of the convection-induced line asymmetry on the resulting ⁶Li abundance as a function of effective temperature, gravity, and metallicity, for a parameter range that covers the stars of the Asplund et al. (2006) sample.

A careful reanalysis of individual objects is under way, in which we consider two alternative approaches for fixing the residual line broadening, V_{BR} , the combined effect of macroturbulence (1D only) and instrumental broadening, for given microturbulence (1D only) and rotational velocity: (i) treating V_{BR} as a free parameter when fitting the Li feature, (ii) deriving V_{BR} from additional unblended spectral lines with similar properties as Li I 6707. We show that method (ii) is potentially dangerous, because the inferred broadening parameter shows considerable line-to-line variations, and the resulting ⁶Li abundance depends rather sensitively on the adopted value of V_{BR} .

2. 3D hydrodynamical simulations and spectrum synthesis

The hydrodynamical atmospheres used in the present study are part of the CIFIST 3D model atmosphere grid (Ludwig et al. 2009). They have been obtained from realistic numerical simulations with the CO⁵BOLD code which solves the time-dependent equations of compressible hydrodynamics in a constant gravity field together with the equations of non-local, frequency-dependent radiative transfer in a Cartesian box representative of a volume located at the stellar surface. The computational domain is periodic in x and y direction, has open top and bottom boundaries, and is resolved by typically $140 \times 140 \times 150$ grid cells. The vertical optical depth of the box varies from $\log \tau_{\text{Ross}} \approx -8$ (top) to $\log \tau_{\text{Ross}} \approx +7.5$ (bottom), and the radiative transfer is solved in 6 or 12 opacity bins. Further information about the models used in the present study is compiled in Table 1. Each of the models is represented by a number of snapshots, indicated in column (6), chosen from the full time sequence of the corresponding simulation.

These representative snapshots are processed by the non-LTE code NLTE3D that solves the statistical equilibrium equations for a 17 level lithium atom with 34 line transitions, fully taking into account the 3D thermal structure of the respective model atmosphere. The photo-ionizing radiation field is computed at 704 frequency points between λ 925 and 32 407 Å, using the opacity distribution functions of Castelli & Kurucz (2004) to allow for metallicity-dependent line-blanketing, including the H I–H⁺ and H I–H I quasi-molecular absorption near λ 1400 and 1600 Å, respectively. Collisional ionization by neutral hydrogen via the charge transfer reaction $\text{H}(1s) + \text{Li}(n\ell) \leftrightarrow \text{Li}^+(1s^2) + \text{H}^-$ is treated according to Barklem et al. (2003). More details are given in Sbordone et al. (2009). Finally, 3D NLTE synthetic line profiles of the Li I λ 6707 Å doublet are computed with the line formation code Linfor3D (http://www.aip.de/~mst/linfor3D_main.html), using the departure coefficients $b_i = n_i(\text{NLTE})/n_i(\text{LTE})$ provided by NLTE3D for each level i of the lithium model atom as a function of geometrical position within the 3D model atmospheres. As demonstrated in Fig. 1, 3D NLTE effects are very important for the metal-poor dwarfs considered here: they strongly reduce the height range of line formation such that the 3D NLTE equivalent width is smaller by roughly a factor 2 compared to 3D LTE. Ironically, the line strength predicted by standard 1D mixing-length models in LTE are close to the results obtained from elaborate 3D NLTE calculations. We note that the half-width of the 3D NLTE line profile, $\text{FWHM}(\text{NLTE}) = 8.5$ km/s, is larger by about 10%: $\text{FWHM}(\text{LTE}) = 7.7$ and 7.5 km/s, respectively, before and after reducing the Li abundance such that 3D LTE and 3D NLTE equivalent widths agree. This is because 3D LTE profile senses the higher photosphere where both thermal and hydrodynamical

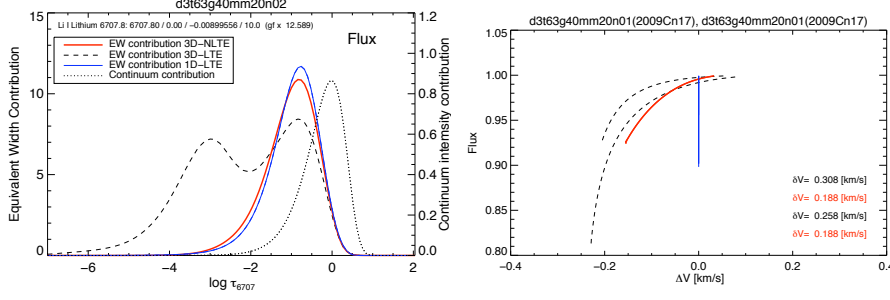


Figure 1. Comparison of 3D LTE (dashed), 3D non-LTE (thick solid), and 1D LTE (thin solid) equivalent width contribution functions (left) and line bisectors (right) of a single ${}^7\text{Li}$ component, computed for a typical metal-poor turn-off halo star ($T_{\text{eff}} = 6215$ K, $\log g = 4.0$, $[\text{Fe}/\text{H}] = -2$). Non-LTE effects strongly reduce the height range of formation and equivalent width of the line ($W: 35.5 \rightarrow 15.6$ mÅ), while differences between 1D LTE and 3D NLTE are much smaller. The line asymmetry is smaller in non-LTE: the velocity span of the bisector is $\delta v(\text{NLTE}) \approx 190$ m/s, while $\delta v(\text{LTE}) \approx 310$ and 260 m/s, respectively, before and after adjusting the equivalent width (by reducing the Li abundance) and the half-width (by Gaussian broadening) of the LTE line to match the values of the NLTE profile (compare the two dashed bisectors).

velocities are lower. However, the NLTE line profile is significantly less asymmetric than the LTE profile, even if the latter is broadened to the same half-width (Fig. 1, right panel).

3. ${}^6\text{Li}$ bias due to convective line asymmetry

As outlined above, the ${}^6\text{Li}$ abundance is systematically overestimated if one ignores the intrinsic asymmetry of the ${}^7\text{Li}$ line components. To quantify this bias theoretically, we rely on synthetic spectra. The idea is as follows: we represent the observation by the synthetic 3D NLTE line profile of the ${}^7\text{Li}$ line blend, computed with zero ${}^6\text{Li}$ content. Except for an optional rotational broadening, the only source of non-thermal line broadening is the 3D hydrodynamical velocity field, which also gives rise to a convective blue-shift and an intrinsic line asymmetry. Now this 3D ${}^7\text{Li}$ line blend is fitted by 'classical' 1D synthetic line profiles composed of intrinsically symmetric components of ${}^6\text{Li}$ and ${}^7\text{Li}$. Four parameters are varied independently to find the best fit (minimum χ^2): in addition to the total ${}^6\text{Li}+{}^7\text{Li}$ abundance, $A(\text{Li})$, and the ${}^6\text{Li}/{}^7\text{Li}$ isotopic ratio, $q(\text{Li})$, which control line strength and line asymmetry, respectively, we also allow for a residual line broadening described by a Gaussian kernel with half-width V_{BR} , and a global line shift, Δv . Note that the four fitting parameters are non-degenerate, since each one has a distinctly different effect on the line profile. The rotational line broadening is fixed to the value used in the 3D spectrum synthesis (we tried $v \sin i = 0$ and 2 km/s). The value $q^*(\text{Li})$ of the best fit is then identified with the correction that has to be *subtracted* from the ${}^6\text{Li}/{}^7\text{Li}$ isotopic ratio derived from the 1D analysis to correct for the bias introduced by neglecting the intrinsic line asymmetry: $q^{(3D)}(\text{Li}) = q^{(1D)}(\text{Li}) - q^*(\text{Li})$. The procedure properly accounts for radiative transfer in the lines, including saturation effects.

Two different sets of 1D profiles were used for this purpose: (a) NLTE line profiles based on the (3D) model, constructed by averaging the 3D model on surfaces of constant optical depth, and (b) LTE line profiles computed from a so-called LHD model, a 1D mixing-length model atmosphere that has the same stellar parameters and uses the same microphysics and radiative transfer scheme as the corresponding 3D model. For both kind of 1D models, the microturbulence was fixed at $\xi_{\text{mic}} = 1.5$ km/s. The mixing length parameter adopted for the LHD models is $\alpha_{\text{MLT}} = 0.5$.

Table 1. List of models used in the present study. Columns (2)-(6) give effective temperature, surface gravity, metallicity, number of opacity bins used in the radiation hydrodynamics simulation, and number of snapshots selected for spectrum synthesis. The equivalent width of the synthetic 3D non-LTE ${}^7\text{Li}$ doublet at $\lambda 6707$ Å, assuming $A(\text{Li})=2.2$ and no ${}^6\text{Li}$, is given in column (7). Columns (8) and (9) show $q_a^*(\text{Li})$ and $q_b^*(\text{Li})$, the ${}^6\text{Li}/{}^7\text{Li}$ isotopic ratio inferred from fitting this 3D non-LTE line profile with two different kinds of 1D profiles, in each case assuming a rotational broadening of $v \sin i = 0.0 / 2.0$ km/s, respectively (see text for details).

Model	$T_{\text{eff}}^{(1)}$ [K]	$\log g$	[Fe/H]	Nbin	Nsnap	$W^{(2)}$ [mÅ]	$q_a^* = n({}^6\text{Li})/n({}^7\text{Li})$ (3D) NLTE [%]	$q_b^* = n({}^6\text{Li})/n({}^7\text{Li})$ 1D LTE [%]
d3t59g40mm30n02	5846	4.0	-3.0	6	20	44.9	1.14 / 1.14	0.88 / 0.88
d3t59g45mm30n01	5924	4.5	-3.0	6	19	39.9	0.75 / 0.75	0.63 / 0.64
d3t63g40mm30n01	6269	4.0	-3.0	6	20	23.9	1.96 / 1.93	1.86 / 1.83
d3t63g40mm30n02	6242	4.0	-3.0	12	20	24.1	1.81 / 1.80	1.63 / 1.62
d3t63g45mm30n01	6272	4.5	-3.0	6	18	24.3	1.07 / 1.06	1.02 / 1.00
d3t65g40mm30n01	6408	4.0	-3.0	6	20	20.0	1.75 / 1.70	1.70 / 1.66
d3t65g45mm30n01	6556	4.5	-3.0	6	12	16.4	1.29 / 1.27	1.25 / 1.22
<hr/>								
d3t59g35mm20n01	5861	3.5	-2.0	6	20	42.8	2.48 / 2.44	2.02 / 2.01
d3t59g40mm20n02	5856	4.0	-2.0	6	20	45.2	1.59 / 1.59	0.96 / 0.98
d3t59g45mm20n01	5923	4.5	-2.0	6	18	42.3	1.12 / 1.13	0.45 / 0.46
d3t63g35mm20n01	6287	3.5	-2.0	6	20	22.1	4.09 / 4.00	4.04 / 3.97
d3t63g40mm20n01	6278	4.0	-2.0	6	16	23.7	1.95 / 1.94	1.79 / 1.78
d3t63g40mm20n02	6215	4.0	-2.0	12	20	25.1	1.92 / 1.92	1.66 / 1.67
d3t63g45mm20n01	6323	4.5	-2.0	6	19	23.0	1.18 / 1.18	0.97 / 0.97
d3t65g40mm20n01	6534	4.0	-2.0	6	19	16.2	2.28 / 2.21	2.22 / 2.16
d3t65g45mm20n01	6533	4.5	-2.0	6	19	17.0	1.31 / 1.29	1.21 / 1.19
<hr/>								
d3t59g40mm10n02	5850	4.0	-1.0	6	20	41.5	1.60 / 1.62	1.45 / 1.47
d3t59g45mm10n01	5923	4.5	-1.0	6	08	38.2	1.14 / 1.15	0.83 / 0.85
d3t63g40mm10n01	6261	4.0	-1.0	6	20	22.0	2.37 / 2.38	2.33 / 2.33
d3t63g40mm10n02	6236	4.0	-1.0	12	20	21.8	2.15 / 2.16	2.05 / 2.06
d3t63g45mm10n01	6238	4.5	-1.0	6	20	23.4	1.36 / 1.37	1.23 / 1.24
d3t65g40mm10n01	6503	4.0	-1.0	6	20	15.5	3.10 / 3.02	3.14 / 3.06
d3t65g45mm10n01	6456	4.5	-1.0	6	19	17.1	1.51 / 1.51	1.44 / 1.43

Notes: ¹⁾ averaged over selected snapshots; ²⁾ averaged over selected 3D non-LTE spectra

We have determined $q^*(\text{Li})$ according to the method outlined above for our grid of 3D model atmospheres. The results are given in Table 1, both for fitting with the (3D) NLTE profiles ($q_a^*(\text{Li})$, col. (8)) and with the 1D LTE profiles of the LHD models ($q_b^*(\text{Li})$, col. (9)). At given metallicity, the corrections are largest for low gravity and high effective temperature. They increase towards higher metallicity. We also note that $q^*(\text{Li})$ is essentially insensitive to the choice of the rotational broadening.

The analysis of Asplund et al. (2006) utilizes 1D LTE profiles computed from MARCS

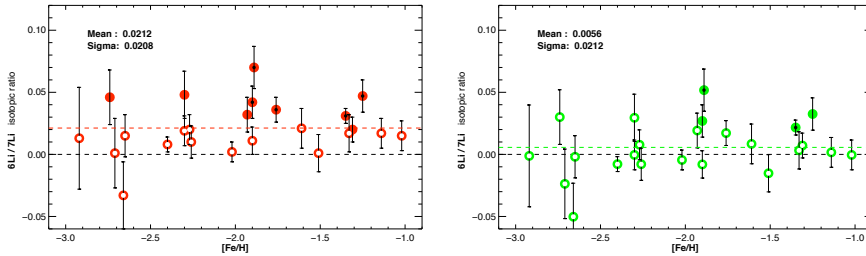


Figure 2. ${}^6\text{Li}/{}^7\text{Li}$ isotopic ratio, and $\pm 1\sigma$ error bars, as a function of metallicity as derived by Asplund et al. (2006) before (left) and after (right) subtraction of $q_a^*(\text{Li})$ (Table 1, col. (8)) to correct for the bias due to the intrinsic line asymmetry. Open circles denote non-detections, filled circles and filled circles with a black dot denote ${}^6\text{Li}$ detections above the 2σ and 3σ level, respectively.

model atmospheres. Hence, the correction $q_b^*(\text{Li})$, computed with the 1D LTE profiles of the 1D LHD models, should be applied to their ${}^6\text{Li}/{}^7\text{Li}$ isotopic ratios. The resulting downward corrections are typically in the range $1\% < q_b^*(\text{Li}) < 2\%$ for the stars of their sample (cf. Steffen et al. 2010, Fig. 2). After subtracting the individual $q_b^*(\text{Li})$ for each of these stars, according to their T_{eff} , $\log g$, and $[\text{Fe}/\text{H}]$, the mean ${}^6\text{Li}/{}^7\text{Li}$ isotopic ratio of the sample is reduced from 0.0212 to 0.0056, as illustrated in Fig. 2. Given the ${}^6\text{Li}/{}^7\text{Li}$ isotopic ratios and their 1σ error bars as determined by Asplund et al. (2006), the number of stars with a ${}^6\text{Li}$ detection above the 2σ and 3σ level is 9 and 5, respectively, out of 24. After correction, the number of 2σ and 3σ detections is reduced to 4 and 2, respectively. One of the stars meeting the 3σ criterion after correction, HD 106038, survives only because of its particularly small error bar of ± 0.006 . The other one is G020-024, which shows the clearest evidence for the presence of ${}^6\text{Li}$ ($q(\text{Li}) = 0.052 \pm 0.017$), while HD 102200 remains the only clear 2σ detection ($q(\text{Li}) = 0.033 \pm 0.013$). The spectra of these stars should be reanalyzed with 3D NLTE line profiles.

4. Analysis of observed spectra: 3D NLTE versus 1D LTE line fitting

As a further exercise, we have fitted the observed Li I $\lambda 6707$ Å spectra of three halo turn-off stars (see Table 2), both with 3D NLTE and 1D LTE synthetic line profiles. Since the parameters of these three stars are very similar, the synthetic spectra were computed in all cases from hydrodynamical model d3t6300g40mm20n01 (see Table 1) and the corresponding 1D LHD model. The standard approach is to vary the four parameters $A(\text{Li})$, $q(\text{Li})$, V_{BR} , and Δv to find the optimum line profile fit, as described above (method I). The results are presented in Table 3. As expected, the 3D analysis yields lower ${}^6\text{Li}/{}^7\text{Li}$ isotopic ratios by about 1.7%. The numbers differ slightly from those given by Steffen et al. 2010 due to an upgrade of the line fitting procedure, but the conclusions remain unchanged: HD 74000 and G271-162 are considered non-detections, while HD 84937 remains a clear ${}^6\text{Li}$ detection with $q^{(3\text{D-NLTE})}(\text{Li}) \approx 5\%$.

For completeness, Table 3 also shows the results of fitting the observed lines with 3D LTE synthetic profiles (not recommended). The ${}^6\text{Li}$ abundances obtained in this way lie between the 3D NLTE and the 1D LTE results. It is not obvious why fitting with the more asymmetric 3D LTE profiles gives higher ${}^6\text{Li}$ than fitting with the slightly more symmetric 3D NLTE profiles, but this is a robust result.

For HD 74000, we also tried an alternative approach (method II), where V_{BR} is determined from other spectral lines, and is then fixed during the fitting of the Li I $\lambda 6707$ Å feature. For this purpose, we rely on a set of 6 clean Fe I lines with similar excitation potential between 2.4 and 2.6 eV: the 5 lines of Cayrel et al. (2007), Table 1, plus Fe I $\lambda 6230.7$ Å, $E_i = 2.559$ eV. Their equivalent widths range from $W \approx 13$ to 30 mÅ, embracing the strength of the Li doublet. Fitting the 6 Fe I lines with 3D LTE synthetic line profiles, we obtain $V_{\text{BR}}(\text{Fe}) = 3.05 (2.15) \pm 0.16 (0.23)$ km/s for $v \sin i = 0 (2)$ km/s, in close agreement with $V_{\text{BR}}(\text{Li})$ inferred from the fitting of the Li I profile. This result may be taken as an indication that, in contrast to Li, the selected Fe I lines are not severely affected by departures from LTE. We note, however, a trend of $V_{\text{BR}}(\text{Fe})$ increasing slightly with W , which remains to be understood. If instead the Fe I lines are

Table 2. Observed Li I $\lambda 6707$ Å spectra of three metal-poor turn-off stars

Star	T_{eff} [K]	$\log g$	$[\text{Fe}/\text{H}]$	$R=\lambda/\Delta\lambda$	S/N	Instrument	Reference
HD 74000	6203	4.03	-2.05	120 000	600	ESO3.6 / HARPS	Cayrel et al. 2007
G271-162	6330	4.00	-2.25	110 000	600	VLT / UVES	Nissen et al. 2000
HD 84937	6300	4.00	-2.30	100 000	630	CFHT / GECKO	Cayrel et al. 1999

Table 3. Fitting the observed spectra of Table 2 with 3D and 1D synthetic line profiles. Columns (4)-(7) show the results for $v \sin i = 0.0 / 2.0$ km/s.

Star	synthetic spectrum	fitting method	$A(\text{Li})$ ¹⁾	$n(^6\text{Li})/n(^7\text{Li})$ [%]	V_{BR} ²⁾ [km/s]	Δv [km/s]
HD 74000	3D NLTE	I	2.25 / 2.25	-1.1 / -1.1	3.1 / 2.1	0.64 / 0.64
	(3D LTE)	I	1.85 / 1.85	-0.4 / -0.5	4.7 / 4.1	0.66 / 0.67
	1D LTE	I	2.23 / 2.23	0.6 / 0.6	5.9 / 5.4	0.43 / 0.43
	3D NLTE	II	2.25 / 2.25	-1.1 / -1.3	3.1 / 2.2	0.64 / 0.65
	(3D LTE)	II	1.84 / 1.84	4.6 / 4.2	3.1 / 2.2	0.46 / 0.47
	1D LTE	II	2.23 / 2.23	1.7 / 1.7	5.6 / 5.1	0.39 / 0.39
G271-162	3D NLTE	I	2.30 / 2.30	0.7 / 0.6	3.7 / 2.9	0.04 / 0.04
	(3D LTE)	I	1.89 / 1.89	1.3 / 1.1	5.2 / 4.6	0.06 / 0.07
	1D LTE	I	2.27 / 2.27	2.3 / 2.4	6.2 / 5.8	-0.17 / -0.17
HD 84937	3D NLTE	I	2.20 / 2.20	5.2 / 5.2	3.3 / 2.4	0.02 / 0.02
	(3D LTE)	I	1.80 / 1.80	5.8 / 5.7	4.8 / 4.3	0.05 / 0.05
	1D LTE	I	2.18 / 2.18	6.9 / 6.9	6.0 / 5.6	-0.19 / -0.19

Notes: ¹⁾ $\log [n(^6\text{Li}) + n(^7\text{Li})] - \log n(\text{H}) + 12$; ²⁾ Gaussian kernel, **bold**: fixed from Fe I lines

fitted with 1D LTE synthetic profiles, we find $V_{\text{BR}}(\text{Fe}) = 5.61 (5.13) \pm 0.07 (0.09)$ km/s, systematically lower than $V_{\text{BR}}(\text{Li})$ by 0.3 km/s. Fixing $V_{\text{BR}} = V_{\text{BR}}(\text{Fe})$, the best fit of the Li I doublet implies $q^{1\text{D LTE}}(\text{Li}) = 1.7\%$, which is 1.1% higher than with method I. Finally, Table 3 demonstrates that applying method II with 3D LTE fitting of Li I leads to a severe overestimation of the $^6\text{Li}/^7\text{Li}$ isotopic ratio: $q^{3\text{D LTE}}(\text{Li}) > 4\%$ compared to $q^{3\text{D NLTE}}(\text{Li}) = -1.1\%$!

5. Conclusions

The $^6\text{Li}/^7\text{Li}$ isotopic ratio derived from fitting of the Li I doublet with 3D NLTE synthetic line profiles is shown to be about 1% to 2% lower than what is obtained with 1D LTE profiles. Based on this result, we conclude that only 2 out of the 24 stars of the Asplund et al. (2006) sample would remain significant ^6Li detections when subjected to a 3D non-LTE analysis, suggesting that the presence of ^6Li in the atmospheres of galactic halo stars is rather the exception than the rule, and hence does not necessarily constitute a *cosmological* ^6Li problem. If we adopt the approach by Asplund et al. (2006), relying on additional spectral lines to fix the residual line broadening, the difference between 3D NLTE and 1D LTE results increases even more, as far as we can judge from our case study HD 74000. Until the 3D NLTE effects are fully understood for all involved lines, we consider this method as potentially dangerous.

References

- Asplund, M., Lambert, D. L., Nissen, P. E., Primas, F., & Smith, V. V. 2006, *ApJ*, 644, 229
Barklem, P.S., Belyaev, A.K., Asplund, M. 2003, *A&A*, 409, L1
Castelli, F., & Kurucz, R. L. 2004, arXiv:astro-ph/0405087
Cayrel, R., et al. 1999, *A&A*, 343, 923
Cayrel, R., et al. 2007, *A&A*, 473, L37
Cayrel, R., et al. 2008, in *Proceedings of Nuclei in the Cosmos (NIC X)*
Christlieb, N. 2008, *Journal of Physics G: Nuclear Physics*, 35, 014001
Freytag, B., Steffen, M., & Dorch, B. 2002, *AN*, 323, 213
Ludwig, H.-G., et al. 2009, *MemSAI*, 80, 708
Nissen, P.E., Asplund, M., Hill, V., D’Odorico, S. 2000, *A&A* 357, L49
Sbordone, L., Bonifacio, P., Caffau, E., et al. 2009, *A&A* (in press)
Steffen, M., et al. 2010, in: K. Cunha, M. Spite, and B. Barbuy (eds.), *Chemical Abundances in the Universe: Connecting First Stars to Planets*, Proc. IAU Symposium No. 265, in press
Wedemeyer, S., Freytag, B., Steffen, M., Ludwig, H.-G., & Holweger, H. 2004, *A&A*, 414, 1121

Beryllium and boron in metal-poor stars

Francesca Primas¹

¹European Southern Observatory,
 KarlSchwarzschild Strasse 2, D-85748, Garching b. München, Germany
 email: fprimas@eso.org

Abstract. Knowledge of lithium, beryllium, and boron abundances in stars of the Galactic halo and disk plays a major role in our understanding of Big Bang nucleosynthesis, cosmic-ray physics, and stellar interiors. ⁹Be and ¹⁰B are believed to originate entirely from spallation reactions in the interstellar medium (ISM) between α -particles and protons and heavy nuclei like carbon, nitrogen, and oxygen (CNO), whereas ¹¹B may have an extra production channel via neutrino-spallation. Beryllium and boron are both observationally challenging, with their main resonant doublets falling respectively at 313 nm and at 250 nm. The advent of 8-10m class telescopes equipped with highly sensitive (in the near-UV/blue) spectrographs has opened up a new era of Be abundance studies. Here, I will review and discuss the most interesting results of recent observational campaigns in terms of formation and evolution of these two light elements.

Keywords. Galaxy: halo, abundances, evolution – stars: Population II, abundances, atmospheres, interiors

1. Introduction

After hydrogen (H), helium (He), and lithium (Li), beryllium (Be) and boron (B) complete the group of the so-called light elements, all covered in great detail during this Symposium. All these elements share a common feature concerning their origin: they can not be produced in stellar interiors, where in fact most of them get destroyed. Deuterium, He, and Li have a strong cosmological component responsible for their formation, hence they offer important insights on the primordial abundances of their isotopes in the early Universe. On the contrary, Be and B are formed via spallation reactions between CNO atoms and α +p particles.

For a long time, it was believed that these reactions take mostly place in the interstellar medium, where alphas and protons (carried by cosmic rays – CR – traveling across the Galaxy) would end up hitting target nuclei like CNO, spallating into atoms of beryllium and boron (cf Reeves et al. 1970, Meneguzzi et al. 1971). One of the earliest observational findings supporting this scenario was the beryllium-to-hydrogen ratios observed in young stars ($\sim 10^{-11}$) in the 70s (e.g. Boesgaard 1976, Boesgaard et al. 1977) which was found to match rather closely the theoretical prediction of Be formation when integrated along the entire history of the Galaxy. In other words, the abundances derived in a few Population I (Pop I) objects were approximately matching the product of the formation rate of Be \dagger \times the abundance ratio of these targets with respect to hydrogen ($\sim 10^{-3}$) in space \times the age of the Galaxy.

Indeed, the observed CR flux, integrated over 10^{10} years of Galactic evolution, seems sufficient to produce the solar abundances of B, Be, and ⁶Li, despite, e.g., the failure in reproducing the observed solar B isotopic ratio. CR spallation in the general ISM has

\dagger described by Reeves et al. (1970) to be the product between the flux of high-energy protons ($\sim 16 \text{ cm}^{-2} \text{ sec}$) \times the cross sections for ⁹Be formation by proton collision on the most abundant targets, ¹⁶O and ¹²C ($\sim 5 \text{ mb}$)

therefore been mostly accepted for 25 years as the main origin of these light elements. However, as I will show in the next section, the first observational studies carried out at 4m ground-based telescopes and with the Hubble Space Telescope (HST) showed some surprising results that triggered a revision of the above described scenario.

Last but not least, the light elements Li, Be, and B, when measured in the same object(s) can be successfully used as diagnostics in the study of stellar mixing. Because they burn at relatively low, but slightly different (and increasing) temperatures, they are expected to show different degrees of depletion and/or dilution at different times. Lithium, which is destroyed at the lowest temperature of all three elements ($T_B \simeq 2.5 \times 10^6$ K) should deplete first, followed by Be ($T_B \simeq 3.5 \times 10^6$ K) and B ($T_B \simeq 5 \times 10^6$ K). Unfortunately, there are large discrepancies in the size of the data samples that have been looked at, which clearly correlate with the observational difficulties in detecting a given transition: lithium, with its main resonant doublet falling in the optical, at 670nm, is the most studied of the three, followed by beryllium (main resonant doublet very close to the atmospheric cut-off, at 313nm), and boron (resonant doublet at 250nm and single feature at 209nm), which requires a telescope in space.

2. A bit of (observational) history

The first attempts to detect beryllium in Population II (Pop II) stars were made in the mid-late 80s (e.g. Molaro et al. 1984, Rebolo et al. 1988) with, respectively, the International Ultraviolet Explorer (IUE) and the 2.5m Isaac Newton Telescope. Unfortunately, these studies succeeded only in measuring beryllium in the Pop I stars of their targeted samples, but failed to detect it in the most metal-poor, Pop II objects, for which only upper limits were derived.

These attempts were then followed by (somewhat larger) observational campaigns in the early 90s (Ryan et al. 1992, Gilmore et al. 1992, Boesgaard & King 1993), which used 4m class telescopes, equipped with spectrographs with a higher sensitivity in the blue. Ryan et al. (1992) and Boesgaard & King (1993) found a quadratic dependence of Be abundances from metallicity and oxygen, thus confirming the CR spallation scenario as the main production channel for beryllium. On the contrary, the study by Gilmore et al. (1992) uncovered a different trend, a linear slope between Be and Fe/O which confirmed some of the very early results obtained with HST for stellar boron abundances (see below).

For boron, after the pioneering work by Boesgaard & Heacox (1973, 1978) who looked at early-type stars (similar to what was done in the very early works for beryllium), one has to wait until the launch of the Hubble Space Telescope for the first measurements of boron abundances in metal-poor stars (Duncan et al. 1992). The sample consisted of 3 metal-poor stars, which these investigators surprisingly found to follow a linear relation. According to the authors, this implied that the evolution of boron cannot depend on metallicity, hence the spallation reactions cannot possibly take place in the interstellar medium, whose metal content keeps increasing as the Galaxy evolves. Instead, they proposed a “reverse” spallation reaction scenario as the one dominating the early phases of the Galaxy, in which it is the CNO (especially oxygen) in the CRs (under the assumption that they remain constant) that hit protons and α -particles in the ISM. For the record, it is important to note that this reverse mechanism had already been mentioned by Reeves and collaborators, but thought to be negligible, hence it had basically been ignored.

Needless to say, both findings (Gilmore et al. 1992 for beryllium and Duncan et al. 1992 for boron) have had a very strong impact on this field of research. In the following sections, I will mostly focus on beryllium, since it is the element for which most progress

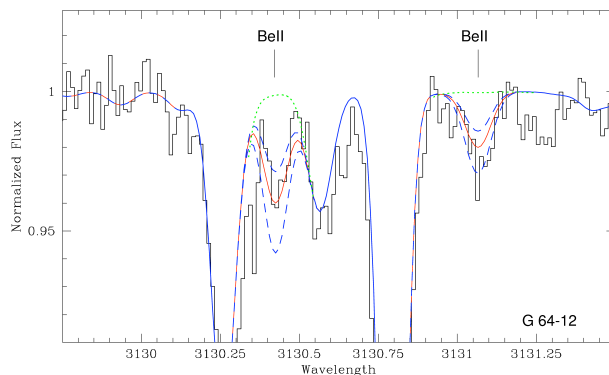


Figure 1. Best-fit spectrum synthesis (continuous curve) of the Be II doublet in one of the most metal-poor stars ever studied for beryllium, G 064-012 ($[\text{Fe}/\text{H}] \simeq -3.2$, histogram). Overplotted are also two spectrum syntheses computed with ± 0.15 dex with respect to the best-fit Be value (dashed curves) and one synthesis computed without any beryllium (dotted curve). (From Primas et al. 2000b)

has been made in the last decade. I will come back to boron towards the end of this review.

3. The impact of 8-10m class telescopes and efficient spectrographs

The advent of high-resolution spectrographs very sensitive in the near-UV on 8-10m class telescopes marked a new observational era, especially for studies of beryllium abundances in metal-poor stars. The observational progress achieved at the Be wavelengths (313 nm) over a bit more than one decade is remarkable: one went from having to integrate 6,000 s on a $V_{\text{mag}}=8$ star in order to obtain a spectrum with a resolving power of $R \simeq 11,000$ and $S/N=37$ (1988, Isaac Newton Telescope) to 3,000 s, $R \simeq 25,000$ and $S/N=55$ (1993, Canada-France-Hawaii Telescope) and to 1,800 s, $R \simeq 45,000$ and $S/N=120$ (2000, Very Large Telescope).

Boesgaard et al. (1999) presented the first systematic analysis of Be in a sample of 22 halo stars plus 5 disk stars observed with HIRES at Keck (Vogt et al. 1994) pushing the detection of Be in stars with metallicities approaching one thousandth less than solar. The major result from this study was a much more robust confirmation of the linear dependence between Be and Fe already found by Gilmore et al. (1992) based only on 6 objects. Furthermore, Boesgaard et al. (1999) confirmed a similar correlation also between Be and O.

Primas et al. (2000a,b) explored the capabilities of the high-resolution echelle spectrograph UVES (Dekker et al. 2000) at the VLT and recorded the first detection of Be in two stars with metallicities below one thousandth solar ($[\text{Fe}/\text{H}] = -3.15$, cf Figure 1).

Finally, Pasquini et al. (2004, 2007) detected for the first time with UVES at the VLT beryllium in turn-off stars of metal-poor globular clusters, like NGC 6397 and NGC 6752.

In more recent years, several Be studies have been conducted, which looked at different aspects of the formation of this light isotope, both in more metal-rich/solar-metallicity stars and metal-poor objects. Very recently, an upper limit has been derived on the Be content of a very metal-poor ($[\text{Fe}/\text{H}] = -3.7$), carbon-rich subgiant star (Ito et al. 2009). The three most recent analyses (Smiljanic et al. 2009, Rich & Boesgaard 2009, Tan et al. 2009) that have looked at stellar samples covering a wide range of metallicities, all

addressed issues like the formation and evolution of Be along the Galactic history. All three studies have presented the trends of Be *vs* iron and *vs* oxygen (or versus an average ratio of the alpha elements) and similar results are found: the correlation coefficient between Be and Fe ranges between 0.97 and 1.2, and they all seem to find a steeper relation when Be is compared to O, which seems to imply a faster increase of Be in the Galaxy with respect to oxygen.

Based on our current understanding of the formation of beryllium, it is indeed more important to relate Be to O: oxygen atoms are the main target nuclei of spallation reactions, hence such a relation should be more straightforward to interpret. In practice, accurate measurements of stellar oxygen abundances remain hard to achieve, due to a variety of oxygen abundance indicators that need to be used in different types of stars and that suffer from different systematic uncertainties that have not always been carefully evaluated. For instance, UV OH lines, basically the only ones available in dwarf stars at very low metallicities, give a very different trend of $[O/Fe]$ *vs* $[Fe/H]$, which seems to be due to the usage of unsuitable model atmospheres and model atoms (ignoring NLTE and 3D effects). The oxygen triplet, on the other hand, possibly detectable in the most metal-poor stars for which a Be detection has been achieved, is highly sensitive to the assumed stellar effective temperature, which in this case becomes the largest source of error on the final determination of the oxygen abundance. The O forbidden line (at 630 nm), the cleanest of all indicators, becomes quickly undetectable in dwarfs as one reaches metallicities around one hundredth less than solar.

3.1. Main recent findings and remaining open issues

All most recent studies of beryllium abundances in Galactic stars seem to agree on a few main findings: *a*) Be closely follows Fe; *b*) the slope between Be and O seems to be slightly steeper than with respect to Fe; *c*) the dispersion around the trends is very small in the most metal-poor stars but it increases at higher metallicities. The metallicity range around the so-called halo-disk transition seems to be characterized by significant scatter.

As already pointed out above, the uncertainty affecting our current determination of stellar oxygen abundances remains one of the main issues in order to properly interpret the Be *vs* O trend, if the correlation is truly different from a linear one. This uncertainty affects also another important test that has been attempted in recent years: the utilization of Be as a cosmic clock. The idea is based on the fact that if Be is produced via a primary process, this process would then become a global one instead of a local one, like, e.g., the production of heavier nuclei in supernovae explosions. Beryllium abundances are then expected to show smaller dispersion compared to elements like O and/or Fe, making Be a possibly more reliable cosmo-chronometer than the commonly used ratios like $[Fe/H]$ and/or $[O/H]$. Pasquini et al. (2005) were the first ones to test this idea, by investigating the evolution of the star formation rate in the early Galaxy using Be and O abundances. In order to do so, they compared O *vs* Be observed trends for stars belonging to two separate kinematical classes, the *accretion* and the *dissipative* components (roughly corresponding to the halo and thick disk populations), as identified by Gratton et al. (2003). They found out that these two samples seem to show different evolutions. Unfortunately, the sample size was rather limited and the sample splitting was not as clean as wished for such a comparison (for instance, they ended up with representatives of the *dissipative* component belonging to the halo, but with kinematical characteristics of the thick disk). This prevented these authors from drawing firm conclusions on the usefulness of Be as a cosmo-chronometer. Subsequent attempts also failed to fully prove the concept. Tan et al. (2009), following Pasquini et al. (2005) did not succeed in obtaining a clearer separation between the *dissipative* and the *accretion* components (cf their

Fig. 9). Smiljanic et al. (2009) presented $[O/Fe]$ and $[\alpha/Fe]$ ratios as a function of Be for a large data sample, and tried to similarly distinguish between halo and thick disk stars. Indeed, they found a possible separation, but also here abundances were too scattered (especially the alpha abundances, since they were taken from the literature) to be able to draw firm conclusions.

4. Shedding new light on Be formation and evolution

Our observational campaign, aimed at investigating the formation and evolution of Be across the Galactic history, has been carried out at the VLT with the UVES spectrograph. The sample includes more than 50 stars, spanning a wide range in metallicities (from -3.3 to -0.5). The objects are mostly dwarf or subgiant stars, belonging to both the halo and disk populations. All observed spectra have a resolving power of at least 40,000 and S/N ratios are of the order of 100 or higher at the Be II transitions. At redder wavelengths (since we took advantage of the dichroic mode of UVES) both S/N ratios and resolving power are higher, respectively, above 2-300 and $R \simeq 55,000$.

Stellar parameters of our sample were determined from Strömgren photometry (effective temperatures, also cross-checked both with V-K colour indices and with H- α fitting), from Hipparcos parallaxes (gravities), and from ionized Fe lines (metallicities). We used 1-D OSMARCS model atmospheres (Gustafsson et al. 2008) and we corrected our derived Be abundances for NLTE corrections (García Pérez, *priv. comm.*). We also derived lithium, oxygen, and other abundances, like Mg.

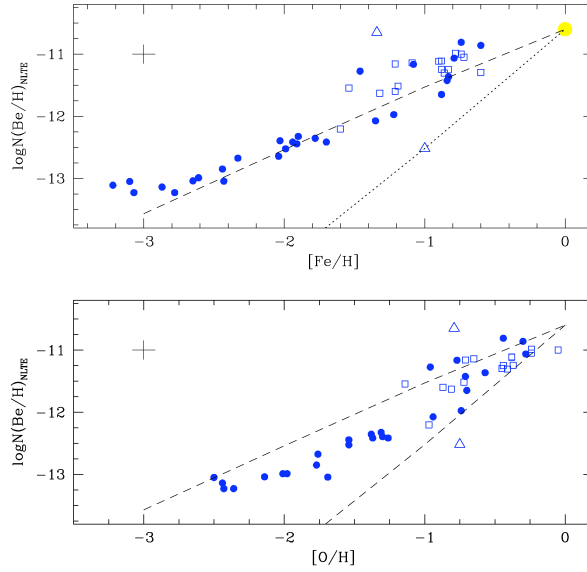


Figure 2. Our derived Be abundances *vs* metallicity (*top*) and $[O/H]$ (*bottom*). Typical errorbars are shown in the upper left corner of each plot. Dashed and dotted line represent respectively a linear and quadratic relation. Symbols: filled circles represent halo stars, open squares disk objects. The two open triangles represent two particular disk objects, one depleted in its Be content and one instead with a very high content of Be (as well as many other elemental abundances).

Figure 2 presents our Be results at large. The Be *vs* Fe trend follows a linear slope,

with very little scatter below a metallicity of $[\text{Fe}/\text{H}] = -1.5$, and a significantly increased dispersion around the halo-disk transition. If we display our Be abundances *vs* oxygen (which is a mix of abundances derived from the forbidden line at 630 nm and the triplet at 770 nm), the slope does not seem to change much but the trend may be more difficult to interpret, especially at higher metallicities (see caption for more details). Furthermore, we have added a few more Be detections below $[\text{Fe}/\text{H}] = -3.0$, which seem to fall a bit above the unitary slope trend identified by the rest of the sample. This feature, together with the need to correctly understand the larger dispersion at higher metallicities, are the main highlights of this study, thus they deserve to be discussed in more detail.

4.1. The very metal-poor tail of the Be evolution

The 4-5 most metal-poor stars of our sample seem to have slightly higher Be abundances with respect to the trend of unitary slope, i.e. the metal-poor tail of the Be *vs* Fe evolutionary trend seems to show some flattening (cf Fig. 2). What does this mean? Certainly, it does not carry any significance for a possible primordial production of beryllium; rather, some of the theoretical scenarios proposed in the past for the production of Be atoms in the early Galaxy predicted the appearance of such a plateau, when the masses of the supernova progenitors were in the range of 40-60 M_{\odot} (cf Vangioni-Flam et al. 1998).

However, before looking for exotic explanations for such feature, it is important to note that one other study that has succeeded in detecting Be in stars with a metallicity less than one thousandth solar does not agree with our finding. At least, not at first sight. Rich & Boesgaard (2009, but also Boesgaard, this volume), in fact, claim that their most metal-poor stars continue to follow the linear trend of the more metal-rich objects (cf their, e.g., Fig. 4). A closer look at both samples shows that most stars are actually in common, but analyzed with very different stellar parameters. If we correct their Be abundances on our stellar parameters scale, we obtain a satisfactory overlap, which demonstrates that the differences between these two sets of results rely only on different input parameters, not on the observed spectra and not on the different model atmospheres and/or analytical tools used during the analysis (reassuring!). Figure 3 shows the results of this test.

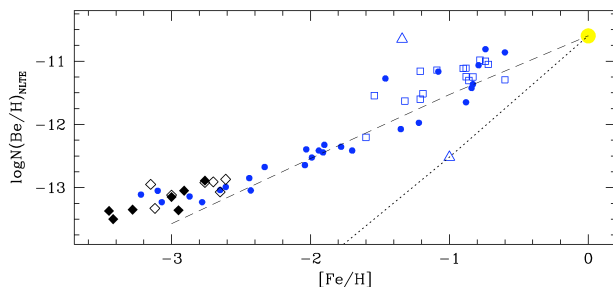


Figure 3. Same as the top panel of Fig. 2, this time with overplotted the most metal-poor data points from Rich & Boesgaard (2009): filled diamonds as in original paper, open diamonds corrected on our stellar parameters scale (see text for more details).

4.2. Be at the halo-disk transition: real scatter?

The larger dispersion detected at higher metallicities is present in both plots of Be trends, *vs* Fe and O. The second plot is certainly more worrisome than the first one, since Be

and O are expected to be well correlated. Figure 2 shows that all in a sudden, when a metallicity of $[\text{Fe}/\text{H}]=-1.5$ or $[\text{O}/\text{H}]=-1.2$ is reached, the tight correlation between, e.g., Be and O becomes looser: there are stars with the same content of oxygen, but with highly different contents of Be.

Since these metallicities map what we commonly call the halo-disk transition, the first attempt to shed some light into this region was to separate the objects kinematically, by associating them to the halo or to the disk component (cf caption of Fig. 2 for symbols coding). Unfortunately, not much was gained. This confirms earlier attempts made by Smiljanic et al. (2009) and Tan et al. (2009) who tried to associate stars to the *dissipative* vs *accretion* components and failed in finding a clear and convincing separation in their Be evolutionary trends.

Nissen & Schuster (2009) have determined very accurate abundances of several alpha elements in a large sample of halo-disk transition stars. The entire analysis has been carried out strictly differentially and this has allowed these authors to achieve very small error-bars on each data point and notably reduce spurious sources of scatter in the data. This work is an extension of Nissen & Schuster (1997), at a much higher accuracy. Their main finding (cf their Figs. 1 and 2) is a clear separation between halo-low and halo-high stars (where low/high refers to a low/high content of α -elements respectively) and with the halo-high overlapping the group of thick disk stars.

If we now use the accurate $[\alpha/\text{Fe}]$ ratios that Nissen & Schuster (2009) have derived for those stars for which we also have Be, we recover as well a very clear separation (in, e.g., a plot of $[\alpha/\text{Fe}]$ vs Be) between halo-low and halo-high, with the latter overlapping the thick disk stars. This splitting now helps us also to interpret the dispersion revealed by Fig. 2. The formerly very confusing halo-disk transition region now appears to be populated by objects that belong to distinct groups: the halo-low stars seem to continue the trend identified by the more metal-poor stars, possibly making the slope a bit steeper, whereas the halo-high stars seem to follow a shallower relation, and at similar oxygen contents have a much higher content of Be. The thick-disk partly overlaps with the halo-high but, with the exclusion of one object, seems to follow a slope more similar to the halo-lows.

Let's make one step further. If we now look at the plot of Be vs $[\alpha/\text{H}]$ (cf Fig. 4), the picture becomes even clearer and confirms what we just said. Halo-lows are a continuation of the more metal-poor stars trend, the thick-disk seems indeed to fall more closely the halo-low than the halo-high, though some overlap is present, especially at the highest metallicities; the halo-high show a flatter trend. As it can be seen in Fig. 4, there are some data points without any α -abundance-group identification (open circles), which are very important in order to confirm or not our preliminary findings. Still, this is an important step forward, in the interpretation of the dispersion now found by several recent studies.

5. Boron: fewer data and slower progress

For boron, the situation has not changed much during the last 10 years. Stellar boron abundances are inferred from the analysis of the BI resonant doublet at 250 nm, hence one needs to go into space. After a burst of studies that followed the launch of the Hubble Space Telescope and that lasted approximately a decade, very few abundance studies in metal-poor halo stars, if any, have been carried out during the last decade. More work has been carried out in stars at higher metallicities (cf Cunha, this volume) and in massive stars (cf Kaufer, this volume).

Therefore, when reviewing the formation and evolution of boron in the early Galaxy,

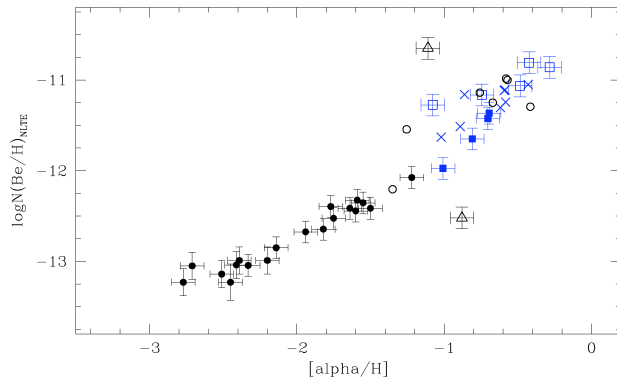


Figure 4. Be vs $[\alpha/H]$ trend, showing a much clearer separation (wrt, e.g., Fig. 2) among the three distinct α -element abundance groups, halo-low (filled squares), halo-high (open squares), and thick disk stars (crosses). Open circles represent disk stars which are not in the sample of Nissen & Schuster (2009); filled circles and open triangles as in Figs. 2 and 3.

one needs to go back to the second half of the 90s, basically to the works of Duncan et al. (1997), García López et al. (1998), and Primas et al. (1998, 1999). The B vs Fe, O relations found by these authors confirmed the earlier results obtained by Duncan et al. (1992) from only three objects, i.e. a primary origin also for this spallative element.

One very recent progress possibly worth mentioning here is the recent re-calculation of the BI lines formation under NLTE conditions carried out by Tan et al (*priv. comm.*). These NLTE corrections seem to differ significantly from those applied in earlier studies (e.g. Kiselman 1994) and to reconcile the B trends (vs Fe and vs O) with the trends recently found also for Be.

6. Constraining stellar mixing with Li, Be, and B

Simultaneous knowledge of Li, Be, and B abundances in the same target(s) is an important diagnostic to investigate mixing mechanisms at work in the outermost layers of stellar photospheres. Because this elemental trio burns at different and slightly increasing temperatures, one expects that Li, which is saved in the outermost layers, will burn first, before Be starts to be affected by any depletion mechanism.

It is important to note that this type of investigations has so far assumed that a Spite-plateau lithium abundance (i.e. the canonical value found in metal-poor Galactic halo stars of $A(\text{Li}) \simeq 2.2$) represents an un-depleted abundance of the lithium stellar content of that given object. But after WMAP (Dunkley et al. 2009 and references therein), we now have a very precise prediction of the primordial lithium abundance in the Standard Big Bang framework ($A(\text{Li}) = 2.72 \pm 0.06$, Cyburt et al. 2008), which instead hints at a rather large depletion of the lithium content that we measure today in the oldest stars of our Galaxy. This of course does not affect the basic depletion/dilution trend of the three light isotopes, but it may have significant implications on how we interpret the comparison of Li, Be, and B abundances in the same objects, especially as far as the amounts of depletion/dilution are concerned.

What still works well is of course a differential analysis among stars that share similar characteristics in, e.g., their stellar parameters. We know several pairs of stars that have an identical lithium content, that are indistinguishable as far as effective temperature, gravity and metallicity are concerned, but have very different Be and B abundances.

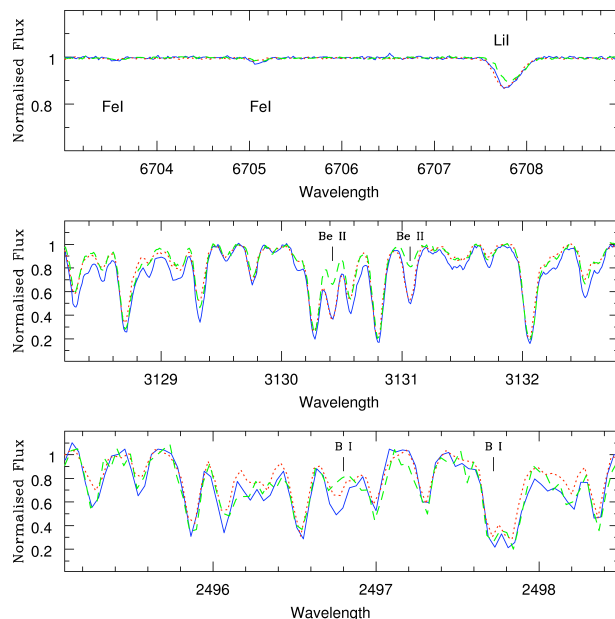


Figure 5. Observed spectra of three different stars overplotted respectively in the Li, Be, and B spectral regions (from *top* to *bottom*). The stars have very similar stellar parameters and Li contents, but show some differences in Be and/or B.

Some of these have the same Be content, but differ in their B signatures (cf Fig. 5, dotted and thin lines – does this imply that there could be another production mechanism for boron, like the often proposed ν -spallation?), others instead have different Be and B contents, for which it then becomes important to see how the degree of depletion of each element compares to the other (cf Fig. 5, dashed and thin line).

An example is given in Fig. 5, where observed spectra of three different objects are shown and overplotted. These three objects have very similar stellar parameters and Li contents, but one of them has much less beryllium and boron (dashed spectrum), and the other two share a similar content of beryllium but have a puzzling different B content!

7. Concluding remarks and acknowledgments

Remarkable observational progress has been made in the last decade, especially as far as Be studies are concerned. In this review, I have shown that the combination of higher quality data and highly accurate measurements of abundances (e.g., α -elements) is now starting to shed new light on the interpretation of some specific features of the Be evolutionary trend (e.g. the dispersion at the halo-disk transition). Progress in studies concerning B abundances has lagged behind, mostly due to the unavailability during the last 4-5 years of the Space Telescope Imaging Spectrograph on board of the Hubble Space Telescope (due to a mechanical/technical failure). But after the successful NASA Service Mission #4, STIS is again operational, therefore new abundance studies of boron in metal-poor stars will hopefully come soon.

Acknowledgments. The author warmly thanks Poul Erik Nissen, for providing the α -

elements abundances discussed in S. 4, and the LOC for the financial support received through the Swiss National Research Foundation.

References

- Boesgaard, A.M. 1976, *ApJ*, 210, 466
 Boesgaard, A. M., & Heacox, W. D. 1973, *ApJ* (Letters), 185, 27
 Boesgaard, A. M., & Heacox, W. D. 1978, *ApJ*, 226, 888
 Boesgaard, A. M., Heacox, W. D., & Conti, P.S. 1977, *ApJ*, 214, 124
 Boesgaard, A. M., & King, J. R. 1993, *AJ*, 106, 2309
 Boesgaard, A. M., Deliyannis, C. P., King, J.R., Ryan, S.G., Vogt, S.S., & Beers, T.C. 1999, *AJ*, 117, 1549
 Cyburt, R. H., Fields, B. D., & Olive, K. A. 2008, *JCAP*, Issue 11, p.012
 Dekker, H., D'Odorico, S., Kaufer, A., Delabre, B. & Kotzlowski, H. 2000 *SPIE*, 4008, 534
 Duncan, D.K., Lambert, D.L., & Lemke, M. 1992, *ApJ*, 401, 584
 Duncan, D. K., Primas, F., Rebull, L. M., Boesgaard, A. M., Deliyannis, C. P., Hobbs, L. M., King, J. R., & Thorburn, J. A. 1997, *ApJ*, 488, 338
 Dunkley, J., Spergel, D. N. Komatsu, E., et al. 2009, *ApJ*, 701, 1804
 García López, R. L., Lambert, D. L., Edvardsson, B., Gustafsson, B., Kiselman, D., & Rebolo, R. 1998, *ApJ*, 500, 241
 Gilmore, G., Gustafsson, B., Edvardsson, B., Nissen, P.E. 1992, *Nature*, 357, 379
 Gratton, R. G., Carretta, E., Desidera, S., Lucatello, S., Mazzei, P., & Barbieri, M. 2003, *A&A*, 406, 131
 Gustafsson, B., Edvardsson, B., Eriksson, K., Jørgensen, U. G., Nordlund, Å, & Plez, B. 2008, *A&A*, 486, 951
 Kiselman, D. 1994, *A&A*, 286, 169
 Ito, H., Aoki, W., Honda, S., & Beers, T. C. 2009, *ApJ* (Letters), 698, 37
 Meneguzzi, M., Audouze, J., & Reeves, H., 1971 *A&A*, 15, 337
 Molaro, P., Beckman, J.E., & Castelli, F. 1984, in *Proceedings of ESA 4th European IUE Conference*, p. 197
 Nissen, P. E. & Schuster, W. E 1997, *A&A*, 326, 751
 Nissen, P. E., & Schuster, W. E. 2009, in: J. Andersen, J. Bland-Hawthorn, & B. Nordström (eds.), *The Galaxy Disk in Cosmological Context* (Proceedings of the International Astronomical Union, IAU Symposium, Vol 254), p. 103
 Pasquini, L., Bonifacio, P., Randich, S., Galli, D., & Gratton, R. G. 2004, *A&A*, 426, 651
 Pasquini, L., Galli, D., Gratton, R. G., Bonifacio, P., Randich, S., & Valle, G. 2005, *A&A* (Letter), 436, 57
 Pasquini, L., Bonifacio, P., Randich, S., Galli, D., Gratton, R. G., & Wolff, B. 2007, *A&A*, 464, 601
 Primas, F., Duncan, D.K., & Thorburn, J. A. 1998, *ApJ* (Letters), 506, 51
 Primas, F., Duncan, D. K., Peterson, R. C., & Thorburn, J. A. 1999, *A&A*, 343, 545
 Primas, F., Molaro, P., Bonifacio, P., & Hill, V. 2000a, *A&A*, 362, 666
 Primas, F., Asplund, M., Nissen, P. E., & Hill, V. 2000b, *A&A* (Letter), 364, 42
 Rebolo, R., Molaro, P., Abia, C., & Beckman, J.E. 1988, *A&A*, 193, 193
 Reeves, H., Fowler, W. A., & Hoyle, F. 1970, *Nature*, 226, 727
 Rich, J.A. & Boesgaard, A.M. 2009, *ApJ*, 701, 1519
 Ryan, S.G., Norris, J.E., Bessell, M.S., & Deliyannis, C.P. 1992, *ApJ*, 388, 184
 Smiljanic, R., Pasquini, L., Bonifacio, P., Galli, D., Gratton, R. G., Randich, S., & Wolff, B. 2009, *A&A*, 499, 103
 Tan, K. F., Shi, J. R., & Zhao, G. 2009, *MNRAS*, 392, 205
 Vangioni-Flam, E., Ramaty, R., Olive, K. A., & Casse, M. 1998, *A&A*, 337, 714
 Vogt, S.S., Allen, S.L., Bigelow, B.C., et al. 1994, *SPIE*, 2198, 362

New Beryllium results in halo stars from Keck/HIRES spectra

Ann Merchant Boesgaard¹, Jeffrey A. Rich¹, Emily M. Levesque¹ &
Brendan P. Bowler¹

¹ University of Hawaii, Institute for Astronomy
2680 Woodlawn Drive, Honolulu, HI 96822, U.S.A.
email: boes@ifa.hawaii.edu, jrich@ifa.hawaii.edu,
emsque@ifa.hawaii.edu, bpbowler@ifa.hawaii.edu

Abstract. We have obtained high-resolution, high signal-to-noise Keck spectra to determine Be abundances in over 100 stars in the Galactic halo. The stellar metallicities range from $[\text{Fe}/\text{H}] = -0.50$ to -3.50 . Using this large sample, we have examined the trends of Be with Fe and Be with O. We find a real dispersion in Be at a given $[\text{O}/\text{H}]$ that indicates that Be may not be a good cosmochronometer. Our results indicate that the dominant production mechanism for Be changes as the Galaxy ages. In the early eras of the Galaxy, when massive stars become supernovae, Be is produced from the acceleration of energetic CNO atoms which bombard protons in the vicinity of supernovae. Later spallation reactions occur as high energy protons bombard CNO atoms in the interstellar gas. The change occurs near $[\text{Fe}/\text{H}] = -2.2$. We have found that Be is deficient in Li-deficient halo stars, which favors the blue straggler analog hypothesis.

Keywords. Stars: abundances, Population II, kinematics, late-type – Galaxy: halo

1. Introduction

The trio of the rare light elements provides excellent probes into many astrophysical issues: cosmology, the chemical evolution of the Galaxy, the origin of the light elements, element destruction in stars, stellar interiors and evolution, cosmic ray theory, hypernovae, etc. For many of these issues Be is the best probe. It has only one long-lived isotope, ⁹Be; the non-LTE effects are negligible; there is only one source for production (spallation); it is less fragile than the Li isotopes; and it has the potential to be a good cosmochronometer.

For our Be studies we have been using the Keck 10-m telescope (with more than 50% more light-gathering power than 8-m telescopes) on the 4200-m Mauna Kea, which is above 40% of Earth's atmosphere. From 1993 to 2003 the CCD on HIRES (Vogt *et al.* 1994) had only 8% quantum efficiency near the Be II lines at 3130.4 and 3131.1 Å. However, after the upgrade of HIRES in 2004, the quantum efficiency on the new “blue chip” rose to 93%. (The upgraded version now has 3 CCDs with 15-μm pixels.) We have been able to take UV spectra of stars almost 3 magnitudes fainter. However, signal-to-noise ratios of more than 100 are needed to find Be abundances in the most metal-poor stars, where the Be II lines are very weak.

Due to the benefits of large aperture and high altitude, we have been able to achieve some interesting results with the original version of HIRES. In our first comprehensive study of Be in halo stars, we found a linear relationship between $[\text{Fe}/\text{H}]$ and $A(\text{Be}) (= \log N(\text{Be})/N(\text{H}) + 12.00)$ with a slope of $+0.96 \pm 0.04$ (Boesgaard *et al.* 1999). We discovered a Be dip like the Li dip in the Hyades F dwarfs (Boesgaard & King 2002), but unlike the

Li decline in the Hyades G dwarfs, there is no decline in Be in the G dwarfs (Boesgaard & King 2002). We followed that up with Be studies in F and G dwarfs in several other open clusters: Pleiades and α Per (Boesgaard *et al.* 2003a), Coma and UMa moving group (Boesgaard *et al.* 2003b), and Praesepe (Boesgaard *et al.* 2004a). In a large study of Li and Be in both field and cluster stars we found that the depletions of Li and Be are correlated in the stars in the Li-Be dip with a slope of $+0.38 \pm 0.03$ (Boesgaard *et al.* 2004b). This could result from rotationally induced mixing. By studying B in stars with large Be deficiencies, we were able to find a correlation between Be and B depletions (Boesgaard *et al.* 2005); the slope for that relationship is 0.22 ± 0.05 .

2. Observations with the upgraded HIRES

The upgraded HIRES has a mosaic of 3 CCDs, each 2048×2048 pixels with a pixel size of $15 \mu\text{m}$. Since September 2004, we have received 16 nights of Keck time with HIRES over a 41-month period to pursue research on Be. Only two of those nights were lost: one due to the closure of the road to the summit from a raging blizzard and one due to two deep undersea earthquakes measuring 6.7 and 6.0 on the Richter scale at just after 7 a.m. on the morning of our one-night run. They caused damage to both Keck telescopes and to the remote-observation rooms. On the other 14 nights, we obtained high signal-to-noise (S/N) spectra of over 100 stars for several different research goals. As Fig. 1 in Rich & Boesgaard (2009) shows, it is important to achieve high S/N in the most metal-poor stars due to the weakness of the Be II lines.

We determined the stellar parameters— T_{eff} , $\log g$, $[\text{Fe}/\text{H}]$, and microturbulence (ξ)—spectroscopically (see Rich & Boesgaard 2009). The values ranged from 5550 to 6400 K, 3.2 to 4.9 in $\log g$, -0.5 to -3.5 in $[\text{Fe}/\text{H}]$, and 0.9 to 1.5 km s^{-1} in ξ . The spectrum synthesis method was used to find abundances; an example is shown in Fig. 1, where both Be and O were varied to achieve the best fit. Oxygen abundances were found from three OH features. The two other OH features (3139, 3140 Å) can be seen in Fig. 3 of Rich & Boesgaard (2009). Each feature contains several OH transitions.

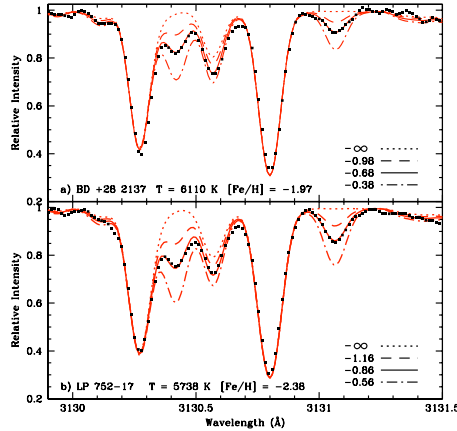


Figure 1. The spectrum synthesis fit for two of our stars: BD +28 2137 at $[\text{Fe}/\text{H}] = -1.97$ and LP 752-17 at $[\text{Fe}/\text{H}] = -2.38$. The dots are the data points and the solid line is the best fit. The dot-dash line has twice as much Be and 0.1 dex more O than the best fit. The dashed line has half the Be and 0.1 dex less O. The dotted line contains no Be and is another 0.1 dex lower in O.

3. Abundances and trends

Be trends with Fe and with O. We have been able to fit the trends of Be with Fe and Be with O with straight lines in the log-log plot. We prefer a two slope fit for both. These fits are shown in Fig. 2. Data from Smiljanic *et al.* (2009) are included in the figure with $[\text{Fe}/\text{H}]$, but not in the figure with $[\text{O}/\text{H}]$ as they did not determine O abundances.

A change in slope would be expected. In the oldest stars, Be would be formed mostly in the vicinity of SN II by the acceleration of CNO nuclei into protons, etc. Thus Be would be proportional to the instantaneous number of supernovae and therefore proportional to O with a slope of ≤ 1 . In the younger stars, the dominant formation mechanism would be traditional GCR spallation from high-energy cosmic rays bombarding CNO in the interstellar gas. The number of O atoms would depend on the cumulative number of supernovae, while the number of energetic cosmic rays is proportional to the instantaneous rate of SN II. The abundance of spallation products is $\int N dN = kN^2$ giving a slope of ≤ 2 . Due to effects such as mass outflow during star formation, the predicted slopes of 1 and 2 would be modified to lower values.

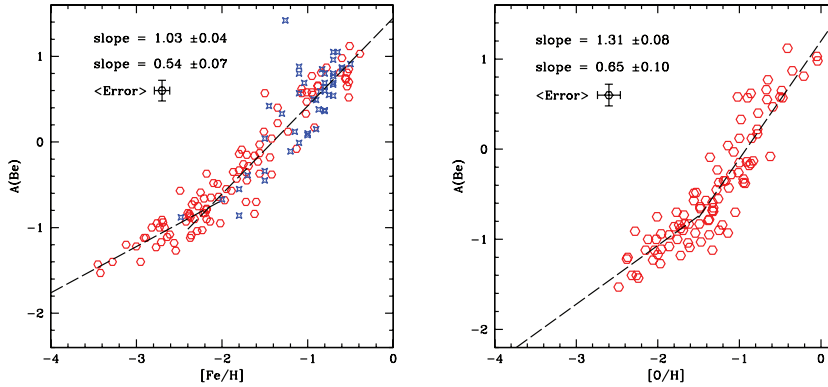


Figure 2. The two-slope fit of $A(\text{Be})$ with $[\text{Fe}/\text{H}]$ and $A(\text{Be})$ with $[\text{O}/\text{H}]$. The open hexagons are from this work and the skeletal squares are from Smiljanic *et al.* (2009).

Beryllium plateau? We find no evidence for a Be plateau at low metallicities comparable to the Li plateau. There may be a steady increase in $[\text{Be}/\text{Fe}]$ at the lowest values of $[\text{Fe}/\text{H}]$, but this may only reflect the paucity of stars (only 5) observed for Be with $[\text{Fe}/\text{H}] < -3.0$.

Beryllium spread. We do find evidence for a real spread in $A(\text{Be})$ at a given $[\text{O}/\text{H}]$ at the 4σ level and probably at a given $[\text{Fe}/\text{H}]$ at the 3σ level. We have done statistical tests using a prediction interval. We start with the null hypothesis that there is no spread in Be abundances in a certain Fe or O interval. We derive slope and offset values from the points outside the metallicity interval under consideration. We then use those data to predict the range of Be values inside our metallicity interval for a given confidence level, and we compare that with the actual data. For example, if there are 25 points in our metallicity interval, and 7 lie outside the 95% confidence level, we can then use the binomial theorem to determine the probability of this occurring by chance. We can try different confidence levels (99%, 95%, 90%) and different size bins for $[\text{Fe}/\text{H}]$ and $[\text{O}/\text{H}]$ (± 0.25 , ± 0.20 , ± 0.10). Fig. 3 shows an example of this. The probability that 7 of 25 stars fall outside the 95% confidence level by chance is 0.015%.

There seems to be little evidence in our data sample of a different distribution of

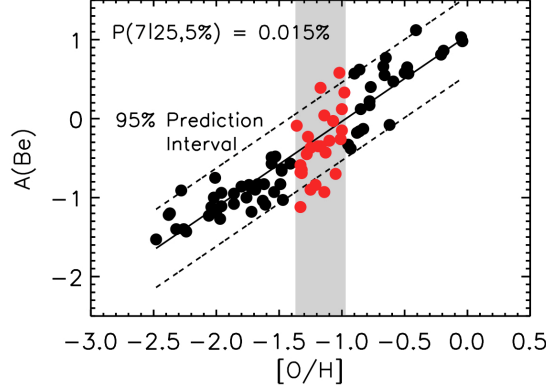


Figure 3. An example of the prediction-interval testing that we did to check for a spread in Be at a given value of $[O/H]$ or $[Fe/H]$.

Be with $[O/Fe]$ for “accretive” vs. “dissipative” stars as determined by the criteria of Gratton *et al.* (2003). Although the errors were large for $[O/Fe]$ in the stars studied by Pasquini *et al.* (2005) and in $[\alpha/Fe]$ in the stars for Smiljanic *et al.* (2009), both groups found intriguing differences in the two sets of stars. They concluded that Be can be used as a chronometer in a subset of stars. They find a large scatter in the dissipative stars and two sequences for the accretive. Our results can be seen in Fig. 4; both accretive and dissipative stars show a spread in $[O/H]$ and no separation of two sequences for the accretive stars. We found an intrinsic spread in Be at a given Fe or O. In addition there is a spread in $[O/Fe]$ of more than 2σ at a given $A(Be)$. We conclude that Be may not fulfill its potential as a chronometer.

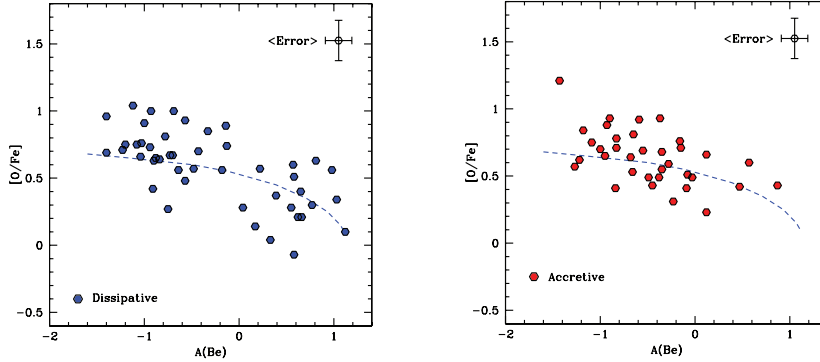


Figure 4. A plot of $[O/Fe]$ vs. $A(Be)$ in stars in the “accretive” and dissipative” populations (as defined by Gratton *et al.* 2003). We see no evidence for a difference in the distribution between the two populations.

4. Beryllium in ultra-Lithium-deficient stars

Although most metal-poor stars have $A(Li)$ values between ~ 1.9 to 2.5, there are a few that are deficient in Li and fall below this plateau. This can be seen in Fig. 5 (left).

These were dubbed "ultra-Li-deficient" stars by Ryan *et al.* (2001). There are at least two plausible explanations for the Li deficiencies. Ryan *et al.* (2001, 2002) suggest that they are blue-straggler analogs in which mass transfer or binary coalescence has occurred that destroyed the Li. Pinsonneault *et al.* (1999, 2002) hypothesize that they are a subset of (once) rapidly rotating stars which have depleted their Li as they spun down their rotation rate. These two ideas make different predictions about Be. In the blue straggler model, most or all of the Be would also be destroyed due to complete internal mixing. In the rotation model some or all of the Be would be preserved because Be is less fragile than Li.

Boesgaard & Novicki (2006) and Boesgaard (2007) determined Be abundances in seven of the nine Li-deficient stars that are indicated in the left panel of Fig. 5. They found that the Li-deficient stars are also Be-deficient as can be seen in the right panel of Fig. 5. Those Be deficiencies are larger than the predictions from the models of rotationally-induced mixing by Pinsonneault *et al.* (1992). This result thus favors the blue-straggler model which predicts large Be deficiencies. Newer models by Pinsonneault *et al.* (2002) predict *smaller* Li depletions, and probably smaller Be depletions as well.

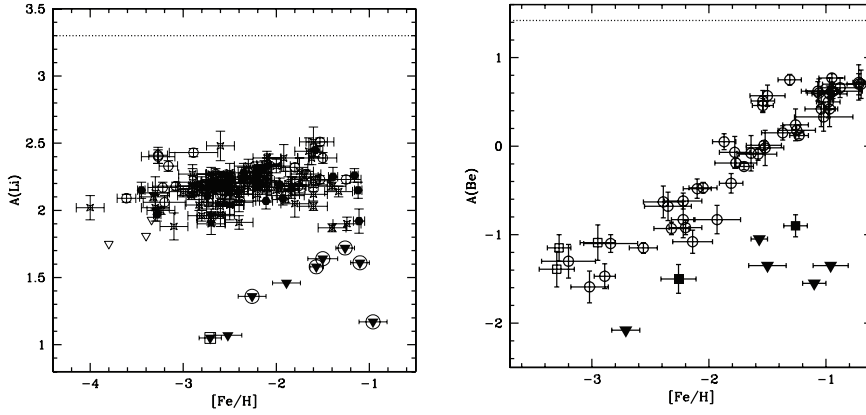


Figure 5. Left: The abundance of Li, $A(\text{Li}) = \log N(\text{Li}) - \log N(\text{H}) + 12.00$, plotted against $[\text{Fe}/\text{H}]$ for halo dwarfs. The upper limits for the Li-deficient stars are indicated by downward triangles; those observed for Be have circles around them (Boesgaard 2007) or a square (Boesgaard & Novicki 2006). See the caption on the similar figure in Figure 1 of Boesgaard (2007) for the detailed references. The horizontal dotted line is the meteoritic Li abundance, $A(\text{Li}) = 3.30$ (Grevesse & Sauval 1998). Right: The Be abundances/limits of the ultra-Li-deficient stars shown in the context of Be abundances in Li-normal stars as a function of $[\text{Fe}/\text{H}]$. The filled squares are the two ultra-Li-deficient stars with detected Be, while the filled triangles represent the upper limits on four ultra-Li-deficient stars. Open circles are from Boesgaard *et al.* (1999), and other references are given in Boesgaard (2007). Open squares (low-metallicity stars) are from Primas *et al.* (2000a, 2000b). Individual error bars on both $A(\text{Be})$ and $[\text{Fe}/\text{H}]$ are shown. The horizontal dotted line is the meteoritic Be abundance, $A(\text{Be}) = 1.42$ (Grevesse & Sauval 1998).

5. Summary of Keck Be results

Our findings from our Keck Be data include the following:

- There are correlated depletions of Li with Be and of Be with B. These observations are well-matched by the predictions of rotationally induced mixing.

- There is a Be dip like the Li dip in the Hyades F stars and in other open clusters. However, for the G stars there is no decline in Be to mirror the decline in Li.
- We have found abundance trends between A(Be) and [Fe/H] and between A(Be) and [O/H] which can be well fit by one straight line or by two. The two-slope fits are preferred and expected if the dominant source of Be production changes during the course of Galactic evolution from core-collapse supernovae (bullets = CNO and targets = p, n) to GCR spallation (bullets = p, n and targets = CNO). There are also tight relationships between [Fe/H] and [O/H] and between [O/Fe] and [Fe/H].
- There appears to be a real spread in Be at a given [Fe/H] and a given [O/H]. We find no difference in the relationships between Be and [O/Fe] for the accretive sample and the dissipative sample. This would seem to indicate that Be cannot be relied on as a cosmochronometer.
- We have found Be abundances and upper limits in those halo stars where the upper limits on the Li abundances put them well-below the Li plateau. A plausible explanation is that these stars are analogs to blue stragglers and have destroyed most or all of their Li and Be through mass transfer or binary coalescence.

Acknowledgements

We gratefully acknowledge support from the National Science Foundation through grant AST-05-05899 to A. M. B.

References

- Boesgaard, A.M. 2007, *ApJ*, 667, 1196
 Boesgaard, A.M. & King, J.R. 2002, *ApJ*, 565, 587
 Boesgaard, A.M. & Novicki, M.C. 2006, *ApJ*, 641, 1122
 Boesgaard, A.M., Armengaud, E. & King, J.R. 2003a, *ApJ*, 582, 410
 Boesgaard, A.M., Armengaud, E. & King, J.R. 2003b, *ApJ*, 583, 955
 Boesgaard, A.M., Armengaud, E., & King, J.R. 2004a, *ApJ*, 605, 864
 Boesgaard, A.M., Armengaud, E., King, J.R., Deliyannis, C.P. & Stephens, A. 2004b, *ApJ*, 613, 1202
 Boesgaard, A.M., Deliyannis, C.P., King, J.R., Ryan, S.G., Vogt, S.S., & Beers, T.C. 1999, *AJ*, 117, 1549
 Boesgaard, A.M., Stephens, A. & Deliyannis, C.P. 2005, *ApJ*, 633, 398
 Gratton, R.G., Carretta, E., Claudi, R., Lucatello, S. & Barbien, M. 2003, *A&A*, 404, 187
 Grevesse, N. & Sauval, A.J. 1998, *Space Sci. Rev.*, 85, 161
 Pasquini, L., Galli, D., Gratton, R.G., Bonifacio, P., Randich, S., & Valle, G. 2005, *A&A* (Letters), 436, 57
 Pinsonneault, M.H., Deliyannis, C.P. & Demarque, P. 1992, *ApJS*, 78, 179
 Pinsonneault, M.H., Steigman, G., Walker, T.P. & Narayanan, V.K. 2002, *ApJ*, 574, 398
 Pinsonneault, M.H., Walker, T.P., Steigman, G. & Narayanan, V.K. 1999, *ApJ*, 527, 180
 Primas, F., Asplund, M., Nissen, P.E. & Hill, V. 2000a, *A&A* (Letters), 364, 42
 Primas, F., Asplund, M., Bonifacio, P. & Hill, V. 2000b, *A&A*, 362, 666
 Rich, J.A. & Boesgaard, A.M. 2009, *ApJ*, 701, 1519
 Ryan, S.G., Beers, T.C., Kajino, T. & Rosolankova, K. 2001, *ApJ*, 547, 231
 Ryan, S.G., Gregory, S.G., Kolb, U., Beers, T.C. & Kajino, T. 2002, *ApJ*, 571, 501
 Smiljanic, R., Pasquini, L., Bonifacio, P., Galli, D., Gratton, R.G., Randich, S. & Wolff, B. 2009, *A&A*, 499, 103
 Vogt, S.S., *et al.* 1994, *SPIE*, 2198, 362

Boron abundances in diffuse interstellar clouds

Adam M. Ritchey¹, S. R. Federman¹, and Y. Sheffer^{1†} and D. L. Lambert²

¹Department of Physics and Astronomy, University of Toledo,
2801 West Bancroft Street, Toledo, OH 43606, USA
email: adam.ritchey@utoledo.edu, steven.federman@utoledo.edu,
ysheffe@utnet.utoledo.edu

²W.J. McDonald Observatory, University of Texas at Austin,
1 University Station, Austin, TX 78712, USA
email: dll@astro.as.utexas.edu

Abstract. We present a comprehensive survey of B abundances in diffuse interstellar clouds from *HST*/STIS observations along 56 Galactic sight lines. Our sample is the result of a complete search of archival STIS data for the B II $\lambda 1362$ resonance line, with each detection confirmed by the presence of absorption from other dominant ions at the same velocity. The data probe a range of astrophysical environments including both high-density regions of massive star formation as well as low-density paths through the Galactic halo, allowing us to clearly define the trend of B depletion onto interstellar grains as a function of gas density. Many extended sight lines exhibit complex absorption profiles that trace both local gas and gas associated with either the Sagittarius-Carina or Perseus spiral arm. Our analysis indicates a higher B/O ratio in the inner Sagittarius-Carina spiral arm than in the vicinity of the Sun, which may suggest that B production in the current epoch is dominated by a secondary process. The average gas-phase B abundance in the warm diffuse ISM [$\log \epsilon(\text{B}) = 2.38 \pm 0.10$] is consistent with the abundances determined for a variety of Galactic disk stars, but is depleted by 60% relative to the solar system value. Our survey also reveals sight lines with enhanced B abundances that potentially trace recent production of ^{11}B either by cosmic-ray or neutrino-induced spallation. Such sight lines will be key to discerning the relative importance of the two production routes for ^{11}B synthesis.

Keywords. ISM: abundances, atoms – nuclear reactions, nucleosynthesis, abundances – ultra-violet: ISM

1. Introduction

Production of the two stable isotopes of boron results from spallation reactions between energetic particles and interstellar nuclei. The less abundant ^{10}B is mainly a product of Galactic cosmic-ray (GCR) spallation (e.g., Meneguzzi, Audouze & Reeves 1971; Ramaty et al. 1997), which typically involves relativistic protons and α -particles impinging on CNO nuclei in the interstellar medium (ISM) but can also occur as accelerated CNO nuclei are spalled from ambient interstellar H and He. While a significant amount of ^{11}B is produced through GCR spallation reactions, an additional source is required to raise the isotopic ratio $^{11}\text{B}/^{10}\text{B}$ from the value predicted by models of cosmic-ray spallation (2.4; Meneguzzi et al. 1971) to the value measured in carbonaceous chondrites (4.0; Lodders 2003). The ν -process, or neutrino-induced spallation in Type II supernovae,

† Present address: Department of Astronomy, University of Maryland, College Park, MD 20742, USA

has often been invoked to account for the discrepancy in the predicted versus measured boron isotopic ratios because, while the yields for ^{11}B are substantial, virtually no ^{10}B is produced (Woosley et al. 1990). Without the ν -process, enhanced synthesis of ^{11}B could be attributed to an increased flux of low-energy cosmic rays, which are unobservable from the Earth due to the modulating effect of the solar wind.

All of the processes that produce boron in significant quantities occur in, or are closely associated with, the interstellar medium. Even the ^{11}B synthesized in core collapse supernovae will quickly be injected into the surrounding interstellar gas. It therefore becomes a critical test of the theoretical ideas concerning boron nucleosynthesis to measure its interstellar abundance. The first detection of interstellar boron was reported by Meneguzzi & York (1980), who used the *Copernicus* satellite to measure B II $\lambda 1362$ along the line of sight to κ Ori. They derived an interstellar abundance of $\log \epsilon(\text{B}) = 2.2 \pm 0.2$, which was consistent with the then-current stellar value of 2.3 ± 0.2 (Boesgaard & Heacox 1978), assumed to be the Galactic value. Federman et al. (1996a), using GHRS on board *HST*, presented the first measurement of $^{11}\text{B}/^{10}\text{B}$ outside the solar system. Their analysis, along with later work by Lambert et al. (1998), showed that the solar system ratio is not anomalous but probably representative of the local Galactic neighborhood. The survey by Howk, Sembach & Savage (2000) expanded the sample of interstellar boron abundances to the extended sight lines accessible to *HST*/STIS. These authors found clear evidence for boron depletion onto interstellar grains and derived a lower limit to the present-day total interstellar boron abundance of $\gtrsim 2.40 \pm 0.13$.

The discovery of newly synthesized lithium toward *o* Per, a line of sight that passes very near to the massive star-forming region IC 348 and has a low $^7\text{Li}/^6\text{Li}$ ratio consistent with predictions of GCR spallation (Knauth et al. 2000a; 2000b), prompted us to seek $^{11}\text{B}/^{10}\text{B}$ ratios along this and other nearby sight lines in the Per OB2 association with STIS. Ultimately, the acquired spectra toward 40 Per, *o* Per, ζ Per, and X Per lacked the signal-to-noise ratio required to yield meaningful results on $^{11}\text{B}/^{10}\text{B}$ but did provide accurate B column densities. Thus, we shifted our focus to determining elemental boron abundances for a much larger Galactic sample.

2. STIS archival survey

All archival STIS datasets employing either the E140H or E140M grating were examined in an effort to find unambiguous interstellar absorption from O I $\lambda 1355$, Cu II $\lambda 1358$, and Ga II $\lambda 1414$. Subsequent searches for absorption from B II $\lambda 1362$ at the same velocity resulted in a sample of 56 Galactic sight lines. All of the above species represent the dominant ionization stage of their particular element in neutral diffuse clouds and are thus expected to coexist. As in our previous work (Federman et al. 1996a; Lambert et al. 1998), the stronger O I, Cu II, and Ga II lines serve as templates of interstellar component structure when determining B II column densities. The STIS spectra acquired with the E140H grating are characterized by velocity resolutions in the range $\Delta v = 2.1\text{--}3.6 \text{ km s}^{-1}$, while E140M spectra have resolutions of $6.5\text{--}7.9 \text{ km s}^{-1}$. Thus, to help constrain the velocity structure along the lines of sight in our sample, we obtained high-resolution ($\Delta v = 1.6\text{--}1.8 \text{ km s}^{-1}$) ground-based data on Ca II $\lambda 3933$ and K I $\lambda 7698$ for many directions either at McDonald Observatory or from the literature (e.g., Welty, Morton & Hobbs 1996; Welty & Hobbs 2001; Pan et al. 2004). We also incorporated into our analysis five sight lines with previous measurements of interstellar B from GHRS (Jura et al. 1996; Lambert et al. 1998; Howk et al. 2000) but did not rederive abundances in these directions.

The full boron sample probes a diverse array of astrophysical environments, including

both high-density regions of massive star formation (e.g., Per OB2 and Cep OB2) as well as low-density paths through the Galactic halo (e.g., the sight lines to HD 156110 and HD 187311). Some directions sample quite local gas (e.g., in Sco OB2 at $d = 160$ pc), while others trace distant spiral arms (e.g., HD 104705, located beyond the Sagittarius-Carina arm at $d = 3.9$ kpc). These characteristics enable a detailed investigation of the effect of physical environment on the observed abundances of boron in diffuse clouds. More information on the boron sample can be found in Ritchey et al. (2010).

3. Abundance analysis

As a first step in the analysis, the absorption profiles of O I, Cu II, and Ga II were synthesized with the rms-minimizing code ISMOD (Y. Sheffer, unpublished). These fits yielded the column density, velocity, and b -value of each absorption component along the line of sight. The B II line was then fitted by holding the b -values, relative velocities, and relative component strengths constant and varying only the absolute velocity of the profile and the total column density. The results of the O I, Cu II, and Ga II fits were each applied separately to the B II line. Additionally, if Ca II and K I data were available, these lines were synthesized and the results were used as a high-resolution template for synthesizing the B II profile. Final B II column densities were determined by taking the mean of these fits, which in all cases were mutually self-consistent.

When a sight line exhibited multiple complexes of absorption components well separated in velocity, the various templates were constructed for each complex and fitted to that portion of the B II profile independently. This technique allows for the possibility that elemental abundance ratios may vary from complex to complex along the line of sight. Indeed, we find suggestive evidence for a higher B/O ratio in components tracing the inner Sagittarius-Carina spiral arm than in those sampling local gas in the same direction. Abundances of secondary elements increase relative to those of primary ones toward the Galactic center due to enhanced rates of star formation and stellar nucleosynthesis. If confirmed, an elevated B/O ratio toward the inner Galaxy would indicate the secondary nature of boron, which in turn would cast doubt on the efficiency of the ν -process, a primary production mechanism.

Under the assumption that all boron in diffuse clouds is singly ionized, the B II column densities derived above can be considered the total boron column densities in the gas phase. Elemental boron abundances can then be determined from knowledge of the total column densities of atomic and molecular hydrogen along the line of sight. The atomic hydrogen data come mainly from the archival study of Lyman- α absorption by Diplas & Savage (1994), while the majority of H₂ column densities were provided by Sheffer et al. (2008). In Figure 1, we plot gas-phase B abundances as a function of the average line-of-sight hydrogen density, defined as $\langle n_H \rangle = [N(\text{H I}) + 2N(\text{H}_2)]/d$, where d is the distance to the background star. Immediately apparent is the trend of decreasing gas-phase abundance with increasing line-of-sight density, a clear signature of the depletion of boron onto interstellar dust grains. Following Jenkins, Savage & Spitzer (1986), we calculated mean B abundances in the warm, low-density gas and in the cold, higher-density clouds based on an idealized model of the neutral interstellar medium (Spitzer 1985). The analysis shows that the depletion (relative to solar) increases from -0.40 dex in lines of sight with the lowest density to -1.20 dex for the directions sampling higher concentrations of cold clouds.

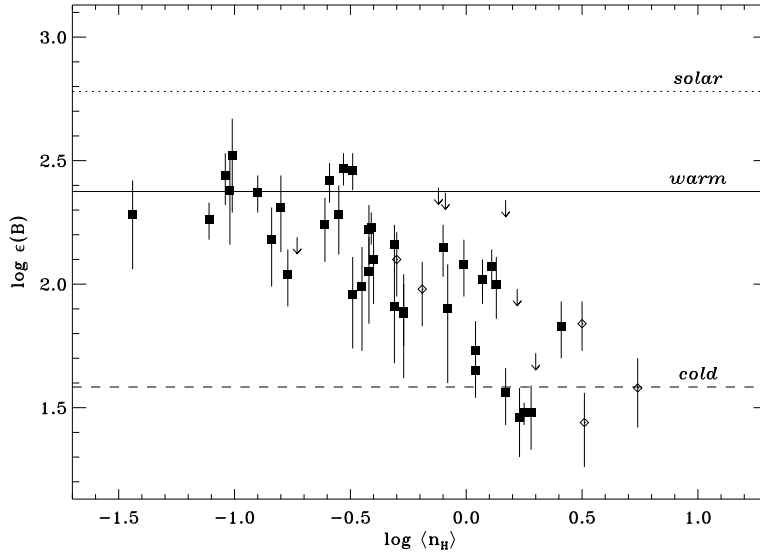


Figure 1. Gas-phase interstellar B abundances versus average line-of-sight hydrogen densities. Solid symbols (and upper limits) denote the STIS boron sample (this work). Open symbols represent GHRS measurements from the literature (see text). The dotted line indicates the solar system abundance (2.78 ± 0.04 ; Lodders 2003), while the solid and dashed lines correspond to the mean abundances in warm gas (2.38 ± 0.10) and cold clouds (1.58 ± 0.16), respectively.

4. Discussion and conclusions

Our result for the mean B abundance in warm diffuse gas, $\log \epsilon(\text{B}) = 2.38 \pm 0.10$, represents a lower limit to the total interstellar B abundance, since some depletion is expected even in the lowest-density phase of the diffuse ISM. This value agrees remarkably well with the lower limit derived by Howk et al. (2000) but is depleted by 60% relative to the solar system (meteoritic) value of 2.78 ± 0.04 (Lodders 2003). The solar abundance is traditionally used as a cosmic standard against which to measure interstellar depletion, although the abundances in F and G field dwarfs of solar metallicity or hot O and B stars are also appropriate references (e.g., Snow & Witt 1996; Sofia & Meyer 2001). Interestingly, our interstellar B abundance for warm gas is fairly consistent with the abundances in a variety of Galactic disk stars (see Table 1). At the very least, if one were to take the F and G dwarf sample of Cunha et al. (2000a) and the sample of B-type stars in Venn et al. (2002) to derive a cosmic B abundance of 2.5, then B would seem to be only lightly depleted along the lowest-density interstellar sight lines. Unless the various solar and stellar abundances can be reconciled, establishing the total interstellar abundance of boron will have to await deeper insight into the gas-grain interactions responsible for removing atoms in diffuse clouds from the gas phase.

While the absolute level of boron depletion will remain controversial without a definitive cosmic standard, the variation in relative depletion has clearly been demonstrated here (Figure 1). It then becomes possible to identify intrinsic variations in abundance superimposed on the general trend due to depletion. Enhanced boron abundances are expected, for example, in regions shaped by Type II supernovae, since these are the sources most likely responsible for the acceleration of Galactic cosmic rays and are also sites of

Table 1. Stellar disk and interstellar boron abundances

	log $\epsilon(\text{B})$	Reference
ISM (warm)	2.38 ± 0.10	This Work
G stars (Orion)	2.35 ± 0.30	Cunha et al. (2000b)
FG stars	2.51 ± 0.20	Cunha et al. (2000a)
B stars	2.54 ± 0.17	Venn et al. (2002)
Solar (photospheric)	2.70 ± 0.17	Cunha & Smith (1999)
Solar (meteoritic)	2.78 ± 0.04	Lodders (2003)

the ν -process. Any recent production of ^{11}B in such a region, due either to cosmic-ray or neutrino-induced spallation, should manifest itself as a local enhancement in the total boron abundance. Depending on the degree of localization, however, the observational signature may be difficult to discern.

Nevertheless, we did find evidence for enhanced boron abundances in a few directions from our large sample of interstellar sight lines. The abundance we derive of $\log \epsilon(\text{B}) = 2.47 \pm 0.06$ for the line of sight to HD 93222, a member of Collinder 228 in the Carina Nebula, is enhanced by 0.27 dex relative to sight lines with similar average densities and is significantly elevated compared to the values for three other sight lines in the Carina Nebula. The stars HD 93205, CPD-59 2603, and HDE 303308, all members of Trumpler 16, have interstellar B abundances of 2.28 ± 0.12 , 2.23 ± 0.06 , and 2.05 ± 0.14 , respectively, and lie just $23'$ to the north of HD 93222. Walborn et al. (2007) discuss high-velocity expanding structures seen in interstellar absorption lines toward many of these cluster members in the context of a supernova remnant (SNR) in this direction. They note that the highest known interstellar velocities in the nebula occur in the spectrum of HD 93222.

For HD 43818, a member of the Gem OB1 association, we derive a B abundance of 2.07 ± 0.07 . The line of sight to this star is characterized by a factor of 4 higher average density than those in Carina. Since higher depletion is therefore expected, the abundance in this direction represents an enhancement, which is found to be 0.26 dex over similarly dense sight lines. The proximity of this line of sight to IC 443, a young SNR known to be interacting with nearby molecular gas, suggests a possible nucleosynthetic origin for the enhancement. The presence of hadronic cosmic rays accelerated by the SNR and their interaction with ambient molecular material was revealed by VERITAS observations of very-high energy γ -ray emission (Acciari et al. 2009). HD 43818, however, lies considerably to the north of the γ -ray source and so may not be related. We are currently pursuing $^7\text{Li}/^6\text{Li}$ ratios and Li and Rb abundances toward stars closer to IC 443 with the Hobby-Eberly Telescope at McDonald Observatory in an effort to constrain the contribution from massive stars to the synthesis of these elements.

Finally, the line of sight to σ Per, which is located just $8'$ to the north of the star-forming region IC 348, has a B abundance enhanced by 0.18 dex relative to the other three sight lines in Per OB2. While the enhancement is only modest (50%), it becomes significant in light of the fact that the other sight lines show very little scatter in $\log \epsilon(\text{B})$. For 40 Per, ζ Per, and X Per, we derive abundances of 1.48 ± 0.11 , 1.46 ± 0.12 , and 1.48 ± 0.04 , while for σ Per we find an abundance of 1.65 ± 0.09 . Considering the low $^7\text{Li}/^6\text{Li}$ ratio in this direction (Knauth et al. 2000a; 2000b; 2003) and an enhanced cosmic-ray flux, which was inferred from measurements of interstellar OH (Federman, Weber & Lambert 1996b) and is consistent with an upper limit derived from observations of H_3^+ (Indriolo et al. 2007), evidence seems to be mounting of the effect of cosmic-ray spallation reactions on the interstellar abundances of Li and B near IC 348. Recently, Li data were obtained toward

the fainter stars of IC 348, itself. Complementary data on interstellar B should now be acquired for these stars, perhaps with the Cosmic Origins Spectrograph, so that the abundance enhancements resulting from cosmic-ray interactions with interstellar clouds can be traced in more detail. In this way, a clearer picture of light element nucleosynthesis will emerge.

Acknowledgements

This research was funded by the Space Telescope Science Institute (STScI) through grant HST-AR-11247.01-A. The data were obtained from the Multimission Archive at STScI, operated by the Association of Universities for Research in Astronomy, Inc. under NASA contract NAS5-26555. A. M. R. would like to thank the Swiss National Science Foundation for a grant provided to cover attendance at the IAU Symposium 268.

References

- Acciari, V. A., Aliu, E., Arlen, T., & VERITAS Collaboration. 2009, *ApJ*, 698, L133
- Boesgaard, A. M., & Heacox, W. D. 1978, *ApJ*, 226, 888
- Cunha, K., & Smith, V. V. 1999, *ApJ*, 512, 1006
- Cunha, K., Smith, V. V., Boesgaard, A. M., & Lambert, D. L. 2000a, *ApJ*, 530, 939
- Cunha, K., Smith, V. V., Parizot, E., & Lambert, D. L. 2000b, *ApJ*, 543, 850
- Diplas, A., & Savage, B. D. 1994, *ApJS*, 93, 211
- Federman, S. R., Lambert, D. L., Cardelli, J. A., & Sheffer, Y. 1996a, *Nature*, 381, 764
- Federman, S. R., Weber, J., & Lambert, D. L. 1996b, *ApJ*, 463, 181
- Howk, J. C., Sembach, K. R., & Savage, B. D. 2000, *ApJ*, 543, 278
- Indriolo, N., Geballe, T. R., Oka, T., & McCall, B. J. 2007, *ApJ*, 671, 1736
- Jenkins, E. B., Savage, B. D., & Spitzer, L. 1986, *ApJ*, 301, 355
- Jura, M., Meyer, D. M., Hawkins, I., & Cardelli, J. A. 1996, *ApJ*, 456, 598
- Knauth, D. C., Federman, S. R., Lambert, D. L., & Crane, P. 2000a, *Nature*, 405, 656
- Knauth, D. C., Federman, S. R., Lambert, D. L., & Crane, P. 2000b, in: L. da Silva, M. Spite & J. R. de Medeiros (eds.), *The Light Elements and Their Evolution*, Proc. IAU Symposium No. 198 (San Francisco: ASP), p. 338
- Knauth, D. C., Federman, S. R., & Lambert, D. L. 2003, *ApJ*, 586, 268
- Lambert, D. L., Sheffer, Y., Federman, S. R., Cardelli, J. A., Sofia, U. J., & Knauth, D. C. 1998, *ApJ*, 494, 614
- Lodders, K. 2003, *ApJ*, 591, 1220
- Meneguzzi, M., Audouze, J., & Reeves, H. 1971, *A&A*, 15, 337
- Meneguzzi, M., & York, D. G. 1980, *ApJ*, 235, L111
- Pan, K., Federman, S. R., Cunha, K., Smith, V. V., & Welty, D. E. 2004, *ApJS*, 151, 313
- Ramaty, R., Kozlovsky, B., Lingenfelter, R. E., & Reeves, H. 1997, *ApJ*, 488, 730
- Ritchey, A. M., Federman, S. R., Sheffer, Y., & Lambert, D. L. 2010, *in preparation*
- Sheffer, Y., Rogers, M., Federman, S. R., Abel, N. P., Gredel, R., Lambert, D. L., & Shaw, G. 2008, *ApJ*, 687, 1075
- Snow, T. P., & Witt, A. N. 1996, *ApJ*, 468, L65
- Sofia, U. J., & Meyer, D. M. 2001, *ApJ*, 554, L221
- Spitzer, L. 1985, *ApJ*, 290, L21
- Venn, K. A., Brooks, A. M., Lambert, D. L., Lemke, M., Langer, N., Lennon, D. J., & Keenan, F. P. 2002, *ApJ*, 565, 571
- Walborn, N. R., Smith, N., Howarth, I. D., Kober, G. V., Gull, T. R., & Morse, J. A. 2007, *PASP*, 119, 156
- Welty, D. E., & Hobbs, L. M. 2001, *ApJS*, 133, 345
- Welty, D. E., Morton, D. C., & Hobbs, L. M. 1996, *ApJS*, 106, 533
- Woosley, S. E., Hartmann, D. H., Hoffman, R. D., & Haxton, W. C. 1990, *ApJ*, 356, 272

Boron abundances in the Galactic disk

Katia Cunha¹

¹NOAO

950 N. Cherry Ave, Tucson , Arizona

email: kcunha@noao.edu

Abstract. When compared to lithium and beryllium, the absence of boron lines in the optical results in a relatively small data set of boron abundances measured in Galactic stars to date. In this paper we discuss boron abundances published in the literature and focus on the evolution of boron in the Galaxy as measured from pristine boron abundances in cool stars as well as early-type stars in the Galactic disk. The trend of B with Fe obtained from cool F-G dwarfs in the disk is found to have a slope of 0.87 ± 0.08 (in a log-log plot). This slope is similar to the slope of B with Fe found for the metal poor halo stars and there seems to be a smooth connection between the halo and disk in the chemical evolution of boron. The disk trend of boron with oxygen has a steeper slope of 1.5. This slope suggests an intermediate behavior between primary and secondary production of boron with respect to oxygen. The slope derived for oxygen is consistent with the slope obtained for Fe provided that [O/Fe] increases as [Fe/H] decreases, as observed in the disk.

Keywords. stars: abundances – Galaxy: disk – ultraviolet: stars

1. Introduction

The light element boron is one of the few elements whose production is not dominated by nucleosynthesis in stars, nor by nucleosynthesis occurring in the Big Bang. In fact, it has been known now for almost 4 decades that Galactic Cosmic Rays are related to the formation of the light elements and, in particular, of boron (Reeves, Fowler & Hoyle 1970). The connection between boron production and cosmic rays spallation reactions, which involve C, N, O atoms, as well as protons and α particles, makes boron an interesting element whose abundance evolution in the Galaxy probes the history of cosmic rays in the galactic environment. In addition, boron is also proposed to be produced by neutrino nucleosynthesis occurring in core collapse of Supernovae Type II (Woosley et al. 1990).

Unveiling the underlying behavior of boron with metallicity (iron and oxygen abundances) is crucial in order to constrain models for boron production. One of the challenges in trying to pin down the behavior of boron with metallicity, however, comes first from the fact that boron is fragile and easily destroyed in stellar interiors (although sturdier than Li and Be) and, in addition, from the difficulty in obtaining boron observations. In this paper we discuss stellar boron abundance results mainly for disk stars which have been published in the literature. Unfortunately, no new boron observations were available in recent years due to the failure of STIS on board HST.

2. Boron transitions and abundance determinations

Boron abundance results are still sparse as boron abundances can only be measured from transitions which fall mainly in the ultraviolet. Boron abundance indicators in different temperature regimes are from three ionization stages: neutral boron in cool stars (B I at 2497.723Å); B II (at 1362Å) mostly in A-type stars and the B III resonance doublet (at 2060Å) in B-type stars.

2.1. Boron in cool stars and the Sun

Boron was measured in the Sun by Kohl, Parkinson & Withbroe (1977). One of the pioneering studies of boron abundances in stars was by Boesgaard & Heacox (1978). A few studies appeared more than a decade later from observations obtained with the Hubble Space Telescope (Duncan, Lambert, & Lemke 1992; Duncan et al. 1997; Primas et al. 1999). The sample analyzed in Duncan et al. (1997) was mostly for halo stars. Their results were particularly important as they found that boron abundances scaled linearly (in log-log space) with the abundance of metals, in contrast with predictions from the standard models of cosmic ray production, which proposed a secondary behavior for boron with metallicity. These predictions from cosmic ray models had remained unchallenged for ~ 20 years.

Following studies focused on samples of stars with disk metallicities and, by the nature of their sample, these probed the behavior of boron in the most metal rich stars in the Galaxy (Boesgaard et al. 1998; Cunha & Smith 1999; Cunha et al. 2000; Boesgaard et al. 2004; Boesgaard et al. 2005). It is important to acknowledge, however, that the line list in the spectral region of the B I transition is a major challenge for the analysis of boron in solar-like stars as the spectral region to be synthesized is covered with strong blending lines for which, in many instances, there is no atomic data available. Note, however,

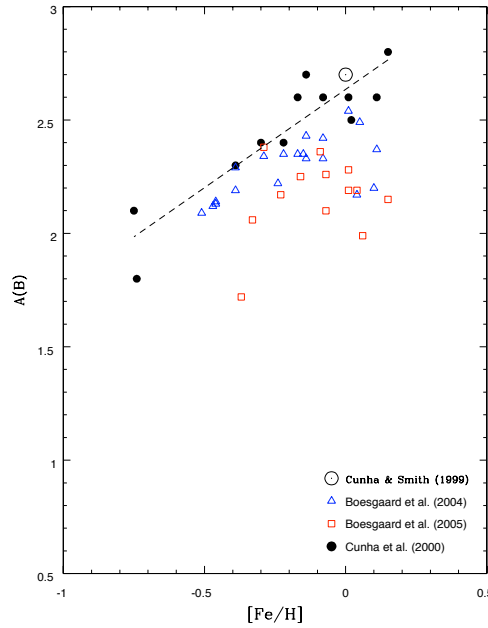


Figure 1. Boron results for the available samples of F-G disk stars. The solar abundance is also plotted. The targets in Boesgaard et al. (2004) and Cunha et al. (2000) are beryllium undepleted, while the stars analyzed in Boesgaard et al. (2005) are mixed showing a degree of Be depletion. For the Be undepleted stars it is clear that there is a systematic abundance offset between the studies of Cunha et al. (2000) and Boesgaard et al. (2004) which can be attributed to the differences in the line lists adopted in the analyses. The slope representing the trend of boron with iron for the disk is 0.87 ± 0.08 (dashed line); this defines the upper envelope (undepleted) of the distribution.

that this does not represent a severe problem for the analysis of halo stars as the metal lines are vanishingly weak. For solar metallicity stars, different studies in the literature constructed and adopted different line lists which resulted in systematic differences in the derived boron abundances. In the following we briefly present some of the boron results in these studies.

Cunha et al. (2000) analyzed dwarf stars with $[\text{Fe}/\text{H}] > -1.0$ (T_{eff} 's between 5650 - 6700K) from HST archival data. One important aspect of that study in comparison with Boesgaard et al. (1998; 2004) is that the line list adopted in the calculation of model spectra in Cunha et al. (2000) was empirically adjusted in order to fit the Sun. In using the Sun as a benchmark in the study of solar-type stars, Cunha & Smith (1999) re-visited the analysis of boron in the solar photosphere. In particular, significant effort was put in that study into evaluating and updating the opacities which are important in the ultraviolet and which affect the derived boron abundances. This resulted in the revision upwards of the boron abundance in the solar photosphere, which was found to be in good agreement with the boron meteoritic value of $A(\text{B}) = 2.79 \pm 0.04$ (see Lodders, Palme & Gail 2009). The agreement between the boron abundances in the solar photosphere and meteorites (implying an *absence* of boron depletion in the Sun) is an important result as it reconciles with the most recent assessment of the beryllium abundance in the solar photosphere by Asplund et al. (2009), indicating no beryllium depletion in the Sun. If Be is indeed not depleted in the solar photosphere, it follows that boron, which is less fragile than Be, cannot be depleted in the solar photosphere.

Boron abundances for disk dwarfs with effective temperatures close to solar are shown in Figure 1. Non-LTE corrections for the B I transition at 2497Å for this temperature range at solar metallicity are deemed to be small (Kiselman & Carlson 1996). In order to have all stars and the Sun on a consistent scale, all disk stars in Cunha et al. (2000) were analyzed homogeneously. The study by Boesgaard et al. (2004) used a different line list which was not fine tuned in order to fit the solar spectrum. It can be seen that the results from Cunha et al. (2000) and Boesgaard et al. (2004), all for targets with undepleted beryllium, have a small systematic offset. It is clear also that the targets analyzed Boesgaard et al. (2005) have significantly lower boron abundances, but this is expected as the target stars were selected in that study to be beryllium depleted in order to further study mixing.

2.2. Boron in early-type stars

Of the light element trio, boron is the only element whose abundance can be measured in early-type stars. One problem in using early-type stars to define the boron Galactic trend, however, is the varying amounts of boron depletion in OB-type stars, as depletion of boron is proportional to stellar mass, age and rotational velocity. In addition, unlike the case of observations of Li and Be in cool stars, there is not a sensitive monitor of depletion in early-type stars. Boron is burnt at temperatures which are lower than those at which the CN cycle takes place and is much more sensitive to mixing than nitrogen.

Some studies in the literature have derived boron abundances from HST observations obtained with the GHRS and STIS spectrographs in relatively small samples of early-type stars (Cunha et al. 1997; Venn et al. 2002; Mendel et al. 2006). Most of these boron abundances, however, were found to be somewhat mixed and therefore not representative of the chemical composition of the gas which formed these young stars. The larger sample analyzed by Proffitt & Quigley (2001) from IUE archival observations of the B III resonance line at 2066Å, although not having the same spectral quality as HST data, found some stars to be boron undepleted which helped define the disk trend.

3. Boron abundance trends in the disk

The evolution of boron with oxygen for metallicities covering the range spanned by the disk is shown in Figure 2. The blue filled circles represent the FG-dwarfs analyzed in Cunha et al. (2000) with the errorbars indicating the estimated abundance uncertainties. Boron results for early-type stars from Proffitt et al. (2001; filled red triangles) and Mendel et al. (2006; filled red squares) are also shown. Most of the B stars shown have roughly undepleted boron and on average follow the disk trend delineated by the cool stars. The general agreement between the results in cool and hot stars is pleasing given that the physical conditions in their stellar atmospheres are quite distinct. The behavior of boron with oxygen can be represented by a linear relation (in the log-log plot) with a slope ~ 1.5 , which can suggest an intermediate behavior between primary and secondary production for boron with respect to oxygen.

In Figure 3 we plot boron abundances versus $[\text{Fe}/\text{H}]$ spanning the metallicity range from the halo to the disk. If we adopt the boron abundances for the Be undepleted stars from Cunha et al. (2000; filled circles) as representative of the disk value, there seems to be a smooth transition between the halo and disk which follows a slope of ~ 0.9 . This slope for the disk + halo is closer to a primary rather than a secondary behavior for boron production. In addition, it is important to note that the slope derived for oxygen (from Figure 2) is consistent with the one obtained for Fe provided that $[\text{O}/\text{Fe}]$ increases as $[\text{Fe}/\text{H}]$ decreases, as observed in the disk.

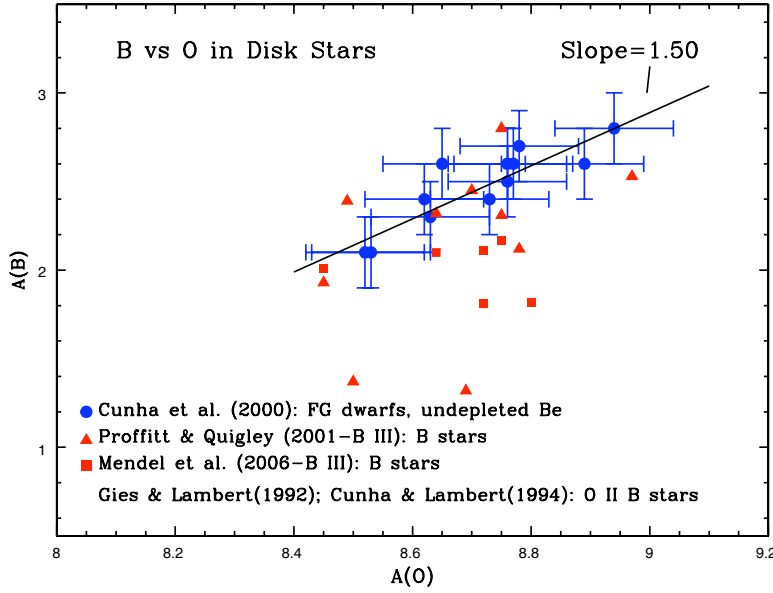


Figure 2. The evolution of boron and oxygen abundances in the Galactic disk. Boron results for cool disk FG-type dwarfs are taken from Cunha et al. (2000); these targets have undepleted Be abundances which indicate that their boron content is not mixed and representative of their natal clouds. The evolution of boron and oxygen from this dataset can be represented by linear relation with slope ~ 1.5 . Boron results for early-type stars from Proffitt & Quigley (2001) and Mendel et al. (2006) are also shown. The lower boron abundances in some of the B-type stars are due to internal mixing and astration.

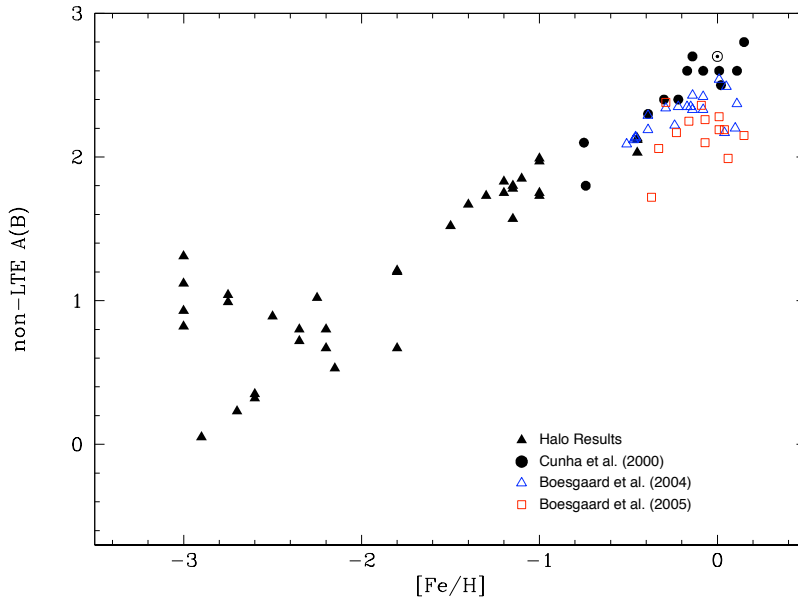


Figure 3. The behavior of boron with metallicity for the Galactic disk in comparison with the trend obtained for the more metal poor stars in the halo. If the abundance results in Cunha et al. (2000) are adopted as representative of the disk (filled circles), there seems to be a smooth transition between the disk and halo. The halo star abundances are taken from Duncan et al. (1997) and García López et al. (1998).

4. How do we move forward?

Probing the behavior of boron with metallicity is crucial for understanding boron production in the Galaxy and the relatively small number of stars analyzed to date could usefully be increased. It is good news that the STIS spectrograph has been recently fixed in a very successful NASA servicing mission (SM4) and that it can now be ready for more boron observations in the UV. In addition, the new UV Cosmic Origins Spectrograph (COS) was deployed on HST during SM4. We also need improvements in the abundance analysis and in particular improvements in the line lists to model the boron region. Full non-LTE treatment is needed, including non-LTE analysis of transitions of all elements contributing to the boron blend; and a complete hydrodynamic 3-D modelling of the stellar atmospheres is also something to look forward to in particular for the cool stars.

References

- Asplund, M., Grevesse, N., Sauval, A. J. & Scott, P. 2009, *ARA*, 47, 481
 Boesgaard, A. M., & Heacox, W. D. 1978, *ApJ*, 226, 888
 Boesgaard, A. M., Deliyannis, C. P., Stephens, A. & Lambert, D. L. 1998, *ApJ*, 492, 727
 Boesgaard, A. M., McGrath, E. J., Lambert, D. L. & Cunha, K. 2004, *ApJ*, 606, 306
 Boesgaard, A. M.; Deliyannis, C. P. & Steinhauer, A. 2005, *ApJ*, 621, 991
 Cunha, K., Lambert, D. L., Lemke, M., Gies, D. R. & Lewis, C. R. 1997, *ApJ*, 478, 211
 Cunha, K. & Smith, V. V. 1999, *ApJ*, 512, 1006
 Cunha, K., Smith, V. V., Boesgaard, A. M. & Lambert, D. L. 2000, *ApJ*, 530, 939
 Duncan, D. K., Lambert, D. L. & Lemke, M. 1992, *ApJ*, 401, 584

- Duncan D. K., Primas, F., Rebull, L. M., Boesgaard, A. M., Deliyannis, C. P., Hobbs, L. M., King, J. R., & Ryan, S. G. 1997, *ApJ*, 488, 338
- García López, R. J., Lambert, D. L., Edvardsson, B., Gustafsson, B., Kiselman, D. & Rebolo, Rafael 1998, *ApJ*, 500, 241
- Kiselman D. & Carlsson M. 1996, *A&A* 311, 680
- Kohl, J. L., Parkinson, W. H. & Withbroe, G. L. 1977, *ApJ*, 212, L101
- Lodders K., Palme H., & Gail H-P. 2009, *Landolt-Bornstein, New Series, Astronomy and Astrophysics*, Ed. Springer Verlag, in press (arXiv:astro-ph/0901.1149)
- Mendel, J. T., Venn, K. A., Proffitt, C. R., Brooks, A. M. & Lambert, D. L. 2006, *ApJ*, 640, 1039
- Primas, F., Duncan, D. K., Peterson, R. C. & Thorburn, J. A. 1999, *A&A*, 343, 545
- Proffitt C. R. & Quigley, M. F. 2001, *ApJ*, 548, 429
- Reeves, H., Fowler, W. A. & Hoyle, F. 1970, *Nature*, 226, 727
- Venn, K. A., Brooks, A. M., Lambert, D. L., Lemke, M., Langer, N., Lennon, D. J. & Keenan, F. P. 2002, *ApJ*, 565, 571
- Woosley, S. E., Hartmann, D. H., Hoffman, R. D. & Haxton, W. C. 1990, *ApJ*, 356, 272

Lithium in globular clusters

Andreas J. Korn

Dept. of Physics and Astronomy, Uppsala University,

Box 516, 75120 Uppsala, Sweden

email: andreas.korn@fysast.uu.se

Abstract. I review recent progress in mapping out and understanding the behaviour of stellar surface abundances of lithium as evidenced by spectroscopic studies of nearby globular clusters (GCs). It will become clear that these observations necessitate revisions to the canonical picture of stellar and globular-cluster evolution: stars evolve with additional non-convective mixing processes and GCs are not simple stellar populations. In spite of these complications, GCs are excellent test beds for chemical-abundance studies. Spectroscopic observations of GC stars of different evolutionary stages reveal systematic trends of surface abundances likely caused by atomic diffusion and mixing. Correcting for their combined effect on surface lithium, a stellar solution to the cosmological lithium discrepancy is likely, if not probable. However, a definitive answer can only be given once we know the effective temperatures of warm subdwarfs and subgiants to high accuracy and understand the processes which give rise to the mixing needed to moderate atomic diffusion.

Keywords. Stars: Population II, atmospheres, abundances – diffusion – line: formation – globular clusters: individual (M 92, NGC 6397, NGC 6752) – cosmology: early universe – techniques: spectroscopic

1. Introduction

Cosmology with stars. This was the implicit promise of the seminal discovery of a uniform lithium abundance among warm halo field stars in 1982 by Monique and Francois Spite (Spite & Spite 1982). A quarter century on, in the era of precision cosmology (PC), heralded by balloon experiments like MAXIMA and BOOMERANG and fully established through the WMAP-satellite all-sky measurements, we realize that the evolution of stellar-surface lithium abundances is more complicated and the inference of its primordial (or Big-Bang nucleosynthesis, BBN) value less direct. As early as 1984, Michaud, Fontaine & Beaudet (1984) cautioned that the Spite plateau of lithium was unlikely to represent the unaltered primordial abundance of lithium, as diffusive processes inside the stars would inevitably deplete the stellar surface layers of heavy elements over the course of the billion-year stellar lifetimes.

It is the intention of this review article to give an overview of the latter half of this time frame of Galactic lithium studies with potential cosmological implications. This is the period when the current generation of 8-10m telescopes became available giving routine access to much fainter Spite-plateau stars. Apart from singular heroic efforts with 4m-class telescopes (e.g. Pasquini & Molaro 1996), lithium in globular clusters (GCs) has been exclusively studied with efficient spectrographs on Keck, the VLT and their siblings. The TOP (turn-off point) stars in even the most nearby low-reddening GCs (e.g. NGC 6397) are no brighter than $V \approx 16.5^m$. In the very metal-poor GC M 92, the TOP stars have $V \approx 18.5^m$ which makes studies at high resolution ($R \approx 40\,000$) and high signal-to-noise ratio ($S/N \approx 100$) a true challenge, even with 50+ square metres of light-collecting area and 90% overall quantum efficiency.

For the sake of a historical assessment, I subdivide the roundabout 12 years to be covered here into two periods: the first six years (1998-2003, Sect. 2) are characterized by a single-star observational approach and small-number statistics, with in part contradicting results; the second six years (2004-2009, Sect. 3) have led to some far-reaching revisions based on multi-object spectroscopy coupled with better observations and better modelling. Some apparent contradictions are discussed. Work in progress is presented in Sect. 4 and concluding remarks are given in Sect. 5.

2. The HIRES and UVES years (1998-2003)

Scientists with access to Keck had a head start to the GC lithium business. Building on observations of Deliyannis, Boesgaard & King (1995), Boesgaard et al. (1998) analysed high-resolution, moderate-S/N spectra of a handful of subgiants in M 92 and concluded that there is a significant dispersion in lithium abundances among otherwise very similar stars. This dispersion was interpreted to be an indication for different levels of lithium depletion taking place in these stars, possibly correlated with the stars' angular-momentum history. This is not necessarily a far-fetched thought (cf. Pinsonneault, these proceedings). But to make sense of a marked dispersion in M 92 on the one hand and no dispersion (plus a few outliers) on the field-star Spite plateau would require to postulate very different angular-momentum conditions for these two groups of stars.

Bonifacio (2002) subsequently analysed the same M 92 data and concluded that there is no compelling evidence for dispersion beyond the level expected from observational uncertainties. Somewhat surprisingly, no one has to this day reinvestigated the chemical signatures of little evolved stars in M 92 (but see Sect. 4).

Across the Atlantic, a team of European researchers used large amounts of observing time at the VLT to systematically explore the nucleosynthesis within a variety of GCs (cf. Bragaglia, these proceedings, for an overview). One of the early targets was the smallish GC NGC 6397. Bonifacio et al. (2002) studied lithium in a dozen TOP stars in this GC and arrived at a common lithium abundance of $\log \varepsilon(\text{Li}) = 2.34 \pm 0.06$ on the customary logarithmic scale that equates $\log \varepsilon(\text{H})$ with 12. It is probably fair to say that in the early years of this century it looked as if the GC Spite plateau behaved just like that of the field stars.

This idea was overthrown by Pasquini et al. (2005) who observed a 0.45 dex tip-to-tip dispersion among nine TOP stars in NGC 6752 at $[\text{Fe}/\text{H}] = -1.5$. They went beyond Boesgaard and collaborators in showing that lithium in this cluster correlates with other elements: sodium, oxygen and nitrogen. Together with other inverse correlations traced down to the main-sequence TOP (O-Na, Mg-Al, Gratton et al. 2001), it thus became clear that a significant fraction of the GC stars we observe today suffer from intra-cluster pollution through a previous generation of (more massive) GC stars. This paradigm shift in GC research paved the way to research on multiple populations in GCs (Piotto et al. 2007, Lee et al. 2009).

3. The FLAMES years (2004-2009)

This period was characterized by several breakthroughs, theoretical and observational ones alike. It became clear that primordial lithium as predicted by standard WMAP-calibrated BBN and the Spite-plateau lithium abundance are irreconcilable at face value, the difference exceeding 0.3 dex (Coc et al. 2004). Building on 20 years of work within the Michaud school, Richard, Michaud & Richer (2005) tuned their stellar-structure models with additional mixing and proposed a stellar-physics solution: the surface lithium

diffuses out of the convective envelope according to the physical laws for inhomogeneous gases in a gravitational field, but this gravitational settling is moderated by an unspecified parametrized mixing process below the convective envelope. It is this (turbulent) mixing that manages to keep the Spite plateau thin and flat, even though the surface abundance is reduced by as much as 0.4 dex. Since this postulated mixing lacks a physical interpretation, the models can be said to lose their predictive power. But it turns out that only a subset of models fulfills the observational constraints: in the language of mixing[†] this is the range from T6.0 to T6.28.

I started to look into the same issue from an observational point as early as 2003. With the vagaries of Paranal weather, it took two years to collect spectroscopic data of sufficient quality to take a fresh look at chemical abundances in NGC 6397. But what a data set it turned out to be! With the advances in instrumentation at the VLT, we not only got high-resolution data for 18 stars along the evolutionary sequence of NGC 6397 with UVES in fibre mode; we also got 100+ spectra of intermediate resolution ($R=25,000$) using FLAMES-MEDUSA. This instrument has really propelled us into a new era of GC research!

In a series of papers, Korn et al. (2006, 2007) and Lind et al. (2008) showed that there are systematic trends of surface abundances with evolutionary stage. The TOP stars show systematically lower abundances (by up to 0.2 dex) than the RGB stars. This is indeed what one would expect from gravitational settling: it is most efficient when the convective envelope (in itself always fully mixed on a convective-turnover time scale) is thinnest and least massive. Once the stars reach the RGB, the convective envelope expands inward and mixes the settled elements back to the surface. With a notable exception.

The run of surface lithium from the TOP to the RGB is instead characterized by a steep surface dilution. Lithium that settles into layers whose temperature exceeds 2 million Kelvin will capture a proton and disintegrate into He-4 and He-3, this lithium is thus lost and cannot replenish the surface abundance. But before the surface dilution sets in, we can see that lithium did actually settle: in the middle of the subgiant branch (SGB), the lithium abundance is higher than among TOP stars. We can understand why by looking at the structure of our model star which apart from the convective envelope has a region below the convection zone that is rich in lithium. This region is created by the mixing we introduced into the model. When the convection zone expands inward, it first encounters this region and brings its lithium content to the surface, the surface lithium abundance increases a little. Indeed, this is seen as a ≈ 0.1 dex abundance difference in lithium between TOP and SGB stars.

Lind et al. (2009) took this work further by analysing several hundred NGC 6397 cluster members with FLAMES-MEDUSA, from the main sequence to beyond the RGB bump. The derived run of lithium as a function of evolution is a textbook result, clearly demonstrating the accuracy with which such work can nowadays be executed. The upturn in the middle of the SGB discussed above and the need for extra mixing around the bump (at $M_V = 0$ for NGC 6397) is seen very clearly. This extra mixing is now believed to be connected to a thermohaline instability that develops in connection with a mean-molecular-weight inversion (Charbonnel & Zahn 2007). We really need more work along these lines, ideally coupling different elements, to verify that we understand all the

[†] There are, in principle, two parameters one can tune: the strengths and the density dependence of mixing. Richard, Michaud & Richer (2005) chose to vary the strength and keep the run with density ρ constant, with an exponent of -3 . The Tx.x notation then specifies the logarithm of the temperature T_0 at which the diffusion coefficient for mixing D_T is connected to the atomic-diffusion coefficient for He D_{He} according to $D_T = 400D_{\text{He}}(T_0)(\rho/\rho(T_0))^{-3}$.

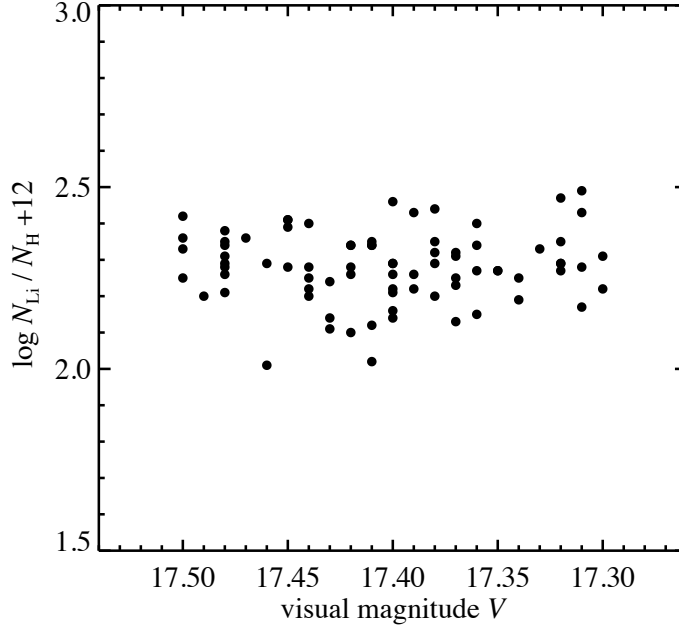


Figure 1. In the subgiant sample of González Hernández et al. (2009), there is little of a correlation between $\log \varepsilon(\text{Li})$ and V magnitude. If anything, there is a slight rise towards the middle of the SGB (brighter stars), like in the other works that studied NGC 6397.

variables at play here. For lithium production in more advanced stages of evolution, the reader is referred to Smith (these proceedings).

Finally, González Hernández et al. (2009) performed a vertical diffusion study comparing the lithium abundances between dwarfs and subgiants at a given $(B - V)$. Like Lind et al. (2009), they find a systematic difference between dwarfs and subgiants with the latter being 0.1 dex more lithium-rich. Working on a newly established effective-temperature scale (Balmer lines in 3D model atmospheres), they derive abundances as high as 2.4 dex for the subgiants. They also find trends with effective temperature that may or may not be significant (since this project was conceived as a vertical study, the T_{eff} range covered is not very large and does not include the TOP; cf. Lind, these proceedings). Without resorting to statistical tests, there seems to be little of a positive trend of $\log \varepsilon(\text{Li})$ with V in Fig. 1. It would be good to see González Hernández and collaborators perform their analysis on all spectroscopically observed stars in NGC 6397 and include other elements into the picture.

4. Ongoing analyses

New evidence in favour of and against atomic diffusion of lithium was presented at IAU 268. Meléndez showed how the field-star Spite plateau can be reconciled with WMAP-calibrated BBN predictions using a T6.25 diffusion-and-mixing model à la Richard. When plotted versus stellar mass, there is a specific morphology that is well-captured by the model predictions. As a cautionary note, it should be said that a single such model (one for $[\text{Fe}/\text{H}] = -2.3$) was used to explain lithium abundances over a large range of

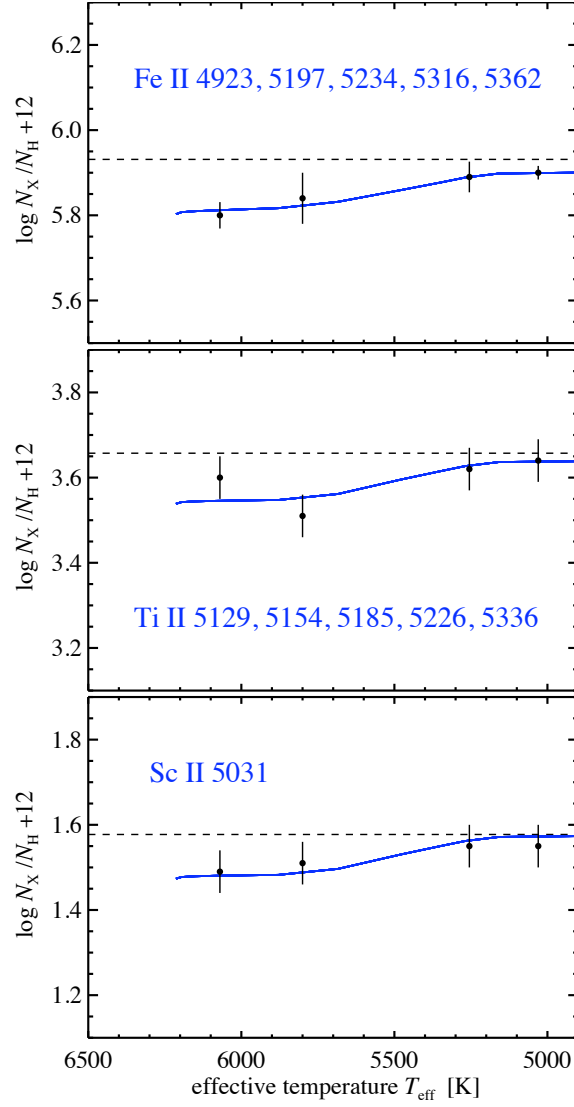


Figure 2. Measured abundance trends for stars in NGC 6752 ($[\text{Fe}/\text{H}] = -1.6$) versus predictions from a T6.2 Richard model. For iron, the star-to-star scatter in each group is given as an error bar, for titanium and scandium which are both measured on the group-averaged spectra, 0.05 dex is assumed.

metallicities. This should be remedied. Bonifacio presented challenging observations of Spite-plateau stars drawn from various populations in ω Cen. Identifying a common Spite plateau for the majority of these stars, he claimed that this must represent an unaltered stellar-birth value, as these different populations have different ages and should thus be affected differently by a temporal process like atomic diffusion. But as long as we do not

know the age difference with certainty (and independent of the unknown helium-content difference), this argument rests on weak foundations.

The ADiOS (Atomic Diffusion in Old Stars) team has begun to analyse VLT/FLAMES-UVES data on NGC 6752 ($[\text{Fe}/\text{H}] = -1.6$) taken last year. The TOP stars in this cluster are faint ($V \approx 17.2^m$) requiring exposure times in excess of 30 h. So far, following a strict quality approach, only lines sensitive to surface gravity have been looked at: Fe II, Ti II and Sc II. Surface-gravity differences between stars can be inferred with high precision based on photometry and estimates of stellar mass and bolometric correction. In addition, both NLTE and 3D corrections are expected to be small for these lines, as they connect levels in the dominant ionization stage and form deep in the atmosphere. The abundance difference between the TOP and RGB stars is found to be $\Delta[\text{Fe}/\text{H}] = -0.10 \pm 0.03$ where the error is the star-to-star scatter in each group propagated into the abundance difference. Similar trends are found for titanium and scandium and all are in good agreement with T6.2 model predictions for this metallicity. With an atomic-diffusion correction of 0.25 dex for Li-7 and face-value surface abundances as high as $\log \varepsilon(\text{Li}) = 2.5$, the primordial lithium abundance can be reached without much ado. Admittedly, it is towards lower metallicities where this game becomes more difficult to play. But beyond the metallicity of M 92 (for which new data was taken with HIRES on Keck last year (PI Cohen), analysis pending) this is not the realm of GC studies.

5. Concluding remarks

Studies of lithium in GCs have led to a number of important discoveries in recent years:

- Apart from intra-cluster Li-Na inverse correlations mainly affecting massive GCs, the behaviour of lithium in single GC stars resembles that of single field stars of the same mass range. This is to be expected assuming that the spin-down of metal-poor stars is fast, i.e. all stars evolve in a homologous manner irrespective of their initial angular momentum (which may well depend on environment).
- Higher surface lithium abundances among warm subgiants are indicative of dredge-up of lithium stored below the convective envelope. This is the most direct signature of atomic diffusion and mixing in such stars. In the presence of a strong Li-Na inverse correlation, atomic diffusion can still be studied using heavier elements.
- Extra mixing around the RGB bump sets in at a well-defined absolute magnitude ($M_V = 0$ for NGC 6397, Lind et al. 2009). Thermohaline mixing is now believed to be the main process responsible. A systematic investigation of how well the best stellar-structure models capture, e.g., the metallicity dependence of this extra mixing is still lacking.

What is almost completely absent from GC (and halo-star) studies so far is insight into rotation, mass loss and magnetic properties and their influence on inferred abundances and stellar evolution. While these “complications” are generally believed to be less prominent in Population II stars, they may still have a non-negligible impact on the quantitative picture.

As is commonplace in modelling of any kind, there are some mismatches between the run of inferred GC surface abundances and those predicted by stellar-structure models with atomic diffusion and mixing. However, given the tests that the atomic-diffusion hypothesis has been subjected to (using different spectrographs, different model atmospheres, different effective-temperature scales, different line-formation theories, different abundance-analysis techniques, spectral lines with different sensitivities to T_{eff} and $\log g$), there can be little doubt that surface abundances of old, low-mass stars are an explicit

function of time. Lithium happens to be one of the elements most affected by atomic diffusion. Surface depletions of 0.25-0.4 dex are predicted by the current generation of sophisticated stellar-structure models (“Richard models”) without an accompanying effect on well-observed elements like calcium or iron exceeding ≈ 0.1 dex. It is difficult to unambiguously establish the reality of such shallow abundance trends (cf. the case of NGC 6752 with a T6.2 mixing model). But even evidence from lithium-only studies is accumulating (Meléndez, these proceedings).

If we convince ourselves that the well-observed TOP-part of the Spite plateau lies at $\log \varepsilon(\text{Li}) = 2.25$, then the atomic-diffusion corrected surface abundance of these stars (around $\log \varepsilon = 2.5$ at $[\text{Fe}/\text{H}] = -2$) are in marginal (1.5σ) agreement with the currently favoured WMAP-calibrated primordial value of 2.72 ± 0.06 (Dunkley et al. 2009). There may, however, be biases both in the stellar-atmosphere, line-formation and stellar-structure modelling that could make the stellar abundances fall short. There may be remaining biases in the BBN predictions (cf. the relatively recent correction of the ${}^7\text{Be}(d, p)2\alpha$ cross-section at BBN energies, Angulo et al. 2005), even though few dare to say so (that would be PC blasphemy!). As an example of the remaining uncertainties of the stellar-atmosphere side, let us recall that an effective-temperature scale hotter by 100 K (as favoured by recent 3D Balmer-profile analyses, González Hernández et al. 2009) would add a further 0.07 dex to the above-mentioned values†.

One may wish to add extra boundary conditions to the picture: the possibility of global Li-7 destruction by decaying super-symmetric particles early on in the Universe (indeed, during the very phase of BBN taking place on the natural time and energy scale for this to happen, cf. Jedamzik, these proceedings); the possibility of global Li-7 destruction by Population III stars (Piau et al. 2006); the observation of fragile Li-6 in some of the classical Spite-plateau halo stars which currently divides the hydro-modelling experts into believers and sceptics (Asplund et al. 2006, Cayrel et al. 2007; cf. the contributions by Asplund and Steffen, these proceedings); the possibility of global Li-6 production by the above-mentioned or a similar cosmological process (e.g. Jedamzik et al. 2006). All these make lithium a fascinating element to observe and model. But until solid evidence is provided for any of these effects, I prefer to settle for the physics we know (Principle of Parsimony): stellar structure and evolution as a remarkably precise theory. This does not free us of the need to develop this theory (and its atmospheric counterpart) to full radiation-hydrodynamic self-consistency.

References

- Angulo, C., Casarejos, E., Couder, M., Demaret, P., Leleux, P., Vanderbist, F., Coc, A., Kiener, J., Tatischeff, V., Davinson, T., Murphy, A. S., Achouri, N. L., Orr, N. A., Cortina-Gil, D., Figuera, P., Fulton, B. R., Mukha, I., Vangioni, E. 2005, *ApJ*, 630, 105
- Asplund, M., Lambert, D. L., Nissen, P. E., Primas, F., Smith, V. V. 2006, *ApJ*, 644, 229
- Boesgaard, A. M., Deliyannis, C. P., Stephens, A., King, J. R. 1998, *ApJ*, 493, 206
- Bonifacio, P. 2002, *A&A*, 395, 515
- Bonifacio, P., Pasquini, L., Spite, F., Bragaglia, A., Carretta, E., Castellani, V., Centurin, M., Chieffi, A., Claudi, R., Clementini, G., D’Antona, F., Desidera, S., Franois, P., Gratton, R. G., Grundahl, F., James, G., Lucatello, S., Sneden, C., Straniero, O. 2002, *A&A*, 390, 91
- Cayrel, R., Steffen, M., Chand, H., Bonifacio, P., Spite, M., Spite, F., Petitjean, P., Ludwig, H.-G., Caffau, E. 2007, *A&A*, 473, L37
- Charbonnel, C. & Zahn, J.-P. 2007, *A&A*, 467, 15
- Coc, A., Vangioni-Flam, E., Descouvemont, P., Adahchour, A., Angulo, C. 2004, *ApJ*, 600, 544

† If you are willing to bet a bottle of wine that the remaining 0.15-0.22 dex are due to new physics, contact the author.

- Deliyannis, C. P., Boesgaard, A. M. & King, J. R. 1995, *ApJ*, 452, L13
- Dunkley, J., Komatsu, E., Nolte, M. R., Spergel, D. N., Larson, D., Hinshaw, G., Page, L., Bennett, C. L., Gold, B., Jarosik, N., Weiland, J. L., Halpern, M., Hill, R. S., Kogut, A., Limon, M., Meyer, S. S., Tucker, G. S., Wollack, E., Wright, E. L. 2009, *ApJS*, 180, 306
- González Hernández, J. I., Bonifacio, P., Caffau, E., Steffen, M., Ludwig, H.-G., Behara, N. T., Sbordone, L., Cayrel, R., Zaggia, S. 2009, *A&A*, 505, L13
- Jedamzik, K., Choi, K.-Y., Roszkowski, L., Ruiz de Austri, R. 2006, *JCAP*, 07, 007
- Korn, A. J., Grundahl, F., Richard, O., Barklem, P. S., Mashonkina, L., Collet, R., Piskunov, N., Gustafsson, B. 2006, *Nature*, 442, 657
- Korn, A. J., Grundahl, F., Richard, O., Mashonkina, L., Barklem, P. S., Collet, R., Gustafsson, B., Piskunov, N. 2007, *ApJ*, 671, 402
- Lee, J.-W., Kang, Y.-W., Lee, J., Lee, Y.-W. 2009, *Nature*, 462, 480
- Lind, K., Korn, A. J., Barklem, P. S., Grundahl, F. 2008, *A&A*, 490, 777
- Lind, K., Primas, F., Charbonnel, C., Grundahl, F., Asplund, M. 2009, *A&A*, 503, 545
- Michaud, G., Fontaine, G. & Beaudet, G. 1984, *ApJ*, 282, 206
- Pasquini, L. & Molaro, P. 1996, *A&A*, 307, 761
- Pasquini, L., Bonifacio, P., Molaro, P., Francois, P., Spite, F., Gratton, R. G., Carretta, E., Wolff, B. 2005, *A&A*, 441, 549
- Piau, L., Beers, T. C., Balsara, D. S., Sivarani, T., Truran, J. W., Ferguson, J. W. 2006, *ApJ*, 653, 300
- Piotto, G., Bedin, L. R., Anderson, J., King, I. R., Cassisi, S., Milone, A. P., Villanova, S., Pietrinferni, A., Renzini, A. 2007, *ApJ*, 661, L53
- Richard, O., Michaud, G. & Richer, J. 2001, *ApJ*, 558, 377
- Spite, M. & Spite, F. 1982, *Nature*, 297, 483

Main-sequence and sub-giant stars in the globular cluster NGC 6397: The complex evolution of the lithium abundance

J. I. González Hernández^{1,2†}, P. Bonifacio^{1,2,3}, E. Caffau¹, M. Steffen⁴,
 H.-G. Ludwig^{1,2}, N. Behara^{1,2}, L. Sbordone^{1,2}, R. Cayrel¹, and
 S. Zaggia⁵

¹GEPI, Observatoire de Paris, CNRS, Université Paris Diderot;
 Place Jules Janssen 92190 Meudon, France
 email: Jonay.Gonzalez-Hernandez@obspm.fr

²Cosmological Impact of the First STars (CIFIST) Marie Curie Excellence Team

³Istituto Nazionale di Astrofisica - Osservatorio
 Astronomico di Trieste, Italy

⁴Astrophysikalisches Institut Potsdam, An der Sternwarte 16,
 D-14482 Potsdam, Germany

⁵INAF - Osservatorio Astronomico di Padova,
 Vicolo dell'Osservatorio 5, Padua 35122, Italy

Abstract.

Thanks to the high multiplex and efficiency of Giraffe at the VLT we have been able for the first time to observe the Li I doublet in the Main Sequence stars of a globular cluster. At the same time we observed Li in a sample of Sub-Giant stars of the same B-V colour.

Our final sample is composed of 84 SG stars and 79 MS stars. In spite of the fact that SG and MS span the same temperature range we find that the equivalent widths of the Li I doublet in SG stars are systematically larger than those in MS stars, suggesting a higher Li content among SG stars. This is confirmed by our quantitative analysis carried out making use of 1D hydrostatic plane-parallel models and 3D hydrodynamical simulations of the stellar atmospheres.

We derived the effective temperatures of stars in our the sample from H α fitting. Theoretical profiles were computed using 3D hydrodynamical simulations and 1D ATLAS models. Therefore, we are able to determined 1D and 3D-based effective temperatures. We then infer Li abundances taking into account non-local thermodynamical equilibrium effects when using both 1D and 3D models.

We find that SG stars have a mean Li abundance higher by 0.1 dex than MS stars. This result is obtained using both 1D and 3D models. We also detect a positive slope of Li abundance with effective temperature, the higher the temperature the higher the Li abundance, both for SG and MS stars, although the slope is slightly steeper for MS stars. These results provide an unambiguous evidence that the Li abundance changes with evolutionary status.

The physical mechanisms responsible for this behaviour are not yet clear, and none of the existing models seems to describe accurately these observations. Based on these conclusions, we believe that the cosmological lithium problem still remains an open question.

Keywords. Stars: abundances, fundamental parameters, Population II – Galaxy: globular clusters: individual: NGC 6397

† Present address: Dpto. de Astrofísica y Ciencias de la Atmósfera, Facultad de Física, Universidad Complutense de Madrid, E-28040 Madrid, Spain. Email: jonay@astrax.fis.ucm.es

1. Introduction

The determination of the baryonic density from the fluctuations of the cosmic microwave background (CMB) by the WMAP satellite (Spergel et al. 2007, Cyburt et al. 2008) implies a primordial Li abundance which is $\log(\text{Li}/\text{H}) + 12 = 2.72 \pm 0.06$, at least 0.3–0.5 dex higher than the Li abundance determined in metal-poor stars of the Galactic halo (Spite & Spite 1982).

Many different models of Li depletion have been proposed to explain discrepancy: (a) Piau et al.(2006) proposed that the first generation of stars, Population III stars, could have processed some fraction of the halo gas, lowering the lithium abundance; (b) other authors suggest that the primordial Li abundance has been uniformly depleted in the atmospheres of metal-poor dwarfs by some physical mechanism (e.g. turbulent diffusion as in Richard et al.(2005), Korn et al.(2006); gravitational waves as in Charbonnel & Talon(2005), etc.); and (c) finally, it has been also suggested that the standard Big Bang nucleosynthesis (SBBN) calculations should be revised, possibly with the introduction of new physics as in e.g. Jedamzik(2004), Jedamzik(2006), Jittoh et al.(2008), Hisano et al.(2009).

Here we present the determination of Li abundances of subgiant (SG) and main-sequence (MS) stars of the cluster NGC 6397. This work provides the first observations of the Li doublet in MS stars of a globular cluster.

2. Observations

We performed spectroscopic observations of the globular cluster NGC 6397 with the multi-object spectrograph FLAMES-GIRAFFE at the VLT on 2007 April, May, June and July, covering the spectral range $\lambda\lambda 6400\text{--}6800 \text{ \AA}$ at resolving power $\lambda/\delta\lambda \sim 17,000$.

We selected subgiant and dwarf stars in the colour range $B - V = 0.60 \pm 0.03$, which ensures that both set of stars fall in a similar and narrow effective temperature range (see Fig. 3 online in González Hernández et al. 2009a).

The spectra were reduced with the ESO pipeline and later on treated within MIDAS. We correct the spectra for sky lines and, barycentric and radial velocity. We typically combine 17 spectra of dwarfs and 4 spectra of subgiants to achieve a similar S/N ratio between 80 and 130 in both sets of stars. The mean radial velocity of the cluster stars is $v_r = 18.5 \text{ km s}^{-1}$.

3. Stellar parameters

We derived the effective temperature by fitting the observed $\text{H}\alpha$ line profiles with synthetic profiles, using 3D hydrodynamical model atmospheres computed with the CO⁵BOLD code. The details of this code are provided in Freytag et al.(2002) and Wedemeyer et al.(2004). The ability of 3D models to reproduce Balmer line profiles has been shown in Behara et al.(2009). In that work, the $\text{H}\alpha$ profiles of the Sun as well as the metal-poor stars HD 84937, HD 74000 and HD 140283 are studied. Ludwig et al.(2009) also quantified, from a purely theoretical point of view, the difference between the effective temperatures derived from $\text{H}\alpha$ fitting using 1D and 3D models.

We also derived the effective temperatures of MS and SG stars using 1D ATLAS 9 model atmospheres (see Kurucz 2005) and the same fitting procedure. In Fig. 1 we display the histograms of the effective temperatures derived for MS and SG stars using both 1D and 3D models. In the 1D case we got similar effective temperatures for both sets of stars. However, using 3D hydrodynamical models we obtained hotter temperatures by

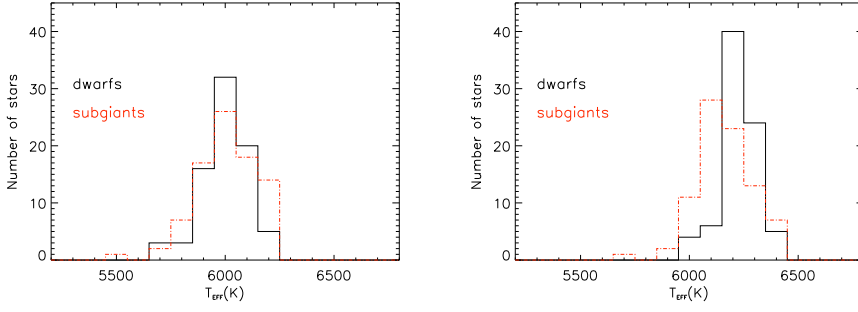


Figure 1. Histograms of 1D (left panel) and 3D (right panel) effective temperatures derived by fitting the observed $H\alpha$ profiles with theoretical profiles computed using 1D (left panel) and 3D (right panel) model atmospheres, in bins of 100 K, in MS (solid line) and SG (dashed-dotted line) stars in the globular cluster NGC 6397.

approximately 250 K in MS stars and 150 K for SG stars. In the 3D case the histogram of SG stars is slightly shifted with respect to the histogram of MS stars to cooler temperatures, as expected from the difference in surface gravity between MS and SG stars and the sensitivity of the $B - V$ colour to the surface gravity.

Fixed values for the surface gravity were adopted for both subgiant and dwarf stars in the sample, according to the values that best match the position of the stars on a 12 Gyr isochrone (Straniero et al. 1997). The adopted values were $\log(g/\text{cm s}^2) = 4.40$ and 3.85 for MS and SG stars, respectively.

4. Li abundances

We measure the equivalent width (EW) of the Li I 6708 Å line in SG and MS stars by fitting synthetic spectra of known EW to the observed Li profiles. González Hernández et al.(2009a) showed the histograms of the EWs measured in SG and MS stars of this cluster (see their Fig. 1). In that figure it is clearly seen that the EWs of SG stars are larger than those of MS stars. They also estimate the weighted mean EW of the SG stars, being ~ 1.1 pm larger than the weighted mean EW of MS stars. Although the colour $B - V$ is sensitive to surface gravity, a priori, this result was not expected, and clearly suggests that subgiants in this cluster have actually higher Li abundances than dwarfs.

We derived Li abundances using 3D model atmospheres. The line formation of Li was treated in non-local thermodynamical equilibrium (NLTE) using the same code and model atom used in Cayrel et al.(2007). The analysis was also done using 1D model atmospheres providing essentially the same picture, even when T_{eff} in 1D are lower (see also Fig. 6 online in González Hernández et al. 2009a). In the 1D case we used the Carlsson et al.(1994) NLTE corrections.

5. Discussion and conclusions

In Fig. 2 we display the histograms of the derived 1D-NLTE and 3D-NLTE Li abundances of dwarf and subgiant stars of the globular cluster NGC 6397. In both 1D and 3D cases, the SG stars have on average larger amounts of Li content in their atmospheres than MS stars. The difference in the mean Li abundance of dwarfs and subgiants is ~ 0.14 dex in the 1D case and ~ 0.07 dex in the 3D case. This difference between the 1D

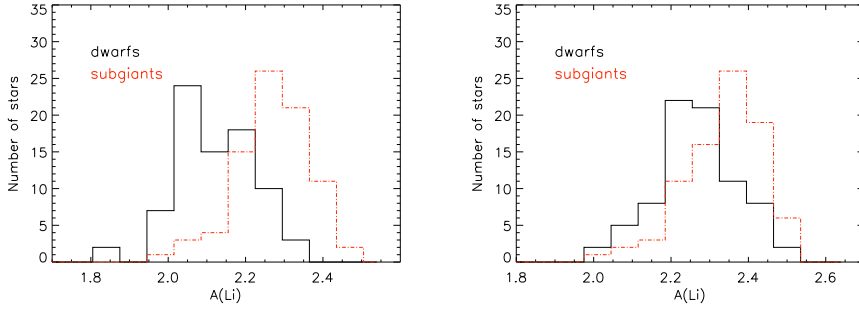


Figure 2. Histograms of 1D (left panel) and 3D (right panel) non-LTE Li abundances, in bins of 0.07 dex, in MS (solid line) and SG (dashed-dotted line) stars in the globular cluster NGC 6397

and the 3D cases is due to the effective temperatures derived using 1D and 3D models, and is not related to the NLTE corrections which were independently computed in the 1D and 3D cases. In fact, due to the cooler temperatures derived in 1D with respect to the 3D case, the mean 1D Li abundance lower by ~ 0.13 dex for the MS stars ~ 0.06 dex for the SG stars than the mean 3D abundance.

Lind et al.(2009) also find different mean Li abundances, using 1D models, in MSs and SGs, but only by 0.03 dex although still significant at 1σ . However, their result is partially affected by the very narrow range of T_{eff} for MSs deduced by Lind et al.(2009) (~ 80 K) compared to the wide range (~ 450 K) for the SGs (see Fig. 7 online in González Hernández et al. 2009a).

González Hernández et al.(2009a) showed, in their Fig. 2, the 3D-NLTE abundances of SG and MS stars versus 3D effective temperatures (see Fig. 1 in González Hernández et al.(2009b) for a similar picture but with T_{eff} and Li abundances computed using 1D models). The points in that figure display a decreasing trend of Li abundance with decreasing temperature. This lithium abundance pattern is different from what is found among field stars (see e.g. Meléndez & Ramírez 2004, Bonifacio et al. 2007, González Hernández et al. 2008).

Our results imply that the Li surface abundance depends on the evolutionary status of the star. In Fig. 2 of González Hernández et al.(2009a), the Li isochrones are shown for different turbulent diffusion models (Richard et al. 2005). These models were shifted up by 0.14 dex in Li abundance to make the initial abundance of the models, $\log(\text{Li}/\text{H}) = 2.58$, coincide with the primordial Li abundance predicted from fluctuations of the microwave background measured by the WMAP satellite (Cyburt et al. 2008). The models assuming pure atomic diffusion, and, among those including low levels of turbulent mixing, in particular the model T6.0, preferred model in Korn et al.(2006) and Lind et al.(2009) are ruled out by our observations, since they predict the Li content in MS stars to be higher than in SG stars. The only model that predicts a Li pattern which is qualitatively similar to that observed, is the T6.25 model. This model shows a decreasing trend of Li abundances with decreasing temperatures and also predicts higher abundances for SG stars than for MS stars although at temperatures lower than 6000 K, which is not consistent with the observed trend even in the 1D case (see Fig. 1 in González Hernández et al. 2009b).

Models including atomic diffusion and tachocline mixing (Piau 2008) do not seem to reproduce our observations either, since they provide a constant Li abundance up to

5500 K. More sophisticated models are required, for instance, those models that besides including diffusion and rotation also take into account the effect of internal gravity waves (Talon & Charbonnel 2004), seem to predict accurately the Li abundance pattern in solar-type stars, at solar metallicity (Charbonnel & Talon 2005), but models at low metallicity are still needed.

The cosmological lithium discrepancy still needs to be solved. Given that none of the existing models of Li evolution in stellar atmospheres matches our observations in the globular cluster NGC 6397, we hope our results will prompt further new theoretical investigations.

References

- Behara, N. T., Ludwig, H.-G., Steffen, M., & Bonifacio, P. 2009, *American Institute of Physics Conference Series*, 1094, 784
- Bonifacio, P., Molaro, P., Sivarani, T., Cayrel, R., Spite, M. 2007, *A&A*, 462, 851
- Carlsson, M., Rutten, R. J., Bruls, J. H. M. J., & Shchukina, N. G. 1994, *A&A*, 288, 860
- Cayrel, R., Steffen, M., Chand, H., Bonifacio, P., Spite, M., Spite, F., Petitjean, P., Ludwig, H.-G., Caffau, E. 2007, *A&A (Letters)*, 473, 37
- Charbonnel, C., & Talon, S. 2005, *Science*, 309, 2189
- Cyburt, R. H., Fields, B. D., & Olive, K. A. 2008, *Journal of Cosmology and Astro-Particle Physics*, 11, 12
- Freytag, B., Steffen, M., & Dorch, B. 2002, *Astronomische Nachrichten*, 323, 213
- González Hernández, J. I., et al. 2008, *A&A*, 480, 233
- González Hernández, J. I., Bonifacio, P., Caffau, E., Steffen, M., Ludwig, H.-G., Behara, N.T., Sbordone, L., Cayrel, R., Zaggia, S. 2009a, *A&A (Letters)*, 505, L13
- González Hernández, J. I., et al. 2009b, *Star Clusters: Basic Galactic Building Blocks Throughout Time And Space*. Edited by R. de Grijs and J. Lepine. Proceedings of IAU Symposium #266, held 10-14 August, 2009 in Brazil, Rio de Janeiro. Cambridge, UK: *Cambridge University Press*, in press
- Hisano, J., Kawasaki, M., Kohri, K., & Nakayama, K. 2009, *Phys. Rev. D*, 79, 063514
- Jedamzik, K. 2004, *Phys. Rev. D*, 70, 083510
- Jedamzik, K. 2006, *Phys. Rev. D*, 74, 103509
- Jittoh, T., Kohri, K., Koike, M., Sato, J., Shimomura, T., & Yamanaka, M. 2008, *Phys. Rev. D*, 78, 055007
- Kurucz, R. L. 2005, *Memorie della Società Astronomica Italiana Supplement*, 8, 14
- Korn, A. J., Grundahl, F., Richard, O., Barklem, P. S., Mashonkina, L., Collet, R., Piskunov, N., & Gustafsson, B. 2006, *Nature*, 442, 657
- Lind, K., Primas, F., Charbonnel, C., Grundahl, F., & Asplund, M. 2009, *A&A*, 503, 545
- Ludwig, H.-G., Behara, N. T., Steffen, M., & Bonifacio, P. 2009, *A&A (Letters)*, 502, 1
- Meléndez, J., & Ramírez, I. 2004, *ApJ (Letters)*, 615, 33
- Piau, L., Beers, T. C., Balsara, D. S., Sivarani, T., Truran, J. W., & Ferguson, J. W. 2006, *ApJ*, 653, 300
- Piau, L. 2008, *ApJ*, 689, 1279
- Richard, O., Michaud, G., & Richer, J. 2005, *ApJ*, 619, 538
- Spergel, D. N., Bean, R. Doré, O., Nolte, M.R., Bennett, C.L., et al. 2007 *ApJS*, 170, 377
- Spite, M. & Spite, F. 1982, *Nature*, 297, 483
- Straniero, O., Chieffi, A., & Limongi, M. 1997, *ApJ*, 490, 425
- Talon, S., & Charbonnel, C. 2004, *A&A*, 418, 1051
- Wedemeyer, S., Freytag, B., Steffen, M., Ludwig, H.-G., & Holweger, H. 2004, *A&A*, 414, 1121



Monique Spite & Katia Cunha



Corinne Charbonnel & Francesca Primas

Observational signatures of lithium depletion in the metal-poor globular cluster NGC6397

Karin Lind¹, Francesca Primas¹, Corinne Charbonnel^{2,3},
Frank Grundahl⁴, and Martin Asplund⁵

¹European Southern Observatory, Karl-Schwarzschild-Strasse 2, 857 48 Garching bei München, Germany

email: klind@eso.org

²Geneva Observatory, 51 chemin des Maillettes, 1290 Versoix, Switzerland

³Laboratoire d'Astrophysique de Toulouse-Tarbes, CNRS UMR 5572, Université de Toulouse, 14, Av. E. Belin, F-31400 Toulouse, France

⁴Department of Physics & Astronomy, Aarhus University, Ny Munkegade, 8000 Aarhus C, Denmark

⁵Max-Planck-Institut für Astrophysik, Karl-Schwarzschild-Strasse 1, 857 41 Garching bei München, Germany

Abstract. The “stellar” solution to the cosmological lithium problem proposes that surface depletion of lithium in low-mass, metal-poor stars can reconcile the lower abundances found for Galactic halo stars with the primordial prediction. Globular clusters are ideal environments for studies of the surface evolution of lithium, with large number statistics possible to obtain for main sequence stars as well as giants. We discuss the Li abundances measured for >450 stars in the globular cluster NGC 6397, focusing on the evidence for lithium depletion and especially highlighting how the inferred abundances and interpretations are affected by early cluster self-enrichment and systematic uncertainties in the effective temperature determination.

Keywords. stars: abundances, atmospheres, evolution, globular clusters: individual (NGC 6397)

1. Introduction

Through the detailed mapping of the cosmic microwave background performed by the *Wilkinson Microwave Anisotropy Probe* (WMAP), a high-precision estimate of the baryon density of the Universe is nowadays possible. When the most up-to-date prediction, $\Omega_b h^2 = 0.02273 \pm 0.00062$ (Dunkley et al. 2009) is entered in standard Big Bang nucleosynthesis (SBBN), the primordial abundance ratios of D, ³He, ⁴He, and ⁷Li with respect to H, are tightly constrained. Cyburt et al. (2008) thus determine a primordial lithium abundance of $N(^7\text{Li})/N(\text{H}) = 5.24^{+0.71}_{-0.67} \times 10^{-10}$ or $A(\text{Li}) = 2.72 \pm 0.06^\dagger$, which can be directly compared to the Li abundances inferred for old, metal-poor Galactic halo stars. Numerous high-resolution studies of Li in these stars have indeed revealed a close-to-constant abundance over a wide range in metallicities (forming the “Spite plateau”, originally found by Spite & Spite 1982). However, the observationally inferred values are typically a factor of 3–5 lower than the primordial prediction. Assuming that both the WMAP+SBBN value and the Spite plateau abundances are correct, this implies that the Population II (Pop II) stars residing in the halo have undergone significant surface depletion of lithium during their life time.

$$^\dagger A(\text{Li}) = \log \left(\frac{N(\text{Li})}{N(\text{H})} \right) + 12$$

That lithium depletion occurs in solar-type main sequence stars is well-known, e.g. since the solar photospheric value is at least two orders of magnitudes lower than what is found in meteorites. Also in Pop I stars that are somewhat hotter than the Sun, characteristic depletion signatures like the famous ‘Li dip’ are seen in open clusters (first identified in the Hyades by Wallerstein et al. 1965). If indeed lithium depletion takes place also in Pop II stars, the process has left little traces behind, since the Spite Plateau is very homogeneous over a wide range in metallicities and effective temperatures, and shows small star-to-star variation. Richard et al. (2005) illustrated clearly how atomic diffusion (gravitational settling) of lithium can qualitatively account for the surface drainage, but needs to be moderated by a mixing process below the outer convective envelope to avoid too much Li depletion in stars lying on the hot end of the Spite Plateau. In a series of papers (Talon & Charbonnel 1998, 2003, 2004), it has been demonstrated that rotation-induced mixing is a plausible source of lithium destruction in both Pop I and II stars, given that the rotation of stars cooler than ~ 6300 K also is efficiently stabilised by gravity waves. This stabilising effect is necessary to avoid a strong dependence of the lithium depletion on the initial angular momentum of the stars, which would result in a non-negligible scatter.

A next generation of stellar evolution models, accounting self-consistently for atomic diffusion, shear turbulence, and meridional circulation, should be confronted with the detailed lithium abundance patterns found for metal-poor stars. Of fundamental importance for constraining the models are Li abundance trends with effective temperature (which for main sequence stars also is indicative of the stellar mass), with metallicity (which constrains the contribution of post-primordial Li), and with evolutionary phase from the main sequence to the very end of the giant stages of evolution. In Lind et al. (2009b) we used FLAMES on VLT/UT2 to investigate the lithium abundances of a very large number of stars in a metal-poor globular cluster (NGC 6397, $[\text{Fe}/\text{H}] = -2.0$), with the primary goals to establish in detail how the abundances depend on evolutionary phase and investigate if there is any significant scatter in abundance for stars in the same phase. In the following we outline our main findings, with focus on the implications and robustness of the observed abundance trends.

Fig. 1 shows how the mean lithium abundance varies with stellar luminosity in NGC 6397, from the dwarfs on the main sequence, over the turn-off point, and on the subgiant branch. This figure highlights the need for smooth turbulence, since the pure diffusive models show large gradients that disagree with the observations (models provided by O. Richard, *priv. comm*). On the other hand, a non-diffusive model is completely flat, which also is a poor match to the observed trend. A moderate degree of turbulence preserves the flat behaviour on the main sequence, while at least qualitatively reproducing the small upturn located prior to the point of strong depletion, although the location of maximum lithium abundance is not matched. However, the predicted level of depletion is only ~ 0.2 dex, which is not enough to reconcile the initial abundance with the cosmological prediction.

2. Li deficient un-evolved stars

Stars in globular clusters are known to show a larger spread in light elements (up to Al) than their counterparts in the halo field. This extra spread is believed to be a result of cluster self-enrichment of the rest products of high-temperature hydrogen burning from an early generation of more massive stars, made possible by the dense intra-cluster environment. Especially N, Na, and Al abundances are enhanced in the most polluted stars,

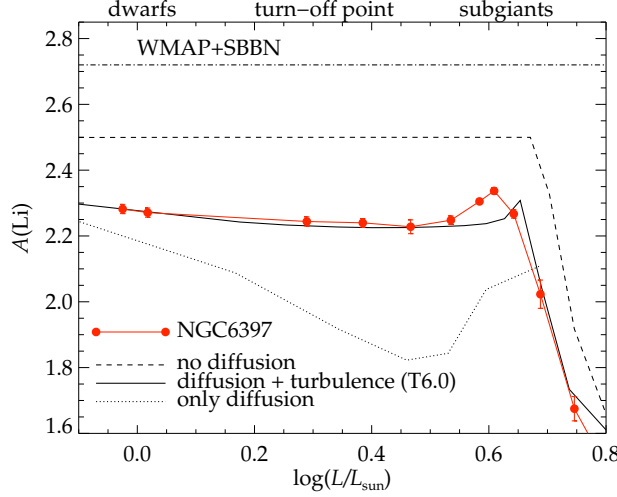


Figure 1. The red bullets represent bin-averaged non-LTE, lithium abundances against stellar luminosity in NGC 6397 (Lind et al. 2009a, 2009b). The dashed line shows the prediction from a model without atomic diffusion (Richard et al. 2005), the dotted line corresponds to a model with only diffusion, and the solid line a model with diffusion moderated by turbulence. The initial abundances of the models are shifted by -0.08 dex to $A(\text{Li}) = 2.50$. The top line shows the prediction from WMAP+SBBN ($A(\text{Li}) = 2.72$, Cyburt et al. 2008). The difference of 0.22 dex in Li abundance is still unaccounted for.

whereas O and Mg levels are depleted. Further, since the stellar ejecta that polluted the cluster gas are presumably void of Li (see e.g. Decressin et al. 2007), the Li abundances are theoretically expected to be lower in more polluted stars. Observational evidence of a Li-Na anti-correlation in the globular cluster NGC 6752 (Pasquini et al. 2005) supports this view.

In NGC 6397 we measured for the first time the Li and Na abundances for a large number (> 100) of turn-off stars and subgiants in a globular cluster. We found indeed, that a handful of rare lithium-deficient stars ($A(\text{Li}) < 2.0$) also are most strongly enhanced in sodium. However, we also realised that a high degree of pollution is actually necessary to significantly affect the lithium abundances, and that the mean Li abundance trends are essentially unbiased by self-enrichment in NGC 6397. We caution however, that this cannot be generalised to other globular clusters, which may have undergone more dramatic enrichment. Lithium abundances in globular clusters should thus preferably be studied in parallel with other light elements.

Limiting the sample to stars with $A(\text{Na}) < 3.9$, having suffered a low degree of pollution, we found that the spread in lithium abundance is very low (0.09 dex), in accordance with what may be expected from observational uncertainty (see Lind et al. 2009b). We therefore expect the real star-to-star scatter in Li abundance in the first generation of cluster stars to be minimal (below 0.05 dex).

Note that both lithium and sodium abundances of metal-poor turn-off stars are sensitive to effective temperature, with ± 100 K corresponding to ± 0.07 dex in Li abundance and ± 0.04 dex in Na abundance. Uncertainties in effective temperature therefore tend to correlate, rather than anti-correlate the abundances. The pollution signature we have identified in NGC 6397 is thus robust in this respect.

3. Li depletion below and above the main sequence turn-off

3.1. Subgiants vs turn-off stars

In canonical models of stellar evolution, assuming convection to be the only mean of particle transport, the surface lithium abundance is constant during the whole main sequence life time, and not until the star has climbed part of the subgiant branch and its convective envelope has expanded to reach Li free layers in the stellar interior, strong surface dilution sets in (the beginning of the “first dredge up”). This view has been challenged, first by Charbonnel & Primas (2005) who detected a difference in lithium abundance between subgiant and less evolved stars in the halo field. That subgiant stars are more Li-rich than turn-off stars also in globular clusters was first discovered by Korn et al. (2007), for stars in NGC 6397. In Lind et al. (2009b) we used unprecedented number statistics to demonstrate the presence of a gradually increasing trend of Li from the turn-off point to the middle of the subgiant branch, which is there interrupted by the onset of the first dredge-up. These results may indicate that the stars that are subgiants today underwent less efficient Li depletion during their time on the main sequence than the slightly less massive stars now sitting at the turn-off point. An alternative scenario would be that the gravitational settling of Li formed a small over-abundance below the convective envelope which is dredged-up in the subgiants by the penetration of the convective envelope.

We found that the subgiants are at most 0.1 dex more Li-rich than the turn-off stars, an estimate which is not suffering from any significant statistical uncertainty, due to the large number of objects (> 200 subgiants and turn-off stars). However, as is always the case with lithium abundance determination, the systematic uncertainties stemming primarily from the effective temperature determination, are dominant. Since errors in effective temperature and lithium abundance are positively correlated, uncertainties in effective temperatures tend to create artificial trends of higher abundance for stars with higher effective temperature and vice versa. Lithium trends with effective temperature should thus be viewed with great caution. In particular, the true range in T_{eff} over which a change in abundance is discussed must be considerably larger than the uncertainty in relative effective temperature determination.

In Lind et al. (2009b) we relied on Strömgren photometry to infer effective temperatures, and based the final scale on the temperature sensitive $b - y$ index, translated to effective temperatures using synthetic colours computed from MARCS model atmospheres (Gustafsson et al. 2008, Önehag et al. 2009). To suppress artificial spread in stellar parameters, caused mainly by photometric uncertainty, we adopted bin-averaged colour-magnitude sequences, constructed from the full photometric catalogue of ~ 5000 stars. The mean locus of the main sequence turn-off point was thus determined to be 6428 K ($(b - y)_0 = 0.303$). In comparison, the new infra-red flux method (IRFM) calibration for dwarfs and subgiants of Casagrande et al. (2010), predicts a turn-off point effective temperature of 6435 K, based on $b - y$. Furthermore, broadband BVI photometry give very similar temperatures when adopting the IRFM calibrations: 6422 K based on $(B - V)_0 = 0.386$, and 6447 K based on $(V - I)_0 = 0.555$. The photometric evidence thus gives a very consistent view, especially when bearing in mind the different sensitivity to reddening of the colour indices, with $b - y$ the least affected, and $V - I$ the most.

The Li abundance difference between subgiants and turn-off stars depends primarily on the temperature difference between the stars. Measuring from the mean locus of the turn-off point ($M_V = 4.07$) to the point where the Li abundance reaches its maximum ($M_V = 3.4$), the different photometric indices and calibrations listed above predict $\Delta T_{\text{eff}} = 312 \pm 40$ K (mean standard deviation). Taking 40 K to be an estimate of the

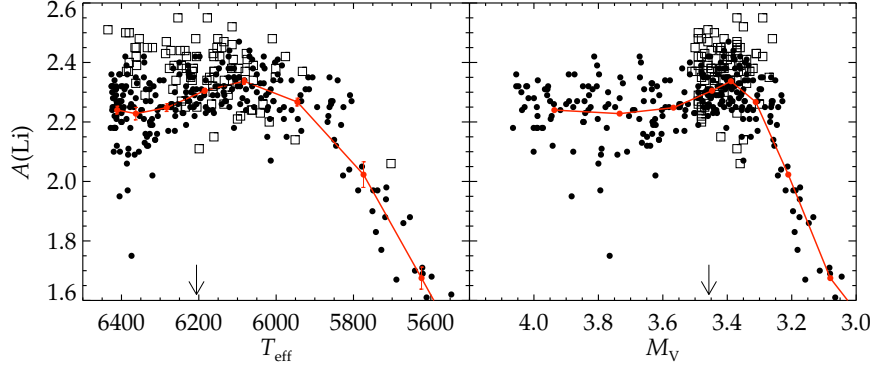


Figure 2. The left hand panel shows lithium abundances vs effective temperature for the post turn-off stars of Lind et al. (2009b, black bullets) and Gonzalez-Hernandez et al. (2009, open squares). In the right hand panel the same abundances are shown vs visual magnitude. The red, bullets connected with a solid line represent the bin-averaged abundances of Lind et al. The turn-off point is located at $M_V \approx 4.07$.

uncertainty, the 0.1 dex difference in $A(\text{Li})$ between turn-off stars and subgiants is significant at the 3σ level.

Spectroscopic effective temperatures have been determined by $\text{H}\alpha$ profile fitting for stars around the turn-off point in NGC 6397 in other studies, with resulting scales that are typically ~ 80 K cooler than our photometric scale (Korn et al. 2007), and ~ 80 K hotter (Gonzalez-Hernandez et al. 2009). The systematic offsets originate in differences in the adopted model atmosphere and likely also in the quality of the spectroscopic observations. It is important to stress that the study by Gonzalez-Hernandez et al. only covered stars above and below but not actually at the turn-off point. The negative slope of $A(\text{Li})$ with decreasing T_{eff} inferred in that study for subgiant branch stars is thus not contradicting the positive increase we identified from the turn-off to the middle of the subgiants branch, contrary to what is claimed by the authors. This is displayed in Fig 2, where the left hand panel shows lithium abundance against effective temperature for post turn-off stars in Lind et al. and Gonzalez Hernandez et al., and the right hand panel shows the same abundances, but with absolute visual magnitude as reference scale. The discrepancies seen in the left panel can partly be explained by the fact that their temperature scale is somewhat hotter. Note that the visual magnitudes listed by Gonzalez Hernandez et al. have been adjusted to agree with our absolute scale as described in Lind et al. (2009b).

3.2. Hot vs cool dwarf stars

In Pop I dwarfs of a certain age, very lithium-deficient stars are found in the range $T_{\text{eff}} = 6400 - 6800$ K, with a gradual increase on the hot as well as the cool end, shaping the so called Li dip. Talon & Charbonnel (2004, see also references therein) describe how the shape and location of the dip can be explained when simultaneously accounting for how the efficiencies of convection, rotational-induced mixing, and gravity waves change

with effective temperature. On the cool side of the dip, gravity waves dominate the transport of angular momentum, which reduces the differential rotation that otherwise would give rise to large lithium destruction. In Pop II stars, an analogous dip is theoretically predicted at the same location, but it has not been detected observationally, because the metal-poor stars that had such hot temperatures on the main sequence have evolved to the giant phases. However, if the hottest metal-poor turn-off stars that exist today (6400-6500 K) show a lower Li abundance than cooler dwarfs, this would indicate the presence of the dip also in Pop II stars.

In Lind et al. (2009b) we indeed found a 0.04 dex deficiency in lithium abundance for the hottest dwarfs just below the turn-off at 6430 K, compared to main sequence stars in the range 6100-6200 K. However, we cautioned that this difference is very small, and sensitive to errors in the effective temperature scale. In fact, using either of the broad-band indices $B - V$ or $V - I$ to determine effective temperatures enhances the temperature span between the groups enough to erase the difference. The main sequence stars in our sample are thus consistent with having the same lithium abundance.

4. Concluding remarks

Stellar lithium depletion remains a promising solution to the cosmological lithium problem, but there are several open issues. Non-standard mixing below the convective envelope is obviously of key importance for the surface evolution of lithium in Pop II stars. Progress on the modelling side as well as the observational side are needed to establish the underlying physical mechanisms and its correct temperature and metallicity dependence. From the point of view of inferring accurate Li abundances in stars, the effective temperature issue is the most crucial to settle, with the development of hydrodynamical model atmospheres for metal-poor stars being an important step in the right direction.

References

- Casagrande, L., Ramírez I., Meléndez, J., Bessel, M. & Asplund, M. 2010, *A&A*, *e-print*: <http://arxiv.org/abs/1001.3142>
- Charbonnel, C. & Primas, F. 2005, *A&A*, 442, 961
- Cyburt, R. H., Fields, B. D., & Olive, K. A. 2008, *JCAP*, 11, 12
- Decressin, T., Charbonnel, C. & Meynet, G. 2007, *A&A*, 475, 859
- Dunkley, J., Komatsu, E., Nolte, M. R., et al. 2009, *ApJs*, 180, 306
- González Hernández, J. I., Bonifacio, P., Caffau, E. et al. 2009, *A&A*, 505, 13
- Gustafsson, B., Edvardsson, B., Eriksson, K., et al. 2008, *A&A*, 486, 951
- Korn, A. J., Grundahl, F., Richard, O., et al. 2007, *ApJ*, 671, 402
- Lind, K., Asplund, M. & Barklem P. S. 2009a, *A&A*, 503, 545
- Lind, K., Primas, F., Charbonnel, C., Grundahl, F. & Asplund, M. 2009b, *A&A*, 503, 545
- Önehag, A., Gustafsson, B., Eriksson, K., & Edvardsson, B. 2009, *A&A*, 498, 527
- Pasquini, L., Bonifacio, P., Molaro, P., et al. 2005, *A&A*, 441, 549
- Richard, O., Michaud, G., & Richer, J. 2005, *ApJ*, 619, 538
- Spite, M. & Spite, F. 1982, *Nature*, 297, 483
- Talon, S. & Charbonnel, C. 1998, *A&A*, 335, 959
- Talon, S. & Charbonnel, C. 2003, *A&A*, 405, 1025
- Talon, S. & Charbonnel, C. 2004, *A&A*, 418, 1051
- Wallerstein, G., Herbig, G. H. & Conti, P. S. 1965, *ApJ*, 141, 610

Lithium in a metal-poor external galaxy: ω Centauri

P. Bonifacio^{1,2}, L. Monaco^{3,4}, L. Sbordone⁵, S. Villanova³, and
E. Pancino⁶

¹GEPI, Observatoire de Paris, CNRS, Université Paris Diderot;
Place Jules Janssen, 92190 Meudon, France
email: Piercarlo.Bonifacio@obspm.fr

²Istituto Nazionale di Astrofisica, Osservatorio Astronomico di Trieste,
Via Tiepolo 11, I-34143 Trieste, Italy

³Universidad de Concepción, Casilla 160-C, Concepción, Chile

⁴European Southern Observatory, Casilla 19001, Santiago, Chile

⁵Max Planck Institut for Astrophysics Karl-Schwarzschild-Str. 1 85741 Garching, Germany

⁶Istituto Nazionale di Astrofisica, Osservatorio Astronomico di Bologna,
Via Ranzani 1, 40127, Bologna, Italy

Abstract. ω Centauri is a massive stellar system which is currently going through the Galactic Halo. Its compact aspect and spheroidal shape have for a long time led to it being classified as a Globular Cluster. However the fact that its stars cover a wide metallicity range ($-0.6 < [\text{Fe}/\text{H}] < -2.1$), points to this object as an external galaxy, satellite of the Milky Way. Lithium among warm metal-poor stars shows a roughly constant abundance, the “Spite Plateau”. This has been interpreted as evidence for a primordial origin of the lithium nucleus, at the time of nucleosynthesis. After the physical conditions under which nucleosynthesis occurred, have been constrained by the observations of the fluctuations of the Cosmic Microwave Background, we are facing a “cosmological lithium problem”, namely the primordial lithium was a factor of three to four higher than what observed in the Spite plateau. Several avenues may be taken to solve this conundrum, either relying on fundamental physics or on stellar physics, however the realm of possibilities may be considerably narrowed by observing stellar populations in different galaxies, which have experienced different evolutionary histories. Some of the proposed “solutions” may be clearly ruled out, depending on the observation of lithium in the metal-poor populations of external galaxies. ω Centauri is the only external galaxy amenable to such an investigation in the era of 8m telescopes. We have pushed to its limits FLAMES at the ESO 8.2m telescope to obtain high resolution spectra of the Li I doublet in 91 Turn-Off and Sub-Giant stars at $V \sim 18$ in ω Centauri. We present our preliminary results on this data which suggest that the Li content in ω Centauri warm stars is comparable to that observed in Galactic Halo field stars of similar metallicities and temperatures. This may effectively rule out a whole class of models which invoke a severe Li depletion through processing of material in an early generation of massive stars.

Keywords. Nuclear reactions, nucleosynthesis, abundances – stars: abundances, Population II – Galaxy: globular clusters: individual (ω Cen) – galaxies: abundances, Local Group – cosmology: observations

1. Introduction

The Spite plateau is the constant Li abundance, observed in warm metal-poor stars of different effective temperature and metallicity. This remarkable feature in the abundance pattern of metal-poor stars was discovered by Monique and François Spite in 1982

(1982a,1982b) and was immediately interpreted as a signature of Big Bang Nucleosynthesis (BBN) and a mean to measure the baryonic density of the Universe. See the review of Spite & Spite (2010) on lithium and that of Steigman (2010) on nucleosynthesis in this volume, for an updated view of the problem. The most striking development came from the accurate measurement of the baryonic density from the WMAP satellite (Dunkley et al. 2009) which, coupled with standard BBN, implied a primordial Li abundance a factor of three to five higher than the Spite plateau. This discrepancy is often referred to as the “cosmological lithium problem”.

Many solutions for this discrepancy have been proposed, including new physics at the time of the Big Bang (see for example Jedamzik 2004, 2006, Jittoh et al. 2008, Hisano et al. 2009), astration in the pristine Galaxy (Piau et al. 2006) and turbulent diffusion to deplete lithium in the stellar atmospheres (Richard et al. 2005). A fresh look at the problem can be afforded by the study of lithium in metal-poor populations of external galaxies. Theories like that of Piau et al. (2006) can be immediately tested and also theories which invoke stellar phenomena can be seriously constrained by the observation of stellar populations with different star formation histories. Unfortunately even nearby galaxies, like the Magellanic Clouds or the Sagittarius dwarf spheroidal are too far to allow such a study with existing telescopes, although they will be within the reach of the next generation of 40m class telescopes.

There is, however, one external galaxy which is, just about, within reach of our telescopes: ω Cen. The complexity of its colour magnitude diagram clearly testifies the existence of multiple stellar populations with a range of metallicities. It is currently generally accepted that ω Cen is not a globular cluster, but a satellite galaxy of the Milky Way. It is more massive than all other globular clusters (about $2.5 \times 10^5 M_{\odot}$, Van de Ven et al. 2006), but was probably more massive in the past and has lost mass due to tidal interaction with the Galaxy. In a galaxy which has such a different mass and history with respect to the Milky Way, one should expect a very different lithium content of the metal-poor populations, if the “cosmological lithium problem” is due to astration by an early population. Also in the case of stellar phenomena, such as diffusion, one may expect different lithium content, if the stars show a consistent age spread. Finally we might be able to capture the results of Li production by super-AGB stars, with $A(\text{Li})$ up to 4 (Ventura & D’Antona 2010, D’Antona & Ventura 2010).

2. Observations

We have selected targets on the turn-off and sub-giant branch of ω Cen, mainly from the high precision FORS/VLT photometry of Sollima et al. (2005) and from the spectroscopic survey of Villanova et al. (2007). Ten targets were selected to trace the faint subgiant branch, called SGB-a in Sollima et al. (2005). Our targets are shown in Fig. 1, where we have used the wide field photometry of Bellini et al. (2009).

The targets were observed on three nights from April 27th to 29th 2007 at ESO Paranal with FLAMES at the Kueyen 8.2m telescope. The fibres in Medusa mode fed the GIRAFFE spectrograph, configured in the HR15n setting, which covers both $H\alpha$ and the LiI resonance doublet at 670.8nm at a resolution of 17000. The same plate configuration was observed for all the three nights, with integration times between one hour and slightly over two hours. Both plates were used alternatively and configured in such a way as to minimise the light loss due to atmospheric refraction. One further plate configuration was observed, with a partial overlap with the main plate configuration. We thus obtained a total integration time between 17 and 19 hours for 91 stars on the MS/SGB

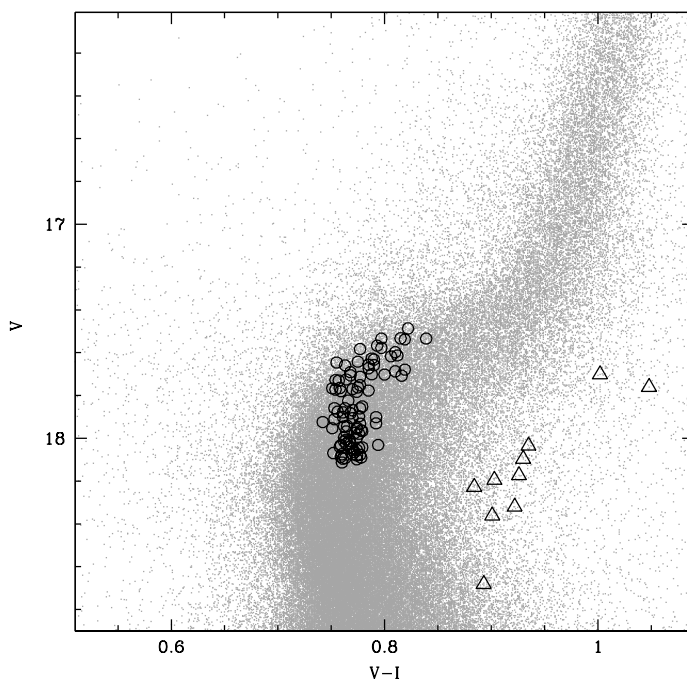


Figure 1. Colour-magnitude diagram of ω Cen from the WFI/2.2m photometry of Bellini et al. (2009). Our targets are shown as open circles, except for the targets on the SGB-a of Sollima et al. (2005), which are shown as open triangles.

and 10 stars on the SGB-a. After data reduction the spectra achieved S/N ratios in the range 30 to 90 with a mean around 60.

3. Analysis

Our analysis is based on one dimensional model atmospheres computed with version 9 of the ATLAS code (Kurucz 2005) in its Linux version (Sbordone 2005, Sbordone et al. 2004). The effective temperature of the stars has been determined by fitting the wings of $H\alpha$. The theoretical profiles were computed with a modified version of the BALMER code [†] which uses the Barklem et al. (2000a,b) self broadening theory and Stehlé & King (1999) Stark broadening. At this stage we assumed $\log g = 4.0$ and a metallicity of -1.5 for all stars, thus ignoring the dependence of the Balmer line profiles on metallicity and surface gravity. The equivalent widths of the Li I resonance doublet were measured by fitting synthetic profiles, as done in Bonifacio et al. (2002). When we could not detect the Li line we estimated an upper limit as $2\sigma_{EW}$, where σ_{EW} was estimated from the Cayrel formula (Cayrel 1988). A model atmosphere with the appropriate effective temperature, $\log g = 4.0$ and metallicity -1.5 was computed for each star and synthetic profiles were iteratively computed with SYNTH until the equivalent width of the Li doublet matched

[†] The original version of R.L. Kurucz is available at <http://kurucz.harvard.edu/>

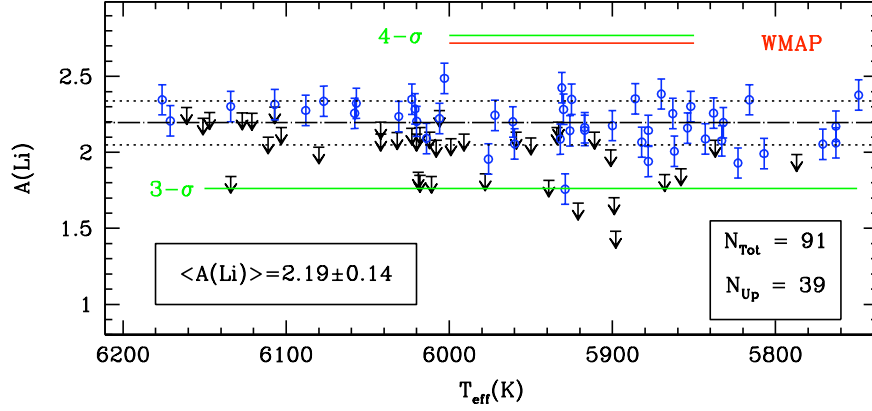


Figure 2. Li abundances in sub-giant and turn-off stars of ω Cen as a function of effective temperature.

the measured equivalent width. A microturbulent velocity of 1 km s^{-1} was assumed, this, like the assumed surface gravity and metallicity, have effects of a few hundredths of dex on the derived Li abundance, this is totally negligible in the current context. Our S/N ratios are high enough that the error on Li abundances is totally dominated by the uncertainty in effective temperatures. The latter is of the order of 150 K and is dominated by the uncertainty in the correction of the blaze function of GIRAFFE. Our estimated total uncertainty on the Li abundance is 0.1 dex.

4. Results

For none of the stars of the SGB-a did we detect the Li doublet. For the other stars our results are summarised in Fig. 2, out of a total of 91 MS/SGB stars for 39 we could not detect any lithium. For the stars with measured Li the abundance appears to be uniform without any trend with effective temperature, the mean value is $A(\text{Li})=2.19$ with a dispersion of 0.14 dex. We verified that if we use effective temperatures based on the V-I colour the mean Li abundance is similar (2.21) and the dispersion is a little smaller (0.11).

The spectral region covered by our observations is not rich of metallic lines, nevertheless we used the Fe I and Ca I to derive the metallicity of the stars, assuming $[\text{Ca}/\text{Fe}]=+0.4$. For the stars in common we get a rather good agreement with the results of Villanova et al. (2007) although we note a small offset of the order of 0.1 dex. Although this is, perhaps, not surprising, given the different spectral range, resolution, model atmospheres and spectrum synthesis codes used, we consider these metallicities yet preliminary and we plan to further investigate these differences in the future. However, even with these preliminary metallicities it is clear that there are no obvious trends of Li abundance with metallicity. Also for the upper limits, there does not appear to be present any clustering of upper limits at a particular range of metallicities.

5. Discussion

It appears that the stars of ω Cen lie on the Spite plateau. Comparison with the Galactic field stars, on the same effective temperature scale (see Sbordone et al. 2010) shows that the stars of ω Cen occupy the same zone of the Galactic stars, both in the $A(\text{Li})$ – T_{eff} and in the $A(\text{Li})$ –metallicity planes. This brings us to two robust conclusions:

- the Spite plateau exists also in other galaxies;
- the mechanism(s) which cause the “cosmological lithium problem” are the same in the Milky Way and in other galaxies.

Although this has only been established for ω Cen, it is simpler to assume that this is true for all galaxies than to assume that all galaxies behave differently and that only ω Cen behaves like the Milky Way. Until Li is measured in further external galaxies, this is an acceptable working hypothesis.

These facts immediately tell us that explanations of the “cosmological lithium problem” which require a special evolution for the Milky Way Halo are immediately ruled out. This is the case of the model by Piau et al. (2006), which requires that from one third to one half of the Galactic Halo ($\sim 10^9 M_{\odot}$) has been processed through massive stars which effectively depleted lithium from the primordial value to the current observed Spite plateau. It would be extremely contrived to assume that another galaxy, of current mass $2.5 \times 10^6 M_{\odot}$, thus of very different type and evolution from the Milky Way, has undergone a similar process with a fine tuning of the mass fraction processed through massive stars so that the Spite plateau results identical to that of the Milky Way. Occam’s razor requires that this theory be discarded.

Among other solutions of the “cosmological lithium problem” all which invoke stellar atmospheric phenomena, such as diffusion might also be tightly constrained by our observations. All such phenomena are time dependent and they may produce a uniform Spite plateau in the Galactic Halo, only because the age-spread in the Halo is very small. So the question is: what is the age spread among the stars observed by us in ω Cen? For the stars in common with Villanova et al. (2007) we may use their age estimates, based on theoretical isochrones, their metallicity estimates and the requirement that, in the colour-magnitude diagram, each sub-giant branch be associated to a Main Sequence which contains the same relative number of stars. Such ages are given in their table 2 and for the stars in common with our study we find the age spread is 5.6 Gyr. If the age spread in ω Cen is indeed so large, then all theories which invoke time-dependent phenomena, such as diffusion, would be ruled out, since it would be impossible for stars of such different ages, which have started their lives with the same (primordial) Li abundance, to still show the same Li abundance.

However the actual age spread in ω Cen is still a matter of debate and the relative ages of Villanova et al. (2007) stand out in the literature for providing the largest spread. Our sample of stars captures essentially the metal-poor population of ω Cen. According to the vast majority of studies, the intrinsic age spread of this population is consistent with zero, from the first photometric estimates (e.g., Hughes et al. 2004, Hilker et al. 2004), to the most recent spectro-photometric studies based on high precision HST CMDs and low resolution spectroscopy of vast samples of SGB and TO stars (such as Sollima et al. 2005, Stanford et al. 2006, Kayser et al. 2006). Theoretical work supports these findings, implying that a first, coeval generation of stars (the metal-poor population) is responsible for at least part of the pollution of the subsequent generations (see e.g., Norris 2004, Lee et al. 2005, Romano et al. 2009). The uncertainties of the experimental age spread determination procedures still allow to accommodate for a maximum spread – within the metal-population – of about 1 Gyr. Besides Villanova et al. (2007), also

the spectroscopic study by Johnson et al. (2009), supports a consistent age spread. In this study the metal-poor stars show different degrees of s-process enrichment (see their Figure 13), implying some 0.1–3 Gyrs (Schaller et al. 1992) for intermediate-mass AGB stars to pollute part of the metal-poor group, depending on the actual mean mass of the AGB population.

It is thus clear that at the present state of understanding of the age spread in ω Cen our observations do not provide a strong constraint on the viability of diffusion-like mechanisms for Li depletion. Future spectroscopic and photometric observations are likely to better pinpoint this issue. It is possible that even a spread of 1 Gyr would prove a strong constraint on possible Li depletion mechanisms

References

- Barklem, P. S., Piskunov, N., & O’Mara, B. J. 2000a, *A&A*(Letters), 355, 5
 Barklem, P. S., Piskunov, N., & O’Mara, B. J. 2000b, *A&A*, 363, 1091
 Bellini, A., Piotto, G., Bedin, L.R., Anderson, J., Platais, I., et al. 2009, *A&A*, 493, 959
 Bonifacio, P., et al. 2002, *A&A*, 390, 91
 Cayrel, R. 1988, in *The Impact of Very High S/N Spectroscopy on Stellar Physics*, G. Cayrel de Strobel and M. Spite eds., IAU Symp. 132, p. 345
 D’Antona, F. & Ventura, P., 2010, this volume
 Dunkley, J., et al. 2009, *ApJS*, 180, 306
 Hilker, M., Kayser, A., Richtler, T., & Willemsen, P. 2004, *A&A*(Letters), 422, 9
 Hisano, J., Kawasaki, M., Kohri, K., & Nakayama, K. 2009, *Phys. Rev. D*, 79, 063514
 Hughes, J., Wallerstein, G., van Leeuwen, F., & Hilker, M. 2004, *AJ*, 127, 980
 Jedamzik, K. 2004, *Phys. Rev. D*, 70, 083510
 Jedamzik, K. 2006, *Phys. Rev. D*, 74, 103509
 Jittoh, T., et al. 2008, *Phys. Rev. D*, 78, 055007
 Johnson, C. I., Pilachowski, C. A., Michael Rich, R., & Fulbright, J. P. 2009, *ApJ*, 698, 2048
 Kayser, A., Hilker, M., Richtler, T., & Willemsen, P. G. 2006, *A&A*, 458, 777
 Kurucz, R. L. 2005, *Memorie della Società Astronomica Italiana Supplementi*, 8, 14
 Lee, Y.-W., et al. 2005, *ApJ*(Letters), 621, 57
 Norris, J. E. 2004, *ApJ*(Letters), 612, 25
 Piau, L., et al. 2006, *ApJ*, 653, 300
 Richard, O., Michaud, G., & Richer, J. 2005, *ApJ*, 619, 538
 Romano, D., Tosi, M., Cignoni, M., Matteucci, F., Pancino, E., & Bellazzini, M. 2009, *MNRAS*, 1604
 Sbordone, L. 2005, *Memorie della Società Astronomica Italiana Supplementi*, 8, 61
 Sbordone, L., Bonifacio, P., Castelli, F., & Kurucz, R. L. 2004, *Memorie della Società Astronomica Italiana Supplementi*, 5, 93
 Sbordone et al. 2010, *A&A* submitted
 Schaller, G., Schaerer, D., Meynet, G., & Maeder, A. 1992, *A&AS*, 96, 269
 Sollima, A., Ferraro, F. R., Pancino, E., & Bellazzini, M. 2005, *MNRAS*, 357, 265
 Spite, M., & Spite, F. 1982a, *Nature*, 297, 483
 Spite, F., & Spite, M. 1982b, *A&A*, 115, 357
 Spite, M. & Spite F. 2010, IAU Symposium 268: “Light elements in the Universe”, C. Charbonnel, M. Tosi, F. Primas & C. Chiappini, eds., this volume
 Steigman, G. 2010, IAU Symposium 268: “Light elements in the Universe”, C. Charbonnel, M. Tosi, F. Primas & C. Chiappini, eds., this volume
 Stanford, L. M., Da Costa, G. S., Norris, J. E., & Cannon, R. D. 2006, *ApJ*, 647, 1075
 Stehle, R., & King, A. R. 1999, *MNRAS*, 304, 698
 van de Ven, G., van den Bosch, R. C. E., Verolme, E. K., & de Zeeuw, P. T. 2006, *A&A*, 445, 513
 Ventura, P., & D’Antona, F. 2010, *MNRAS*, in press, arXiv:0912.4399
 Villanova, S., et al. 2007, *ApJ*, 663, 296

Lithium and beryllium in Population I dwarf stars

Sofia Randich¹

¹INAF-Osservatorio Astrofisico di Arcetri

Largo E. Fermi, 5, I-50125, Firenze, Italy

email: randich@arcetri.astro.it

Abstract. In the last few years a variety of lithium and beryllium surveys have been carried out among Pop. I stars in the field and open clusters, with the goal to trace the dependence of these element abundances on stellar mass, age, metallicity, and to understand the physical processes that lead to their depletion. I summarize here the most recent results, focusing on stars with temperatures similar to the Sun. In particular, I will discuss Li measurements in solar-type members of old open clusters, which definitively show that the low solar lithium is not the standard for a star of that age and mass.

Keywords. Stars: abundances, interiors – open clusters and associations: general

1. Introduction

Several papers in this conference have addressed the question whether metal poor Pop. II stars deplete some lithium (Li) during their lifetime and the issue is indeed still open and highly debated. On the contrary, a large number of observational evidences indicate that more metal rich Pop. I stars do deplete their initial Li content; this is indeed expected on theoretical grounds, due their thicker convective envelopes. However, understanding when and how Li depletion occurs in Pop. I stars of different masses is still a major challenge and several unsolved problems exist.

Among the most puzzling ones, I mention the so-called “Lithium-dip”, a sharp decrease of Li abundance in a very narrow temperature range around 6500 K, first discovered in the Hyades (Boesgaard & Tripicco 1986) and then found in several other clusters older than a few hundred Myr; the dispersion in Li seen among stars cooler than ~ 5000 K in the Pleiades and other young clusters (e.g., Jeffries 2006 and references therein); the main sequence (MS) Li depletion observed in the Sun and similar stars. In this paper I shall focus on the latter issue.

Li and Be are depleted from the stellar atmosphere when a mechanism exist which is able to transport surface material down in the stellar interior, where the temperature is high enough for Li/Be reactions. Standard models of stellar evolution (those including convection only as mixing mechanism) predict that solar-type stars should undergo a considerable amount of Li depletion during the pre-main sequence phases; on the contrary, these stars are not predicted to destroy any Li during the MS, since the base of the convective zone does not reach the layer where the temperature is high enough for Li burning to occur. Also, the amount of Li depletion should tightly depend on mass, age, and metallicity.

It is now well established on observational grounds that the Li pattern in solar-type stars contradicts standard model predictions. The Sun has undergone a factor of about 160 Li depletion with respect to its initial abundance witnessed by meteorites, and it is now well ascertained that solar depletion occurs during the MS, rather than in the

PMS phase. Indeed early observations of solar analogs in the Pleiades (100 Myr) and Hyades (600 Myr) clusters already suggested almost forty years ago that solar-analogs undergo less PMS depletion than predicted by models and that Li depletion must take place during the MS (Zappalà 1972).

Furthermore, as first found by Spite et al. (1987) and confirmed by several other studies (García López et al. 1988; Pasquini et al. 1997; Jones et al. 1999), otherwise similar members of the solar-age, solar-metallicity M 67 cluster are characterized by different Li abundances: part of them are similar to the Sun, while another fraction have a factor of ~ 10 larger Li, suggesting that the amount of MS depletion is not necessarily the same for stars with the same mass, metallicity, and age. Similar results were achieved for field stars: different studies reported both a dispersion in Li and relatively high Li abundances in old (as indicated by chromospheric activity or rotation) solar analogs (Duncan 1981; Spite & Spite 1982; Pallavicini et al. 1987; Pasquini et al. 1994).

All these findings support the idea that Li depletion in solar-type stars is not driven by age and mass only, but that some additional parameter likely plays a role. Several models including non standard physics (rotation, magnetic fields, gravity waves, termohaline instability) have indeed been developed, but so far no consensus has been reached neither on the extra-mixing mechanism, nor on the additional parameter(s).

In the last decade several new and more modern measurements of Li in solar-type stars have been performed both in the field and in clusters, allowing us to draw more solid conclusions on the Li depletion pattern in solar-type stars. I will summarize those results by addressing a few specific questions; Namely, **i.** Is the solar Li content typical for a star of that age and mass? **ii.** Is the dispersion seen among solar analogs in M 67 also observed in other open clusters? **iii.** What are the timescales of Li depletion for solar-type stars? **iv.** Does depletion depend on metallicity? **v.** Do solar analogs deplete Be along with Li?

I finally mention that, whereas I will follow here an empirical approach and I will not attempt any direct comparison between theoretical predictions and observed patterns, I encourage theoreticians to use the latter to put constraints on the different extra-mixing models and/or to discern among them.

2. Lithium in solar analogs in the field

New measurements of Li in field stars similar to the Sun were recently carried out by Lambert & Reddy (2009) and Meléndez et al. (2009), who reached discrepant conclusions.

The first authors compared the Sun and stars with mass around one solar mass and found that none of their sample stars was as Li-poor as the Sun; actually all of them showed a factor of ~ 10 larger abundance. Based on this, Lambert & Reddy concluded that the solar Li might not represent the standard. On the other hand, Meléndez et al. measured Li in a very small sample of solar twins (defined as stars with mass within 3% and $[\text{Fe}/\text{H}]$ within ± 0.1 dex solar). Stars in their sample showed a decline of Li with age and, in particular, all the old solar twins were characterized by a low Li abundance. This led them to the conclusion that the solar Li is not abnormal and to the claim that previous results (i.e., the finding of Li-rich old solar-type stars) were due to biases in the samples and to considering young stars and/or stars that are not strict solar-twins.

Most obviously, ages of field stars are highly uncertain. A definitive answer to the question whether the solar Li is normal can only come from Li measurements in stars in old open clusters whose age is much better constrained.

3. Open clusters

Since the early study of Zappalá (1972), a huge amount of observational effort has been dedicated to Li measurements in open cluster stars. Sestito & Randich (2005) reanalyzed in a homogeneous fashion modern observations, putting together a sample of 22 open clusters from the literature, in order to derive the timescales of Li evolution in stars in different temperature intervals. They confirmed that solar-type stars deplete lithium during the MS phases; however, they evidenced that Li depletion slows down after the Hyades age and eventually stops for most of the stars after ~ 1 Gyr. Noticeably, solar-type members of the very old (6 Gyr) cluster NGC 188 showed a less than a factor of 2 lower abundance than similar stars in the ten times younger Hyades (see also Randich et al. 2003). At that time M 67 was the only known old cluster characterized by a dispersion and showing the presence of severely depleted stars. However, the sample of old clusters was small and only a few stars (typically less than 10) per clusters had Li measurements available.

Taking advantage of available multiplex facilities on 8m class telescopes, in the last five years new, high quality Li measurements in open clusters were obtained. Some of them focused on low- or very-low mass stars (e.g., Manzi et al. 2008; Jeffries et al. 2009) or on F-type stars (Anthony-Twarog et al. 2009), while others concentrated on solar-type stars (Prisinzano & Randich 2007; Pasquini et al. 2008; Randich et al. 2009; Pace et al. 2010, these Proceedings). In the following, the latter ones will be discussed in more detail.

3.1. A new analysis of M 67

Pasquini et al. (2008) carried out VLT/FLAMES observations of a large sample of MS stars in M 67 in order to identify true solar analogs. At variance with previous studies, effective temperature were derived by spectroscopic means, rather than from photometry. The Li vs. T_{eff} distribution based on these observations still show a dispersion, which however is more evident for stars in the temperature range $5850 \text{ K} \leq T_{\text{eff}} \leq 6000 \text{ K}$, rather than for members within $\pm 50 \text{ K}$ from the solar temperature. Most of these stars appear indeed Li-poor and only one of them has a high Li content. This apparently supports the claim of Meléndez et al. (2009) that the solar Li abundance is normal. However, we note that the sample of Pasquini et. al. includes only one of the high-lithium solar-type cluster members analyzed by Jones et al. (1999); hence, the inferred Li distribution for solar analogs is based on an incomplete sample and Li-rich stars might be missing. Indeed Randich et al. (2006) spectroscopically confirmed the solar-like temperature of star S969 ($T_{\text{eff}} = 5800 \text{ K}$); this star has a high Li ($\log n(\text{Li})=2.06$) and is not included in the sample of Pasquini et al. (2008).

3.2. The VLT/FLAMES survey

We have very recently carried out a VLT/FLAMES spectroscopic survey of a large sample of Galactic open clusters (Randich et al. 2005; Pallavicini et al. 2006). UVES fibers were allocated to evolved cluster members in order to obtain their chemical composition and investigate the issue of the radial metallicity gradient. The Giraffe spectrograph was instead used to obtain high resolution spectra ($R \sim 20,000$) of unevolved cluster candidates; our primary goals were membership determination and Li measurements among confirmed members. A total of 11 clusters were observed, nine of which are close enough to allow us to obtain good quality spectra of their solar-type members. In Table 1 I list the seven sample clusters whose Li analysis has been completed. Analysis for the remaining two clusters (NGC 2324 and To 2) is in progress. As the table shows, the clusters cover the age interval between ~ 0.7 and 8 Gyr and the metallicity range $[\text{Fe}/\text{H}] = -0.38 - +0.35$. After excluding radial velocity non members, each cluster sample typically consists of

Table 1. The sample clusters. I list ages, metallicities, and number of members for which we derived Li abundances.

Cluster	age (Gyr)	[Fe/H]	N _{stars}
NGC 3960	0.7	0.02±0.04	36
NGC 2477	1.0	0.07±0.04	73
NGC 2506	2.2	-0.20 ± 0.02	71
NGC 6253	3.0	0.36±0.07	54
Melotte 66	4.0	-0.33 ± 0.03	53
Be 32	6.0	-0.29 ± 0.04	57
Cr 261	8.0	0.13±0.05	135

~40-140 stars. The analysis of the data was homogeneously carried out as following Sesito & Randich (2005) and Randich et al. (2009). Briefly, effective temperatures (T_{eff}) were derived employing the T_{eff} vs. B-V calibration of Soderblom et al. (1993a) for solar metallicity stars or that of Alonso et al. (1996) for stars with non-solar [Fe/H] content. Li abundances were then derived from equivalent widths and using curves of growths. For more details on the Li analysis (in particular on the estimate of the contribution of the Fe I 670.74 nm line to the Li I 670.8 nm feature) I refer to Randich et al. (2009).

I mention that Pace et al. (2010, these Proceedings) warn that effective temperatures estimated from colors might be in error, due to uncertain knowledge of reddening. However, I note that for all the FLAMES clusters reddening is known relatively well (in several cases has been estimated from spectroscopy). Also, whereas one cannot exclude that T_{eff} values of individual stars might be somewhat in error, we can exclude that the overall temperature distribution within a given cluster is shifted towards lower/higher temperatures. If this was indeed the case, there would be an inconsistency with cluster ages derived from turn-off stars. In conclusion, use of photometric temperatures, should not greatly affect our results and conclusions.

3.2.1. *Li vs. temperature distribution*

In Fig. 1, I compare the $\log n(\text{Li})$ vs. T_{eff} distributions of M 67 and NGC 188 with those of four FLAMES clusters (Be 32 -6 Gyr, [Fe/H]=-0.29; Collinder 261 -6 Gyr, [Fe/H]=0.13; Melotte 66 -4 Gyr, [Fe/H]=-0.31, and NGC 6253 -3 Gyr, [Fe/H]=+0.36). The comparison of the four panels in the figure clearly shows that the upper envelope of the Li vs. T_{eff} distribution is very similar for the six clusters; however, each of them behaves in a different way as far as the dispersion and the fraction of Li-poor and Li-rich stars around the solar temperature is concerned. The distribution of the metal poor Be 32 is similar to that of NGC 188: at variance with M 67, it is characterized by virtually no dispersion and all stars have a Li abundance more than a factor of 10 larger than the Sun. Cr 261 shows a larger amount of dispersion, but none of its members is as Li depleted as the Sun or the lower envelope of M 67. Viceversa, most members of Mel 66 are heavily Li depleted and only five stars (out of 53) have $\log n(\text{Li}) > 2$. Finally, the very metal rich NGC 6253 exhibits an intermediate behaviour, more similar to the pattern of M 67: a fraction of stars shares the same low Li as the Sun, while another fraction has a much higher Li. As to the other three (younger) FLAMES clusters (NGC 3960, NGC 2477 and NGC 2506), all of them show almost no dispersion and all their members are Li-rich ($\log n(\text{Li}) \sim 2.2 - 2.4$). Note that all these would hold true even if considering a very narrow (± 50 K) temperature interval around the solar value.

I believe that these results confirm on solid and statistically significant grounds that old stars with temperatures close to the Sun are not necessarily as Li poor as the Sun.

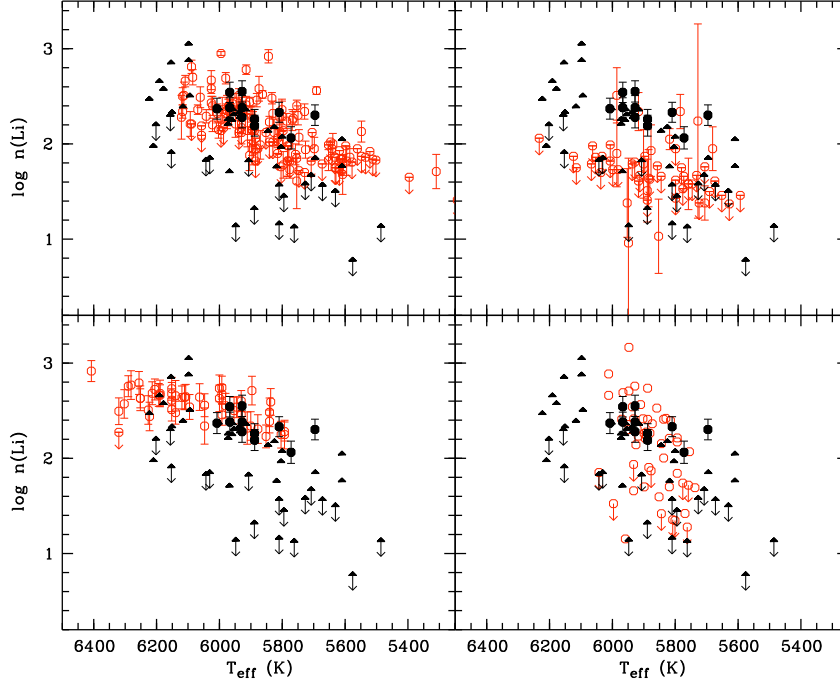


Figure 1. Li abundances ($\log n(\text{Li})$ – in the usual logarithmic scale where $\log n(\text{H})=12$) vs. effective temperature distributions of different FLAMES clusters (red open circles) are compared to M 67 (black filled triangles) and to NGC 188 (black filled circles). Namely, in the top panels the distributions of Collinder 261 (left-hand) and Melotte 66 (right-hand) are plotted, while in the bottom panels Berkeley 32 (left-hand) and NGC 6253 (right-hand) are shown. Li abundances for NGC 188 and M 67 have been retrieved from Sestito & Randich (2005) and had been derived in the same fashion as for the FLAMES sample clusters.

Old open cluster members show a variety of Li patterns and there is not a 'standard'. In a few clusters Li-rich and Li-poor stars are both present, while in others only the Li rich population exist. This provides strong support to the idea that the solar Li is not representative of the Li content of solar-type stars at the solar age and that other parameters, besides age and mass, drive Li depletion during the MS. Also note that the Li pattern of the clusters shown in Fig. 1 does not apparently depend on the cluster metallicity, since clusters with similar age and $[\text{Fe}/\text{H}]$ (e.g., Be 32 and Mel 66) are characterized by completely different distributions, while clusters with significantly different metallicity (e.g. Be 32 and NGC 188) have similar Li patterns.

Our conclusion is that some initial cluster condition or property might have affected the following evolution of Li. Unfortunately, at the old ages of the clusters memory of that is lost, but Li might represent an important fossil record.

3.2.2. Evolution of Li with age

In Fig. 2 I show the evolution of Li with age as inferred from available open clusters measurements. For each cluster I consider stars in the temperature interval $5750 \text{ K} \leq$

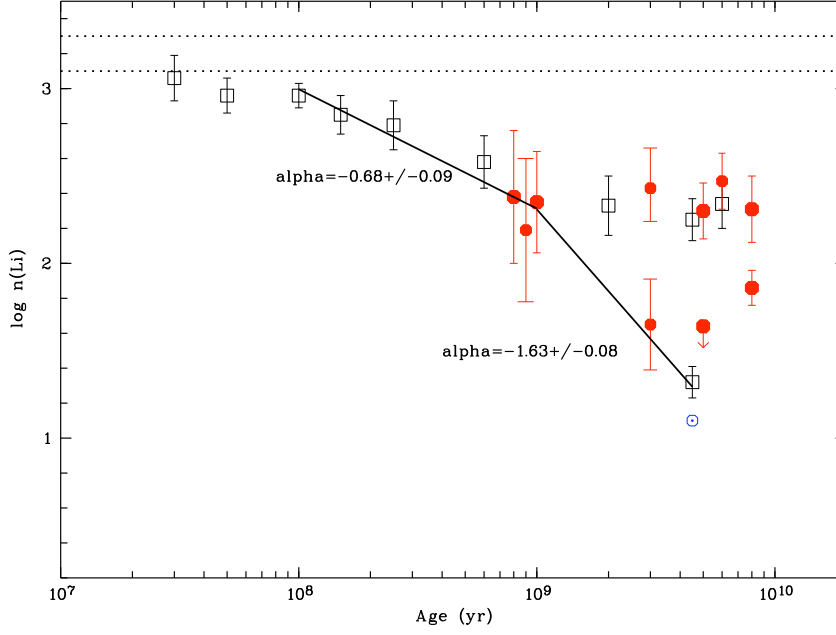


Figure 2. Average Li abundance as a function of age for solar-type stars ($5750 \text{ K} \leq T_{\text{eff}} \leq 6050 \text{ K}$). Open symbols indicate clusters from Sestito & Randich (2005), while filled circles denote the new FLAMES clusters. Error bars indicate the 1σ deviation from the average. Symbols at the same age indicate the average of the upper and lower envelopes of the Li vs. T_{eff} distribution of clusters characterized by a dispersion. The two dotted lines limit the range of initial Li abundances for Pop. I stars. The Sun is also plotted. The best fit exponential decays ($\log n(\text{Li}) \propto t^{-\alpha}$) between 100 Myr and 1 Gyr, and between 1 and 4.5 Gyr are also shown.

$T_{\text{eff}} \leq 6050 \text{ K}$, i.e. solar-type stars and slightly warmer ones. Note that the 300 K temperature interval was chosen as to have relatively large samples of stars. Fig. 1 however indicates that the results would not change very much if considering a narrower temperature range around the solar value.

Fig. 2 confirms, based on a much larger sample of clusters, the results of Sestito & Randich: very little depletion (less than a factor of 2) occurs up to 100 Myr. Then, a phase of continuous depletion follows up to an age of about 1 Gyr; the decay of Li abundance is well fitted with an exponential law $\log n(\text{Li}) \propto t^{-\alpha}$ with $\alpha = -0.68 \pm 0.09$. After 1 Gyr depletion becomes bimodal: part of the stars do not undergo any additional depletion and Li abundances converge towards a plateau value. I mention in passing that this plateau value is surprisingly similar to the Spite plateau of Pop. II stars. Another fraction of the stars, including the Sun, instead continue depleting Li at a very fast rate ($\alpha = -1.63 \pm 0.08$).

4. Beryllium

Be is destroyed at a higher temperature than Li (3.0 vs 2.5 MK) and thus simultaneous observations of Li and Be allow us to understand how deep in the stellar interior the mixing process extends and to put tighter constraints on models. Different models indeed predict different patterns of Be vs. Li depletion. Measurements of beryllium however rely on the resonant lines of Be II which are located in the near-UV spectral region at $\lambda\lambda = 3130.420, 3131.064$. Hence, the capability of observing these lines and measuring abundances is lower than for Li (see also Primas, these Proceedings). For this reason, until very recently much fewer surveys of Be have been performed, mostly focusing on bright F-type stars in the field and in the closest clusters (Hyades, Coma Ber, Ursa Major, Pleiades). These measurements have shown that such stars undergo Be depletion (a Be dip has indeed been identified) and show a tight Be vs. Li correlation holds (Boesgaard et al. 2004a and references therein).

4.1. Beryllium in solar-type stars

As mentioned, the Sun has suffered a large amount of Li depletion. Until 10 years ago it was commonly believed that it had also undergone some (a factor of two) Be depletion. Balachandran & Bell (1998) performed a new analysis of the near-UV solar spectrum, correctly taking into account continuous opacity. They showed that the Sun has instead not depleted any Be, implying that mixing in the solar photosphere is more superficial than previously supposed.

The availability of state-of-the art high resolution spectrographs with high near-UV efficiency has made it possible to measure Be not only in bright stars in close-by clusters, but also in fainter members of more distant, old clusters (Randich et al. 2002, 2007; Smiljanic et al. 2009). In particular, Be has been measured in solar-analogs in two clusters older than the Hyades: IC 4651 (2 Gyr) and M 67. Furthermore, in a very recent paper Boesgaard & Krugler (2009) present Be measurements for the one solar mass stars of the sample of Lambert & Reddy (2004). All these new data give us the possibility to study the behaviour of Be depletion in old stars similar to our Sun.

In Fig. 3 I show Li vs. Be abundance for members of different clusters in two temperature regimes, as indicated in the caption. The figure evidences distinct behaviors for stars in the two subsamples. Namely, stars warmer than 6000 K in both young and old clusters deplete some amount of Be and a clear correlation between Li and Be abundances is present, in agreement with the results of Boesgaard and collaborators. I mention that Be depletion was also found by Smiljanic et al. (2009) among F-type stars in IC 4651. On the other hand, virtually all the stars in the range $5700 \leq T_{\text{eff}} \leq 6000$ K, including the Sun, show, within the errors, the same Be abundance. While some star-to-star dispersion is present, possibly due to the adoption of different abundance scales and to non-uniform initial abundance, the stars in the right-hand panel of the figure do not follow any Be vs. Li correlation. These stars span two orders of magnitude in Li abundances, they have different ages and metallicities, but they share the same Be content. The Sun also has a very similar Be abundance. I stress that stars in the old M 67 have virtually the same Be abundance as members of the 50 Myr old IC 2391 and the 100 Myr old NGC 2516 clusters. Also, stars in M 67 showing different amount of Li depletion have the same Be content (see also Randich et al. 2002, 2007). This in turn implies that *i.* solar-type stars do not deplete any beryllium at least up to the solar and M 67 age, in spite of the fact that they do deplete lithium; *ii.* at variance with the warmer star regime, where Be depletion is correlated to Li depletion, the mixing mechanism responsible for MS Li

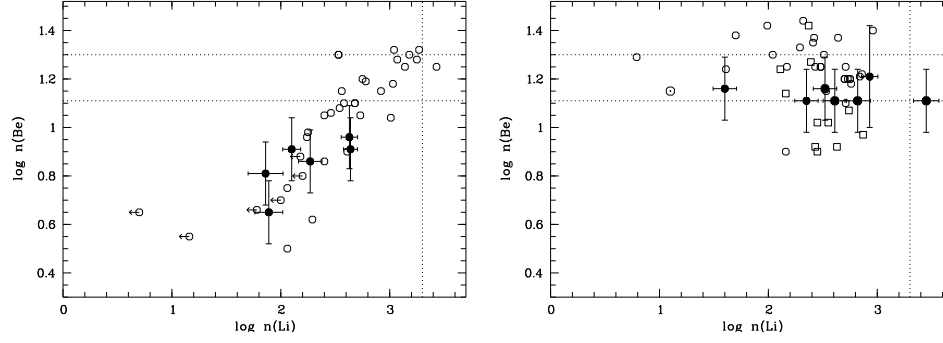


Figure 3. Be vs. Li abundances for stars with $T_{\text{eff}} > 6000$ K (left-hand panel) and for stars with $5700 \leq T_{\text{eff}} \leq 6000$ K (right-hand panel). Open circles are Hyades, Praesepe, Coma members from Boesgaard et al. (2002, 2003, 2004b), while filled circles denote M 67, IC 4651, IC 2391 and NGC 2516 members from Randich et al. (2007). Finally, open squares are solar mass field stars from Boesgaard et al. (2009). The position of the Sun is also shown. The horizontal lines bound the range of initial Be abundances in the different scales, while the vertical line indicates the initial Li abundance.

depletion in this temperature range is rather shallow and does not extend deep enough to cause also Be depletion.

5. Concluding remarks

I conclude by answering the five questions raised in the introduction.

Observations of solar-type stars in open clusters strongly suggest that the solar Li content is not typical. Whereas stars showing the same severe Li depletion as the Sun are found in the field and in clusters, otherwise similar old stars are present with a factor of at least ten higher Li. Part of the old open clusters so far observed show a dispersion similar to M 67, while the Li distribution in other clusters is very narrow. Solar-type stars deplete Li on the MS up to an age of about 1 Gyr; afterward, depletion either stops or becomes considerably more efficient, like in the Sun. The reasons why otherwise similar stars deplete Li at different rates after 1 Gyr and why similar cluster behave differently is so far not understood. The hypothesis that the Li behaviour might be related to the presence of a planetary system (Israeli, these Proceedings) is very tempting. In any case, this empirical evidence suggests that Li is a good age tracer for these stars up to about 1 Gyr. After that age, a 'low' solar-like Li abundance is indicative of an old age, plus, possibly, a peculiar evolution. Viceversa, a 'high' Li content (~ 10 times the solar value) only allows inferring a lower limit to the age.

Li vs. T_{eff} patterns and the presence of severely depleted stars do not depend on the cluster metallicity. I mention however that metallicity affects stellar structure and a given effective temperature corresponds to lower masses for lower metallicities (and viceversa). Therefore, similar Li vs. T_{eff} distributions do not correspond to similar Li vs. mass patterns, if the metallicity of the clusters is not the same (see Randich et al. 2009).

Finally, Be observations in solar-type stars in old clusters show that, like the Sun, they do not deplete any Be, in spite of the fact that they deplete [different amount of] Li. This indicates that the mixing process must be a shallow one.

References

- Alonso, A., Arribas, S., Martinez-Roger, C. 1996, *A&A*, 313, 873
- Anthony-Twarog, B.J., Deliyannis, C.P., Twarog, B., Croxall, K.V., Cummings, J.D. 2009, *AJ*, 138, 1171
- Balachandran, S.C., Bell, R.A. 1998, *Nature*, 392, 791
- Boesgaard, A.M., Tripicco, M.J. 1986, *ApJ*, 302, L49
- Boesgaard, A.M., King, J.R. 2002, *ApJ*, 565, 587
- Boesgaard, A.M., Armengaud, E., King, J.R. 2003, *ApJ*, 583, 955
- Boesgaard, A.M., Armengaud, E., King, J.R., Deliyannis, C.P., Stephens, A. 2004a, *ApJ*, 613, 1202
- Boesgaard, A.M., Armengaud, E., King, J.R. 2004b, *ApJ*, 605, 864
- Boesgaard, A.M., Krugler, H.J. 2009, *ApJ*, 691, 1412
- Duncan, D.K. 1981, *ApJ*, 248, 651
- García López, R.J., Rebolo, R., Beckmann, J.E. 1988, *PASP*, 100, 1489
- Jeffries, R. 2006, in *Chemical Abundances and Mixing in Stars in the Milky Way and its Satellites*, ESO Astrophysics Symposia, S. Randich, L. Pasquini (eds), (Springer-Verlag), p. 163
- Jeffries, R., Jackson, R.J., James, D.J., Cargile, P.A. 2009, *MNRAS*, 400, 317
- Jones, B.F., Fisher, D., Soderblom, D.R. 1999, *AJ*, 117, 330
- Lambert, D., Reddy, B. 2004, *MNRAS*, 349, 757
- Manzi, S., Randich, S., de Wit, W.J., Palla, F. 2009, *A&A*, 479, 141
- Meléndez, J., Ramírez, I., Casagrande, L. et al. 2009, *Ap&SS*, in press
- Pallavicini, R., Cerruti-Sola, M., Duncan, D.K. 1987, *ApJ*, 174, 116
- Pallavicini, R., et al. 2006, in *Chemical Abundances and Mixing in the Milky Way and its Satellites*, ESO Astrophysics Symposia, S. Randich, L. Pasquini (eds), Springer-Verlag, p. 181
- Pasquini, L., Liu, Q., Pallavicini, R. 1994, *A&A*, 287, cw191535
- Pasquini, L., Randich, S., Pallavicini, R. 1997, *A&A*, 325, 535
- Pasquini, L., Biazzo, K., Bonifacio, P., Randich, S., Bedin, L. R. 2008, *A&A*, 489, 677
- Prisinzano, L., Randich, S. 2007, *A&A*, 475, 535
- Randich, S., Primas, F., Pasquini, L., Pallavicini, R. 2002, *A&A*, 387, 222
- Randich, S., Sestito, P., Pallavicini, R. 2003, *A&A*, 399, 133
- Randich, S., et al. 2005, *ESO Messenger*, 121, 18
- Randich, S., Sestito, P., Primas, F., Pallavicini, R., Pasquini, L. 2006, *A&A*, 450, 557
- Randich, S., Primas, F., Pasquini, L., Sestito, P., Pallavicini, R. 2007, *A&A*, 469, 163
- Randich, S., Pace, G., Pastori, L., Bragaglia, A. 2009, *A&A*, 496, 441
- Sestito, P., Randich, S. 2005, *A&A*, 442, 615
- Smiljanic, R., Pasquini, L., Charbonnel, C., Lagarde, N. 2009, *A&A*, in press
- Soderblom, D.R., Stauffer, J.R., Hudon, J.D., Jones, B.F. 1993, *ApJS*, 85, 113
- Spite, M., Spite, F. 1982, *A&A*, 115, 351
- Spite, F., Spite, M., Peterson, R. C., Chaffee, F. H., Jr. 1987, *A&A* 171, L8
- Zappalà, R.R. 1972, *ApJ*, 72, 57



Andreas Kaufer



Garik Isrealian

Lithium in stars with exoplanets

Garik Israelian

Instituto de Astrofísica de Canarias,
Calle Via Lactea s/n, E38200, La Laguna, Tenerife, Canary Islands, Spain
email: gil@iac.es

Abstract. Our recent study of solar-type stars from the HARPS GTO sample provides highly accurate information with regard to Lithium abundances in stars with and without detected planets (Israelian et al. 2009). When the Li abundances of planet bearing stars are compared with the “single” stars, we find an excess of Li depletion in planet hosts with effective temperatures in the range 5700–5850 K. We also found that small amounts of Li have survived in the atmospheres of some planet-host solar analogs. Enhanced Li depletion in planet host stars puts constraints on mixing processes responsible for this phenomenon. We show that neither age nor metallicity are responsible for this observational fact.

Keywords. Stars: abundances, late-type, planetary systems

1. Introduction

The enhanced depletion of lithium in the Sun discovered more than 60 years ago remains the epitome of the Li puzzle. The base of the surface convective layer of the Sun is not hot enough for nuclear reactions to destroy Li, and yet the surface Li abundance is about 140 times less than the initial protosolar abundance which is the meteoritic value (Anders & Grevesse 1989). A large dispersion in Li abundance observed in solar-type stars of the same age, mass and metallicity is inconsistent with classical models of stellar evolution (D’Antona & Mazzitelli 1994) and has reinforced the idea that the presence of planets may be responsible for this effect (King et al. 1997, Gonzalez & Laws 2000, Israelian et al. 2004).

King et al. (1997) were first to propose that the low Li abundances of the Sun and 16 Cyg B with respect to 16 Cyg A may be related to the presence of a planetary companion. Many studies have attempted to separate the effects of planets on Li abundance. Gonzalez & Laws (2000) corrected Li abundances in planet hosts for linear trends with age, metallicity, and T_{eff} , and concluded that planet hosts contain less Li than field stars. This result was debated by Ryan (2000) who proposed that these differences were not significant. Many authors have revisited this topic since then (Israelian et al. 2004, Chen & Zhao 2006, Luck & Heiter 2006, Takeda et al. 2007, Gonzalez 2008) and all of them, except Luck & Heiter (2006) have concluded that stars with planets tend to have smaller Li abundance. However, stellar samples used in these studies were not homogeneous. It was possible that the planet host stars are Li poor because they are more metal rich. Moreover, neither of these authors could provide a homogeneous comparison sample of “single” stars without detected giant planets. These tasks have been undertaken by our group (Israelian et al. 2009) who recently has demonstrated that, indeed, stars with giant exoplanets contain less Li than “single” stars without (so far) detected planets in the HARPS GTO sample.

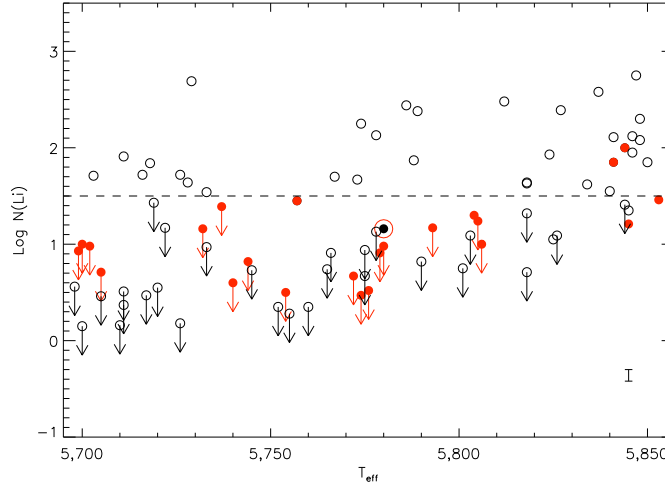


Figure 1. Lithium abundance against effective temperature in solar-analogue stars with and without detected planets. The planet-hosts are red filled circles. The minimum detectable Li abundance varies among the stars used in this study because their spectra have different signal-to-noise ratios. The straight line $\log N(\text{Li})=1.5$ matches the upper envelope of the lower limits corresponding to a minimum $S/N = 200$ in a typical solar twin. We employ this line as a cut-off for selecting Li-depleted stars in our sample. The mean statistical errors (1σ) for the $\log N(\text{Li})$ and T_{eff} averaged over all stars are 0.06 dex and 30 K, respectively (Sousa et al. 2008). Errors in $\log N(\text{Li})$ include uncertainties in T_{eff} and equivalent width measurements.

2. New analysis

To establish a definitive relation between the presence of planets and enhanced Li depletion in solar-type stars requires high quality observations and unbiased abundance analysis of Li for a large sample of stars with and without planets. We obtained Li abundances from high resolution, high S/N spectra for a sample of 451 stars in the HARPS high precision radial velocity survey (precision better than 1 m/s; Mayor et al. 2003) spanning the effective temperature range between 4900 and 6500 K. These are unevolved, slowly rotating non-active stars from a CORALIE catalogue (Mayor et al. 2003). Of these 451 stars, 70 are reported to host planets and the rest (often we call them single stars) have no detection so far. Our abundance analysis, which followed standard prescriptions for stellar models, spectral synthesis code and stellar parameter determination (Sousa et al. 2008), confirm a peculiar behavior of Li in the effective temperature range 5600-5900 K. To put this in a more solid statistical basis these two samples in the T_{eff} window 5600-5900 K were extended by adding 16 and 13 planet host and “single” stars, respectively, with Li abundances from our previous work where the same spectral synthesis tools have been employed (Israelian et al. 2004). It is remarkable that the immense majority of planet host stars have severely depleted lithium while in the comparison sample large fraction partially inhibited depletion. The Li abundance of 20 % of stars with exoplanets in the temperature range 5600-5900 K has $\log N(\text{Li}) \geq 1.5$ while for the 116 comparison stars the Li abundance shows a rather large dispersion with some 43 % of the stars displaying Li abundances $\log N(\text{Li}) > 1.5$. This result becomes more obvious in solar analog stars where some 50 % of 60 single stars in narrow window of $T_{\text{sun}} \pm 80$ K appear with $\log N(\text{Li}) \geq 1.5$ while only one planet host, out of 24, has

$\log N(\text{Li}) \geq 1.5$ (Fig 1). Lithium survival at $T_{\text{eff}} > 5850$ K is explained by the fact that the convective layers of stars more massive than the Sun are shallow and too far to reach the Li-burning layers. On the other hand, lower mass stars with $T_{\text{eff}} < 5700$ K have deeper convective layers and destroy Li more efficiently. We note that subgiants were not included in this study because they undergo dramatic changes in their internal structure that alters surface abundance of Li. The Li over-depletion in planet bearing main sequence stars is a generic feature over T_{eff} restricted range from 5700 to 5850 K. Let us now investigate if Li abundance in solar analog stars is determined by their age and/or metallicity.

3. Ages, metallicity, and rotation

3.1. Metallicities

Most of the planet-host stars discovered to date are metal-rich (Santos, Israelian & Mayor 2004). The metallicity excess could result from either the accretion of planets/planetesimals on to the star or the protostellar molecular cloud. This metallicity excess is also present in the solar analogue planet-bearing stars (see Fig. 2c). It is very important to investigate if a high metallicity is responsible for enhanced Li depletion in these stars. The increase of metal opacities in solar-type stars is responsible for the transition between radiative and convective energy transport. The main contributors to the total opacity at the base of the convective zone are oxygen and iron (Piau & Turck-Chièze 2002). Our data (Fig 2c) show that the fraction of single stars with $\log N(\text{Li}) > 1.5$ is 50% at $[\text{Fe}/\text{H}] < 0$ and $[\text{Fe}/\text{H}] > 0$. This suggests that the Li depletion mechanism does not depend on the metallicity in the range $0.5 < [\text{Fe}/\text{H}] < +0.5$. Apart from this, we have investigated the dependence of $\log N(\text{Li})$ on $[\text{O}/\text{Fe}]$ (Piau & Turck-Chièze 2002) for planet-host stars, using oxygen abundances in planet-host stars from the literature (Ecuivillon et al. 2006), and again found no correlation. We conclude that the metallicity or $[\text{O}/\text{Fe}]$ ratio is not responsible for an enhanced Li depletion in metal-rich planet-host stars.

3.2. Chromospheric ages and rotation

It is often stated that the lithium abundance of solar-type main sequence stars decreases progressively with age (Sestito & Randich 2005). If that were the case, we should expect a correlation between lithium and stellar age indicators. Chromospheric activity is a reliable age indicator for solar-type stars from young ages to about 1 Gyr (Pace et al. 2009), or perhaps even to the age of the Sun (Wright et al. 2004). Abundances of Li versus chromospheric activity indices, R_{HK} , for the solar analogue stars with and without detected planets are shown in Fig. 2a. We find no correlation between Li and the activity index and conclude that the solar analogue stars with and without planets considered in this work have similar ages. This conclusion is valid as long as the chromospheric activity index R_{HK} can be used as an age indicator. It means our stars are older than 1 Gyr (Pace et al. 2009) or perhaps as old as 4.5 Gyr (Wright et al. 2004).

It is known (Cutispoto et al. 2003) that chromospheric activity correlates with stellar rotation ($v \sin i$). If the planet hosts were older than the comparison sample, their rotational velocities would be smaller than in the comparison sample. This is not observed either (Fig 2b), adding support to our conclusion that the ages of planet hosts and “single” stars in our sample exceed 1 Gyr.

We have compiled previously published isochrone ages for Li-rich ($\log N(\text{Li}) > 1.9$) stars shown in Fig 1. One may think that these main sequence solar analogue stars are young since their atmospheres contain a lot of Lithium. However, the average isochrone

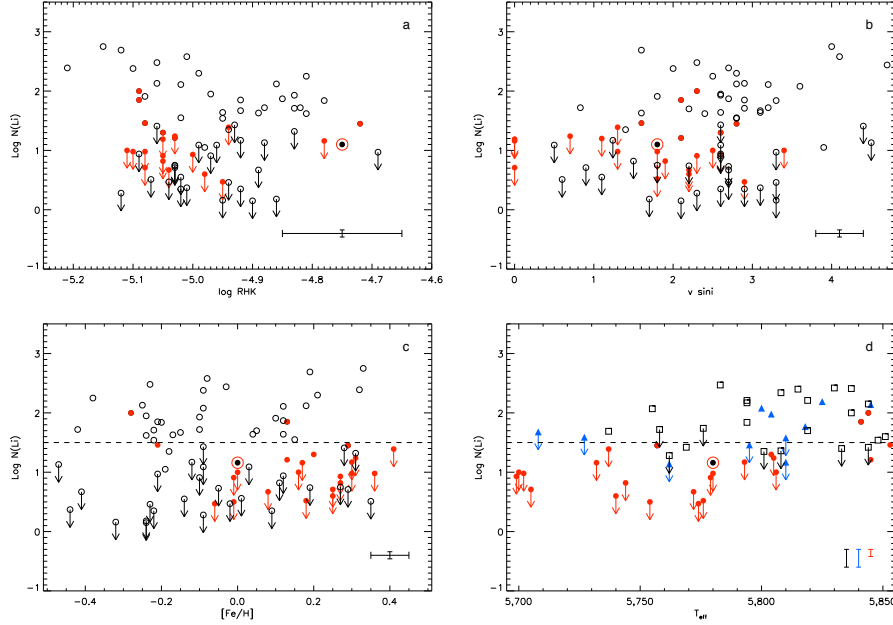


Figure 2. Panels (a) and (b). Lithium abundances in solar-analogue stars with and without detected planets versus chromospheric activity indices ($\log R_{HK}$) and rotational velocity ($v \sin i$). R_{HK} values were taken from the literature (Wright et al. 2004, Saffe et al. 2005, Gray et al. 2006) while rotational velocities of the comparison sample stars and many planet hosts were measured from CORALIE and HARPS spectra using a cross correlation function (Santos et al. 2002). Typical 1σ uncertainties for $\log R_{HK}$ and $v \sin i$ are 0.1 dex and 0.3 km/sec, respectively (Wright et al. 2004, Santos et al. 2002). Rotational velocities of several planet-hosts were taken from the literature (Valenti & Fischer 2005). Panel (c). Li abundances for the same stars versus metallicity. The latter was measured (Sousa et al. 2008) with a precision of 0.03 dex (1σ). Panel (d). Li abundances in planet hosts and stars of the open clusters M67 and NGC 6253. In this panel we plot Li abundances versus effective temperature in planet hosts (red filled circles), and stars of the open clusters M67 (blue triangles) and NGC 6253 (open squares). The data for M67 were taken from the literature. Li abundances in NGC 6253 have been derived from VLT/Giraffe spectra using standard methods (Randich et al., in preparation). Typical 1σ error bars for cluster stars are 0.15 dex and 100 K for $\log N(\text{Li})$ and T_{eff} , respectively.

ages of our planet-hosts and “single” stars are found in the window 5 to 9 Gyr (Holmberg et al. 2009). Nevertheless, stellar ages derived from isochrones cannot be used since they are very uncertain with the dispersion as large as 4 Gyr (Saffe et al. 2005).

3.3. Lithium and ages in planet hosts and open clusters

Observations of solar-type stars in the temperature range 5700-6100 K in open clusters (Sestito & Randich 2005, Randich 2008) show that the Li depletion continuously occurs from the Zero Age Main Sequence (ZAMS) up to ~ 1 Gyr, with a time scale of 1.4 Gyr. It becomes bimodal at > 1 Gyr as the fraction of stars continue depleting Li at higher rate. Our Sun is perhaps the best representative of this group. The Li depletion completely stops for the majority of stars and all cluster average abundances converge to a plateau value close to the Spite plateau of Pop II stars (see Sestito & Randich 2005, Randich 2008, Randich, S. this proceedings).

We have seen (Fig. 2) that the comparison with field stars leads to the conclusion that neither age nor metallicity is responsible for the excess Li depletion. This is reinforced by observations of Li in solar-type stars in old solar metallicity and/or metal-rich open clusters, which indeed show a wide dispersion of Li abundances with values ranging from $\log N(\text{Li}) = 2.5$ down to 1.0 and lower (Sestito et al. 2007, Randich 2008, Pasquini et al. 2008). This is the case for M67 (age 3.5–4.8 Gyr and $[\text{Fe}/\text{H}] = 0.06$) (Pasquini et al. 2008) and NGC 6253 (age 3 Gyr and $[\text{Fe}/\text{H}] = 0.35$) (Yadav et al. 2008, Sestito et al. 2007), as is clearly seen in Fig 2d. These two clusters offer a homogeneous sample of solar analogues in terms of age and metallicity. Both high and low Li abundance solar analogues are present in these two clusters. The high Li abundance in a large fraction of old metal-rich stars in NGC 6253 and M67 supports our conclusion that high metallicity and/or age are not the main cause for the systematic low Li abundances in solar analogue planet-host stars. Two other clusters, Cr261 (age 6 Gyr and $[\text{Fe}/\text{H}] = 0.13$) and NGC 188 (age 8 Gyr and $[\text{Fe}/\text{H}] \sim 0$) show significant Li dispersion (Sestito & Randich 2005, Randich 2008, Randich, S., this conference). Slow mixing models of solar-type stars predict Li abundances $\log N(\text{Li}) \leq 1$ and cannot explain a large fraction of Li-rich solar analogues in these clusters with $\log N(\text{Li}) \sim 2.4$. The analysis of several old open clusters observed with FLAMES confirm that the Li dispersion does not depend on age or metallicity. (S. Randich, this conference).

4. Conclusions

We propose that the low Li abundance of planet-host solar analogue stars is associated with the presence of planets. The presence of a planetary system may affect the angular momentum evolution of the star and the surface convective mixing, thereby causing enhanced lithium depletion. Planet migration could possibly trigger angular momentum transfer in the convective zone, leading to additional mixing below this zone. Theoretical models (Pinsonneault et al. 1989) show how magnetic braking scales with rotational velocity leading to turbulent diffusion mixing and enhanced lithium depletion. In this case we would expect severely Li-depleted stars to host planets with shorter orbital periods. On the other hand, long-lasting star–disc interaction during the pre-main sequence may cause planet-host stars to be slow rotators and develop a high degree of differential rotation between the radiative core and the convective envelope. This process may lead to enhanced lithium depletion too (Bouvier 2008).

We know that all stars used in the HARPS GTO program are non-active, slow rotators. Thus, from the RV point of view they are all equally good planet-host candidates. It is impossible to explain why HARPS was unable to detect the relatively young planetary systems with ages between (for example) 1 and 3 Gyr. This fact alone suggests that planet-host and “single” stars in our sample come from groups with the same age distribution. Thus, our finding presented in Fig. 1 can be considered as an independent confirmation of the well-known Li puzzle discovered in open clusters (Randich 2008). We confirm that factors other than age, mass, and metallicity, such as angular momentum (which planets may alter), can affect stellar lithium abundance.

Studying young stars to identify the effect that planets have on their rotation is the next step to explain the correlation between lithium abundance and planets. Young stars and planets are more difficult to observe, but they reveal more than old stars do about how fast they rotated in their infancy. In the future, it may be possible to test the hypothesis that altering stars’ rotation affects lithium depletion. Discovery of planets in open clusters will certainly help to understand the Li puzzle.

References

- Anders, E. & Grevesse, N. 1989, *Geochim. Cosmochim. Acta*, 53, 197
- Bouvier, J. 2008, *A&A* (Letters), 489, 53
- Chen, Y. Q. & Zhao, G. 2006, *AJ*, 131, 1861
- Cutispoto, G., Tagliaferri, G., de Medeiros, J. R., Pastori, L., Pasquini, L. & Andersen, J. 2003, *A&A*, 397, 987
- D'Antona, F. & Mazzitelli, I. 1994, *ApJS*, 90, 467
- Ecuvillon, A., Israelian, G., Santos, N. C., Shchukina, N. G., Mayor, M. & Rebolo, R. 2006, *A&A*, 445, 633
- Gonzalez, G. 2008, *MNRAS*, 386, 928
- Gonzalez, G. & Laws, C. 2000, *AJ*, 119, 390
- Gray, R.O., Corbally, C.J., Garrison, R.F., McFadden, .T., Bubar, E.J., McGahee, C.E., O'Donoghue, A.A., Knox, E.R., 2006, *AJ*, 132, 161
- Holmberg, J., Nordström, B. & Andersen, J. 2009, *A&A*, 501, 941
- Israelian, G., Santos, N., Mayor, M. & Rebolo, R. 2004, *A&A*, 414, 601
- Israelian, G., Delgado Mena, E., Santos, N., Sousa, S., Mayor, M., Udry, S., Dominguez Cerdena, C., Rebolo, R. & Randich, S. 2009, *Nature*, 462, 189
- King, J.R., Deliyannis, C.P., Hiltgen, D.S., Stephen A., Cunha, K., Boesgaard, A.M. 1997, *AJ*, 113, 1871
- Luck, E. & Heiter, U. 2006, 131, 3069
- Mayor, M. et al. 2003, *Messenger*, 114, 20
- Pace, G., Melendez, J., Pasquini, L., Carraro, G., Danziger, J., François, P., Matteucci, F., Santos, N.C. 2009, *A&A* (Letters), 499, 9
- Pasquini, L., Biazzo, K., Bonifacio, P., Randich, S. & Bedin, L. R. 2008, *A&A*, 489, 677
- Piau, L. & Turck-Chièze, S. 2002, *A&A*, 566, 419
- Pinsonneault, M., Kawaler, S. D., Sofia, S. & Demarque, P. 1989, *ApJ*, 338, 424
- Randich, S. 2008, *Mem. Soc. Astr. It.*, 79, 516
- Ryan, S. 2000, *MNRAS* (Letters), 316, 35
- Saffe, C., Gomez, M. & Chavero, C. 2005, *A&A*, 443, 609
- Santos, N.C., Mayor, M., Naef, D., Pepe, F., Queloz, D., et al. 2002, *A&A*, 392, 215
- Santos, N. C., Israelian, G., Mayor, M. 2004, *A&A*, 415, 1153
- Sestito, P. & Randich, S. 2005, *A&A*, 442, 615
- Sestito, P., Randich, S. & Bragaglia, A. 2007, *A&A*, 465, 185
- Sousa, S.G., Santos, N.C., Mayor, M., Udry, S., Casagrande, L. et al. 2008, *A&A*, 487, 373
- Takeda, Y., Kawanomoto, S., Honda, S., Ando, H. & Sakurai, T. 2007, *A&A*, 468, 663
- Valenti, J. & Fischer, D. 2005, *ApJS*, 159, 141
- Wright, J., Marcy, G. W., Butler, R. P. & Vogt, S. S. 2004, *ApJS*, 152, 261
- Yadav, R.K.S., Bedin, L.R., Piotto, G., Anderson, J., Cassisi, S., et al. 2008, *A&A*, 484, 609

Light elements in stars with exoplanets

N.C. Santos¹, E. Delgado Mena², G. Israelian², J. I. González-Hernández³, M. C. Gálvez-Ortiz⁴, M. Mayor⁵, S. Udry⁵, R. Rebolo^{2,6}, S. Sousa¹ and S. Randich⁷

¹Centro de Astrofísica, Universidade do Porto, Rua das Estrelas, 4150-762 Porto, Portugal.
email: Nuno.Santos@astro.up.pt

²Instituto de Astrofísica de Canarias, E-38200 La Laguna, Tenerife, Spain.

³Departamento de Astrofísica, Facultad de Ciencias Físicas, Universidad Complutense de Madrid, E-28040, Spain.

⁴Centre for Astrophysics Research, Science and Technology Research Institute, University of Hertfordshire, Hatfield AL10 9AB, UK.

⁵Observatoire de Genève, 51 ch. des Maillettes, CH-1290 Sauverny, Switzerland.

⁶Consejo Superior de Investigaciones Científicas, E-28006, Madrid, Spain.

⁷INAF/Osservatorio Astrofisico di Arcetri, Largo Enrico Fermi 5, I-50125 Firenze, Italia.

Abstract. It is well known that stars orbited by giant planets have higher abundances of heavy elements when compared with average field dwarfs. A number of studies have also addressed the possibility that light element abundances are different in these stars. In this paper we will review the present status of these studies. The most significant trends will be discussed.

Keywords. Stars: abundances, fundamental parameters, atmospheres – planetary systems: formation

1. Introduction

Since the discovery of the first exoplanet around 51 Peg (Mayor & Queloz 1995) the number of known exoplanets orbiting solar type stars did not stop growing, being currently of more than 400 (including more than 30 multi-planetary systems)[†]. In addition, more than 50 planets are now known to transit their host stars. Finally, in the last few years about 30 planets with masses between 2 and 20 M_{Earth} have been discovered. Present results strongly suggest that planets are common around solar-type stars.

One remarkable characteristic of planet host stars is that they are considerably metal-rich when compared with single field dwarfs (Gonzalez 1998; Santos et al. 2000; Santos et al. 2004a; Fischer & Valenti 2005). As we can perfectly see in Fig.1, the probability of finding a giant planet depends strongly on the metallicity of the star. Interestingly, as discussed in Santos et al. (2004a), there seems to be two regimes in this distribution. For super solar metallicities the presence of planets is a steep rising function of metallicity, while for metal poor stars there is no significant dependence with metallicity.

Two main explanations have been suggested to explain the observed metallicity “excess”. In the first one it is considered that its origin is primordial, so the more metals you have in the proto-planetary disk, the higher should be the probability of forming a planet. Alternatively, this excess could be produced by accretion of rocky material by the star sometime after it reached the main-sequence.

In the right panel of Fig.1 metallicity is shown as a function of the stellar convective envelope mass. If pollution were the main responsible for the enhanced metallicity of

[†] See tables at <http://www.exoplanet.eu>

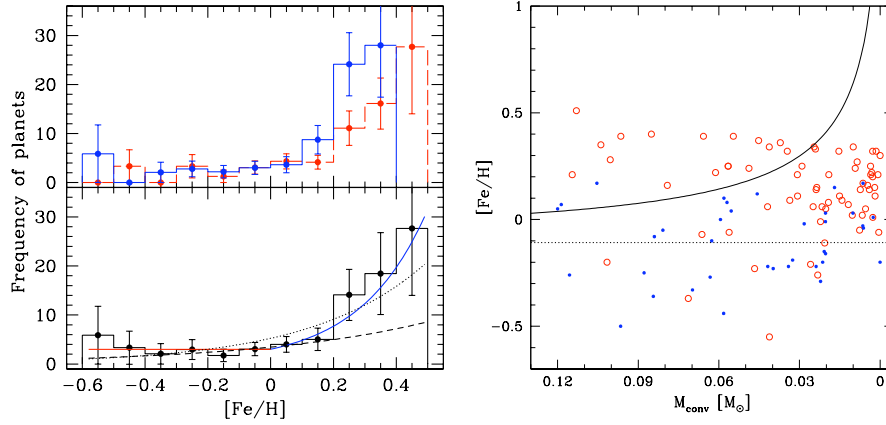


Figure 1. *Left panel:* Frequency of planet hosts as a function of stellar metallicity. Blue points are from Santos et al. (2004a) and red points are from Fischer & Valenti (2005). From Udry & Santos (2007). *Right panel:* Metallicity as a function of convective envelope mass for stars with planets (open symbols) and field stars (points). The $[Fe/H] = \text{constant}$ line represents the mean $[Fe/H]$ for the non-planet hosts stars from Santos *et al.* (2001). The curved line represents the result of adding 8 earth masses of iron to the convective envelope of stars having an initial metallicity equal to the non-planet hosts mean $[Fe/H]$. The resulting trend has no relation with the distribution of the stars with planets. From Santos et al. (2003).

planet hosts, we would expect to find higher metallicities as the convective envelope mass decreases. We do not find such a trend. Observations of stars arriving at the main sequence in open clusters do not show this correlation either (Shen et al. 2005). Another point against pollution is that we would need too high accretion rates to explain the metallicity observed in K-dwarfs. In addition, transit detections showed that the mass of heavy elements in the planets appears to be correlated with the metallicity of their parent stars (Guillot et al. 2006). The stars that are the most metal-rich host the most metal-rich planets. Finally, a recent work by Mordasini et al. (2009) finds that the distributions of planetary properties are well reproduced using core-accretion models (see below), which are dependent on dust content of the disk, thus supporting the primordial origin of overmetallicity in stars with planets.

These results have important implications for the models of giant planet formation and evolution. Two major giant planet formation models have been proposed. The core accretion model (Pollack et al. 1996) and the disk instability model (Boss 1997). In the former case, planets are formed by the collisional accumulation of planetesimals by a growing solid core, followed by accretion of a gaseous envelope onto the core. In the second one, a gravitationally unstable region in a protoplanetary disk forms self-gravitating clumps of gas and dust (Boss 1997). In the core accretion model, planet formation is critically dependent of the dust content of the disk (Pollack et al. 1996) while in the disk instability model it is not (Boss 2002). Present observations are thus more compatible with core accretion model, though do not exclude disk instability.

Although most data suggest that pollution is not the major source of the high metallicity levels in planet host stars, this issue is still not settled. In contrast with main sequence stars, planet-hosting giants do not show a tendency of being more metal-rich. Pasquini et al. (2008a) proposed that the lack of a metallicity-planet connection among giant stars

is due to pollution of the star while on the main sequence, followed by dilution during the giant phase. Moreover, if hydrogen-poor material is accreted in the early phases of stellar evolution, during planet formation, the metal excess in the convective zone could be diluted, first by dynamical convection, then by thermohaline mixing, on a timescale much shorter than the stellar lifetime (Vauclair 2004).

Although the primordial origin of metallicity seems to be the more compatible explanation, pollution might have been able to alter more or less significantly the global metallicity of stars. In fact, though at low levels, cases of $[\text{Fe}/\text{H}]$ pollution exist (e.g. Laws & Gonzalez 2001). In a different context, some Li-rich giants have been found (Brown et al. 1989), stars which should have depleted their lithium due to their deep convective envelopes, and that perhaps might have accreted metal-rich material. However, none of the Li-rich giants studied by Melo et al. (2005) were found to have detectable Be, something incompatible with an engulfment scenario (see also review by V.V. Smith in this book).

The key to understand these issues may be in the study of light element abundances. Light element should be particularly sensitive, since they are normally depleted in solar-type stars. If they are present in large quantities, a external origin might be the best explanation, rather than stellar evolution. Furthermore, light elements are important tracers of internal structure and mixing in stars and they can give us information about the rotational history of the star. It is indeed plausible that the planet formation process is able to alter the rotational history of a star, thus inducing changes in the observed abundances of light elements.

In this paper we will review the major results of the study of the light elements Li and Be in stars with planets.

2. ^6Li : Tracing pollution events.

The lithium isotope ^6Li is produced by spallation reactions in the interstellar medium while it is easily destroyed in stellar interiors at a temperature of 2 million K. According to standard models (Forestini 1994, Montalbán & Rebolo 2002), at a given metallicity there is a mass range, where ^6Li but not ^7Li is being destroyed. These models predict that no ^6Li can survive pre-MS mixing in metal-rich solar-type stars. We note, however, that the mass and the depth of the convection zone also depend on the metal content of the star, and for this reason several old metal-poor stars have preserved a fraction of their initial ^6Li nuclei (Cayrel et al. 1999). In any case, these results suggests that any detected ^6Li in a metal-rich solar-type star would most probably be a signal of an external source, that is, accretion of planetary-like material (Sandquist et al. 2002). It is worth mentioning that ^6Li cannot be produced in large quantities in stellar flares, although some is produced (Ramaty et al. 2000).

The first ^6Li detection in a planet host star was reported by Israelian et al. (2001, 2003) in HD82943, a star which hosts two planets. This is an old and non active G0 dwarf with an effective temperature of 6010 K, $[\text{Fe}/\text{H}]=+0.32$ and $\log N(\text{Li}) \sim 2.5$. They found an isotopic ratio $^6\text{Li}/^7\text{Li} \sim 0.05$ (see Fig. 2), which may be explained by infall of $1 M_J$ or equivalent, a value that would not significantly alter the stellar metallicity.

Observations of ^6Li are very difficult because it is a weak component of the much stronger doublet of ^7Li . Moreover, in metal-rich stars, blending with other weak absorptions becomes important. This makes the detection of this isotope a controversial fact. For instance, Reddy et al.(2002) did not find signatures of ^6Li in HD82943, although they were using a blend of TiI in the Li region, instead of the SiII line used by Israelian et al. (2003). Other authors have also not found similar detections in other

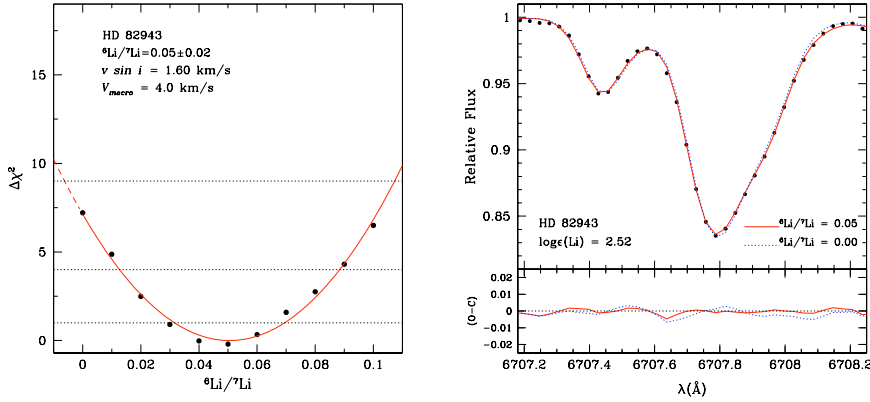


Figure 2. *Left panel:* Results from the χ^2 analysis for the ${}^6\text{Li}/{}^7\text{Li}$ ratio. $\Delta\chi^2 = 1, 4$, and 9 correspond to $1, 2$ and 3σ confidence limit (dotted lines). Continuum adjustments were allowed within 0.2% . *Right panel:* Comparison of the observed (filled large dots) and synthetic spectra of HD 82943 corresponding to ${}^6\text{Li}/{}^7\text{Li} = 0.05$ (continuous) and ${}^6\text{Li}/{}^7\text{Li} = 0$ (dotted) isotopic ratios. They correspond to the best fits with $f({}^6\text{Li}) = 0$ and a wavelength offset of -0.65 km s^{-1} (small dots) and to the $f({}^6\text{Li}) = 0.05$ with a wavelength offset of -0.44 km s^{-1} (continuous line). Fits to the blue wing of the Li profile can be improved if we adopt the wavelengths of CN lines from Brault & Mueller (1975). The CN lines observed in the arc spectrum by these authors appear at 6707.55 \AA while Reddy et al. (2002) and Lambert et al. (1993) list them between 6707.464 and 6707.529 \AA . The residuals (O-C) of the observations after subtraction of the synthetic spectra are shown. Both plots are from Israelian et al. (2003).

planet host stars (Mandell et al. 2004, Ghezzi et al. 2009). Uncertainties in the line lists can indeed lead to wrong determinations of ${}^6\text{Li}$ abundance. Perhaps most importantly, the use of 3D models may change this panorama, since convection will produce an asymmetry in the ${}^7\text{Li}$ line similar to the one produced by the presence of ${}^6\text{Li}$ (Cayrel et al. 2008, Ghezzi et al. 2009). This problem may affect the determination of ${}^6\text{Li}$ abundances not only for metal-rich planet host stars but also for their metal poor counterparts (see discussion in reviews by Asplund, Spite, Melendez, and Steffen, this Volume).

In any case, present results suggest that signs of “massive” pollution are not generalized in planet host stars.

3. ${}^7\text{Li}$

The more common lithium isotope ${}^7\text{Li}$ was produced during Big Bang nucleosynthesis and it can be produced in stellar interiors during AGB phase. It is depleted at a temperature of 2.5 million K primarily during the PMS in solar-type stars but it can also be destroyed in stellar envelopes during MS if any mixing process exists.

The light element ${}^7\text{Li}$ can also be used to trace pollution events. For instance, Deliyannis et al. (2002) discovered an extremely Li-rich dwarf, J37, a F-star in the open cluster NGC6633 (see Fig.3). Firstly they suggested upward, radiatively driven diffusion as the best explanation for this Li overabundance. However, later studies demonstrated a high Be abundance too (Ashwell et al. 2005), a result that is in contradiction with radiative diffusion models. Furthermore, Laws & Gonzalez (2003) showed that refractory elements

were also overabundant, arriving at the conclusion that this star had accreted volatile-depleted material.

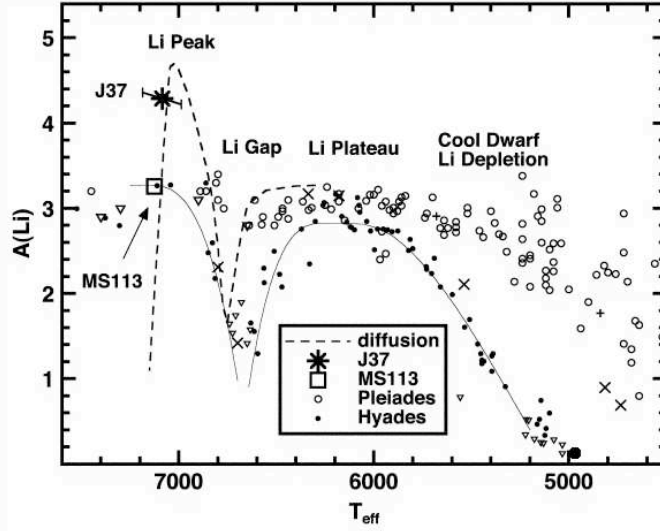


Figure 3. *Left panel:* Li abundances in the Hyades (detections: filled circles; upper limits: small inverted triangles; short-period binaries: multi crosses) and Pleiades (detections: open circles; upper limits: large inverted triangles; short-period binaries: plus signs) open clusters, in J37, and in MS113. From Deliyannis et al. (2002).

A study of the differences of Li abundances in stars with and without planets was first carried out by King et al. (1997). In that work they measured Li abundances for the binary system formed by 16CygA, a star without planets and a detectable Li abundance, and 16CygB, a planet-host that is Li depleted. This work was followed by several studies claiming that stars with planets have different Li abundances when compared to stars without detected companions (Cochran et al. 1997; Gonzalez & Laws 2000; Takeda & Kawanomoto 2005; Chen & Zhao 2006; Israelian et al. 2004, 2009), though these results are not consensual (e.g. Ryan 2000; Luck & Heiter 2006). A recent uniform study by Israelian et al. (2009) seems to confirm, however, that planet host stars have lower Li abundances in the solar temperature region (see Fig.4) and exclude metallicity, age, $v \sin i$, or activity as the cause of this anomaly (for more details see review by Israelian in this volume).

To explain the observed difference several possibilities exist. Pollution should be ruled out because it would have the opposite effect. On the other hand, it seems that stars with planets might have a different evolution. Extra mixing due to planet-star interaction, like migration, could take place (Castro et al. 2009). The infall of planets might also affect the mixing processes of those stars (Theado et al., *in prep.*). Finally a long-lasting star-disc interaction during PMS may cause planet hosts to be slow rotators and develop a high degree of differential rotation between the radiative core and the convective envelope, also leading to enhanced lithium depletion (Bouvier 2008).

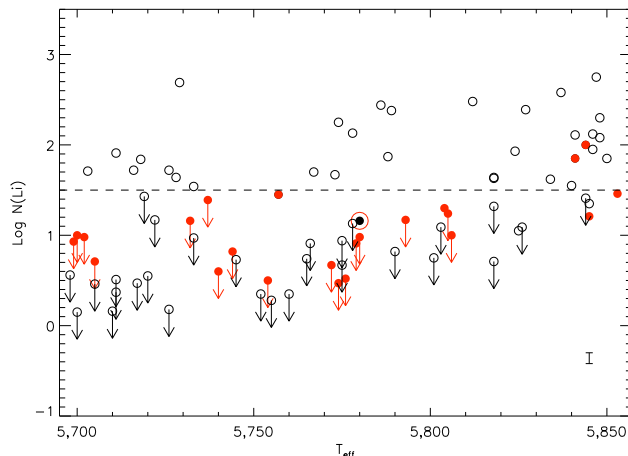


Figure 4. Li abundances as a function of effective temperature for stars with (red filled circles) and without known planets (open circles), from Israelian *et al.* (2009).

4. Be

Be is mainly produced by spallation reactions in the interstellar medium while it is burned in the hot stellar furnaces at a temperature of 3.5 million K. Li is depleted at much lower temperatures than Be. Thus, by measuring Li in stars where Be is not depleted (early-G and late-F) and Be in stars where Li is depleted (late-G and K) we can obtain crucial information about the mixing, diffusion and angular momentum history of exoplanets hosts (Santos *et al.* 2002). Measurements of the abundance of this element are however difficulted by the fact that the only available lines are in the near-UV, a very blended region in metal-rich stars (Fig.5).

There are not many works about Be abundances in planet host stars in the literature. Some of the first works made (García López & Pérez de Taoro 1998; Deliyannis *et al.* 2000), had a very small number of objects. In Fig.6 the largest samples made at the moment are plotted together, showing Be abundances as a function of effective temperature (Santos *et al.* 2002, 2004b; Gálvez-Ortiz *et al.* 2009; Delgado Mena *et al.*, *in prep.*).

At a first sight, there are not clear differences between stars with and without planets. Globally, Be abundances decrease from a maximum at 6100 K towards both higher and lower temperatures, in a similar way as Li abundances behave. In the high temperature domain, the steep decrease with increasing temperature resembles the well-known Be gap for F-stars (Boesgaard *et al.* 1999). The decrease of the Be content towards lower temperatures is smoother and may show evidence for continuous Be-burning during the main-sequence evolution of these stars.

In the temperature range where Li abundances are different in stars with and without planets, we do not observe any difference in Be abundances. This is something we can expect because for those temperatures, convective envelopes are not deep enough to bring the material of the convective envelope down to the layers where the temperature is high enough to burn Be. On the other hand, for the lowest temperatures of the range it seems that stars with planets have lower abundances when compared with stars for which no planet has been discovered. Unfortunately, the number of comparison stars in that temperature regime is still small to allow us to take a strong conclusion.

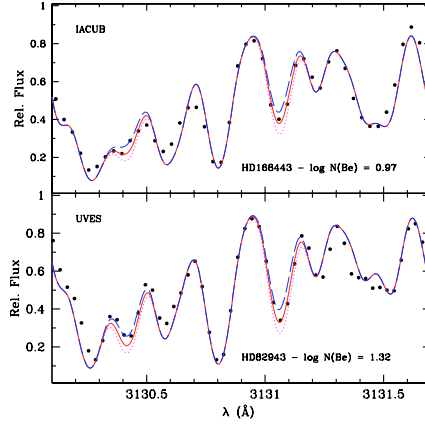


Figure 5. Spectra in the BeII region (dots) for HD168443 and HD82943, and three spectral synthesis with different abundances, corresponding to the best fit (solid line) and to changes of ± 0.2 dex, respectively. From Santos et al. (2002).

In addition, in the low temperature region we find very low abundances of Be, in contradiction with models of Be depletion. In Fig.6, models with different initial rotation rates have been overplotted (Pinsonneault et al. 1990). As already noticed in Santos et al. (2004b,c), these models agree with the observations above roughly 5600 K, but while the observed Be abundance decreases towards lower temperatures when $T_{eff} < 5600$, these models predict either constant or increasing Be abundances. Even taking into account mixing by internal waves (Montalbán & Schatzman 2000), Be depletion is still lower than observed. Although uncertainties in Be abundances for the coolest stars are large (significant systematic errors are not excluded), Be abundances are still overestimated by models.

5. Conclusions

In this paper we reviewed the main results concerning the study of light element abundances in stars with planets. The main conclusions can be listed as follows.

- ^6Li shows evidence that stars with planets may suffer (isolated) pollution events. However, the difficulty in deriving reliable abundances of this isotope makes this a very debatable issue. An improvement of the line lists and in the determination of convective blue shifts is needed to understand how frequent are pollution events.
- ^7Li has been found to be more depleted in stars with planetary companions in contrast with what happens in stars without detected planets. This trend is only observable in stars with temperatures in the solar range. This result suggests that some mechanisms is acting that is responsible for a higher Li depletion in planet-host stars.
- Be abundances in stars with and without planets do not follow the trend found for Li. No clear Be abundance differences seem to exist between the two groups of stars. More data is needed, specially for cooler stars, to understand the actual disagreements with the models for those temperatures.

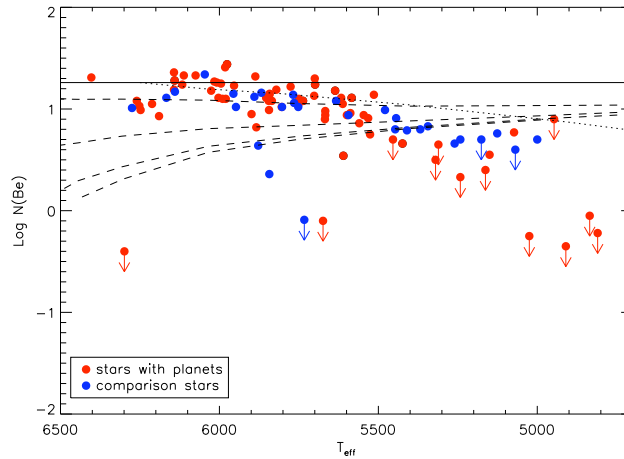


Figure 6. Be abundances as a function of effective temperature for stars with (red circles) and without planets (blue circles). The dashed lines represent 4 Be depletion models of Pinsonneault et al. (1990) (Case A) with different initial angular momentum for solar metallicity and an age of 1.7 Gyr. The solid line represents the initial Be abundance of 1.26. The dotted line represents the Be depletion isochrone for 4.6 Gyr taken from the models including mixing by internal waves of Montalbán & Schatzman (2000).

Acknowledgements

NCS would like to thank the support by the European Research Council/European Community under the FP7 through a Starting Grant, as well from Fundação para a Ciência e a Tecnologia (FCT), Portugal, through a Ciência2007 contract funded by FCT/M CTES (Portugal) and POPH/FSE (EC), and in the form of grants reference PTDC/CTE-AST/098528/2008 from FCT/MCTES.

References

- Ashwell, J. F., Jeffries, R. D., Smalley, B., Deliyannis, C. P., Steinhauer, A. & King, J. R. 2005, *MNRAS*, 363, 81
- Boesgaard, A. M., Deliyannis, C. P., King, J. R., Ryan, S. G., Vogt, S. S. & Beers, T. C. 1999, *AJ*, 117, 1549
- Boss, A. P. 1997, *Science*, 276, 1836
- Boss, A. P. 2002, *ApJ*, 567, 149
- Bouvier, J. 2008, *A&A*, 489, 53
- Brault, J.W., & Mueller, E.A. 1975, *Solar Physics*, 41, 43
- Brown, J. A., Sneden, C., Lambert, D. L. & Dutchover, E. Jr. 1989, *ApJS*, 71, 293
- Castro, M., Vauclair, S., Richard, O. & Santos, N. C. 2009, *A&A*, 494, 663
- Cayrel, R., Lebreton, Y. & Morel, P. 1999, *Ap&SS*, 265, 87
- Cayrel, R., Steffen, M., Bonifacio, P., Ludwig, H.-G. & Caffau, E. 2008, *nuco.conf*, E, 2C
- Chen, Y. Q. & Zhao, G. 2006, *Aj*, 131, 1816
- Cochran, W. D., Hatzes, A. P., Butler, R. P. & Marcy, G. W. 1997, *ApJ*, 483, 457
- Deliyannis, C. P., Cunha, K., King, J. R. & Boesgaard, A. M. 2000, *AJ*, 119, 2437
- Deliyannis, C. P., Steinhauer, A. & Jeffries, R. D. 2002, *ApJ*, 577, 39
- Gálvez-Ortiz, M. C., Delgado Mena, E., González Hernández J. I., Israelian, G., Santos, N.C. & Rebolo, R. 2009, *A&A*, submitted
- García López, R. J. & Pérez de Taoro, M. R. 1998, *A&A*, 334, 599

- Fischer, D.A. & Valenti, J. 2005, *AJ*, 622, 1102
- Forestini, M. 1994, *A&A*, 285, 473
- Ghezzi, L., Cunha, K., Smith, V. V., Margheim, S., Schuler, S., de Arajo, F. X. & de la Reza, R. 2009, *ApJ*, 698, 451
- Gonzalez, G. 1998, *A&A*, 334, 221
- Gonzalez, G. & Laws, C. 2000, *AJ*, 119, 390
- Guillot, T., Santos, N. C., Pont, F., Iro, N., Melo, C. & Ribas, I. 2006 *A&A* (Letters), 453, 21
- Israelian, G., Santos, N. C., Mayor, M. & Rebolo, R. 2001, *Nature*, 411, 163
- Israelian, G., Santos, N. C., Mayor, M. & Rebolo, R. 2003, *A&A*, 405, 753
- Israelian, G., Santos, N. C., Mayor, M. & Rebolo, R. 2004, *A&A*, 414, 601
- Israelian, G., Delgado Mena, E. Santos, N. C., Sousa, S. G.; Mayor, M., Udry, S., Domnguez Cerdea, C., Rebolo, R. & Randich, S. 2009, *Nature*, 462, 189
- King, J. R., Deliyannis, C. P., Hiltgen, D. D., Stephens, A., Cunha, K. & Boesgaard, A. M. 1997 *AJ*, 113, 1871
- Laws, C & Gonzalez, G. 2001, *ApJ*, 553, 405
- Laws, C & Gonzalez, G. 2003, *ApJ*, 595, 1148
- Luck, R. E. & Heiter, U. 2006, *AJ*, 131, 3069
- Mandell, A. M., Ge, J. & Murray, N. 2005, *AJ*, 127, 1147
- Mayor, M. & Queloz, D. 1995, *Nature*, 378, 355
- Melo, C. H. F., de Laverny, P., Santos, N. C., Israelian, G., Randich, S., Do Nascimento, J. D., Jr. & de Medeiros, J. R. 2005, *A&A*, 439, 227
- Montalbán, J. & Schatzman, E. 2000, *A&A*, 354, 943
- Montalbán, J. & Rebolo, R. 2002, *A&A*, 386, 1039
- Mordasini, C., Alibert, Y., Benz, W. & Naef, D. 2009, *A&A*, 501, 1161
- Pasquini, L., Dllinger, M. P., Hatzes, A., Setiawan, J., Girardi, L., da Silva, L., de Medeiros, J. R. & Weiss, A. 2008a, *IAUS*, 249, 209
- Pasquini, L., Biazzo, K., Bonifacio, P., Randich, S. & Bedin, L. R. 2008b, *A&A*, 489, 677
- Pinsonneault, M. H., Kawaler, S. D. & Demarque, P. 1990, *ApJS*, 74, 501
- Pollack, J. B., Hubickyj, O., Bodenheimer, P., Lissauer, J. J., Podolak, M. & Greenzweig, Y. 1996, *Icarus*, 124, 62
- Ramaty, R., Tatischeff, V., Thibaud, J. P., Kozlovsky, B. & Mandzhavidze, N., 2000, *ApJ* (Letters), 534, 207
- Reddy, B. E., Lambert, D. L., Laws, C., Gonzalez, G. & Covey, K. 2002, *MNRAS*, 335, 1005
- Ryan, S. G. 2000, *MNRAS*, 316, 35
- Sandquist, E. L., Dokter, J. J., Lin, D. N. C. & Mardling, R. A. 2002, *ApJ*, 572, 1012
- Santos, N. C., Israelian, G. & Mayor, M. 2000, *A&A*, 363, 228
- Santos, N. C., Israelian, G. & Mayor, M. 2001a, *A&A*, 373, 1019
- Santos, N. C., García López, R. J., Israelian, G., Mayor, M., Rebolo, R., García-Gil, A., Pérez de Taoro, M. R. & Randich, S. 2002, *A&A*, 386, 1028
- Santos, N. C., Israelian, G., Mayor, M., Rebolo, R. & Udry S. 2003, *A&A*, 398, 363
- Santos, N. C., Israelian, G. & Mayor, M. 2004a, *A&A*, 415, 1153
- Santos, N. C., Israelian, G., Randich, S., García López, R. J. & Rebolo, R. 2004b, *A&A*, 425, 1013
- Santos, N. C., Israelian, G., García López, R. J., Mayor, M., Rebolo, R., Randich, S., Ecuivillon, A. & Domnguez Cerdea, C. 2004c, *A&A*, 427, 1085
- Shen, Z.-X., Jones, B., Lin, D. N. C., Liu, X.-W. & Li, S.-L. 2005, *ApJ*, 635, 608
- Takeda, Y. & Kawanomoto, S. 2005, *PASJ*, 57, 45
- Udry, S. & Santos, N.C. 2007, *ARAA*, 45, 397
- Vauclair, S. 2004, *ApJ*, 605, 874



George Wallerstein



Verne Smith and Evan Skillman

Observations of Lithium in red giant stars

Verne V. Smith¹

¹National Optical Astronomy Observatory
950 N. Cherry Ave., Tucson, AZ 85719 USA
email: vsmith@noao.edu

Abstract. Connections between observations of the lithium abundance in various types of red giants and stellar evolution are discussed here. The emphasis is on three main topics; 1) the depletion of Li as stars ascend the red giant branch for the first time, 2) the synthesis of ⁷Li in luminous and massive asymptotic giant branch stars via the mechanism of hot-bottom burning, and 3) the possible multiple sources of excess Li abundances found in a tiny fraction of various types of G and K giants.

Keywords. Stars: abundances, late-type

1. Introduction

The connection between lithium and evolution along the red giant branch has a long history, going back to early work by Bonsack (1959), who noted that lithium abundances declined towards later spectral types, which was interpreted as astration of Li in deepening convective envelopes in cooler stars. A quantitative analysis and comparison with models of the effect of red giant evolution on lithium abundances was carried out by Wallerstein (1966), who was able to identify the Li I $\lambda 6707\text{\AA}$ line in both components of the double-lined spectroscopic binary Capella. Wallerstein found that the more luminous G-giant in the system had 60 times less Li than the less-evolved F-star component: the larger convective envelope of the G-giant had diluted its Li. The factor of 60 in dilution was in excellent agreement with predictions from stellar models by Iben (1965). Lithium had now become an important quantitative test of stellar evolution.

The simple evolution of the dilution of lithium from main sequence to red giant branch is not the whole story of “Lithium in Red Giants”, however, due to the complex evolution of stars, initially up the first ascent of the red giant branch (which is referred to here as RGB), followed by evolution along the asymptotic giant branch (AGB), with both destruction and possible synthesis of lithium taking place during different evolutionary phases.

This short summary of lithium in red giants is divided into three sections:

- observations of Li in predominantly RGB stars, where mostly dilution/destruction occurs.
- the behavior of Li in AGB stars, where both destruction, as well as synthesis of ⁷Li (via so-called “hot bottom burning”) can take place.
- the nature of Li-rich G- and K-giant stars, where only dilution is nominally expected.

2. Lithium in first-ascent red giants

Due to the deepening convective envelope that occurs as stars evolve from the main sequence to the RGB, it is expected that the lithium abundance in RGB stars, in general, will be much lower than that observed in main sequence stars that have not destroyed their surface Li. By and large, this simple prediction has been born out by surveys of red

giants; two early quantitative abundance surveys contained 81 stars of spectral types G, K, and M by Lambert, Dominy, & Sivertson (1980) and Luck & Lambert (1982).

A more extensive survey of 644 G and K giants was presented by Brown et al. (1989) and their abundance results are summarized in histogram form in Figure 1. In Figure 1 the number of stars is plotted versus the lithium abundance, where $A(\text{Li})$ is the standard spectroscopic definition of $A(x) = \log[N(x)/N(\text{H})] + 12.0$. The arrow indicates the solar system meteoritic abundance ($A(\text{Li}) = 3.25$) and the shift of the red giants to lower abundances is clear. Below abundances of about $+0.50$ in $A(\text{Li})$, the histogram is dominated by upper limits (that is, non-detections of the Li I $\lambda 6707\text{\AA}$ line), so the real abundance distribution tails off to even lower Li abundances. There are two main points to take from Figure 1, the first of which is that the overall abundance distribution contains a large fraction of red giants with lower Li abundances than were predicted from standard convective dilution, thus suggesting that extra-mixing processes on the RGB removed more Li from the surface. The second point is that Brown et al. (1989) were able to quantify the percentage of G and K giants which contain more Li than predicted (giants with $A(\text{Li}) \geq 1.5$ are considered to be “Li rich”); this small number of Li-rich giants can be seen in Figure 1. The number of Li-rich giants is roughly $\sim 1\%$ of the total (this topic will be discussed further in Section 4).

Gratton et al. (2000) conducted a survey of field metal-poor giants to study mixing, with lithium being included as one of their tests. One of the advantages in the Gratton et al. study, was that the luminosities of their sample giants could be estimated reasonably well, so that $A(\text{Li})$ could be investigated as a function of position on the RGB. The top panel of Figure 2 summarizes the results from Gratton et al. (2000), with $A(\text{Li})$ shown versus luminosity. The vertical dashed lines indicate the approximate luminosity of two important locations in an HR diagram; the first one shows the approximate location of the base of the RGB (at $\log(L/L_\odot) \sim +0.8$), while the second illustrates roughly where the RGB luminosity “bump” falls in low-mass low-metallicity giants. The dramatic drop in the Li abundance at the beginning of evolution up the RGB stands out clearly, with the abundance of lithium then remaining roughly constant, until another drop at the RGB bump. Displayed as in Figure 2, the evolution of the lithium abundance in most RGB stars seems reasonably well-defined.

Recent work on Li depletion along the RGB has focused on the globular cluster NGC6397, with studies by Korn et al. (2007) or Lind et al. (2009). In the case of a globular cluster, such as NGC6397, the advantage is that the luminosity (or put another way, the position on the RGB) is very well determined. The bottom panel of Figure 2 shows results from the Korn et al. (2007) study, where their results for 18 stars are averaged into 4 distinct evolutionary points: in increasing luminosity, the subgiant branch, the base of the RGB, the lower RGB, and the upper RGB. The overall behavior of $A(\text{Li})$ in the NGC6397 stars closely matches that for the metal-poor low-mass field giants from Gratton et al. (2000—the top panel of Figure 2). The recent work on NGC6397 (Korn et al. 2007; Lind et al. 2009) includes diffusion in their modelling and the results between Li depletion predicted by theory and what is observed is quite good.

Progress continues to be made using lithium to probe RGB evolution, e.g. Lagarde et al. (2009, this symposium) presents Li abundances in a large sample of field red giants, with luminosities derived from Hipparcos parallaxes, which were not available to Brown et al. (1989). It can be stated that our understanding of the behavior of Li abundances along the RGB is much better than it was compared to just a few years ago.

3. Lithium in hot-bottom burning asymptotic giant branch stars

Asymptotic Giant Branch stars are well-known producers of ^{12}C , with this primary carbon-12 produced during phases of shell- ^4He -burning in thermal pulses, which drive convective mixing of ^{12}C -rich material to the stellar surface. This mixing results in the evolutionary sequence running from the oxygen-rich ($\text{C}/\text{O} \leq 1$) M-type giants to the carbon stars ($\text{C}/\text{O} \geq 1$). In addition to the production of ^{12}C , the mixing between He-burning shell and H-rich envelope results in the release of free neutrons via the chain $^{12}\text{C}(\text{p}, \gamma)^{13}\text{N}(\beta^+, \nu)^{13}\text{C}(\alpha, \text{n})^{16}\text{O}$. These neutrons drive the s-process and synthesize the neutron-rich nuclei heavier than Fe (such as Zr or Ba).

The synthesis of ^{12}C and the s-process elements, followed by dredge-up (the so-called “third dredge-up”) to produce C- and s-process-rich AGB stars, occurs in a large fraction of AGB stars from $M \sim 1\text{--}8M_{\odot}$, with the exact mass limits depending on stellar metallicity. Another process, referred to as “hot-bottom burning” (HBB), first studied in model stars by Scalo, Despain, & Ulrich (1975), occurs in the more massive AGB stars (say $M \geq 4M_{\odot}$) and can result in the production of ^7Li via the Cameron-Fowler mechanism (Cameron & Fowler 1971).

As a result of HBB, very Li-rich AGB stars can be created and observations pointed

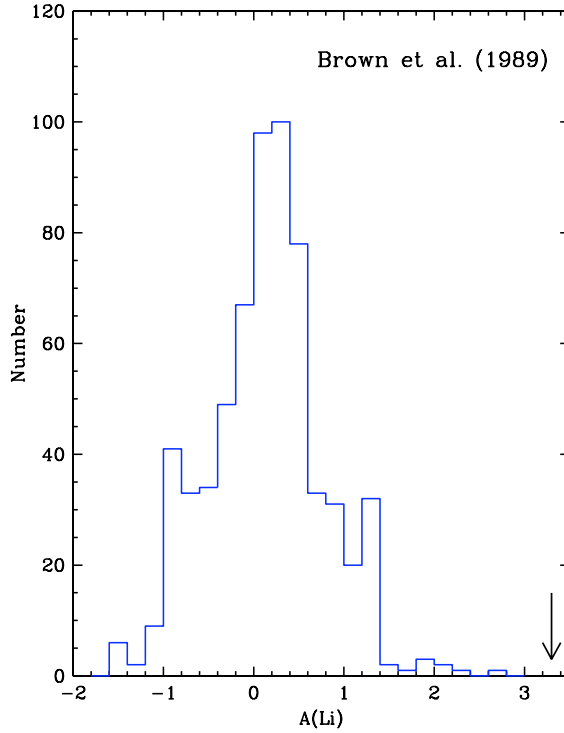


Figure 1. The distribution of lithium abundances in 644 G and K giants from Brown et al. (1989). Note that non-detections dominate the statistics below $A(\text{Li}) \sim +0.5$. The distribution of abundances suggests that extra-mixing and more astration of Li occurs on the RGB, with about $\sim 1\%$ of the giants being “Li rich”. The arrow indicates the solar system value of $A(\text{Li})$.

in this direction long before any understanding of internal nucleosynthesis in AGB stars. McKellar (1940) observed a very strong Li I $\lambda 6707\text{\AA}$ line in the carbon star WZ Cas and suggested that this star had “an unusually high abundance of lithium”. A survey of 30 disk carbon stars was conducted by Torres-Peimbert & Wallerstein (1966), who found some 16 of these stars to exhibit substantial Li I lines. The phenomenon of Li-rich AGB stars was extended to the S-stars (AGB stars with enhanced s-process and carbon-12 abundances, but with C/O still less than 1.0) with Keenan’s (1967) detection of a strong Li I line in T Sgr.

Quantitative lithium abundance analyses of S stars began with Boesgaard (1970), who found very large abundances in a few S stars (including T Sgr), with values as large as $A(\text{Li}) \sim 4.0$ ($\sim 10\times$ the solar system abundance). Observationally measured luminosities of HBB Li-rich AGB stars was placed on a firmer footing by observations of such stars in

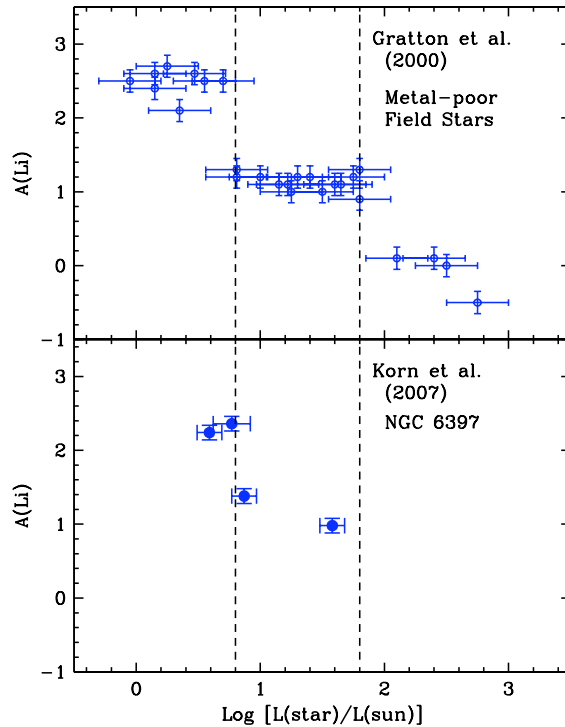


Figure 2. The top panel shows results from Gratton et al. (2000) lithium abundances in metal-poor low-mass field stars plotted versus luminosity. The vertical dashed lines mark the approximate luminosities of the base of the RGB (left line) and the RGB luminosity bump (right line). The precipitous drop on $A(\text{Li})$ as stars evolve onto the RGB is clear, with another decline near the location of the RGB bump. The bottom panel illustrates lithium abundances in stellar members of the globular cluster NGC6397 from Korn et al. (2007). The 4 points are averages from a sample of 18 stars, with the points representing stars on the subgiant branch, the base of the RGB, the lower RGB, and upper RGB. The behavior of the lithium abundance in the low-mass low-metallicity stars in NGC6397 is similar to those in the field-star sample from Gratton et al. (2000).

the Magellanic Clouds (Smith & Lambert 1989; 1990; Plez et al. 1993; Smith et al. 1995), since the distances to the LMC and SMC are quite well known. More recently, attention has turned back to the Milky Way, with work by Garcia-Hernandez et al. (2007), who determined Li abundances (along with other elements, including the s-process) in luminous Galactic AGB stars. A convenient way to view the combined lithium abundances in Galactic, LMC, and SMC luminous AGB stars is illustrated in Figure 3, where $A(\text{Li})$ is plotted versus pulsational period (all of these cool stars are long period variables). The overall trend is for the period to increase with increasing luminosity, so this figure shows the somewhat abrupt increase in lithium for periods greater than about 300-400 days. This figure also demonstrates that although ${}^7\text{Li}$ can be produced in amounts larger than that found in the current disk ISM, it can also be destroyed, so there is a wide distribution of lithium abundances in the luminous AGB stars; the exact net amount of ${}^7\text{Li}$ that might be contributed by these types of stars to chemical evolution remains uncertain, primarily due to uncertainties in how mass loss occurs along the AGB. Stellar models of HBB along the AGB by Sackmann & Boothroyd (1992) can produce the upper envelope of $A(\text{Li})$ observed in Figure 3 for stellar masses of $4\text{-}6M_{\odot}$ at $M_{\text{Bol}} \sim -6.2$ to -6.8 .

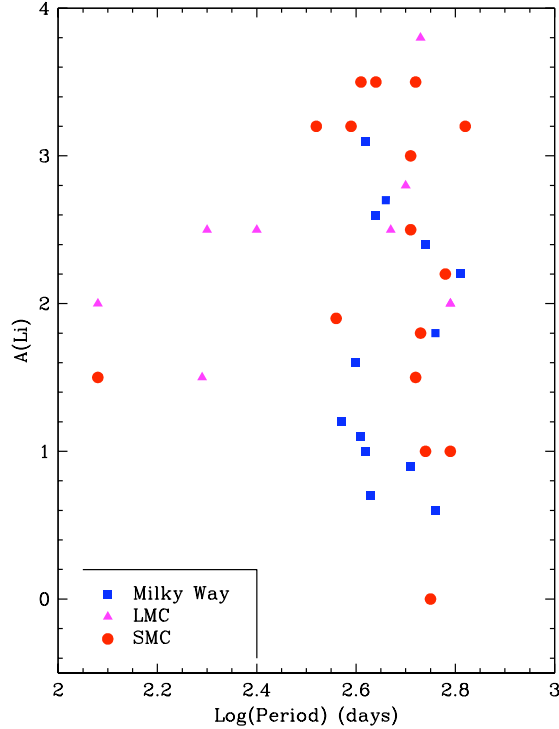


Figure 3. Lithium abundances versus pulsational period for luminous Galactic AGB stars from Garcia-Hernandez et al. (2007; filled blue squares) and for luminous SMC and LMC AGB stars from Smith et al. (1995); filled red circles for the SMC and filled magenta triangles for the LMC. The upper envelope of $A(\text{Li})$ is predicted by models of HBB in AGB stars by Sackmann & Boothroyd (1992).

One interesting consequence of HBB in AGB stars is the conversion of primary ^{12}C (sometimes lots of it) into ^{14}N via the CN-cycle taking place within the deep convective envelope itself. The drop in ^{12}C abundance can result in the surface C/O ratio falling below 1.0, and the transformation of a carbon star back into an oxygen-rich star (in this case, since it would be s-process enriched star, it would be an S-star). This effect is illustrated in Figure 4 for the LMC, where the C-star luminosity function from Iben (1981) is shown compared to the location, in luminosity space (with luminosity indicated by M_{Bol}), of the Li-rich S-stars. At the bolometric luminosity at which the number of C-stars drops to zero, the appearance of Li-rich S-stars takes place, with the lithium indicating the onset of HBB. With enough conversion of ^{12}C to ^{14}N in the hot envelopes of these stars, the C/O ratio is driven back down below unity and former carbon stars transform to S-stars.

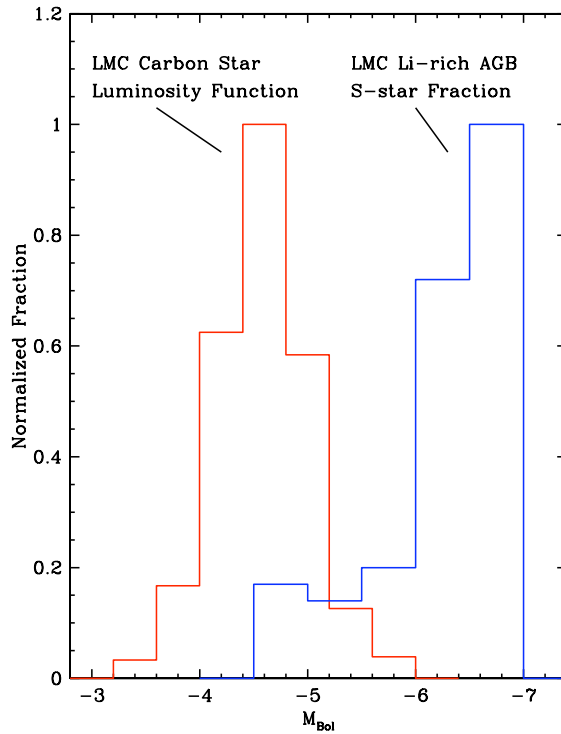


Figure 4. The carbon-star luminosity function for the LMC from Iben (1981) is shown as the lefthand histogram. On the right is plotted the fraction of AGB S-stars that are Li-rich in the LMC (Smith et al. 1995). Note that the fraction of Li-rich AGB stars with $\text{C}/\text{O} \geq 1.0$ increases at about the same luminosity that the C-star luminosity function falls to zero; this transition between the two distributions represents the onset of hot bottom burning, the production of lithium and the conversion of carbon stars to luminous S-stars.

4. The mysterious Lithium-rich red giants

As discussed in Section 2, stellar evolutionary models predict that lithium will be depleted during the first ascent of the RGB, with the amount of this depletion being 1 to 2 orders of magnitude. It was not expected that there would be significant sources of Li in stars evolving along the RGB, until the possible onset of HBB in massive, luminous AGB stars (the subject of Section 3). However, the discovery of an unexpectedly high lithium abundance ($A(\text{Li})=2.7$) in the K-giant HD112127 by Wallerstein & Sneden (1982) demonstrated that the behavior of Li in RGB stars was not simple. The subsequent survey by Brown et al. (1989—see Figure 1) showed that about 1% of G and K giants exhibit excess Li abundances (i.e., $A(\text{Li}) \geq 1.5$).

Continuing studies found additional examples of Li-rich RGB stars, with the interesting observation by Fekel & Balachandran (1993) that a significant fraction of the Li-rich giants are rapidly rotating (with $v \sin i \geq 8 \text{ km-s}^{-1}$). In addition, de la Reza et al. (1996) found that these peculiar giants were surrounded by spatially extended, faint dust shells, as revealed in IRAS colors. Charbonnel & Balachandran (2000) found that the so-called “super Li-rich” giants (with $A(\text{Li}) \geq 3.3$) tended to be found in a specific location of the H-R Diagram, near the luminosity bump at $\log(L/L_\odot) \sim 1.4 - 1.9$ and $T_{\text{eff}} \sim 4450 - 4600 \text{ K}$. The combination of rapid rotation, dust shells which suggest mass-loss episodes, and location in a single part of the HR Diagram has led to a picture in which the excess Li has been produced within the RGB star (via the Cameron Fowler mechanism) and carried to the surface. This dredge-up episode also carried angular momentum from the more rapidly rotating interior and drove a mass loss event. The exact physical mechanism remains elusive, but may be the only viable hypothesis to explain the location of the super Li-rich giants near the luminosity bump.

In addition to the Li-rich RGB stars found in the disk, 3 Li-rich giants have been found in globular clusters; one each in the clusters M5 (Carney et al. 1998), NGC362 (Smith et al. 1999), and M3 (Kraft et al. 1999). Since the globular clusters have well-defined stellar populations and distances, it is straightforward to place these stars in an H-R Diagram. Figure 5 summarizes the locations of the Li-rich G and K giants in a $\log L - T_{\text{eff}}$ plane and it is immediately clear that the super Li-rich giants (filled circles) are in a distinctly different evolutionary state than the Li-rich globular cluster giants, which turn out to be AGB, or even post-AGB stars. Since the globular cluster AGB stars are not massive enough to have undergone HBB, the source of the lithium must be from a different mechanism. It is also worth noting that there is no evidence of rapid rotation in the 3 Li-rich globular cluster giants. One is tempted to conclude that different physical mechanisms are driving the mixing (if it is internal mixing) in these two classes of Li-rich giants.

Finally in Figure 5, we note the filled squares which represent rapidly rotating Li-rich G and K giants found by Carlberg et al. (2009b), and which extend to luminosities well below the luminosity bump. Carlberg et al. (2009b) speculate that these objects may result from the ingestion of closely orbiting large planets or brown dwarfs as the parent star evolves up the RGB. Simulations of the future evolution of known star-hot Jupiter systems by Carlberg et al. (2009a) suggest that such ingestion will occur, typically near the base of the RGB, and would result in an increase in the stellar surface Li abundance, as well as spin-up of the convective envelope.

With such a variety of low-mass giants exhibiting enhanced lithium abundances spread across the H-R Diagram, it may well be that the phenomenon of the Li-rich G and K giants is caused by a number of different mechanisms. Observers and modelers have much to sort out in this particular area.

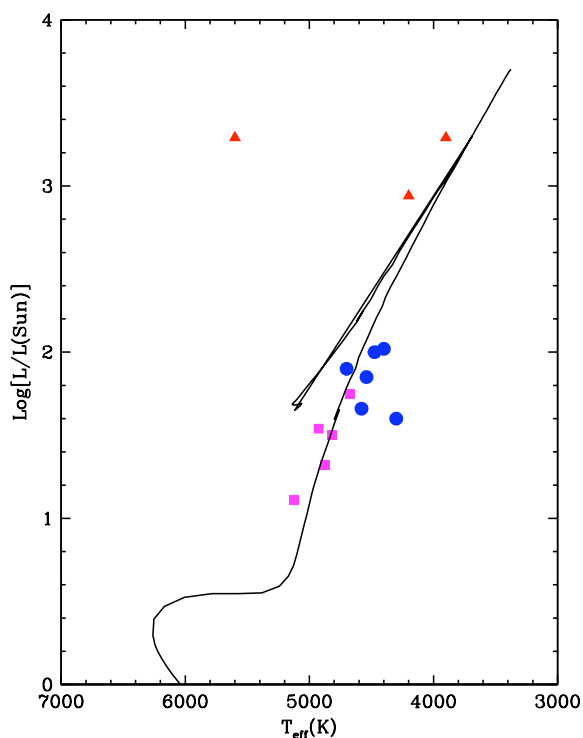


Figure 5. Luminosities and effective temperatures for samples of K-giants with enhanced lithium abundances. The filled triangles are stars in globular clusters from Carney et al. (1998) for M5, Smith et al. (1999) for NGC362, and Kraft et al. (1999) for M3. Filled circles are field K-giants discussed in Kumar & Reddy (2009), while the filled squares are rapidly-rotating Li-rich giants noted in Carlberg et al. (2009b). This type of diagram suggests that the “lithium-rich K-giant” phenomenon occurs over a wide evolutionary range and may be due to different processes, depending on the evolutionary state of the red giant. The solid line is a sample isochrone for a metallicity of -0.5 and an age of 9 Gyr (or a giant mass of about $1.3M_{\odot}$), not very different from the plotted giants; this stellar evolutionary track indicates that the Li-rich giants are found from near the base of the red giant branch to well along and past the AGB.

Acknowledgements

I wish to thank the meeting organizers for inviting me to present this review of a truly fascinating and rich topic, involving lithium and stellar evolution. I would also like to note that of the 3 main issues that were covered here, George Wallerstein (one of the meeting attendees) played key roles in the early stages of each one of them: he is an observational pioneer in this area. Since GW was my thesis advisor, I would also like to take this opportunity to thank him for introducing me, in his own unique style, to each of these topics and providing a background that stressed the key role of spectroscopy.

References

Boesgaard, A. M. 1970, *ApJ*, 161, 1003

- Bonsack, W. K. 1959, *ApJ*, 130, 843
- Brown, J. A., Sneden, C., Lambert, D. L., & Dutchover, E., Jr. 1989, *ApJS*, 71, 293
- Cameron, A. G. W., & Fowler, W. A. 1971, *ApJ*, 164, 111
- Carlberg, J. K., Majewski, S. R., & Arras, P. 2009a, *ApJ*, 700, 832
- Carlberg, J. K., Majewski, S. R., Smith, V. V., Cunha, K., Patterson, R. J., Bizyaev, D., Arras, P., Rood, R. T. 2009b, in: K. Cunha, M. Spite, & B. Barbuy (eds.), *Chemical Abundances in the Universe: Connecting First Stars to Planets* (Cambridge: Cambridge University Press), p.408
- Carney, B. W., Fry, A. M., & Gonzalez, G. 1998, *AJ*, 116, 2984
- Charbonnel, C., & Balachandran, S. 2000, *A&A*, 359, 563
- de La Reza, R., Drake, N. A., & da Silva, L. 1996, *ApJ* (Letters), 456, 456
- Fekel, F. C., & Balachandran, S. 1993, *ApJ*, 403, 708
- Garcia-Hernandez, D. A., Garcia-Lario, P., Plez, B., Manchando, A., D'Antona, F., Lub, J., Habing, H. 2007, *A&A*, 462, 711
- Gratton, R. G., Sneden, C., Carretta, E., Bragaglia, A. 2000, *A&A*, 354, 169
- Iben, I., Jr. 1965, *ApJ*, 142, 1447
- Iben, I., Jr. 1981, *ApJ*, 243, 987
- Keenan, P. C. 1967, *AJ*, 72, 808
- Korn, A. J., Grundahl, F., Richard, O., Mashonkina, L., Barklem, P. S., Collet, R., Gustafsson, B., Piskunov, N. 2007, *ApJ*, 671, 402
- Kraft, R. P., Peterson, R. C., Guhathakurta, P., Sneden, C., Fulbright, J. P., Langer, G. E. 1999, *ApJ*, 518, L53
- Kumar, Y. B., & Reddy, B. E. 2009, *ApJ* (Letters), 703, 46
- Lambert, D. L., Dominy, J. F., & Sivertsen, S. 1980, *ApJ*, 235, 114
- Lind, K., Primas, F., Charbonnel, C., Grundahl, F., Asplund, M. 2009, *A&A*, 503, 545
- Luck, R. E., & Lambert, D. L. 1982, *ApJ*, 256, 189
- McKellar, A. 1940, *PASP*, 52, 407
- Plez, B., Smith, V. V., & Lambert, D. L. 1993, *ApJ*, 418, 812
- Sackmann, I.-J., & Boothroyd, A. I. 1992, *ApJ*, 392, 71
- Scalo, J. M., Despain, K. H., & Ulrich, R. K. 1975, *ApJ*, 196, 805
- Smith, V. V., & Lambert, D. L. 1989, *ApJ* (Letters), 345, 75
- Smith, V. V., & Lambert, D. L. 1990, *ApJ* (Letters), 361, 69
- Smith, V. V., Plez, B., Lambert, D. L., Lubowich, D. A. 1995, *ApJ*, 441, 735
- Smith, V. V., Shetrone, M. D., & Keane, M. J. 1999, *ApJ* (Letters), 516, 73
- Torres-Peimbert, S., & Wallerstein, G. 1966, *ApJ*, 146, 724
- Wallerstein, G. 1966, *ApJ*, 143, 823
- Wallerstein, G., & Sneden, C. 1982, *ApJ*, 255, 577



Sofia Randich



Andreas Korn & Jeffrey Linsky

Mass loss and luminosities of S and C AGB stars with and without Li

Roald Guandalini¹, Sara Palmerini^{1,2}, Maurizio Busso^{1,2}, Enrico Maiorca^{1,2}, and Stefan Uttenthaler³

¹ Dipartimento di Fisica, Università degli Studi di Perugia,
via Pascoli, 06123, Perugia, Italy
email: guandalini@fisica.unipg.it

² I.N.F.N. sezione di Perugia

³ Instituut voor Sterrenkunde, K. U. Leuven,
Celestijnenlaan 200D, 3000 Leuven, Belgium

Abstract. We present the preliminary results of an analysis performed on two samples of thermally pulsing Asymptotic Giant Branch stars from our Galaxy, the first made of carbon-rich sources and the second of S-type stars. We have estimated their absolute luminosities and updated rates of the stellar winds through methods based on their infrared spectrophotometry and on updated estimates of their variability and distance.

We then focus on those sources in our database showing Li in their spectra looking for correlations between the Li abundance and the other physical parameters, in the aim of establishing observational criteria for understanding the conditions for the occurrence of the deep mixing phenomena to which the production of Li is currently attributed.

Keywords. Stars: evolution, AGB, post-AGB – infrared: stars

1. Introduction on Li and evolved giant stars

Stars evolving along the red giant branch are on average depleted in lithium. We remind here that, for low-metallicity objects, an upper limit on the Li content was set by Gratton et al. (2000), stating that low-mass stars on the upper RGB have $\log \epsilon(\text{Li}) \leq 0$. Mixing processes on the Main Sequence and up to the first dredge-up imply that Li be gradually carried down from the photosphere to regions of high temperature and destroyed; at the same time new Li is not produced, because any mixing mechanism occurring is so slow that the parent nucleus ${}^7\text{Be}$ has time to capture protons on the path. This explains why red giants are mainly Li-poor. It was further established (Sweigart & Mengel 1979) and confirmed by observations (Gilroy 1989, Gilroy & Brown 1991, Kraft 1994) that there must be slow mixing episodes in low-mass stars also after the first dredge-up. They gradually carry to the surface a considerable amount of ${}^{13}\text{C}$, so that the ${}^{12}\text{C}/{}^{13}\text{C}$ ratio decreases. These mixing phenomena can happen because after dredge-up, the H-burning shell advances into a homogeneous region, so that the natural barrier opposed to mass transport by a chemical stratification is not present. This happens in the so-called “L-bump phase”. Slow mixing processes occurring at or after the L-bump would further reduce the Li abundance. However, a few red giants (about 2%) show enhanced Li abundances at levels sometimes higher than in the present Interstellar Medium ($\log \epsilon(\text{Li}) \simeq 3.3$). Amongst the various explanations attempted, the most common assumption is that some form of fast extra-mixing might transport ${}^7\text{Be}$ from above the H-burning shell to the envelope at a speed sufficient to overcome the rate of p-captures. This is the so-called Cameron-Fowler mechanism (Cameron & Fowler 1971). The attempts at

involving stellar rotation as source for these extra-mixing processes were frustrated by the understanding that the stellar structure reacts to rotational distortions too quickly to induce significant mixing on long time scales (Palacios et al. 2006).

It has been suggested (Busso et al. 2007a, Wasserburg & Busso 2008, Nordhaus et al. 2008) that the processes that cause the mass transport might be linked to the buoyancy of magnetized H-burning ashes, based on the fact that magnetic bubbles are lighter than the stellar environment, due to the unbalance generated by magnetic pressure ($B^2/8\pi$). This requires a magnetic dynamo to occur in red giants, as indeed observed (Andrews et al. 1988). Magnetic buoyancy is an interesting possibility especially because it can occur at different speeds, depending on the amount of heat exchanged with the environment (Denissenkov et al. 2009, Palmerini & Busso 2008). Therefore, Li could experience production or destruction according to different mixing velocities.

In order to perform an accurate analysis on Li abundances and to attribute them to the correct evolutionary phases, we need reliable estimates of absolute luminosities and mass loss rates. Therefore, we here apply bolometric corrections for evolved stars, as derived in our recent work, to infer reliable estimates of these parameters (and of the distance) for stars having measurements of Li abundances in their photosphere. This helps in setting constraints on where extra-mixing is active. In Section 2 we discuss the analysis we performed and link it with our models. Instead, in Section 3 preliminary conclusions are illustrated.

2. Luminosities and mass loss rates of red giants showing Li

2.1. *The AGB sub-sample*

In order to improve our understanding of the evolutionary properties of Asymptotic Giant Branch stars (hereafter AGB) we need to study in an accurate way two crucial parameters: luminosities and mass loss rates. For both, determinations are hampered by the large distance uncertainties and by the fact that most of the radiation emitted by these sources can be observed only at infrared wavelengths and therefore depends on space-borne facilities, or on the exploitation of special ground-based locations.

In the last years we performed an extensive analysis of the photometric properties of AGB stars, using available infrared data from the ISO, MSX and IRAS-LRS experiments and looking for relations between their luminosities and their main chemical and physical parameters. In this way we are trying to find crucial tools that could help us in the improvement of the evolutionary models for AGB sources.

In the particular case of Li-bearing stars the formation of our sub-sample starts from the previous work by Uttenthaler et al. (2007) on AGB stars in the Galactic bulge with Li. We extend it to the Galactic AGB stars of the disk, already examined in their photometrical properties in our previous works (Guandalini et al. 2006, Guandalini & Busso 2008), with the aim of creating a homogeneous sub-sample with good estimates for mass and Li-abundances, good measurements of the distance and reliable near-to-mid infrared photometry. The resulting list of sources and all the details on the analysis performed are presented in Guandalini et al. (2009; Table 1). All sources come from large samples of C-rich or S-type AGB stars; the photometric data used and the techniques adopted are from Guandalini & Busso (2008), Busso et al. (2007b), and Guandalini et al. (2006).

2.2. *Luminosities and mass loss rates*

Figure 1 presents the selected sample of AGB stars showing Li in their spectra as compared with the luminosities obtained through the bolometric corrections from Guandalini

et al. (2006) [C-rich] and Guandalini & Busso (2008) [S-type]. The sources richest in Li are all of CJ type: we believe, also thanks to our analysis performed on C-rich galactic sources in Guandalini et al. (2006), that they are all source with peculiar evolutionary properties. Their high Li abundance can be produced either by a relatively fast extra-mixing in low-mass stars or by hot bottom burning in more massive AGB stars. Going down along the axis of the Li-abundance we find the four stars from the Galactic bulge discussed by Uttenthaler et al. (2007): they are all O-rich. We have marked by dashed lines the region occupied by “standard” C(N) sources (circles). They are divided into two groups according to the higher (full circles) or lower (empty circles) reliability of their distance estimate. For this group we can see that there seems to be a pattern for which more luminous sources are more depleted in Li and fainter ones are instead less depleted. This could be originated by two concurring phenomena: 1) more luminous Carbon stars are on average more evolved, so had more time to destroy Li; 2) more luminous Carbon stars could be the most massive ones (in a relatively small range of masses), therefore they could destroy Li more efficiently due to higher H-burning temperatures. If we look at the vertical dashed lines, they indicate the range of the luminosity function for Galactic C-rich sources from Guandalini et al. (2006). Our stars belong to the typical luminosity range of normal C-stars and cover all the interval, therefore we can conclude that our sample is a good representative for the standard galactic Carbon stars from the disk. We believe that also their Li abundances should represent typical trends. Finally, we see that the few S-type (or M) sources we have in our sample are more depleted in Li than the average standard Carbon star.

If we look at Figure 1 we see a pattern for which the more luminous C-rich AGBs are the more depleted in Li. In order to study this property we have to consider in the

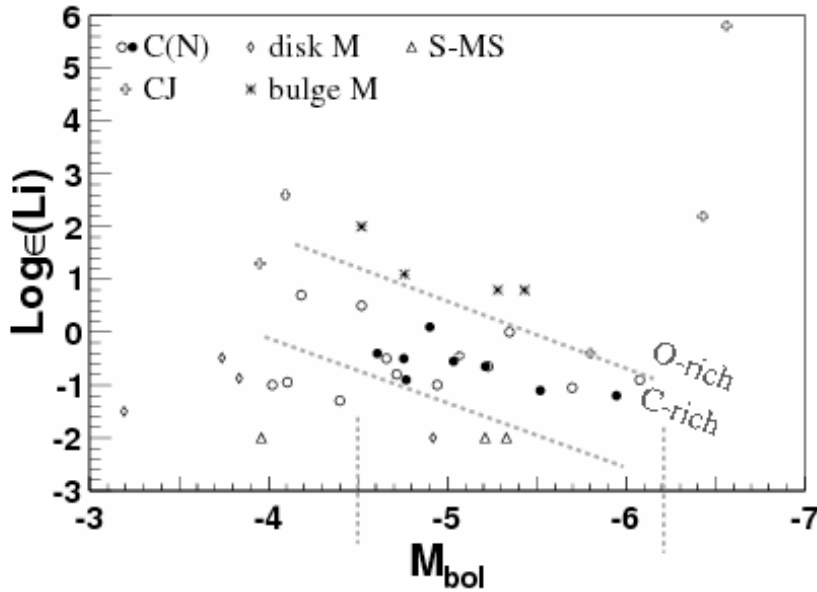


Figure 1. The sample of AGB stars showing Li in their spectra. Dashed lines roughly limit the region occupied by C(N) giants and their range of luminosities as inferred from the empirical Luminosity Function of Guandalini et al. (2006) (vertical lines).

picture also Red Giant Branch stars (hereafter RGB). Therefore, we add in the analysis a second sub-sample of RGB stars quite close to us, whose distances and Li-abundances are well-studied. The data for this group of K- and G-type sources are reported in Table 2 of Guandalini et al. (2009). In Figure 2 we consider both sub-samples in the same plot: RGB stars are the less luminous on the left side. The stars at the left of the plot, with $\log \epsilon(\text{Li}) \simeq 2$, are K giants with luminosities typical of the L-bump on the RGB. We consider them as being stars newly enriched in Li in agreement with Charbonnel & Balachandran (2000). After the extensive depletion of Li on the Main Sequence and on the early RGB phases, their envelopes must have seen some form of rapid mixing implementing a Cameron-Fowler mechanism. The second moderately Li-rich group is considered by us as being in the upper part of the RGB itself. Instead, Charbonnel & Balachandran (2000) interpreted this group as formed by early-AGB stars, producing Li (after some destruction in the late RGB phases). Inspection of stellar models, however, reveals that the early-AGB stages suitable to reproduce the luminosities and temperatures of these K giants fall in a temporal phase where the H-shell is extinguished, so that no ${}^7\text{Be}$ survives to be carried to the surface. We must therefore tentatively conclude that a new production of Li on the early-AGB at temperatures and luminosities compatible with observations does not occur and therefore the observed Li should be a relic of the previous production on the RGB. G-type stars show values of Li-abundance ranging between 0 and 1. They are not totally depleted but don't show the high values of K-type Li-rich sources. Finally, K-type sources without Li could be intermediate-mass stars with no hot bottom burning or low-mass stars with strong phenomena of depletion.

We searched also for possible relations between the rates of the stellar winds and Li-abundances for AGB stars. In order to estimate the rates, we adopted the methods

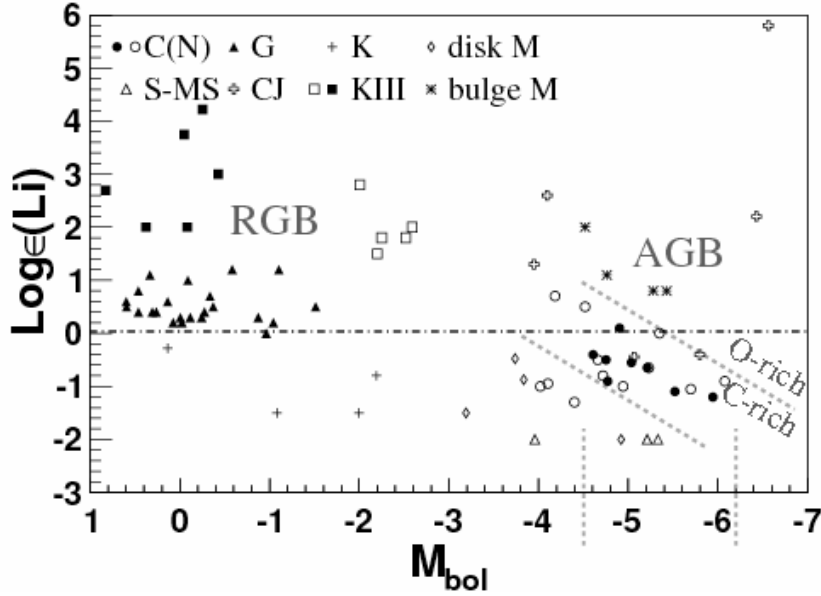


Figure 2. The same plot already presented in Figure 1, but including also the RGB sub-sample. See text and Guandalini et al. (2009) for details.

explained in detail in Guandalini et al. (2006) and Guandalini (2010). Unfortunately, we didn't find any apparent relation between these two parameters: the data have a too large scatter to draw any conclusion.

2.3. Link with the models

Our interpretation of the above results can be summarized in the following points [see Palmerini et al. (2010), this conference, for more details on this part]:

1) We observe in Figures 1 and 2 that Li is produced at the Luminosity bump and then is depleted with different rates during the successive evolution of the sources along the RGB and AGB stages.

2) We have so far no clear evidence for another phase of production after the L-bump.

3) This could be explained by the model presented by Palmerini et al. (2009) that suggests two types of extra-mixing. i) Fast Mixing, due to the buoyancy of small magnetized parcels, generated by detached magnetic instabilities. This causes ${}^7\text{Be}$ transport at rates faster than its decay lifetime (53 days) and therefore produces Li. This appears to happen at the bump of the Luminosity function following the first dredge-up. ii) Slow Mixing, due to the slower buoyancy of larger magnetized domains, which efficiently exchange heat with the environment, hence slowing down their motion. This happens during the remaining evolution and causes depletion of Li.

3. Conclusions

We have examined a sub-sample of Galactic AGB stars of moderate luminosity (Bolometric Magnitude fainter than -6) having phenomena of extra-mixing for Li. The study of this sub-sample gives us the chance to refine our previous studies made on larger and more general samples thanks to their higher homogeneity and to the presence of another constraint: the Li-abundance.

The relation between the Li abundance and the luminosity, examined for different classes of stars along the RGB and the AGB branches, shows us that, for stars of moderate luminosity, Li is produced at the Bump of the L-function and then is depleted at different rates during the successive evolution of the sources.

No clear correlation of Li abundances with mass loss rates emerged so far.

The behaviour of Li in evolved stars seems to be explained by the model presented in Palmerini et al. (2010), this conference, thanks to two different phenomena of extra-mixing:

- Fast Mixing, at the bump of the L-function, causing production of Li (buoyancy, at speeds close to the Alfvén Velocity, of small bubbles formed by magnetic instabilities).
- Slow Mixing, during the remaining evolution, which causes depletion of Li (buoyancy of larger magnetized structures exchanging heat efficiently with the environment).

Acknowledgments

This research was supported by the Italian Ministry of Research under contract PRIN2006-022731 and by INFN (sezione di Perugia) through the funds of Research Group n. 3. The idea of mixing by magnetic buoyancy was developed in common with G.J. Wasserburg and K.M. Nollett. R.G. wishes to thank the organizers of IAU Symposium 268 for the chance of giving a talk and for the wonderful conference.

References

- Andrews, A.D., Rodonó, M., Lensky, J.L. et al. 1988, *A&A*, 204, 177
- Busso, M., Wasserburg, G. J., Nollett, K. M., & Calandra, A. 2007a, *ApJ*, 671, 802
- Busso, M., Guandalini, R., Persi, P., Corcione, L., & Ferrari-Toniolo, M. 2007b, *AJ*, 133, 2310
- Cameron, A. G. W., & Fowler, W. A. 1971, *ApJ*, 164, 111
- Charbonnel, C., & Balachandran, S. C. 2000, *A&A*, 359, 563
- Denissenkov, P. A., Pinsonneault, M., & Mac Gregor, K. B. 2009, *ApJ*, 696, 1823
- Gilroy, K. K. 1989, *ApJ*, 347, 835
- Gilroy, K. K., & Brown, J. A. 1991, *ApJ*, 371, 578
- Gratton, R. G., Carretta, E., Matteucci, F., & Sneden, C. 2000, *A&A*, 358, 671
- Guandalini, R., Busso, M., Ciprini, S., Silvestro, G., & Persi, P. 2006, *A&A*, 445, 1069
- Guandalini, R., & Busso, M. 2008, *A&A*, 488, 657
- Guandalini, R., Palmerini, S., Busso, M., & Uttenthaler, S. 2009, *PASA*, 26, 168
- Guandalini, R. 2010, *A&A*, in press
- Kraft, R. P. 1994, *PASP*, 106, 553
- Nordhaus, J., Busso, M., Wasserburg, G. J., Blackman, E. G., & Palmerini, S. 2008, *ApJ* (Letters), 684, 29
- Palacios, A., Charbonnel, C., Talon, S., & Siess, L. 2006, *A&A*, 453, 261
- Palmerini, S., & Busso, M. 2008, *New AR*, 52, 412
- Palmerini, S., Busso, M., Maiorca, E., & Guandalini, R. 2009, *PASA*, 26, 161
- Palmerini, S., et al. 2010, this conference
- Sweigart, A. V., & Mengel, J. G. 1979, *ApJ*, 229, 624
- Uttenthaler, S., Lebzelter, T., Palmerini, S., Busso, M., Aringer, B., & Lederer, M. T. 2007, *A&A* (Letters), 471, 41
- Wasserburg, G. J., & Busso, M. 2008, *AIPC*, 1001, 295

Observations of light elements in massive stars

A. Kaufer

European Southern Observatory,
Alonso de Cordova 3107, Casilla 19001, Santiago de Chile
email: akaufer@eso.org

Abstract. Observations of light elements in hot massive stars are limited to few transitions of boron in the satellite-ultraviolet; lithium and beryllium are not observable at all. But because of its high sensitivity to the effects of rotational mixing, boron abundance determinations in massive stars have excelled as the definite test for evolutionary models with rotation. In this paper the observational evidence for rotational mixing in massive stars is reviewed and alternative interpretations are discussed.

Keywords. Stars: abundances, massive, rotation

1. Introduction

Despite their small number (only three stars out of a thousand have a mass larger than $8 M_{\odot}$) and their small mass fraction (only 14% of the mass of all stars is found in massive stars with $M > 8 M_{\odot}$), massive stars are important because they inject into the ISM large amounts of radiation, mass, and mechanical energy in shortest time (3–30 Myr) (Meynet 2008). Massive stars hence drive the chemical and dynamical evolution of the galaxies through nucleosynthesis and (re-)distribution of elements. Consequently, accurate galaxy evolution models require a detailed understanding of the internal and core properties of massive stars.

The observation of surface abundances of non-radioactive elements is an efficient probe for studying stellar evolution and verifying internal nuclear processes. The consideration of rotation in stellar evolution models predicts significant effects on the evolutionary tracks and surface abundances of massive stars (cf. Heger & Langer 2000 and Maeder & Meynet 2000). In particular the light trace elements lithium, beryllium, and boron are strongly affected by effects of rotationally induced mixing. Hence their observations and detailed surface abundance analyses are critical to test effects of rotational mixing. In the following an overview of the available observations of light elements in massive stars is given and the methods and achievable accuracies of abundance determinations from the observations are described. Then the observed light-element abundance patterns and their interpretation in context of stellar evolution models with rotation are discussed.

2. Observations

Lithium has been crucial to test models of cool stars at all possible stages of evolution, from pre-main sequence to the post-AGB stage and is conveniently observed through the resonance doublet at 6706 Å. Beryllium is observable in cool stars through the Be II $\lambda 3130$ resonance doublet but of limited use because of the considerably more difficult access from the ground to this spectral region in the near-UV. Boron is the most difficult light element to observe since all transitions of B I, B II, and B III are below the atmospheric

cut-off at 300 nm in the satellite ultraviolet. Unfortunately, boron is at the same time the only light element observable in hot massive stars. Boron can be observed either through the B II $\lambda 1362$ resonance line or the B III $\lambda 2066$ resonance doublet line.

After a 5-year forced hiatus, STIS onboard *HST* is today and the mid-term future the only observational resource to study boron in hot massive stars. In the past boron abundances have been determined using the B II $\lambda 1362$ line by Boesgaard & Heacox (1978) using *Copernicus* observations of 16 'normal' A and B stars, by Venn, Lambert, & Lemke (1996) using *IUE* observations of 6 B and A sub/giants and supergiants, and by Cunha et al. (1997) using GHRS data from *HST* of 4 B stars in Orion.

The B II $\lambda 1362$ line turns out to be rather problematic for accurate abundance determinations: the line is blended with Si III, Ni II, V II, Zn III, and Fe III and the line is sensitive to NLTE corrections as reported by Cunha et al. (1997) and Venn et al. (2002). For the temperature range of mid-B type stars and earlier, where B III is the dominant ion above a temperature of 18 kK, the B III $\lambda 2066$ doublet line appears better suited: the lines are not blended and NLTE effects are small compared to the B II line.

Proffitt et al. (1999) were the first to move to the B III $\lambda 2066$ line to determine boron abundances and $^{11}\text{B}/^{10}\text{B}$ isotopic ratios for 3 B stars using very high-SNR GHRS spectra. Proffitt et al. (1999) find isotopic ratios of the 3 B stars of $^{11}\text{B}/^{10}\text{B} \sim 4$ consistent with the solar-system value (Anders & Grevesse 1989). Proffitt & Quigley (2001) explored the *IUE* archive for high-resolution spectra of B-type stars and determined boron abundances (and upper limits) for 45 early B-type stars. Venn et al. (2002) determine 4 boron upper limits from 7 B-type main sequence stars using STIS onboard *HST*. Mendel et al. (2006) observe 7 additional B-type main sequence stars with STIS and find most of them boron depleted. Brooks et al. (2002) add to this handful of boron abundances of hot massive galactic B-type stars upper limits for boron abundances for two B-type stars in the Small Magellanic Cloud (SMC) obtained with STIS and the *HST* ($V \approx 15$ mag).

3. Abundance analysis of hot stars

To convert an observation of a stellar spectrum into an abundance measurement requires to carry out a detailed abundance analysis using atmosphere models and line-formation codes. For the early- to mid-B type main sequence stars, which are primarily observed in the context of light element abundances, the stellar atmospheres can be assumed to be plane-parallel and non-expanding, i.e., stellar winds are considered to be negligible. Then the stellar atmospheres can be described by 1D line-blanketed LTE models. Information on the gravity is obtained from the shape of the Balmer-line wings, which are broadened by the gravity-sensitive Stark effect. The line wings are fit with 1D (N)LTE Balmer line formation models. Effective temperature is derived from the so-called *ionisation equilibrium* of different ions of the same element (like Si II/III/IV) to reproduce the observed line profiles and equivalent widths for a given element abundance. Depending of the individual lines used for the analysis this requires 1D LTE line formation plus NLTE corrections or – if available – 1D NLTE line formation computations. Despite of sophisticated NLTE line-formation codes, for early-type B stars, usually a slight dependency of the computed line-by-line abundance on the strength of the lines remains, which is attributed to an additional line-broadening, the so-called microturbulence. It is determined from lines of ions that span a large range in equivalent widths, i.e., O or Fe in early B-type stars. Once effective temperature, gravity, and microturbulence have been determined in a quasi self-consistent way, the line-by-line element abundances can be determined using again 1D (N)LTE line formation.

Nieva & Przybilla (2007) and Nieva & Przybilla (2008) have pushed this hybrid NLTE approach for detailed abundance analyses of early B-type stars to a high level of perfection. Przybilla, Nieva, & Butler (2008) demonstrate that for a carefully selected sample of early-type B stars in the solar neighborhood with high-quality spectral observations, individual element abundances with 1 sigma errors clearly less than 0.1 dex can be obtained for all observable ions in the optical spectra of these stars.

A direct comparison of the proto-solar abundances of Asplund et al. (2009) with the B-star abundances of Przybilla, Nieva, & Butler (2008) shows nearly perfect agreement:

B stars	X=0.715	Y=0.271	Z=0.014	Z/X = 0.020	(Przybilla et al. 2008)
proto-solar	X=0.7154	Y=0.2703	Z=0.0142	Z/X = 0.0198	(Asplund et al. 2009)

Considering these advances and the improved accuracies that can be obtained with such state-of-the-art abundance determination techniques, it seems advisable to make the effort to reanalyse all available (but still few) spectra of early-type B stars for which satellite ultraviolet observations of light elements, i.e., of boron are available.

4. Boron abundances patterns in hot stars

Most of the boron abundance studies of hot massive stars aim to establish the present-day boron abundance to constrain the Galactic chemical evolution models. Cunha (2010) reviews the implications of these observations of cool and hot stars for chemical evolution models and constraints on the boron production mechanisms.

The latter is of particular interest since boron is the only light element whose production is neither due to nucleosynthesis in stellar interiors nor due to big-bang nucleosynthesis but is produced through cosmic ray spallation reactions in the interstellar gas. Boron abundance trends as function of oxygen provide constraints on the possible spallation reactions at work.

Cunha et al. (2000) and Smith, Cunha, & King (2001) find a linear trend for the boron abundances as function of oxygen abundances for galactic FG disk stars that show no beryllium depletion. The measured slope of 1.50 ± 0.08 (Cunha 2010) indicates a combination of primary source (expected slope 1) and secondary source (expected slope 2) production of boron in the Galaxy.

If the boron – oxygen abundances patterns determined for galactic hot stars by Proffitt & Quigley (2001) and Mendel et al. (2006) are compared with the galactic FG disk stars, a good agreement is found for the non-boron depleted hot stars.

Interestingly, an extrapolation of the boron – oxygen trend with a slope of 1.5 to low-metallicity environments is in excellent agreement with the abundance determinations (upper limits) of two B stars in the SMC by Brooks et al. (2002) (cf. their Fig. 6). The fact that boron in hot stars is frequently found to be severely depleted however complicates the rigorous interpretation of this interesting result. An increase in the sample size in the MCs would be the obvious demand to tighten the constraints on boron production by spallation in the MCs in comparison with the Galaxy but at the same time appears almost prohibitive considering the excessive amount of required STIS observing time (some 15 hours of *HST* integration time per star to obtain a S/N ~ 50).

Additional constraints on cosmic ray spallation theory could be obtained through high resolution, high SNR observations of the B III $\lambda 2066$ line, which allows to determine $^{11}\text{B}/^{10}\text{B}$ isotopic ratios from the predicted isotopic shift of 42 mÅ. The solar-system value of $^{11}\text{B}/^{10}\text{B} \sim 4$ (Anders & Grevesse 1989) is larger than the prediction from current cosmic ray spallation theory ($^{11}\text{B}/^{10}\text{B} \sim 2.5$, Meneguzzi, Audouze, & Reeves 1971). An observational determination of the isotopic ratio from hot massive stars would there-

fore provide strong constraints on the ^{11}B production processes. Again, such observations are possible with STIS but demanding in observing time.

5. Boron depletion in hot stars

The light elements lithium, beryllium, and boron are very sensitive to destruction by proton capture at temperatures much lower than those where the H-burning CN-cycle is effective. This makes the light elements a sensitive tracer of mixing of stellar surface layers to deeper layers and can be observed as apparent depletion of the respective element. Lithium and beryllium have been intensively used in this context to study stellar evolution processes in cool stars but cannot be observed in hot stars. For hotter stars, boron is the only observable light element as discussed before.

Boron is a very fragile element and destroyed by proton capture already at temperatures of $< 6 \times 10^6 \text{ K}$, which corresponds to about $1 M_{\odot}$ below the surface of a B-type main-sequence star. Due to this sensitivity of boron to moderate temperatures, any mild mixing of surface layers to deeper layers would already deplete boron while keeping less fragile elements like nitrogen unchanged. In more evolved stages of the star the same mixing process may enhance other elements like nitrogen (progressive mixing). Therefore, the determination of boron – nitrogen abundance patterns in hot stars of different evolutionary stage is a sensitive method to test stellar evolution models.

Venn, Lambert, & Lemke (1996) were the first to explore this possibility in a dedicated study of a sample of A and B stars of different evolutionary stage. Contrary to the expectation to find boron depletion for the more evolved stars showing at the same time nitrogen enrichment, the authors found severe boron depletion for all stars of their sample including for the non-evolved stars near the main sequence that show only little nitrogen enrichment. The finding of boron depletion without nitrogen enhancement could only be explained by invoking an additional mixing process. Based on their evolutionary tracks of massive stars including the effects of rotation, Fliegner, Langer, & Venn (1996) proposed rotationally induced mixing acting in the radiative zones of massive main star-sequence stars to explain the observations of Venn, Lambert, & Lemke (1996).

Figure 1 compiles all to date available boron and nitrogen abundance data of B-type stars from Venn et al. (2002), Lemke, Cunha, & Lambert (2000), Proffitt et al. (1999), and Proffitt & Quigley (2001). The dashed (blue) line shows an evolutionary track according to Heger & Langer (2000) for a fast rotating massive star of $12 M_{\odot}$ and $v_{\text{eq}} = 200 \text{ km/s}$, which nicely demonstrate the rapid depletion of boron by a factor of ~ 50 while nitrogen enhances by a factor of ~ 2.5 only. The newer boron observations have added three measurement of the two stars HD 36591 and HD 30836 to the group of stars showing strong boron depletion with virtually no nitrogen enrichment (group II in the classification of Morel, Hubrig, & Briquet (2008)). These observations still remain difficult to explain by rotational mixing. However, new models of the Geneva stellar evolution code with rotational mixing and an extended reaction network including lithium, beryllium, and boron by Frischknecht (2010) promise to obtain an even faster boron depletion and therefore a better match to the observations.

It should be mentioned here that also other effects than rotational mixing can alter the stellar surface composition of hot massive stars: mass loss and mass transfer in binary systems are the primary candidates. While mass loss does not play a strong role in B-type main-sequence stars, the mass transfer in a close binary could produce considerable effects to the measured abundance patterns. For a detailed discussion of the latest results on element depletion and enhancements through binary interaction in massive stars see Langer (2010).

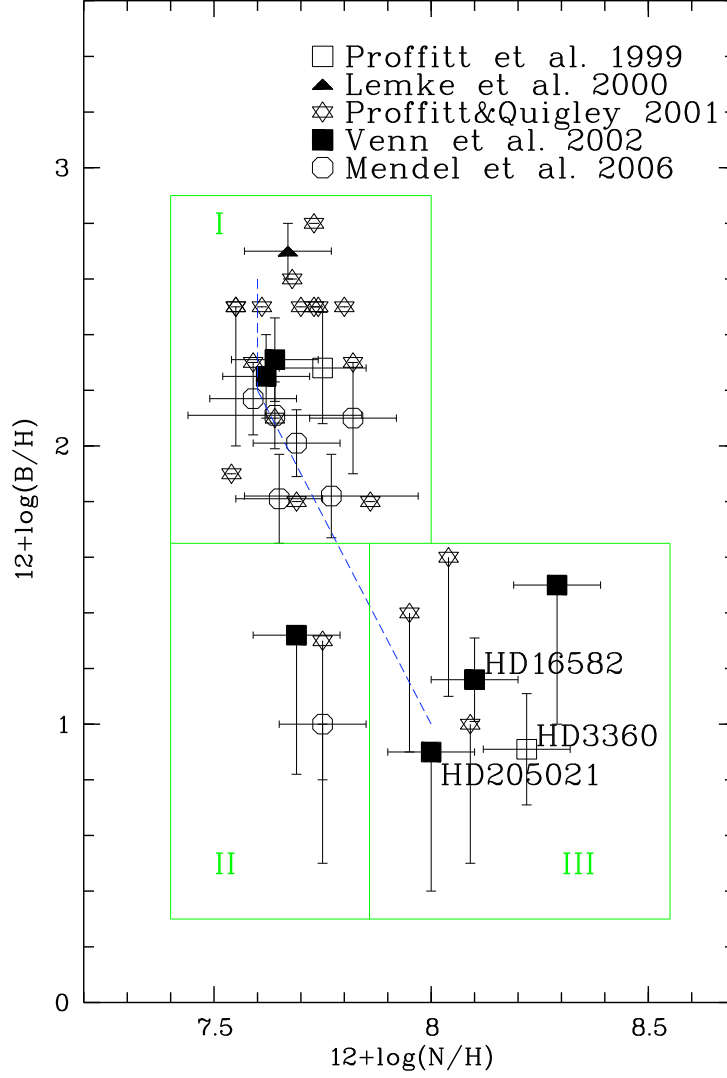


Figure 1. Boron and nitrogen abundances in B stars. Error bars of $+0/-0.5$ dex indicate upper limits. The dashed (blue) line shows an evolutionary track according to Heger & Langer (2000) for a rotating star of $12 M_{\odot}$ and $v_{\text{eq}} = 200$ km/s and an initial nitrogen and boron abundance of 7.6 and 2.6, respectively. The (green) boxes indicate the different groups described in Morel, Hubrig, & Briquet (2008), i.e., I - unaltered, close to solar nitrogen and boron abundances, II - boron depleted but nitrogen unchanged, and III - boron depleted and nitrogen enhanced. Three stars are indicated with their HD number for which independent observations have established that these stars are slow rotators. See text for discussion.

Despite the compelling results from boron – nitrogen abundance measurements and the striking evidence for rotational mixing in massive stars, further observations and precise abundance analyses would be highly desirable to verify that rotational mixing increases with age, rotation rates, and stellar mass. The revival of STIS during the spectacular service mission to *HST* in 2009 opens up new possibilities for such observations on larger samples of hot massive stars.

6. Boron abundances and rotational velocities

Observational tests of rotational mixing suffer from a fundamental dilemma: while measurable effects of altered abundance pattern are only predicted for fast rotating stars with $v_{\text{eq}}/v_{\text{crit}} > 0.2$, detailed abundance analyses require sharp-lined stellar spectra. Therefore, abundance analyses are strongly biased towards sharp-line stars with $v_{\text{eq}} \sin i < 20$ km/s, i.e., stars either seen pole-on or real slow rotators. Considering that the median equatorial rotational velocity of B-type main-sequence stars is ~ 200 km/s (Howarth 2004), slow rotators cannot be considered representative of their class.

It is therefore crucial to include true *fast* rotators in future boron abundance studies by expanding the samples with stars showing rotationally broadened lines. Precise abundance analyses can still be carried out from spectra with rotationally broadened lines up to $v_{\text{eq}} \sin i \sim 100$ km/s if the SNR of the spectra is increased accordingly (cf. e.g. Kaufer et al. 1994 and references therein).

It is further crucial to determine true stellar rotation rates for the stars under examination to allow direct comparison with evolutionary models of rotating stars. The rotation of stellar surface patterns like stellar spots or non-radial pulsation patterns or the rotation of wind patterns locked to the stellar surface (cf. e.g. Prinja, Massa, & Fullerton (1995), Fullerton et al. (1997), Kaufer et al. (2006)) can provide direct measurements of true stellar rotation rates. Rotational modulation can be more or less easily observed through spectral or photometrical time series studies of the respective bright galactic early-type B stars.

Morel, Hubrig, & Briquet (2008) have applied this idea to the sample of early-type B stars for which boron and nitrogen abundances have been determined and which are shown in Fig. 1. The authors identify three boron depleted and nitrogen enriched stars (their group III) which are true slow rotators as determined from the modulation of UV wind lines (UV) or asteroseismological (AS) determination of the rotation rate:

HD 3360	ζ Cas	$v_{\text{eq}} = 55$ km/s	UV	SPB + magn.field	Neiner et al. (2003)
HD 16582	δ Cet	$v_{\text{eq}} = 14$ or 28 km/s	AS	β Cep + magn.field	Aerts et al. (2006)
HD 205021	β Cep	$v_{\text{eq}} = 26$ km/s	UV	β Cep + magn.field	Henrichs et al. (2000)

The fact that all three stars are either slowly pulsating B stars or β Cephei stars for which the presence of a weak magnetic field has been established leads Morel, Hubrig, & Briquet (2008) to propose that magnetic phenomena are important in altering the photospheric abundances of early B dwarfs, even for surface field strengths as low as at the one hundred Gauss level. The authors further argue that these stars only suffered a moderate amount of angular momentum loss along the main sequence and that they were likely slow rotators already on the ZAMS. At least in the cases of these three stars, the boron depletion can therefore not be explained by rotational mixing, which otherwise nicely reproduces the transition from group I to group III as illustrated in Fig. 1 by the evolutionary track from Heger & Langer (2000).

7. Conclusions

Undoubtedly the observational discovery of an additional mixing process to explain the boron depletion in the surface layers of non-evolved hot B stars on or near the main sequence by Venn, Lambert, & Lemke (1996) has been the most notable contribution by the studies of the light elements in massive stars. The subsequent identification of this mixing process to be due to rotationally induced mixing in the radiative layers of massive stars by Fliegner, Langer, & Venn (1996) has to be considered a major milestone in the development of stellar evolution models of massive stars. The understanding of the importance of stellar rotation for the evolution of massive stars has revolutionised the whole field of hot star research. Still, the number of actual measurements of boron in massive stars remains scarce due to the observational limitation imposed by the diagnostic lines in the satellite ultraviolet. The recent return of STIS onboard *HST* into science operation presents a rather unique opportunity to intensify the studies of rotational mixing as function of age, mass, and rotational rates of massive stars. Large and carefully selected samples of early-type stars should be examined to establish statistically significant dependencies on the relevant evolution parameters. The Galactic and MC samples already studied by the VLT-FLAMES survey of massive stars (Hunter et al. 2009) appear to be best suited for such future studies since they cover a large range of rotational velocities up to 300 km/s and a wide range of ages and masses.

References

- Aerts, C., et al. 2006, *ApJ*, 642, 470
 Anders, E., & Grevesse, N. 1989, *GeCoA*, 53, 197
 Asplund, M., Grevesse, N., Sauval, A. J., & Scott, P. 2009, *ARA&A*, 47, 481
 Boesgaard, A. M., & Heacox, W. D. 1978, *ApJ*, 226, 888
 Brooks, A. M., Venn, K. A., Lambert, D. L., Lemke, M., Cunha, K., & Smith, V. V. 2002, *ApJ*, 573, 584
 Cunha, K., Lambert, D. L., Lemke, M., Gies, D. R., & Roberts, L. C. 1997, *ApJ*, 478, 211
 Cunha, K., Smith, V. V., Parizot, E., & Lambert, D. L. 2000, *ApJ*, 543, 850
 Cunha, K. 2010, *these proceedings*
 Fliegner, J., Langer, N., & Venn, K. A. 1996, *A&A*, 308, L13
 Frischknecht, U. 2010, *these proceedings*
 Fullerton, A. W., Massa, D. L., Prinja, R. K., Owocki, S. P., & Cranmer, S. R. 1997, *A&A*, 327, 699
 Heger, A., & Langer, N. 2000, *ApJ*, 544, 1016
 Henrichs, H. F., et al. 2000, *ASPC*, 214, 324
 Howarth, I. D. 2004, *IAUS*, 215, 33
 Hunter, I., et al. 2009, *A&A*, 496, 841
 Kaufer, A., Szeifert, T., Krenzlin, R., Baschek, B., & Wolf, B. 1994, *A&A*, 289, 740
 Kaufer, A., Stahl, O., Prinja, R. K., & Witherick, D. 2006, *A&A*, 447, 325
 Langer, N. 2010, *these proceedings*
 Lemke, M., Cunha, K., & Lambert, D. L. 2000, *LIACo*, 35, 223
 Maeder, A., & Meynet, G. 2000, *A&A*, 361, 159
 Mendel, J. T., Venn, K. A., Proffitt, C. R., Brooks, A. M., & Lambert, D. L. 2006, *ApJ*, 640, 1039
 Meneguzzi, M., Audouze, J., & Reeves, H. 1971, *A&A*, 15, 337
 Meynet, G. 2008, *EAS Publication Series*, 32, 187
 Morel, T., Hubrig, S., & Briquet, M. 2008, *A&A*, 481, 453
 Neiner, C., Geers, V. C., Henrichs, H. F., Floquet, M., Frémat, Y., Hubert, A.-M., Preuss, O., & Wiersema, K. 2003, *A&A*, 406, 1019
 Nieva, M. F., & Przybilla, N. 2008, *A&A*, 481, 199

- Nieva, M. F., & Przybilla, N. 2007, *A&A*, 467, 295
- Prinja, R. K., Massa, D., & Fullerton, A. W. 1995, *ApJ*, 452, L61
- Proffitt, C. R., Jönsson, P., Litzén, U., Pickering, J. C., & Wahlgren, G. M. 1999, *ApJ*, 516, 342
- Proffitt, C. R., & Quigley, M. F. 2001, *ApJ*, 548, 429
- Przybilla, N., Nieva, M.-F., & Butler, K. 2008, *ApJ*, 688, L103
- Smith, V. V., Cunha, K., & King, J. R. 2001, *AJ*, 122, 370
- Venn, K. A., Lambert, D. L., & Lemke, M. 1996, *A&A*, 307, 849
- Venn, K. A., Brooks, A. M., Lambert, D. L., Lemke, M., Langer, N., Lennon, D. J., & Keenan, F. P. 2002, *ApJ*, 565, 571

Lithium abundances in Bulge-like SMR stars

Beatriz Barbuy¹, M. Trevisan¹, B. Gustafsson², K. Eriksson², M. Grenon³, and L. Pompéia⁴

¹Universidade de São Paulo, Brazil
 email: barbuy@astro.iag.usp.br

²Uppsala Universitet, Sweden

³Observatoire de Genève, Switzerland

⁴Universidade do Vale do Paraíba, Brazil

Abstract. We analyze a sample of 21 super-metal-rich (SMR) stars, using high-resolution échelle spectra obtained with the FEROS Spectrograph at the 1.5m ESO telescope. The metallicities are in the range $0.15 < [\text{Fe}/\text{H}] < 0.5$, 3 of them in common with Pompéia et al. (2002). Geneva photometry, astrometric data from *Hipparcos*, and radial velocities from CORAVEL are available for these stars. The peculiar kinematics suggests the thin disk close to the bulge as the probable birthplace of these stars (Grenon 1999). From *Hipparcos* data, it appears that the turnoff of this population indicates an age of 10-11 Gyr (Grenon 1999). Detailed analysis of the sample stars is carried out. Lithium abundances of these stars were derived, and their behaviour with effective temperature is shown.

Keywords. Stars: abundances, formation - Galaxy: formation

1. Introduction

Grenon (1989, 1999) selected a sample of about 6000 dwarf stars from the NLTT catalogue (see Grenon 1999), and studied them by means of Geneva photometry, radial velocity and Hipparcos astrometry. A sub-sample of super-metal-rich (SMR) stars was revealed (Grenon 1972, 1989, 1990, 1998, 2000). Optical spectra were obtained for 21 among the most metal-rich dwarfs of the sample, with the FEROS Spectrograph at the 1.52m telescope at ESO, La Silla. The total wavelength coverage is 3560-9200 Å with a resolving power $R = 48,000$.

The surface gravities $\log g$ were derived using *Hipparcos* parallaxes π with bolometric correction relations given in Alonso et al. (1995). The parameters $[T_{\text{eff}}, v_t]$ were obtained by fixing trigonometric surface gravities and imposing excitation equilibrium for Fe I lines and ionization equilibrium for Fe I and Fe II. Independence between equivalent widths and the abundances of Fe I lines was imposed to determine v_t . Derivations of metallicity were carried out through the Meudon code ABON2, and the code by the Uppsala group BSYN/EQWI. We are going through iterative checks, by computing FeI and FeII in the Sun, with both codes, and then for the stars, using the same tailored MARCS models. The codes are found to generate similar results, although some minor differences, which are not expected to affect the present results, are still being explored. The comparison, and more abundance results will be presented by Trevisan et al. (2009, in prep.). Lithium abundances were derived from the LiI 6707.8 Å line for the sample stars, by fitting the synthetic to the observed spectra. The spectrum synthesis code is described in Cayrel et al. (1991) and Barbuy et al. (2003). Photospheric 1D models for the sample were extracted from the MARCS grid (Gustafsson et al. 2008).

Comparisons are presented in Fig. 1 with the results by Pompéia et al. (2002), obtained

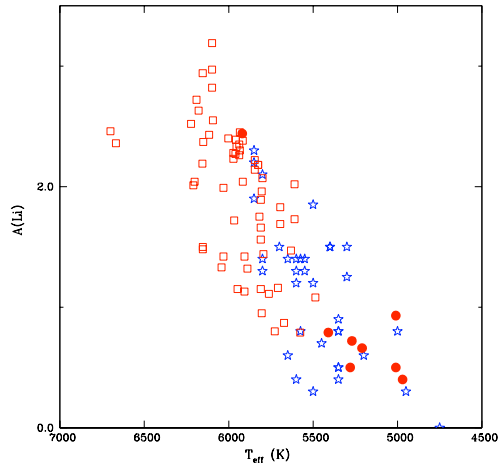


Figure 1. Log (Li/H) vs. effective temperature for the sample stars (red filled circles), compared with data for another sub-sample of bulgelike SMR stars by Pompéia et al. (2002) (open stars), and the metal-rich open cluster M67 (open squares, with results from Jones et al. (1999).

for another sub-sample of bulgelike dwarfs, therefore compatible in terms of age and kinematics with the present sample, and with M67, a metal-rich open cluster of 4.5 Gyr, with data from Jones et al. (1999). Jones et al. had also shown that older stars deplete their Li with time, and it is more efficient in the cooler stars.

In conclusion, lithium abundances in our sample of very metal-rich stars are somewhat higher than in M67, and those found by Pompéia et al. (2002) for similar stars. One star HD 90054 shows a high Li abundance, compatible with being the hottest star of the sample.

Acknowledgements

The observations were carried out within Brazilian time in a ESO-ON agreement, and within an IAG-ON agreement funded by FAPESP project n° 1998/10138-8.

References

- Alonso, A., Arribas, S., Martinez-Roger, C. 1995, *A&A*, 297, 197
- Barbuy, B., Perrin, M.-N., Katz, D., et al. 2003, *A&A*, 404, 661.
- Cayrel, R., Perrin, M.-N., Barbuy, B., & Buser, R. 1991, *A&A*, 247, 108.
- Grenon, M. 1972, in IAU Colloq. 17, Age des Etoiles, eds. G. Cayrel de Strobel & A. M. Deplace (Paris : Obs. de Paris-Meudon), 55.
- Grenon, M. 1989, *Ap&SS*, 156, 29.
- Grenon, M. 1990, in ESO Workshop and Conf. Proc. 35, Bulges of Galaxies, 1st ESO / CTIO Workshop, ed. B. Jarvis & D. Terndrup (Garching : ESO), (Sunspot : NSO), 143.
- Grenon, M. 1998, *Highlights of Astronomy*, Vol.11A, ed. J. Andersen (Dordrecht:Kluwer), 560.
- Grenon, M. 1999, *Ap&SS*, 265, 331.
- Grenon, M. 2000, in The Evolution of the Milky Way, ed. F. Matteucci & F. Giovannelli (Dordrecht : Kluwer), 47.
- Gustafsson, B., Edvardsson, B., Eriksson, K. et al. 2008, *A&A*, 486, 951
- Jones, B.F., Fischer, D., Soderblom, D.R. 1999, *AJ*, 117, 330
- Pompéia, L., Barbuy, B., Grenon, M., Castilho, B.V. 2002, *ApJ*, 570, 820

Survey for Li-rich K giants

Y. Bharat Kumar and Bacham E. Reddy

Indian Institute of Astrophysics, Bengaluru.
email: bharat@iiap.res.in, ereddy@iiap.res.in

Abstract. We present results from an ongoing survey of searching Li-rich K giants among low mass giants along the Red Giant Branch (RGB). A sample of 2500 stars with accurate astrometry have been selected from Hipparcos catalogue covering both the RGB luminosity bump and the red clump regions on the HR diagram. Lithium abundances have been determined for half of the sample from low resolution spectra using line depth ratio method. Results confirm the rarity of Li-rich K giants, just under 1%, in the solar neighbourhood. This study increased the total number of known Li-rich K giants by a factor of two. The analysis of high resolution spectra of candidate Li-rich K giants showed that the K giant HD 77361 is highly enriched in lithium ($\log \epsilon(\text{Li}) = 3.82$) and at the same time has anomalously low carbon isotopic ratio ($^{12}\text{C}/^{13}\text{C} = 4.3$). The results put important constraints on the theoretical modelling of the stellar structure and the mixing process, particularly, of the K giants.

Keywords. stars: late-type, abundances, individual (HD 77361), statistics – surveys

1. Li-rich K giants

Lithium is an important indicator of mixing processes in the stars on the Red Giant Branch (RGB). The expansion of convective envelope alters the surface chemical composition of lighter elements in the red giants. According to the classical stellar evolution theory (Iben 1967), any K giant with a surface lithium abundance exceeding $\log \epsilon(\text{Li}) \sim 1.4$ can be characterized as Li-rich K giant (hereafter LRKG). The discovery of first LRKG (Wallerstein & Sneden 1982) has challenged the concept of gradual depletion of lithium on RGB. Since then, a dozen K giants were identified as LRKG. Charbonnel & Balachandran (2000) located all the known Li-rich stars on the Hertzsprung-Russell diagram using the Hipparcos parallaxes (Perryman et al. 1997). Most of them are fast rotators and show infrared excess. The origin of the anomalous lithium in these stars is not well understood. We have initiated a systematic survey to search for LRKG along the RGB, to pin down the source of lithium by studying the correlations between high lithium and other stellar parameters, and to estimate the fractional content of lithium contribution from the K giants to the Galaxy.

2. Samples and observations

We have selected 2500 sample giants along the RGB, sourced from Hipparcos catalog (Perryman et al. 1997, van Leeuwen 2007). We have restricted the survey to bright ($m_v \leq 8$) and nearby stars ($d \leq 200$ pc), with accurate parallaxes ($\leq 15\%$ error). Further, the sample stars were subjected to the following criteria: declination ($-60 \leq \delta \leq +80$), spectral type (K or late G) or T_{eff} ($4200 \leq T_{\text{eff}} \leq 5000$ K) and luminosity ($1.0 \leq \log (L/L_{\odot}) \leq 2.5$). The last two criteria (luminosity and temperature) ensure that the sample covers the luminosity bump and/or red clump region on the HR diagram.

High quality low resolution spectra of sample stars were obtained using 2 m Himalaya Chandra Telescope (HCT), Hanle, 1 m Carl Zeiss telescope, and 2.34 m Vainu Bappu Telescope (VBT), Kavalur with resolution $R \sim 3500$, $R \sim 6000$, $R \sim 1500$, respectively. Along with the sample stars, we also made observations of known Li-rich giants, for which Li abundance was independently determined from high resolution spectra. An empirical relation is obtained between known Li-abundance and the ratios of line depths between Li I 6707 Å and Ca I 6717 Å. The derived relation is good to use for K giants with Li abundance $\log \epsilon(\text{Li}) \geq 1.0$. The method is useful to efficiently eliminate K giants with low Li abundance and select LRKG based on line depth ratios.

3. Results & discussion

Preliminary results from the analysis of 1100 spectra are presented here. We could detect Li I line at 6707 Å for Li abundances exceeding 0.6 dex. Li I line is seen in only 39% of the sample stars. The remaining 60% of stars in the sample are considered normal with $\log \epsilon(\text{Li}) < 0.6$. The corresponding uncertainty in the derived abundance from the empirical relation is significantly large owing to the uncertainty in the line depth ratios. We found a dozen new K giants with Li significantly above the expected value and considered them as Li-rich K giants, which confirm the rarity of LRKG.

Detailed analysis from high resolution ($R \sim 65000$) spectra of one of the new LRKG HD 77361 at the RGB bump shows anomalous high lithium ($\log \epsilon(\text{Li}) = 3.82$) and low carbon isotopic ratio ($^{12}\text{C}/^{13}\text{C} = 4.3$), which is different from the other known super Li-rich K giants. Results for HD 77361 do not fit with any of the explanations put forward for the source of enhanced Li in the photospheres of K giants: first dredge-up, extra deep mixing associated with cool bottom processing, lithium flash scenario, extra mixing triggered by spinning up the K giants with external angular momentum. The free mixing of material between hydrogen burning shell and the bottom of convective outer layer due to erasing the μ -barrier seems to be favored for the enrichment of products in the envelope, and hence the enhancement of surface lithium abundance and ^{13}C . We refer to Kumar & Reddy (2009) for a detail discussion.

4. Acknowledgement

We are grateful to the IAU, DST, and IIA for support to attend this meeting.

References

- Charbonnel, C., & Balachandran, S. C. 2000, *A&A*, 359, 563
- Iben, I. J. 1967, *ApJ*, 147, 624
- Kumar, Y. B., & Reddy, B. E. 2009, *ApJ* (Letters), 703, L46
- Perryman, M. A. C., Lindegren, L., Kovalevsky, J., et al. 1997, *A&A*, 323, L49
- van Leeuwen, F. 2007, *A&A*, 474, 653
- Wallerstein, G., & Sneden, C. 1982 *ApJ*, 255, 577

A 3D-NLTE study of the 670 nm solar lithium feature

Elisabetta Caffau¹, Hans-Günter Ludwig^{2,1}, Matthias Steffen³, and Piercarlo Bonifacio¹

¹GEPI, Observatoire de Paris, CNRS, Université Paris Diderot; 92195 Meudon Cedex, France
Elisabetta.Caffau@obspm.fr

²ZAH-Landessternwarte, Königstuhl 12, D-69117 Heidelberg, Germany

³Astrophysikalisches Institut Potsdam, An der Sternwarte 16, D-14482 Potsdam, Germany

Abstract. We derive the 3D-NLTE lithium abundance in the solar photosphere from the Li I line at 670 nm as measured in several solar atlases. The Li abundance is obtained from line profile fitting with 1D/3D-LTE/3D-NLTE synthetic spectra, considering several possibilities for the atomic parameters of the lines blending the Li feature. The 670 nm spectral region shows considerable differences in the two available disc-centre solar atlases, while the two integrated disc spectra are very similar. We obtain $A(\text{Li})_{3\text{D-NLTE}}=1.03$. The 1D-LTE abundance is 0.07 dex smaller. The line-lists giving the best fit for the Sun may fail for other stars, while some line-lists fail to reproduce the solar profile satisfactorily. We need a better knowledge of the atomic parameters of the lines blending the Li feature in order to be able to reproduce both the solar spectrum and the spectra of other stars. An improved line-list is also required to derive reliable estimates of the isotopic Li ratio in solar-metallicity stars.

Keywords. Sun: abundances – stars: abundances – hydrodynamics – line: formation

1. Introduction

For determining the lithium abundance in the solar photosphere one has to rely on the absorption feature of Li I at 670.7 nm. While the surrounding wavelength region is very clean in metal-poor stars making the abundance determination straightforward, this is not the case for the Sun and stars of comparable metallicity. The Li 670 nm feature is immersed in a forest of atomic and molecular lines whose atomic data are unfortunately not well known. Several line-lists for the blending components have been proposed. We applied them in 3D-NLTE spectral syntheses of the Li profile. The substantial differences among the resulting spectra indicate that for determining the Li abundance in stars of metallicity greater than 1/10 solar a major effort should be devoted to the search for data of the blending lines which are able to simultaneously reproduce the observed spectra over a wide range of effective temperatures and surface gravities.

Somewhat surprisingly, among the applied high-quality solar atlases we found noticeable differences in the Li range between the two disc-centre spectra of Neckel & Labs (1984) and Delbouille et al. (1973). While the lack of knowledge concerning the lines blending the Li 670 nm doublet is discussed in several papers, we could not find any information about this disagreement of the observed spectra in the literature.

2. Atomic and molecular data

In our analysis we assume that no ^6Li is present in the solar photosphere. For ^7Li we take into consideration ten line components. For the blending lines in the range, we

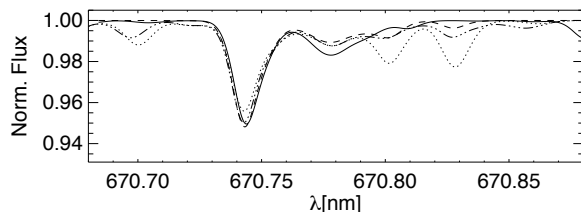


Figure 1. Synthetic, disc-integrated (flux) spectra for the Li I wavelength range and solar parameters: Li is modelled identically in 3D-NLTE in all syntheses while the blending components are computed in 3D-LTE, with line parameters from Hiltgen (1996) (solid), Reddy et al. (2002) (dash), Mandell et al. (2004) (dotted), and Ghezzi et al. (2009) (dash-dot).

used the line-lists of Hiltgen (1996), of Reddy et al. (2002), of Mandell et al. (2004), and the most recent work of Ghezzi et al. (2009). We computed the 3D spectral synthesis, taking into account the NLTE effects for the Li contribution. In Fig. 1, we compare the resulting synthetic profiles using the different line-lists. The disagreement between the profiles is evident, and can be explained by the fact that they have been optimised to analyse different stars.

3. The solar photospheric abundance of lithium

In the analysis of the solar Li abundance we only applied the line-lists for the blending components by Reddy et al. (2002) and Ghezzi et al. (2009). These authors applied and optimised their lists for the Sun, which naturally leads to a better agreement with the observed solar spectra. We further modified the line-lists slightly by changing the oscillator strength of the involved transitions to better reproduce the observations with our synthetic spectra based on 3D simulations. Performing a comprehensive fitting with synthetic 3D spectra is a computationally so demanding task that we had to restrict our approach to these small, manually introduced changes.

The abundances we obtain for the solar spectra of Neckel & Labs (1984) and of Kurucz (2005) are in close agreement. Despite that the parameters of the blending components in the two line-lists of Reddy et al. (2002) and Ghezzi et al. (2009) are different, the Li abundance does not change very much (within 0.04 dex). For the abundance determination we gave preference to the line-list of Ghezzi et al. (2009), and our result is $A(\text{Li})_{3\text{D-NLTE}} = 1.03 \pm 0.03$ where the uncertainty reflects the dispersion among the results for the different observed spectra.

The 1D-LTE abundance of lithium is 0.07 dex lower than the 3D-NLTE value. However, the synthetic 1D spectrum does not reproduce the observed line profile, in part because the parameters of the blending lines have been optimised for the 3D synthesis.

References

- Delbouille, L., Roland, G., & Neven, L. 1973, Liege: Universite de Liege, Institut d'Astrophysique, 1973
- Ghezzi, L., Cunha, K., Smith, V. V., Margheim, S., Schuler, S., de Araújo, F. X., & de la Reza, R. 2009, *ApJ*, 698, 451
- Hiltgen, D.D. 1996, Ph.D. Thesis
- Kurucz, R. L. 2005, *MemSAI* (Supplement), 8, 189
- Mandell, A. M., Ge, J., & Murray, N. 2004, *AJ*, 127, 1147
- Neckel, H., & Labs, D. 1984, *Solar Phys.*, 90, 205
- Reddy, B. E., Lambert, D. L., Laws, C., Gonzalez, G., & Covey, K. 2002, *MNRAS*, 335, 1005

Ultra-lithium-deficient halo stars

Lisa M. Elliott¹ and Sean G. Ryan²

¹Centre for Stellar and Planetary Astrophysics, School of Mathematical Sciences
 Building 28, Monash University, Victoria, 3800, Australia
 email: Lisa.Elliott@sci.monash.edu.au

²School of Physics, Astronomy and Mathematics, and Centre for Astrophysics Research,
 University of Hertfordshire,
 College Lane Hatfield AL10 9AB, United Kingdom
 email: s.g.ryan@herts.ac.uk

Abstract. While most warm halo dwarfs show lithium abundances at the level of the Spite Plateau, a small number ($\sim 5\%$) have undetectable lithium lines. The existence of these stars has long raised questions when interpreting the plateau abundances: are they an extreme example of a depletion mechanism that has affected the plateau stars, or do they have an entirely different history? We provide an overview of what is currently known about the lithium-poor halo stars and discuss a possible origin for the lithium deficiency in this unique group of stars.

Keywords. stars: abundances, blue stragglers – Galaxy: halo

1. Introduction

The existence of warm halo dwarfs with lithium abundances significantly below the Spite Plateau was first noted by Spite et al. (1984). These stars have undetectable lithium lines, with inferred upper limits for $A(\text{Li})$ more than 0.4 dex below the level of the plateau (eg. Hobbs & Mathieu 1991; Thorburn 1992). Previous studies of lithium-deficient halo stars have revealed various abundance anomalies that affect some, although not all, stars (eg. Norris et al. 1997; Ryan et al. 1998). More recently, many of these objects were found to be deficient in Be (Boesgaard & Novicki 2005; Boesgaard 2007). Ryan et al. (2002) discovered that three out of four lithium-poor stars studied showed spectral line broadening and attributed this to rotation. Coupled with a high incidence of binarity, these findings have led to suggestions that the lithium-poor stars may be a product of the same mechanism that is responsible for the formation of field blue-stragglers. Understanding the origin of the lithium-poor stars is crucial for studies of the Spite Plateau: if they do have a different history to normal halo dwarfs they should be ruled out of future studies of lithium depletion in the general halo population.

Following the rotation study of Ryan et al. (2002), a further investigation of abundance trends and rotation properties in the lithium-poor stars was undertaken (Elliott & Ryan 2010; Ryan et al. 2010). Here we draw on results from these studies, along with previous results, to provide an overview of the observed characteristics of the lithium-poor halo stars.

2. Overview of results

A summary of observed properties for nine lithium-deficient halo stars is presented in Table 1. The key properties are as follows:

Abundances Two cool, metal-poor lithium-poor stars show abundance ratios that differ from the mean trends in the general halo population. This includes enhancements in the

Table 1. Overview of properties of lithium-deficient halo stars

Star	T _{eff}	[Fe/H]	Abundance Anomalies?	Rotation	Binary ¹
HD97916	Warm*	High*	No	Yes	Yes
G202-65	Warm	High	No	Yes	Yes
G66-30	Warm	High	No	Yes	Yes
BD+51°1817	Warm	High	No	Yes ²	Yes
BD+25°1981	Warm ³	High ³	No	Yes? ¹	Yes?
CD-31°19466	Cool	Med	No	No ²	?
G122-69	Cool	Low	No	Yes	No
G139-8	Cool	Low	Yes	No	No
G186-26	Cool	Low	Yes	No	No

Notes:

* Warm refers to stars with T_{eff} \gtrsim 6300 K, high refers to stars with [Fe/H] \gtrsim -1.50

¹From Carney et al. 1994; Carney et al. 2001; Latham et al. 2002 ²From Ryan et al. (2002). ³From Ryan et al. 2001.

neutron-capture element ratios [Sr/Fe], [Y/Fe] and [Ba/Fe] in G186-26 and deficiencies in [Na/Fe], [Mg/Fe], [Al/Fe], [Sr/Fe] and [Ba/Fe] in G139-8.

Rotation At least five stars show evidence of line broadening indicative of rotation rates exceeding that expected in old halo dwarfs. Inferred projected rotation velocities for these five stars are between 4.7 and 10.4 km s⁻¹. At least four of the rotating stars are in binary systems, with periods ranging from 168 to 688 days (Carney et al. 1994; Carney et al. 2001; Latham et al. 2002). Rapid rotation is common in the warm, metal-rich subset of lithium-poor stars while only one of the cooler stars, G122-69, shows mildly enhanced rotation.

3. Conclusions

The high incidence of rotation among the lithium-poor stars suggests that these stars do have a different history to the lithium-normal halo population. Our results, particularly for the warm subset of lithium-poor stars, support a scenario in which mass and angular momentum have been transferred from a now evolved companion, similar to the mechanism that may be responsible for the formation of field blue-stragglers.

References

- Boesgaard, A. M., & Novicki, M. C. 2005, *ApJ* (Letters), 633, L125
Boesgaard, A. M. 2007, *ApJ*, 667, 1196
Carney, B. W., Latham, D. W., Laird, J. B., & Aguilar, L. A. 1994, *AJ*, 107, 2240
Carney, B. W., Latham, D. W., Laird, J. B., Grant, C. E., & Morse, J. A. 2001, *AJ*, 122, 3419
Elliott, L. M. & Ryan S. G. 2010, *in prep.*
Hobbs, L. M., & Mathieu, R. D. 1991, *PASP*, 103, 431
Latham, D. W., Stefanik, R. P., Torres, G., Davis, R. J., Mazeh, T., Carney, B. W., Laird, J. B., & Morse, J. A. 2002, *AJ*, 124, 1144
Norris, J. E., Ryan, S. G., Beers, T. C., & Deliyannis, C. P. 1997, *ApJ*, 485, 370
Ryan, S. G., Norris, J. E., & Beers, T. C. 1998, *ApJ* 506, 892
Ryan, S. G., Gregory, S. G., Kolb, U., Beers, T. C., & Kajino, T. 2002, *ApJ* 571, 501
Ryan, S. G., Elliott, L. M., Ford, A. & Gregory, S. G. 2010, *in prep.*
Spite, M., Maillard, J. P., & Spite, F. 1984, *A&A*, 141, 56
Thorburn, J. A. 1992, *ApJ* (Letters), 399, L83

Li-rich giants in the Galactic Bulge. Is Li linked only to evolutionary status?

Oscar A. Gonzalez¹

¹Southern Observatory, Karl-Schwarzschild-Strasse 2, D-85748 Garching, Germany
email: ogonzale@eso.org

Abstract. In our detailed study of chemical abundances in the Galactic bulge (see Zoccali et al. 2008 for a description of the entire project) we have measured Li abundances by fitting synthetic spectra to the ${}^7\text{Li}$ (6707.18Å) line for ~ 400 giants in Baade’s Window and a field at $b=-6$ (Gonzalez et al. 2009). We have found 13 stars showing strong ${}^7\text{Li}$ lines in complete contrast to the rest of the sample for which only upper limits could be obtained. Our sample is at least 1.2 mag brighter than the expected RGB bump, therefore we interpreted our results as evidence for stars that might have avoided the observed extra-mixing process or undergoing a Li enrichment process not necessarily linked to the RGB bump.

Keywords. stars: abundances, late-type – Galaxy: bulge

1. Introduction

Even with the increasing number of low mass Li-rich giants found to date, we have not been able to fully understand their origin. The main reason is that is becoming difficult to relate Li-rich stars with a single evolutionary status. Charbonnel & Balachandran (2000) presented a first evidence for a connection between Li-rich stars and evolutionary status showing that a significant number of Li-rich giants fall close to the RGB bump, where an extra-mixing process is expected to act, affecting abundances of C, ${}^{12}\text{C}/{}^{13}\text{C}$ and ${}^7\text{Li}$ (Gratton et al. 2000). In particular, after the RGB bump, ${}^7\text{Li}$ abundances are expected to be close to $A(\text{Li})=0$ as the material from the convective envelope is brought to higher temperatures in which Li is expected to be destroyed. However, in a very short stage prior to its destruction, ${}^7\text{Li}$ could be produced by Cameron-Fowler mechanism (Cameron & Fowler 1971). In complete contrast, the number of Li-rich stars not fulfilling the RGB bump connection has been recently increased (Monaco et al. 2007; Uttenthaler et al. 2007; Gonzalez et al. 2009) requiring stellar models to explain a Li production phase almost at any instance along the giant evolutionary sequence.

2. Can we really constrain Li-rich giants to a single phenomena?

While 11 stars in our sample show $A(\text{Li})$ within 0.8 and 2.3 following a well defined trend with T_{eff} (Fig. 1), 2 of them have $A(\text{Li})\sim 2.8$ and fall away from this relation. From their location in the CMD (nearly 1 mag. above the red clump), Li-rich stars in our sample are not compatible with a Li production phase in the RGB bump, even considering the Bulge distance spread. However, the Li content in the remaining ~ 400 stars is in agreement with an extra-mixing process diluting Li at the RGB bump to a value of $A(\text{Li})\sim 0$. Therefore, these Li-rich giants might be stars which have avoided the extra-mixing at the RGB bump and show the Li abundance expected from standard dilution ($A(\text{Li})\sim 1.5$) which would explain the observed trend between ${}^7\text{Li}$ and T_{eff} . However, in this scenario, the problem remains for the two Li-rich stars showing $A(\text{Li})\sim 2.8$ for

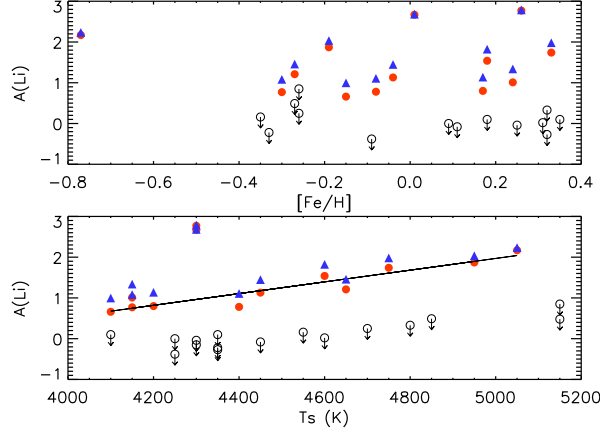


Figure 1. Relation between Li abundances and effective temperature (lower panel). Red filled circles are Li abundances measured under LTE and empty circles are upper limits. Blue triangles are $A(\text{Li})$ with NLTE corrections. No relation is observed between $A(\text{Li})$ and metallicity (upper panel).

which the high Li content could only be explained by an undergoing Li production phase. Models have shown that Li evolution in low-mass giants is highly dependent on magnetic field properties (Guandalini et al. 2009). By taking into account these magnetic properties, stars avoiding the extra-mixing process in the RGB bump might be explained (Charbonnel & Zahn 2007) as well as Li production in other instances of the giant evolution. A different approach must be considered as well, as Li has been probed to be affected by the presence of planets, at least in main sequence stars. In more evolved stars, this might also be the case. The engulfment of a planet would hardly contain enough material to enrich the surface of the star, but according to the models presented by Denissenkov & Herwig (2004), the addition of angular momentum might be enough to trigger a short Li production phase which might explain Li enriched giants at any moment during their giant evolution.

In conclusion, as the number of Li-rich stars has increased, it has become clear that their occurrence cannot be confined to a single evolutionary phase. Other parameters such as magnetic field properties or the presence of planets, might also be playing an important role.

References

- Cameron, A.G.W., & Fowler, W.A. 1971, *ApJ*, 164, 111
 Charbonnel, C., & Balachandran S.C. 2000, *A&AS*, 359, 563
 Charbonnel, C., & Zahn, J.P. 2007b, *A&A*, 476, L29
 Denissenkov, P.A. & Herwig, F. 2004, *ApJ*, 612, 1081
 Gonzalez, O.A., Zoccali, M., Monaco, L., Hill, V. et al. 2009, *A&A*, 508, 289
 Gratton, R.G., Snenen, C., Carretta, E., Bragaglia, A. 2000, *A&A*, 354, 169
 Guandalini, R., Palmerini, M., Busso, M. & Uttenthaler, S. 2009, *PASA*, 26, 168
 Monaco, L., Bellazzini, M., Bonifacio, P., Buzzoni, A., Ferraro, F. R., Marconi, G., Sbordone, L., & Zaggia, S. 2007, *A&A*, 464, 201
 Monaco, L. & Bonifacio, P., 2008, *MemSAI*, 79, 1
 Uttenthaler, S., Lebzelter, T., Palmerini, et al. 2007, *A&A*, 471, L41
 Zoccali, M., Lecureur, A., Hill, V. et al. 2008, *A&A*, 486, 177

Interstellar Lithium as a probe of the primordial abundance

J. Christopher Howk¹

¹Department of Physics,
University of Notre Dame,
Notre Dame, IN, USA
email: jhowk@nd.edu

Abstract.

The cosmic abundance of lithium continues to represent a conundrum, as predictions from BBN theory are inconsistent with measurements in the atmospheres of the lowest-metallicity stars. While there are worries that modifications of the stellar Li abundances may play a role in this discrepancy, no satisfactory solution has yet been found. We suggest an alternate approach to studying the cosmic abundance of Li: measurements of interstellar gas-phase Li in low-metallicity environments.

Keywords. ISM: abundances, clouds – galaxies: abundances – nuclear reactions, nucleosynthesis, abundances

1. Introduction

The primordial Li abundance predicted by standard Big Bang nucleosynthesis (BBN) is a factor of $\gtrsim 2-4$ above the best estimates of the Li abundance in halo star atmospheres (cf., summary in Cyburt et al. 2008). Several possibilities for this discrepancy exist, including destruction of Li within the stars themselves or the intriguing possibility of new physics (e.g., inhomogeneous nucleosynthesis, Li destruction in the first stars, non-thermal production by particle decays) as discussed elsewhere in these proceedings.

A new approach to estimating the primordial abundance of Li would be extremely useful. Here we reintroduce such an approach, the measurement of *interstellar* lithium abundances in low-metallicity galaxies. Estimating Li/H in the interstellar medium (ISM) of galaxies carries its own potential systematic uncertainties (see Steigman 1996), *but they are independent of those that may affect stellar abundance estimates*. In addition, the small velocity dispersions of interstellar gas makes it possible to measure the ${}^6\text{Li}/{}^7\text{Li}$ isotopic ratio (Kawanomoto et al. 2009), which can further constrain the origin of Li.

Previous searches for interstellar Li in external galaxies were limited to the SN 1987A sight line in the Large Magellanic Cloud as reported in Vidal-Madjar et al. (1987), ?, and Baade et al. (1991), which had somewhat limited usefulness for placing a limit on the absolute abundance measurements (Steigman 1996). More recently Prodanović & Fields (2004) suggested it may be possible to measure the gas-phase Li abundances in Galactic high velocity clouds, which are low-metallicity clouds that appear to be falling onto the Galaxy for the first time. While their calculations are overly optimistic (as described below), the rationale for such a measurement is clearly stated. With today's large aperture telescopes, however, it is possible to detect interstellar Li in other galaxies, and we will report on the first detection of interstellar Li in the Small Magellanic Cloud in an upcoming publication.

2. Interstellar lithium abundances

Measurements of Li in ISM clouds rely on the measurement of neutral lithium in absorption against background light sources using the Li I doublet near 6707 Å. However, the direct comparison of the column density of Li I with that of H I measured in the same way does not directly yield the interstellar Li abundance, because 1) Li^0 is not the dominant ionization stage of Li in the ISM (that being Li^+); and 2) Li may be incorporated into interstellar dust grains. These effects are such that $\text{Li I}/\text{H I} \ll \text{Li}/\text{H}$. Thus, the abundance of Li in the ISM is given by

$$\text{Li}/\text{H} = N(\text{Li I})N(\text{H})^{-1}x(\text{Li}^0)^{-1}\delta_{\text{Li}}^{-1}, \quad (2.1)$$

where $N(\text{H}) \equiv N(\text{H I}) + 2N(\text{H}_2)$ is the total hydrogen column density, $x(\text{Li}^0)$ is the ionization fraction of neutral lithium, and δ_{Li} is the fraction of all Li present in the gas phase (the “depletion” due to dust). The ionization fraction in this case depends on the density of electrons (and perhaps of dust grains; see) and the strength of the radiation field.

These corrections can be quite large, with likely values $x(\text{Li}^0)^{-1} \gtrsim 100$ and $\delta_{\text{Li}}^{-1} \sim 4-5$ (Welty et al. 2003). Although the ionization corrections are typically derived in a relative sense using observed ratios of adjacent ions from other elements (e.g., Ca I/Ca II) so that the absolute strength of the radiation field is not important, these can still be quite uncertain. Steigman (1996) has argued that the ratio of Li I/K I can be a better approach to studying the interstellar abundance of Li, given the similar ionization characteristics of these two elements, although one is then in a position of estimating or assuming the K/H ratio if one is to estimate Li/H.

The recent work of Prodanović & Fields (2004) did not consider the strong effects of photoionization of Li I in their feasibility arguments when discussing measurements in high velocity clouds. The very small amounts of neutral lithium expected for such clouds, coupled with the relatively low column densities of these clouds makes the measurements extremely difficult. It will not be possible to probe Li in interstellar environments as metal poor as the halo star sample, but by probing gas in a range of metallicities, we will eventually be able to use the interstellar abundances to complement our understanding of the stellar results. Indeed, our first measurement beyond the Milky Way is in the gas of the Small Magellanic Cloud, which has a metallicity $\sim 0.25Z_{\odot}$. The next generation of very large aperture telescopes should allow us to push this approach to lower metallicity damped Lyman- α systems, although significant uncertainties in the absolute abundances derived through ionization analyses will likely persist.

References

- Baade, D., Cristiani, S., Lanz, T., Malaney, R.A., Sahu, K.S., & Vladilo, G. 1991, *A&A*, 251, 253
 Cyburt, R.H., Fields, B.D., & Olive, K.A. 2009, *J. Cosmology & Astroparticle Physics*, 11, 012
 Kawanomoto, S., et al. 2009, *ApJ*, 701, 1506
 Prodanović, T., & Fields, B.D. 2004, *ApJ* (Letters), 616, L115
 Steigman, G. 1996, *ApJ*, 457, 737
 Vidal-Madjar, A., Andreani, P., Cristiani, S., Ferlet, R., Lanz, T., Vladilo, G. 1987, *A&A*, 177, L17
 Welty, D.E., Hobbs, L.M., & Morton, D.C. 2003, *ApJS*, 147, 61

A very low upper limit for a Be abundance of a carbon-enhanced metal-poor star

Hiroko Ito^{1,2}, Wako Aoki^{1,2}, Satoshi Honda³,
Timothy C. Beers⁴, and Nozomu Tominaga⁵

¹Department of Astronomical Science, School of Physical Sciences, The Graduate University for Advanced Studies (SOKENDAI), 2-21-1, Osawa, Mitaka, Tokyo, 181-8588, Japan
email: hiroko.ito@nao.ac.jp

²National Astronomical Observatory of Japan, Mitaka, Tokyo, Japan

³Gumma Astronomical Observatory, Agatsuma, Gunma, Japan

⁴Michigan State University, East Lansing, MI 48824-1116, USA

⁵Konan University, Kobe, Hyogo, Japan

Abstract. We performed a 1D LTE chemical abundance analysis of an extremely metal-poor star BD+44°493 ($[\text{Fe}/\text{H}] = -3.7$), and set a very low upper limit for its Be abundance: $A(\text{Be}) < -2.0$. It may indicate that the decreasing trend of Be abundances with lower $[\text{Fe}/\text{H}]$ still holds at $[\text{Fe}/\text{H}] < -3.5$, and demonstrate that high C and O abundances do not necessarily imply high Be abundances. However, since the star is a subgiant with $T_{\text{eff}} \sim 5500\text{K}$, Be may be depleted.

Keywords. stars: abundances, individual (BD+44°493), Population II

1. Observation and analysis

High-resolution spectroscopy of BD+44°493 was carried out with Subaru/HDS. The atmospheric parameters that we adopt are $T_{\text{eff}} = 5510\text{K}$, and $\log g = 3.7$. Our 1D LTE abundance analysis derives $[\text{Fe}/\text{H}] = -3.7$, $[\text{C}/\text{Fe}] = +1.3$, and $[\text{O}/\text{Fe}] = +1.6$, indicating that this star is a carbon-enhanced metal-poor (CEMP) star. Its abundance pattern implies that a first-generation "faint" supernova (e.g., Tominaga et al. 2007) is the most likely origin of its carbon excess. See Ito et al. (2009) for detail.

2. Implications of its low beryllium abundance

We set a very low upper limit for its Be abundance ($A(\text{Be}) < -2.0$). This is the Be abundance reported at the lowest metallicity yet achieved, and is the lowest Be limit so far for metal-poor dwarfs or subgiants that have normal Li abundances. The result indicates that the decreasing trend of Be abundances with lower $[\text{Fe}/\text{H}]$, which was revealed by previous studies (e.g., Boesgaard et al. 1999), still holds at $[\text{Fe}/\text{H}] < -3.5$ (Fig. 1).

Our analysis is the first attempt to measure a Be abundance for a CEMP star. Since Be is produced via the spallation of CNO nuclei, their abundances, especially O abundances, have been expected to correlate with Be abundances. However, our low Be upper limit shows that the high C and O abundances in BD+44°493 are irrelevant to its Be abundance (Fig. 1), which offers a new insight into the origin of CEMP stars.

3. Possibility of depletion

Previous studies of Be abundances in metal-poor subgiants indicate that Be is depleted in those with $T_{\text{eff}} < 5500\text{K}$, so BD+44°493 is at the boundary (Fig. 2). In Ito et al. (2009),

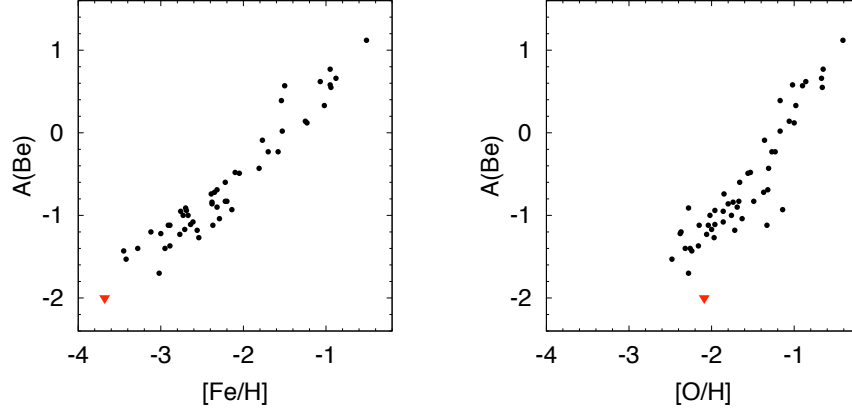


Figure 1. $A(\text{Be})$ vs. $[\text{Fe}/\text{H}]$ and $A(\text{Be})$ vs. $[\text{O}/\text{H}]$. Our upper limit for BD+44°493 is shown by the red triangle. The filled circles indicate results of Rich & Boesgaard (2009).

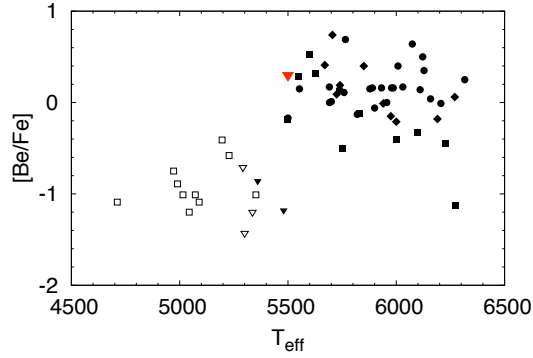


Figure 2. $[\text{Be}/\text{Fe}]$ as a function of T_{eff} . Our upper limit for BD+44°493 is shown by the red (bigger) triangle above the centre of the figure. Filled circles and diamonds indicate results of Rich & Boesgaard (2009) and Tan et al. (2009), respectively. Filled squares and (smaller) triangles those of Smiljanic et al. (2009), and the open ones those of García Pérez & Primas (2006). All triangles represent upper limits. Only subgiants ($\log g < 4.0$) are plotted.

we adopt $T_{\text{eff}} = 5510$ K determined by Carney et al. (2003), and assumed that Be in the star is not depleted. However, Carney et al. (2003) seems to overestimate the reddening, and our re-estimate lowers its temperature by about 100K (Ito et al. in prep.), increasing the possibility of Be depletion. We cannot conclude whether its Be is depleted, but if it is, our interpretation of its low Be abundance needs to be revised.

References

- Boesgaard, A. M., Deliyannis, C. P., King, J. R., Ryan, S. G., et al. 1999, *AJ*, 117, 1549
 Carney, B. W., Latham, D. W., Stefanik, R. P., Laird, J. B., & Morse, J. A. 2003, *AJ*, 125, 293
 García Pérez, A. E., & Primas, F. 2006, *A&A*, 447, 299
 Ito, H., Aoki, W., Honda, S., & Beers, T. C. 2009, *ApJ* (Letters), 698, L37
 Rich, J. A., & Boesgaard, A. M. 2009, *ApJ*, 701, 1519
 Smiljanic, R., Pasquini, L., Bonifacio, P., Galli, D., et al. 2009, *A&A*, 499, 103
 Tan, K. F., Shi, J. R., & Zhao, G. 2009, *MNRAS*, 392, 205
 Tominaga, N., Maeda, K., Umeda, H., Nomoto, K., et al. 2007, *ApJ* (Letters), 657, L77

Lithium abundances in the α Persei Cluster

Sushma V. Mallik¹, Suchitra C. Balachandran², and David L. Lambert³

¹Indian Institute of Astrophysics, Bangalore 560034, India

email: sgvmlk@iiap.res.in

²Astronomy Department, University of Maryland, College Park, MD 20742-2421, USA

email: suchitra@astro.umd.edu

³W.J. McDonald Observatory, The University of Texas, Austin, TX 78712-0259, USA

email: dll@astro.as.utexas.edu

Abstract. As a sequel to the Li observations by Balachandran, Lambert & Stauffer (1988, 1996) in 35 stars of the 50 Myr old cluster α Persei, we have obtained and analyzed high resolution spectra of another 51 stars. Following a reconsideration of the cluster membership of the stars (Prosser 1992, Makarov 2006, Mermilliod et al. 2008, and Patience et al. 2002), we discuss the Li abundances for 70 stars. With our larger sample, we reexamine the question of whether the scatter in Li abundance at a given T_{eff} seen in young clusters at cool temperatures is real or not.

Keywords. Galaxy: open clusters – stars: abundances

1. Observations, abundances and their interpretation

High S/N echelle spectra were obtained for 30 stars at the 2.7m telescope at the McDonald Observatory at $R=60,000$ and for 21 stars at the 4m telescope at KPNO at $R=40,000$. The Li abundance as determined from the 6707.8 Å feature is singularly sensitive to the adopted T_{eff} . For an error of ± 200 K in T_{eff} , the uncertainty in $\log N(\text{Li})$ varies from 0.28 to 0.14 over the temperature range from 4500 K to 6500 K. We choose (V–K) colour index as our principal indicator of T_{eff} . Our fresh estimates of reddening for stars with available Stromgren photometry yield $E(b-y)$ in the range of 0.02 to 0.12 with an average of 0.075 (± 0.05). We adopt this average that translates to $E(V-K) = 0.284$ and use the (V–K) - T_{eff} calibration of Alonso et al. (1986) to derive $T_{\text{eff}}(V-K)$ for all the stars. A mean Fe abundance of 7.40 ± 0.08 dex was obtained for the 26 slowly rotating stars from a fine spectroscopic analysis; the standard error comparable to the estimate of the precision of a single determination. As is apparent from Fig.1, Li abundance in the hottest stars approaches a constant value (taken as the initial value for young open clusters), close to the meteoritic value of 3.25 ± 0.06 , as also to the abundance derived of T Tauri stars suggesting it has changed little in the last 4.5 Gyrs.

1589, 1604, 56 and 93 (> 5300 K) and # 1612, 1735 (< 5300 K) are outliers that do not define the mean relation. This could possibly be either because their assigned T_{eff} is too low or they are non-members that have experienced normal Li depletion for their age or an unusual amount of Li depletion has occurred. At $T_{\text{eff}} < 5300$ K, Li vs. T_{eff} relation plunges steeply and develops a scatter in Li abundance; it widens into a band with a lower envelope defined by low *vsini* stars from Li of 2.1 at 5000 K to -0.4 at 4500 K and an upper envelope defined by high *vsini* stars from Li of 2.5 at 4700 K to 0.6 at 4300 K; width of the band at $T_{\text{eff}} < 4700$ K is ~ 1.5 dex, as is observed in the Pleiades.

Pre-Main Sequence (PMS) depletion of Li is ineffective for the hotter stars of α Per. In cooler stars it is best mappable by looking at the youngest of clusters, for, stars in α Per have experienced PMS depletion that is essentially complete. A Li abundance

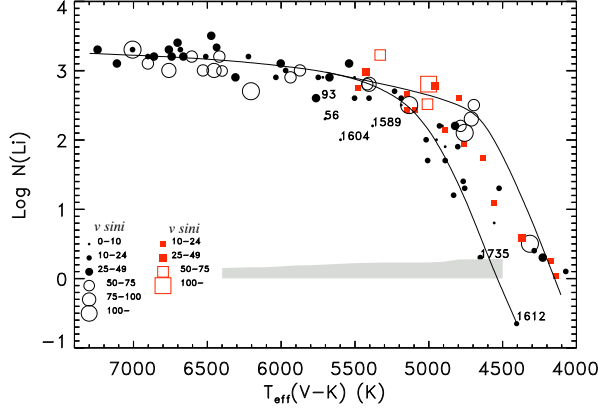


Figure 1. T_{eff} vs Li abundance for α Per with data (red squares) added from Randich et al. (1998). $v\text{ sini}$ is represented according to the legend of the figure. The shaded strip shows the Li spread resulting from an uncertainty of $\pm 100\text{K}$ in T_{eff} . The labelled stars are possible outliers. Suggested upper and lower envelopes to the relation are indicated.

study of 5 associations with age ranging from 10 to 100 Myr (Mentuch et al. 2008) suggests increasing Li depletion with age as predicted for the PMS phase. The peak-to-peak scatter increases from ± 0.3 (for β Pic) to $\pm 0.5 - \pm 0.8$ (for Tucanae-Horologium and the AB Doradus), less than that seen for α Per. Clusters younger than α Per - IC 2602, IC 2391, NGC 4665, NGC 2547 also have smaller star-to-star scatter in Li. The older cluster, the Pleiades (70 Myr) has a similar scatter as α Per and in fact M 34 (250 Myr) has as much. These observations imply that that spread in Li among cooler stars is not well developed in the youngest clusters/associations and it may take 20 Myr or so to develop fully. Li depletion seems to be dominated by that occurring in the PMS phase for clusters up to the ages of 50-100 Myr. For older clusters, it is the Main Sequence depletion that begins to reduce Li in the coolest stars. Very apparent, *e.g.*, in M 34 where the star-to-star scatter remains similar to the Pleiades and α Per but the mean abundances are noticeably reduced.

The large scatter observed at cooler temperatures is far larger than could be explained by the standard sources of uncertainty. Several studies in the past report a strong correlation between the Li scatter and stellar activity. We have to have contemporaneous indicators of stellar activity for pairs of stars with maximum and minimum Li abundance but similar observed properties such as colour and rotation period. In the absence of these, the debate continues on whether the star-to-star spread is due to real differences in Li abundances or arises due to atmospheric effects.

References

- Alonso, A., Arribas, S., & Martínez-Roger, C. 1996, *A&A*, 313, 873
- Balachandran, S., Lambert, D.L., & Stauffer, J.R. 1988, *ApJ*, 333, 267
- Balachandran, S., Lambert, D.L., & Stauffer, J.R. 1996, *ApJ*, 470, 1243
- Makarov, V.V. 2006, *AJ*, 131, 2967
- Mentuch, E. et al. 2008, *ApJ*, 689, 1127
- Mermilliod, J.-C., Queloz, D., & Mayor, M. 2008, *A&A*, 488, 409
- Patience, J., Ghez, A.M., Reid, I.N., & Matthews, K. 2002, *AJ*, 123, 1570
- Prosser, C.F. 1992, *AJ*, 103, 488
- Randich, S., Martín, E.L., García López, R.J., & Pallavicini, R. 1998, *A&A*, 333, 591

Lithium in other Suns: no connection between stars and planets

Jorge Meléndez¹, Iván Ramírez², Martin Asplund², and Patrick
Baumann²

¹Centro de Astrofísica, Universidade do Porto, Rua das Estrelas, 4150-762 Porto, Portugal
email: jorge@astro.up.pt

²Max-Planck-Institut für Astrophysik, Germany

Abstract. An unbiased sample of solar twins shows that the Sun has a normal Li abundance for its age and that a low Li abundance does not imply the presence of planets. We find a tight correlation between Li and age, which holds for all stars analyzed in our sample: solar twins, stars with and without detected giant planets, and stars that may host terrestrial planets.

Keywords. Sun: abundances – stars: abundances, planetary systems

1. Lithium vs. age for solar twins in the field and clusters

The sample consists of more than one hundred stars similar to the Sun observed at McDonald (2.7m) and Las Campanas (6.5m Magellan Clay telescope). Most of them are from our solar twin survey (Meléndez et al. 2009a,b; Ramírez et al. 2009). We have also included ~ 20 solar analogs with and without detected giant planets.

Our high quality spectra ($R = 60,000$; $S/N = 200-450$) allows the determination of Li abundances in stars as Li-poor as the Sun. Due to the similarity between the Sun and the twins, accurate stellar parameters can be determined, thus reliable ages can be obtained from isochrones. For young stars ($<1\text{Gyr}$) whenever possible we use precise rotation periods to estimate ages. Both methods agree, but the rotational ages are more precise. In Fig. 1 we show only solar twins (open circles) with good ages ($3-\sigma$ or better).

There is a clear correlation between Li and Age in our sample of solar twins (open circles). The one-solar-mass stars in solar-metallicity open clusters (filled triangles) also follow the same correlation. Note that we have only used clusters with reliable data, which are very few for old solar-metallicity open clusters. For example, the cluster Collinder 261 seems old but its age, reddening and metallicity are very uncertain (Spanò et al. 2005). Furthermore, only relatively high upper limits in the Li abundances of solar twins in Cr 261 are available (Spanò et al. 2005). NGC 188 is another potentially interesting old solar metallicity open cluster, but there is only one star that may be as cool as the Sun in the study of Randich et al. (2003, Fig. 2). Furthermore, according to Sestito & Randich (2005), the NGC 188 stars analyzed by Randich et al. (2003) have a S/N of only 20-35, which would be too low to detect the Li feature in a star like the Sun.

2. No planet connection

Our sample of solar twins without detected giant planets follows the same Li vs. Age as other solar twins. We have also studied 18 solar analogs included in radial velocity planet surveys; six of them with detected giant planets and 12 of them without detected giant planets. Both samples seem to follow the Li vs. Age correlation shown in Fig. 1.

We have recently found a signature that may indicate the presence of terrestrial planets

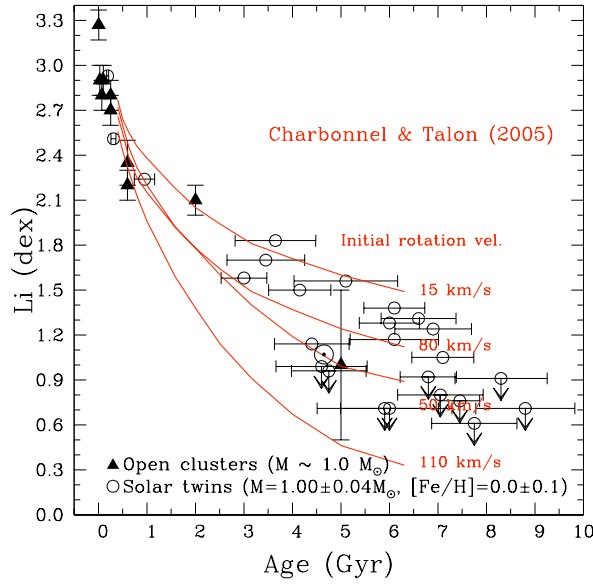


Figure 1. Li for our solar twins with one solar mass ($\pm 4\%$) and solar $[\text{Fe}/\text{H}]$ (± 0.1 dex), and for one-solar-mass stars in solar metallicity (± 0.15 dex) open clusters selected from Sestito & Randich (2005), although for M67 we used the sample of Pasquini et al. (2008). Field stars are shown as circles while open clusters with triangles. Figure updated from Meléndez et al. 2009b.

around other stars (Meléndez et al. 2009a; Ramírez et al. 2009). Solar twins showing the same terrestrial planet signature as our Sun also follow the same Li vs. Age relation as solar twins without the signature of other earths.

In conclusion, we find no relation between low levels of Li and the presence of planets. The low Li observed in the Sun is normal for a star of its age, mass, and metallicity.

As already suggested by other authors (see Meléndez et al. 2009b for a review), Israelian et al. (2009) have recently claimed that planet host stars in a narrow range around solar T_{eff} , have enhanced depletion of lithium due to the presence of planets. Our work suggests as alternative explanation that the low Li in planet host stars around the solar T_{eff} may be due an age effect instead of the presence of planets.

References

- Charbonnel, C., & Talon, S. 2005, *Science*, 309, 2189
 Israelian, G., et al. 2009, *Nature*, 462, 189
 Meléndez, J., Asplund, M., Gustafsson, B., & Yong, D. 2009a, *ApJ* (Letters), 704, L66
 Meléndez, J., et al. 2009b, *ApJSS*, 221, in press
 Pasquini, L., Biazzo, K., Bonifacio, P., Randich, S., & Bedin, L. R. 2008, *A&A*, 489, 677
 Ramírez, I., Meléndez, J., & Asplund, M. 2009, *A&A* (Letters), 508, L17
 Randich, S., Sestito, P., & Pallavicini, R. 2003, *A&A*, 399, 133
 Sestito, P., & Randich, S. 2005, *A&A*, 442, 615
 Spanò, P., Pallavicini, R., & Randich, S. 2005, *IAU Symp.*, 228, 111

Li abundances and chromospheric activity of BY Dra type stars

Tamara V. Mishenina^{1,2}, Caroline Soubiran¹, Valery V. Kovtyukh²,
and Stanislav I. Belik²

¹Université de Bordeaux - CNRS - Laboratoire d'Astrophysique de Bordeaux,
BP 89, 33271 Floirac Cedex, France,
email: caroline.soubiran@obs.u-bordeaux1.fr

²Astronomical observatory, Odessa National University,
T.G.Shevchenko Park, Odessa 65014 Ukraine
email: tamar@deneb1.odessa.ua

Abstract. Atmospheric parameters and Li abundances have been determined for 162 stars observed at high resolution, high signal to noise ratio with the ELODIE echelle spectrograph (OHP, France). Among them, about 70 stars are active stars with a large fraction of BY Dra type stars. For all stars, rotational velocities were obtained with a calibration of the cross-correlation function, effective temperatures by the line depth ratio method, surface gravities by the parallax method and by the ionization balance of iron. The frequency of stars with observed lithium is significantly higher in active stars than in non active stars. Among active stars, no clear correlation has been found between different indicators of activity for our sample stars, but some correlation of an index R'_{HK} and $v \sin i$ is observed.

Keywords. Stars: abundances, fundamental parameters, activity

1. Introduction

Lithium abundances are of a particular interest, as reflecting various processes in stars and at the stellar surface and as a possible indicator of chromospheric activity. It is important also because the Sun is suspected to belong to the BY Dra type.

2. Observations, parameters, and Li determinations

The spectra of 162 stars were obtained using the 1.93 m telescope at Observatoire de Haute-Provence (OHP, France) equipped with the echelle spectrograph ELODIE (Baranne et al. 1996) which gives a resolving power of $R = 42\,000$. The spectral processing was performed according to Katz et al. (1998). Rotational velocities $v \sin i$ were measured with a relation calibrated by Queloz et al. (1998).

The determination of T_{eff} , $\log g$, $[\text{Fe}/\text{H}]$ was performed following Mishenina et al. (2004, 2008) and Kovtyukh et al. (2004). Li abundances $\log A(\text{Li})$ were determined by LTE spectral synthesis code STARS (Tsymbal 1996). The list of lines in the region of Li I line 6707 Å was taken from Mishenina & Tsymbal (1997).

3. Results and discussion

Stars of BY Dra type are young stars. In their spectra the lines of lithium show different intensities not always correlating with other indicators of stellar activity. Sometimes Li lines are absent. The dependence of $\log A(\text{Li})$ on T_{eff} , is presented in Fig.1 (the top value of an estimation of $\log A(\text{Li})$ are marked by symbols with arrows).

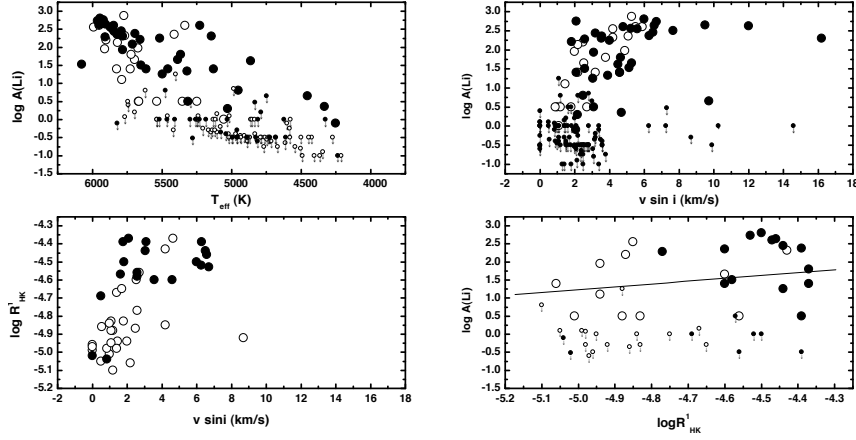


Figure 1. Connection between $\log A(\text{Li})$, T_{eff} , $v \sin i$, and R'_{HK} .

We have detected the lithium in 19 stars among the 91 non active dwarfs and 39 stars among the 73 stars with chromospheric activity, corresponding to about 20% and 54%, respectively. We confirm our earlier result (Mishenina et al. 2008) with almost doubled quantity of active stars. The behavior of $\log A(\text{Li})$ with $v \sin i$ is similar for active and non-active stars (see Fig.1). To search for correlations between the lithium abundance and chromospheric activity we have used as an indicator of chromospheric activity the index R'_{HK} (Wright et al. 2004) for stars in a range of colours $0.4 < B - V < 0.9$. We have checked R'_{HK} versus rotation and lithium abundance versus R'_{HK} (see Fig. 1). We observe some correlation of R'_{HK} and $v \sin i$, but the correlation between $\log A(\text{Li})$ and R'_{HK} is not so obvious.

4. Conclusions

I. The frequency of stars with observed lithium is significantly higher in active stars than in non active stars.

II. Active stars exhibit no clear correlation between $\log A(\text{Li})$ and $v \sin i$ and the index R'_{HK} , but we observe some correlation of the index R'_{HK} and $v \sin i$.

References

- Baranne, A., Queloz, D., Mayor, M. et al. 1996, *A&AS*, 119, 373
- Katz, D., Soubiran, C., Cayrel, R. et al. 1998, *A&A*, 338, 151
- Kovtyukh, V.V., Soubiran, C., & Belik, S.I. 2004, *A&A*, 427, 923
- Mishenina, T.V., & Tsymbal, V.V. 1997, *Pis'ma v AZh*, 23, 693
- Mishenina, T.V., Soubiran, C., Kovtyukh, V.V., & Korotin, S. A. 2004, *A&A*, 418, 551
- Mishenina, T.V., Soubiran, C., Bienayme, O., Kovtyukh, V.V., & Korotin, S. A. 2008, *A&A*, 489, 923
- Queloz, D., Allain, S., Mermilliod, J.-C. et al. 1998, *A&A*, 335, 183
- Tsymbal, V.V. 1996, *ASP Conf. Ser.*, 108, 198
- Wright, J.T., Marcy, G.W., Butler, R.P., & Vogt, S.S. 2004, *ApJS*, 152, 261

Lithium abundances in dwarfs of intermediate age open clusters

Giancarlo Pace¹ and Jorge Mélendez¹

¹Centro de Astrofísica, Universidade do Porto,

Rua das Estrelas, 4150-762, Porto, Portugal

email: gpace@astro.up.pt

Abstract.

Lithium abundance measurements in dwarf stars in open clusters are of crucial importance for our understanding of the mixing mechanism and have allowed us to achieve important conclusions on the matter. However, in order to further our understanding of what drives lithium depletion, lithium abundance measurements have to be coupled with accurate temperature determinations, which are best achieved when the analysis of iron lines is employed. Effective temperature estimations from photometry, on the contrary, can be affected by errors as large as several hundred kelvins due to uncertain open cluster reddening, especially when studying old open clusters, which tend to be more distant. We present lithium abundance in 12 dwarfs belonging to 4 open clusters at about 1 or 2 Gyr. The stellar effective temperatures, along with the other parameters, were estimated from the analysis of about 60 Fe I lines and 10 Fe II. Even though the few datapoints call for caution, we notice that stars in the open cluster IC 4651 seem to present a steep decline with temperature below 6000 K.

Keywords. Galaxy: open clusters – stars: low-mass, abundances

1. Data sample and analysis

The sample consists of 12 dwarf stars in the following 4 open clusters whose ages, as found by Salaris *et al.* (2004), are indicated in the legend of Figure 1. The spectra were taken with UVES @ VLT, they have a resolution of about $R \approx 100\,000$ and S/N of about 100 in the range between 4800 and 6800 Å.

Stellar parameters, namely temperature, gravity, metallicity, and microturbulence, were obtained (Pace et al. 2008, 2010) with the classical equivalent width analysis of the iron lines (about 60 for Fe I and about 10 for Fe II). Apart of the precision achievable, especially when, as in our case, spectra with high resolution and good S/N are available, this method has the great advantage of being independent of the cluster reddening.

We find differences of several hundred Kelvin between the temperatures as evaluated from the spectroscopic analysis and the temperatures evaluated by means of photometry and published calibration. Most of this difference is probably due to the error in the reddening of the cluster and in the zero point errors in the calibration of the photometry.

Lithium abundances were measured by comparing the observed spectrum of the lithium doublet at 6707.8 Å with the synthetic one, and changing the assumed abundance until a match between the two was obtained. The typical errors are between 0.05 and 0.15 dex. Using the same procedure, we also compared the synthetic spectrum of the Sun with the UVES-archive solar spectrum, and we obtained the best match by assuming $A(\text{Li}) = 1$ rather than the canonical $A(\text{Li}) = 1.1$.

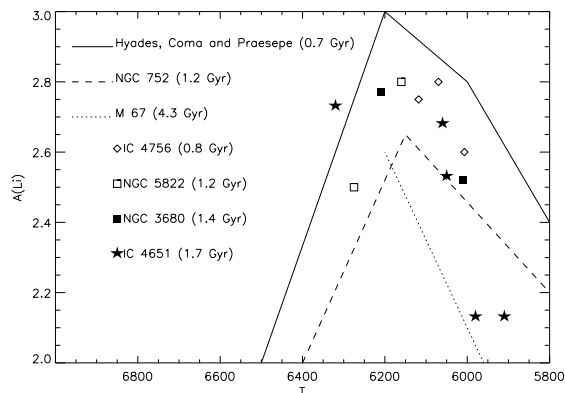


Figure 1. Our data on dwarfs in intermediate age open clusters compared with literature data about young open clusters and NGC 752 (also about 1 Gyr old) and the much older M 67.

2. Results and conclusions

In the Figure we show a temperature versus lithium abundance diagram, in which we compare the 12 data points from the present analysis with published open cluster data at 3 different ages. Hyades, Coma, and Praesepe data are depicted in one single curve, another represents NGC 752 and the third M 67. M 67 data are taken from Pasquini *et al.* (2008), the remainder from the compilation in Xiong & Deng (2009). The curves that represent the published cluster data at the 3 different ages, are fits by eye to the datapoints. The temperatures for the Hyades age clusters and NGC 752 are derived from photometry. For the former the uncertainty in the colour excess should not play a major role, since they are nearby clusters. The curve representing the clusters at the Hyades age form an upper envelope to the distribution of the other datapoints. The curve representing M 67 and, for temperatures higher than 6000 K, that of NGC 752, form, instead, a possible lower envelope. Only one datapoint falls slightly outside the region defined by the two envelopes. Even though the few datapoints call for caution, we notice that IC 4651 seems to present a steep decline below 6000K.

When studying the dependence of lithium abundances as a function of temperatures in stars in open clusters, the use of temperature measurements by spectroscopic analysis is essential to avoid errors due to uncertain reddening.

References

- Pace, G., Danziger, J., Carraro, G., Melendez, J., François, P., Matteucci, F. & Santos N.C. 2010 *A&A*, accepted
- Pace, G., Pasquini, L., & François, P. 2008, *A&A* (Letters), 489, 403
- Pasquini, L., & Biazzo, K., Bonifacio, P., Randich, S., & Bedin, L. R. 2008, *A&A*, 489, 677
- Salaris, M., Weiss, A., & Percival, S. M. 2004, *A&A*, 414, 163
- Xiong, D. R., & Deng, L. 2009 *MNRAS*, 395, 2013

HD 232 862 : a magnetic and lithium-rich giant star

A. Palacios¹, A. Lèbre¹, J.D. do Nascimento Jr², R. Konstantinova-Antova³, D. Kolev³, M. Aurière⁴, P. de Laverny⁵ and J.R. de Medeiros²

¹ GRAAL-CNRS/Université Montpellier II, France
email: palacios@graal.univ-montp2.fr

²DFTE - Universidade Federal do Rio Grande do Norte, Natal, Brazil

³ Institute of Astronomy, Bulgarian Academy of Sciences, Sofia, Bulgaria

⁴LATT - Observatoire Midi-Pyrénées, Toulouse, France

⁵ Cassiopée, Observatoire de la Côte d'Azur, Nice, France

Abstract. Using spectropolarimetric data acquired with the ESPaDOnS and NARVAL instruments at CFHT and at TBL, we present a detailed spectral synthesis analysis of HD 232 862, a field giant classified as a G8II star hosting a magnetic field. This star is the first lithium-rich field giant hosting a magnetic field. Stellar evolution models suggest that HD 232 862 should be a 1.5 to 2.0 M_{\odot} star at the bottom of the red giant branch. Its unusually high lithium content ($A(\text{Li}) = 2.45 \pm 0.25$ dex) is even more puzzling and challenges our understanding of the evolution of this star.

Keywords. Stars: spectroscopy, spectropolarimetry, abundances, evolution, magnetic fields

1. Observations and main features

HD 232 862 is classified as a G8II star in the SIMBAD database. This corresponds to a bright giant star in the mass range $[2.5 M_{\odot}; 9 M_{\odot}]$. With no Hipparcos parallax, a better determination of its mass and evolutionary status is not available in the literature. HD 232 862 presents several intriguing features : (a) rotational velocity $v \sin i = 20.6$ km/s, ten times larger than the mean value for luminosity class II objects (de Medeiros & Mayor 1999); (b) is an X-ray source in the ROSAT database and presents coronal and chromospheric activity (IUE spectra); (c) is a visually tight binary (Couteau 1988).

The spectropolarimetric data acquired with ESPaDOnS (CFHT, Hawaii) in circular polarization mode between the 7 and 10 Dec. 2006, allowed us to characterize the Stokes V and I parameters. We could detect a complex and time-variable Stokes V profile, pointing to the existence of a magnetic field at the surface of this moderate rotating giant. On the other hand, thanks to the subarcsec conditions reached, we were able to separate the components of the binary and obtain the first high resolution and high S/N spectra for the main component alone. MARCS models atmospheres (Gustafsson et al. 2008) were used to derive the following fundamental parameters and Li abundance : $T_{\text{eff}} = 5000 \pm 250$ K, $\log g = 3.0 \pm 0.5$, $[\text{Fe}/\text{H}] = -0.3 \pm 0.1$ dex, $A(\text{Li}) = 2.45 \pm 0.2$ dex.

2. Evolutionary status

Lacking from any parallax, we use the gravity and temperature derived from the spectral synthesis to estimate the mass and evolutionary status of HD 232 862. To do so we use a grid of standard stellar evolution models computed with the STAREVOL code,

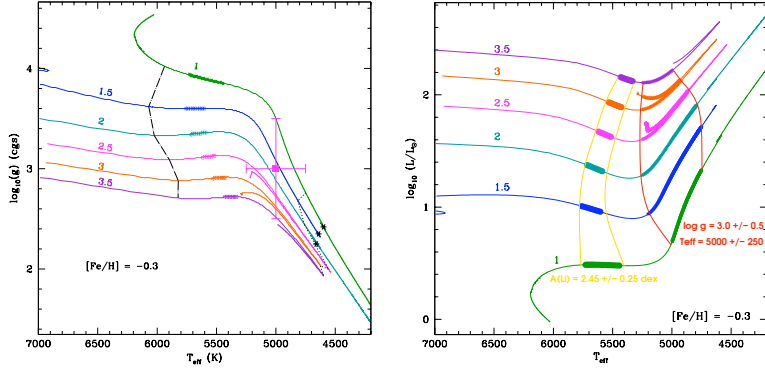


Figure 1. Evolutionary status of HD 232 862. *Left:* Dashed (left) and dotted (right) lines on the figure indicate the beginning and the end of the first dredge-up resp. The asterisks indicate the position of the bump. The bold parts on the tracks indicate the location where $A(\text{Li}) \in [2.7; 2.2]$ dex.

with masses ranging from $1 M_{\odot}$ to $3.5 M_{\odot}$. No diffusion, rotation nor magnetic fields are included in these models. We adopt $[\text{Fe}/\text{H}] = -0.3$, $A(\text{Li})_{\text{init}} = 2.976$ dex and Grevesse & Sauval (1998) for the solar chemical composition. Figure 1 shows the $(T_{\text{eff}}, \log g)$ diagram. HD 232 862 appears to be undergoing the first dredge-up. During this phase, the deepening convective envelope reaches regions where lithium is depleted by nuclear processes, and in the temperature and gravity range estimated for HD 232 862, the surface abundance of this nuclide is predicted to have dropped by a factor of 60 to 100 (depending on the stellar mass), in contradiction with the determined abundance of $A(\text{Li}) = 2.45 \pm 0.25$ dex. Marking the regions in the theoretical HR diagram, where the surface Li abundance and $(T_{\text{eff}}, \log g)$ vary within the derived errorbars (Fig 1 right), we can see that there is no overlap of these regions : standard stellar evolution models cannot account for the high Li abundance found in HD 232862.

HD 232 862 appears to be a giant, more likely of luminosity class III, at the bottom of the red giant branch. Its surface gravity and effective temperature indicate a mass between 1 and $3.5 M_{\odot}$. The high lithium abundance found at its surface is incompatible with the predictions of standard stellar evolution. It is even more intriguing since HD 232 862 should be at the end of the first dredge-up, a stage where the surface Li drops dramatically. As a comparison, the other known Li-rich giants are either at the beginning of the first dredge-up, or at the bump, an evolutionary point well beyond that of HD 232 862. HD 232 862 is also the first Li-rich giant with a detected surface magnetic field. This, together with its binary status, could be important to explain the unusual Li abundance of this star.

References

- Grevesse, N., & Sauval, A.J. 1998, *Space Science Review*, 85, 161
 de Medeiros, J.R., & Mayor, M. 1999, *A&A*, 139, 443
 Couteau, P. 1988, *A&AS*, 75, 163
 Gustafsson, B., Edvardsson, B., Eriksson, K. Jorgensen, U.G., Nordlund, A., & Plez, B. 2008, *A&A*, 486, 951

Beryllium abundances in metal-rich stars

Ruth C. Peterson¹

¹UCO/Lick Observatories and Astrophysical Advances

email: peterston@ucolick.org

Abstract. In metal-rich stars as cool as the Sun, beryllium abundance determinations are difficult due to heavy line blanketing in the near-UV 3130 Å region where the accessible BeII lines reside. We can now attempt such determinations based on improved lists of atomic line identifications and gf-values in the near-UV. Here we report Be determinations for three metal-rich A, F, and G stars plus three solar-metallicity standards. All six stars have beryllium-to-hydrogen ratios at or below solar. More such determinations would provide stronger constraints on trends in Be abundance with temperature, metallicity, and age.

Keywords. Stars: abundances, individual (HD 61421, HD 72660, HD 165341, HD 179949, HD 217107)

Previous analyses of stellar beryllium abundances have shed light on both the production of beryllium in the interstellar medium, and its destruction in non-standard mechanisms within and among stars. However, except for members of the young Hyades open cluster (age 600 Myr), existing beryllium abundance determinations are for stars of solar metallicity and lower. Consequently little is known about beryllium production and depletion among old metal-rich stars.

The problem has been the extreme crowding by the rich assortment of spectral lines in the ultraviolet spectra of stars of type F and later. As reported by ? we have empirically improved the lists of optical and near-UV atomic line parameters to the point where near-UV abundance analyses of such stars are tractable.

We first extracted from the ESO UVES and Keck HIRES archives the spectra for two slowly-rotating metal-rich stars from ?, HD 179949 (F8.5V) and HD 217107 (G8IV), and for the solar-metallicity standard HD 165341 (K0V; 70 Oph A). We analyzed these together with ground-based spectra of the Sun (G2V) and with space-based HST STIS E230H spectra of two ? Hubble Treasury standards, HD 61421 (F5IV-V; Procyon) and the metal-rich HD 72660 (A1IV).

Beryllium abundances were determined by comparing the observed echelle spectra to calculations run with the Kurucz program SYNTHE and our updated atomic line list, using ? ODFNEW models. First, the stellar temperature T_{eff} , gravity $\log g$, and metallicity $[Fe/H]$ were found from the optical region of the spectra, except for HD 72660 where the near-UV continuum is seen. Our results confirm Takeda et al.'s parameters for the two cool metal-rich stars. We then matched the entire region near the BeII doublet with a small grid of calculations, to ensure that continuum placement and spectral resolution were determined as reliably as possible. Fig. ?? shows the results of these comparisons.

All stars are found to have a Be abundance of solar or less, including the two cool metal-rich stars. We are unaware of any previous Be determinations in metal-rich stars, nor in A stars. Before concluding that stellar beryllium never exceeds the solar value, more stars need to be analyzed, to understand what role may be played by the destruction of Be in cool or hot metal-rich stars.

This work was supported in part by NASA HST grants GO-9455 and AR-10970.

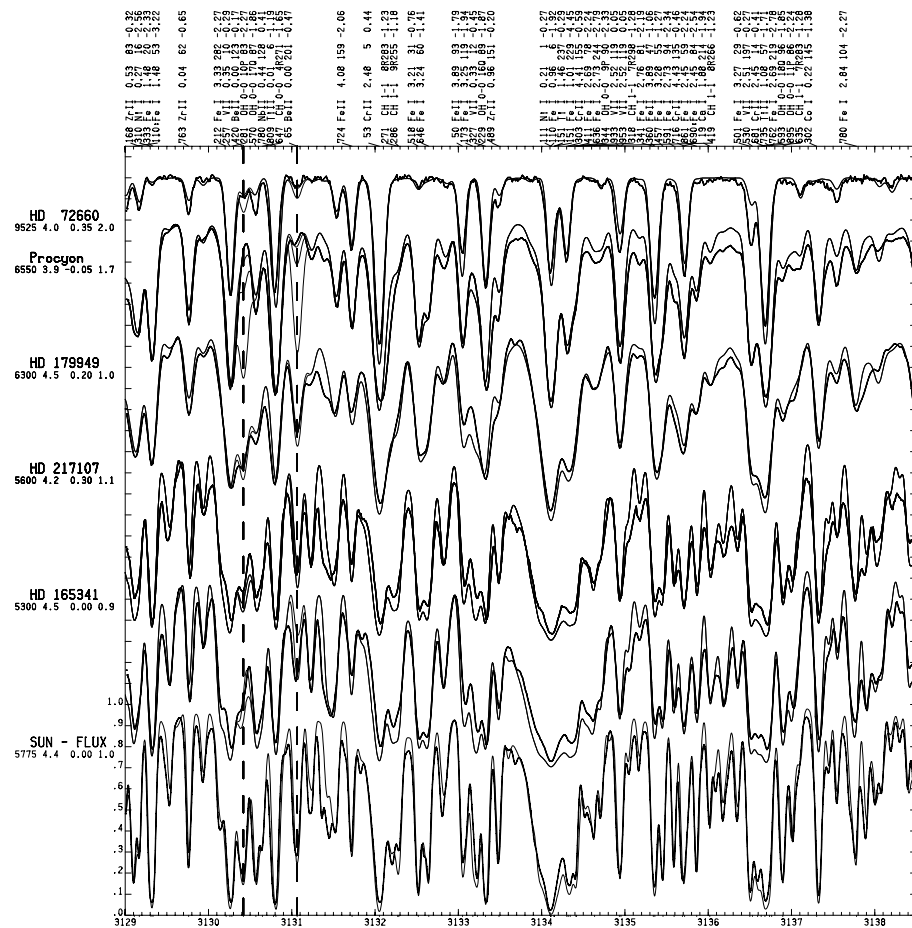


Figure 1. Comparisons between observed spectra (dark lines) and calculated spectra (light lines) are shown in an 11Å region including the Be II lines. Their positions are indicated by the vertical dashed lines. Each comparison is offset vertically for clarity; ticks denote 10% of the continuum level. Each star is identified on the left, with the T_{eff} , $\log g$, and $[\text{Fe}/\text{H}]$ values of the model used in its calculation. For each star, calculations are shown for two assumed Be abundances: one scaled to the stellar iron abundance, and one adopting the solar Be value itself (half this for HD 165341). For Procyon, which is severely Be-depleted (??), three calculations show Be abundances of 1/10 and 1/40 solar as well as solar. Identifications of the strongest lines in the calculation appear at the top.

References

- Boesgaard, A.M. 1976, *ApJ*, 210, 466
 Castelli, F., & Kurucz, R.L. 2003, *IAU Symp. No. 210*, poster A20; models are at <http://wwwuser.oat.ts.astro.it/castelli/grids.html>
 Peterson, R.C., Carney, B.W., Dorman, B., Green, E.M., Landsman, W., Liebert, J., O'Connell, R.W., Rood, R.T., & Schiavon, R.P. 2004, *STSCI Newsletter*, 21, no. 4, p. 1
 Stephens, A., Boesgaards, A.M., King, J.R., & Deliyannis, C.P. 1997, *ApJ*, 491, 339
 Takeda, Y., Ohkubo, M., Sato, B., Kambe, E., & Sadakane, K. 2005, *PASJ*, 57, 27

New results of the spectral observations of CP stars

N.S. Polosukhina¹, A.V. Shavrina², N.A. Drake³, D.O. Kudryavtsev⁴,
M.A. Smirnova¹

¹ Crimean Astrophysical Observatory, Nauchnyi, Crimea, Ukraine – email:
polo@crao.crimea.ua

² Main Astronomical Observatory of NAS of Ukraine, Kyiv, Ukraine

³ Sobolev Astronomical Institute, St. Petersburg State University, Russia

⁴ Special Astrophysical Observatory, Russian Academy of Sciences, Russia

Abstract. The lithium problem in Ap-CP stars has been, for a long time, a subject of debate. Individual characteristics of CP stars, such as high abundance of the rare-earth elements presence of magnetic fields, complicate structure of the surface distribution of chemical elements, rapid oscillations of some CP-stars, make the detection of the lithium lines and the determination of the lithium abundance, a difficult task. During the International Meeting in Slovakia in 1996, the lithium problem in Ap-CP stars was discussed. The results of the Li study carried out in CrAO Polosukhina (1973-1976), the works of Hack & Faraggiana (1963), Wallerstein & Hack (1964), Faraggiana et al. (1992-1996) formed the basis of the International project ‘Lithium in the cool CP-stars with magnetic fields’. The main goal of the project was, using systematical observations of Ap-CP stars with phase rotation in the spectral regions of the resonance doublet Li I 6708 Å and subordinate 6104 Å lithium lines with different telescopes, to create a database, which will permit to explain the physical origin of anomalous Li abundance in the atmospheres of these stars.

Keywords. Stars: magnetic fields, abundances

1. First results in the framework of the international Project: ‘Lithium in cool CP stars with magnetic fields’

The first observations of roAp stars in a frame of the International Project, showed abnormally high Li abundances for some of these stars as well as different behavior of the Li doublet with stellar rotation. The most important result of the observations was the discovery of the profile variability of the Li I 6708 Å line with the rotation phase in the spectra of two southern roAp stars HD 83368 and HD 60435 (North et al. 1998) (see Figs. 1 and 2). The Doppler shift of the Li I line in the spectrum of HD 83368 is about 0.7 Å ($v \sin i = \pm 27.6$ km/s) and is the result of the rotation-modulation of the spotted stellar surface (Fig. 3). We have shown also that Li spots are situated near the magnetic poles of dipole stellar magnetic field (Polosukhina et al. 1999).

1.1. BTA program for Lithium observations and data treatment

Observations have been carried out with the 6-m telescope and the echelle spectrometer ‘NES’ of the Special Astrophysical Observatory of RAS, Russia, (Panchuk and Klochkova, 1999) in the spectral region 6000 - 6800 Å with a signal-to-noise ratio $S/N = 60-100$. For the reduction of obtained spectra we used the package ‘Reduce’ (Piskunov and Valenti 2002).

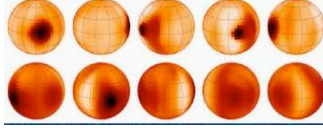


Figure 2. The test D.I. of Lithium 6708 Å blend (using CAT and FEROS telescopes) observations was made assuming that it consists only of Li I and Pr III (Kochukhov et al. 2004)

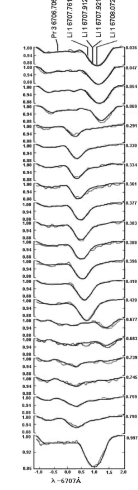


Figure 1. Observed and computed profiles of Li I 6708 Å with rotational phases for HD 83368.

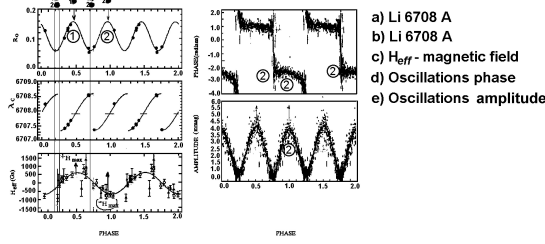


Figure 3. The observations 33Lib in CraO and in ESO

Test observations permitted us to discover some new stars with the detectable Li I 6708 Å line: HD 62140, HD 65339, HD 176232, HD 107612, HD 149822, HD 169842. Some of these stars have short rotational periods and we plan to carry out spectral monitoring of these objects in order to study the behavior of the Li I line with stellar rotation.

1) roAp-CP stars with sharp lines. The stars 33 Lib, HD134214, HD 166473 are low rotors ($v \sin i < 10$ km/s). They have spectra rich REE lines and strong magnetic fields (1500 - 5000 G). Spectra of these stars confirmed the results obtained early and did not show any rotational variability of the strong Li I 6708 Å line.

2) Rapidly-rotating Ap-CP stars ($v \sin i > 10$ km/s): HD 65339, HD 169842, HD12098. Among these stars, HD 12098 deserves a special attention. In the spectrum of this star we detected a strong and variable Li I 6708 Å, indicating that Li spots must exist on the surface of this star, which is the first roAp star discovered on the northern hemisphere. Quantitative analysis of this star is presented in Shavrina et al. (2008).

1.2. Variability spectra (dispersograms).

We used the method of dispersograms for detection of the variable details in the stellar spectra. In order to present more clearly the variability of the spectrum, we calculated the spectrum of 'variability' (Malanushenko et al. 1992 as a value of the dispersion of intensity in each wavelength λ from the mean intensity value I_{mean} ,

$$\sigma_{obs} = \frac{1}{I_{mean}} \sqrt{\frac{\sum (I_i - I_{mean})^2}{n-1}} \quad (1.1)$$

where I_i - intensity of the spectrum in selected wavelengths (i), I_{mean} - mean value of the intensity in corresponding wavelengths, n - the number of observed spectra (Fig. 5).

1.3. Analysis of observed and synthetic spectra

The stars with strong 6708 Å lithium doublets are very poorly studied. We study their spectra in detail in a narrow range near 6708 Å and 6103 Å, by the method of synthetic spectra, taking into account the Zeeman magnetic splitting and blending

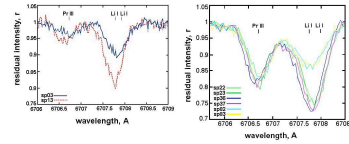


Figure 4. Original spectra of HD 12098 and HD 60435 (classical roAp-CP star with the lithium spots)

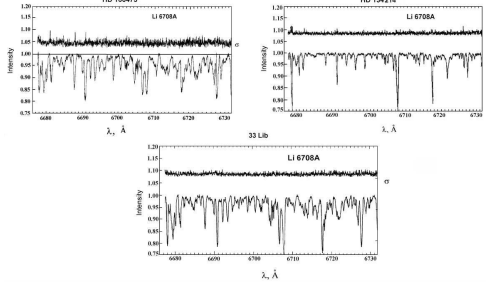


Figure 5. We present examples of the dispersograms for the sharp-lined stars with unvariable Li I 6708 Å line: HD 134214, HD 166473, and 33 Lib.

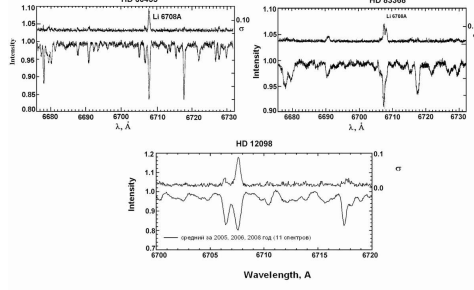


Figure 6. Dispersograms for the stars HD 60435, HD 83368 and HD 12098 in the Li I 6708 Å region.

Table 1. Lithium abundance sharp-lined stars roAp-CP stars.

	HD 101065	HD 134214	HD 137949	HD 137949	HD 166473	HD 201601
$T_{eff}/\log g$	6600/4.2	7500/4.0	7750/4.5	7250/4.5	7750/4.0	7750/4.0
$N(\text{Li})6708\text{\AA}$	3.1	3.9	4.1	3.6	3.3	3.8
$N(\text{Li})6103\text{\AA}$	3.5	4.1	4.4	4.4	4.0	4.0
${}^6\text{Li}/{}^7\text{Li}$	0.4:	0.3:	0.2:	0.3:	0.4:	0.5:

by REE lines. To calculate synthetic spectra we applied the magnetic spectrum synthesis code SYNTHM (Khan, 2004) which is similar to Piskunov's code SYNTHMAG. We also used the code STARSF of Tzymbal (1996).

Results of modeling observed and accounting profiles to lines 6708 Å Li I for stars HD 83368, HD 60435 and HD 12098 (Shavrina et al, 2001, 2006):

- **HD 83368** for $i = 90^\circ$, $v_e = 35$ km/s, and a lithium content in the photosphere $\log \varepsilon(\text{Li}) = 1,8$
 - **Spots 1:** $l_1 = 173^\circ \pm 6^\circ$, $\varphi_1 = 0^\circ \pm 6^\circ$, $R_1 = 33^\circ \pm 6^\circ$, $\log \varepsilon_1(\text{Li}) = 3.6 \pm 0.2$
 - **Spots 2:** $l_2 = 337^\circ \pm 6^\circ$, $\varphi_2 = 0^\circ \pm 6^\circ$, $R_2 = 35^\circ \pm 6^\circ$, $\log \varepsilon_2(\text{Li}) = 3.5 \pm 0.2$
- **HD 60435** for $i = 47^\circ$ (133°), $v_e = 15$ km/s, and a lithium content in the photosphere $\log \varepsilon_2(\text{Li}) = 1,8$
 - **Spots 1:** $l_1 = 11^\circ \pm 6^\circ$, $\varphi_1 = -15^\circ \pm 6^\circ$, $R_1 = 44^\circ \pm 3^\circ$, $\log \varepsilon_1(\text{Li}) = 3.8 \pm 0.2$
 - **Spots 2:** $l_2 = 205^\circ \pm 10^\circ$, $\varphi_1 = 15^\circ \pm 6^\circ$, $R_2 = 40^\circ \pm 7^\circ$, $\log \varepsilon_2(\text{Li}) = 2.7 \pm 0.2$
- **HD 12098**
 - **Spot 1:** $l_1 = 30^\circ$, $\varphi = -20^\circ$, $R_1 = 40^\circ$, $\log \varepsilon_1(\text{Li}) = 5.0$
 - **Spot 2:** $l_2 = 180^\circ$, $\varphi = 25^\circ$, $R_2 = 70^\circ$, $\log \varepsilon_2(\text{Li}) = 4.2$
 - **Spot 3:** $l_3 = 290^\circ$, $\varphi = -20^\circ$, $R_3 = 40^\circ$, $\log \varepsilon_3(\text{Li}) = 4.4$

Analyses of the lithium lines 6708 Å and 6103 Å in spectra of these sharp-lined stars roAp stars were carried out. All stars are characterized by strong overabundance of REE and by surface magnetic fields from 2 KG to 6.8 KG (Shavrina et al 2004).

2. Conclusions

- The experience with spectra of roAp-CP stars in 6708 Å region shows that Li doublet is main contributor.
- Dispersograms clearly showed a different behavior of the lithium line in the spectra of

slowly and rapidly rotating roAp-Cp stars. Dispersograms obtained for HD 12098 and the 'Li-spotted' stars HD 83368 and HD 60435, clearly show the variability of their spectra in the region of the Li I line 6708 Å. The dispersograms show also that the amplitude of the intensity variations of the Li line is sufficiently higher than that of the lines of the rare-earth elements Nd III, Pr III, Ce II etc. This fact is an additional evidence that the blend at 6708 Å belongs to the lithium. - Observations of CP stars with the 6-m BTA telescope confirmed a non-variability of the Li I 6708 Å line in the spectra of the slowly rotating stars in comparison to the spectra observed at ESO in 1996. Analysis of the observed and synthetic spectra for the sharplined stars HD 134214, 33 Lib, HD 166473 showed table 1.

- The lithium abundance derived from the secondary Li I 6104 Å line is slightly higher than that derived from the resonance Li I 6708 Å line for all stars of this group.
- Lithium isotopic ratio ($^6\text{Li}/^7\text{Li}$) differs slightly from one star to another and is higher than $^6\text{Li}/^7\text{Li}$ ratio in the solar atmosphere and in the interstellar medium.
- Observations of HD 12098 with the BTA 6-m telescope in the Li I 6708 Å region revealed strong variations of this line testifying that one more Ap-Cp star with the Li spots was discovered. Figure 4 clearly shows the identical behavior of HD 12098 and HD 60435 spectra (HD 60435 is a classical roAp star with the Li spots on the magnetic poles).
- High Li abundance can be explained by means of physical processes which prevent the mixing in the stellar atmosphere and maintain its high initial abundance, suppression of convective motions by strong magnetic fields and action of the ambipolar diffusion. The observed lithium may also be produced in stellar atmospheres, for example by spallation reactions at the stellar surface in the regions of the magnetic poles, where lithium spots are found (Goriely 2007). The creation of a database of observational data in the region of the Li lines is very important for the CP-stars studies, and our new results on lithium abundances in Ap-CP stars and their interpretation, open new perspectives in the research of the physical nature of these stars.

References

- Faraggiana, R. 1992-1996, *Mem.S.A.I.*
 Goriely 2007, *A&A*, 466, 619
 Hack, M., Faraggina, R. 1963, *PASP*
 Khan 2004, *JQSRT*, 88, N1-3, 71
 Kochuknov, O., Hoppe, P., & Zinner, E. 2004, *A&A.*, 424, 935
 Malanushenko, V. et al. 1992, *A&A.*, 259, 567
 North et al. 1998, *A&A*, 333, 644
 Panchuk and Klochkova, 1999.
 Piskunov and Valenti 2002, *A&A.*, 385, 109
 Polosukhina, N. 1973-1976, *Izv. CrAO*
 Polosukhina, N. et al. 1999, *A&A*, 351, 283
 Shavrina, A. V. et al. 2008, *Astrophysics*, Vol. 51, p. 517
 Shavrina, A. V. et al. 2006 in *Physics of Magnetic Stars. Proceedings of the Int. Conf.*, p. 341
 Shavrina, A. V. et al. 2004, in *The A-Star Puzzle, IAU Symp.*, 224, p. 711
 Shavrina, A. V. et al 2001 *A&A*, 372, 571
 Tzymbal, V. 1996, *ASP Conf. Ser.*, 108, 198
 Wallerstein, G. and Hack, M. 1964, *The Observatory*, Vol. 84, p.160

The metal–poor end of the Spite plateau: gravity sensitivity of the H α wings fitting.

L. Sbordone^{1,2,3}, P. Bonifacio^{1,2,4}, E. Caffau², H.-G. Ludwig^{1,2},
N. Behara^{1,2}, J. I. Gonzalez-Hernandez^{1,2,4}, M. Steffen⁵, R. Cayrel²,
B. Freytag⁶, C. Van’t Veer², P. Molaro³, B. Plez⁷, T. Sivarani⁸,
M. Spite², F. Spite², T. C. Beers⁹, N. Christlieb¹⁰, P. François²,
and V. Hill^{2,11}

¹ CIFIST Marie Curie Excellence Team,

² GEPI – Observatoire de Paris – France

³ Max-Planck Institut für Astrophysik, Garching – Germany

⁴ INAF – Osservatorio Astronomico di Trieste – Italy

⁵ Universidad Complutense de Madrid – Spain

⁶ Astrophysikalische Institut Potsdam – Germany

⁷ Centre de Recherche Astrophysique de Lyon, UMR 5574 – France

⁸ Université Montpellier 2 – France

⁹ Indian Institute of Astrophysics, Bangalore – India

¹⁰ Michigan State University and JINA, Lansing, MI – USA

¹¹ Landessternwarte Heidelberg – Germany

¹² Cassiopée, Observatoire de la Cote d’Azur, Nice – France

Abstract. We recently presented (Sbordone et al., 2009a) the largest sample to date of lithium abundances in extremely metal-poor (EMP) Halo dwarf and Turn-Off (TO) stars. One of the most crucial aspects in estimating Li abundances is the T_{eff} determination, since the Li I 670.8 nm doublet is highly temperature sensitive. In this short contribution we concentrate on the T_{eff} determination based on H α wings fitting, and on its sensitivity to the chosen stellar gravity.

Keywords. Nuclear reactions, nucleosynthesis – Galaxy: halo – stars: abundances, Population II

1. Introduction

In Sbordone et al. (2009a) we present lithium abundances for a sample of 28 stars in the $-3.6 < [\text{Fe}/\text{H}] < -2.4$ range, 10 of which have $[\text{Fe}/\text{H}] \leq -3.0$. We derived four different T_{eff} scales: H α wings fitting against a grid of synthetic profiles from 1D models using Barklem et al. (2000) or Ali & Griem (1966) self-broadening theories (BA and ALI scales); H α fitting against a 3D-hydrodynamical grid based on CO⁵BOLD models (Freytag et al. 2002; Wedemeyer et al. 2004) with Barklem et al. (2000) self-broadening (3D scale); InfraRed Flux method (IRFM, González Hernández & Bonifacio 2009).

2. The H α gravity sensitivity

Effective temperature (T_{eff}) is the most crucial stellar atmosphere parameter influencing Li abundance determination: Li abundances derived from the Li I 670.75nm line are sensitive to T_{eff} at a level of about 0.03 dex for each 50 K variation in T_{eff} . Being mostly temperature sensitive, the H α wings are also influenced by the adopted surface gravity,

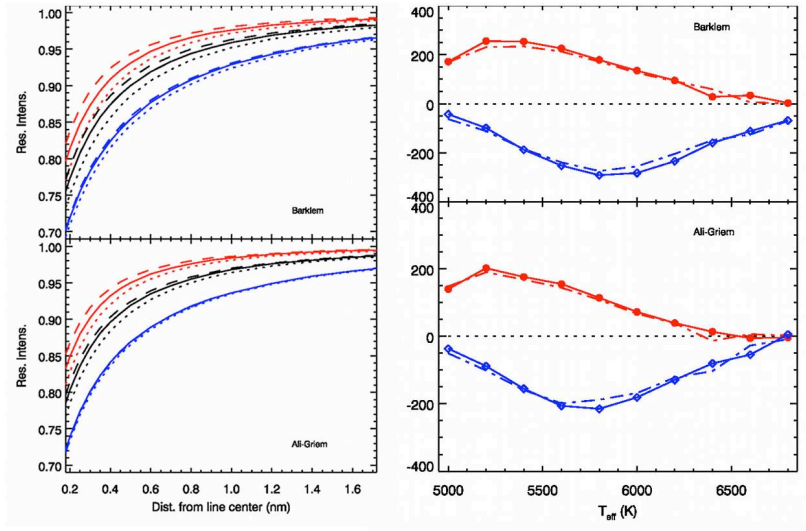


Figure 1. Left panel, for BA and ALI scales, 1D synthetic profiles of the H α red wing are plotted for $T_{\text{eff}}=5400$ K, 6000 K, and 6600 K (red, black and blue respectively). Line type identify gravity, dashed for $\log g=3.5$, solid for $\log g=4.0$, dotted for $\log g=4.5$. In the right panel, the effect of gravity offsets on T_{eff} estimate are shown. Theoretical profiles computed with $\log g=4.0$ have been fitted with $\log g=3.5$ profiles (red lines, filled circles) and $\log g=4.5$ profiles (blue lines, open diamonds). The temperature difference (recovered-real) is plotted against the real temperature. Solid lines refer to $[\text{Fe}/\text{H}]=-3$, dotted to $[\text{Fe}/\text{H}]=-2.5$.

to a level which might be significant in the present scope. In this short contribution we concentrate on this effect. Barklem et al. (2002) already reported estimates of such a sensitivity down to $[\text{Fe}/\text{H}]=-2$. The effect is always in the sense of higher gravity leading to broader profiles, and appears generally stronger at lower metallicities, and for the BA profiles compared to the ALI profiles. The effect is shown in Fig. 1, where we show both the shape of the H α red wing and the temperature offset deriving from adopting the wrong gravity estimate in measuring effective temperature. As it can be seen, in the temperature range 6000-6500K, most significant for Li measurement in EMP TO and dwarf stars, significant (>100 K) offsets can arise from neglecting the gravity dependence in fitting H α profiles, which can appreciably skew the results when Li abundances are measured over a fairly broad temperature range (see Sbordone et al. 2009b).

References

- Ali, A. W., & Griem, H. R. 1966, *Physical Review*, 144, 366
 Barklem, P. S., Stempels, H. C., Allende Prieto, C., Kochukhov, O. P., Piskunov, N., & O'Mara, B. J. 2002, *A&A*, 385, 951
 Barklem, P. S., Piskunov, N., & O'Mara, B. J. 2000, *A&A (Letters)*, 355, 5
 Freytag, B., Steffen, M., & Dorch, B. 2002, *Astronomische Nachrichten*, 323, 213
 González Hernández, J. I., & Bonifacio, P. 2009, *A&A*, 497, 497
 Sbordone, L., et al. 2009a, proceedings of IAU Symposium 265 "Chemical Abundances in the Universe: Connecting First Stars to Planets", K. Cunha, M. Spite & B. Barbuy, eds., in press.
 Sbordone, L., et al. 2009b, *A&A*, submitted
 Wedemeyer, S., Freytag, B., Steffen, M., Ludwig, H.-G., Holweger, H., 2004, *A&A*, 414, 1121

Beryllium abundances along the evolutionary sequence of the open cluster IC 4651

Rodolfo Smiljanic^{1,2}, L. Pasquini², C. Charbonnel^{3,4}, and N. Lagarde³

¹IAG, University of São Paulo, Brazil, ² ESO, Germany,

email: rsmiljan@eso.org

³ Geneva Observatory, Switzerland, ⁴ LATT, CNRS, Université de Toulouse, France

Abstract. The simultaneous investigation of Li and Be in stars is a powerful tool in the study of the evolutionary mixing processes. Here, we present beryllium abundances in stars along the whole evolutionary sequence of the open cluster IC 4651. This cluster has a metallicity of $[Fe/H] = +0.11$ and an age of 1.2 or 1.7 Gyr. Abundances have been determined from high-resolution, high signal-to-noise UVES spectra using spectrum synthesis and model atmospheres. Lithium abundances for the same stars were determined in a previous work. Confirming previous results, we find that the Li dip is also a Be dip. For post-main-sequence stars, the Be dilution starts earlier within the Hertzsprung gap than expected from classical predictions, as does the Li dilution. Theoretical hydrodynamical models are able to reproduce well all the observed features.

Keywords. Stars: abundances, evolution, rotation – Open clusters and associations: individual: IC 4651

1. Introduction

In contradiction with standard stellar evolution models, where convection is the only mechanism driving mixing episodes, field and cluster F- and early G-type stars (including the Sun) deplete Li abundances during the main sequence (Lambert & Reddy 2004; Sestito & Randich 2005, and references therein). Different physical mechanisms have been proposed to explain these observations: atomic diffusion, mass loss, rotation-induced mixing, internal gravity waves, or combinations of these (see Charbonnel & Talon 2008 and references therein).

As Li and Be burn at different temperatures (2.5×10^6 K for Li and 3.5×10^6 K for Be), i.e. at different depths in the stellar interior, they help in constraining the transport mechanisms by performing a stellar tomography. In the study of mixing processes as a function of mass and evolutionary status cluster stars are ideal because they have well defined masses and share the same age and initial chemical composition. We derived Be abundances along the whole evolutionary sequence of the open cluster IC 4651, including solar-type, Li-dip, turn-off, subgiant, and red giant stars. With these new results, we investigate in detail the mixing processes in different stellar masses.

2. Discussion

The sample analyzed here is composed of 22 stars; 21 with atmospheric parameters and Li abundances from Pasquini et al. (2004) and 1 from Randich et al. (2002). The spectra have $40 \leq S/N \leq 100$ (per resolution element) and $R \sim 45000$.

Be abundances were determined using synthetic spectra and the same codes and line lists used in Smiljanic et al. (2009a). As some of the sample stars are fast rotators, we first carefully modeled the slow-rotating stars and tested the effects in the abundances

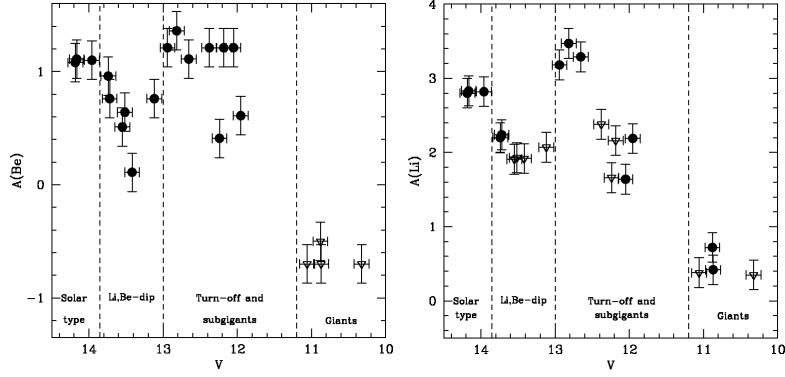


Figure 1. Abundances of Be (left panel) and Li (right panel) as a function of the V magnitude. Detections are shown as full circles and upper limits as open triangles.

of artificially broadening the spectra (see Smiljanic et al. 2009b for details). Beryllium was detected in all the sample stars except for the giants.

New evolutionary models for stars on the hot side of the dip, including atomic diffusion, meridional circulation, and shear turbulence, were calculated with STAREVOL V3.1 by Lagarde & Charbonnel (in preparation, see also Charbonnel & Lagarde this volume) for a range of stellar masses and initial rotation velocities. For stars on the cool side of the Li dip we use the $1.2 M_{\odot}$ model computed by Talon & Charbonnel (2005) which has an initial rotation velocity of 50 km s^{-1} .

Beryllium abundances are found to follow closely the behavior of the Li abundances (Fig. 1). In a sequence of increasing mass we have first the coolest main-sequence stars that do not present a Be abundance dispersion. This is expected to be due to the impact of internal gravity waves. After that, a well-defined Be dip is seen. This confirms previous results that the Li dip is also a Be dip (Boesgaard & King 2002, Boesgaard et al. 2004). For post-main-sequence stars we confirm that Be dilution starts earlier than the expected classically. The Be abundances also present a significant dispersion.

The dispersion of Li and Be abundances on the blue side of the dip and in evolved stars is very well explained by the models when accounting for a dispersion in the initial values of the stellar rotational velocities. The models reproduce all the Li and Be features along the CMD of IC 4651. The success in explaining the Li and Be abundances along the whole evolutionary sequence shows that important steps have been taken towards the proper understanding of the physical mechanisms acting during the stellar evolution.

References

- Boesgaard, A. M., Armengaud, E., King, J. R. 2004, *ApJ*, 605, 864
- Boesgaard, A. M. & King, J. R. 2002, *ApJ*, 565, 587
- Charbonnel, C. & Talon, S. 2008, in Proceedings of IAUS 252, 163
- Lambert, D. L. & Reddy, B. E. 2004, *MNRAS*, 349, 757
- Pasquini, L., Randich, S., Zoccali, M. et al. 2004, *A&A*, 424, 951
- Randich, S., Primas, F., Pasquini, L. et al. 2002, *A&A*, 387, 222
- Sestito, P. & Randich, S. 2005, *A&A*, 442, 615
- Smiljanic, R., Pasquini, L., Bonifacio, P., et al. 2009a, *A&A*, 499, 103
- Smiljanic, R., Pasquini, L., Charbonnel, C., Lagarde, N. 2009b, arXiv:0910.4399, *A&A*, in press
- Talon, S. & Charbonnel, C. 2005, *A&A*, 440, 981

Using lithium to estimate ages for solar-type stars

David R. Soderblom¹

¹Space Telescope Science Institute,
3700 San Martin Drive, Baltimore MD 21218 USA
email: drs@stsci.edu

Abstract. Can observations of Li in F, G, and K stars be used to derive an age for an individual star or a group? This is a brief progress report on using Li for age estimation in PMS and ZAMS stars.

Keywords. Stars:ages, solar-type, convection

The decline of the surface Li abundance with age is well known for stars near and below $1 M_{\odot}$. Observations and models of this phenomenon should provide constraints on convection in these stars, the process believed to be the underlying cause of the Li depletion. This is a progress report on an effort to invert the problem to use observations of Li in F, G, and K dwarfs to estimate their ages.

A full understanding of Li depletion involves some complex and not well understood physics and requires accurate determinations of basic stellar quantities such as temperature and composition. Also, transforming an observation of Li to an abundance is very sensitive to temperature as well as non-LTE effects. However, when estimating ages these quantities are often only poorly constrained and I wished to address a simpler question: If observations of the Li equivalent width (W_{λ}) and color ($(B - V)$, say, or the equivalent derived from another color or from T_{eff}) are at hand, how well can an age be estimated? Can an age be determined at all for a single star, or is some minimum number in a group required?

The data used will be described fully and illustrated in a forthcoming paper, and here I will summarize the key points:

- The youngest stars with good Li observations are T Tauri stars in Taurus-Auriga, the Orion Nebula Cluster, and NGC 2264, all with ages of 5 Myr or less. The scatter in W_{λ} among these stars is small and consistent with the observational errors. The consistency

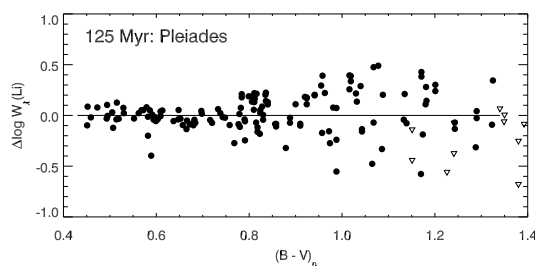


Figure 1. Lithium equivalent widths for F, G, and K stars in the Pleiades. A mean relation has been fitted and subtracted to show how the scatter in W_{λ} varies with color.

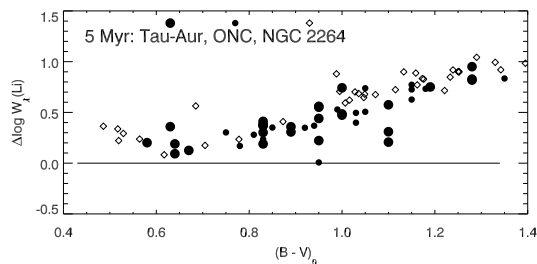


Figure 2. Li equivalent widths for T Tauri stars in Tau-Aur, the Orion Nebula Cluster, and NGC 2264, relative to the Pleiades.

in Li among these different groups suggests stars in the present epoch all form with the same initial Li abundance, and the agreement with the primordial solar Li abundance (from meteorites) indicates that that value has not changed significantly in ~ 5 Gyr.

- By contrast, the Pleiades is a well-observed cluster with an age of 125 Myr and it exhibits an inherent spread in W_λ that grows in going to cooler stars, becoming as much as 1 dex for K dwarfs (see Fig. 1). This spread is much larger than the observing errors and also significantly larger than the scatter seen among T Tauri stars. The fact that T Tauris show little scatter implies that inhomogeneous stellar atmospheres (i.e., spots) are not the cause of the spread in Li in the Pleiades because the T Tauris are expected to be at least as spotted as ZAMS stars.

- The run of W_λ with color for the α Persei cluster and NGC 2451 at about 80 Myr is indistinguishable from that of the Pleiades (see Fig. 2). This implies that Li depletion – at least on average – goes through plateau stages where little or nothing happens for an extended time.

- There are clusters with ages between those of the T Tauris and α Persei but they are sparse and so the data are less well defined. Nevertheless, W_λ declines in progression with age as expected, although there can again be plateaus where little difference in the average W_λ is seen despite a significant difference in age.

- Li continues to decline in stars after they reach the ZAMS, as seen in 200 Myr-old clusters (M35, NGC 2516 and Blanco 1), and at 300 Myr (M34 and NGC 6475).

- Stars in the Hyades and other clusters of that age (Praesepe, Coma, and NGC 6633) have well-defined runs of W_λ with color and with little scatter. This suggests that the large scatter seen in the Pleiades may later lessen, but there is no known mechanism to achieve that. Also, stars in the 4 Gyr-old cluster M67 show an appreciable spread in Li. The Hyades may possibly be misleading because it is metal-rich.

There are trends of declining average W_λ for the F and G stars but they are comparable to the scatter seen. For the K dwarfs, however, the decline in W_λ is large and rapid up to 200-300 Myr or so. The large scatter seen among stars of a single age (notably the Pleiades) means that for a single star one can only set limits to age, but if data for a group of 10-20 stars exist then a more precise age can be set. This makes it possible to use observations of Li in K dwarfs to at least set the age ordering of young kinematic groups such as β Pictoris, η Cha, TW Hya, etc.

Lithium in metal-poor red giants

Laimons Začs and Arturs Barzdis

Faculty of Physics and Mathematics, University of Latvia,
Raiņa bulvāris 19, LV-1586 Rīga, Latvia
email: zacs@latnet.lv

Abstract. The lithium abundance was calculated for five metal-poor red giant stars from Li I doublet at 6707 Å by fitting the observed high-resolution spectra with synthetic spectra. The lithium abundance was found to be low in all stars, $\log \varepsilon(\text{Li}) \leq 1.8$, confirming lithium depletion on the red giant and asymptotic giant branch.

Keywords. Stars: abundances, Population II, late-type, binaries: spectroscopic, stars: individual (HD 30443, HD 187216, HD 209621, HD 218732, HD 232078)

1. Observations and analysis

High resolution spectra for three analyzed stars (HD 209621, HD 218732, HD 232078) were observed with the cross-dispersed high-resolution échelle spectrograph FIES installed on NOT (Canary Islands) with a spectral resolution of $R = 67\,000$. HD 187216 was observed using the fiber-fed échelle spectrograph BOES attached to the 1.8-m telescope of Bohyunsan Observatory (Korea) with a spectral resolution of $R = 45\,000$. HD 30443 was observed using the coude échelle spectrometer MAESTRO on the 2 m telescope at the Observatory on the Terskol Peak in Northern Caucasus (Russia) with a resolving power of 45 000. The basic data for all targets are provided in Table 1. Spectral classification was adopted from Yamashita (1975) and the SIMBAD database. All stars are first-ascent red giants or on the asymptotic giant branch. HD 30443 and HD 209621 are spectroscopic long period binaries ($P = 2954$ & 407.4 days; McClure & Woodsworth 1990). HD 218732 was suspected to be a long period binary ($P = 567$ days; Carney et al. 2003).

Synthetic spectra for some lithium abundances around the final value are calculated and convolved with the instrumental profile using spectrum synthesis technique which based on the R.L.Kurucz's code SYNTHE and the Uppsala atmospheric models. Figure 1 illustrates iterations (± 0.1 dex for HD 30443, ± 0.2 dex for HD 187216, HD 209621, and HD 232078, ± 0.5 dex for HD 218732) around the accepted lithium value. The accepted lithium abundances are provided in Table 1. The line list was examined using the databases VALD and DREAM. Significant blending of Li doublet was expected because of low effective temperature and peculiar chemical composition of stellar atmospheres. C_2 and CN lines are strong in the spectra of HD 30443, HD 187216, and HD 209621 (see Figure 1) and lines of neutron capture elements are enhanced.

2. Conclusions

Five red giants in the metallicity range $-1 < [\text{Fe}/\text{H}] < -2$ display $\log \varepsilon(\text{Li}) \leq 1.8$, confirming a substantial lithium depletion on the red giant and asymptotic giant branch. Neutron capture elements are significantly enhanced in the atmospheres of three analyzed giants.

Table 1. Basic data for the program stars. Accepted effective temperature (K), gravity (cgs), iron abundance relative to the solar value, lithium abundance and averaged abundance of neutron capture elements relative to the solar value are given.

Star	Sp.type	T_{eff}	$\log g$	[Fe I/H],[Fe II/H]	$\log \varepsilon(\text{Li})$	[n/Fe II]	binary
HD30443	R, C4,3 CH	4100	1.5	-1.1,-1.1	1.8	+1.6	yes
HD187216	R, C3,3 CH	4000	0.75	-2.6,-1.7	0.45	+1.2	
HD209621	C, C1,2 CH	4300	-0.4	-2.0,-2.0	1.2	+1.3	yes
HD218732	G7 Ib	4200	0.50	-1.5,-1.5	-1.1	0.0	yes
HD232078	K3 IIp	4000	0.00	-1.4,-1.4	-0.55	+0.3	

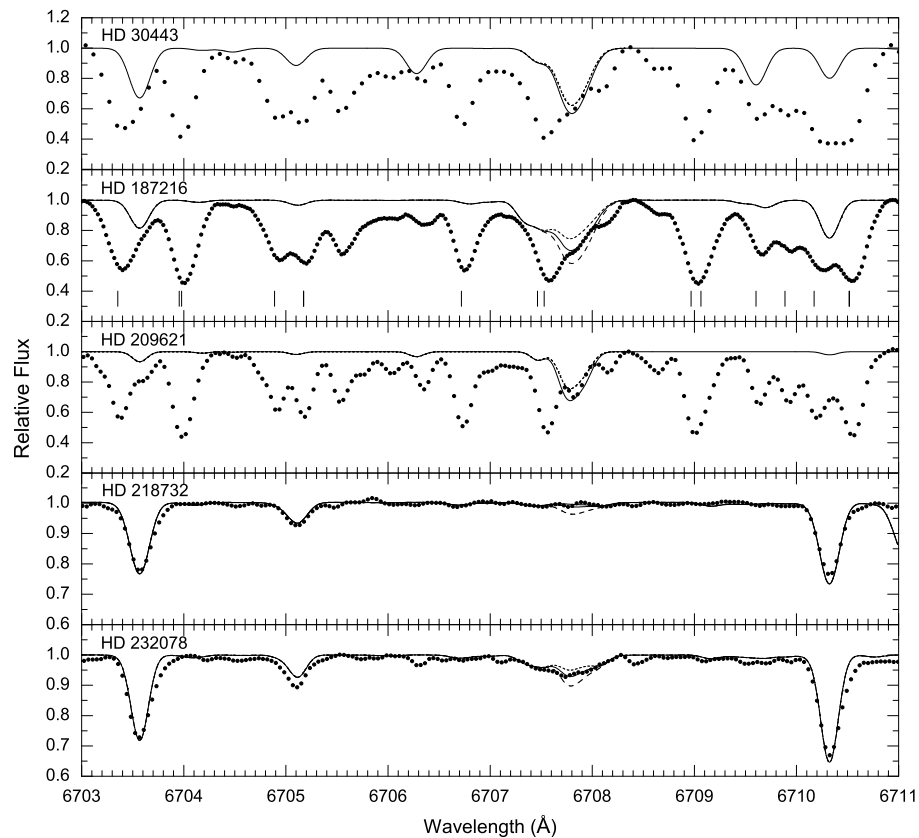


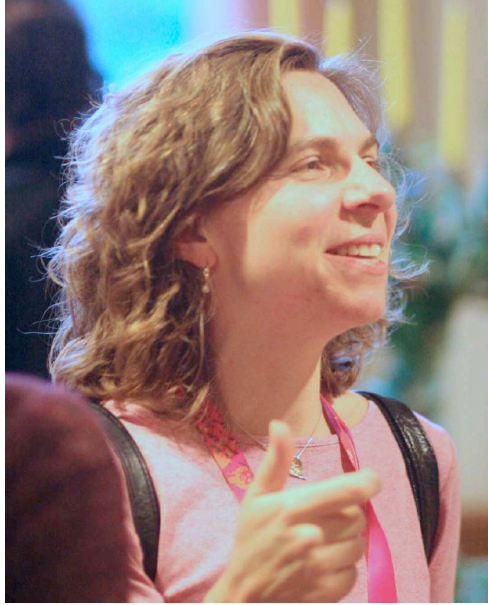
Figure 1. The observed spectra (dots) of red giants in spectral region around Li doublet at 6707 Å. The positions of CN Red system lines are marked for HD 187216. Synthesized atomic line spectra for the accepted lithium abundances are displayed by thick solid lines.

References

- Carney, B.W., Latham, D.W., Stefanik, R.P., Laird, J.B., Morse, J.A. 2003, *AJ*, 125, 293
 McClure, R.D., & Woodsworth, A.W. 1990, *ApJ*, 352, 709
 Yamashita, Y. 1975, *PASJ*, 27, 325

Session IV

Sources and sinks of light elements



Suzanne Talon



Takuji Tsujimoto

Light elements as diagnostics on the structure and evolution of low-mass stars

Suzanne Talon¹ and Corinne Charbonnel^{2,3}

¹ RQCHP, Département de physique, Université de Montréal, C.P. 6128, succ. centre-ville, Montréal, Québec, H3C 3J7
email: suzanne.talon@umontreal.ca

² Geneva Observatory, University of Geneva, ch. des Maillettes 51, 1290 Versoix, Switzerland
email: Corinne.Charbonnel@unige.ch

³ Laboratoire d'Astrophysique de Toulouse-Tarbes, Université de Toulouse, CNRS UMR 5572, 14 Av. E. Belin, 31400 Toulouse, France

Abstract. Low-mass stars exhibit, at all stages of their evolution, the signatures of complex physical processes that require challenging modelling beyond standard stellar theory. In this review, we focus on lithium depletion in low-mass stars. After dissecting the Li dip, we discuss how large scale mixing due to rotation and internal gravity waves may interact to explain this feature. We also briefly discuss the impact that is expected on Population II stars.

Keywords. Hydrodynamics – instabilities – turbulence – waves – stars: abundances, evolution, interiors, rotation

1. The lithium dip, atomic diffusion and rotation-induced mixing

During the last couple of decades, it became obvious that the art of modeling stars in the 21st century strongly relies on the art of modelling transport processes. Observational evidences now give precise clues on the various processes that transport angular momentum and chemical elements in the radiative regions of low-mass stars, at various stages of their evolution. One of the most striking signatures of transport processes in low-mass stars is the so-called Li dip (see Fig. 1). This drop-off in the Li content of main-sequence F-stars in a range of ~ 300 K centered around 6700 K was discovered in the Hyades by Wallerstein et al. (1965); its existence was later confirmed by Boesgaard & Tripicco (1986). This feature appears in all open clusters older than ~ 200 Myr, as well as in field stars (Balachandran 1995), an indication that it is a phenomenon occurring on the main sequence.

Michaud's (1986) original suggestion that this structure is shaped by gravitational settling (causing the drop in Li abundance on the cool side of the dip as the surface convection zone shrinks) and radiative levitation (which explains the rise on the warm side of the dip) suffers from two serious drawbacks:

- The expected concomitant underabundances of heavier elements (C, N, O, Mg, Si) are not observed in cluster stars (Takeda et al. 1998; Varenne & Monier 1999; Gebran et al. 2008).
- In this framework, Li is not destroyed; it settles and accumulates in a buffer zone below the convective envelope. Li should thus be dredged-up as a star enters the Hertzsprung gap and this is not observed, neither in the field nor in open cluster stars (Pilachowski et al. 1988; Deliyannis et al. 1997).

Boesgaard (1987) noticed that the effective temperature of the dip is also associated with a sharp drop in rotation velocities (see Fig. 1). Rotation was then suggested to play a

dominant role in this mass range. To properly model rotation-induced mixing, one must follow the time evolution of the angular momentum distribution within a star, taking into account *all* relevant physical processes: contraction/expansion caused by stellar evolution, mass loss or accretion, tidal effects, as well as internal redistribution of angular momentum through meridional circulation, turbulence, magnetic torques and waves.

1.1. *Shaping the warm side of the dip with wind driven circulation*

The description of the internal physical processes related to stellar rotation greatly improved during the last two decades. Here, we review the results of the application of Zahn's (1992) model of rotation-induced mixing, using the same free parameters as those required to explain abundance anomalies in more massive stars (see Maeder & Meynet 2000). In this framework, transport of angular momentum is dominated by the Eddington-Sweet meridional circulation and shear instabilities.

In the dip region, the evolution of a star's angular momentum is influenced by various mechanisms depending on its effective temperature.

- Stars with T_{eff} higher than ~ 6900 K have a shallow convective envelope and are not spun down by a magnetic torque. These stars soon reach a stationary regime where there is no net flux of angular momentum[†], in which meridional circulation and shear-induced turbulence counterbalance each other. The associated weak mixing is just sufficient to counteract atomic diffusion. These rotating models account nicely for the observed constancy of Li and CNO in these stars, and they also explain the Li and Be behaviour in subgiant stars (Palacios et al. 2003; Pasquini et al. 2004; Smiljanic et al. 2009; see also Charbonnel & Lagarde, this Volume). Talon, Richard, & Michaud (2006) showed that the transport coefficients related to rotation-induced mixing lead to normal A stars for rotation velocities above $\sim 100 \text{ km s}^{-1}$, and permit Am anomalies below with a mild correlation with rotation, provided a reduction of turbulent mixing by horizontal turbulence is taken into account. Fossati et al. (2008) have confirmed observationally this correlation with rotation.

- Between ~ 6900 and 6600 K, the convective envelope deepens and a weak magnetic torque, associated with the apparition of a surface dynamo, spins down the outer layers of the star. This creates internal shears and the transport of angular momentum by meridional circulation and shear turbulence increases, leading to a larger destruction of Li and Be, in agreement with the data. The rotating model thus perfectly fits the blue side of the Li and Be dips (Talon & Charbonnel 1998, Charbonnel & Talon 1999, Palacios et al. 2003, Pasquini et al. 2004; Smiljanic et al. 2009).

- Stars on the cool side of the Li dip ($T_{\text{eff}} < 6600$ K) have an even deeper convective envelope sustaining a very efficient dynamo, which produces a strong magnetic torque that spins down the outer layers very efficiently. If we assume that all the angular momentum transport is assured by the wind-driven circulation in these stars[‡], we obtain too much Li depletion compared to the observations (see Fig.2). *On the basis of these results, Talon & Charbonnel (1998) suggested that the Li dip corresponds to a transition region where the efficiency of another process for angular momentum transport rises.*

This signature of the existence of new physics can be drawn from studies performed by two other groups. In Théado & Vauclair (2003), where rotation-induced mixing is assumed to be linked to meridional circulation in a solid-body rotating star, the two free parameters associated with this mixing have to be varied by factors of 2 and 260 to fit

[†] In fact, there remains a small flux of angular momentum, just sufficient to counteract the effect of stellar contraction/expansion.

[‡] Let us mention that in the case of large shears meridional circulation is far more efficient than shear for angular momentum transport.

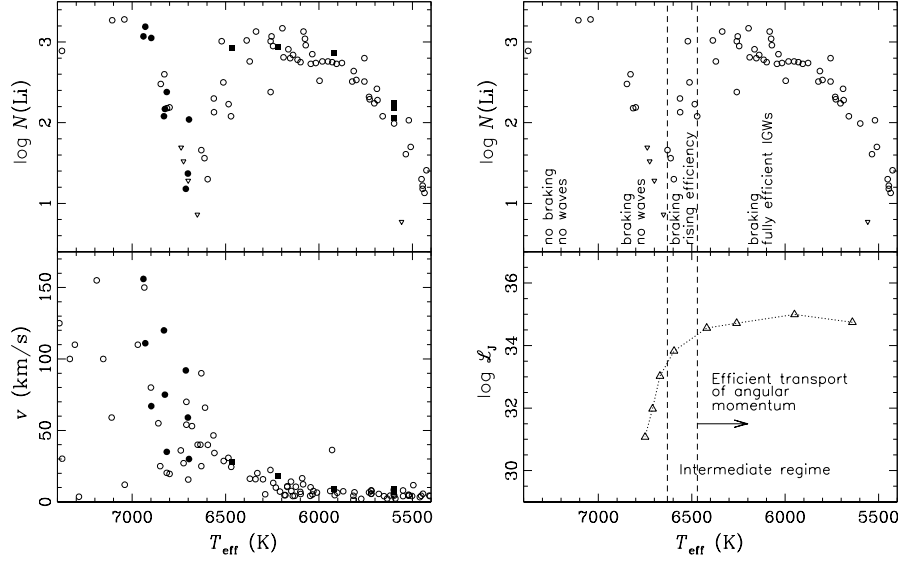


Figure 1. (Left) (top) Lithium abundance in the Hyades versus effective temperature (open symbols, data from Burkhardt & Coupry 2000) plus model data (filled symbols). Circles: models where internal gravity waves (hereafter IGWs) are negligible. Squares: models where IGWs are significant (Charbonnel & Talon 2005; Talon & Charbonnel 2005). (bottom) Rotational velocity in the Hyades - unprojected (open symbols, data from Gaigé 1993) plus model data (filled symbols). **(Right)** (top) Lithium abundance plus approximate dependence of surface braking on effective temperature and the requirements for angular momentum transport for rotational mixing to lead to the formation of the lithium dip (Talon & Charbonnel 1998). (bottom) Filtered angular momentum luminosity of waves below the SLO measuring the efficiency of wave induced angular momentum transport. Adapted from Talon & Charbonnel (2003).

the Li dip. Similarly, Richard et al. (priv. comm.) have to change the ad-hoc turbulence they add to reduce atomic diffusion by an order of magnitude along along the Li dip. The strong variation of these *fudge factors* is actually an indication that the *physical processes* at play inside these stars change in that region.

1.2. A link with the Sun's rotation

The proposition by Talon & Charbonnel (1998) may be linked to another observation that fails to be reproduced by the pure hydrodynamic models, namely the flat solar rotation profile revealed by helioseismology (Brown et al. 1989; Kosovichev et al. 1997; Couvidat et al. 2003; García et al. 2007). At the solar age, models relying only on turbulence and meridional circulation for momentum transport predict large angular velocity gradients that are not present in the Sun (Pinsonneault et al. 1989; Chaboyer et al. 1995; Talon 1997; Matias & Zahn 1998). This indicates that another process participates to the transport of angular momentum in solar-type stars.

Two candidates have been examined. The first rests on the possible existence of a magnetic field within the radiation zone (Charbonneau & MacGregor 1993; Eggenberger et al. 2005). The second invokes traveling internal gravity waves (hereafter IGWs) generated at the base of the convection envelope (Schatzman 1993; Zahn et al. 1997; Kumar & Quataert 1997; Talon, Kumar & Zahn 2002). For either of these solutions to be convinc-

ing, they must be tested with numerical models coupling these processes with rotational instabilities and should explain all the aspects of the problem, including the lithium evolution with time.

The Li data suggest that the efficiency of the additional process is linked to the growth of the convective envelope in stars with effective temperatures around $T_{\text{eff}} \simeq 6600$ K. As we shall see below, this is a characteristic of IGWs.

2. IGWs generation and momentum extraction in low-mass stars

In the Earth's atmosphere, wave-induced momentum transport is a key process in the understanding of several phenomena, the best known being the quasi-biennial oscillation of the stratosphere. In astrophysics, IGWs have initially been invoked as a source of mixing for chemicals (Press 1981; García López & Spruit 1991; Schatzman 1993; Montalbán 1994; Montalbán & Schatzman 1996, 2000; Young et al. 2003). Ando (1986) studied the transport of angular momentum associated with standing gravity waves in Be stars. He was the first to clearly state, in the stellar context, that IGWs carry angular momentum from the region where they are excited to the region where they are dissipated. Traveling IGWs have since been invoked as an important source of angular momentum redistribution in single stars (Schatzman 1993; Kumar & Quataert 1997; Zahn, Talon & Matias 1997, Talon et al. 2002; Charbonnel & Talon 2005).

2.1. IGWs generation and wave spectrum

Two different processes contribute to IGWs excitation at the border of convective regions: convective overshooting in an adjacent stable region (García López & Spruit 1991; Kiraga et al. 2003; Rogers & Glatzmaier 2005a, 2005b), and Reynolds stresses in the convection zone (Goldreich & Kumar 1990; Balmforth 1992; Goldreich, Murray & Kumar 1994). In our studies, we shall use the second mechanism, which has been calibrated on solar p-modes and, thus, seems more reliable at this time. This gives a lower limit to the correct/total wave flux although neglecting the other excitation mechanism remains the weakest point of wave-induced transport models (see Charbonnel & Talon 2007 for a complete discussion on wave excitation and numerical simulations).

If we assume that prograde and retrograde waves are produced with the same efficiency and if they are damped in the same way as they propagate inside the star, then waves have no net impact on the angular momentum distribution. It is thus important to treat wave damping properly. In Talon et al. (2002), we showed that the development of a double-peaked shear layer (SLO, for Shear Layer Oscillation), acts as a filter for waves and that, when the core is rotating faster than the surface, the asymmetry of this filter produces momentum extraction.

In Talon & Charbonnel (2005), we developed a formalism to incorporate the contribution of IGWs to the transport of angular momentum and chemical elements in stellar models on secular time-scales. Using only this filtered flux, it is possible to follow the contribution of internal waves over long (evolutionary) time-scales. We use the formalism developed by Goldreich & Kumar (1990) and Goldreich et al. (1994) to estimate the angular momentum luminosity \mathcal{L}_J below the convective envelope (see also Kumar & Quataert 1997). The local momentum luminosity of waves is then given by

$$\mathcal{L}_J(r) = \sum_{\sigma, \ell, m} \mathcal{L}_{J\ell, m}(r_{\text{cz}}) \exp[-\tau(r, \sigma, \ell)] \quad (2.1)$$

where 'cz' refers to the base of the convection zone. τ corresponds to the integration of

the local damping rate, and takes into account the mean molecular weight stratification

$$\tau(r, \sigma, \ell) = [\ell(\ell + 1)]^{\frac{3}{2}} \int_r^{r_c} (K_T + \nu_v) \frac{N N_T^2}{\sigma^4} \left(\frac{N^2}{N^2 - \sigma^2} \right)^{\frac{1}{2}} \frac{dr}{r^3} \quad (2.2)$$

(Zahn et al. 1997). In this expression, N_T^2 is the thermal part of the Brunt-Väisälä frequency, K_T is the thermal diffusivity and ν_v the (vertical) turbulent viscosity. σ is the local, Doppler-shifted frequency

$$\sigma(r) = \omega - m [\Omega(r) - \Omega_{cz}] \quad (2.3)$$

and ω is the wave frequency in the reference frame of the convection zone. Let us mention that, in this expression for damping, only the radial velocity gradients are taken into account. This is because angular momentum transport is dominated by the low frequency waves ($\sigma \ll N$) for which horizontal gradients are much smaller than vertical ones.

When meridional circulation, turbulence, and waves are all taken into account, the evolution of angular momentum follows

$$\rho \frac{d}{dt} [r^2 \Omega] = \frac{1}{5r^2} \frac{\partial}{\partial r} [\rho r^4 \Omega U] + \frac{1}{r^2} \frac{\partial}{\partial r} \left[\rho \nu_v r^4 \frac{\partial \Omega}{\partial r} \right] - \frac{3}{8\pi} \frac{1}{r^2} \frac{\partial}{\partial r} \mathcal{L}_J(r), \quad (2.4)$$

(Talon & Zahn 1998) where U is the radial meridional circulation velocity. This equation takes into account the advective nature of meridional circulation rather than modeling it as a diffusive process and assumes a “shellular” rotation (see Zahn 1992 for details). Horizontal averaging was performed, and meridional circulation is considered only at first order. When we calculate the fast SLO’s dynamics, U is neglected in this equation. This is justified by the fact that when shears are large such as in the SLO, angular momentum redistribution is dominated by the (turbulent) diffusivity rather than by meridional circulation. However, the complete equation is used when we compute full evolution models as in Charbonnel & Talon (2005).

2.2. Shear layer oscillation (SLO) and filtered angular momentum luminosity

One key feature of the wave-mean flow interaction is that the dissipation of IGWs produces an increase in the local differential rotation: this is caused by the increased dissipation of waves that travel in the direction of the shear (see Eqs. 2.2 and 2.3). In conjunction with viscosity, this leads to the formation of an oscillating doubled-peak shear layer that oscillates on a short time-scale (Gough & McIntyre 1998; Ringot 1998; Kumar, Talon & Zahn 1999). This oscillation is similar to the Earth quasi-biennial oscillation that is also caused by the differential damping of internal waves in a shear region.

This SLO occurs if the deposition of angular momentum by IGWs is large enough when compared with (turbulent) viscosity (Kim & MacGregor 2001)[†]. To calculate the turbulence associated with this oscillation, we rely on a standard prescription for shear turbulence away from regions with mean molecular weight gradients

$$\nu_v = \frac{8}{5} Ri_{\text{crit}} K \frac{(rd\Omega/dr)^2}{N_T^2} \quad (2.5)$$

which takes radiative losses into account (Townsend 1958; Maeder 1995). This coefficient is time-averaged over a complete oscillation cycle (for details, see Talon & Charbonnel 2005).

In the presence of differential rotation, the dissipation of prograde and retrograde waves in the SLO is not symmetric, and this leads to a finite amount of angular momentum

[†] If viscosity is large, a stationary state can be reached.

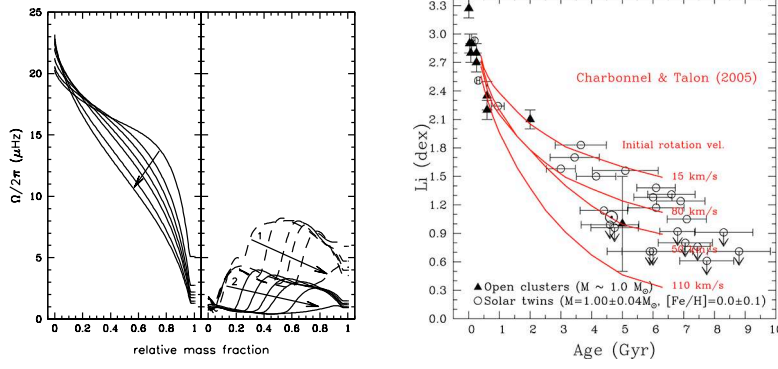


Figure 2. (Left) Evolution of the rotation profile in a solar-mass model with and without IGWs. The initial equatorial rotation velocity is 50 km s^{-1} , and identical surface magnetic braking is applied. (left) Model without IGWs. Curves correspond to ages of 0.2, 0.5, 0.7, 1.0, 1.5, 3.0 and 4.6 Gy that increase in the direction of the arrow. (right) When IGWs are included, low-degree waves penetrate all the way to the core and deposit their negative angular momentum in the whole radiative region. Curves labelled 1 correspond to ages of 0.2, 0.21, 0.22, 0.23, 0.25 and 0.27 Gy and those labelled 2 to 0.5, 0.7, 1.0, 1.5, 3.0 and 4.6 Gy. From Charbonnel & Talon (2005). (Right) Evolution of surface lithium abundance with time for solar-mass models including gravity waves compared with observations in solar analogues. Updated from Meléndez et al. (2009).

being deposited in the radiative interior beyond the SLO. This is the filtered angular momentum luminosity $\mathcal{L}_J^{\text{fil}}$. Let us mention that in fact, the existence of a SLO is not even required to obtain this differential damping between prograde and retrograde waves, and thus, as long as differential rotation exists at the base of the convection zone, waves will have a net impact of the rotation rate of the interior.

The SLO's dynamics is studied by solving Eq. (2.4) with small time-steps and using the whole wave spectrum while for the secular evolution of the star, one has to use instead the filtered angular momentum luminosity. Let us stress that in the case of the secular evolution we do not follow the SLO dynamics, because of its very short time scale. Rather, we only consider the filtered angular momentum luminosity beyond the SLO, and its effect on chemicals is given by a local turbulence calculated from a study of the SLO's dynamic over very short time-scales. Let us also mention here that, for both the SLO and the filtered angular momentum luminosity, differential damping is required. Since this relies on the Doppler shift of the frequency (see Eqs. 2.2 and 2.3), angular momentum redistribution will be dominated by the low frequency waves that experience a larger Doppler shift, but that are not so low that they will be immediately damped. Numerical tests indicate that this occurs around $\omega \simeq 1 \mu\text{Hz}$.

3. The case of Population I low-mass stars, the Li dip and the Sun

An important property of IGWs is that their generation and efficiency in extracting angular momentum from stellar interiors depend on the structure of their convective envelope, which varies strongly with the effective temperature of the star. Figure 1 shows the T_{eff} -dependence of the filtered angular momentum luminosity of waves below the SLO, which directly measures the efficiency of wave-induced angular momentum extraction in zero-age main sequence stars around the Li dip. It appears that the net momentum luminosity slightly increases with increasing T_{eff} , presents a plateau, and suddenly drops

at the T_{eff} of the dip. This clearly indicates that the momentum transport by IGWs has the proper T_{eff} -dependence to be the required process to explain the cool side of the Li dip (Talon & Charbonnel 2003).

Talon et al. (2002) have shown, in a static model, that waves can efficiently extract angular momentum from a star that has a surface convection zone rotating slower than the interior. Charbonnel & Talon (2005) then calculated the evolution of the internal rotation profile for a solar-mass star with surface spin-down. We showed that, in that case, waves tend to slow down the core, creating “slow” fronts that propagate from the core to the surface (Fig. 2). These calculations confirmed, in a complete evolution of solar-mass models evolved from the pre-main sequence to 4.6 Gy, that IGWs play a major role in braking the solar core. This momentum transport reduces rotational mixing in low-mass stars, leading to a theoretical surface lithium abundance in agreement with observations made in solar analogues of various ages (Fig. 2).

Figure 1 shows our predictions for rotation velocities and Li surface abundances together with the observed data at the age of the Hyades. On the left side of the dip, IGWs play no role and the predictions are taken from Charbonnel & Talon (1999). On the cool side of the dip IGWs are at act and lead to the rise of the surface Li. The model at ~ 5800 K corresponds to a $1.0 M_{\odot}$ star. It was computed for 3 initial rotation velocities of 50, 80 and 110 km s^{-1} (Charbonnel & Talon 2005). Models with IGWs are in perfect agreement with the observations, both regarding the amplitude of the Li depletion and the dispersion at a given effective temperature.

4. The case of Population II low-mass stars

In the context of primordial nucleosynthesis, it has long been debated whether Pop II stars could have depleted their surface Li abundance, just as their metal-rich counterpart did. Recent results on cosmic microwave background anisotropies, and especially those of the WMAP experiment, have firmly established that the primordial Li abundance is ~ 3 to 5 times higher than the measured Li value in dwarf stars along the so-called Spite plateau (Charbonnel & Primas 2005). The main theoretical difficulty to reproduce these data is that the Li abundance is remarkably constant in halo dwarfs, while it seems at first sight that depletion should lead to a larger dispersion.

A re-examination of Li data in halo stars available in the literature has led to a very surprising result: the mean Li value as well as its dispersion appear to be lower for the dwarfs than for the subgiant stars (Charbonnel & Primas 2005). In addition, all deviant stars, i.e. those with a strong Li deficiency or an abnormally high Li content, lie on or originate from the hot side of the Li plateau. These results indicate that halo stars that have now just passed the turnoff have experienced a Li history slightly different from that of their less massive counterparts.

This behaviour is the signature of a transport process for angular momentum whose efficiency changes on the extreme blue edge of the plateau and it corresponds to the generation and filtering of IGWs in Pop II stars (Fig. 3, Talon & Charbonnel 2004), just as it does in the case of Pop I stars.

Indeed and as discussed previously, the generation of IGWs and, consequently, their efficiency in transporting angular momentum, depend on the structure of the stellar convective envelope, which in turn depends on the effective temperature of the star as can be seen in Fig. 3. As in the case of Pop I stars on the red side of the Li dip, the net angular luminosity of IGWs is very high and constant in Pop II stars along the plateau up to $T_{\text{eff}} \sim 6300$ K. There, IGWs should dominate the transport of angular momentum and enforce quasi solid-body rotation of the stellar interior on very short timescale. As

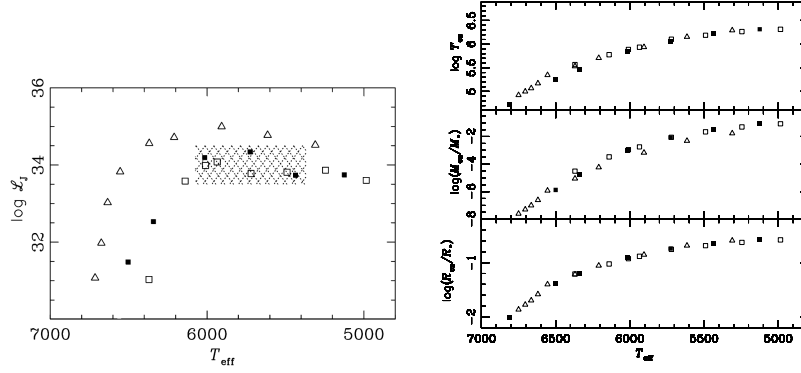


Figure 3. (Left) Net momentum luminosity at $0.03 R_*$ below the surface convection zone as a function of T_{eff} for an initial differential rotation of $\delta\Omega = 0.01 \mu\text{Hz}$ over $0.05 R_*$. The Li plateau region is dashed. From Charbonnel & Talon (2004). (Right) (top) Temperature at the base of the convection zone (T_{cz}), (middle) mass of the convection zone and (bottom) radius of the convection zone as a function of T_{eff} . Squares: Pop II stars on the zams (open squares) and at 10 Gyr (black squares); Triangles: Pop I stars on the zams. From Charbonnel & Talon (2004).

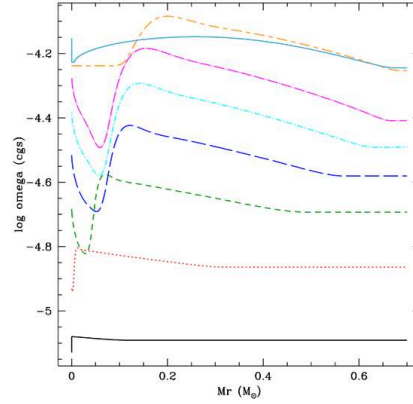


Figure 4. Evolution of the rotation profile inside a $0.7 M_\odot$ Pop II star during the pre-main sequence. Curves correspond to 2, 5, 10, 15, 20, 25, 35 and 237 My, from bottom to top (acceleration is related to the star's overall contraction). The ZAMS velocity is 25 km s^{-1} .

a result, the surface Li depletion is expected to be independent of the initial angular momentum distribution, implying a very low dispersion of the Li abundance from star to star.

In more massive stars however the efficiency of IGWs decreases and internal differential rotation is expected to be maintained under the effect of meridional circulation and turbulence. Consistently, variations of the initial angular momentum from star to star would lead to more Li dispersion and to more frequent abnormalities in the case of the most massive stars where IGWs are not fully efficient, as required by the observations. We note that the mass-dependence of the IGWs efficiency also leads to a natural explanation of fast horizontal branch rotators.

Let us stress here that the absence of a Li dip in Pop II stars reflects the facts that Pop II dip stars already evolved past the main sequence.

We started the computation of complete stellar evolution models of Pop II stars from the pre-main sequence. Preliminary results show that the spin-down fronts that are observed in Pop I stars are also seen in Pop II stars during the PMS (see Fig. 4). Lithium depletion remains negligible during that phase. Calculation of the main sequence evolution is underway.

5. Conclusions

IGWs have a large impact on the evolution of low-mass stars, especially through their effect on the rotation profile, which then modifies meridional circulation and shear turbulence, and thus, the mixing of chemical elements. Within this framework, hydrodynamical models including the combined effects of meridional circulation, shear turbulence and internal gravity waves (using an excitation model that fits solar p-modes) successfully reproduce several observations:

- the time evolution of lithium in solar analogues (Fig. 2);
- the shape of the Li and Be dips (Fig. 1);
- the Li and Be behaviour in evolved stars (see Charbonnel & Lagarde, this Volume);
- the small amount of differential rotation measured by helioseismology (Fig. 2).

Up to now, no other theoretical model has achieved similar results. We also expect that IGWs can reduce the impact of the variety of initial rotation velocities during the spin-down phase of Pop II stars and thus, could be an important element in the understanding of the small amount of dispersion measured on the Li plateau.

Our comprehensive picture should have implications for other difficult unsolved problems related to the transport of chemicals and angular momentum in stars. We think in particular to the stars on the horizontal and asymptotic giant branches that exhibit unexplained abundance anomalies. No doubt that all these so-called “non-standard” physical processes must be part of the art of modelling stars in the 21st century. In this context, light elements such as Li and Be play a crucial role.

Acknowledgements

We acknowledge financial support from IAU, from the French “Programme National de Physique Stellaire” of CNRS/INSU, and from the Swiss National Science Foundation.

References

- Ando, H. 1986, *A&A*, 163, 97
 Balachandran, S. 1995, *ApJ* 446, 203
 Balmforth, N.J. 1992, *MNRAS* 255, 639
 Bøsgaard, A.M. & Tripicco, M.J. 1986, *ApJ*, 302, L49
 Bøsgaard, A.M. 1987, *PASP* 99, 1067
 Brown, T.M., Christensen-Dalsgaard, J., Dziembowski, W.A., Goode, P., Gough, D.O., Morrow, C.A. 1989, *ApJ* 343, 526
 Burkhardt, C. & Coupry, M.F. 2000, *A&A* 354, 216
 Chaboyer, N., Demarque, P., Guenther, D.B., Pinsonneault, M.H. 1995, *ApJ* 446, 435
 Charbonneau, P. & Mac Gregor, K.B. 1993, *ApJ* 417, 762
 Charbonnel, C. & Primas, F. 2005, *A&A* 442, 961
 Charbonnel, C. & Talon, S. 1999, *A&A* 351, 635
 Charbonnel, C. & Talon, S. 2005, *Science* 309, 2189
 Charbonnel, C. & Talon, S. 2007, AIP Conference Proceedings, Volume 948, pp. 15-26
 Couvidat, S., García, R. A., Turck-Chièze, S., Corbard, T., Henney, C. J., Jiménez-Reyes, S. 2003, *ApJ* 597, L77

- Deliyannis, C.P., King, J.R., Boesgaard, A.M. 1997, Kontikas E., et al. (eds), “*Wide-field spectroscopy*”, p. 201
- Eggenberger, P., Maeder, A., Meynet, G. 2005, *A&A*, 440, L9
- Fossati, L., Bagnulo, S., Landstreet, J., Wade, G., Kochukhov, O., Monier, R., Weiss, W., Gebran, M. 2008, *A&A*, 483, 891
- Gaigé, Y. 1993, *A&A* 269, 267
- García, R.A., Turck-Chièze, S., Jiménez-Reyes, S.J., Ballot, J., Pallé, P.L., Eff-Darwich, A., Mathur, S., Provost, J. 2007, *Science*, 316, 1591
- García López, R.J. & Spruit, H.C. 1991, *ApJ* 377, 268
- Gebran, M., Monier, R., Richard, O. 2008, *A&A*, 479, 189
- Goldreich, P. & Kumar, P. 1990, *ApJ* 363, 694
- Goldreich, P., Murray, N., Kumar, P. 1994, *ApJ* 424, 466
- Gough, D.O. & McIntyre, M.E. 1998, *Nature* 394, 755
- Kim, E., & MacGregor, K.B. 2001, *ApJ*, 556, L117
- Kiraga, M., Jahn, K., Stepien, K., Zahn, J.-P. 2003, *Acta Astronomica* 53, 321
- Kosovichev, A., et al. 1997, *Sol. Phys.* 170, 43
- Kumar, P. & Quataert, E.J. 1997, *ApJ* 575, L143
- Kumar, P., Talon, S., Zahn, J.-P. 1999, *ApJ* 520, 859
- Maeder, A. 1995, *A&A*, 299, 84
- Maeder, A. & Meynet, G. 2000, *ARAA* 38, 143
- Matias, J. & Zahn, J.-P. 1998, Provost & Schmider (eds), “*Sounding solar and stellar interiors*”, IAU Symp. 181
- Meléndez, J., Ramírez, I., Casagrande, L., Asplund, M., Gustafsson, B., Yong, D., Do Nascimento, J.D., Castro, M., Bazot, M. 2009 *Ap&SS*, tmp, 221
- Michaud, G. 1986, *ApJ* 302, 650
- Montalban, J. 1994 *A&A*, 281, 421
- Montalban, J. & Schatzman E. 1996 *A&A*, 305, 513
- Montalban, J. & Schatzman E. 2000 *A&A*, 354, 943
- Palacios, A., Talon, S., Charbonnel, C., Forestini, M. 2003, *A&A* 399, 603
- Pasquini, L., Randich, S., Zoccali, M., Hill, V., Charbonnel, C., Nordström, B. 2004, *A&A* 424, 951
- Pilachowski, C.A., Saha, A., Hobbs, L.M. 1988, *PASP* 100, 474
- Pinsonneault, M.H., Kawaler, S.D., Sofia, S., Demarque, P. 1989 *ApJ* 338, 424
- Press, W.H. 1981 *ApJ*, 245, 286
- Ringot, O. 1998, *A&A* 335, 89
- Rogers, T.M. & Glatzmaier, G.A. 2005a, *ApJ*, 620, 432
- Rogers, T.M. & Glatzmaier, G.A. 2005b, *MNRAS*, 364, 1135
- Schatzman, E. 1993 *A&A* 279, 431
- Smiljanic, R., Pasquini, L., Charbonnel, C., Lagarde, N., 2009 arXiv0910.4399, A&A, in press
- Takeda, Y., Kawanomoto, S., Takada-Hidai, M., Sadakane, K. 1998, *PASJ* 50, 509
- Talon S. 1997 *PhD Thesis*, Université Paris VII
- Talon, S., Kumar, P., Zahn, J.-P. 2002, *ApJL* 574, 175
- Talon, S. & Charbonnel, C. 1998, *A&A* 335, 959
- Talon, S. & Charbonnel, C. 2003, *A&A* 405, 1025
- Talon, S. & Charbonnel, C. 2004, *A&A* 418, 1051
- Talon, S. & Charbonnel, C. 2005, *A&A* 440, 981
- Talon, S., Richard, O., Michaud, G. 2006, *ApJ* 645, 634
- Talon, S. & Zahn, J.P. 1998, *A&A*, 329, 315
- Théado, S. & Vauclair, S. 2003, *ApJ*, 587, 795
- Townsend A.A., 1958, *J. Fluid Mech.* 4, 361
- Varenne, O. & Monier R. 1999 *A&A* 351, 247
- Wallerstein, G., Herbig G.H., Conti, P.S. 1965, *ApJ*, 141, 610
- Young, P.A., Knierman, K.A., Rigby, J.R., Arnett, D. 2003, *ApJ*, 585, 1114
- Zahn, J.P. 1992, *A&A* 265, 115
- Zahn, J.P., Talon, S., Matias, J. 1997, *A&A* 322, 320

Rotational mixing and Lithium depletion

M. H. Pinsonneault¹

¹Ohio State University, Dept. of Astronomy 140 W. 18th Ave. Columbus, OH 43210 USA

email: pinsonneault.1@osu.edu

Abstract. I review basic observational features in Population I stars which strongly implicate rotation as a mixing agent; these include dispersion at fixed temperature in coeval populations and main sequence lithium depletion for a range of masses at a rate which decays with time. New developments related to the possible suppression of mixing at late ages, close binary mergers and their lithium signature, and an alternate origin for dispersion in young cool stars tied to radius anomalies observed in active young stars are discussed. I highlight uncertainties in models of Population II lithium depletion and dispersion related to the treatment of angular momentum loss. Finally, the origins of rotation are tied to conditions in the pre-main sequence, and there is thus some evidence that environment and planet formation could impact stellar rotational properties. This may be related to recent observational evidence for cluster to cluster variations in lithium depletion and a connection between the presence of planets and stellar lithium depletion.

Keywords. Hydrodynamics – stars: abundances, rotation, spots

1. Introduction

Lithium is an extraordinarily sensitive diagnostic of stellar structure and evolution. The observed lithium abundances in stars, not surprisingly, reveal an extremely complex picture, and it can sometimes be difficult to remember why rotational mixing is a useful framework for interpreting this data. I therefore begin by briefly summarizing the case for rotation as the physical ingredient responsible for light element depletion in stars.

1.1. Evidence for rotational mixing

The first and most important point is that stellar rotation is capable of driving mild envelope mixing at the observationally required rates (Pinsonneault et al. 1989.) Rotation induces a departure from spherical symmetry which generates meridional circulation currents, and both structural evolution and angular momentum loss from magnetized winds generate shears which can drive mild turbulence. Lithium is easily destroyed in stellar interiors, and such mild mixing can therefore generate surface lithium depletion.

This leads directly to a second important feature of rotational mixing which is observationally required: namely, stars which rotate at different rates will have different mixing histories. Rapid rotators experience stronger torques and larger shears than slow rotators, and they also are less spherical. It is therefore a basic prediction of rotational mixing that there should be a dispersion in mixing rates which can manifest itself as a dispersion in lithium at fixed mass, composition, and age. Lithium is observed to have a significant dispersion in many clusters (see Pinsonneault 1997 for a theoretical review and Sestito & Randich 2005 for a more recent observational synthesis) while other elements in open clusters are very uniform (Paulson et al. 2003). Other mechanisms, such as gravity waves and microscopic diffusion, can generate depletion but not dispersion, so this observed feature allows us to discriminate between physical processes.

Finally, both the mass dependence and time dependence of the observed depletion pattern strongly implicate rotationally driven mixing as the culprit. Rotation declines with age, and so does lithium depletion. By contrast, processes such as gravitational settling tend to be more independent of age, or even increase in rate as stars get older. Rotational mixing also extends through stellar envelopes, and as a result it can simultaneously mix different elements and be present in stars with very different surface convection zone depths. We observe lithium depletion in all low mass open cluster stars, which would not be expected if lithium depletion were a phenomenon confined to the convection zone boundary. This does not rule out interesting interactions with other physics processes, such as magnetic or wave-driven angular momentum transport (see the contribution by Talon in these proceedings), but it does require rotation as a component of the solution.

However, the physics of stellar angular momentum evolution is extremely challenging, and it has proven difficult to develop a rigorous physical model. This has led to a sort of stasis in our understanding of phenomena such as rotational mixing. Fortunately, there have been positive developments, which I summarize below, which reveal a dynamic and more complete picture of stellar evolution. In Section 2 recent advances in our understanding of angular momentum evolution are reviewed; Section 3 then discusses three areas where there are either new observational or theoretical features in stellar lithium depletion. A discussion of some recent developments is given in section 4.

2. Angular momentum evolution

Stellar rotation is an initial value problem, and the initial conditions are set by the details of the star formation process. The angular momentum distribution is subsequently modified by angular momentum loss (via star-disk interactions) and internal angular momentum transport. The physics of the latter is vigorously debated in the literature, with three distinct mechanisms (hydrodynamic, wave-driven, and magnetic) all being in principle important. Rotational mixing is a natural byproduct of angular momentum transport in stellar radiative interiors, especially from hydrodynamic mechanisms. This is a rich field, so I will summarize the main developments relevant for rotational mixing.

Stars appear at the deuterium-burning birthline (Stahler 1988) with a range of rotation rates, typically well below that expected for accretion from a Keplerian disk. The currently favored explanation is that magnetic coupling between the protostar and the accretion disk regulates the rotation (Shu et al. 1994.) In this framework, the initial rotation rate can be thought of as related to the mass accretion rate in the early hydrodynamic stages of star formation. However, the predicted rotation rates on the main sequence are both too rapid and too uniform if models with the observed rotation rates are evolved to the main sequence, even if torques from solar-like winds are included.

However, if a coupling between protostars and their accretion disks exists, the initial spread of rotation rates can be amplified and stars can reach the main sequence as relatively slow rotators. Much observational work has also been invested in the question of star-disk coupling, with a diversity of results largely centered around the proper choice of disk proxies and disentangling evolutionary effects. However, recent Spitzer studies (Rebull et al. 2006) have provided strong evidence for a relationship between rotation and the presence of disks. This may reflect a coupling between the protostar and accretion disk similar to that operating at the earlier stages, or it could be induced by an enhanced stellar wind tied to accretion. In either case, the lifetime of accretion disks and their degree of coupling to the parent star is crucial for establishing the main sequence rotation. Rotation is therefore now perceived as a product of environment, and this raises the

interesting possibility that rotational mixing may also depend on where a star was born or on how the accretion disk evolved.

There are also now very large databases of stellar rotation periods, ranging from star forming regions (Rodríguez-Ledesma et al. 2009) to extensive open cluster surveys such as the Monitor program (Irwin et al. 2009) and transit studies such as the one which yielded a large database of rotation periods in the 550 Myr system M37 (Hartman et al. 2009). The latter study in particular indicates the ability of modern campaigns to infer rotation periods caused by spot modulation for large stellar samples at small amplitude.

These samples can in turn be used to reconstruct the angular momentum evolution of stellar populations, in particular the dependence of angular momentum loss on rotation rate and mass, as well as the coupling timescale between core and envelope (e.g. Irwin et al. 2007, Denissenkov et al. 2009). Different groups agree on the essential features. Angular momentum loss scales as the rotation rate cubed at low rotation rates, then saturates at a threshold which decreases as mass decreases. The net effect is that lower mass stars take longer to spin down and longer for their rotation rates to converge. The cores of the slowly rotating population couple to their envelopes with a timescale of order 100 Myr, while rapidly rotating stars appear to be more strongly coupled. These results are consistent with helioseismic data indicating that the rotation of the solar interior is strongly coupled to that of the surface convection zone.

This combination of theoretical advances and improved rotational data and empirical constraints therefore has significant promise for more robust rotational mixing predictions in the future.

3. Lithium depletion and rotational mixing revisited

The basic rotational mixing picture can be simply defined. Stars experience a mass-dependent pre-main sequence lithium burning epoch, which ends when they develop substantial radiative cores. They then experience rotational mixing on the main sequence, induced either by shears generated by angular momentum loss or their departure from spherical symmetry. As the stars spin down the rate of lithium depletion decreases. This overall picture is reasonable, but a number of phenomena defy easy categorization within it. This is in large part because of the interaction of rotation with other phenomena typically neglected in stellar models. Below are three examples.

3.1. *Structural effects of starspots*

There is a striking dispersion in lithium abundances among late-type stars in young open clusters; the Pleiades is the clearest example (Soderblom et al. 1993.) This trend is not expected from rotational mixing in such young stars, and the relative effect is also the opposite of the one expected: namely, the least depleted stars are the most active and heavily spotted. Much subsequent work has focused on whether the dispersion is real or induced by the heavily spotted nature of the stars in question; the model atmospheres used to interpret the data typically neglect the large changes in the strength of the lithium feature which would be associated with a substantial fraction of the surface covered with cool spots with ample neutral lithium. However, in recent work (King et al. 2009) we found that the scatter in K I was much less than the scatter in Li I, indicating that the bulk of the dispersion is real. The likely origin in our view is actually a different mechanism altogether, and it is motivated by recent data on radius anomalies in active stars from interferometric and eclipsing binary studies.

Eclipsing binaries such as YY Gem (Torres & Ribas 2002) were found to have radii significantly larger than those predicted by interiors theory. Subsequent work traced out

a radius anomaly pattern. More recent interferometric data permits the measurement of radii for inactive field stars, which are found to be in accord with theoretical predictions (Demory et al. 2009.) High activity, such as that found in tidally synchronized short-period binaries, therefore appears to puff up stars. A similar effect during the fully convective protostellar phase would reduce the degree of pre-main sequence lithium depletion; if this varied from star to star it could generate a dispersion with characteristics remarkably like the data. This is illustrated in Fig.1., where Pleiades data from Soderblom et al. (1993) is compared with standard stellar models (lower line) and models with a radius inflated by 10 percent, the level inferred in highly active stars (upper line). In addition to being an attractive solution for a longstanding problem, this leads to an interesting insight. Stellar activity is not a mere detail; it can impact the entire structure of a star and change its mixing history.

3.2. Blue stragglers and halo Lithium depletion

The lithium depletion pattern in metal-poor stars poses a different problem; the majority of stars exhibit little dispersion and the observed abundances appear to be nearly independent of surface temperature or metallicity. One striking counter-example is the presence of a small but real population of highly depleted stars (Thorburn 1994.) In recent work on blue stragglers we find that a population of sub-turnoff merger products, presumably highly lithium depleted, is predicted to arise from such mergers; the number expected is close to that observed in halo stars (Andronov et al. 2006). This confirms the suggestion in Ryan et al. (2001) that these highly depleted stars should not be regarded as the tail of a rotational mixing distribution, but rather that they have a distinct origin.

This does not, however, require that mixing be absent in halo stars. The nature of the dispersion predicted depends on both the distribution of initial conditions and the angular momentum loss history. At present we can only extrapolate Population I conditions to Population II stars. Their torques and initial conditions could very well have been different; for example, planet formation may be less common in them, and this could impact the distribution of accretion disk coupling timescales (see Section 4.) Future work on the activity properties of tidally synchronized halo stars may prove diagnostics of the braking law, while we may need rotation data in more metal-poor outer disk systems to test the metallicity dependence of the initial conditions.

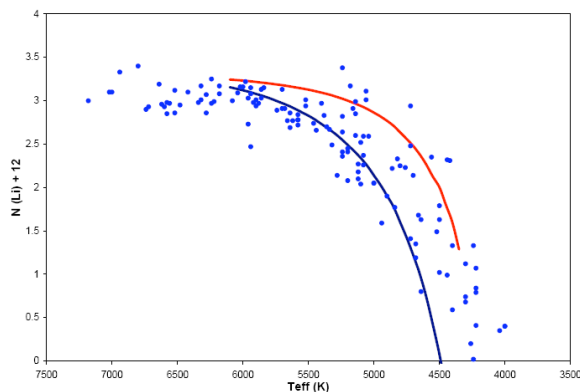


Figure 1. Lithium abundances as a function of effective temperature in the Pleiades cluster compared with standard models (lower line) and models which were inflated during the pre-main sequence lithium depletion epoch (upper line).

3.3. *Interaction of diffusion and rotational mixing*

Microscopic diffusion (or gravitational settling and thermal diffusion) is a basic physical process expected to occur in stars, typically over a very long timescale. The net effect is that heavy species tend to sink relative to light ones, although radiation pressure can drive some heavier elements upwards in sufficiently thin surface convection zones (Michaud 1970). There is clear evidence for diffusion in the Sun (Bahcall & Pinsonneault 1992), both in the sound speed profile and in the detection of a surface helium abundance lower than that initially required to reproduce the solar luminosity.

Diffusion can induce lithium depletion directly, but it also has interesting interactions with rotational mixing (see Richard et al. 1996 for a nice example in the solar context). Gravitational settling operates over shorter timescales for thinner convection zones, and it produces mean molecular weight gradients at the base of the surface convection zone. It is energetically unfavorable to mix in the presence of a μ gradient, and mixing can erase composition gradients; there is thus a natural competition between the two processes. Furthermore, the timescale for mixing increases with age, while the timescale for settling changes very slowly (and tends to decrease as stars evolve to higher effective temperatures). One might therefore expect rotational mixing to predominate earlier while diffusion suppresses mixing at later ages, and for this interaction to depend on mass and composition. This may be related to the apparent stalling of lithium depletion in older open clusters (discussed by Randich in these proceedings), and could be an additional source of lithium depletion in halo stars as well. Recent evidence for settling in multiple elements (Korn, these proceedings) of globular cluster stars provides evidence that diffusion sets in for older stars; an earlier epoch of depletion is certainly permitted by theory, although establishing this observationally will require additional work as discussed in the angular momentum evolution section. Observations of multiple elements, as already done in globulars, could be used to establish the diffusion signature in old open clusters and the interaction between mixing and separation.

4. Future directions

In closing I'd like to note some other wrinkles which may prove important for understanding lithium depletion: differences in depletion patterns from cluster to cluster (see the presentation by Randich) and an apparent excess lithium depletion in stars which host planets (see the talks by Israelian and, for a contrary view, Melendez.) Both can be interpreted in the framework where stellar rotation properties are determined by interactions between protostars and accretion disks. In dense stellar environments the timescale for interactions can be comparable to the lifetimes inferred for accretion disks, raising the possibility that stars born in such regions might have a different distribution of disk lifetimes than stars born in loose associations. This hypothesis is testable in the measured rotation rates of young systems, and this is an important potential effect (especially if we use clusters as an evolutionary sequence!) which needs to be explored.

The recent report that stars with planets have excess lithium depletion (Israelian et al. 2009) may be a fascinating example of how the formation of planets can impact the properties of stars. Bouvier (2008) has proposed a linkage, arguing that systems with planets should have long-lived accretion disks. These in turn become slow rotators, with large relative shears, which in turn could drive excess mixing. He thus argued that there may be a connection between lithium overdepletion and planet formation. Such a link is certainly plausible, but the opposite correlation appears to be required by rotational mixing. More rapid rotators experience larger absolute torques (and in

any case subsequently evolve to become slow rotators, thus in effect adding the mixing from the rapid to that of the slow phase). They also experience larger departures from spherical symmetry; both imply stronger mixing. However, the rotation is set primarily by the coupling between star and disk, not necessarily in the disk lifetime itself, and this may explain the apparent contradiction between “massive disk required for planets” and “weak star-disk interaction required for rapid rotation and lithium depletion.” This avenue may prove promising to explore, and it would be a delightful turn of events if the planetary tail could wag the stellar dog.

References

- Andronov, N., Pinsonneault, M.H. & Terndrup, D.M. 2006, *ApJ*, 646, 1160
- Bahcall, J.N. & Pinsonneault, M.H. 1992, *RMP*, 64, 885
- Bouvier, J. 2008, *A&A* (Letters), 489, 53
- Demory, B.-O., Ségransan, D., Forveille, T., Queloz, D., Peuzit, J.L., et al. 2009, *A&A*, 505, 205
- Denissenkov, P., A., Pinsonneault, M.H., Terndrup, D.M. & Newsham, G. 2009, submitted *ApJ* (astro-ph/0911.1121)
- Hartman, J.D., Gaudi, B.S., Pinsonneault, M.H., Stanek, K.Z., Holman, M.J., McLeod, B.A., Meibom, S., Barranco, J.A. & Kalirai, J.S. 2009, *ApJ*, 691, 342
- Irwin, J., Hodgkin, S., Aigrain, S., Hebb, L., Bouvier, J., Clarke, C., Moraux, E. & Bramich, D.M., 2007, *MNRAS*, 377, 741
- Irwin, J., Aigrain, S., Bouvier, J., Hebb, L., Hodgkin, S., Irwin, M. & Moraux, E. 2009, *MNRAS*, 392, 1456
- Israelian, G., Delgado Mena, E., Santos, N.C., Sousa, S.G., Mayor, M., Udry, S., Dominguez Cerdena, C., Rebolo, R. & Randich, S. 2009, *Nature*, 462, 189
- King, J.R., Schuler, S.C., Hobbs, L.M. & Pinsonneault, M.H. 2009, *ApJ* in press (astro-ph/1001.2796)
- Michaud, G. 1970, *ApJ*, 160, 641
- Paulson, D.B., Sneden, C. & Cochran, W.D. 2003, *AJ*, 125, 3185
- Pinsonneault, M.H. 1997, *ARAA*, 35, 557
- Pinsonneault, M.H., Kawaler, S.D., Sofia, S. & Demarque, P. 1989, *ApJ*, 338, 424
- Rebull, L.M., Stauffer, J.R., Megeath, S.T., Hora, J.L. & Hartmann, L. 2006, *ApJ*, 646, 297
- Richard, O., Vauclair, S., Charbonnel, C. & Dziembowski, W.A.. 1996, *A&A*, 312, 1000
- Rodriguez-Ledesma, M.V., Mundt, R. & Eisloffel, J. 2009 *A & A*, 502, 883
- Ryan, S.G., Beers, T.C., Kajino, T. & Rosolankova, K. 2001, *ApJ*, 547, 231
- Sestito, P. & Randich, S. 2005, *A&A*, 442, 615
- Shu, F.H., Najita, J., Ostriker, E., Wilkin, F., Ruden, S. & Lizano, S. 1994, *ApJ*, 429, 781
- Soderblom, D., Jones, B.F., Balachandran, S., Stauffer, J.R., Duncan, D.K., Fedele, S.B. & Hudon, J.D. 1993, *AJ*, 106, 1059
- Stahler, S.W. 1988, *ApJ*, 332, 804
- Thorburn, J.A. 1994, *ApJ*, 421, 318
- Torres, G. & Ribas, I. 2002, *ApJ*, 567, 1140

Effects of rotation and magnetic fields on the structure and surface abundances of solar-type stars

P. Eggenberger, A. Maeder, and G. Meynet

Observatoire de Genève, Université de Genève,
 51 Ch. des Maillettes, CH-1290 Versoix, Suisse
 email: [patrick.eggenberger;andre.maeder;georges.meynet]@unige.ch

Abstract. The effects of shellular rotation on the modelling of solar-type stars (in particular internal structure, evolutionary tracks in the HR diagram, lifetimes and surface abundances) are first examined. Then the effects of a dynamo possibly occurring in the internal stellar radiative zone by imposing nearly solid body rotation are studied. These results are finally discussed in the context of the rotational history of exoplanet host stars and the link between lithium depletion and the presence of exoplanets.

Keywords. Stars: rotation, magnetic fields, interiors, abundances

1. Introduction

Rotation is one of the key processes that changes the internal structure and global properties of stellar models with a peculiarly strong impact on the physics and evolution of massive stars (see e.g. Maeder 2009). In this work, we first focus on the effects of rotational mixing on the global properties and surface abundances of solar-type stars by comparing stellar models including shellular rotation to non-rotating models. We then investigate the effects of a dynamo in the radiative zone of a solar-type star on the efficiency of rotational mixing by computing models with shellular rotation and the Tayler-Spruit dynamo (Spruit 2002). A comparison between models of solar-type stars including rotation only and both rotation and magnetic fields is made in the framework of a scenario proposed by Bouvier (2008) that relates the enhanced lithium depletion in exoplanet host stars to their rotational history.

2. Effects of rotation

To investigate the effects of rotational mixing on the properties of solar-type stars, $1 M_{\odot}$ models are computed with the Geneva stellar evolution code (Eggenberger et al. 2008). These models are computed with a solar chemical composition as given by Grevesse & Noels (1993) and a solar calibrated value for the mixing-length parameter. The main-sequence evolution of non-rotating models with and without atomic diffusion of helium and heavy elements is compared to the main-sequence evolution of a rotating model with an initial velocity of 50 km s^{-1} on the zero age main sequence (ZAMS). We adopt the braking law of Kawaler (1988) to account for the magnetic braking undergone by solar-type stars when arriving on the main sequence. Two parameters enter this braking law: the saturation velocity Ω_{sat} and the braking constant K . Following Bouvier et al. (1997), Ω_{sat} is fixed to $14 \Omega_{\odot}$ and the braking constant K is calibrated so that a $1 M_{\odot}$ star with an initial velocity of 50 km s^{-1} on the ZAMS reproduces the solar surface rotational velocity after 4.57 Gyr. The rotating model also includes the effects of atomic diffusion

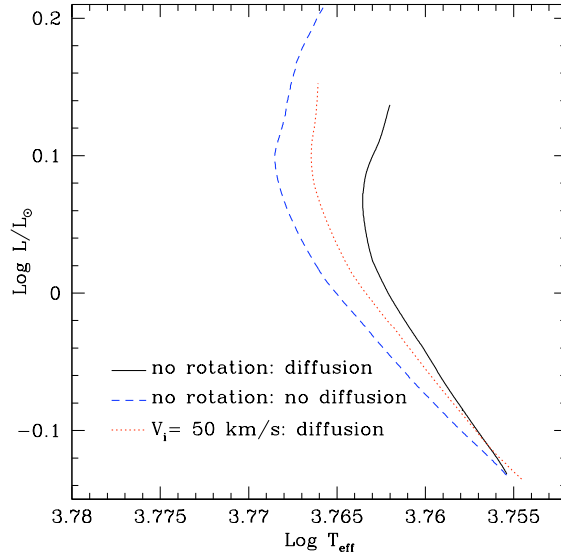


Figure 1. Main-sequence evolution of $1 M_{\odot}$ models with and without rotation. The continuous and dashed lines correspond to non-rotating models computed with and without atomic diffusion, respectively. The dotted line indicates a rotating model computed with an initial velocity of 50 km s^{-1} on the ZAMS and with atomic diffusion.

of helium and heavy elements. All three $1 M_{\odot}$ models share therefore exactly the same initial parameters except for the inclusion of shellular rotation and atomic diffusion.

The evolutionary tracks in the HR diagram corresponding to the main-sequence evolution of these models are shown in Fig. 1. By comparing the rotating model (dotted line) to the non-rotating model computed with the same initial parameters except for the inclusion of shellular rotation (continuous line), we see that the rotating model exhibits larger effective temperatures and slightly larger luminosities than the non-rotating one. This results in a shift of the evolutionary track to the blue part of the HR diagram when rotation is included in the computation. Concerning atomic diffusion, Fig. 1 shows that the non-rotating model including atomic diffusion (continuous line) is characterised by lower effective temperatures and luminosities compared to the non-rotating model without atomic diffusion (dashed line). The inclusion of atomic diffusion is thus found to shift the evolutionary track towards the red part of the HR diagram.

These changes observed in the HR diagram can be related to differences in the surface chemical composition of the models. Fig. 2 shows the helium surface mass fraction Y_s as a function of time during the main-sequence evolution for the three models shown in Fig. 1. The model computed without atomic diffusion and rotation (dashed line) exhibits a constant value of the helium surface abundance since no mixing mechanisms are at work in the radiative zone. The inclusion of atomic diffusion leads to a decrease of the helium mass fraction at the stellar surface. By comparing the models including atomic diffusion computed with and without rotation (dotted and continuous lines), we note a lower decrease of the helium surface abundance for the rotating model than for the non-rotating one. Rotational mixing is thus found to counteract the effects of atomic diffusion in the external layers of the star. As a result, rotating models exhibit larger

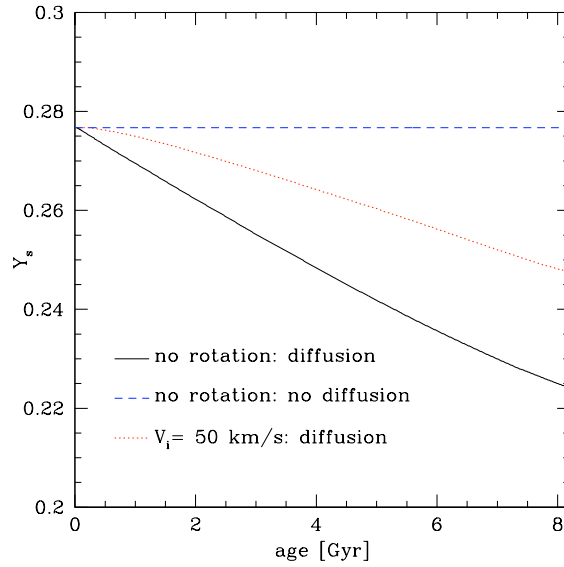


Figure 2. Surface helium mass fraction during the evolution on the main sequence for the $1 M_{\odot}$ models shown in Fig. 1.

values of helium abundances at the surface. This leads to a decrease of the opacity in the external layers of the star and explains the shift towards the blue part of the HR diagram observed in Fig. 1.

The effects of rotation are of course not restricted to the external layers of the star. Rotational mixing has indeed a large impact on the properties of the central layers by bringing fresh hydrogen fuel to the central stellar core. As a result, the central hydrogen mass fraction at a given age is found to be larger for rotating models than for models without rotation. The inclusion of atomic diffusion leads to the opposite effect, since a non-rotating model computed with atomic diffusion exhibits a more rapid decrease of the central hydrogen abundance than a model without atomic diffusion. It is interesting to note that the efficiency of rotational mixing relative to atomic diffusion is found to be larger in the central layers of a solar-type star than in its external layers. In the external layers, rotation only reduces the efficiency of atomic diffusion but does not completely counteract these effects (see Fig. 2), while in the central layers the increase of the hydrogen abundance due to rotation is larger than the decrease related to atomic diffusion. Due to rotational mixing, the main-sequence lifetime is then larger for stellar models including rotation.

Rotational effects change the structure of a solar-type star and hence its asteroseismic properties. In particular, the change of the central chemical gradients and the increase of the central hydrogen abundance induced by rotational mixing lead to an increase of the values of the asteroseismic small separation for rotating models compared to non-rotating models (Eggenberger et al. 2006; Eggenberger & Carrier 2006). The effects of rotation on the external layers are of course reflected in the change of the surface abundances but can also be revealed by asteroseismic measurements. As discussed above, the inclusion of rotation results in a significant increase of the effective temperature. At a given luminosity, this leads to smaller radii for rotating models than for non-rotating

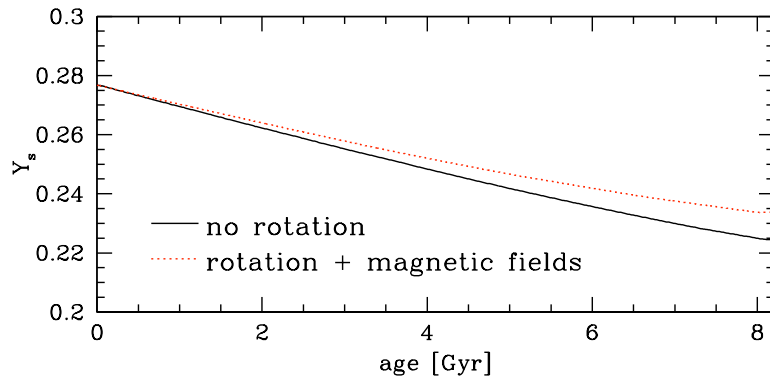


Figure 3. Surface helium mass fraction during the main-sequence evolution of a non-rotating model (continuous line) and a model including rotation and magnetic fields (dotted line). Both models are computed with atomic diffusion of helium and heavy elements.

models. Consequently, a rotating model will be characterised by a larger mean density and hence a larger value of the asteroseismic mean large separation than a non-rotating model. It is thus interesting to note that spectroscopic measurements of the surface abundances and asteroseismic measurements can give us valuable insights about the effects of rotational mixing on the properties of solar-type stars.

3. Effects of magnetic fields

After the effects of rotation, the effects of magnetic fields and in particular of a dynamo possibly occurring in the radiative zone of the star are studied. These effects are particularly interesting to consider in the context of the internal rotation of the Sun, since models including only shellular rotation predict a rapidly rotating core in disagreement with helioseismic measurements. Models of solar-type stars including both shellular rotation and the Tayler-Spruit dynamo (Spruit 2002) are then computed. We recall here that the theoretical formulation of this dynamo is still a matter of debate (see e.g. Denisov & Pinsonneault 2007; Zahn et al. 2007; Rüdiger et al. 2009). It is however worth investigating the effects of such an efficient process for the transport of angular momentum on the properties of solar-type stars, since models including both the effects of shellular rotation and magnetic fields as prescribed by the Tayler-Spruit dynamo are found to correctly reproduce the helioseismic measurements of the solar rotation profile (Eggenberger et al. 2005).

Figure 3 shows the comparison between the helium surface abundance during the main sequence for a $1 M_{\odot}$ model including both shellular rotation and the Tayler-Spruit dynamo computed with an initial velocity on the ZAMS of 50 km s^{-1} and the corresponding non-rotating model. Both models include atomic diffusion of helium and heavy elements. The inclusion of both rotation and magnetic fields results in a slight increase of the helium mass fraction at the stellar surface compared to a non-rotating model including only atomic diffusion. This increase is however much lower than for a model computed with rotation only (compare Fig. 2 and Fig. 3). The efficiency of rotational mixing is thus found to be strongly reduced when the effects of the Tayler-Spruit dynamo are taken into account. The near solid body rotation of models including this dynamo leads indeed to a low value of the diffusion coefficient associated to the shear turbulent mixing. The transport of chemicals by shear mixing is thus strongly reduced when the effects of the

Taylor-Spruit are included in the computation. Compared to the case with rotation only, we also note a slight increase of the transport of chemicals by the meridional circulation for models with magnetic fields. This increase is however much smaller than the strong decrease of the shear turbulent mixing leading to a net decrease of the global efficiency of rotational mixing for a rotating model of a solar-type star computed with the Taylor-Spruit dynamo.

4. Rotational history of exoplanet host stars

Finally, the effects of rotation and magnetic fields are briefly discussed in the context of the rotational history of exoplanet host stars and in particular in the framework of a scenario suggested by Bouvier (2008). This scenario is first based on the fact that observations of rotational periods of young solar-type stars suggest that slow rotators develop a high degree of differential rotation between the radiative core and the convective envelope, while solid-body rotation is favoured for fast rotators (see e.g. Irwin et al. 2007; Bouvier 2008). This result implies that slow rotators can be modelled with shellular rotation only, while fast rotators are modelled with both rotation and the Taylor-Spruit dynamo in order to produce a sufficient internal coupling to ensure solid body rotation. As discussed in the preceding section, this leads to different surface chemical compositions for slow and fast rotators, since the efficiency of rotational mixing is strongly reduced when the effects of magnetic fields are taken into account. Slow rotators will then exhibit lower values of surface lithium abundance than fast rotators.

As discussed by Bouvier (2008), the rotation of the star on the ZAMS depends on the initial velocity of the star and on the disk lifetime during the pre-main sequence. A longer disk lifetime enables the star to lose a larger amount of angular momentum during the pre-main sequence leading to a lower rotation rate on the ZAMS. As mentioned above, slow rotators are characterised by lower surface abundances of lithium than fast rotators. We thus obtain a relationship between the surface lithium abundance and the rotation rate on the ZAMS which seems to be in good agreement with observations in the Pleiades (Soderblom et al. 1993). Moreover, longer disk lifetimes may favor the formation and migration of giant exoplanets. This leads to an interesting relationship between the abundance of lithium and the presence of giant exoplanets. In this scenario, a longer disk lifetime leads indeed simultaneously to a lower lithium abundance (due to the smaller rotation rate on the ZAMS) and a higher probability to detect giant exoplanets. This seems to be in good agreement with observations of lithium depletion in exoplanet host stars as reported by Israelian et al. (2009).

One may wonder whether other observational trends are predicted in the framework of this scenario. As mentioned in Sect. 2, the effects of rotation on the properties of the central layers of a solar-type star can be revealed by asteroseismic observations and in particular by changes of the small separation. In the scenario outlined here, the efficiency of rotational mixing is larger for slow rotators on the ZAMS than for fast rotators. Since the presence of giant exoplanets is favored for stars with slow rotation rates on the ZAMS, the efficiency of rotational mixing is then predicted to be larger in exoplanet host stars than in stars without planets. This explains the different lithium abundances of stars with and without planets but this also leads to changes in the structure and chemical composition of the central layers and hence to different values of the small separation. In the scenario proposed by Bouvier (2008) we thus expect larger values of the asteroseismic small separation for exoplanet host stars than for stars without planets. It will be particularly interesting to investigate this point in the light of new

asteroseismic observations coming from space missions dedicated simultaneously to the search of exoplanets and asteroseismology like CoRoT and Kepler.

References

- Bouvier, J. 2008, *A&A*, 489, L53
Bouvier, J., Forestini, M., & Allain, S. 1997, *A&A*, 326, 1023
Denissenkov, P. A. & Pinsonneault, M. 2007, *ApJ*, 655, 1157
Eggenberger, P. & Carrier, F. 2006, *A&A*, 449, 293
Eggenberger, P., Carrier, F., Maeder, A., & Meynet, G. 2006, *Memorie della Societa Astronomica Italiana*, 77, 309
Eggenberger, P., Maeder, A., & Meynet, G. 2005, *A&A*, 440, L9
Eggenberger, P., Meynet, G., Maeder, A., et al. 2008, *Ap&SS*, 316, 43
Grevesse, N. & Noels, A. 1993, in *Origin and evolution of the elements: proceedings of a symposium in honour of H. Reeves, held in Paris, June 22-25, 1992*. Edited by N. Prantzos, E. Vangioni-Flam and M. Casse. Published by Cambridge University Press, Cambridge, England, 1993, p.14, ed. N. Prantzos, E. Vangioni-Flam, & M. Casse, 14
Irwin, J., Hodgkin, S., Aigrain, S., et al. 2007, *MNRAS*, 377, 741
Israelian, G., Delgado Mena, E., Santos, N. C., et al. 2009, *Nature*, 462, 189
Kawaler, S. D. 1988, *ApJ*, 333, 236
Maeder, A. 2009, *Physics, Formation and Evolution of Rotating Stars*, ed. A. Maeder
Rüdiger, G., Gellert, M., & Schultz, M. 2009, *MNRAS*, 399, 996
Soderblom, D. R., Jones, B. F., Balachandran, S., et al. 1993, *AJ*, 106, 1059
Spruit, H. C. 2002, *A&A*, 381, 923
Zahn, J., Brun, A. S., & Mathis, S. 2007, *A&A*, 474, 145

The light elements in a helio- and asteroseismic perspective

Sylvie Vauclair¹

¹ Laboratoire d'Astronomie de Toulouse-Tarbes, Université de Toulouse,
14 Avenue Edouard Belin, 31400 Toulouse, France
email: sylvie.vauclair@ast.obs-mip.fr

Abstract. Asteroseismology is a powerful tool to derive stellar parameters, including the helium content and internal helium gradients, and the macroscopic motions which can lead to lithium, beryllium, and boron abundance variations. Precise determinations of these parameters need deep analyses for each individual stars. After a general introduction on helio and asteroseismology, I first discuss the solar case, the results which have been obtained in the past two decades, and the crisis induced by the new determination of the abundances of heavy elements. Then I discuss asteroseismology in relation with light element abundances, especially for the case of main sequence stars.

Keywords. Sun: abundances, heliosismology – stars: interiors

1. Introduction

The general study of stellar oscillations began long before the advent of the so-called helio and asteroseismology. In the past, astronomers only detected large amplitude oscillations and they spoke of “variable stars” or “pulsating stars”. Nowadays, new techniques allow to detect very small amplitude oscillations, and variable stars are known all over the HR diagram. They can be classified according to:

- the type of waves which leads to their oscillations, either pressure or gravity waves or both
- their amplitudes
- their excitation mechanisms

Before the first discovery of solar oscillations, solar-type stars were not supposed to be variable, as the acoustic waves are damped in their interiors. We now know that stochastic excitation induced by convective motions leads to permanent destabilisation so that these stars behave like resonant cavities in spite of the waves damping.

The first report of a periodic solar velocity field was given by Leighton et al. (1962). Evidences of the five minute oscillations were later confirmed by Ulrich (1970) and Leibacher & Stein (1971). Some 10 millions p-modes are observed in the Sun, with frequencies around 2 to 4 mHz, velocity amplitudes about one cm.s^{-1} (max 20 cm.s^{-1}), relative variations of brilliance 10^{-7} , mode lifetimes of a few hours up to a few months.

All the solar-type stars which have been observed for seismology do oscillate with frequencies in the interval 0.1 to 10 mHz. However, only global modes can be detected, as stellar surfaces cannot be resolved. A few tens of modes only can typically be identified in such stars, so that the inversion techniques and the precision on the results are quite different from the solar case.

In this framework, light elements are related to helio- and asteroseismology in various ways. Helium 4, the second most abundant element in stars, is the only one which

directly influences the oscillation scheme, as modifying its abundance changes the stellar structure. The helium abundance and abundance gradients may be derived from seismic studies. It can also be the cause for seismic destabilisation of the star through κ -mechanism.

On the other hand, the light elements lithium, beryllium, boron, and helium 3 are only indirectly related to asteroseismology, as they are destroyed by nuclear reactions in a way determined by macroscopic motions (convective zones, overshooting, internal mixing) which themselves have seismic signatures. As for deuterium, I do not think that any relation can be found between its abundance evolution and helio or asteroseismology.

2. The solar case

Helioseismology consists in analysing the sound waves that propagate throughout the Sun and using them to measure, by inversion procedures, the solar internal parameters like temperature, pressure, density, helium abundance, partial ionisation regions, zones of convection and macroscopic motions, internal rotation.

The oscillation modes are trapped in spherical-shell cavities extending between the surface and their “turning points”, which are consequences of the refraction of the waves due to the inwardly increasing sound velocity. The angular component of the wave function of these oscillations is described by the spherical harmonics, characterized by their two quantum numbers: the degree l and the azimuthal-order m . The number l corresponds to the number of null circles around the sphere, and m to the number of these null circles which cross the poles (meridional circles). In the radial direction, the number of null spheres is characterized by the third quantum number n . The depth of a given cavity depends on both the oscillation frequency and the spherical-harmonic degree l of the associated mode. Modes with large l are confined near the surface, while modes with small l extend much deeper, those with $l = 0$ and $l = 1$ reaching the center of the Sun itself. Consequently, all these modes sample different, although overlapping, regions of the solar interior.

Various observational techniques have been developed to detect and precisely observe the solar oscillation frequencies. To obtain the needed precision, the observations must go on uninterrupted during at least one month (a solar rotation), which may be reached by three different solutions: instruments at the Earth’s poles (Antarctica), space observations (e.g. SOHO: sohowww.nascom.nasa.gov) and networks of instruments dispatched in longitude all around the Earth (e.g. GONG: gong.nso.edu).

Inversion procedures have been developed to obtain very precisely the sound velocity throughout the Sun, and the individual internal parameters by comparison with models. Owing to the very large number of observed resonant modes, and to their propagations in different internal cavities, at different depths, it is possible to derive the solar internal parameters with an accuracy of 0.1 percent in most of the internal Sun (see Basu et al. 2009 and references therein). The first important success of helioseismology was that the seismic profile of the sound velocity inside the Sun clearly indicated the exact depth of the convective zone, at a fractional radius 0.713 ± 0.03 (Christensen-Dalsgaard et al. 1996). It also showed that overshooting was not present or extended on a very small depth if any.

In the early phases of seismic inversion and comparison with solar models, around 1995, discrepancies of order one percent were found. Then it was realized that helium diffusion, which decreases the helium abundance in the convective zone by about 20 percent compared to the internal one, had to be added to obtain better agreement. Other physical processes were improved, motivated by these new constraints: opacities

and equations of state (e.g. OPAL, Iglesias & Rogers 1996, Rogers & Nayfonov 2002) and nuclear reaction rates (Angulo et al. 1999). It was also found that a mild turbulence below the convective zone, which could smoothen the diffusion-induced helium gradient, was necessary to obtain a good fit between the seismic and model sound velocity in this special region. This mild turbulence was able to account for the lithium deficiency observed in the solar outer layers, as well as the constraints imposed by beryllium (Balachandran & Bell 1997) and helium 3 (Geiss & Gloecker 1998)(see Richard et al. 1996, Brun et al. 2002).

Precise analysis of the rotational splitting of the solar mode frequencies allowed to discover that, while the outer solar layers undergo a well-known differential rotation, the internal Sun, below the convective zone, rotates as a solid body. This offered an important challenge to hydrodynamicists and is not entirely solved. It may be related to internal gravity waves (Charbonnel & Talon 2005, Talon & Charbonnel 2008), or to the internal solar magnetic field (Turck-Chieze et al. 2005).

The picture of our Sun seemed to have well improved during about 20 years, with very good results, until a crisis came with the new determinations of the solar chemical composition by Asplund et al (2005). Using 3D simulations of the atmospheric solar motions, they determined heavy element abundances significantly smaller than obtained before (Grevesse & Sauval 1998). Although these abundances have recently been revised and slightly increased (Asplund et al. 2009), the discrepancy between the models computed with the new abundances and the seismic inversions is unacceptable. As the new determinations of abundances seem convincing, there is a real challenge about solar physics (see Serenelli et al. 2009).

Several ideas have emerged to try and solve this discrepancy. None of them worked. The most promising one may be the idea of accretion by the young Sun of metal-poor material coming from the planetary disc gas (Castro et al. 2007). However, this leads to a steep abundance gradient below the convective zone, incompatible with the present sound velocity. New studies are under work, to see how this steep gradient could be smoothed, without modifying too much the internal Sun. Another solution could be that a systematic error occurred in the determinations of the new abundances, but at the present time it does not seem to be the case.

3. The stellar case

Asteroseismology can give much more precise values of the stellar parameters, including age, mass, radius, stellar gravity, effective temperature, metallicity, helium abundance value, depth of convective regions, than any other means. Such precise determinations need deep seismic analyses of individual stars, and cannot be obtained with approximate theories only, although these approximate theories are very useful for first insights.

The stellar oscillations may be observed either by spectroscopic observations, using Doppler effect on lines, or by photometric method, which gives access to the global luminosity variations of the star. For technical reasons, the first method is used on the ground (e.g. HARPS and SOPHIE spectrographs) while the second one is used on satellites, like COROT or KEPLER. In any case, only global modes can be detected, with l values ranging from 0 to 3. Typically a few tens of modes at most can be identified in stars, far from the ten millions observed in the Sun.

The inversion techniques used for the solar case cannot be applied to stars. In particular, the outer layers are not scanned by the different waves as it is in the Sun, as all the observed modes travel deep inside. However, if the waves encounter regions of rapid variation of the sound velocity on their way, they are partially reflected, creating sec-

ondary periods. This phenomenon is very helpful in the determination of internal stellar characteristics, as will be seen below.

Tassoul (1980) derived an asymptotic analytical expression for the mode frequencies in stellar cavities, which is widely used as a first approximation:

$$\nu_{n,\ell} \simeq 2\pi\Delta\nu_0\left(n + \frac{\ell}{2} + \epsilon\right) \quad (3.1)$$

with

$$\Delta\nu_0 = \left[2 \int_0^R \frac{1}{r} dr \right]^{-1}, \quad (3.2)$$

which is the inverse of twice the time needed by the sound waves to travel from the stellar surface down to the center. This quantity is named the mean large separation.

One must be aware however that this theory is a crude approximation, valid only for small ℓ and large n values, and only in stars in which the sound velocity varies smoothly as in the Sun. In a real star, there may be strong deviations from this theory and these deviations do provide important information about specific regions of the star (Soriano et al. 2007, see below).

In the first order approximation, two p-modes of successive radial order n , with the same degree ℓ are approximately separated by $\Delta\nu_0$. If we define the large separation by:

$$\Delta\nu = \nu_{n+1,\ell} - \nu_{n,\ell} \quad (3.3)$$

we have $\Delta\nu_{n,\ell}$ equal to $\Delta\nu_0$. But deviations from the asymptotic theory induce deviations of $\Delta\nu$ from $\Delta\nu_0$.

It is also useful to define the small separations as:

$$\delta\nu = \nu_{n,\ell} - \nu_{n-1,\ell+2} \quad (3.4)$$

At first order we clearly have $\delta\nu_{n,\ell} \simeq 0$. But in a real star, there are deviations from this theory and the small separations are not equal to zero. These quantities are very sensitive to the deep stellar interior (Gough 1986, Roxburgh 2009, and references therein) and can give us precious informations about the stellar core. These quantities, and in particular for the degrees $\ell = 0$ - $\ell = 2$, can even become negative (Soriano et al. 2007, Soriano & Vauclair 2008). This specific behaviour is related to the presence of a convective core or to a helium core with sharp edges. We can use this phenomenon to characterize helium-rich cores and to give strong constraints on the possible overshooting.

Finally, in regions with an important gradient of the sound velocity, like the boundary of the convective zone or the HeII ionization zone, there is partial reflexions of the waves that create modulations on the frequencies. These modulations clearly appear in the so-called second differences (Gough 1990, Vauclair & Theado 2004) which are defined by:

$$\delta_2\nu = \nu_{n+1,\ell} + \nu_{n-1,\ell} - 2\nu_{n,\ell} \quad (3.5)$$

The modulation period of the oscillations is equal to twice the acoustic depth, which is the time needed for the sound waves to travel from the considered region to the stellar surface:

$$t_s = \int_{r_s}^R \frac{dr}{c(r)} \quad (3.6)$$

$c(R)$ is the sound velocity at the radius r , and r_s the radius of the considered region.

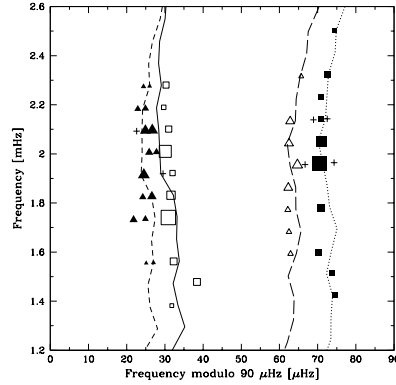


Figure 1. Example of echelle diagram: the star μ Arae. The symbols represent the observed modes, empty squares, $l = 0$, filled squares, $l = 1$, filled triangles, $l = 2$ and empty triangles, $l = 3$. The lines correspond to a stellar model. When two symbols are present, they correspond to two peaks due to rotational splitting.

A useful representation of the oscillation frequencies is the echelle diagram (Figure 1). In ordinates are plotted the frequencies and in abscissas, the same frequencies modulo the mean large separation. According to the asymptotic expressions, we should obtain straight lines corresponding to each value of the degree ℓ . In real stars, the specific features observed in the echelle diagram structure are indicative of their internal structure.

4. Helium determinations from asteroseismology

4.1. Helium in stellar outer layers and helium gradients

Rapid variations of the sound velocity in the outer stellar layers lead to partial reflections of the sound waves, which appear as frequency modulations in the “second differences”. The periods of these modulations are equal to $2t_s$ where t_s is the time needed for the acoustic waves to travel between the surface and the considered region (acoustic depth).

These rapid variations can be due to the boundary of the outer convective zone, to helium ionisation regions and to diffusion-induced helium gradients. In practice, when helium settling is taken into account, the importance of helium gradients is larger than those of the convective boundary and helium ionisation regions (Vauclair & Theado 2004, Castro & Vauclair 2006).

Similar computations can be done for evolutionary models in which helium diffusion is introduced or suppressed. The resulting second differences are quite different. When diffusion is suppressed, they show signatures of the helium ionization zones while the signatures of helium gradients have, of course, disappeared.

Houdek & Gough (2007) have shown in detail how to determine the helium abundance in stars from the observed helium-ionisation-induced features observed in the second differences. It gives interesting and precise results, but one must keep in mind that the obtained value corresponds to the helium abundance inside the convective zone, not the original one, as it has been decreased by gravitational settling.

4.2. Determinations of the internal helium abundance from model comparisons

Stars have to be observed during a sufficiently long time, typically eight nights or more with the HARPS spectrograph, several months for space observations, to allow precise

comparisons with models. The Fourier analysis may lead to mode identification, as discussed in Bouchy et al. (2005), and frequency determinations. Meanwhile evolutionary tracks are computed, with various input parameters (mass, chemical composition, presence or not of overshooting, etc...). The computed mode frequencies are compared with the observed ones in a rigorous way. In this framework, departures from the “asymptotic theory” give fundamental information on the stellar parameters and internal structure.

For a given set of abundances (metallicity and helium value), only one model may reproduce the observed frequencies in a satisfying way (Soriano et al. 2007, Vauclair et al. 2008). The various models obtained in this way for different chemical composition have similar ages, gravities, and radii. The other parameters are then constrained with the help of the spectroscopic observational boxes.

In this way, it becomes possible to determine the internal helium abundance of the stars. Up to now, it has been done for two main-sequence exoplanet-host stars, which are both overmetallic compared to the Sun. The results for the helium abundance are quite different.

The exoplanet-host star μ Arae (HD160691) is a G5V star which has been observed for seismology during 8 nights in August 2004 with HARPS. The observations allowed to identify 43 oscillation modes of degrees $l = 0$ to $l = 3$ (Bouchy et al. 2005). They have been analysed by Bazot et al. (2005), and by Soriano et al. (2007) after revision of its Hipparcos parallax. The metallicity of this star, compared to the solar one, is $[Fe/H] = 0.30 \pm 0.01$, and the helium abundance is correspondingly high, $Y = 0.301 \pm 0.01$.

Solar-type oscillations of the exoplanet-host star ι Hor (HD17051) were detected with HARPS in November 2006. Up to 25 oscillation modes could be identified and compared with stellar models. The analysis is discussed in detail in Laymand & Vauclair (2007) and Vauclair et al. (2008). Contrary to μ Arae, which has a high helium value, as expected from the normal evolution of the chemical abundance of galaxies, according to its high metallicity, ι Hor has a very small helium value, comparable to that of the Hyades: $Y = 0.255 \pm 0.015$, for a metallicity $[Fe/H] = 0.16 \pm 0.02$. As we also know that this star has the same kinematics as the cluster in the Galaxy, this is an indication that it was formed with the cluster and evaporated.

5. Helium abundance variations and kappa mechanism

Helium is an important element in the framework of oscillation stars, as it may in some cases lead to wave amplification through kappa mechanism. Here I only discuss the Am - δ -Scuti case.

Among the main sequence stars which lie inside the instability strip, many chemically peculiar stars are found. The so-called Am stars are found in the H.R. diagram at the same place as the δ -Scuti stars. Generally speaking, the former ones show abundance peculiarities, namely a general overabundance of metals (except calcium and scandium), but no oscillations, while the later ones are pulsating but chemically normal. As discussed by Turcotte et al. (2000), in A-type stars, almost 70% of non chemically peculiar stars are δ -Scuti variables at current levels of sensitivity while most non-variable stars are Am stars. Furthermore, Am stars are slower rotators than δ -Scuti stars. In this region of the H.R. diagram, the stars display two different convective zones in their outer layers : the upper one due to the HI and HeI ionisations and the lower one to the HeII ionisation. The δ -Scuti stars pulsate due to a κ -mechanism which takes place in the second convective zone. When microscopic diffusion occurs, this convective zone disappears due to helium depletion and the κ -mechanism cannot take place anymore (Vauclair et al. 1974).

Some oscillating Am stars have been discovered (Kurtz 1989), which challenge the

previously accepted theory. Richer et al. (2000) and Turcotte et al. (2000) computed models of Am stars in the framework of the Montreal models. They found that, due to the iron accumulation in the radiative zone below the H and He convective zone, a new convective region appears which increases the diffusion time scales compared to the previous models. In these new models, helium is still substantially present in the helium convective zone at the ages of the considered stars. They claim that it is possible to account for the existence of oscillating Am stars close to the cool boundary of the instability strip.

These computations ignored however an important process which occurs in case of μ -gradient inversion : thermohaline convection, or double-diffusive convection (Vauclair 2004, Charbonnel & Zahn 2007). Recently, Theado et al. (2009) have done precise computations of such diffusion-induced accumulation of elements, including thermohaline convection. The accumulation is much smaller than previously thought, but still present. This study will lead to many applications concerning element abundances in stars.

6. Conclusion

From the few examples already available, asteroseismology has proved to be a powerful tool for determining stellar parameters and constraints on their internal structure. However, tests have to be done for individual stars, observed during long periods. Usual approximate theories are not precise enough to obtain such results.

Only helium can be directly determined from asteroseismology. Lithium, beryllium, and boron, whose abundances are obtained from spectroscopy, are related to the macroscopic motions at work below the outer convective zones in solar-type stars. Asteroseismology can be used to constrain these macroscopic motions, in some cases. At least the depth of the convective zones can be derived somewhat precisely. Other kinds of mixing, like rotation-induced mixing, can influence the mode frequencies (e.g. Eggenberger 2009), but up to now the observed precision in the modes identifications and frequencies is not enough to measure it. Maybe in the future?

References

- Angulo C., Arnould M., Rayet M., (NACRE collaboration) 1999, *Nuclear Physics A*, 656, 1
 Asplund, M., Grevesse, N. & Sauval, J. 2005, Cosmic Abundances as Records of Stellar Evolution and Nucleosynthesis, 336, 25
 Asplund, M., Grevesse, N., Sauval, J. & Scott, P. 2009, *ARA&A*, 47, 481
 Balachandran, S. & Bell, R.A. 1997, *AAS meeting* 29, 1325
 Basu, S., Chaplin, W.J., Elsworth, Y., New, R. & Serenelli, A.M. 2009, *ApJ*, 699, 1403
 Bazot, M., Vauclair, S., Bouchy, F. & Santos, N. C. 2005, *A&A*, 440, 615
 Brun, A. S., Antia, H. M., Chitre, S. M. & Zahn, J.-P. 2002, *A&A*, 391, 725
 Bouchy, F., Bazot, M., Santos, N. C., Vauclair, S., & Sosnowska, D. 2005, *A&A*, 440, 609
 Castro, M. & Vauclair, S. 2006, *A&A*, 456, 611
 Castro, M., Vauclair, S. & Richard, O. 2007, *A&A*, 463, 755
 Charbonnel, C. & Talon, S. 2005, *Science*, 309, 2189
 Charbonnel, C. & Zahn, J.P. 2007, *A&A* (Letters), 467, 15
 Christensen-Dalsgaard J. et al. 1996, *Science*, 272, 1286
 Eggenberger, P. 2009, this conference
 Geiss, J. & Gloecker, G. 1998, *Space Science Reviews*, 84, 239
 Gough, D. O. 1986, in Hydrodynamic and magnetohydrodynamic problems in the Sun and stars, ed. Y. Osaki (Uni. of Tokyo Press), p. 117
 Gough, D. O. 1990, In Progress of Seismology of the Sun and Stars, Proc. Oji International

- Seminar (Hakone) (Japan : Springer Verlag), *Lect. Notes Phys.*, 367, 283, eds Y. Osaki, H. Shibahashi
- Grevesse, N. & Sauval, A.J. 1998, *Space Science Reviews*, 85, 161
- Houdek, G. & Gough, D.O. 2007, *MNRAS*, 375, 861
- Iglesias, C. A. & Rogers, F. J. 1996, *ApJ*, 464, 943
- Kurtz, D.W. 1989, *MNRAS*, 238, 1077
- Laymand, M. & Vauclair, S. 2007, *A&A*, 463, 657
- Leibacher, J. W. & Stein, R. F. 1971, *APL*, 7, 191L
- Leighton, R. B., Noyes, R. W. & Simon, G. W. 1962, *ApJ*, 135, 474
- Richard, O., Vauclair, S., Charbonnel, C. & Dziembowski, W.A. 1996, *A&A*, 312, 1000
- Richer, J., Michaud, G. & Turcotte, S. 2000, *ApJ*, 529, 338
- Rogers, F. J. & Nayfonov, A. 2002, *ApJ*, 576, 1064
- Roxburgh, I. W 2009, *A&A*, 493, 185
- Serenelli, A.M., Basu, S., Ferguson, J.W. & Asplund, M. 2009, *ApJ*, 705, L123
- Soriano, M., Vauclair, S., Vauclair, G. & Laymand, M. 2007, *A&A*, 471, 885
- Soriano, M. & Vauclair, S. 2008, *A&A* 488, 975
- Talon, S. & Charbonnel, C. 2008, *A&A*, 482, 597
- Tassoul, M. 1980, *ApJS*, 43, 469
- Theado, S., Vauclair, S., Alecian, G. & Le Blanc, F. 2009, *ApJ*, 704, 1262
- Turck-Chieze, S., Appourchaux, T., Ballot, J., et al., 2005, *ESASP*, 588, 193
- Turcotte, S., Richer, J., Michaud, G. & Christensen-Dalsgaard, J. 2000, *A&A*, 360, 603
- Ulrich, R. K. 1970, *ApJ*, 162, 993
- Vauclair, G., Vauclair, S. & Pamjatnikh, A. 1974, *A&A*, 31, 63
- Vauclair, S. 2004, *ApJ*, 605, 874
- Vauclair, S. & Théado, S. 2004, *A&A*, 425, 179
- Vauclair, S., Laymand, M., Bouchy, F., Vauclair, G., Hui Bon Hoa, A., Charpinet & S., Bazot, M. 2008, *A&A* (Letters), 482, 5

Lithium factories in the Galaxy: novae and AGB stars

Francesca D’Antona¹ and Paolo Ventura¹

¹INAF – Osservatorio di Roma,

via di Frascati 33, I-00040 Monteporzio, Italy

email: dantona@oa-roma.inaf.it ventura@oa-roma.inaf.it

Abstract. We review the state of the art in modelling lithium production, through the Cameron–Fowler mechanism, in two stellar sites: during nova explosions and in the envelopes of massive asymptotic giant branch (AGB) stars. We also show preliminary results concerning the computation of lithium yields from super–AGBs, and suggest that super–AGBs of metallicity close to solar may be the most important galactic lithium producers. Finally, we discuss how lithium abundances may help to understand the modalities of formation of the “second generation” stars in globular clusters.

Keywords. Stars: AGB and post-AGB, novae; convection, nuclear reactions, nucleosynthesis; Globular Clusters: general

1. Introduction

Although lithium is very fragile, its galactic abundance increases from $\log \epsilon(\text{Li})^\dagger \sim 2.2$ at the surface of Population (Pop) II stars to $\log \epsilon(\text{Li}) \sim 3.3$ or more in Pop I. Even if lithium is hidden in the atmospheres of Pop II, and its true primordial abundance is ~ 2.7 , a galactic production by $\sim 0.7\text{dex}$ is necessary.

The mechanism responsible for lithium production has been proposed by Cameron & Fowler (1971): ${}^7\text{Be}$ is produced by fusion of ${}^3\text{He}$ with ${}^4\text{He}$, and rapidly transported to stellar regions where it can be converted into ${}^7\text{Li}$ by k -capture. Notice, then, that the lithium production may last only until there is ${}^3\text{He}$ available in the region of burning, and that the production ends when the ${}^3\text{He}$ is all consumed.

There are two main physical situations where this mechanism can produce enough lithium that it is important to investigate their role in the galactic production: the first one is the explosive hydrodynamical formation during the outbursts of novae (Arnould & Norgaard 1975, Starrfield et al. 1978), the second one is the hydrostatic, slow formation in the envelopes of asymptotic giant branch (AGB) stars, for which it was first proposed. In envelope models of AGB stars (Scalo et al. 1975), in which the bottom of the convective envelope reaches the hydrogen burning layers, and its temperature (T_{bce}) becomes as large as $T_{\text{bce}} \sim 40\text{MK}$, the ${}^3\text{He}(\alpha, \gamma){}^7\text{Be}$ chain acts. These models were able to explain the high lithium abundances found in some luminous red giants, and the process took the name of Hot Bottom Burning (HBB).

In Section 2 we will resume the state of the art of the modelling of lithium production during nova outbursts, and in Section 3 we will deal with the AGB models, to understand whether they can account for the lithium galactic evolution. In addition, we will show new models of lithium production in super–AGB stars (Ventura & D’Antona 2010) and speculate on the possible role of these stars as efficient lithium factories. Finally, in Section 4 we will shortly summarize the problem of lithium in the “second generation”

[†] we use the notation $\log \epsilon(\text{Li}) = \log(N_{\text{Li}}/N_{\text{H}}) + 12$.

stars of globular clusters. We will not consider here the different, slow mixing process also based on the Cameron & Fowler (1971) mechanism and named “cool bottom burning” (e.g. Nollett et al. 2003). This process can explain the lithium abundances seen in lower luminosity red giants (e.g. Wasserburg et al. 1995, Sackmann & Boothroyd 1999), but its physical reasons are not well studied, while the nucleosynthesis in HBB is based on straightforward time-dependent mixing in standard convective regions.

2. Nova outbursts

Schatzman (1951) was the first to propose that the isotope ^3He could play a role in nova explosion, in the context of a theory of novae powered by thermonuclear detonations. Arnould & Noergaard (1975) proposed that the Cameron–Fowler mechanism, acting at the nova outburst, would produce a lithium abundance proportional to the ^3He abundance in the nova envelope. Starrfield et al. (1978) showed that the mechanism could be efficient for outburst temperatures $>150\text{MK}$, and the fast ejection of the ^7Be rich nova shell leads to ^7Li production; they quantified the expected linear relation, between lithium and the ^3He initial mass fraction X_{3i} , as:

$$[Li/H] \simeq 200 \times X_{3i}/X_{3\odot} \quad (2.1)$$

where $X_{3\odot}$ is the solar ^3He mass fraction. D’Antona & Matteucci (1991) modelled the galactic evolution of lithium, including the contribution of novae according to this result. The argument below their modelization was very simple: the nova explosion occurs when a critical hydrogen rich envelope is reached on the white dwarf component of the nova binary, by accretion from its low mass companion. By losing mass, low mass stars expose the stellar regions in which the hydrogen burning p–p chain is incomplete, and thus bring to the surface the ^3He accumulated in the envelope during the period preceding the mass transfer phase, and during the (slow) mass transfer phase itself (e.g. D’Antona & Mazzitelli 1982). Thus D’Antona & Matteucci (1991) linked the lithium abundance produced in the outburst to the “delay time” between the formation of the white dwarf and the occurrence of nova outbursts. As a result, mainly the novae containing an “old” white dwarf, and therefore an old and ^3He -rich low mass companion contribute to the galactic production of lithium, in agreement with the Li vs. $[\text{Fe}/\text{H}]$ galactic relation.

Motivated by the D’Antona & Matteucci (1991) paper, Boffin et al. (1993) revisited the influence of ^3He on the nova outbursts with simple one-zone models, but found out that equation 2.1 was a large overestimate, due to two main reasons: 1) the neglect of the reaction $^8\text{B}(p, \gamma)^9\text{C}$ in the Starrfield et al. (1978) network, and 2) the increasing influence of the competitive reaction $^3\text{He}(^3\text{He}, 2p)^4\text{He}$ when ^3He is enhanced in the nova envelope. Consequently, they found a milder dependence on the lithium production on the ^3He :

$$\frac{X(^7\text{Li})}{X_0(^7\text{Li})} \simeq 1 + 1.5 \log \frac{X(^3\text{He})}{X_{\odot}(^3\text{He})} \quad (2.2)$$

where X represents mass fractions, and $X_0(^7\text{Li})$ is the lithium production when the solar ^3He abundance is adopted. Afterwards, Hernanz et al. (1996) and Jose & Hernanz (1998) re-examined the problem with an implicit hydro-code including a full reaction network, able to treat both the hydrostatic accretion phase and the explosion stage. They considered both the case of white dwarfs having a carbon–oxygen core and the case of oxygen–neon cores, showing that C–O cores are more efficient in the lithium production, as they have a shorter accretion phase, so that ^3He is not destroyed efficiently, and more ^7Be is produced. Overproduction of lithium is found, but its dependence on the initial ^3He abundance still follows Boffin et al. (1993) prescription. Including this revised lithium

production in the galactic chemical evolution model, novae appear to be a modest lithium producer (Romano et al. 1999).

3. Luminous AGB stars

Above a luminosity of $\sim 2 \times 10^4 L_\odot$, the bottom of the convective envelope during the AGB evolution reaches the H-shell burning region, and the nuclear reaction products are transported to the surface by convection. This is the perfect site of lithium production through the Cameron–Fowler mechanism (Iben 1973, Sackmann et al. 1974). While we have seen that $T_{\text{bce}} \sim 40\text{MK}$ is sufficient to produce lithium by HBB, if T_{bce} becomes larger, other important reactions take place.

About 65MK are necessary to convert carbon to nitrogen. The very luminous ($M_{\text{bol}} < -6$, that is $L > 2 \times 10^4 L_\odot$) lithium-rich giants of the Magellanic Clouds (Smith & Lambert 1989, 1990, Smith et al. 1995) are indeed M-stars, and not carbon stars. Their carbon star features may have been lost by CN processing in HBB. Carbon stars in the Clouds, in fact, populate only the region at $M_{\text{bol}} > -6$. Lithium rich – oxygen rich AGB stars embedded in thick circumstellar envelopes have also been discovered in a Galactic sample, in a survey by García-Hernández et al. (2007), aimed at obtaining spectroscopy of very massive AGB candidates.

A third possible processing occurs at even larger $T_{\text{bce}} (> 80\text{MK})$, where H burns through the full CNO cycle. These very high temperatures are reached in low metallicity massive AGBs, and are possibly at the basis of the self-enrichment process in globular clusters (Ventura et al. 2001). The oxygen abundance in the envelopes of these AGB stars, and consequently in the matter ejected by wind or planetary nebula, is reduced, as we see in the “anomalous” stars of galactic globular clusters, see Sect.4.

Modelling of lithium rich AGB stars first of all requires to treat non-instantaneous mixing in the envelope, coupling the nuclear reaction network with the mixing process. This can be easily done by treating mixing as a diffusion. In Figure 1 we show the total phase of lithium production in a $5 M_\odot$ star of metallicity $Z=10^{-3}$ (left side), and a zoom of the same figure between two thermal pulses (right side). We see that, when T_{bce}

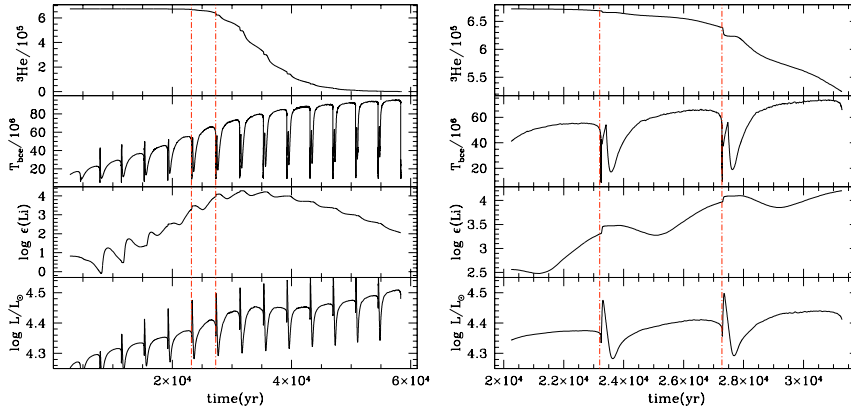


Figure 1. From bottom to top panel we plot the luminosity, surface lithium, HBB temperature and ^3He surface content along the AGB evolution of a star of $5 M_\odot$, metallicity $Z=10^{-3}$. The total duration of the phase of the most important lithium production lasts $\sim 20 \times 10^3 \text{yr}$. The two vertical lines delimit the time interval displayed in the right panel.

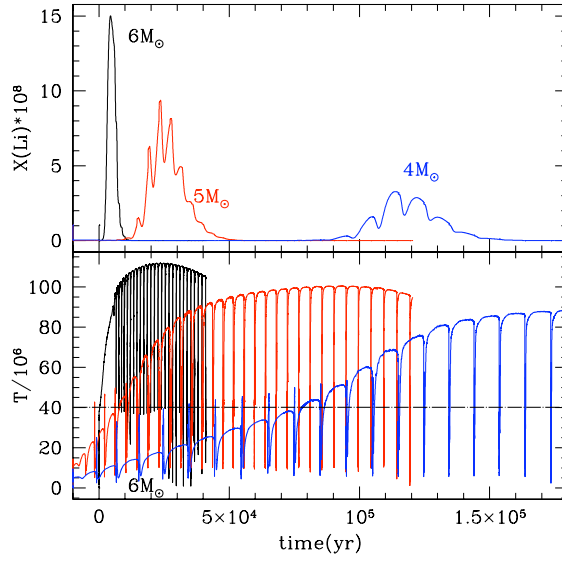


Figure 2. Temperature at the bottom of the convective layer (bottom) and lithium surface abundance (top) as a function of the time for the masses 6, 5 and $4 M_{\odot}$, $Z=10^{-3}$, from left to right. Time is computed from the beginning of the AGB phase, when the H-shell burning is reignited. The horizontal line at $T=40\text{MK}$ limits the temperature region for lithium production.

decreases, due to the ignition of the thermal pulse and the expansion of the envelope, the lithium abundance decreases. We can appreciate the delay time between the physical conditions in the burning region and the surface lithium, due to the non instantaneous mixing. The total phase of lithium production lasts more than $50 \times 10^3 \text{yr}$, but the phase in which $\log \epsilon(\text{Li}) \gtrsim 3$ lasts only $\sim 20 \times 10^3 \text{yr}$. Once the initial ^3He present in the envelope is depleted, lithium production is over.

Lithium production and destruction depend on

- (a) the physical inputs, and mainly on the convection model: the higher is the convection efficiency, the larger is T_{bce} and the larger is the efficiency of HBB (see, e.g. Ventura & D'Antona 2005);
- (b) the initial mass (or, better, the initial core mass): it must be large enough to get HBB;
- (c) the chemical inputs, mainly the metallicity and the envelope opacity. Fixed the mass, the higher is the opacity (or the metallicity) the smaller is T_{bce} and the lower is the efficiency of HBB.

Figure 2 shows the mass dependence for a fixed chemical composition: the larger is the mass, the larger is T_{bce} and the stronger and faster is lithium production.

Figure 3 shows the dependence on the metallicity, at fixed mass $M=6 M_{\odot}$. Increasing the opacity (and Z), T_{bce} decreases, and the lithium production is lower but more extended in time.

The computation of lithium production during the super-AGB evolution has been recently achieved by Ventura & D'Antona (2010) for $Z=10^{-3}$. The results are very interesting, as we see in Fig. 4 for a mass of $7.5 M_{\odot}$. Lithium achieves very large abundances,

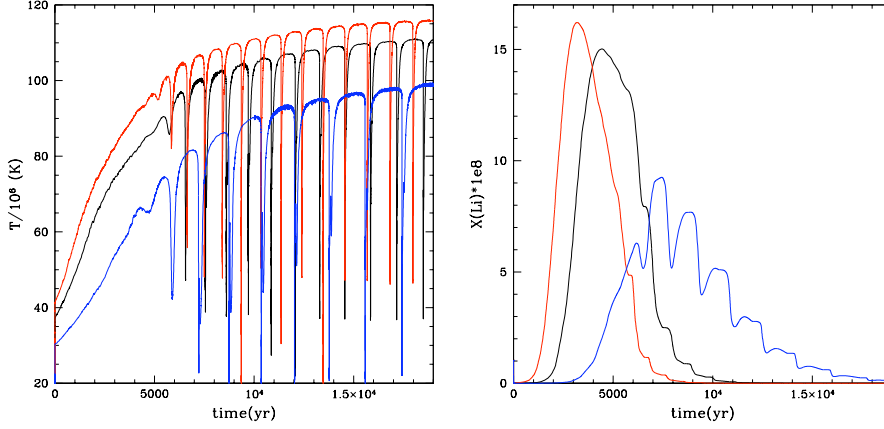


Figure 3. The evolution of $6 M_{\odot}$ for metallicities $Z=0.0006$, $Z=0.001$ and $Z=0.004$ from top to bottom is displayed. On the left side, we plot T_{bce} , on the right side the lithium mass fraction $X(\text{Li})$.

due to the very high T_{bce} , and the Li-rich phase occurs even before the star begins the thermal pulse phase.

Of course ‘production’ does not mean ‘yield’: two ingredients are important: how much lithium is made, and how long it lasts, so that mass loss can recycle it into the interstellar medium. Consequently, the lithium yield is very dependent on the mass loss rate: larger rates during the phase of lithium production provide a higher lithium yield. Unfortunately, mass loss is another great uncertainty in the computation of stellar models. In Figure 6 we show as open (red) circles at $[\text{Fe}/\text{H}]=-1.3$ the average lithium abundance in the ejecta of models of 4, 5 and $6 M_{\odot}$ with three different mass loss formulations: the middle points refer to the mass loss rate suggested by Blöcker (1995), who extends Reimers’ recipe to describe the steep increase of mass loss with luminosity as the stars

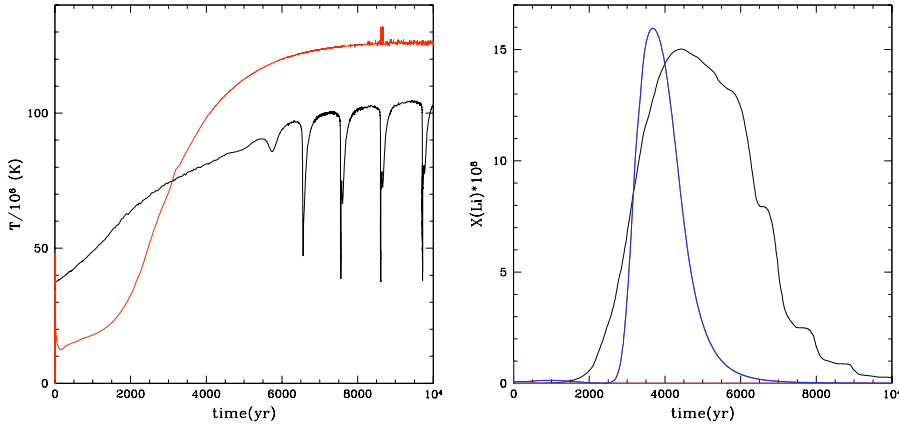


Figure 4. The same as Fig. 3 for $Z=0.001$ and masses $6 M_{\odot}$ (lower curve) and a super-AGB model of $7.5 M_{\odot}$.

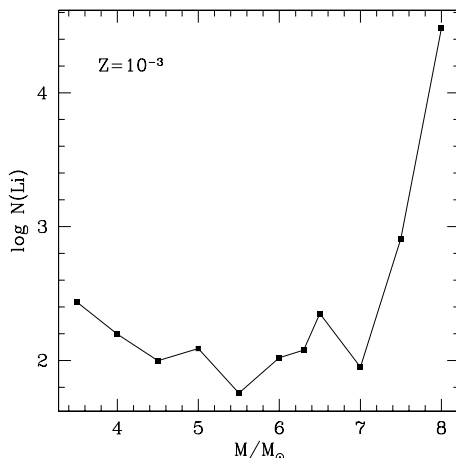


Figure 5. Lithium abundance averaged on the ejected envelope mass as a function of the total mass for $Z=0.001$

“climb” the AGB. The full expression, for Mira’s periods exceeding 100d, is

$$\dot{M} = 4.83 \times 10^{-22} \eta_R M^{-3.1} L^{3.7} R \quad (3.1)$$

where η_R is the free parameter entering the Reimers’ (1977) prescription. In the “standard” models of Fig. 6 we adopt $\eta_R = 0.02$, according to a calibration based on the luminosity function of lithium rich stars in the Magellanic Clouds given in Ventura et al. (2000). The highest points in the figure are obtained for the extreme value of $\eta_R = 0.1$, while the models adopting the Vassiliadis & Wood (1993) mass loss rate are the lowest ones. We see then that the absolute values of the lithium yields must be considered highly uncertain (see also Ventura et al. 2002). The global behaviour of the average lithium abundance in the ejecta, as a function of the initial mass is given in Fig. 5 for the models computed with the standard mass loss ($\eta_R=0.02$) prescription and $Z=10^{-3}$. Increasing the mass, the average abundance first decreases, due to the faster consumption of ${}^3\text{He}$, in spite of the larger abundances reached in the phase of production. For the super-AGB masses, the average abundance increases, and may also become very large, both due to the stronger production and to the huge mass loss rate achieved by the largest core masses.

Based on these first computation of the super-AGB phase, we can make a prediction on the lithium galactic evolution: which are the best producers? The larger is the mass, the higher is lithium during the production phase. On the other hand, the shorter is the duration of the Li rich phase, the smaller is the lithium yield. Increasing the metallicity, T_{bce} becomes smaller, and the duration of the lithium production phase is longer. For large core mass (and thus high luminosity) the mass loss rates become larger and larger. So we should expect that the Li yield is positively correlated both with metallicity and core mass, and that the super-AGB stars of metallicity close to solar are possibly great producers. The possible consequences for galactic Li production are described in the talk by Francesca Matteucci in this book.

4. Lithium and AGB stars in globular clusters

Globular Clusters (GCs) so far examined show spectroscopic evidence for the presence of two stellar generations: a First Generation (FG) having “normal” abundances, similar to those of halo stars of the same metallicity, and a Second Generation (SG) whose abundances are more spreaded, and bear the sign of hot CNO processing, with an often very significative oxygen reduction, evidence for the action of the Ne–Na cycle and sometimes of the Mg–Al cycle (see, e.g. Gratton et al. 2004). The SG contains at least 50% of the cluster stars (Carretta et al. 2009a,b). At low metallicity, in the most massive AGB stars, T_{bce} becomes larger than $\sim 80\text{MK}$, and the ON chain of the CNO cycle becomes active. In these envelopes, oxygen is cycled to nitrogen, and its abundance can be dramatically reduced. Thus some models for the formation of the different populations attribute the presence of “anomalous” stars with low oxygen and high sodium, to a SG including matter processed by HBB (e.g. Ventura et al. 2001). Other models attribute the formation of the SG to the ejecta of fast rotating massive stars (FRMS, see e.g. Decressin et al. 2007a), or even to pollution from gas expelled during highly non conservative evolution of massive binaries (De Mink et al. 2009), although this latter model in particular can not explain the very high fraction of SG stars present in most of the GCs so far examined.

The lithium yield from AGB stars of different mass may contribute to understand the role (if any) of these stars in the formation of the SG in GCs. It is commonly believed that the polluting matter must be diluted with pristine matter to explain the abundance patterns, such as the Na–O anticorrelation (Prantzos & Carbonnel 2006, D’Antona & Ventura 2007). If the progenitors of the SG stars are massive stars, they have destroyed their original lithium, and the lithium in the SG must be due to the mixing with pristine gas. If instead the progenitors are massive AGB stars, they may have a non negligible lithium yield, that must be taken into account in the explanation of the SG abundances.

Figure 6 shows a compact summary of what we know about lithium abundances in the halo and in GCs in the plane $\log \epsilon(\text{Li})$ versus $[\text{Fe}/\text{H}]$. The halo stars are plotted as triangles, from Meléndez et al. (2009) (their non LTE abundances are plotted). The data for three clusters are added, at their $[\text{Fe}/\text{H}]$ content, taken from Carretta et al. (2009c) scale. The references for the clusters data are in the figure label. Notice that the three open triangles of NGC 6397, at much lower $\epsilon(\text{Li})$ than the other points, refer to subgiants, in which lithium can be reduced by mixing. Although the data analysis is not homogeneous among the different samples, the figure shows interesting trends. The lithium spread of the halo stars in the range of metallicities of the clusters NGC 6397 and NGC 6752 is very small around a plateau value $\log \epsilon(\text{Li}) \sim 2.2$. In fact the full triangles at $\log \epsilon(\text{Li}) < 2$ are lower mass stars for which depletion is expected (Meléndez et al. 2009). The WMAP – big bang nucleosynthesis “standard” abundance, $\log \epsilon(\text{Li}) = 2.72$ (e.g. Cyburt et al. 2009) is much larger than the plateau abundance. The lithium spread in the clusters appears a bit larger, although Lind et al. (2009) point out that in NGC 6397 it is consistent with the observational error. We should expect a larger lithium spread among GC stars if there are SG stars, even if the pollutors’ gas (AGB or massive stars envelopes) has been diluted with pristine gas (Decressin et al. 2007b, Prantzos et al. 2007). The dilution is very plausible if there is a direct correlation between lithium and sodium abundances, as convincingly shown in NGC 6752 (Pasquini et al. 2005). A similar correlation also appears in NGC 6397, but it is based only on the high sodium abundance of the three subgiants plotted as open triangles (Lind et al. 2009). A possible anticorrelation among the stars of 47 Tuc (Bonifacio et al. 2007) is not convincing, as these stars may be subject to lithium depletion mechanisms due to their larger iron content (D’Orazi, these proceedings). In addition, according to Pasquini et al. (2008),

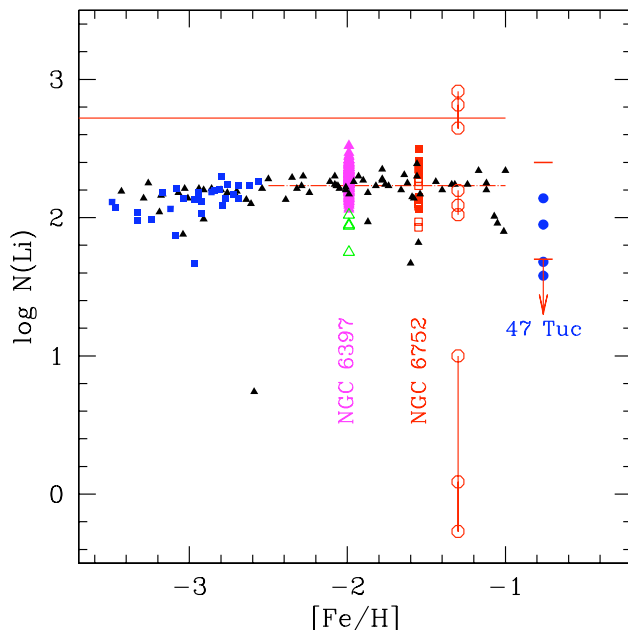


Figure 6. Lithium abundances as a function of $[\text{Fe}/\text{H}]$ in halo stars and in scarcely evolved stars in three GCs. Halo data are from Meléndez et al. (2009), represented as black triangles (non LTE models). (Blue) full squares are from Sbordone et al. (2009), analyzed by 3D non LTE models. The top horizontal line represent a WMAP – standard Big Bang nucleosynthesis value $\log \epsilon(\text{Li})=2.72$, the dot-dashed line represents an eye fit of the Meléndez et al. (2009) data in the range of the GC metallicities. Data for NGC 6397 are from Lind et al. (2009). The three open triangles are relative to the data for three subgiants, and may not represent the turnoff abundances in this cluster. Data for NGC 6752 are from Pasquini et al. (2005), plotted as open or full squares according to the two different temperature scales used in their work. The full circles are the data for 47 Tuc by Bonifacio et al. (2007). The limits of the lithium range in the 50 stars recently examined by D’Orazi (these proceedings) are also given. Open circles at $[\text{Fe}/\text{H}]=-1.3$ represent the average abundances in the ejecta of models of 4, 5 and $6 M_{\odot}$ for three different mass loss rate formulations (see text).

two stars in NGC 6397 differ by ~ 0.6 dex in oxygen, but have “normal” $\log \epsilon(\text{Li}) \sim 2.2$: this is certainly not easily compatible with a simple dilution model, and may require that the polluters are also important lithium producers. In fact, if the AGB polluters produce enough lithium, a dilution model must take it into account.

Notice that the dilution model is not so straightforward as we may think a priori: it will include a fraction α of matter with pristine Li, plus a fraction $(1-\alpha)$ having the Li of the ejecta (so, either the abundance of the AGB ejecta in the AGB mass range involved in the SG formation, or zero Li for the FRMS model). The dilution required to explain a given range in observed Li is different if we assign to the pristine Li the value $\log \epsilon(\text{Li})=2.72$ (see above), or the atmospheric Pop II value (~ 2.2), or some intermediate value. In addition, if we are assuming that the uniform surface abundance of Li in Pop II is due to a depletion mechanism, also the abundance resulting from the dilution model must be decreased to take into account a similar depletion factor.

If we take our “standard mass loss” results of Fig. 6 at face value, ignoring the big

question mark on mass loss, the yields can be used to predict the lithium expected in the SG, if the SG is a result of star formation from AGB ejecta diluted with pristine gas. The abundances will depend mainly on the mass range of the AGB progenitors: if the ejecta of masses in the range $4.5 - 6 M_{\odot}$ are involved, their abundance is $\log \epsilon(\text{Li}) \sim 2, 0.7$ dex smaller than the Big Bang abundance. In order to explain the abundances observed in NGC 6397 or in NGC 6752, a dilution model including the ejecta of these AGB stars will require a percentage of pristine matter only *slightly smaller* than in a model including the lithium free FRMS, and we will not be able to discriminate between the two models. The case is different if the Big Bang abundance is “non standard” and closer to the observed halo stars average value.

A different interesting problem is posed by the GCs in which a “blue” main sequence (MS) has been revealed from precise HST photometry, namely ω Cen (Bedin et al. 2004) and NGC 2808 (D’Antona et al. 2005, Piotto et al. 2007). The blue MS can only be interpreted as a very high helium MS (mass fraction $Y \sim 0.38$) (Norris 2004, Piotto et al. 2005). Actually, in NGC 2808 three MS well separated each other in color are present (Piotto et al. 2007), corresponding to three main helium content values, and in agreement with the predictions made from the distribution of stars in the very extended and multimodal horizontal branch (see, e.g. D’Antona & Caloi 2004, D’Antona et al. 2005). Pumo et al. (2008) noticed that the helium abundances of super-AGB stars envelopes are within the small range $0.36 < Y < 0.38$ (Siess 2007) and D’Ercole et al. (2008) have shown that a full chemo-hydrodynamical model of the cluster can provide a reasonable interpretation of the three MSs of NGC 2808, *provided that the blue MS is formed directly by matter ejected from the super-AGB range, undiluted with pristine gas*. In the future, spectroscopic observations of the blue MS in ω Cen and NGC 2808 will provide a falsification of this hypothesis, e.g. by means of the oxygen and sodium abundance revealed. In particular lithium can be an important test too, as it could provide an independent calibration of the mass loss rate in the super-AGB phase. Already some observations of the turnoff stars in ω Cen are available (Bonifacio, in this book), but it is not clear whether stars belonging to the blue MS have been observed. The “standard mass-loss” super-AGB models shown in Fig. 5 predict that lithium in these stars may become very large if some blue MS stars are formed from the ejecta of the upper mass range of super-AGB stars. We need observations of the blue MS to falsify this prediction.

We thank Corinne Charbonnel and the organizing committees for the invitation and for the successful and intense meeting. We are grateful to J. Meléndez and L. Sbordone for allowing us to use their data in advance of publication, and to V. D’Orazi and D. Romano for useful information.

References

- Arnould, M., & Norgaard, H. 1975, *A&A*, 42, 55
 Bedin, L. R., Piotto, G., Anderson, J., Cassisi, S., King, I. R., Momany, Y., Carraro, G. 2004, *ApJ*, 605, L125
 Blöcker, T. 1995, *A&A*, 297, 727
 Boffin, H. M. J., Paulus, G., Arnould, M., & Mowlavi, N. 1993, *A&A*, 279, 173
 Bonifacio, P., et al. 2007, *A&A*, 470, 153
 Cameron, A. G. W., & Fowler, W. A. 1971, *ApJ*, 164, 111
 Carretta, E., et al. 2009a, *A&A*, 505, 117
 Carretta, E., Bragaglia, A., Gratton, R., & Lucatello, S. 2009b, *A&A*, 505, 139
 Carretta, E., Bragaglia, A., Gratton, R., D’Orazi, V., & Lucatello, S. 2009c, arXiv:0910.0675

- Cybert, R. H., Ellis, J., Fields, B. D., Luo, F., Olive, K. A., & Spanos, V. C. 2009, *Journal of Cosmology and Astro-Particle Physics*, 10, 21
- D'Antona F., Caloi V., 2004, *ApJ*, 611, 871
- D'Antona, F., Bellazzini, M., Caloi, V., Pecci, F. F., Galleti, S., & Rood, R. T. 2005b, *ApJ*, 631, 868
- D'Antona, F., & Mazzitelli, I. 1982, *ApJ*, 260, 722
- D'Antona, F., & Matteucci, F. 1991, *A&A*, 248, 62
- D'Antona, F., & Ventura, P. 2007, *MNRAS*, 379, 1431
- Decressin, T., Meynet, G., Charbonnel, C., Prantzos, N., & Ekström, S. 2007a, *A&A*, 464, 1029
- Decressin, T., Charbonnel, C., & Meynet, G. 2007b, *A&A*, 475, 859
- D'Ercole, A., Vesperini, E., D'Antona, F., McMillan, S. L. W., & Recchi, S. 2008, *MNRAS*, 391, 825
- de Mink, S. E., Pols, O. R., Langer, N., & Izzard, R. G. 2009, *A&A*, 507, L1
- García-Hernández, D. A., García-Lario, P., Plez, B., Manchado, A., D'Antona, F., Lub, J., & Habing, H. 2007, *A&A*, 462, 711
- Gratton, R., Sneden, C., & Carretta, E. 2004, *ARA&A*, 42, 385
- Hernanz, M., Jose, J., Coc, A., & Isern, J. 1996, *ApJ Letters*, 465, L27
- Iben, I. J. 1973, *ApJ*, 185, 209
- Jose, J., & Hernanz, M. 1998, *ApJ*, 494, 680
- Lind, K., Primas, F., Charbonnel, C., Grundahl, F., & Asplund, M. 2009, *A&A*, 503, 545
- Meléndez, J., Casagrande, L., Ramirez, I., & Asplund, M., submitted
- Nollett, K. M., Busso, M., & Wasserburg, G. J. 2003, *ApJ*, 582, 1036
- Norris, J. E. 2004, *ApJ Letters*, 612, L25
- Pasquini, L., Bonifacio, P., Molaro, P., Francois, P., Spite, F., Gratton, R. G., Carretta, E., & Wolff, B. 2005, *A & A*, 441, 549
- Pasquini, L., Ecuivillon, A., Bonifacio, P., & Wolff, B. 2008, *A&A*, 489, 315
- Piotto, G., et al. 2005, *ApJ*, 621, 777
- Piotto, G., et al. 2007, *ApJ Letters*, 661, L53
- Prantzos, N., & Charbonnel, C. 2006, *A&A*, 458, 135
- Prantzos, N., Charbonnel, C., & Iliadis, C. 2007, *A&A*, 470, 179
- Pumo, M. L., D'Antona, F., & Ventura, P. 2008, *ApJ Letters*, 672, L25
- Reimers, D. 1977, *A&A*, 61, 217
- Romano, D., Matteucci, F., Molaro, P., & Bonifacio, P. 1999, *A&A*, 352, 117
- & D'Antona, F. 2001, *A&A*, 374, 646
- Sackmann, I.-J., & Boothroyd, A. I. 1999, *ApJ*, 510, 217
- Sackmann, I.-J., Smith, R. L., & Despain, K. H. 1974, *ApJ*, 187, 555
- Siess, L. 2007, *A&A*, 476, 893
- Sbordone et al. 2009 *A&A* submitted
- Scalo, J. M., Despain, K. H., & Ulrich, R. K. 1975, *ApJ*, 196, 805
- Schatzman, E. 1951, *Annales d'Astrophysique*, 14, 294
- Smith, V. V., & Lambert, D. L. 1989, *ApJ Letters*, 345, L75
- Smith, V. V., & Lambert, D. L. 1990, *ApJ Letters*, 361, L69
- Smith, V. V., Plez, B., Lambert, D. L., & Lubowich, D. A. 1995, *ApJ*, 441, 735
- Starrfield, S., Truran, J. W., Sparks, W. M., & Arnould, M. 1978, *ApJ*, 222, 600
- Vassiliadis, E., & Wood, P. R. 1993, *ApJ*, 413, 641
- Ventura, P., D'Antona, F., & Mazzitelli, I. 2000, *A&A*, 363, 605
- Ventura, P., D'Antona, F., Mazzitelli, I., & Gratton, R. 2001, *ApJ Letters*, 550, L65
- Ventura, P., D'Antona, F., & Mazzitelli, I. 2002, *A&A*, 393, 215
- Ventura, P., & D'Antona, F. 2005, *A&A*, 431, 279
- Ventura, P., & D'Antona, F. 2010, *MNRAS Letters*, in press
- Wasserburg, G. J., Boothroyd, A. I., & Sackmann, I.-J. 1995, *ApJ Letters*, 447, L37

Lithium production by thermohaline mixing in low-mass, low-metallicity asymptotic giant branch stars

Richard J. Stancliffe, George C. Angelou and John C. Lattanzio

Centre for Stellar and Planetary Astrophysics, Monash University, VIC 3800, Australia

email: Richard.Stancliffe@sci.monash.edu.au

Abstract. We examine the effects of thermohaline mixing on the composition of the envelopes of low-metallicity asymptotic giant branch (AGB) stars. We have evolved models of 1, 1.5 and $2 M_{\odot}$ and of metallicity $Z = 10^{-4}$ from the pre-main sequence to the end of the thermal pulsing asymptotic giant branch with thermohaline mixing applied throughout the simulations. We find that the small amount of ^3He that remains after the first giant branch is enough to drive thermohaline mixing on the AGB and that the mixing is most efficient in the early thermal pulses, with the efficiency dropping from pulse to pulse. We note a surprising increase in the ^7Li abundance, with $\log_{10} \epsilon(^7\text{Li})$ reaching values of over 2.5 in the $1.5 M_{\odot}$ model. It is thus possible to get stars which are both C- and Li-rich at the same time. We compare our models to measurements of carbon and lithium in carbon-enhanced metal-poor stars which have not yet reached the giant branch. These models can simultaneously reproduce the observed C and Li abundances of carbon-enhanced metal-poor turn-off stars that are Li-rich.

Keywords. Stars: evolution, AGB and post-AGB, Population II, carbon

1. Introduction

It has long been known that models of asymptotic giant branch (AGB) stars that only include mixing in convective regions are incomplete. These canonical models cannot account for observations such as: the low $^{12}\text{C}/^{13}\text{C}$ ratios in low-mass AGB stars (Abia & Isern 1997; Lebzelter et al. 2008), Li and C-rich stars in our Galaxy (Abia & Isern 1997; Uttenthaler et al. 2007), isotopic ratios measured in pre-solar grains (e.g. Nollett et al. 2003, and references therein). It has therefore been suggested that material might circulate below the base of the convective envelope into regions where nuclear burning can happen. This process is often referred to as ‘cool bottom processing’.

There have been detections of lithium in carbon-enhanced metal-poor (CEMP) stars (e.g. Thompson et al. 2008) and this is difficult to reconcile with standard models of AGB stars. Canonical AGB models produce Li via the Cameron-Fowler mechanism (Cameron & Fowler 1971), which involves the production of beryllium deep in the hydrogen burning shell via the reaction $^4\text{He}(^3\text{He}, \gamma)^7\text{Be}$ and the immediate transport of this to cooler regions of the star where the ^7Li that forms (once the beryllium has undergone electron capture) is stable against proton captures. This takes place in the more massive stars which undergo hot bottom burning (HBB, where the base of the convective envelope lies in the top of the hydrogen-burning shell). Such stars would be rich in nitrogen, not carbon. These observations suggest that something is missing from the AGB models and an extra mixing mechanism must be at work.

Lithium is a particularly important element from the point of view of mixing processes in CEMP stars, especially those that are enriched in *s*-process elements. These CEMP-*s* stars are believed to have formed in binary systems where mass has been transferred

from an AGB star which is no longer visible on to a companion that we now observe as carbon rich. Stancliffe et al. (2007) pointed out that material accreted on to a low-mass companion does not just remain at the surface of the companion star and that thermohaline mixing could efficiently mix this material deep into the stellar interior. However, detection of lithium in the CEMP binary system CS 22964-161 led Thompson et al. (2008) to suggest that the mixing efficiency could not be so high. Li is a fragile element and is easily destroyed at temperatures in excess of about 2.5×10^6 K. Even a modest depth of mixing can lead to efficient Li-depletion (Stancliffe 2009) and hence the measurement of Li in CEMP stars could be a good test of the efficiency of thermohaline mixing. It is therefore crucial that we understand the origin of this element.

Despite the apparent need for extra mixing on both the giant branches, the physical nature of the mechanism (or mechanisms) has proved illusive. Recently, Eggleton et al. (2006) showed that the lowering of the mean molecular weight by the reaction ${}^3\text{He}({}^3\text{He}, 2\text{p}){}^4\text{He}$ could lead to mixing in red giants via the thermohaline instability. This can potentially explain the change in abundances seen in giants above the luminosity bump (Charbonnel & Zahn 2007; Eggleton et al. 2008). In this work, we wish to examine what the consequences of thermohaline mixing are for low-mass, low-metallicity AGB stars.

2. The stellar evolution code

Calculations in this work have been carried out using the STARS stellar evolution code (see Stancliffe & Eldridge 2009, for a detailed description of the code). Thermohaline mixing is included throughout all the evolutionary phases via the prescription of Kippenhahn, Ruschenplatt & Thomas (1980), with the mixing coefficient being multiplied by a factor of 100 as suggested by the work of Charbonnel & Zahn (2007). These authors find that with a factor of this magnitude they are able to reproduce the abundance trends observed towards the tip of the red giant branch. Stancliffe et al. (2009) also showed that a coefficient of this magnitude could reproduce the observed mixing trends in both low-mass metal-poor stars and carbon-enhanced metal-poor stars on the upper part of the first giant branch.

We evolve stars of 1, 1.5 and $2 M_{\odot}$ from the pre-main sequence to the end of the thermally pulsing asymptotic giant branch (TP-AGB) using 999 mesh points. Reimers (1975) mass-loss prescription, with $\eta = 0.4$, is used from the Main Sequence up to the TP-AGB; the Vassiliadis & Wood (1993) mass-loss law is employed during the TP-AGB. A mixing length parameter of $\alpha = 2.0$ is employed. The metallicity of each model is $Z = 10^{-4}$ ($[\text{Fe}/\text{H}] \approx -2.3$) and the initial abundances are assumed to be solar-scaled according to Anders & Grevesse (1989), with the exception of ${}^7\text{Li}$, for which we adopt a value of $X_{7\text{Li}} = 1.05 \times 10^{-9}$ which is equivalent to the Spite plateau value.

3. Lithium production on the AGB

While lithium is destroyed on the red giant branch, we find that it can be produced during the TP-AGB phase. Lithium production occurs in each of the models in the following way. First, the deepening of the convective envelope that occurs after every thermal pulse (referred to as third dredge-up) homogenises the envelope and flattens out the mean molecular weight above the burning shell (top left panel of Fig. 1). This is an essential precursor to thermohaline mixing. The reaction ${}^3\text{He}({}^3\text{He}, 2\text{p}){}^4\text{He}$ can only produce a small reduction of the mean molecular weight and its effects will only be apparent in a region of zero mean molecular weight gradient.

After the convective envelope has reached its maximum depth, it begins to retreat and

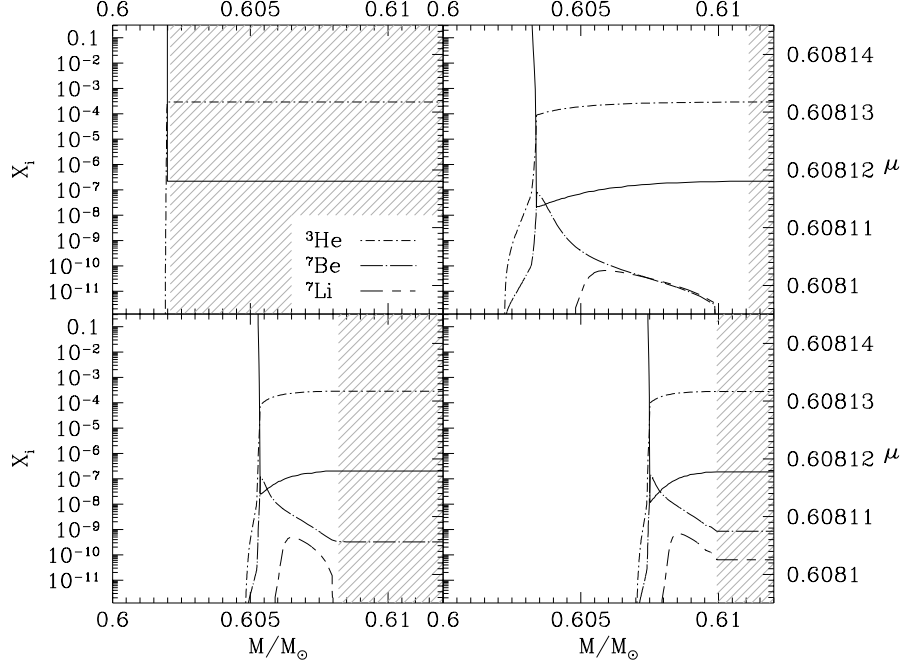


Figure 1. Abundance profiles of the $1.5 M_{\odot}$ model after its second thermal pulse. In each panel, the abundances are: ^3He (dot-short dash line), ^7Be (dot-long dash line) and ^7Li (dashed line). The mean molecular weight, μ , is displayed by a solid line. The grey shading indicates convective regions. **Top left:** Just after the end of third dredge-up. **Top right:** Retreat of the convective envelope. Therohaline mixing leads to the formation of a pocket of beryllium and lithium. **Bottom left:** The hydrogen shell moves outward and the envelope comes back in again. **Bottom right:** Just before the beginning of the next thermal pulse.

hydrogen burning re-ignites. At the top of the hydrogen burning shell, two important reactions are occurring. The $^3\text{He}(^3\text{He}, 2p)^4\text{He}$ lowers the mean molecular weight and therohaline mixing starts to occur. In addition, the fusion of ^3He with ^4He produces ^7Be . Therohaline mixing transports this newly synthesised beryllium toward the convective envelope. En route, ^7Be undergoes electron capture to produce ^7Li . While it remains deep in the star, this lithium is destroyed by proton captures. Therohaline mixing is not efficient enough to transport the lithium to the envelope before it is destroyed. Pockets of ^7Be and ^7Li (top right panel of Fig. 1) are thus formed and their abundances depend on the rate at which fresh beryllium is transported up from hydrogen burning shell and the rate at which both species are being destroyed.

As the star settles into the interpulse phase, the convective envelope retreats inward again but not to the same extent as it did during third dredge-up. The envelope reaches into the lithium pocket that has been formed and a surface enrichment of lithium occurs. In addition the distance between the hydrogen burning shell and the convective envelope has now been reduced and therohaline mixing is now able to transport lithium into the envelope before it is destroyed (bottom panels of Fig. 1). The lithium abundance thus continues to increase during the interpulse phase.

We find that the $1.5 M_{\odot}$ model obtains the greatest lithium enrichment of the three

models we have run. By the time the star enters the superwind phase the surface lithium abundance has reached $\log_{10} \epsilon(^7\text{Li}) = 2.51$. The $2 M_{\odot}$ model reaches a peak surface lithium enrichment of $\log_{10} \epsilon(^7\text{Li}) = 1.44$ after 7 thermal pulses but then suffers a slight decline as the base of the convective envelope becomes sufficiently deep for some lithium destruction to take place. At the onset of the superwind phase, the surface lithium abundance is $\log_{10} \epsilon(^7\text{Li}) = 1.38$. The $1 M_{\odot}$ model is the least enriched by this mechanism and only reaches $\log_{10} \epsilon(^7\text{Li}) = 1.03$ by the end of the TP-AGB.

4. Discussion

The surprising outcome of these simulations is the high Li abundances that can be produced. It is usually supposed that only the higher mass AGB stars which undergo hot bottom burning are able to produce Li via the Cameron-Fowler mechanism (Cameron & Fowler 1971). This work shows that it is possible that *low-mass AGB stars could be producers of lithium-7*. We also note that the action of thermohaline mixing on the AGB is subtly different from its action of the RGB. On the RGB, it leads to a depletion of Li with the star leaving the RGB with virtually no lithium left. However, on the AGB thermohaline mixing can substantially increase the surface Li abundance above the Spite plateau value. It is therefore possible that low-mass AGB stars have contributed to the Galaxy's Li budget. The effect of a population of low-mass, low-metallicity lithium producers on Galactic chemical evolution models should be investigated.

These models do improve the agreement of the AGB models with observations of Li in carbon-enhanced metal-poor stars. We have extracted from the Stellar Abundances for Galactic Archaeology (SAGA) database (Suda et al. 2008) those CEMP stars that are both C-rich and have measured Li-abundances, and also that are still close to the main sequence turn-off (because first dredge-up will significantly reduce the surface Li abundance). We select only those stars in the metallicity range $-3 < [\text{Fe}/\text{H}] < -2$ as the models presented herein may be expected to apply only over a limited range in metallicity. In particular, at very low metallicities, AGB stars can undergo additional mixing events not present in our models (see e.g. Fujimoto et al. 1990; Campbell & Lattanzio 2008; Lau et al. 2009, among many others for a discussion of these mixing events). SAGA lists 5 turn-off objects with measured lithium abundances, the properties of which are displayed in Table 1.

One caveat should be added to the following discussion. The scenario of mass transfer from an AGB primary star on to a lower mass secondary in a binary system is expected to apply to those stars belonging to the CEMP-*s* subclass, i.e. those stars which have $[\text{Ba}/\text{Fe}] > 1$ and $[\text{Ba}/\text{Eu}] > 0.5$ according to the definitions given by Beers & Christlieb (2005). The origin of the *r + s* subclass of CEMP stars, which have $0 < [\text{Ba}/\text{Eu}] < 0.5$, is currently unknown. It is possible that their *s*-process enrichment has come from a binary mass transfer event, in which case the models presented herein would apply, but the enrichment may have another source entirely (see e.g. Lugaro et al. 2009, for a possible alternative formation scenario). This should be borne in mind throughout the following discussion.

We model CEMP stars by accreting material of the composition of the ejecta from our AGB models on to low-mass stars on the main sequence (see Stancliffe & Glebbeek 2008, for details). We accrete 0.001, 0.01 and $0.1 M_{\odot}$ of material on to a companion so that its final mass is $0.8 M_{\odot}$, equivalent to the turn-off mass of the Halo. The model is then evolved until the star reaches the main-sequence turn-off, i.e. the point at which the Li-rich CEMP stars are observed. An example of accretion from the $1.5 M_{\odot}$ model is shown in Fig. 2. We find that a model that includes thermohaline mixing, gravitational settling and the

Object	[Fe/H]	[C/Fe]	$\log_{10} \epsilon(\text{Li})$	$\log g$	Refs.
CS 22964-161A	-2.41	1.35	2.09	3.7	1
CS 22964-161B	-2.39	1.15	2.09	4.1	1
HE 0024-2523	-2.7	2.6	1.5	4.3	2
CS 31080-095	-2.85	2.69	1.73	4.5	3
CS 31062-012	-2.53	2.14	2.3	4.3	4

Table 1. Properties of CEMP turn-off stars with measured Li-abundances, as extracted from the SAGA database. References: 1 – Thompson et al. (2008), 2 – Lucatello et al. (2003), 3 – Sivarani et al. (2006), 4 – Aoki et al. (2008)

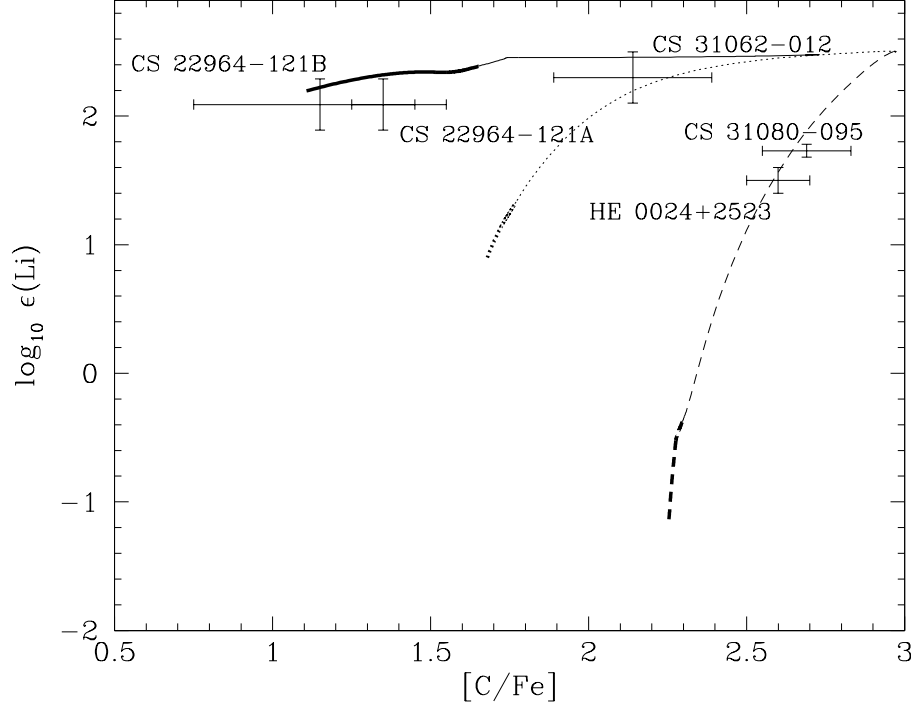


Figure 2. The evolution of $\log_{10} \epsilon(\text{Li})$ with $[\text{C}/\text{Fe}]$ when accreting material from a $1.5 M_{\odot}$ companion. The cases displayed are for when $0.001 M_{\odot}$ (solid line), $0.01 M_{\odot}$ (dotted line) and $0.1 M_{\odot}$ (dashed line) is accreted. In each case, the secondary is left with a total mass of $0.8 M_{\odot}$. Bold lines indicate where $\log g$ passes from 4.5 to 3.5 as the object evolves off the main sequence. The errorbars denote the locations of specific observed systems. The secondary is modelled including thermohaline mixing, gravitational settling and an extra turbulent process.

ad hoc turbulent mixing of Richard et al. (2005) can reproduce the observed properties of CS 22964-121 if $0.001 M_{\odot}$ of material is accreted, while for CS 31062-012 around $0.002 M_{\odot}$ of material would have to be accreted. For CS 31080-095 and HE 0024+2523 a companion of between 1 and $1.5 M_{\odot}$ mass is most likely required, though based on the high carbon abundance in these objects, it seems unlikely that the accreted material would have undergone any mixing.

5. Conclusions

We have investigated the effect that thermohaline mixing has on the abundances of low-mass, low-metallicity AGB stars. We find that enough ^3He remains after the first giant branch that thermohaline mixing can still take place on the AGB. Thermohaline mixing can lead to substantial production of ^7Li – even up to abundances above the Spite plateau value. Thus it is possible to reconcile C- and Li-rich metal-poor stars with having come from a binary mass transfer scenario. The possibility that low-mass, low-metallicity stars could be producers of lithium is intriguing and their role in Galactic chemical evolution should be investigated.

6. Acknowledgements

RJS is funded by the Australian Research Council’s Discovery Projects scheme under grant DP0879472. This work was supported by the NCI National Facility at the ANU.

References

- Abia C., Isern J., 1997, *MNRAS*, 289, L11
 Anders E., Grevesse N., 1989, *Geo.Cosmo.Acta*, 53, 197
 Aoki W., Beers T. C., Sivarani T., Marsteller B., Lee Y. S., Honda S., Norris J. E., Ryan S. G., Carollo D., 2008, *ApJ*, 678, 1351
 Beers T. C., Christlieb N., 2005, *ARA&A*, 43, 531
 Cameron A. G. W., Fowler W. A., 1971, *ApJ*, 164, 111
 Campbell S. W., Lattanzio J. C., 2008, *A&A*, 490, 769
 Charbonnel C., Zahn J.-P., 2007, *A&A*, 467, L15
 Eggleton P. P., Dearborn D. S. P., Lattanzio J. C., 2006, *Science*, 314, 1580
 Eggleton P. P., Dearborn D. S. P., Lattanzio J. C., 2008, *ApJ*, 677, 581
 Fujimoto M. Y., Iben I. J., Hollowell D., 1990, *ApJ*, 349, 580
 Kippenhahn R., Ruschenplatt G., Thomas H.-C., 1980, *A&A*, 91, 175
 Lau H. H. B., Stancliffe R. J., Tout C. A., 2009, *MNRAS*, 396, 1046
 Lebzelter T., Lederer M. T., Cristallo S., Hinkle K. H., Straniero O., Aringer B., 2008, *A&A*, 486, 511
 Lucatello S., Gratton R., Cohen J. G., Beers T. C., Christlieb N., Carretta E., Ramírez S., 2003, *AJ*, 125, 875
 Lugaro M., Campbell S. W., de Mink S. E., 2009, *PASA*, 26, 322
 Nollett K. M., Busso M., Wasserburg G. J., 2003, *ApJ*, 582, 1036
 Reimers D., 1975, *Memoires of the Societe Royale des Sciences de Liege*, 8, 369
 Richard O., Michaud G., Richer J., 2005, *ApJ*, 619, 538
 Sivarani T., Beers T. C., Bonifacio P., Molaro P., Cayrel R., Herwig F., Spite M., Spite F., Plez B., Andersen J., Barbuy B., Depagne E., Hill V., François P., Nordström B., Primas F., 2006, *A&A*, 459, 125
 Stancliffe R. J., 2009, *MNRAS*, 394, 1051
 Stancliffe R. J., Church R. P., Angelou G. C., Lattanzio J. C., 2009, *MNRAS*, 396, 2313
 Stancliffe R. J., Eldridge J. J., 2009, *MNRAS*, 396, 1699
 Stancliffe R. J., Glebbeek E., 2008, *MNRAS*, 389, 1828
 Stancliffe R. J., Glebbeek E., Izzard R. G., Pols O. R., 2007, *A&A*, 464, L57
 Suda T., Katsuta Y., Yamada S., Suwa T., Ishizuka C., Komiya Y., Sorai K., Aikawa M., Fujimoto M. Y., 2008, *PASJ*, 60, 1159
 Thompson I. B., Ivans I. I., Bisterzo S., Sneden C., Gallino R., Vauclair S., Burley G. S., Shectman S. A., Preston G. W., 2008, *ApJ*, 677, 556
 Uttenhaler S., Lebzelter T., Palmerini S., Busso M., Aringer B., Lederer M. T., 2007, *A&A*, 471, L41
 Vassiliadis E., Wood P. R., 1993, *ApJ*, 413, 641

Light elements in massive single and binary stars

N. Langer^{1,2}, I. Brott², M. Cantiello², S.E. de Mink², R.G. Izzard³,
and S.-C. Yoon¹

¹Argelander-Institut für Astronomie, Universität Bonn,
Auf dem Hügel 71, Germany

²Sterrenkundig Instituut, University of Utrecht,
Postbus 80000, NL-3508TA, Utrecht, the Netherlands

³Institut d'Astronomie et d'Astrophysique, Université Libre de Bruxelles,
Boulevard du Triomphe, 1050 Brussels

Abstract. We highlight the role of the light elements (Li, Be, B) in the evolution of massive single and binary stars, which is largely restricted to a diagnostic value, and foremost so for the element boron. However, we show that the boron surface abundance in massive early type stars contains key information about their foregoing evolution which is not obtainable otherwise. In particular, it allows to constrain internal mixing processes and potential previous mass transfer event for binary stars (even if the companion has disappeared). It may also help solving the mystery of the slowly rotating nitrogen-rich massive main sequence stars.

Keywords. Stars: abundances, binaries

1. Introduction

A large effort has been undertaken in the last decades to measure and understand the surface chemical composition of massive main sequence stars. In particular, the detection of nitrogen enhancements in quite a number of such stars (e.g., Gies & Lambert 1992) has triggered the idea that internal mixing processes can bring material from the stellar core to the surface in rapid rotators (Meynet & Maeder 2000, Heger & Langer 2000).

The picture has become more complicated by the recent analysis of a large sample of early B type main sequence stars of Hunter et al. (2008b), who showed that the nitrogen-rich stars found by Gies & Lambert (1992), who restricted their analysis to objects with low projected rotational velocities, are likely part of a population of *intrinsically* slowly rotation main sequence stars. This view is supported by the work of Morel et al. (2006, 2008), who indeed identifies such a population in our Galaxy (see also Morel 2009). The origin of the nitrogen enrichment in these stars is not understood, but as they are slow rotators it appears difficult to reconcile them with the idea of rotational mixing.

On the other hand, Hunter et al. (2008b) also identified a nitrogen-rich population of rapidly rotating early B stars, which appears to be well in line with the predictions of theoretical models including rotational mixing (cf., Maeder et al. 2008). The caveat here is that evolutionary models of massive close binaries — whether or not they include rotationally induced chemical mixing (Langer et al. 2008) — appear to predict essentially the same trend of nitrogen enrichment with rotational velocity as the single star models (Meynet & Maeder 2000, Heger & Langer 2000).

The light elements lithium, beryllium and boron may play a key role to resolve this issue. They are so rare in the interstellar medium that they can not influence the course of stellar evolution, and thus are often neglected in massive star models. Furthermore,

they are fragile nuclei which are generally not synthesised in stars, but rather destroyed, at least certainly on the main sequence. In the cool low-mass stars, lithium is most interesting, as it can be observed rather easily, and it is indeed used extensively to constrain internal mixing processes as can be seen in many contributions to this book. In massive stars this role can be played by boron as will be outlined below.

2. Single stars

Other than helium and the major CNO nuclei, the light elements Li, Be, and B are destroyed by proton capture relatively close to the stellar surface. For both stable boron isotopes, ^{10}B and ^{11}B , the life time against proton capture is equal to the main sequence life time of a $10M_{\odot}$ star (10^7 yr) at a temperature of roughly $7 \cdot 10^6$ K. Fliegner et al. (1996) have computed the evolution of stars of $15M_{\odot}$, and found this temperature to occur sufficiently deep inside the stellar envelope (i.e. roughly $1M_{\odot}$ below the surface; cf. Fig. 1) that its surface abundance can not be altered due to mass loss alone on the main sequence in the B star regime. Thus, the boron abundance in B stars is a critical test of mixing processes in the upper stellar envelope, while CNO and helium abundances additionally trace the mixing in deeper layers.

Models which include rotational mixing show that boron depletion at the stellar surface is predicted for initial rotational velocities above 50 km/s. However, while in low-mass stars, the rotational velocity is a strong function of age, and so is the lithium abundance, a clear correlation of boron with stellar age is not expected in a population which contains initially fast and slow rotators (cf. Gies & Lambert 1992). However, a population synthesis

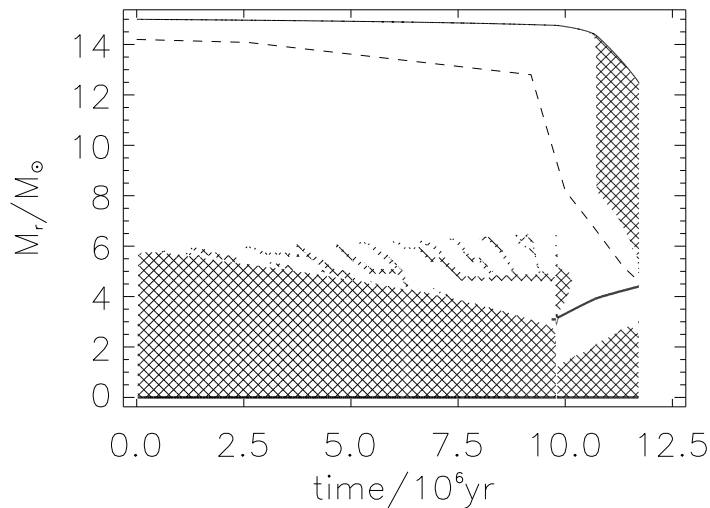


Figure 1. Internal structure of a $15M_{\odot}$ star during core hydrogen and helium burning. The solid line on top indicates the total mass of the star as function of time. Hatched areas designate convectively unstable mass zones in the star. The full drawn line at $M_r \simeq 4M_{\odot}$ and $t \gtrsim 10^7$ yr designates the location of the H-burning shell during core helium burning. The dashed line indicates the threshold temperature for boron destruction (cf. Fliegner et al. 1996).

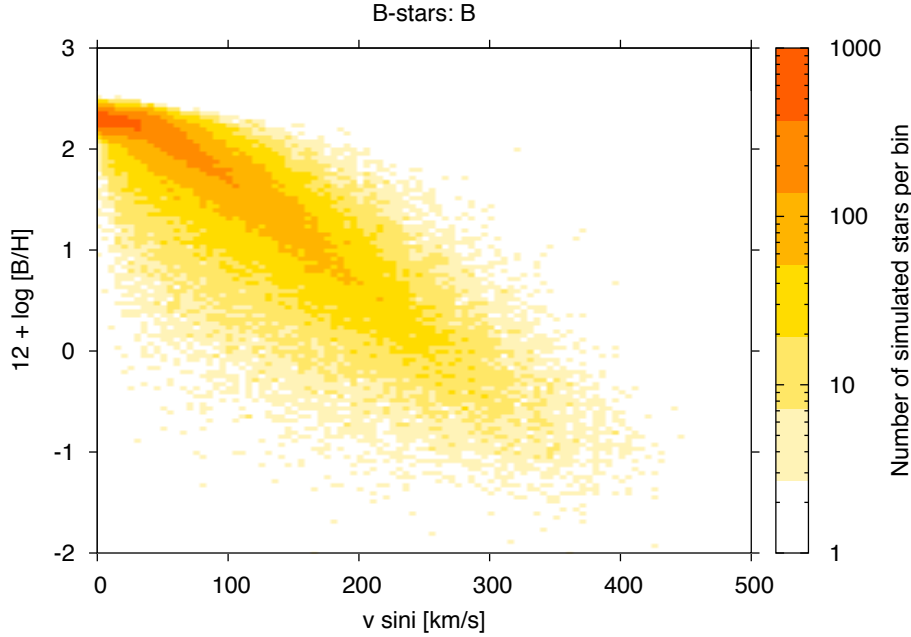


Figure 2. Result of a population synthesis calculation for massive main sequence stars (Brott et al., in prep.), employing a Salpeter initial mass function, and a distribution of initial stellar rotation rates as derived by Hunter et al. (2008a), and a constant star formation rate, based on single star evolution models which include rotational mixing. A random Gaussian error of 0.2 dex was added to the predicted boron abundances.

simulation by Ines Brott shows (Fig. 2), that a clear correlation of the surface boron depletion with the stellar rotation rate can be expected in early B type single stars.

Figure 3 shows the behaviour of the surface abundances of a rotating $15M_{\odot}$ in a plot of boron depletion versus nitrogen enhancement. Interestingly, it predicts that boron depletion happens essentially *before* nitrogen enrichment occurs. Thus, stars which are already depleted in boron, but which are still nitrogen normal are expected. Indeed, in the sample of Venn et al. (1996), several such stars seem to exist. The importance of this finding becomes more clear in the next section.

3. Binary stars

The binary fraction of massive stars is very high, and it may be futile to try to understand their surface abundances without considering effects of binarity (Langer et al. 2008). The issue of binarity is not easily resolved, because of two reasons.

Firstly, after a strong binary interaction, the object may not appear to be a binary any more. This is so since many mass transfer systems will produce a rejuvenated main sequence star which dominates the light of the system, with a faint helium star in a wide orbit. In fact, many such objects ought to exist, as we see many of their descendants, the Be-X-ray binaries. However, for the stage where the main sequence star has a helium star companion, we practically do not know any counterpart. Also, there will be many cases

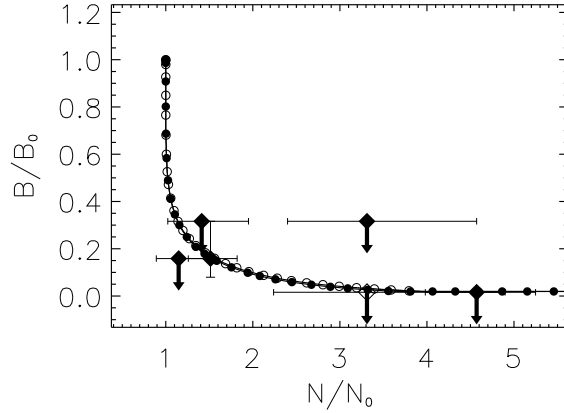


Figure 3. Boron depletion versus nitrogen enrichment for rotating stars of $10M_{\odot}$ during the main sequence evolution (Fliegner et al. 1996). Open circles correspond to a moderately, filled circles to a fast rotating model. Two neighbouring symbols on each line indicate a constant distance in time of 10^6 yr. Diamonds indicate the location of the five B main sequence stars (filled symbols) and one B giant (open symbol) of Venn et al.’s (1996) sample (see also Venn et al. 2002). Arrows designate upper limits.

where the post-interaction system is in fact a single star. E.g., in many systems consisting of a main sequence star and a helium star companion, the supernova explosion of the helium star will disrupt the binary (instead of leading to a Be-X-ray binary stage). And furthermore, as many as 10% of all massive stars may actually merge with their close companion during the main sequence evolution. Therefore, most of the binaries which we detect in massive main sequence star populations may have in fact not yet interacted, while on the other hand, many apparent single stars may be the result of a strong binary interaction.

Secondly, binary interaction has many complex branches, and it is a big theoretical enterprise to even fully consider the most important ones in a population study. So far, no such study exists which takes the physics of rotation fully into account — which is what appears to be needed in order to demonstrate that rotational mixing works in Nature.

However, there are some binary evolution models available which include all the required physics, and while they will not allow to obtain a full view of the picture, they may give indications in one or the other direction. To that purpose, Fig. 4 shows the time evolution of the surface rotational velocity and of the surface boron abundance of the mass gainer (i.e. the star which will be visible after the mass transfer) of a close massive binary. The lower most panel also shows the boron depletion factor as function of the rotational velocity in this star.

The model shown in Fig. 4 does include rotational mixing, which produces the mild boron depletion before the first mass transfer event (at about $t = 8.5$ Myr). The mass transfer event itself, which occurs on a time scale of some 10^4 yr, puts boron depleted layers on the surface of the mass gainer, and subsequent thermohaline mixing brings the surface boron abundance back to a level of one per mille of the initial boron abundance.

Consecutively, the mass gainer is spun down by tidal interaction, while rotational mixing reduces the surface boron abundance slightly more. As a result of this phase, one

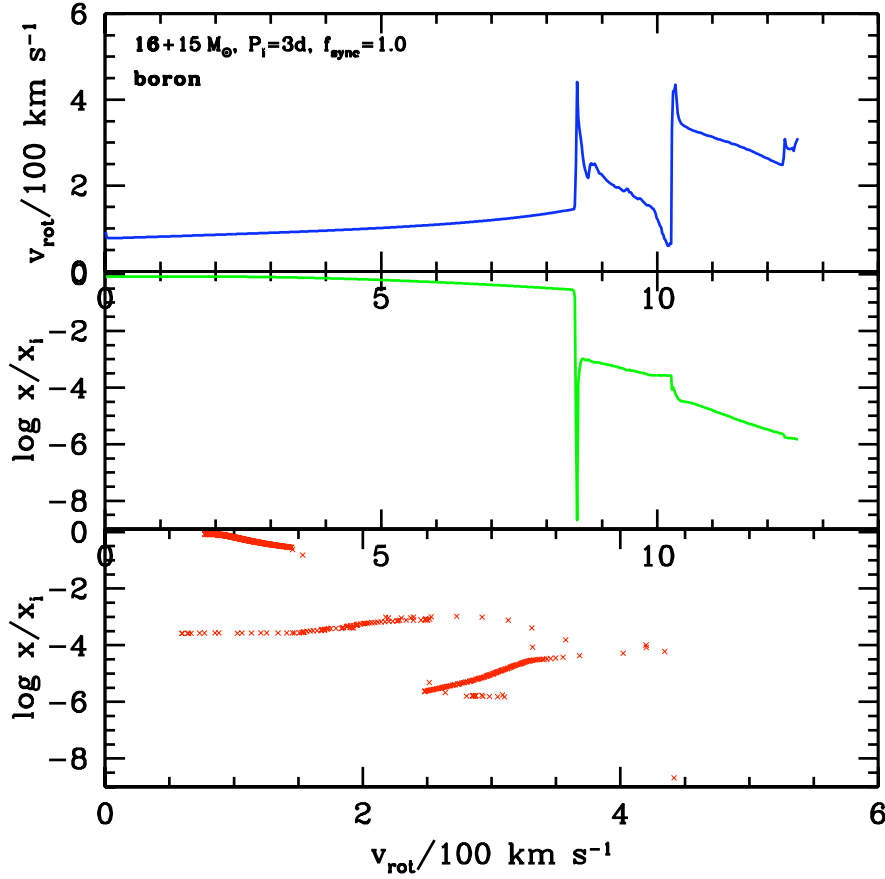


Figure 4. Equatorial rotational velocity (upper panel) and surface boron mass fraction relative to the initial value (middle panel) as function of time (in Myr), for the mass gainer in a solar metallicity $16M_{\odot} + 15M_{\odot}$ binary with an initial orbital period of 3 days. The computations include the physics of rotation for both components as in Heger et al. (2000), and Spin-Orbit coupling as in Detmers et al. (2008) with the nominal coupling parameter $f_{\text{sync}} = 1$, and rotationally enhanced stellar wind mass loss (Langer 1998). Internal magnetic fields are not included. The bottom panel shows the evolution of the mass gainer in the boron depletion versus rotational velocity diagram, where each data point represents a duration of 20 000 yr. The spin-down of the star after the first accretion event ($t = 8.5\text{--}10$ Myr) is mostly due to tidal effects.

obvious result from Fig. 4 is that in mass gainers of close binaries, one can *not* generally expect a correlation of the boron depletion factor with the surface rotation rate. Here, a slowly rotating main sequence star is produced which shows a surface boron depletion by 3 to 4 orders of magnitude. Fig. 2 shows that such a strong depletion is only expected in single stars with rotation rates above 300 km/s.

The model in Fig. 4 suffers from a second mass transfer at $t \simeq 10.2$ Myr, which leads to a second spin-up of the mass gainer and a further strong reduction of the surface boron abundance. As the orbit widens strongly during the second mass transfer phase, no tidal

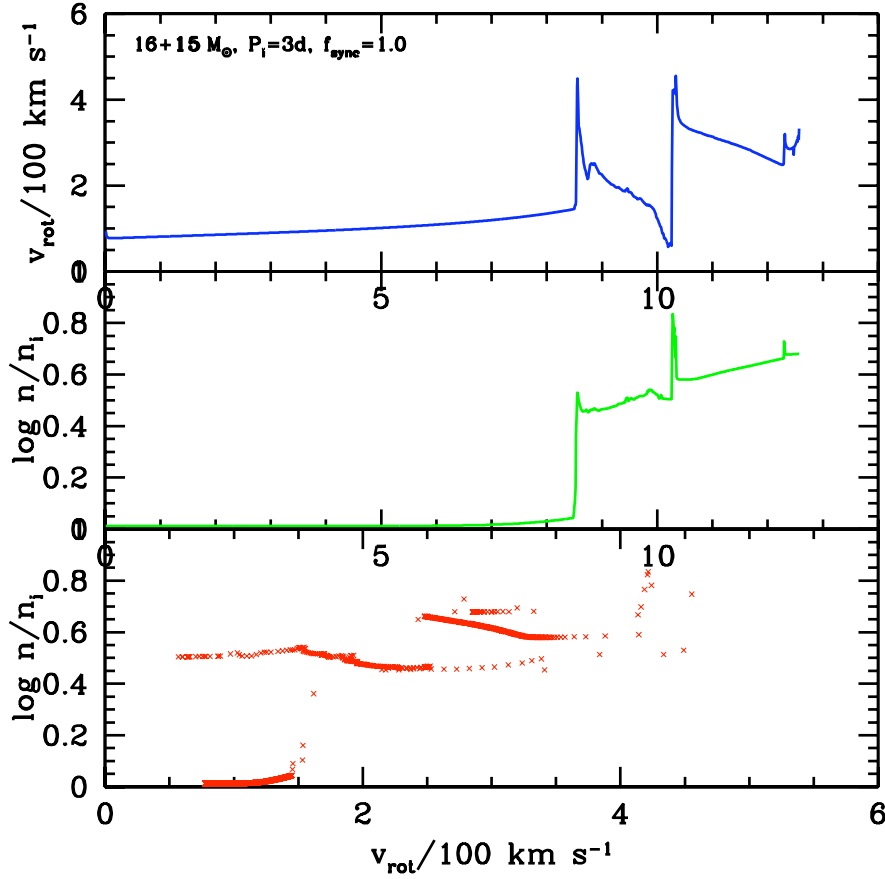


Figure 5. As Fig. 4, but showing the surface nitrogen abundance.

spin-down occurs thereafter. The mass gainer is now a rapidly rotating main sequence star which is strongly boron depleted.

While rotational mixing is included in this model, we want to point out that the effects of rotational mixing and of mass transfer (and thermohaline mixing) are well separable in Fig. 4. The steps in the time evolution of the boron abundance are produced by the mass transfer, and the long time scale changes are due to rotational mixing. We conclude that the main features of the boron evolution of this model would not change if rotational mixing were switched off. From this consideration, we can argue that if rotational mixing would not operate in Nature, then perhaps binary models would not predict main sequence stars with only a mild boron depletion (unless one considered masses much higher than $15M_{\odot}$, where mass loss can gradually uncover boron-depleted layers).

The situation becomes more clear when nitrogen is considered at the same time. Fig. 5 shows the nitrogen surface abundances of the same binary model described above. The nitrogen surface abundance increases abruptly due to the mass transfer. Thus, from

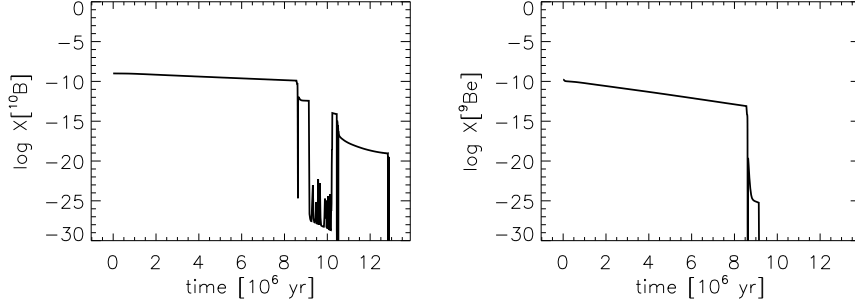


Figure 6. Surface abundance of boron 10 (left) and of beryllium (right) as function of time during core hydrogen burning, for the mass gainer in a solar metallicity $16M_{\odot} + 15M_{\odot}$ binary with an initial period of 3 days. In contrast to the models shown in Figs. 4 and 5, the stellar models shown here have been computed including angular momentum transport by internal magnetic fields (Yoon et al., in prep.).

this sequence, one would not expect to observe stars which are boron depleted but not nitrogen enriched unless rotational mixing operates. The corresponding stars in Fig. 2 thus indicate that rotational mixing is perhaps operating as we expect.

However, this is not yet a definite conclusion. The example binary displayed in Figs. 4 and 5 evolves rather conservatively, i.e. about 70% of the transferred matter is actually accepted by the mass gainer (while the rest is ejected due to its excess angular momentum). We know from observations and predict theoretically that many mass transfer systems evolve rather non-conservatively (Petrovic et al. 2005ab). We can currently not exclude that some of these systems produce boron depletion with only mild or no nitrogen enhancement.

It is also interesting to consider boron as a test of rotational mixing in very close and very massive pre-mass transfer binaries, as explored by de Mink et al. (2009). In such very tight binaries, tidal synchronisation can enforce very rapid rotation of both stars. While de Mink et al. point out that generally the nitrogen surface abundance is the prime observable for such test, their results on boron depletion appear particularly interesting for Galactic binaries, since in those boron has a larger predicted relative change than nitrogen.

Finally, in Fig. 6, we show the surface abundances of boron and of beryllium in a similar binary as the one discussed above (even though some physics assumptions were different, which is not essential for our discussion here). Fig. 6 indicates that also beryllium is very interesting from the theoretical point of view. However, beryllium abundance determinations in hot main sequence stars appear to be difficult.

4. Unknown mixing processes

We have seen in the previous sections, that the surface abundances of massive main sequence stars are not yet fully understood, and that unambiguous evidence for the existence of rotationally induced mixing in massive stars is still lacking. Of particular worry is the solid evidence for a population of nitrogen-rich slowly rotating massive main sequence stars (Hunter et al. 2008b, 2009; Morel et al. 2006, 2008; Morel 2009). While the binary models discussed above do show a way to produce such stars (Langer et al., 2008; cf. Fig. 5), the Galactic fraction of this population contains well investigated β Cephei pulsators (Morel et al. 2006, 2008) none of which seems to show any indication

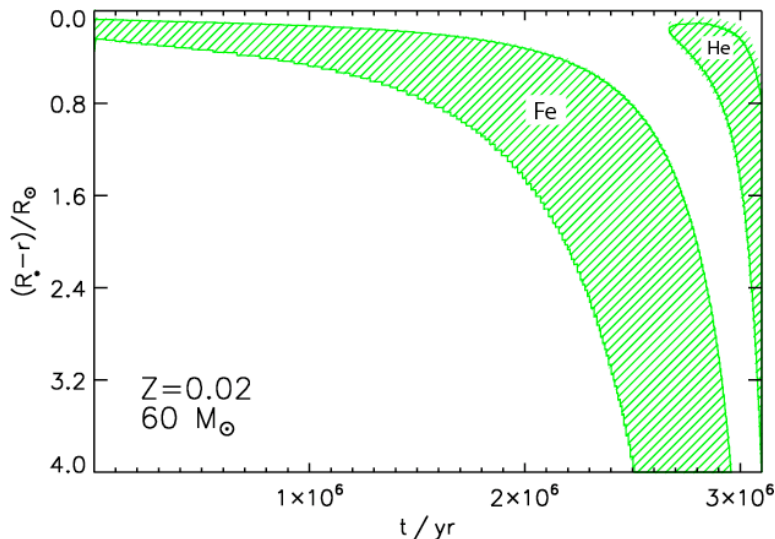


Figure 7. Evolution of the radial extent of the subsurface helium and iron convective regions (hatched) as function of time, from the zero age main sequence to roughly the end of core hydrogen burning, for a $60 M_{\odot}$ star (Cantiello et al. 2009). The top of the plot represents the stellar surface. Only the upper $4 R_{\odot}$ of the star are shown in the plot, while the stellar radius itself increases during the evolution. The star has a metallicity of $Z=0.02$, and its effective temperature decreases from 48 000 K to 18 000 K during the main sequence phase.

of binarity. Despite the warning above that binarity might be difficult to detect in post-mass transfer systems, the lack of any indication of a companion in well-studied nearby stars could imply that binarity is not the (only) answer to this question. It also remains to be seen whether binary evolution could produce enough of these objects, which may have a frequency of about 15% of all main sequence stars (Hunter et al. 2008b).

So we may face the situation that so far completely unaccounted mixing processes may operate in stars (see also Brott et al., in preparation). Perhaps, they could be related to magnetic fields in the interior of massive stars. Also gravity waves could be excited in massive stars, as Talon & Charbonnel (2008) employ them for angular momentum transport in intermediate-mass stars. However, we want to end with a related possibility, for which recent observational evidence has accumulated.

Cantiello et al. (2009) investigated the subsurface convection zones which occur in the envelopes of hot massive stars due to the iron opacity peak (cf. Fig. 7). They found that the occurrence of strong subsurface convective motion predicted by the models correlates with observed large microturbulent velocities deduced from stellar spectroscopy. While this may not be sufficient to conclude that subsurface convection causes observable motion at the stellar surface, it appears to be a possibility. This could mean that the subsurface layers of massive stars, independent of their rotation, could be in motion, and perhaps lead to some mixing near the surface; this might produce a surface boron depletion without changing nitrogen.

5. Conclusions

It remains a major challenge to the theory of massive star evolution to explain the observed surface abundances of massive main sequence stars. While until recently, the

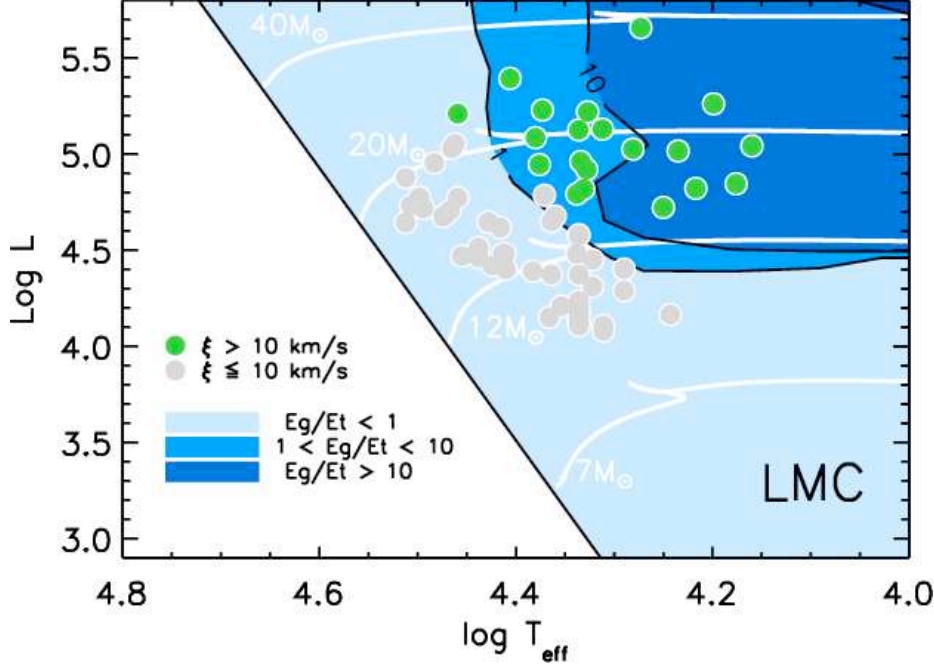


Figure 8. Values of the ratio E_g/E_s of the kinetic energy in the form of gravity waves above the iron convection zone, to the kinetic energy of the surface velocity field, as a function of the location in the HR diagram (Cantiello et al. 2009). This plot is based on evolutionary models between $5 M_\odot$ and $100 M_\odot$ for LMC metallicity. The ratio E_g/E_s (see Eq. (9) of Cantiello et al. 2009) is estimated using a value $v_s = 10 \text{ km s}^{-1}$ for the surface velocity amplitude. Overplotted as filled circles are stars which have photospheric microturbulent velocities ξ derived in a consistent way by Hunter et al. (2008a). Only data for stars with an apparent rotational velocity of $v \sin i < 80 \text{ km s}^{-1}$ is plotted. Solid white lines are reference evolutionary tracks, and the full drawn black line corresponds to the zero age main sequence.

incorporation of rotational mixing was thought to lead to a much better agreement, the discovery that a significant fraction of early B dwarfs are nitrogen-rich and intrinsically slowly rotating has cast some doubts on the previous ideas. We argue that boron observations of early type main sequence stars, as performed by Venn et al. (1996, 2002) and Morel et al. (2006, 2008), have the potential to move towards a solution. Clearly, binary evolution needs to be considered at the same time. Finally, we may be facing the situation that still not all mixing processes which can operate in massive main sequence stars have been described. Amongst possible candidates is mixing due to magnetic processes, and mixing induced by subsurface convection zones in hot massive stars.

References

- Cantiello, M., Langer, N., Brott, I., de Koter, A., Shore, S. N., Vink, J. S., Voegler, A., Lennon, D. J. & Yoon, S.-C. 2009, *A&A*, 499, 279
 de Mink, S. E., Cantiello, M., Langer, N., Pols, O. R., Brott, I. & Yoon, S.-Ch. 2009, *A&A*, 497, 243
 Detmers, R. G., Langer, N., Podsiadlowski, Ph. & Izzard, R. G. 2008, *A&A*, 484, 831
 Fliegner, J., Langer, N. & Venn, K. A. 1996, *A&A* (Letters), 308, 13

- Gies D.R. & Lambert D.L 1992, *ApJ*, 387, 673
- Heger, A. & Langer, N. 2000, *ApJ*, 544, 1016
- Heger, A., Langer, N. & Woosley, S. E. 2000, *ApJ*, 528, 368
- Hunter, I., Brott, I., Lennon, D. J., Langer, N., Dufton, P. L., Trundle, C., Smartt, S. J., de Koter, A., Evans, C. J. & Ryans, R. S. I. 2008b, *ApJ* (Letters), 676, 29
- Hunter, I., Lennon, D. J., Dufton, P. L., Trundle, C., Simon-Diaz, S., Smartt, S. J., Ryans, R. S. I. & Evans, C. J. 2008a, *A&A*, 479, 541
- Hunter, I., Brott, I., Langer, N., Lennon, D. J., Dufton, P. L., Howarth, I. D., Ryans, R. S. I., Trundle, C., Evans, C. J., de Koter, A. & Smartt, S. J. 2009, *A&A*, 496, 841
- Langer, N. 1998, *A&A*, 329, 551
- Langer, N., Cantiello, M., Yoon, S.-C., Hunter, I., Brott, I., Lennon, D., de Mink, S. & Verheijdt, M. 2008, IAU Symposium 250, p. 167
- Maeder, A., Meynet, G., Ekström, S. & Georgy, C. 2009, *Communications in Asteroseismology*, 158, 72
- Meynet, G. & Maeder, A. 2000, *A&A*, 361, 101
- Morel, T. 2009, *Communications in Asteroseismology*, 158, 122
- Morel, T., Butler, K., Aerts, C., Neiner, C. & Briquet, M. 2006, *A&A*, 457, 651
- Morel, T., Hubrig, S. & Briquet, M. 2008, *A&A*, 481, 453
- Petrovic, J., Langer, N., Yoon, S.-C. & Heger, A. 2005a, *A&A*, 435, 247
- Petrovic, J., Langer, N. & van der Hucht, K. A. 2005b, *A&A*, 435, 1013
- Talon, S. & Charbonnel, C. 2008, *A&A*, 482, 597
- Venn, K.A., Lambert, D.L. & Lemke, M. 1996, *A&A*, 307, 849
- Venn, K. A., Brooks, A. M., Lambert, David L., Lemke, M., Langer, N., Lennon, D. J. & Keenan, F. P. 2002, *ApJ*, 565, 571

Boron depletion in 9 to 15 M_{\odot} stars with rotation

U. Frischknecht¹, R. Hirschi², G. Meynet³, S. Ekström³, C. Georgy³,
 T. Rauscher¹, C. Winteler¹ and F.-K. Thielemann¹

¹Department of Physics, University of Basel, CH-4056 Basel, Switzerland
 email: urs.frischknecht@unibas.ch

²Astrophysics Group, Keele University, UK-ST5 5BG Keele and Institute for the Physics and
 Mathematics of the Universe, University of Tokyo, Japan

³Geneva Observatory, University of Geneva, CH-1290 Sauverny, Switzerland

Abstract. The treatment of mixing is still one of the major uncertainties in stellar evolution models. One open question is how well the prescriptions for rotational mixing describe the real effects. We tested the mixing prescriptions included in the Geneva stellar evolution code (GENEC) by following the evolution of surface abundances of light isotopes in massive stars, such as boron and nitrogen. We followed 9, 12 and 15 M_{\odot} models with rotation from the zero age main sequence up to the end of He burning. The calculations show the expected behaviour with faster depletion of boron for faster rotating stars and more massive stars. The mixing at the surface is more efficient than predicted by prescriptions used in other codes and reproduces the majority of observations very well. However two observed stars with strong boron depletion but no nitrogen enrichment still can not be explained and let the question open whether additional mixing processes are acting in these massive stars.

Keywords. Stars: rotation, abundances, interiors

1. Introduction

Rotation is beside the stellar mass and the initial chemical composition the most important parameter in the evolution of single stars. It affects the physical and chemical structures of the stars and therefore quantities such as lifetime, luminosity, surface temperature etc. Recent models including rotation reproduce a wide range of observations better than those without (e.g. Meynet & Maeder 2003, 2005; Vázquez et al. 2007; Georgy et al. 2009). Still, the treatment of transport of angular momentum and chemical species is thought to be one of the main uncertainties in stellar evolution models.

Light elements and in particular boron and nitrogen can constrain the mixing induced by rotation and help distinguish between single stars and interacting binaries (Brott et al. 2009). Boron is destroyed at relatively low temperatures ($6 \cdot 10^6$ K) where the CNO-cycles are not yet efficient. Therefore shallow mixing due to rotation leads to a depletion of light elements such as Li, Be and B at the surface without considerable nitrogen enrichment. This effect can not be explained by mass transfer in a binary system, since there the accreted material is depleted in boron and enriched in nitrogen. An increasing number of boron surface abundances from O- and early B-type stars became available in the last few years (Proffitt & Quigley 2001; Venn et al. 2002; Mendel et al. 2006). The comparison in Mendel et al. (2006) of observational data with the models of Heger & Langer (2000) shows a good agreement with the exception of two stars. The strong boron depletion in these two young B-type stars raises the question if the efficiency of surface mixing due to rotation should be stronger or if there is another mixing effect which should be

accounted for. We examined this question because GENEC includes the effect of rotation in a different way. The main difference comes from the fact that the transport of angular momentum is properly accounted for as an advection process and not as diffusion.

2. Models and comparison

We calculated 9, 12 and 15 M_{\odot} models, each with different rotational velocities, to study the influence of rotational mixing on the light elements. A detailed description of the treatment of the transport of chemical species and angular momentum in GENEC can be found e.g. in Hirschi et al. (2004). In all our models shear turbulence is the dominant mixing process close to the stellar surface. In radiative zones, the gradient in angular momentum leading to shear mixing results from the concomitant effects of meridional currents, shear turbulence and from envelope expansion occurring on the main sequence.

In massive stars boron is only destroyed. The observations of boron in young massive stars in the solar vicinity show variations in $\log(B/H)$ from 2.9 down to unobservable quantities below 1. The large boron surface variations cannot be explained only by variation of initial composition (Venn et al. 2002). The boron vs nitrogen relation of the models is almost independent of the rotation velocity and initial stellar mass and therefore a good way to compare with observations since usually only $v \cdot \sin(i)$ is known from them. The early boron depletion and only subsequent enrichment of CN-cycle processed material is the main characteristic of rotational mixing. Most of the observations can be well reproduced. However the observed stars with boron depletion of about 1.5 dex or more and no enrichment of CNO-processed material at the surface are hard to explain with our and previous models. To reproduce these stars (HD 30836, HD 36591) the models would have to mix very efficiently the outermost envelope to destroy boron while at the same time not dredging nitrogen from the central regions up to the surface. Rotational mixing as it is treated in the current models does not seem to explain all the observations, meaning that additional physics like magnetic fields could play a role.

In comparison to the models of Heger & Langer (2000) ours show considerably more mixing for the outer part of the envelope at the end of central hydrogen burning, i.e. boron is in general more depleted at the end of the main sequence in our models with similar initial angular momentum. This means also that observed stars are better reproduced with our models since most of them are intrinsically slow rotators (Morel et al. 2008). The stronger surface mixing in our models originates in the meridional circulation, which is implemented as an advective process, whereas it is treated as a diffusive process in the models of Heger & Langer (2000). This allows meridional circulation to build stronger angular velocity gradients in the envelope instead of just diffusing the gradient away.

References

- Brott, I., Hunter, I., de Koter, A., et al. 2009, *Communications in Asteroseismology*, 158, 55
 Georgy, C., Meynet, G., Walder, R., Folini, D., & Maeder, A. 2009, *A&A*, 502, 611
 Heger, A. & Langer, N. 2000, *ApJ*, 544, 1016
 Hirschi, R., Meynet, G., & Maeder, A. 2004, *A&A*, 425, 649
 Mendel, J. T., Venn, K. A., Proffitt, C. R., et al. 2006, *ApJ*, 640, 1039
 Meynet, G. & Maeder, A. 2003, *A&A*, 404, 975
 Meynet, G. & Maeder, A. 2005, *A&A*, 429, 581
 Morel, T., Hubrig, S., & Briquet, M. 2008, *A&A*, 481, 453
 Proffitt, C. R. & Quigley, M. F. 2001, *ApJ*, 548, 429
 Vázquez, G. A., Leitherer, C., Schaerer, D., Meynet, G., & Maeder, A. 2007, *ApJ*, 663, 995
 Venn, K. A., Brooks, A. M., Lambert, D. L., et al. 2002, *ApJ*, 565, 571

Li survey in giant stars : probing non-standard stellar physics

N. Lagarde¹, C. Charbonnel^{1,2}, G. Jasiewicz³, P. North⁴, M. Shetrone⁵, J. Hollek⁵, and V. V. Smith⁶

¹ Geneva Observatory, University of Geneva, Switzerland
email: Nadege.Lagarde@unige.ch

² CNRS UMR 5572, Université de Toulouse, France

³ Université de Montpellier II, CNRS/UM2 UMR 5024, France

⁴ Laboratoire d'astrophysique, Ecole Polytechnique Fédérale de Lausanne, Switzerland

⁵ University of Texas, McDonald Observatory, USA

⁶ National Optical Astronomy Observatory, Tucson, USA

Abstract. Lithium has long been known to be a good tracer of non-standard mixing processes occurring in stellar interiors. Here we present the results of a large survey aimed at determining the surface Li abundance in a sample of about 800 giant (RGB and AGB) stars with accurate Hipparcos parallaxes. We compare the observed Li behaviour with that predicted by stellar models including rotation and thermohaline mixing.

Keywords. Hydrodynamics, instabilities, Stars: abundances, evolution, rotation

1. Introduction

Red giant stars present surface abundance anomalies that are not explained by classical stellar evolution models and that reveal the existence of extra-mixing (i.e., non convective) processes inside stellar interiors. Thermohaline mixing (Charbonnel & Zahn 2007) has been recently identified as the dominating process that governs the photospheric composition of low-mass bright giant stars, affecting in particular the surface Li abundances in red giants more luminous than the RGB bump. In order to test this assessment we present Li observations in a large sample of about 800 giant stars with Hipparcos parallaxes and compare our data for the solar-metallicity subsample with models computed with the evolutionary code STAREVOL and including thermohaline mixing and rotation-induced processes (see Charbonnel & Lagarde, this volume).

Observations were carried out with: (1) Standiford Cassegrain Echelle Spectrometer on the T2.1m at McDonald Observatory (2) Fiber-fed Extended Range Optical Spectrograph (FEROS) on the T1.52m at ESO ; (3) AURELIE spectrometer on the T1.52m at Haute-Provence Observatory.

2. Solar metallicity subsample

In Fig. 1 we compare our observations with the predictions of the solar metallicity models described in Charbonnel & Lagarde (this volume) and Lagarde & Charbonnel (in preparation) that were computed with the code STAREVOL taking into account (1) rotation-induced processes following the formalism by Zahn (92) and Maeder & Zahn (98), (2) thermohaline mixing as described by Charbonnel & Zahn (07), and (3) atomic diffusion. We also use these models to determine the mass and evolutionary status of each sample star.

On the main sequence and early-RGB, rotation-induced processes lead to stronger Li

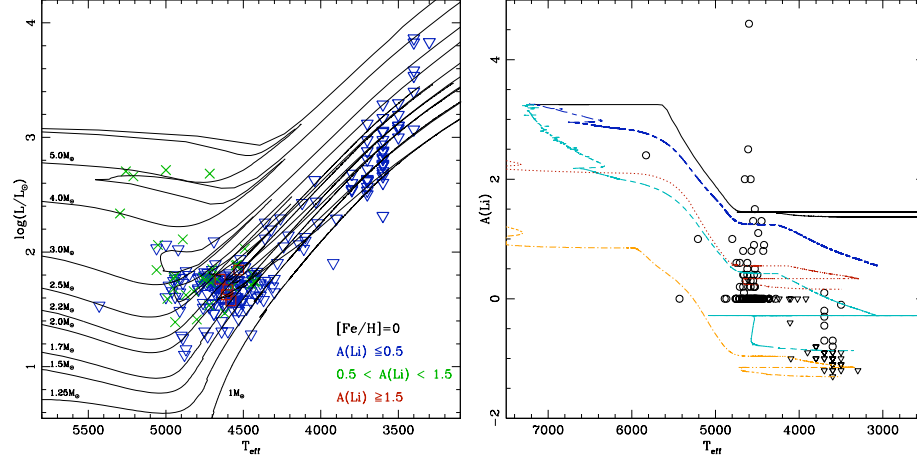


Figure 1. Comparison between models and data for the solar metallicity subsample. (Left:) HR diagram with indications on the surface Li abundance. Triangles : $A(Li) \leq 0.5$, square : $0.5 < A(Li) < 1.5$, crosses : $A(Li) \geq 1.5$. (Right:) Lithium as a function of Teff for stars with masses lower than $2M_{\odot}$ (Circles and triangles for actual determinations and upper limits respectively). Solid line, short dashed - long dashed line, and dashed line represent $1.5M_{\odot}$ stars in standard model, with thermohaline mixing and rotation $V_{ZAMS} = 50km/s$ and $V_{ZAMS} = 110km/s$ respectively. Dotted line and dot - short dashed line represent $2.0M_{\odot}$ with thermohaline mixing and rotation $V_{ZAMS} = 110km/s$ and $V_{ZAMS} = 250km/s$ respectively.

depletion than in the standard case, in agreement with observations, and the observed Li dispersion reflects dispersion in the initial rotation velocity (see also Charbonnel & Talon 1999, Palacios et al. 2003, Smiljanic et al. 2009). After the end of the first dredge-up (Teff $\sim 4800K$), the Li abundance remains temporarily constant. When thermohaline mixing becomes efficient at the bump in the luminosity function (which corresponds here to Teff $\sim 4200K$), the Li abundance is predicted to drop again in drastic manner, explaining very well the Li upper limits obtained for the brightest RGB and AGB sample stars.

References

- Charbonnel, C. & Zahn, J.P. 2007, *A&A*, 467, L15
 Charbonnel, C. & Talon, S. 1999, *A&A*, 351, 635
 Maeder, A. & Zahn, J.P. 1998, *A&A*, 334, 1000
 Palacios, A., Talon, S., Charbonnel, C., & Forestini, M. 2003, *A&A*, 399, 603
 Smiljanic, R., Pasquini, L., Charbonnel, C., Lagarde, N. 2009, *A&A*, in press, astro-ph 0910.4399
 Zahn, J.P. 1992, *A&A*, 265, 115

Li and CNO isotopes from magnetically induced extra-mixing in evolved stars

Sara Palmerini^{1,2}, Maurizio Busso^{1,2}, Roald Guandalini¹ and Enrico Maiorca^{1,2}

¹ Dipartimento di Fisica, Universtit  degli Studi di Perugia,
via Pascoli, 06125, Perugia, Italy
email: sara.palmerini@fisica.unipg.it

²I.N.F.N. sezione di Perugia, Italy

Abstract. Evolved low mass stars (LMS) contribute not only to the synthesis of s-process nuclei, but also to modifications in the isotopic mix of light elements (Li and CNO especially), induced by proton captures. In particular, RGB and AGB stars show a wide range of Li abundances. This spread is currently attributed to deep phenomena of non-convective mixing. These processes can, in principle, either produce or destroy Li, depending on their velocity. This is due to the fact that Li production requires preserving the unstable ⁷Be, which has a half-life of only 53 days. Physical mechanisms devised so far to explain the existence of deep mixing in low mass stars generally fail in accounting for fast transport and in avoiding ⁷Be destruction; on the contrary, this is easily obtained in Intermediate Mass Stars, where Hot Bottom Burning can occur. However, as Li-rich low-mass red giants do exist, we propose here a scenario where both production and destruction of Li are possible in LMS, thanks to the buoyancy of magnetized parcels of processed matter, traveling from the H shell to the envelope at different speeds (depending on their size). Consequences of this transport for CNO nuclei are also discussed.

Keywords. Nucleosynthesis – Stars: abundances, AGB, evolution, low-mass, magnetic fields

From the original poloidal field of a rotating star, a toroidal field of similar strength can be generated by the dynamo mechanism (Parker 1974). Indeed, the differential rotation of the external layers wraps the fields, aligning them to the equator (Spruit 1999). Toroidal flux tubes then develop, with their magneto hydrodynamics instabilities, and float to the surface (Spruit & van Ballegoijen 1982). This is so because a pressure term and a tension term (acting as an elastic force) are both created by the magnetic field. Torsion due to the Coriolis force then helps detaching portions of the tubes, or "bubbles". They move outward, with a relatively high speed, close to the Alfvén velocity (Case A; Busso *et al.* 2007). Due to their small size, the bubbles undergo minimal heat exchanges. When the average stellar magnetic field is strong enough to induce the buoyancy of a large portion of a flux tube, the resulting mixing velocity will be reduced (by heat exchanges) down to near the diffusion one (Case B; Palmerini & Busso 2008, Denissenkov *et al.* 2009). Hence magnetic buoyancy offers a scenario for the occurrence of both fast and slow mixing episodes.

A possible scenario for the evolution of the Li abundance in low mass red giants, as a function of their bolometric magnitude, on the basis of a new estimate for their distances and evolutionary status was suggested by Guandalini *et al.* (2009), to which we refer for details. These authors considered a phase of magnetic field growth, at the L-bump, where field strengths were assumed to be not strong enough to promote the buoyancy of entire magnetic flux tubes, but only to generate the intermittent detaching of fast bubbles (Case A). Hence, the induced fast mixing may induce Li enrichment, as shown

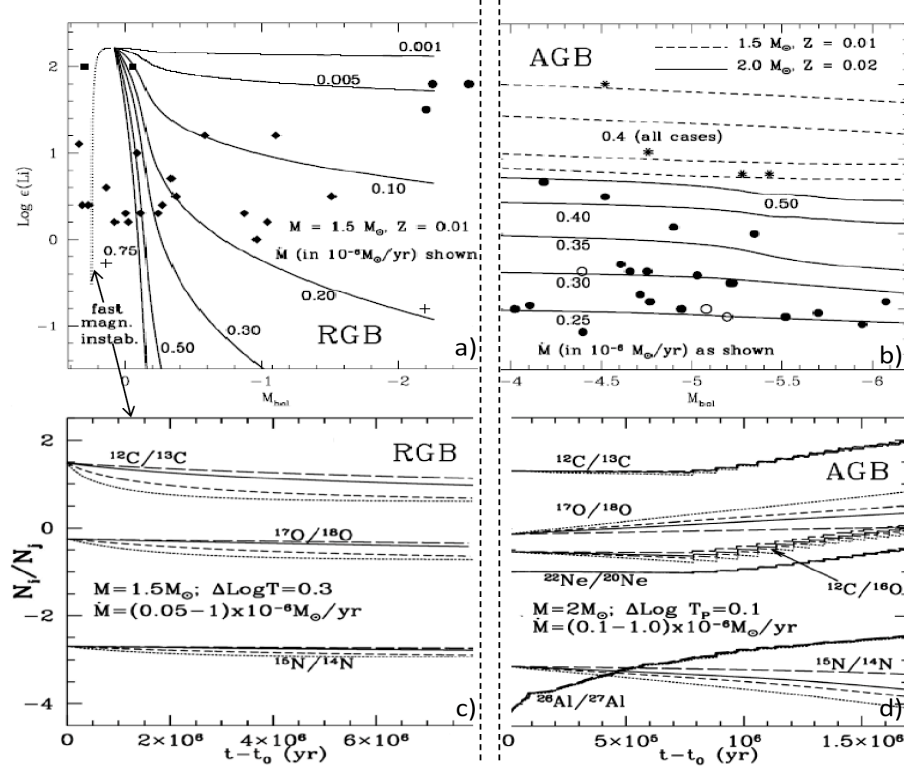


Figure 1. The evolution of Li (upper panels) and CNO isotopic ratios (lower panels) according to mixing cases A and B, see text for details.

by several red giants in this evolutionary phase (Fig.1 panel a). When the fields have grown sufficiently, larger magnetized structures can become buoyant, driving a slower mass circulation (case B), which depletes Li during the rest of the RGB phase and the whole AGB phase (Fig.1 panel a and b). The temporal evolution of Li is accompanied by modifications of CNO isotopic ratios during both fast and slow mixing episodes. Panel c of Fig.1 reports them at different values of the mixing rate (\dot{M}), for a $1.5M_{\odot}$, $Z = Z_{\odot}/2$ RGB model (Palmerini *et al.* 2009). Panel d instead shows temporal evolutions of CNO and Al isotopic ratios, in a $2M_{\odot}$, $Z = Z_{\odot}$ AGB model, due to both slow mixing (case B, at different \dot{M}) and convective third dredge-up, whose contribution results in the step-wise trend of $^{12}\text{C}/^{13}\text{C}$, $^{12}\text{C}/^{16}\text{O}$ and $^{20}\text{Ne}/^{22}\text{Ne}$ ratios.

References

- Busso, M., Wasserburg, G. J., Nollett, K. M., Calandra, A., 2007, *ApJ*, 671, 802
 Denissenkov, P. A., Pinsonneault, M., Mac Gregor K. B. 2009, *ApJ*, 696, 1823
 Guandalini, R., Palmerini, S., Busso, M., Uttenthaler, S. 2009, *PASA*, 26, 168
 Palmerini, S., Busso M., 2008, *New AR*, 52, 412
 Palmerini, S., Busso, M., Maiorca, E., Guandalini, R. 2009, *PASA*, 26, 161
 Parker, E. N. 1974, *ApJSS*, 31, 261
 Spruit, H. C. 1999, *A&A*, 349, 189
 Spruit H. C., van Ballegoijen, A. 1982, *A&A*, 106, 58

Lithium destruction induced by planetary accretion in solar-type stars

Sylvie Théado¹, Elise Bohuon¹, and Sylvie Vauclair¹

¹Laboratoire d'Astrophysique de Toulouse et Tarbes, CNRS, Université de Toulouse ; 14
avenue Edouard Belin, 31400 Toulouse, France
email: sylvie.vauclair@ast.obs-mip.fr

Abstract. Accretion of planetary (metal-rich) material onto a star in its early phases can produce episodes of thermohaline convection below the outer convective zone. These extra-mixing phases lead to rapid lithium destruction. The observed dispersion of lithium abundances in solar-type stars can be related to such events.

Keywords. Stars: abundances

Lithium depletion in solar-type stars remains a challenge for stellar models. Extra-mixing below the outer convective zone is needed to explain the observed abundances in the Sun, the solar analogs and the solar twins (e.g., Do Nascimento et al. 2009). Several processes have been invoked in the past to account for this lithium depletion, like rotational induced mixing, but they fail to account for all the observed features and observed abundance dispersion. Meanwhile recent detailed observations of heavy elements in the Sun and solar-type stars show systematic differences, which lead to the idea that accretion may play an important role in their early phases (e.g. Meléndez et al. 2009).

Although no precise statistics can yet be given, it seems possible that many solar-type stars were born with disks, some of them, but not all, leading to observable planets. According to the parameters of the disk and of the central star, matter with abundances

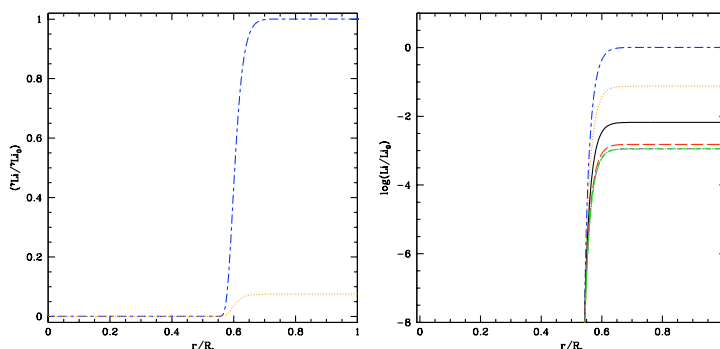


Figure 1. Lithium profiles in $1.10 M_{\odot}$ stars with planetary accretion. The left panel displays the ratio of the lithium mass fraction to its initial value at 2 Myrs (evolution with atomic diffusion, blue line) and 4 Myrs (after the first accretion episode of $0.03 M_{Jup}$, orange line). The right panel presents the same ratio in logarithmic units at 2 Myrs (blue line) and after each accretion episode (at 4, 6, 8, 10 and 12 Myrs). Thermohaline mixing strongly decreases the lithium surface abundance. However the depletion saturates after 4 or 5 events. This occurs when the accreted amount of lithium becomes comparable to the depleted one.

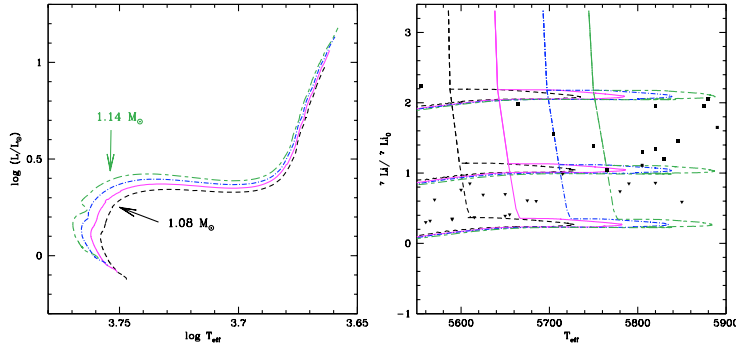


Figure 2. Lithium destruction in stars of various masses : 1.08 (dashed line), 1.10 (solid line), 1.12 (dashed-dotted line) and 1.14 M_\odot (long dashed-dashed line) models. The left panel displays the evolutionary tracks. The right panel shows the lithium abundance variations along the evolutionary tracks, as a function of the effective temperature for the same models, including either one, two, or three accretion events of 0.03 M_{Jup} each. The points correspond to the lithium observations by Israelian et al. (2004).

different from those of the star can be accreted onto it. It may be either disk gaseous matter (metal-poor) or matter already condensed in the form of planetesimals or planets (metal-rich). The idea that such metal rich-accretion could be the reason for the observed metal overabundances in exoplanet-host stars has now been ruled out (e.g. Vauclair et al. 2008). However, such accretion processes can happen, even if it does not lead to observable metal enrichment, and it may have important consequences on the lithium abundances.

Accretion of planetary matter onto a star in its early phases leads to mean molecular weight inversion below the outer convective zone, unstable against thermohaline convection (e.g. Vauclair 2004). Every time the star accretes planetary material, extra mixing induced by this hydrodynamical instability leads to lithium destruction. We first present computations for a 1.10 M_\odot star with $[Fe/H] = 0.20$ suffering 1 to 5 accretion events of 0.03 M_{Jup} beginning at 2 Myrs and occurring every 2 Myrs afterwards. Then we show examples of other stellar masses and other accreted masses. In all these computations, thermohaline mixing is computed as described in Théado et al. (2009a). Clearly such events can completely modify the lithium abundance and its subsequent evolution. More detailed computations will be given in Théado et al. (2009b).

References

- Do Nascimento, J.D., Castro, M., Meléndez, J., Bazot, M., Théado, S., Porto de Mello, G.F. & de Medeiros, J.R. 2009, *A&A*, 501, 687
- Israelian, G., Santos, N.C., Mayor, M. & Rebolo, R. 2004, *A&A*, 414, 601
- Meléndez, J., Asplund, M., Gustafsson, B. & Yong, D. 2009, *ApJ* (Letters), 704, 66
- Théado, S., Vauclair, S., Alecian, G. & LeBlanc, F. 2009a, *ApJ*, 704, 1262
- Théado, S., Bohuon, E. & Vauclair, S. 2009b, *in preparation*
- Vauclair, S. 2004, *ApJ*, 605, 874
- Vauclair, S., Laymand, M., Bouchy, F., Vauclair, G., Hui Bon Hoa, A., Charpinet, S. & Bazot, M. 2008, *A&A* (Letters), 482, 5

Session V

**Evolution of light elements
in the Universe**



Donatella Romano



Patrick Eggenberger

Galactic evolution of D, ^3He and ^4He

Donatella Romano

Dept. of Astronomy, Bologna University,
Via Ranzani 1, I-40127, Bologna, Italy
and

INAF-Bologna Observatory,
Via Ranzani 1, I-40127, Bologna, Italy
email: donatella.romano@oabo.inaf.it

Abstract. The uncertainties which still plague our understanding of the evolution of the light nuclides D, ^3He and ^4He in the Galaxy are described. Measurements of the local abundance of deuterium range over a factor of 3. The observed dispersion can be reconciled with the predictions on deuterium evolution from standard Galactic chemical evolution models, if the true local abundance of deuterium proves to be high, but not too high, and lower observed values are due to depletion onto dust grains. The nearly constancy of the ^3He abundance with both time and position within the Galaxy implies a negligible production of this element in stars, at variance with predictions from standard stellar models which, however, do agree with the (few) measurements of ^3He in planetary nebulae. Thermohaline mixing, inhibited by magnetic fields in a small fraction of low-mass stars, could in principle explain the complexity of the overall scenario. However, complete grids of stellar yields taking this mechanism into account are not available for use in chemical evolution models yet. Much effort has been devoted to unravel the origin of the extreme helium-rich stars which seem to inhabit the most massive Galactic globular clusters. Yet, the issue of ^4He evolution is far from being fully settled even in the disc of the Milky Way.

Keywords. Galaxy: abundances, Galaxy: evolution, nuclear reactions, nucleosynthesis, abundances

1. Introduction

The discovery of the cosmic microwave background (CMB) by Penzias & Wilson (1965) in the mid sixties set the stage for a quantitative exploitation of the Big Bang nucleosynthesis theory. In their pioneer studies, Peebles (1966) and Wagoner et al. (1967) demonstrated that D, ^3He and ^4He could well have been produced in solar-system abundances in the ‘primordial fireball’.

In the framework of the standard Big Bang nucleosynthesis (SBBN) theory, the baryon-to-photon ratio, η , is the only parameter regulating the amounts of D, ^3He and ^4He which emerge from the hot, early Universe (see Fig. 1 and contribution by G. Steigman, this volume). In the nineties, observations, seeking to constrain the primordial abundances of D, ^3He and ^4He – and, hence, the value of η – by probing the most metal-poor environments in the Universe, did not come up with consistent results. Both high and low values were suggested for the primordial deuterium abundance as measured in high-redshift, low-metallicity quasar absorption-line systems (QSOALS), $(\text{D}/\text{H})_{\text{P}} = 2.5 \times 10^{-4}$ (Carswell et al. 1994, Songaila et al. 1994) or a few times 10^{-5} (Burles & Tytler 1998a,b). Similarly, both low and high values were suggested for the primordial ^4He abundance, e.g., $Y_{\text{P}} = 0.234 \pm 0.002$ (Olive et al. 1997) or 0.244 ± 0.002 (Izotov & Thuan 1998).

The difficulty to determine $(\text{D}/\text{H})_{\text{P}}$ from observations led to turn the problem upside down and try to infer that quantity by using Galactic chemical evolution (GCE) models.

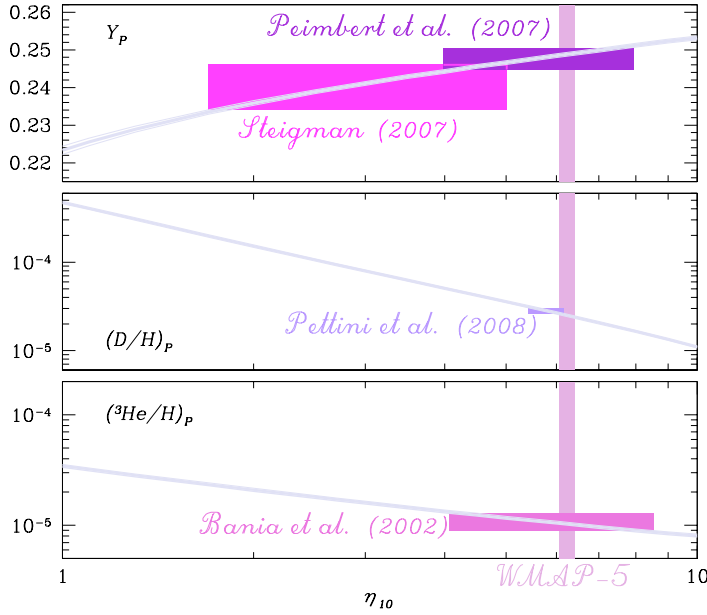


Figure 1. SBBN-predicted primordial mass fraction of ${}^4\text{He}$ (Y_p) and abundances of D and ${}^3\text{He}$ (relative to hydrogen by number), as functions of the η_{10} parameter, $\eta_{10} \equiv 10^{10}(n_B/n_\gamma)$. Theoretical predictions are from Hata et al. (1995), as updated by G. Steigman (courtesy of G. Steigman). The widths of the curves reflect the uncertainties in the nuclear and weak-interaction rates. The vertical band crossing all panels corresponds to the η_{10} value derived from analysis of five-years *WMAP* data on the CMB anisotropy (Dunkley et al. 2009). Also shown are the most recent estimates of the primordial abundances of D, ${}^3\text{He}$ and ${}^4\text{He}$ from observations, along with the allowed ranges of values for η_{10} (boxes; Bania et al. 2002, Peimbert et al. 2007, Steigman 2007, Pettini et al. 2008).

GCE models put stringent limits on the degree of astration suffered by deuterium in the solar vicinity over a Hubble time. Assuming that the local pre-solar (Geiss & Reeves 1972, Geiss & Gloeckler 1998) and current (Linsky 1998) D abundances are reasonably well known, they could settle tight limits to the primordial deuterium abundance, and definitively ruled out a high primordial deuterium.

Modelling the Galactic evolution of deuterium is a straightforward task. Since D is completely destroyed as gas cycles through stars and there are no known sources of substantial production other than BBN (Epstein et al. 1976, Prodanović & Fields 2003), its evolution is obtained for free from GCE models. Good models for the solar neighbourhood – i.e., models which satisfy the majority of the observational constraints available for the solar neighbourhood – have always predicted astration factors $f_D \equiv (D/H)_P/(D/H)_{\text{LISM}}$ not in excess of 2–3 for deuterium (Audouze & Tinsley 1974, Steigman & Tosi 1992, Edmunds 1994, Galli et al. 1995, Prantzos 1996, Tosi et al. 1998, Chiappini et al. 2002, Romano et al. 2003, 2006). Attempts to accommodate larger astration factors (Vangioni-Flam et al. 1994, Scully et al. 1997) have resulted in models which failed to reproduce important observational constraints. Moreover, the more D is burnt in the Galaxy, the more ${}^3\text{He}$ is produced. Since the abundance of ${}^3\text{He}$ is observed to stay rather constant with both

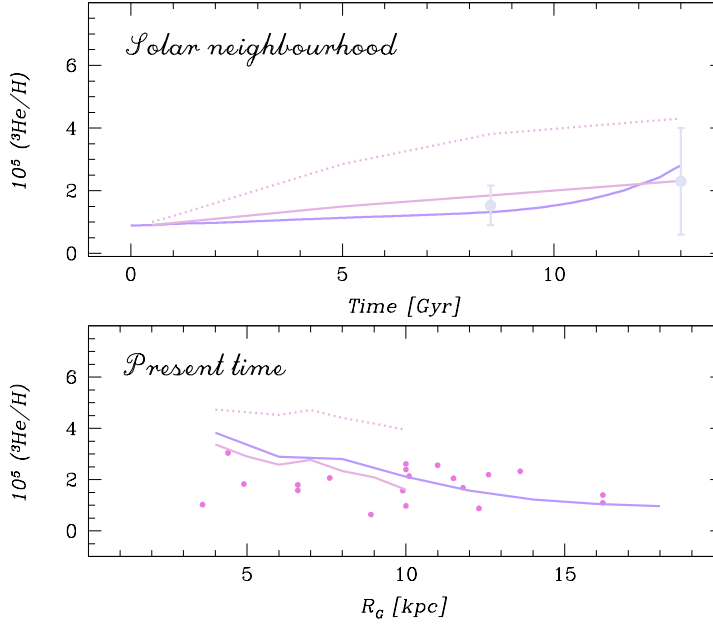


Figure 2. Evolution of ${}^3\text{He}/\text{H}$ in the solar neighbourhood (upper panel) and distribution of ${}^3\text{He}/\text{H}$ across the Galactic disc at the present time (lower panel) for different GCE models, assuming either $(D/H)_P = 2.5 \times 10^{-5}$ (solid lines) or $(D/H)_P = 20 \times 10^{-5}$ (dotted lines). All models assume zero net production of ${}^3\text{He}$ from 93% of low-mass stars ($1-2 M_\odot$) in order to fit the observations (filled circles; upper panel: local pre-solar and current values from Geiss & Gloeckler 1998; lower panel: H II region abundances from Bania et al. 2002). Figure adapted from Romano et al. (2003).

time and position in the Milky Way (Bania et al. 2002), GCE models which overproduce this isotope must be discarded.

As first recognized by Truran & Cameron (1971), GCE models adopting standard prescriptions for the synthesis of ${}^3\text{He}$ in stars dramatically overestimate its abundance in the Milky Way (see also Rood et al. 1976). According to standard stellar models, ${}^3\text{He}$ is most efficiently produced on the main sequence (MS) of $1-2 M_\odot$ stars through the action of the p-p chains. In order not to overproduce ${}^3\text{He}$ in the course of Galactic evolution, it has become customary to assume that some unknown ${}^3\text{He}$ -destruction mechanism is at work in more than 90% of low-mass stars (Dearborn et al. 1996, Galli et al. 1997, Chiappini et al. 2002, Romano et al. 2003). Hogan (1995) and Charbonnel (1995) have suggested ‘extra mixing’ during the red giant branch (RGB) phase of low-mass stars as a possible solution (see also Charbonnel & Do Nascimento 1998, Sackmann & Boothroyd 1999). In Fig. 2, we compare the predictions of two successful models for the chemical evolution of the Milky Way (the one by Chiappini et al. 2002 and Model 1 of Tosi 1988) to ${}^3\text{He}$ data for the solar neighbourhood (upper panel) and the Galactic disc (lower panel). Despite different assumptions about the infall law, star formation rate and stellar initial mass function (IMF), both models need to assume that at least 93% of low-mass stars burn the ${}^3\text{He}$ they have produced on the MS in later evolutionary phases in order to fit the

Table 1. Abundances of D, ^3He and ^4He at different epochs

Nuclide	Units	SBBN+ <i>WMAP</i> ^a (13.7 Gyr ago)	Low- <i>Z</i> systems (10–13 Gyr ago)	Pre-solar matter (4.5 Gyr ago)	LISM (Today)
D	10 ⁵ (D/H)	2.49 ± 0.17 ⁽¹⁾	2.8 ± 0.2 ⁽²⁾	2.1 ± 0.5 ⁽³⁾	2.31 ± 0.24 ⁽⁴⁾ 0.98 ± 0.19 ⁽⁵⁾ 2.0 ± 0.1 ⁽⁶⁾
^3He	10 ⁵ ($^3\text{He}/\text{H}$)	1.00 ± 0.07 ⁽¹⁾	1.1 ± 0.2 ⁽⁷⁾	1.5 ± 0.2 ⁽³⁾	2.4 ± 0.7 ⁽⁸⁾
^4He	Y	0.2486 ± 0.0002 ⁽¹⁾	0.2477 ± 0.0029 ⁽⁹⁾ 0.240 ± 0.006 ⁽¹⁰⁾	0.2703 ⁽¹¹⁾	

Notes:

^a Using $\eta_{10} = 6.23 \pm 0.17$ from analysis of 5-years *WMAP* data (Dunkley et al. 2009).

References:

(1) Cyburt et al. (2008); (2) Pettini et al. (2008); (3) Geiss & Gloeckler (1998); (4) Linsky et al. (2006); (5) Hébrard et al. (2005); (6) Prodanović et al. (2009); (7) Bania et al. (2002); (8) Gloeckler & Geiss (1996); (9) Peimbert et al. (2007); (10) Steigman (2007); (11) Asplund et al. (2009).

observations. It is worth noticing that the good agreement between model predictions and observations depends also on the adopted value of the primordial deuterium abundance: if $(\text{D}/\text{H})_{\text{P}} = 20 \times 10^{-5}$, rather than 2.5×10^{-5} (dotted versus solid lines in Fig. 2), both the local behaviour of ^3He with time and its present distribution across the Galactic disc can not be reproduced by the models, independently of how many low-mass stars burn their ^3He on the RGB.

As far as ^4He is concerned, there has been a general consensus that the relative helium-to-metal enrichment ratio in the solar neighbourhood is $\Delta Y/\Delta Z \sim 2$, both from a theoretical (Chiosi & Matteucci 1982, Maeder 1992, Chiappini et al. 2003) and an observational point of view (e.g., Casagrande et al. 2007). Yet, hints for very different values of this ratio were reported early on in the literature (Danziger 1970, and references therein).

The determination of the parameter η from *WMAP* data (see text by J. Dunkley, this volume) has allowed to fix, with unprecedented precision, the primordial abundances of the light elements in the framework of the SBBN model (see Cyburt et al. 2008 for recent work). The primordial abundances of D, ^3He and ^4He determined indirectly from the CMB anisotropies agree very well with those inferred from recent, direct observations (see Fig. 1 and Table 1), although one must be aware that the latter actually provide only lower/upper limits to the true primordial abundances. Above all, it is clear that the determination of the primordial abundance of deuterium is converging towards a low value, beautifully confirming earlier findings from GCE models.

In the following sections, the remaining (major) causes of uncertainty, which hamper our current understanding of the Galactic chemical evolution of the light elements D, ^3He and ^4He , are discussed, element by element.

2. Deuterium

The joint determinations of the primordial and pre-solar deuterium abundances (Table 1) point to a small depletion of deuterium from the Big Bang up to the solar system formation 4.5 Gyr ago. However, the present-day abundance of deuterium in the solar vicinity is currently under debate. The *FUSE* satellite has measured the deuterium abundance along the lines of sight to several stars in the Local Bubble as well as beyond it, up to 1–2 kpc away. The dispersion (by a factor of 3) which has been found in the measurements (Linsky et al. 2006) makes it hard to interpret the data in the context of standard GCE models. It has been suggested (Hébrard et al. 2005, Linsky et al. 2006) that either the lowest (see also text by G. Hébrard, this volume) or the highest (see also text by J. Linsky, this volume) observed abundances are indicative of the actual value of

the deuterium abundance in the local ISM (LISM). However, neither of these values can be reproduced by GCE models in agreement with all the major observational constraints for the solar neighbourhood (Romano et al. 2006). Very recently, using a Bayesian analysis approach, Prodanović et al. (2009) have provided another estimate of the true LISM deuterium abundance, which places it very close to the D abundance at the time of the formation of the Sun (see Table 1).

In Fig. 3 we show the evolution of deuterium in the solar vicinity and the deuterium abundance profile across the Milky Way disc. The adopted GCE model, from Romano et al. (2006), is the one which allows for the lowest D astration factor in the solar vicinity ($f_D = 1.39$). Here it has been recomputed assuming $(\text{D}/\text{H})_P = 2.8 \times 10^{-5}$ rather than 2.6×10^{-5} as in Romano et al. (2006). Extrapolation of the theoretical results towards the Galaxy center has been performed by taking into account the detailed results of a model for the Galactic bulge by Matteucci et al. (1999). Data are from Table 1 for local values (at a radius $R_G = 8$ kpc), from Rogers et al. (2005) for the outer disc and from Lubowich et al. (2000) for a region at 10 pc distance from the Galactic center.

The agreement of the model predictions with the data is striking, especially if the true value for the local abundance of deuterium is the one suggested by Prodanović et al. (2009; see also contribution by T. Prodanović, this volume). In this context, lower observed local abundances of deuterium would be due to D depletion onto dust grains

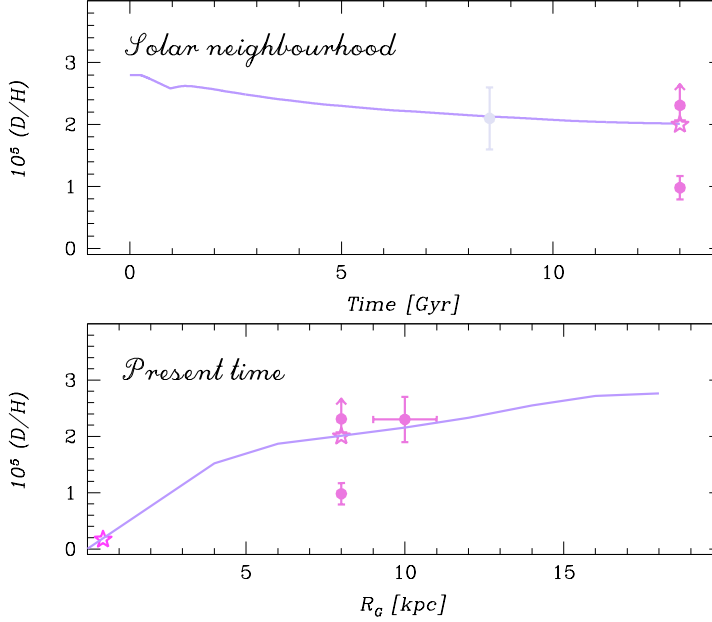


Figure 3. Evolution of D/H in the solar neighbourhood (upper panel) and distribution of D/H across the Galactic disc at the present time (lower panel) for the GCE model (solid lines in both panels) of Romano et al. (2006) with the lowest D astration factor, assuming $(\text{D}/\text{H})_P = 2.8 \times 10^{-5}$. Data are from Table 1 for local values, from Rogers et al. (2005) for the outer disc (filled circle at $R_G = 10 \pm 1$ kpc, bottom panel) and from Lubowich et al. (2000) for the inner Galaxy (star at $R_G = 10$ pc, bottom panel).

(Linsky et al. 2006, Steigman et al. 2007, and references therein). The highest observed local D values are marginally consistent with the estimate of the true D value by Prodanović et al. (2009).

3. Helium-3

As far as ^3He is concerned, we must recognize that the problems raised in pioneering works by people such as Truran & Cameron (1971), Reeves et al. (1973) and Tinsley (1974) (to name a few) are still unsolved: we must postulate that some unknown ^3He -destruction mechanism is at work in not less than 90% of low-mass stars in order not to overproduce ^3He in the course of Galactic evolution (see discussion in Sect. 1). But which is the physical mechanism responsible for that? In a coherent picture, one must also be able to explain the existence of a few planetary nebulae (PNe) with high ^3He content, consistent with predictions from standard stellar models (e.g., Balser et al. 1999). Recently, the inclusion of thermohaline mixing in detailed stellar evolutionary models (Charbonnel & Zahn 2007) has shown that this is likely to be the ‘extra mixing’ mechanism we have been searching for years. Indeed, thermohaline mixing is able to efficiently destroy ^3He on the RGB of low-mass ($1\text{--}2\text{ M}_\odot$) stars, when not inhibited by magnetic fields. Details on this interesting process can be found in the contribution by N. Lagarde and C. Charbonnel to these conference proceedings (see also text by R. Stancliffe, this volume). The expected output of stellar models including thermohaline mixing are complete grids of yields. New GCE models computed with such new yields will hopefully lead the so-called ^3He problem to an end.

4. Helium-4

As far as ^4He is concerned, there are many open issues to be discussed.

First of all, it is worth stressing that, when dealing with the evolution of ^4He in the Galactic disc, we can rely on only a few data (see also M. Peimbert et al., this volume), namely, the abundance of ^4He in the Sun at the time of its birth, which is by now quite well established (Asplund et al. 2009), the abundance of ^4He in M 17, an H II region located in the inner Galaxy, and the helium-to-metal enrichment ratio as derived from nearby K-dwarf stars. The latter quantity, however, is affected by a rather large error and can only be trusted around solar metallicity (see Casagrande et al. 2007 and contribution by L. Casagrande, this volume).

Fig. 4 shows the behaviour of Y as a function of metallicity [10^6 (O/H)] in the solar neighbourhood, as predicted by the two-infall model of Chiappini et al. (1997). The model has been computed with different prescriptions on the stellar yields and primordial mass fraction of ^4He (see figure caption for details). Although the models adopting the ^4He yields from rotating, mass-losing stellar models (Fig. 4, dotted and dashed lines) provide a good fit to the available solar neighbourhood data, performing definitely better than the model using stellar yields without stellar rotation and mass loss (Fig. 4, solid line), it has to be reminded that the data for M 17 cannot be satisfactorily reproduced by any GCE model yet (see M. Peimbert et al., this volume, their figure 1).

Another debated topic is the extreme He enhancement in Galactic globular clusters (GCs). The presence of multiple MSs in the GCs $\omega\text{ Cen}$ and NGC 2808 (Piotto et al. 2005, 2007), indeed, is most convincingly explained in terms of an extreme He enhancement of the bluest MS population (Norris 2004). Helium abundances as high as $Y \sim 0.4$ are suggested, which for $\omega\text{ Cen}$ imply a helium-to-metal enrichment ratio $\Delta Y/\Delta Z \geq 70$ (Piotto et al. 2005). Such a value is outstandingly larger than that quoted for the solar

neighbourhood around and above solar metallicity from a sample of nearby K-dwarf stars, $\Delta Y/\Delta Z = 2.1 \pm 0.9$ (Casagrande et al. 2007). Attempts have been made to explain such extreme ^4He abundances in the framework of two main competing scenarios, the so-called ‘asymptotic giant branch (AGB) self-pollution scenario’ (P. Ventura, this volume) and the so-called ‘fast rotating massive star (FRMS) self-pollution scenario’ (T. Decressin, this volume). Both scenarios have to reproduce other chemical peculiarities of GC stars besides the ‘anomalous’ ^4He abundances, and both have advantages and disadvantages. As a common limitation, they are presently able to deal only with two-population clusters. However, in ω Cen – the object for which the most compelling evidence for the need for a *huge* helium enrichment is found – there is clear-cut evidence of the presence of complex, multiple populations (e.g., Pancino et al. 2000). We (Romano et al. 2010) have recently proposed that the presence of extreme He-rich stars in ω Cen can be explained in the context of a model where the cluster is the remnant of a much more massive parent system, that evolved in isolation for a relatively long time – 3 Gyr, with the bulk of the stars forming during the first 1 Gyr. The system was then captured and partially disrupted by the Milky Way (see contribution by D. Romano et al., this volume). The

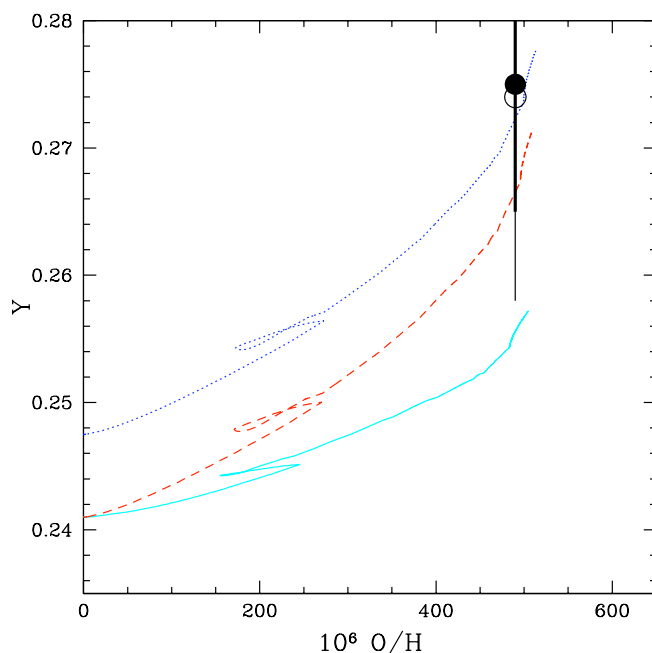


Figure 4. Y versus $10^6 (O/H)$ in the solar neighbourhood predicted by the *two-infall* model of Chiappini et al. (1997) with different prescriptions on the stellar nucleosynthesis. Solid line: the model adopts the van den Hoek & Groenewegen (1997) yields for low- and intermediate-mass stars and the Woosley & Weaver (1995) yields for massive stars; dashed line: the model is computed with the yields of Meynet & Maeder (2002), taking into account the effects of rotation on stellar evolution, for the whole range of stellar masses; dotted line: same model as the previous one, but starting from a higher primordial ^4He abundance, $Y_P = 0.248$ rather than 0.241. The model predictions are compared with the solar value (oxygen from Allende-Prieto et al. 2001, Y from Anders & Grevesse 1989 – open circle with thin errorbar – and Grevesse & Sauval 1998 – filled circle with thick errorbar). Figure from Chiappini et al. (2003).

key ingredient in our model is the development of a differential galactic wind, which selectively removes from the progenitor galaxy mostly the elements restored to the ISM through fast polar winds from massive stars and supernova (SN) explosions. Elements restored to the ISM through gentle winds from both AGB and FRMSs are, instead, mostly retained in the cluster potential well, where they enter the formation of successive stellar generations. Since, according to the latest stellar evolutionary computations, ^4He is dispersed in the ISM by means of low-energy stellar winds by both AGBs and FRMSs, while metals are mostly expelled through SN explosions, a high $\Delta Y/\Delta Z$ is naturally obtained in the framework of our model. Other important observational constraints can also be satisfactorily reproduced.

Since differential galactic winds do, as a matter of fact, modify somewhat arbitrarily the true (effective) yields of the various elements, a better assessment of the stellar yields of ^4He is mandatory.

Finally, it is worth reminding that the usually quoted value of $Y \sim 0.4$ for the extreme He-rich GC stars could be revised downwards to as low as $Y \sim 0.3$ (L. Casagrande, this volume).

5. Conclusions

We have reviewed the evolution of the light elements D, ^3He and ^4He in the Milky Way, emphasizing recent developments and open problems. We summarize our conclusions as follows:

(a) GCE models are consistent with the relatively high value of $(\text{D}/\text{H})_{\text{LISM}} = (2.0 \pm 0.1) \times 10^{-5}$ suggested by Prodanović et al. (2009) from their Bayesian analysis of *FUSE* data. Standard GCE models are instead unable to explain values of $(\text{D}/\text{H})_{\text{LISM}}$ significantly higher/lower than this.

(b) The need for some 'extra mixing' to destroy ^3He in most ($> 90\%$) of 1-2 M_{\odot} stars came from GCE arguments more than 30 years ago. The way to the understanding of the physical processes underlying this assumption has been a long one, but now thermohaline mixing seems to be a good candidate to solve the long-standing issue of ^3He evolution. Stellar yields taking this mechanism into account are needed for use in GCE models.

(c) It is still debated whether the chemical peculiarities seen in a fraction of Galactic globular cluster stars – first of all an impressive helium enrichment – are due to self-pollution from AGBs or FRMSs. In the very peculiar case of ω Cen, which likely suffered a complicated star formation history as the nucleus of a larger system, both stellar categories should have polluted the ISM. In such a scenario, the observed chemical 'anomalies' would be driven by the action of differential galactic outflows, venting out preferentially metals. However, it is still unclear if such an extreme scenario could apply to other GCs as well.

Acknowledgements

I thank the organizers for their kind invitation and for giving me the opportunity to attend such a lively conference. I would like to express my gratitude to Francesca Matteucci and Monica Tosi for advice over the years, and to Johannes Geiss and Gary Steigman for helpful discussions. Generous financial support from IAU is also gratefully acknowledged. The author's research at Bologna University is supported by Italian MIUR under grant PRIN 2007, prot. 2007JJC53X_001.

References

- Allende-Prieto, C., Lambert, D.L., & Asplund, M. 2001, *ApJ*, 556, L63
- Anders, E., & Grevesse, N. 1989, *Geochim. Cosmochim. Acta*, 53, 197
- Asplund, M., Grevesse, N., Sauval, A.J., & Scott, P. 2009, *ARA&A*, 47, 481
- Audouze, J., & Tinsley, B.M. 1974, *ApJ*, 192, 487
- Balser, D., Rood, R.T., & Bania, T.M. 1999, *ApJ*, 522, L73
- Bania, T.M., Rood, R.T., & Balser, D.S. 2002, *Nature*, 415, 54
- Burles, S., & Tytler, D. 1998a, *ApJ*, 499, 699
- Burles, S., & Tytler, D. 1998b, *ApJ*, 507, 732
- Carswell, R.F., Rauch, M., Weymann, R.J., Cooke, A.J., & Webb, J.K. 1994, *MNRAS*, 268, L1
- Casagrande, L., Flynn, C., Portinari, L., Girardi, L., & Jimenez, R. 2007, *MNRAS*, 382, 1516
- Charbonnel, C. 1995, *ApJ*, 453, L41
- Charbonnel, C., & Do Nascimento, J.D., Jr. 1998, *A&A*, 336, 915
- Charbonnel, C., & Zahn, J.-P. 2007, *A&A*, 467, L15
- Chiappini, C., Matteucci, F., & Gratton, R. 1997, *ApJ*, 477, 765
- Chiappini, C., Matteucci, F., & Meynet, G. 2003, *A&A*, 410, 257
- Chiappini, C., Renda, A., & Matteucci, F. 2002, *A&A*, 395, 789
- Chiosi, C., & Matteucci, F. 1982, *A&A*, 105, 140
- Cybert, R.H., Fields, B.D., & Olive, K.A. 2008, *JCAP*, 11, 012
- Danziger, I.J. 1970, *ARA&A*, 8, 161
- Dearborn, D.S.P., Steigman, G., & Tosi, M. 1996, *ApJ*, 465, 887
- Dunkley, J., et al. 2009, *ApJS*, 180, 306
- Edmunds, M.G. 1994, *MNRAS*, 270, L37
- Epstein, R.I., Lattimer, J.M., & Schramm, D.N. 1976, *Nature*, 263, 198
- Galli, D., Palla, F., Ferrini, F., & Penco, U. 1995, *ApJ*, 443, 536
- Galli, D., Stanghellini, L., Tosi, M., & Palla, F. 1997, *ApJ*, 477, 218
- Geiss, J., & Gloeckler, G. 1998, *Space Sci. Rev.*, 84, 239
- Geiss, J., & Reeves, H. 1972, *A&A*, 18, 126
- Gloeckler, G., & Geiss, J. 1996, *Nature*, 381, 210
- Grevesse, N., & Sauval, A.J. 1998, *Space Sci. Rev.*, 85, 161
- Hata, N., Scherrer, R.J., Steigman, G., Thomas, D., Walker, T.P., Bludman, S., & Langacker, P. 1995, *Phys. Rev. Lett.*, 75, 3977
- Hébrard, G., Tripp, T.M., Chayer, P., Friedman, S.D., Dupuis, J., Sonnentrucker, P., Williger, G.M., & Moos, M.W. 2005, *ApJ*, 635, 1136
- Hogan, G. 1995, *ApJ*, 441, L17
- Izotov, Y.I., & Thuan, T.X. 1998, *ApJ*, 500, 188
- Linsky, J.L. 1998, *Space Sci. Rev.*, 84, 285
- Linsky, J.L., et al. 2006, *ApJ*, 647, 1106
- Lubowich, D.A., Pasachoff, J.M., Balonek, T.J., Millar, T.J., Tremonti, C., Roberts, H., & Galloway, R.P. 2000, *Nature*, 405, 1025
- Maeder, A. 1992, *A&A*, 264, 105
- Meynet, G., & Maeder, A. 2002, *A&A*, 390, 561
- Matteucci, F., Romano, D., & Molaro, P. 1999, *A&A*, 341, 458
- Norris, J.E. 2004, *ApJ*, 612, L25
- Olive, K.A., Skillman, E., & Steigman, G. 1997, *ApJ*, 483, 788
- Pancino, E., Ferraro, F.R., Bellazzini, M., Piotto, G., & Zoccali, M. 2000, *ApJ*, 534, L83
- Peebles, P.J.E. 1966, *Phys. Rev. Lett.*, 16, 410
- Peimbert, M., Luridiana, V., & Peimbert, A. 2007, *ApJ*, 666, 636
- Penzias, A.A., & Wilson, R.W. 1965, *ApJ*, 142, 419
- Pettini, M., Zych, B.J., Murphy, M.T., Lewis, A., & Steidel, C.C. 2008, *MNRAS*, 391, 1499
- Piotto, G., et al. 2005, *ApJ*, 621, 777
- Piotto, G., Bedin, L.R., Anderson, J., King, I.R., Cassisi, S., Milone, A.P., Villanova, S., Pietrinferni, A., & Renzini, A. 2007, *ApJ*, 661, L53
- Prantzos, N. 1996, *A&A*, 310, 106

- Prodanović, T., & Fields, B.D. 2003, *ApJ*, 597, 48
- Prodanović, T., Steigman, G., & Fields, B.D. 2009, preprint (arXiv:0910.4961)
- Reeves, H., Audouze, J., Fowler, W.A., & Schramm, D.N. 1973, *ApJ*, 179, 909
- Rogers, A.E.E., Dudevoir, K.A., Carter, J.C., Fanous, B.J., Kratzenberg, E., & Bania, T.M. 2005, *ApJ*, 630, L41
- Romano, D., Tosi, M., Matteucci, F., & Chiappini, C. 2003, *MNRAS*, 346, 295
- Romano, D., Tosi, M., Chiappini, C., & Matteucci, F. 2006, *MNRAS*, 369, 295
- Romano, D., Tosi, M., Cignoni, M., Matteucci, F., Pancino, E., & Bellazzini, M. 2010, *MNRAS*, in press (arXiv:0910.1299)
- Rood, R.T., Steigman, G., & Tinsley, B.M. 1976, *ApJ*, 207, L57
- Sackmann, I.-J., & Boothroyd, A.I. 1999, *ApJ*, 510, 217
- Scully, S., Cassé, M., Olive, K.A., & Vangioni-Flam, E. 1997, *ApJ*, 476, 521
- Songaila, A., Cowie, L.L., Hogan, C.J., & Rugers, M. 1994, *Nature*, 368, 599
- Steigman, G. 2007, *Annu. Rev. Nucl. Part. Sci.*, 57, 463
- Steigman, G., & Tosi, M. 1992, *ApJ*, 401, 150
- Steigman, G., Romano, D., & Tosi, M. 2007, *MNRAS*, 378, 576
- Tinsley, B.M. 1974, *ApJ*, 192, 629
- Tosi, M. 1988, *A&A*, 197, 33
- Tosi, M., Steigman, G., Matteucci, F., & Chiappini, C. 1998, *ApJ*, 498, 226
- Truran, J.W., & Cameron, A.G.W. 1971, *Ap&SS*, 14, 179
- van den Hoek, L.B., & Groenewegen, M.A.T. 1997, *A&AS*, 123, 305
- Vangioni-Flam, E., Olive, K.A., Prantzos, N. 1994, *ApJ*, 427, 618
- Wagoner, R.V., Fowler, W.A., & Hoyle, F. 1967, *ApJ*, 148, 3
- Woosley, S.E., & Weaver, T.A. 1995, *ApJS*, 101, 181

Thermohaline mixing in stars : solving the long-standing ^3He problem

Corinne Charbonnel^{1,2} and Nadège Lagarde¹

¹Geneva Observatory, University of Geneva

Chemin des Maillettes 51, 1290 Versoix, Switzerland

email: Corinne.Charbonnel@unige.ch, Nadege.Lagarde@unige.ch

²CNRS UMR 5572, Toulouse University

14, av.E.Belin, 31400 Toulouse, France

Abstract. Thermohaline mixing has been recently identified as the dominating process that governs the photospheric composition of low-mass bright giant stars (Charbonnel & Zahn 2007a). Here we present the predictions of stellar models computed with the code STAREVOL that takes into account this mechanism together with rotational mixing and atomic diffusion. We compare our theoretical predictions with recent observations and discuss how the corresponding yields for ^3He are compatible with the observed behaviour of this light element in our Galaxy.

Keywords. Hydrodynamics, instabilities, Stars: abundances, evolution, rotation, Galaxy: abundances

1. The “ ^3He problem”

The classical theory of stellar evolution predicts a very simple Galactic destiny to ^3He , dominated by a large production of this isotope by low-mass stars (Iben 1967; Rood 1972; Rood et al. 1976; Dearborn et al. 1996; Weiss et al. 1996). As a consequence, one expects a large increase of ^3He with time in the Galaxy with respect to its primordial abundance (e.g., Tosi 1996). However, the ^3He content of Galactic HII regions (Balser et al. 1994, 1999; Bania et al. 1997, 2002) is very similar to that of the Sun and solar system (Geiss & Reeves 1972; Geiss 1993; Mahaffy et al. 1998), and very close to the BBN value (Coc et al. 2004; Cyburt 2004; Serpico et al. 2004). This is the so-called “ ^3He problem” that could be resolved if only $\sim 10\%$ or less of the low-mass stars were releasing ^3He as predicted by classical stellar theory (Tosi 1998, 2000; Palla et al. 2000; Charbonnel 2002; Romano et al. 2003).

Charbonnel & Zahn (2007a) showed that thermohaline mixing drastically reduces the ^3He production in low-mass, low-metallicity stars. Simultaneously, this mechanism changes the surface carbon isotopic ratio as well as the abundances of lithium, carbon and nitrogen.

2. Stellar models including thermohaline convection, rotation-induced mixing, and atomic diffusion

Here we present the predictions of new stellar models computed with the code STAREVOL for solar metallicity and stellar masses between 1 and 4 M_{\odot} . Computations include the transport of chemical species in the radiative regions due to thermohaline instability, rotational mixing, and atomic diffusion. For thermohaline transport we use the diffusion coefficient advocated by Charbonnel & Zahn (2007a) based on Ulrich (1972) arguments

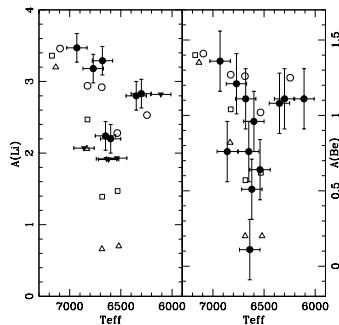


Figure 1. Li and Be abundances in IC 4651 main sequence and turnoff stars (black points and triangles for actual determinations and upper limits respectively). Open circles, squares, and triangles show model predictions for initial rotation velocities of 50, 80, and 110 km s^{-1} respectively. On the cool side of the Li and Be dip the model with $T_{\text{eff}} \sim 6250$ K is from Talon & Charbonnel (2005) and takes into account additional transport of angular momentum by internal gravity waves. Adapted from Smiljanic et al. (2009b)

for the aspect ratio of the salt fingers as supported by laboratory experiments (Krishnamurti 2003) and on Kippenhahn et al. (1980) extended expression for the case of a non-perfect gas. The evolution of the internal angular momentum profile and the associated transport of chemicals are accounted for with the complete formalism developed by Zahn (1992) and Maeder & Zahn (1998) that takes into account advection by meridional circulation and diffusion by shear turbulence (see Palacios et al. 2003, 2006, and Decressin et al. 2009 for a description of the implementation in STAREVOL). Typical initial (i.e., ZAMS) surface rotation velocities are chosen for all the models depending on the stellar mass. We assume magnetic braking on the early main sequence for the stars with T_{eff} on the ZAMS lower than ~ 6900 K that have relatively thick convective envelopes (Talon & Charbonnel 1998). The adopted braking law follows the description of Kawaler (1988). Rotational velocity further decreases when the stars evolve on the subgiant branch due to radius expansion. Atomic diffusion is included in the form of gravitational settling as well as that related to thermal gradients, using the formulation of Paquette et al. (1986).

3. Model predictions for the surface abundances

The model predictions for the evolution of the surface abundances of various species have been validated all along the evolutionary sequence. They reproduce for example very nicely the surface abundances of Li and Be along the colour-magnitude diagram of the open cluster IC 4651 as shown in Fig.1 and 2. Note that thermohaline mixing is efficient only when RGB stars reach the so-called bump in the luminosity function, which is located at $T_{\text{eff}} \sim 4200$ K in the present case. For stars less evolved than the bump as those shown in both figures, the Li and Be behaviours are thus dictated by rotation-induced mixing (see Smiljanic et al. 2009b for more details and Smiljanic et al., this volume; see also Charbonnel & Talon 1999 and Palacios et al. 2003).

Predictions for the evolution of the surface carbon isotopic ratio are shown in Fig. 3 for models of 1.25 and 2 M_{\odot} stars, and compared with observations in the open cluster M67 (turnoff mass $\sim 1.2 M_{\odot}$). We note that rotation-induced mixing on the main sequence slightly lowers the post-dredge-up $^{12}\text{C}/^{13}\text{C}$ value compared to the classical case (i.e., no rotation, diffusion, nor thermohaline mixing). At the luminosity of the bump

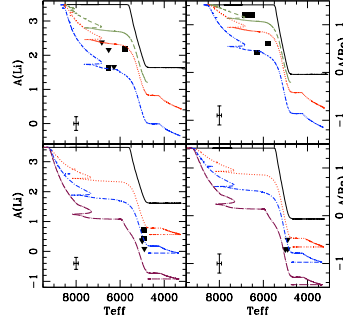


Figure 2. Li and Be abundances in IC 4651 evolved stars. Theoretical predictions for 1.8 and 2 M_{\odot} models are compared to observations of subgiant and giant stars (upper and lower pannels respectively). Solid lines are for the classical case. Other lines correspond to different initial rotation velocities (80, 110, and 180 km s^{-1} for the 1.8 M_{\odot} star; 110, 180, and 250 km s^{-1} for the 2.0 M_{\odot} star). Adapted from Smiljanic et al. (2009b)

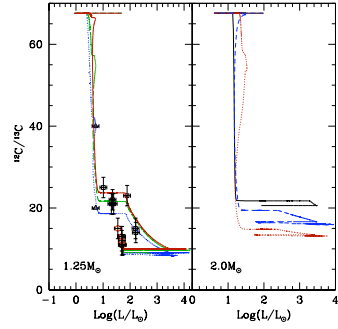


Figure 3. Evolution of the surface $^{12}\text{C}/^{13}\text{C}$ value as a function of stellar luminosity for models of 1.25 and 2 M_{\odot} stars (left and right respectively). Different tracks are for different initial rotation velocities (50, 80, and 110 km.s^{-1} for the 1.25 M_{\odot} star, and 0, 110, and 250 km.s^{-1} for the 2 M_{\odot} star). Observations by Gilroy & Brown (1991) in evolved stars of the open cluster M67 (turnoff mass $\sim 1.2 M_{\odot}$) are also shown (triangle, squares, and circles for subgiant, RGB, and clump stars respectively). Adapted from Lagarde & Charbonnel (in preparation)

($\log(L/L_{\odot}) \sim 2$ for the 1.25 M_{\odot} star), thermohaline mixing leads to further decrease of the carbon isotopic ratio, in excellent agreement with M67 data. In the case of the 2 M_{\odot} star, thermohaline mixing becomes efficient at the bump in the luminosity function only when rotation in earlier phases is accounted for. Importantly we note that at solar metallicity, the $^{12}\text{C}/^{13}\text{C}$ values reached when thermohaline mixing ceases are higher than in the case of metal-poor stars where the carbon isotopic ratios almost always reach the equilibrium value (see Fig. 3 of Charbonnel & Zahn 2007a). This metallicity-dependence is in perfect agreement with the observational behaviour (see Fig. 1 of Charbonnel & Do Nascimento 1998).

In Fig. 4 we show the predictions for the $^{12}\text{C}/^{13}\text{C}$ surface ratio at the tip of the RGB and of the AGB for our models over the whole considered mass range and compare them with observations in stars belonging to open clusters of various turnoff masses. We see that in models for stars with masses below $\sim 1.7 M_{\odot}$, thermohaline mixing is the main physical process governing the photospheric composition of evolved giants, while rotation

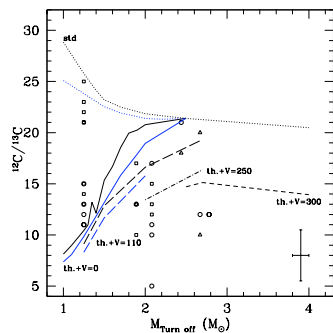


Figure 4. Theoretical predictions compared with observations of $^{12}\text{C}/^{13}\text{C}$ in open clusters spanning a large turnoff mass range. Data are from Smiljanic et al. (2009a) and Gilroy & Brown (1991). Squares, triangles and circles are for RGB, clump, and early-AGB stars respectively. Typical observational errors are indicated. Classical models (i.e., non-rotating and without thermohaline mixing) are shown as dotted lines. The solid lines are for models including thermohaline mixing only, while all the other models include rotation-induced mixing (with initial rotation velocities as indicated), thermohaline convection, and atomic diffusion. Black and blue lines correspond to model predictions at the tip of the RGB and AGB respectively. Adapted from Lagarde & Charbonnel (in preparation)

plays only a minor role on the red giant branch (see Palacios et al. 2006). In fact, the thermohaline diffusion coefficient at the RGB bump is several order of magnitudes higher than the total rotation-induced diffusion coefficient.

For more massive stars, thermohaline mixing occurs in the advanced phases when rotation-induced mixing is accounted for, but in a much less efficient manner. In this case, the final carbon isotopic ratio depends mainly on rotation-induced mixing on the main sequence that modifies the abundance profiles, and in particular the ^{13}C peak inside the stars, before the occurrence of the first dredge-up. Overall, the present models explain very well the observed abundance patterns over the considered mass range.

4. Model predictions for ^3He

On the main sequence, a ^3He peak builds up due to pp-reactions inside low-mass stars (Iben 1967), and is engulfed in the stellar envelope during the first dredge-up. As a consequence the surface abundance of ^3He strongly increases on the lower RGB as can be seen in Fig. 5 for various stellar masses. Its value reaches a maximum when the whole peak is engulfed. After the first dredge-up, the temperature at the base of the convective envelope is too low for ^3He to be nuclearly processed. As a result in canonical models this fresh ^3He is preserved until the ejection of the planetary nebula when it is released into the interstellar matter. This classical view is however contradicted by observations and chemical evolution models as discussed in § 1.

After the bump however, thermohaline mixing brings ^3He from the convective envelope down to the hydrogen-burning shell where it burns. This leads to a rapid decrease of the surface abundance (and thus of the corresponding yield) of this element as can be seen in Fig. 5, and as already shown by Charbonnel & Zahn (2007a) for low-metallicity stars. This confirms the early suggestion by Rood et al. (1984) that the variations of the carbon isotopic ratio and of ^3He are strongly connected (see also Charbonnel 1995; Charbonnel & Do Nascimento 1998; Eggleton et al. 2006). It is important to note that in the models presented here ^3He decreases by a large factor in the ejected material with respect to

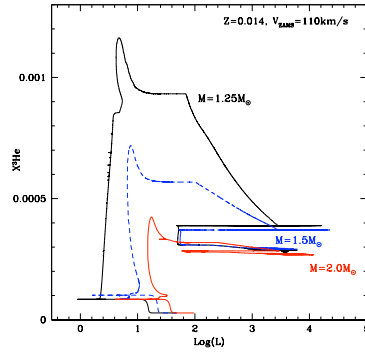


Figure 5. Evolution of the surface abundance of ^3He (in mass fraction) for stars of various initial masses and solar metallicity. Figure from Lagarde & Charbonnel (in preparation)

the canonical evolution predictions, but that low-mass stars remain net producers (while far much less efficient than in the canonical case) of ^3He . As already depicted by the $^{12}\text{C}/^{13}\text{C}$ behaviour that traces the dependance of the thermohaline mixing efficiency with metallicity, the destruction of fresh ^3He by this process is much more efficient in low-metallicity stars (see Fig. 4 of Charbonnel & Zahn 2007a).

Computations for a larger grid in stellar masses and metallicities are now being performed in order to quantify the actual contribution of low-mass stars to Galactic ^3He in the framework proposed here (Lagarde et al., in preparation). We are confident that the corresponding ^3He yields will help reconciling the primordial nucleosynthesis with measurements of $^3\text{He}/\text{H}$ in Galactic HII regions (Charbonnel 2002).

5. The peculiar case of “thermohaline deviant stars”: Ap star descendants?

However a couple of planetary nebulae, namely NGC 3242 and J320, have been found to behave “classically” (see Bania, this volume): slightly more massive than the Sun, they are currently returning fresh ^3He to the interstellar medium, in the amount predicted by classical stellar models (Rood et al. 1992; Galli et al. 1997; Balser et al. 1999, 2006).

To reconcile the $^3\text{He}/\text{H}$ measurements in Galactic HII regions with the high values of ^3He in NGC 3242 and J320, Charbonnel & Zahn (2007b) proposed that thermohaline mixing is inhibited by a fossil magnetic field in RGB stars that are descendants of Ap stars. They obtained a threshold for the magnetic field of 10^4 - 10^5 Gauss, above which it inhibits thermohaline mixing in red giant stars located at or above the L-bump. Fields of that order are expected in the descendants of Ap stars, taking into account the contraction of their core when they become red giants.

Charbonnel & Zahn (2007b) thus concluded that in a large fraction of descendants of Ap stars thermohaline mixing does not occur. As a consequence these objects should produce ^3He as predicted by the standard stellar theory and as observed in the planetary nebulae NGC 3242 and J320. The relative number of such stars with respect to non-magnetic objects that undergo thermohaline mixing is consistent with the statistical constraint coming from observations of the carbon isotopic ratio in red giant stars (Charbonnel & Do Nascimento 1998). It satisfies also the Galactic requirements for the evolution of the ^3He abundance.

Acknowledgements

We acknowledge financial support from IAU, from the French “Programme National de Physique Stellaire” of CNRS/INSU, and from the Swiss National Science Foundation.

References

- Balser, D.A., Bania, T.M., Brockway, C.J., Rood, R.T., Wilson, T.L., 1994, *ApJ*, 430, 667
 Balser, D.A., Bania, T.M., Rood, R.T., Wilson, T.L., 1999, *ApJ*, 510, 759
 Balser, D.A., Goss, W.M., Bania, T.M., Rood, R.T., 2006, *ApJ*, 640, 360
 Bania, T.M., Balser, D.A., Rood, R.T., Wilson, T.L., Wilson, T.J., 1997, *ApJS*, 113, 353
 Bania, T.M., Rood, R.T., Balser, D.A., 2002, *Nature*, 415, 54
 Charbonnel, C. 1995, *ApJ*, 453, L41
 Charbonnel, C. 2002, *Nature*, 415, 27
 Charbonnel, C. & Do Nascimento, J.D. 1998, *A&A*, 336, 915
 Charbonnel, C. & Talon, S. 1999, *A&A*, 351, 635
 Charbonnel, C. & Zahn, J.P. 2007a, *A&A Letters*, 467, L15
 Charbonnel, C. & Zahn, J.P. 2007b, *A&A Letters*, 476, L29
 Coc, A., Vangioni-Flam, E., Descouvemont, P., Adahchour, A., & Angulo, C. 2004, *ApJ*, 600, 544
 Cyburt, R.H. 2004, *Phys.Rev.D*, 70, 023 505
 Dearborn, D.S.P., Steigman, G., Tosi, M., 1996, *ApJ*, 465, 887
 Decressin, T., Mathis, S., Palacios, A., et al. 2009, *A&A*, 495, 271
 Eggleton, P.P., Dearborn, D.S.P., Lattanzio, J.C 2006 *Science*, 314, 5805, 1580
 Galli, D., Stanghellini, L., Tosi, M., Palla, F. 1997, *ApJ*, 477, 218
 Geiss, J. & Reeves, H., 1972, *A&A* 18, 126
 Geiss, J., 1993, in Origin and evolution of the elements, eds. N.Prantzos et al., p.89
 Gilroy, K.K., & Brown, J.A. 1991, *ApJ*, 371, 578
 Iben, I., 1967, *ApJ*, 143, 642
 Kawaler, S.D., 1988, *ApJ*, 333, 236
 Kippenhahn, R., Ruschenplatt, G., & Thomas, H.C. 1980, *A&A*, 91, 175
 Krishnamurti, R. 2003, *J. Fluid Mech.*, 483, 287
 Maeder, A., & Zahn, J.P. 1998, *A&A*, 334, 1000
 Palacios, A., Charbonnel, C., Talon, S., & Forestini, M. 2003, *A&A*, 399, 603
 Palacios, A., Charbonnel, C., Talon, S., & Siess, L. 2006, *A&A*, 453, 261
 Palla, F., Bachiller, R., Stanghellini, L., Tosi, M., Galli, D., 2000, *A&A*, 355, 69
 Paquette, C., Pelletier, C., Fontaine, G., & Michaud, G., 1986, *ApJS*, 61,177
 Rood, R.T., 1972, *ApJ*, 177, 681
 Rood, R.T., Steigman, G., Tinsley, B.M., 1976, *ApJ*, 207, L57
 Rood, R.T., Bania, T.W., Wilson, T.L. 1984, *ApJ*, 280, 629
 Rood, R.T., Bania, T.W., Wilson, T.L. 1992, *Nature*, 355, 618
 Romano, D., Tosi, M., Matteucci, F., Chiappini, C. 2003, *MNRAS*, 346, 295
 Smiljanic, R., Gauderon, R., North, P., Barbuy, B., Charbonnel, C., Mowlavi, N. 2009a, *A&A* 502, 267
 Smiljanic, R., Pasquini, L., Charbonnel, C., Lagarde, N. 2009b, *A&A*, in press, astro-ph 0910.4399
 Talon, S. & Charbonnel, C 1998, *A&A*, 335, 959
 Talon, S. & Charbonnel, C 2005, *A&A*, 440, 981
 Tosi, M. 1996, *ASP Conference Series*, Vol. 98, 299
 Tosi, M. 1998, *Space Science Reviews*, Vol. 84, 207
 Tosi, M. 2000, IAUS 198, 525
 Ulrich, R.K. 1972, *ApJ*, 172, 165
 Weiss, A., Wagenhuber, J., Denissenkov, P.A., 1996, *A&A*, 313, 581
 Zahn, J.P. 1992, *A&A*, 265, 115

Theoretical stellar $\Delta Y/\Delta O$ in the early Universe

Sylvia Ekström¹, Georges Meynet¹, André Maeder¹, Cristina
Chiappini^{1,2}, Cyril Georgy¹ and Raphael Hirschi^{3,4}

¹Astronomical Observatory of the Geneva University
Maillettes 51 - Sauverny, 1290 Versoix GE, Switzerland
email: Sylvia.Ekstrom@unige.ch

²Osservatorio Astronomico di Trieste
OAT/INAF, Via G. B. Tiepolo 11, 34131 Trieste TS, Italy

³Astrophysics group, Keele University,
Lennard-Jones Lab., Keele, ST5 5BG, UK

⁴IPMU, University of Tokyo,
Kashiwa, Chiba 277-8582, Japan

Abstract. Population III stars initiated the chemical enrichment of the Universe. Chemical evolution models seem to favour fast rotators among the very low-metallicity population. When a star rotates fast, it ejects significant quantities of He and its nucleosynthetic products are modified compared to the case without rotation. The value of $\Delta Y/\Delta O$ is explored from a theoretical point of view through stellar models of zero- or very low-metallicity.

Keywords. nucleosynthesis, stars: rotation, early universe

1. Introduction

About a quarter of an hour after the Big Bang, the Universe has finished all possible nucleosynthesis leaving its chemical composition devoid of metals (see for example Iocco et al. 2007). Only when the first stars form does nucleosynthesis take place again, in their cores and envelopes, and the enrichment of the Universe in heavy elements can start.

In the very early Universe, the chemical enrichment follows the nucleosynthetic path of massive stars for the first few millions of years. Of course, in the galaxies we can observe now, the contribution of the first generations of stars has been overwhelmed by the following generations, where intermediate- or low-mass stars contribute actively to the nucleosynthesis. However, should we be able one day to observe galaxies with metallicities as low as $Z = 10^{-8}$, we would certainly observe a medium enriched only by massive stars and it is interesting to study how this enrichment would take place. Currently it is in the Milky Way halo that the most metal poor objects are observed. These low-mass, second generation stars retain the memory of the unique nucleosynthesis in the first generations of massive stars.

We have recently shown that only chemical evolution models adopting stellar yields from rotating star models can successfully explain some of the puzzling imprints of the first stellar generations, such as the production of primary nitrogen and ^{13}C in the early Universe (before intermediate-mass stars have had time to contribute to the chemical enrichment - see Chiappini et al. 2008, 2006). Here we address the following question: would fast rotators eject significant larger quantities of helium in the early chemical enrichment than present-day massive stars? Here, we explore the theoretical dY/dO value obtained by massive star models with rotation at extremely low or zero metallicities. We

consider only stellar model results, since at those extreme metallicities only a few massive stars would have had time to contribute to the chemical enrichment.

2. Stellar models

In the present study, we use the same fast-rotating models of extremely-low metallicity ($Z = 0$ and $Z = 10^{-8}$) massive stars considered in our previous papers (Chiappini et al. 2008, 2006). The stellar models are described in Hirschi (2007) for $Z = 10^{-8}$ and in Ekström et al. (2008) for $Z = 0$. The mass range covered goes from 9 to 85 M_{\odot} . We let the interested reader refer to the original papers for the detailed physics of the models, we will just summarize here the main ingredients of the calculation:

- non-solid rotation is treated as in Hirschi et al. (2004), with the horizontal turbulence coefficient from Zahn (1992) and the shear diffusion coefficient from Talon & Zahn (1997);
- the radiative mass loss prescription is Kudritzki (2002) for the $Z = 0$ models, with the same adaptations as in Marigo et al. (2003), and Vink et al. (2001) for the $Z = 10^{-8}$ models;
- when (if) the star reaches the critical velocity[†], a mechanical mass loss is applied as in Meynet et al. (2006), so the supercritical layers are removed;
- an important reaction rate for the results of $\Delta Y / \Delta O$ is the $^{12}\text{C}(\alpha, \gamma)^{16}\text{O}$ rate, which is still a subject of controversy. Here the models are computed with the NACRE recommended rate;
- the convection criterion applied is the Schwarzschild (1958) criterion.

The models start on the ZAMS with a ratio v/v_{crit} around 0.5.

2.1. Nucleosynthesis

There are some peculiarities of the nucleosynthesis at extremely-low or zero metallicity. The stars are very compact, because of the lack of metals in their envelope, thus the hydrogen burning takes place at higher temperature in the core. Pop III stars even burn some helium during the main sequence. The compactness favours a mixing between the different burning zones, for example between the helium-burning convective core and the hydrogen burning radiative shell. This leads to the production of primordial nitrogen, for example (see Meynet & Maeder 2002). While the non-rotating models undergo this phenomenon only at specific mass domains (~ 25 and $\sim 85 M_{\odot}$), the rotating models present the primary nitrogen production at all masses. Later, some of this nitrogen can diffuse towards the core and increase the production of ^{22}Ne , which is an interesting source of neutrons for the s -process nucleosynthesis (Pignatari et al. 2008).

Rotation also leads to modifications in the yields of the elements that interest us here. At non-zero metallicity, the mass loss is enhanced, saving some helium from further burning. Fast rotators are thus expected to be strong helium producers (see the contribution of G. Meynet in this proceedings). When some C and O are diffused from the core to the H-burning shell, it drives a boost of the energy production in it (passing suddenly from the pp -chains to the CNO cycle). The boost of energy reduces the size of the core, and since the O yield is closely related to the core size, the O production is reduced in this case.

2.2. Yields

Figure 1 and Table 1 present the yields of O and He of all the models. The $Z = 0$ very massive (above 40 M_{\odot}) models produce more O and less He than the $Z = 10^{-8}$ models.

[†] *i.e.* the velocity at which the centrifugal force counterbalances exactly the gravitational force at the surface

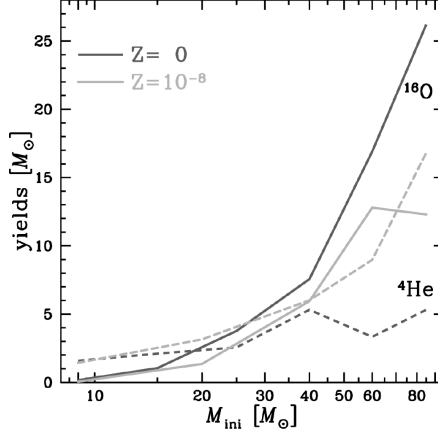


Figure 1. Yields in He (dashed lines) and O (solid lines): $Z = 0$ models (dark grey) and $Z = 10^{-8}$ (light grey).

This is mainly due to the difference in the mass loss rate: the Pop III models lose almost no mass at all while the $Z = 10^{-8}$ models experience a strong surface enrichment and the mass loss is largely increased thanks to the diffused metals. The evolution at almost constant mass and the extreme compactness of Pop III stars lead to very large CO cores, which favours a high O production at the expense of He.

As we mentioned previously, rotation enhances the mass loss. This is particularly interesting at very low metallicity, where radiative mass loss is supposed to be extremely weak. Also, according to Heger et al. (2003), some of the low-metallicity massive stars could end their life without the explosion of a supernova. The formation of a direct black hole would swallow the whole star without any ejection, except the winds the star lost during its life. In this case, the chemical contribution of the star would be of the ‘wind-only’ type. Table 1 shows the ‘wind-only’ contribution in parenthesis. We see that the wind is rich in He and very poor in O, as expected.

3. $\Delta Y/\Delta O$

Figure 2 shows the dY/dO values obtained by stellar models. The more massive the model, the earlier the contribution is expected. Since high-mass models yield a low dY/dO value, the dY/dO ratio increases with time. The range of $\Delta Y/\Delta O$ values observed in the most metal-poor HII regions of the present-day Universe is indicated on the figure. Though metal-poor, those regions already bear the imprint of many stellar generations, including intermediate- and low-mass stars. The values are deduced from observations under the hypothesis that the IMF doesn’t change at low metallicity (see Izotov et al. 2007). This hypothesis needs yet to be ascertained. In the very early Universe, it is thought that either the slope of the IMF is still valid but there is a mass-cut under $\simeq 10 M_{\odot}$ (Nakamura & Umemura 1999), either the IMF is flat, or it is doubled-peaked (Nakamura & Umemura 2001).

If we assume that all the stars die at the same moment (which is reasonable given that the less massive stars live less than 30 million years), we can integrate their yields with an IMF and get a mean value for a first burst of primordial stars. For this, we use

Table 1. Yields in He and O for the $Z = 0$ and $Z = 10^{-8}$ models. All masses are in M_{\odot} . The values given in parenthesis are the ‘wind-only’ contribution (see text).

Mass	$Z = 0$			$Z = 10^{-8}$		
	^4He	^{16}O	dY/dO	^4He	^{16}O	dY/dO
9	1.59	0.17	9.35	1.43	0.06	24.2
				(2.80e-5)	(2.33e-8)	(1200)
15	2.10	1.05	2.00			
	(3.59e-4)	(1.79e-15)	(2.0e11)			
20				3.15	1.35	2.33
				(2.36e-4)	(2.54e-10)	(9.3e5)
25	2.57	3.76	0.68			
	(2.13e-3)	(2.06e-13)	(1.0e10)			
40	5.32	7.57	0.70	6.01	5.94	1.01
	(5.48e-2)	(4.09e-8)	(1.3e6)	(0.33)	(2.42e-3)	(136)
60	3.37	16.90	0.20	8.97	12.80	0.70
	(4.11e-2)	(8.88e-8)	(4.6e5)	(1.21)	(5.48e-5)	(2.2e4)
85	7.09	26.20	0.27	16.80	12.30	1.37
	(1.78)	(5.98e-5)	(3.0e4)	(20.0)	(3.02)	(6.62)
IMF integrated						
S55†			1.39			2.82
MS79‡			2.14			4.18
IMF integrated, with ‘realistic’ fate¶ for the stars						
S55			2.36			5.16
MS79			3.51			7.28

† Salpeter (1955)

‡ Miller & Scalo (1979)

¶ Heger et al. (2003)

the following formula:

$$\frac{dY}{dO} = \frac{\int_{M_{\text{down}}}^{M_{\text{up}}} dY \Phi(M) dM}{\int_{M_{\text{down}}}^{M_{\text{up}}} dO \Phi(M) dM}$$

where $\Phi(M) = AM^{-(1+x)}$ is the IMF. Since we consider only massive stars, we use $M_{\text{down}} = 9 M_{\odot}$ and $M_{\text{up}} = 120 M_{\odot}$.

The results are given in the middle panel of Table 1. Depending on the IMF used, the results change because different mass domains are favoured. Compared to Salpeter’s, the slope $x = 2.30$ (for $M > 10 M_{\odot}$) of Miller & Scalo is steeper and favours the lowest masses, leading to a higher value of dY/dO. The case of Pop III stars seems very peculiar, lower dY/dO values than the case of $Z = 10^{-8}$ stars. It reflects the peculiarities of the yields commented in section 2.2. When the metallicity grows slightly, the nucleosynthesis changes, and even with a metallicity as low as $Z = 10^{-8}$, the stars present a higher dY/dO value. The ‘wind-only’ case leads to extremely high dY/dO values.

Now let us take into account the ‘realistic’ fate of the star as determined by Heger et al. (2003). According to these authors, all stars with M_{α} † between 9 and $40 M_{\odot}$ are supposed to end their life by collapsing into a black hole, without a supernova explosion. For such stars, the only contribution to the chemical enrichment of the Universe would be made by the winds they experienced during their life. At $Z = 0$ the 25, 40, and 60

† M_{α} , the He core mass at the end of a star’s evolution, is the mass coordinate at which the hydrogen abundance drops below 10^{-3} .

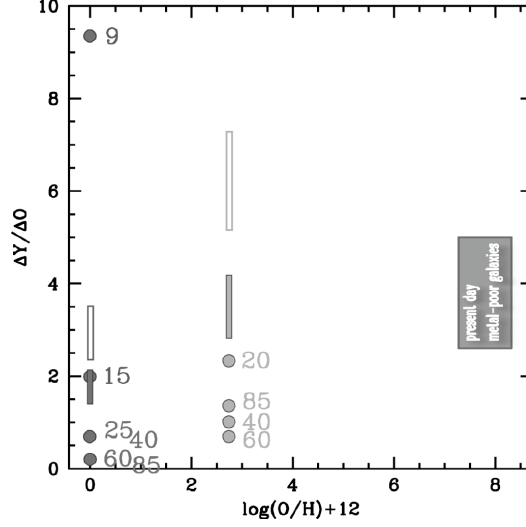


Figure 2. $\Delta Y/\Delta O$ values obtained with the total yields of the models as a function of the oxygen abundance: $Z = 0$ models (dark grey) and $Z = 10^{-8}$ (light grey). The IMF integrated values are given as a filled rectangle (range of values between S55 and MS79), and the ones obtained by taking into account the supposed fate of the models are shown with an empty rectangle. The range of values for the most metal-poor HII regions observed in the present-day Universe is also shown (data from Olive & Skillman 2004, Izotov et al. 2007 and Peimbert et al. 2007).

M_{\odot} come into this category. At $Z = 10^{-8}$ the 40, 60, and 85 M_{\odot} are concerned. Using these limits, we can compute more realistic dY/dO stellar ratios, which are given in the bottom panel of Table 1. Because of the high He and low O content of the winds, the dY/dO is much larger in this mixed case (i.e. winds+SN yields for stars with He core mass below 9 M_{\odot} and only winds above that value).

4. Discussion

Here we computed the expected $\Delta Y/\Delta O$ ratio from a generation of $Z=0$ and ultra metal poor ($Z=10^{-8}$) massive stars. The stellar values presented here give the starting point for the further evolution of the $\Delta Y/\Delta O$ ratio. With time, the $\Delta Y/\Delta O$ ratio will increase thanks to the contribution to the helium of intermediate and low-mass stars. The evolution of $\Delta Y/\Delta O$ will depend on the star formation history, IMF and selective outflows of the particular galaxy under study.

We show how the initial $\Delta Y/\Delta O$ obtained from the first stars depend upon the fate of these stars. If the most massive stars do contribute to the chemical enrichment only via their stellar winds, the expected $\Delta Y/\Delta O$ ratio is larger due to the high helium and low oxygen content of the stellar winds. Under the hypothesis that all massive $Z=0$ stars ended up into black holes, contributing to the chemical enrichment only via their stellar winds, we get unrealistic high $\Delta Y/\Delta O$ ratios (due to a very low contribution to oxygen). A mixed scenario where, even at $Z=0$, only stars with helium core mass between 9 and 40 M_{\odot} do implode directly as black holes seems more likely.

References

- Bromm, V. & Larson, R. B. 2004, *ARA&A* 42, 79
- Chiappini, C., Ekström, S., Meynet, G., Hirschi, R., Maeder, A., & Charbonnel, C. 2008, *A&A* 479, L9
- Chiappini, C., Hirschi, R., Meynet, G., Ekström, S., Maeder, A., & Matteucci, F. 2006, *A&A* 449, L27
- Ekström, S., Meynet, G., Chiappini, C., Hirschi, R., & Maeder, A. 2008, *A&A* 489, 685
- Heger, A., Fryer, C. L., Woosley, S. E., Langer, N., & Hartmann, D. H. 2003, *ApJ* 591, 288
- Hirschi, R. 2007, *A&A* 461, 571
- Hirschi, R., Meynet, G., & Maeder, A. 2004, *A&A* 425, 649
- Iocco, F., Mangano, G., Miele, G., Pisanti, O., & Serpico, P. D. 2007, *Phys. Rev. D* 75(8), 087304
- Izotov, Y. I., Thuan, T. X., & Stasińska, G. 2007, *ApJ* 662, 15
- Kudritzki, R. P. 2002, *ApJ* 577, 389
- Maeder, A. 1992, *A&A* 264, 105
- Marigo, P., Chiosi, C., & Kudritzki, R.-P. 2003, *A&A* 399, 617
- Meynet, G., Ekström, S., & Maeder, A. 2006, *A&A* 447, 623
- Meynet, G. & Maeder, A. 2002, *A&A* 390, 561
- Miller, G. E. & Scalo, J. M. 1979, *ApJS* 41, 513
- Nakamura, F. & Umemura, M. 1999, *ApJ* 515, 239
- Nakamura, F. & Umemura, M. 2001, *ApJ* 548, 19
- Olive, K. A. & Skillman, E. D. 2004, *ApJ* 617, 29
- Peimbert, M., Luridiana, V., & Peimbert, A. 2007, *ApJ* 666, 636
- Peimbert, M., Peimbert, A., Luridiana, V., & Ruiz, M. T. 2003, in E. Perez, R. M. Gonzalez Delgado, & G. Tenorio-Tagle (eds.), *Star Formation Through Time*, Vol. 297 of *Astronomical Society of the Pacific Conference Series*, p. 81
- Pignatari, M., Gallino, R., Meynet, G., Hirschi, R., Herwig, F., & Wiescher, M. 2008, *ApJ* 687, L95
- Salpeter, E. E. 1955, *ApJ* 121, 161
- Schwarzschild, M. 1958, *Structure and evolution of the stars*.
- Talon, S. & Zahn, J.-P. 1997, *A&A* 317, 749
- Vink, J. S., de Koter, A., & Lamers, H. J. G. L. M. 2001, *A&A* 369, 574
- Zahn, J.-P. 1992, *A&A* 265, 115

Galactic evolution of ${}^7\text{Li}$

Francesca Matteucci^{1,2}

¹ Department of Physics, Astronomy Division, Trieste University, Italy
 Via G.B. Tiepolo, 11 34134 Trieste, Italy,
 email: matteucc@oats.inaf.it

² INAF, Trieste
 Via G.B. Tiepolo, 11 34134 Trieste, Italy

Abstract.

Lithium represents a key element in cosmology, as it is one of the few nuclei synthesized during the Big Bang. The primordial abundance of ${}^7\text{Li}$ allows us to impose constraints on the primordial nucleosynthesis and on the baryon density of the universe. However, ${}^7\text{Li}$ is not only produced during the Big Bang but also during galactic evolution: measures of stellar Li in our Galaxy suggest an almost constant Li abundance (the so-called Spite plateau) at low metallicities and a subsequent increase in the disk stars, leading to a Li abundance in Population I stars higher by a factor of ten than in Population II stars. This means that there must exist several possible stellar sources of ${}^7\text{Li}$: asymptotic giant branch stars, supernovae, novae, red giant stars. ${}^7\text{Li}$ is also partly produced in spallation processes while ${}^6\text{Li}$ is entirely produced by such processes. All of these sources have been included in galactic chemical evolution models and constraints have been derived on the primordial ${}^7\text{Li}$ and its evolution, as well on stellar models. I will review these models and their results and what we have learned about ${}^7\text{Li}$ evolution. Some still open problems, such as the disagreement between the primordial ${}^7\text{Li}$ abundance as derived by WMAP and as measured in Population II stars, and the uncertainties about the main sources of stellar ${}^7\text{Li}$ will be discussed.

Keywords. Stars: abundances – Galaxy: evolution

1. Introduction

Standard Big Bang nucleosynthesis predicts the abundances of ${}^2\text{D}$, ${}^3\text{He}$, ${}^4\text{He}$ and ${}^7\text{Li}$ and if these abundances are in agreement with the observationally derived primordial abundances, then we can derive the baryon to photon ratio and the baryonic density parameter Ω_b . This was the case until WMAP results became available (Spergel et al. 2003), suggesting directly a value for the baryon to photon ratio $\eta_{10} = 6.1^{+0.3}_{-0.2}$. More recently, the last release of WMAP (Hinshaw et al. 2009) suggests a revised value of $\eta_{10} = 6.23 \pm 0.17$. This value of η_{10} gives primordial abundances of ${}^2\text{D}$, ${}^3\text{He}$ and ${}^4\text{He}$ in good agreement with observations except for ${}^7\text{Li}$, for which the primordial abundance estimated from WMAP is higher by a factor of 3-4 than the abundance of ${}^7\text{Li}$ measured in low-metallicity halo stars, always interpreted as the primordial one. If the WMAP value is correct, we therefore should revise our interpretation of the ${}^7\text{Li}$ abundance in halo stars (Population II stars) and assume that some Li astration has taken place in these stars. In recent years some suggestions were put forward to explain the low Li abundance in metal-poor stars, such as diffusion and turbulence in the presence of weak turbulence (e.g. Richard et al. 2005; Melendez et al. 2009) and rotational mixing (Pinsonneault, this conference). Alternatively, this discrepancy could be solved by Li destruction during the Big Bang (Jedamzik, this conference). In this review we will focus on the interpretation of the plot $\text{Log}\epsilon(\text{Li})$ versus $[\text{Fe}/\text{H}]$ in terms of Galactic production of ${}^7\text{Li}$. We will review the main sources of ${}^7\text{Li}$: stars, cosmic rays, and Big Bang. Then we will describe how

to model the Galactic evolution of ${}^7\text{Li}$ by taking into account in detail all the various ${}^7\text{Li}$ sources. The most important results from 1990 up to now will be described, and the constraints derived from the comparison theory-observations as well as the still existing uncertainties will be summarized. Finally, we will discuss the ${}^7\text{Li}$ discrepancy originated by the difference between the primordial Li abundance derived from WMAP and the measured one.

2. ${}^7\text{Li}$ production in stars

There is only one way to produce ${}^7\text{Li}$ during normal stellar evolution and it is by means of the nuclear reaction ${}^3\text{He}(\alpha, \gamma){}^7\text{Be}$. The fresh ${}^7\text{Be}$ should be then transported by convection into stellar regions of lower temperature, where it decays into ${}^7\text{Li}$ by k-capture. This mechanism was originally proposed by Cameron & Fowler (1971). However, ${}^7\text{Li}$ is also destroyed during stellar evolution, and in general it is assumed that all the original Li present in the star is destroyed in the course of the evolution. From the observational point of view, K giants and M supergiants are Li-rich (Smith & Lambert 1989, 1990) indicating that ${}^7\text{Li}$ is produced by asymptotic giant branch stars (AGBs) (see Gratton 1991, for an exhaustive review on the subject). Theoretical models of AGB stars (Sackmann & Boothroyd 1999) have suggested that stars in the mass range $(4-6)M_{\odot}$ can produce noticeable quantities of ${}^7\text{Li}$ ($\text{Log}\epsilon(\text{Li}) \sim 4-4.5$, with $\text{Log}\epsilon(\text{Li})$ being the number density of Li in the unit system $\text{Log}(\text{X}/\text{H}) + 12$, where 12 is the hydrogen). This result was later confirmed by Travaglio et al. (2001). On the other hand, Ventura et al. (1998) found a negligible ${}^7\text{Li}$ production from AGB stars, so the situation is still unclear. Classical novae could also in principle be ${}^7\text{Li}$ producers, although so far only one detection of ${}^7\text{Li}$ in novae has been reported (Della Valle et al. 2002). From the theoretical point of view, Starrfield et al. (1978) had suggested novae as possible ${}^7\text{Li}$ producers and that the amount of freshly produced Li would depend crucially on the amount of ${}^3\text{He}$ present in the matter accreted onto the white dwarf. Later on, José & Hernanz (1978) recomputed the ${}^7\text{Li}$ yields from novae and confirmed that these objects can be Li producers but their predicted Li was not as high as in Starrfield et al. (1978). In particular, José & Hernanz (1998) suggested an average mass of Li produced in a nova outburst $\langle M_{\text{Li}} \rangle = (1.8 - 7.5) \cdot 10^{-7} M_{\odot}$, and considering that each nova has $\sim 10^4$ outbursts during its life, this leads to an average total mass of Li produced by a nova $\langle M_{\text{Li}} \rangle = (1.8 - 7.5) \cdot 10^{-3} M_{\odot}$. Another possible stellar ${}^7\text{Li}$ source are supernovae (SN) II: neutrino-induced nucleosynthesis can produce ${}^7\text{Li}$ (Woosley & al. 1990). In particular, SNe II can produce ${}^7\text{Li}$ in the He-shell by excitation of He by μ and τ neutrinos, produced during the formation of the neutron star in the pre-explosion phase, followed by de-excitation with emission of a proton or a neutron which in turn reacts with He and forms ${}^7\text{Li}$. Woosley & Weaver (1995) computed detailed ${}^7\text{Li}$ yields from SNe II as functions of the initial stellar metallicity. Unfortunately, no detection of ${}^7\text{Li}$ in SNe has been reported so far. Finally, low-mass giants could in principle produce ${}^7\text{Li}$ since in some of them it has been measured a high Li abundance. The production of ${}^7\text{Li}$ in this case should occur during the upper part of the red giant branch (RGB), between the first episode of dredge-up and the tip of the RGB, coupled with mass loss (see de la Reza et al. 2000). Unfortunately, only a very small fraction of these stars ($< 5\%$) show overabundances of ${}^7\text{Li}$ in their atmospheres ($\text{Log}\epsilon(\text{Li}) \sim 4$).

3. ${}^7\text{Li}$ production in the Big Bang and cosmic rays

During the Big Bang a tiny fraction of ${}^7\text{Li}$ was produced, whereas ${}^6\text{Li}$ has been entirely produced by cosmic rays (Reeves 1994). The isotope ${}^6\text{Li}$ has been detected in halo stars (Asplund et al. 2006), thus suggesting that also some of the original ${}^7\text{Li}$ in the same stars originates from Galactic cosmic rays (GCRs). Calculations of the amount of ${}^7\text{Li}$ produced by GCRs can be found in Lemoine et al. (1988).

4. Galactic chemical evolution of ${}^7\text{Li}$

The abundance of ${}^7\text{Li}$ measured in the stellar atmospheres of stars which have not yet depleted their original Li should provide, in principle, the history of the Galactic evolution of this element. In fact, the measured ${}^7\text{Li}$ abundance in very metal-poor halo stars is lower by a factor of ten than the ${}^7\text{Li}$ abundance measured in young stars, such as the Pleiades. This means that ${}^7\text{Li}$ has been produced by stars and cosmic rays during Galactic evolution. In Figure 1 we show the famous plot $\text{Log } \epsilon(\text{Li})$ vs. $[\text{Fe}/\text{H}]$, where the ${}^7\text{Li}$ evolution is given by the upper envelope of the data. The large spread in the disk stars is clearly due to the fact that Li is depleted in different ways in different stars. On the other hand, the halo stars ($[\text{Fe}/\text{H}] < -1.0$) show a quite remarkable plateau and a small spread. Such a plateau was discovered first by Spite & Spite (1982) and confirmed later on by other authors with some exceptions (Thornburn 1994; Ryan et al. 1999) and the primordial ${}^7\text{Li}$ value was fixed ($\text{Log } \epsilon(\text{Li}) = 2.1 - 2.3$, e.g. Bonifacio et al. 2002). More recently, the newest data (28 halo dwarfs observed with UVES at the VLT) seem to indicate that the plateau does not exist any more for $[\text{Fe}/\text{H}] < -3.0$ (Sbordone et al. 2009, this conference). So the “Spite-plateau” does not exist any more and we should understand how Li has been depleted at an almost constant level in all stars with $-3.0 < [\text{Fe}/\text{H}] < -1.0$, and then how the depletion increases for $[\text{Fe}/\text{H}] > -3.0$. Anyway, the diagram of Figure 1 is the one that was adopted by all the chemical evolution modelists up to now and we will start this review by describing the history of the interpretation of this important diagram. In particular, chemical evolution models should aim at fitting the upper envelope of the diagram of Figure 1. Detailed chemical evolution models follow the evolution in time of the gas abundances in the Galaxy by taking into account the star formation history, the stellar yields and possible gas flows (infall/outflows) (see Matteucci 2001).

4.1. The interpretation of the $\text{Log } \epsilon(\text{Li})$ vs. $[\text{Fe}/\text{H}]$

In principle, two possible interpretations can be suggested for the diagram of Figure 1: i) the ${}^7\text{Li}$ abundance of the plateau is the primordial Li value, whereas the Li abundance of young stars is the effect of Li production by stars and GCRs during Galactic evolution, ii) the primordial ${}^7\text{Li}$ abundance is the one measured in young stars, whereas that of the plateau is the consequence of Li depletion in stars. This second hypothesis, however, would require a non-standard Big Bang nucleosynthesis. Mathews et al. (1990) explored these two possibilities by means of a detailed chemical evolution model for the Milky Way and concluded that, on the basis of only chemical evolution models, it is difficult to distinguish which hypothesis works better. In Figure 2 we show the model predictions for the two cases: in case i) they started from the primordial abundance of the Spite plateau and assumed carbon stars (low-mass giants) and SNe II as possible ${}^7\text{Li}$ producers and explored different star formation rates. They found that the observed data could be reproduced by assuming ad hoc yields for both stellar sources, since at that time detailed Li yields were missing. In case ii) Mathews et al. (1990) started with a high ${}^7\text{Li}$ primordial

abundance and then assumed a gradual exponential main-sequence destruction of this element. Also in this case the agreement with data is good. In the following years, case ii) was abandoned since it requires a non-standard Big Bang nucleosynthesis not supported by the primordial abundances of the other light elements, and since now on we will refer only to case i). D'Antona & Matteucci (1991) produced a chemical evolution model for the Milky Way, well reproducing the majority of observational constraints, and computing the Galactic evolution of the ${}^7\text{Li}$ abundance by considering Li production from novae and AGBs. The results are shown in Figure 3 where one can notice how the inclusion of novae as Li producers, reproduces very well the steep rise off the spite-plateau for $[\text{Fe}/\text{H}] > -1.0$. This is due to the fact that novae are long-living systems (white dwarfs in binary systems) and contribute to Galactic chemical enrichment with time delays as long as 1-5 Gyr. These authors computed the nova formation rate by assuming that it is a fraction of the rate of formation of the white dwarfs. Then they assumed that each nova has 10^4 bursts during its life and adopted the yields for Li as suggested by Starrfield et al. (1978). Under these assumptions the evolution of the ${}^7\text{Li}$ abundance could be well reproduced just by assuming novae and AGBs as Li producers. In particular, each nova was assumed to produce from 10^{-8} to $10^{-5}M_{\odot}$ per outburst, thus contributing to more than 50% of the total Li production.

In Figure 4 we show the results of a more recent model from Romano et al. (2001), who took into account novae, SNeII, low-mass giants, AGBs, and cosmic rays as ${}^7\text{Li}$ producers. Here, low-mass giants ($M=1-2.5M_{\odot}$) are assumed to produce a fair fraction of the total ${}^7\text{Li}$: in fact, it is assumed that each star produces $\text{Log}\epsilon(\text{Li}) = 4.0$, whereas the AGB stars are producing a negligible amount of Li, as suggested by Ventura et al. (1998). Novae produce a non negligible amount of Li, as suggested by José & Hernanz (1998). The Li yields from SNe II are from Woosley & Weaver (1995) and the ${}^7\text{Li}$ from GCRs is taken from Lemoine et al. (1998). It should be noted that the yields of Woosley

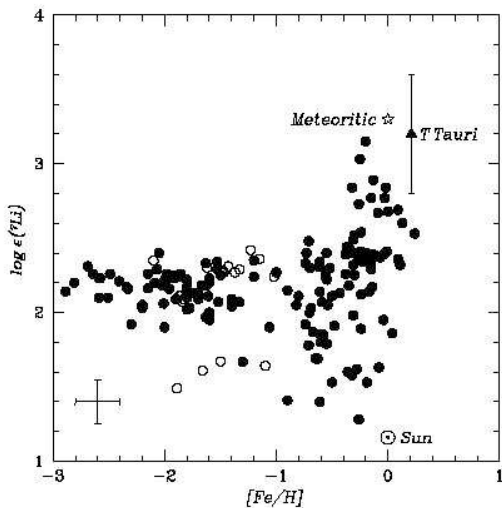


Figure 1. $\text{Log}\epsilon(\text{Li})$ versus $[\text{Fe}/\text{H}]$ for stars in the solar vicinity. The plateau value of $\text{Log}\epsilon(\text{Li}) \sim 2.2$ for $[\text{Fe}/\text{H}] < -1.0$ is interpreted as the primordial value, whereas the highest Li abundance relative to young stars and meteorites is $\text{Log}\epsilon(\text{Li}) = 3.3$. The value of the Li abundance in the Sun is indicated.

& Weaver (1995) have been halved in order not to overproduce boron, in agreement with results from Duncan et al. (1997.) In Figure 4 the contributions from the different sources are separated. Again, we should note that assuming ${}^7\text{Li}$ sources with only short lifetimes (SNeII and AGBs) does not reproduce the steep rise off the Spite plateau which is instead obtained by long-living Li producers, such as novae and low-mass stars. In Figure 4 we show also the predictions considering all sources together but the GCRs. The conclusions of Romano et al. (2001) were that most of Li in the solar system was produced by low-mass stars ($\sim 41\%$), that novae contribute by $\sim 18\%$, SNeII by $\sim 9\%$, AGB stars by only $\sim 0.5\%$ and finally that GCRs contribute for roughly 25%. The same conclusions were not shared by Travaglio et al. (2001,) who concluded that the major contributors to ${}^7\text{Li}$ in the Galaxy are AGB stars with minor contributions from low-mass stars, novae and SNe II. The different approach of Romano et al. (2001) and Travaglio et al. (2001) about ${}^7\text{Li}$ production from AGB stars was due to different assumptions about the mass loss

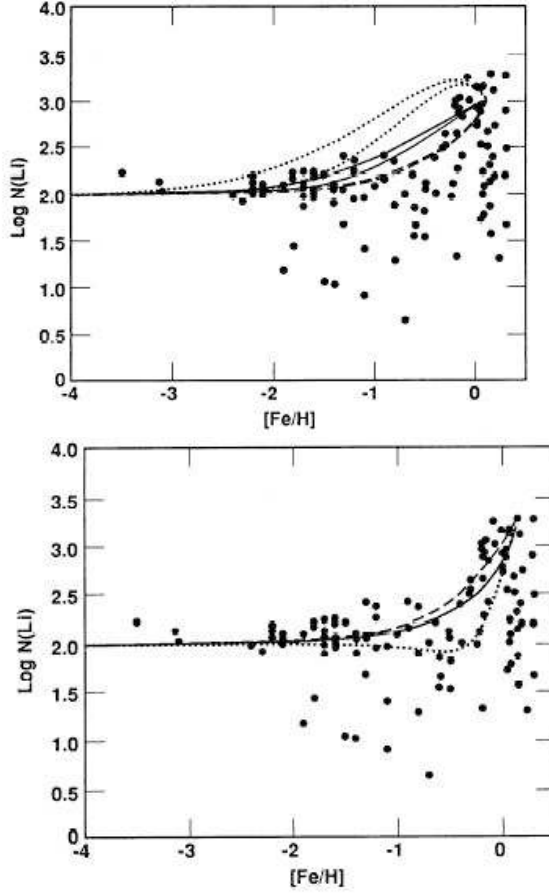


Figure 2. $\text{Log } N(\text{Li})$ (the equivalent of $\text{Log } \epsilon(\text{Li})$) versus $[\text{Fe}/\text{H}]$ for stars in the solar vicinity compared with chemical evolution models. Data are from Rebolo et al. (1988). In the upper panel are shown model results for case i) and different star formation histories, in the lower panel are shown model results for case ii) and the same star formation rates as for case i). Figure from Mathews et al. (1990).

in these stars made by these authors. However, not considering long-living Li producers as important, the Travaglio et al. model cannot reproduce the steep rise of the Spite plateau. In the following years, the advent of WMAP changed the situation depicted up to now. In particular, the primordial value suggested was $\text{Log } \epsilon(\text{Li}) = 2.6$ (Spergel et al. 2003), higher by a factor of ~ 2 than the value of the Spite plateau, thus implying that the Li abundance in metal-poor stars is not the primordial one. This can be explained if the primordial Li is depleted in these stars, and some papers suggested that this is possible by means of gravitational settling and also that the amount of depletion is the same in all metal-poor stars, thus explaining the plateau (Richard et al. 2005). This was confirmed by observations of globular clusters where this depletion was measured (Korn et al. 2006). Unfortunately, more recently new data have appeared (Sbordone et al. 2009, this conference) and the situation has become even more complicated since the data have shown that the Spite plateau exists only down to $[\text{Fe}/\text{H}] = -3.0$, for lower metallicities a decreasing trend is evident. This finding implies that the Li depletion in very metal-poor stars must be a function of metallicity. In Figure 5 we show a more recent model (Romano et al. in preparation) where cosmic rays, novae, SNe II, super-AGBs ($7-11 M_{\odot}$) but not low-mass stars are considered as Li producers. The prescriptions for Li production in GCRs, SNeII and novae are like in Romano et al. (2001, 2003) but the Li produced by super-AGBs is a function of stellar metallicity, and increases with metallicity. The yields for Li from super-AGBs are taken from D'Antona (this conference). As one can see, the steep rise off the Spite plateau is well reproduced even without low-mass stars because of novae and AGBs becoming important Li producers only for $[\text{Fe}/\text{H}] > -1.0$.

5. Conclusions

We have traced the history of the computation of the evolution of the abundance of ${}^7\text{Li}$ in our Galaxy. We started from the diagram tracing the evolution of the Li abundance as a function of $[\text{F}/\text{H}]$ measured in stars of the solar neighbourhood, and interpreted the lower Li abundance in Pop II stars as the primordial Li abundance and that of Pop I stars as the effect of Li production during the galactic lifetime. Several models in the past eleven years have attempted to fit the upper envelope of the $\text{Log}\epsilon(\text{Li})$ vs. $[\text{Fe}/\text{H}]$, and although the uncertainties still existing in the ${}^7\text{Li}$ yields from stars are preventing us from drawing firm conclusions, we have understood the following:

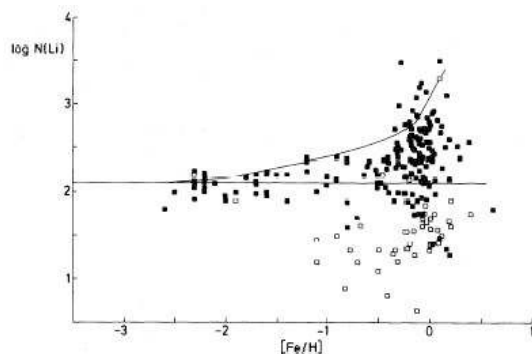


Figure 3. $\text{Log } N(\text{Li})$ versus $[\text{Fe}/\text{H}]$ for stars in the solar vicinity compared with the chemical evolution model of D'Antona & Matteucci (1991) in the framework of case i). The assumed Li producers are novae and ABG stars.

- one or more delayed stellar Li sources are necessary to reproduce the steep rise off the Spite plateau,
- possible candidates are classical novae and low-mass stars although these latter are unlikely since only a small fraction shows an overabundance of ${}^7\text{Li}$ in the atmosphere.
- On the other hand, super-AGB stars ($7\text{--}11M_{\odot}$) producing more and more ${}^7\text{Li}$ with increasing stellar metallicity, can be very promising candidates.

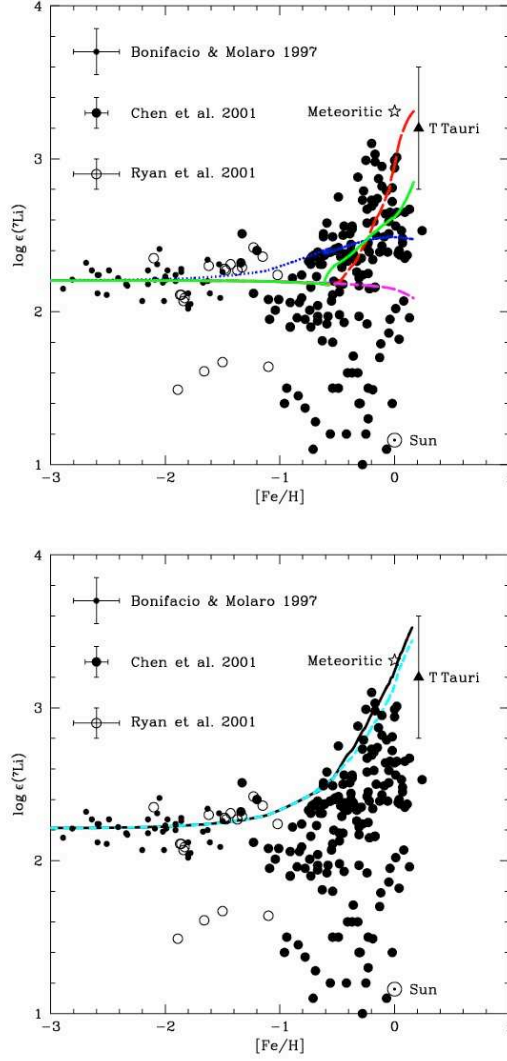


Figure 4. $\text{Log} \epsilon(\text{Li})$ versus $[\text{Fe}/\text{H}]$ for stars in the solar vicinity compared with the chemical evolution model of Romano et al.(2001) in the framework of case i). The assumed Li producers are novae, SNeII, low-mass stars, AGB stars and cosmic rays. The data sources are indicated in the figure.

- The primordial Li abundance derived from WMAP is higher than the Li abundance of the Spite plateau, thus suggesting that the primordial Li abundance has been depleted in Pop II stars. Several mechanisms to explain such a depletion have been suggested but there is still a potential problem related to the possible detection of ${}^6\text{Li}$ in Pop II stars (Asplund et al. 2006), which should have been more heavily depleted than ${}^7\text{Li}$.
- The Li abundance characterizing the Spite plateau seems to be constant only for $-3.0 < [\text{Fe}/\text{H}] < -1.0$, then for very low metallicity the Li abundance seems to decrease. This suggests the existence of a depletion mechanism which is a function of metallicity.

Acknowledgements

I thank Donatella Romano for computing the new model and for reading the manuscript and for all the work done together with me in the past years. I also want to thank Luca Sbordone for allowing me to show his data before publication.

References

- Asplund, M., Lambert, D. L., Nissen, P. E., Primas, F. & Smith, V. V. 2006, *ApJ*, 644, 229
 Bonifacio, P. & Molaro, P. 1997, *MNRAS*, 285, 874
 Bonifacio, P. Pasquini, L., Spite, F., Bragaglia, A., Carretta, E., et al. 2002, *A&A*, 390,91

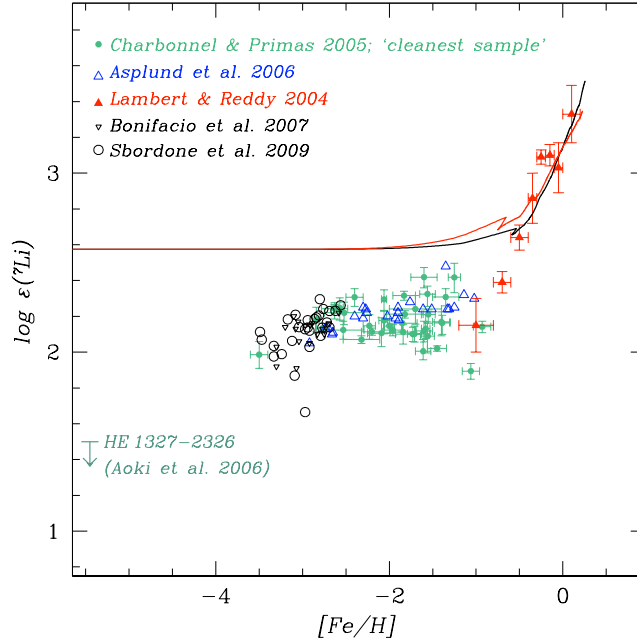


Figure 5. $\text{Log}\epsilon(\text{Li})$ versus $[\text{Fe}/\text{H}]$ for stars in the solar vicinity compared with the chemical evolution model of Romano et al. (in preparation) (upper line) and with the Romano et al. (2001) (lower line), in the framework of case i). The assumed Li producers are novae, SNeII, AGB stars, and cosmic rays, as described in the text. Note that the theoretical curve starts with the primordial Li value from WMAP which lies well above the Li abundances of halo stars. The data sources are indicated in the figure.

- Bonifacio, P., Pasquini, L., Molaro, P., Carretta, E., François, P., Gratton, R. G., James, G., Sbordone, L., Spite, F. & Zoccali, M. 2007, *A&A*, 470, 153
- Cameron, A.G.W. & Fowler, W.A. 1971, *ApJ*, 164, 111
- Charbonnel, C. & Primas, F. 2005, *A&A*, 442, 961
- Chen, Y.Q., Nissen, P.E., Benoni, T. & Zhao, G. 2001, *A&A*, 371, 943
- D’Antona, F. & Matteucci, F. 1991, *A&A*, 284, 62
- de la Reza, R., da Silva, L., Drake, N.A. & Terra, M.A. 2000, *ApJ* (Letters), 535, 115
- Della Valle, M., Pasquini, L., Daou, D. & William, R.E. 2002, *A&A*, 155, 166
- Duncan, D.K., Primas, F., Rebull, L.M., Boesgaard, A.M., Delyannis, C.P., & al. 1997, *ApJ*, 488, 338
- Gratton, R. 1991, *Mem. S.A.It.*, 62, 53
- Hinshaw, G., Weiland, J.L., Hill, R.S., Odegard, N., Larson, D. & al. 2009, *ApJS*, 180, 225
- José, J. & Hernanz, M. 1998, *ApJ*, 494, 680
- Korn, A. Grundohl, F., Richard, O., Barklem, P.S., Mashonkina, L., Collet, R., Piskunov, N. & Gustafsson, B. 2006, *Nature*, 442, 657
- Lambert, D.L. & Reddy, B.E. 2004, *MNRAS*, 349, 757
- Lemoine, M., Vangioni-Flam, E. & Cassé, M. 1998, *ApJ*, 499, 735
- Mathews, G.J., Alcock, C.R. & Fuller, G.M. 1990, *ApJ*, 449, 457
- Matteucci, F. 2001, “The chemical evolution of the Galaxy”, *AASSL*, Kluwer Academic Publishers
- Melendez J., Ramirez, I., Casagrande, L., Asplund, M., Gustafsson, B., Yong, D., do Nascimento, J. D., Jr. et al. 2009, astro-ph/090105845
- Rebolo, R., Beckman, J. E. & Molaro, P. 1988, *A&A*, 192, 192
- Reeves, H. 1994, *Rev.Mod.Phys.*, 66, 193
- Richard, O., Michaud, G. & Richer, J. 2005, *ApJ*, 619, 538
- Romano, D., Matteucci, F., Ventura, P. & D’Antona, F. 2001, *A&A*, 374, 646
- Romano, D., Tosi, M., Matteucci, F. & Chiappini, C. 2003, *MNRAS*, 346, 295
- Ryan, S. G., Kajino, T., Beers, T.C., Suzuki, T. K., Romano, D., Matteucci, F. & Rosolankova, K. 2001, *ApJ*, 549, 55
- Ryan, S. G., Norris, J.E. & Beers, T. C. 1999, *ApJ*, 523, 654
- Sackmann, I.-J. & Boothroyd, A. I. 1999, *ApJ*, 510, 217
- Smith, V.V. & Lambert, D.L. 1989, *ApJ* (Letters), 354, 75
- Smith, V.V. & Lambert, D.L. 1990, *ApJ* (Letters), 361, 69
- Spergel, D.N., Verde, L., Peiris, H.V., Komatsu, E., Nolte, M.R., et al. 2003, *ApJS*, 148, 175
- Spite, F. & Spite, M. 1982, *A&A*, 115, 357
- Starrfield, S., Truran, J.W., Sparks, W.M. & Arnould, M. 1978, *ApJ*, 222, 600
- Thorburn, J.A. 1994, *ApJ*, 421, 318
- Travaglio, C., Randich, S., Galli, D., Lattanzio, J., Elliott, L.M., Forestini, M., Ferrini, F. 2001, *ApJ*, 559, 909
- Ventura, P., Zepieri, A., Mazzitelli, I. & D’Antona, F. 1998, *A&A*, 334, 953
- Woosley, S.E., Hartman, D.H., Hoffman, R.D. & Haxton, W.C. 1990, *ApJ*, 356, 272
- Woosley, S.E. & Weaver, T.A. 1995, *ApJS*, 101, 181



Sylvia Ekström & Cyril Georgy



Ruth Peterson

Lithium, beryllium, and boron production in core-collapse supernovae

Ko Nakamura¹, Takashi Yoshida², Toshikazu Shigeyama^{2,3}
 and Toshitaka Kajino^{1,2}

¹National Astronomical Observatory of Japan,
 Osawa 2-21-1, Mitaka, Tokyo, 181-8588 Japan
 email: nakamura.ko@nao.ac.jp

²Department of Astronomy, Graduate School of Science, University of Tokyo,
 Hongo 7-3-1, Bunkyo-ku, Tokyo, 113-0033 Japan

³Research Center for the Early Universe, Graduate School of Science, University of Tokyo

Abstract. Type Ic supernova (SN Ic) is the gravitational collapse of a massive star without H and He layers. It propels several solar masses of material to the typical velocity of 10,000 km/s, a very small fraction of the ejecta nearly to the speed of light. We investigate SNe Ic as production sites for the light elements Li, Be, and B, via the neutrino-process and spallations. As massive stars collapse, neutrinos are emitted in large numbers from the central remnants. Some of the neutrinos interact with nuclei in the exploding materials and mainly ${}^7\text{Li}$ and ${}^{11}\text{B}$ are produced. Subsequently, the ejected materials with very high energy impinge on the interstellar/circumstellar matter and spall into light elements. We find that the ν -process in the current SN Ic model produces a significant amount of ${}^{11}\text{B}$, consistent with observations if combined with B isotopes from the following spallation production.

Keywords. Neutrinos, nuclear reactions, nucleosynthesis, abundances – Supernovae: general

1. Introduction

Most of metals up to iron are synthesized inside main sequence stars via nuclear reactions called nuclear burning. Newly-synthesized elements are ejected into interstellar space and pollute the interstellar gas primitively consisted of hydrogen and helium. However, light elements such as Li, Be, B and their isotopes (LiBeB) are hardly produced by nuclear burning partly because of Li fragile property and absence of stable nuclei with atomic mass number of eight. Some processes considered to mainly produce these elements are briefly summarized below.

Shortly after the Big Bang, protons and neutrons combine and produce hydrogen and helium isotopes. Subsequently, tritium and ${}^3\text{He}$ combine with α -particle to form ${}^7\text{Li}$ (and ${}^7\text{Be}$ eventually decaying to ${}^7\text{Li}$), which make an almost constant Li abundance observed on the surfaces of metal-poor halo stars, the so-called Spite Plateau (Spite & Spite 1982).

After star formation and its gravitational contraction, hydrogen burning reaction is ignited at the center. Although light elements synthesized at the hot regions of stars are fated to be broken by surrounding hot protons, an escape route for them are known. Cameron proposed a mechanism (Cameron 1955) available for AGB stars, called Be-transport mechanism, where ${}^7\text{Be}$ in hydrogen burning shell are brought to cool envelopes by the circulation currents during a thermal pulse phase. A fraction of survived ${}^7\text{Be}$ (${}^7\text{Li}$) capture α -particle and form ${}^{11}\text{B}$, both of them are ejected into the interstellar space through stellar winds. This mechanism is effective for stars with masses in the

range $4 \leq M/M_{\odot} \leq 6$. Some computational works, however, have revealed that lithium from AGB stars are not important for the Galactic chemical evolution (Romano et al. 2001; Ventura et al. 2002). Note that in some cases AGB stars show low, not high, lithium abundances caused by dilution during the previous evolutionary phases (Maceroni et al. 2002). For more massive stars, they are known to collapse and explode as supernovae at the end of their lives. Most of the gravitational energy released at the explosion of a massive star is carried away by neutrinos emitted from the central remnant. Their number is achieved to more than 10^{58} . Although cross sections of neutrino-nucleus reactions are very small, such a huge number of neutrinos enable to contribute the increase in the yields of some species of nuclei. This is called the ν -process (Woosley et al. 1990). The ν -process mainly contributes to the production of ${}^7\text{Li}$ and ${}^{11}\text{B}$ among light elements (e.g. Woosley et al. 1990; Heger et al. 2005; Yoshida et al. 2005, 2008).

The processes described above predominantly produce ${}^7\text{Li}$ and ${}^{11}\text{B}$, while cosmic-ray (CR) nucleosynthesis produces all stable isotopes of LiBeB (e.g. Meneguzzi et al. 1971; Suzuki & Inoue 2002; Rollinde et al. 2008). In CR nucleosynthesis, low-energy CRs accelerated in shocks interact with the ambient medium and produce LiBeB via spallations ($\text{H}, \alpha + \text{C}, \text{N}, \text{O} \rightarrow \text{LiBeB}$) or fusion reaction of α -particles ($\alpha + \alpha \rightarrow {}^6, {}^7\text{Li}$). Theoretical CR nucleosynthesis models predict strong correlations between BeB abundances and metallicity, consistent with observations although it is difficult to explain the observed linear dependences if the Galactic CRs consist of protons and α -particles.

Despite a great deal of efforts to investigate these processes, the origins of LiBeB are not fully understood and there remain some observational features conflicting with theoretical predictions. For instance, theoretical predictions for LiBeB production from Galactic CRs indicate quadratic relations between B(Be) abundances and metallicity, while observations clearly show linear relations. To consist with observational trend, CNO CRs from superbubbles (Higdon et al. 1998) and Type Ic supernovae (Fields et al. 2002; Nakamura & Shigeyama 2004) have been suggested. However, the CR spallations cannot be the only source of boron isotopes because the CR spallations do not reproduce the high ratio of ${}^{11}\text{B}$ to ${}^{10}\text{B}$ observed in meteorites. Therefore another ${}^{11}\text{B}$ source is necessary.

To solve these unsolved problems and consider the Galactic chemical evolution concerning with the light elements, it is necessary to accurately evaluate the contribution of each LiBeB productive process. Here we focus on the B isotopes from core-collapse SNe, in particular energetic Type Ic SNe (SNe Ic). The progenitor of an SN Ic is a C/O star and its H and He envelopes have been stripped during the stellar evolution. Although the explosion mechanism of SNe Ic has not clarified, neutrinos should be one of main carriers of the gravitational energy released from the collapsing core. The neutrino emission from a collapsing proto-neutron star evolved from a $\sim 40M_{\odot}$ star has been investigated (Sumiyoshi et al. 2006). Even in the case that the central core of such a star becomes a black hole, a temporally formed proto-neutron star emits a huge amount of neutrinos before collapsing to the black hole. On the other hand, after the black hole formation, neutrinos are considered to be emitted from accretion disk surrounding the newly formed black hole (e.g. Kohri et al. 2005; Surman & McLaughlin 2005). Therefore, a huge amount of neutrinos are emitted from the central region of an SN Ic and the ν -process is expected to occur in the exploding supernova material. We investigate the ν -process in SN Ic for the first time. In addition, LiBeB production through spallations between the SN ejecta and the interstellar/circumstellar matter is considered. In §2, we present our calculations of supernova explosion (§2.1), nucleosynthesis by the ν -process (§2.2), and by spallations (§2.3). Section §3 discusses our results and clarifies the important role of SNe Ic in the light element synthesis.

2. Calculations and results

2.1. Supernova explosion

Here we consider a very energetic explosion of a $15 M_{\odot}$ C/O star with the explosion energy $E_{\text{ex}} = 3 \times 10^{52}$ ergs corresponding to SN 1998bw (Nakamura et al. 2001). The explosion energy is released at the center of the progenitor star as thermal energy. Resulting shock wave accelerates the stellar materials and explode the progenitor as a supernova. Time evolution of physical quantities in the progenitor are calculated with 1-dimensional hydrodynamic code taking the effects of special relativity into account. We solve the special relativistic hydrodynamic equations in Lagrangian coordinates with an ideal equation of state involving gas and radiation pressure. Adiabatic indices are treated as functions of pressure and gas density. Details on the numerical code are described in Nakamura & Shigeyama (2004).

2.2. The Neutrino-Process

Light element synthesis in the Type Ic supernova is calculated as a post process. We use a nuclear reaction network consisting of 291 species of nuclei and taking into account the ν -process (Yoshida et al. 2008).

Neutrinos are considered to be emitted from a collapsing proto-neutron star (e.g. Sumiyoshi et al. 2006) and/or the innermost region just above a black hole (e.g. Surman & McLaughlin 2005). However, properties of the neutrinos, particularly in SNe Ic, are still uncertain. So, we use the following neutrino model extended from a supernova neutrino model taken in Yoshida et al. (2008). We suppose that neutrino luminosity decreases exponentially with the decay time of 3 s while the neutrino temperature of each species does not change with time. The total energy carried out by neutrinos is assumed to be 3×10^{53} ergs.

We consider two models for these constant neutrino temperatures. In the first model, the temperatures of ν_e , $\bar{\nu}_e$, and $\nu_{\mu,\tau}$ and $\bar{\nu}_{\mu,\tau}$ are set to be $T_{\nu_e} = 3.2$ MeV, $T_{\bar{\nu}_e} = 5$ MeV, and $T_{\nu_{\mu,\tau}} = 6$ MeV, respectively. This temperature model is referred to as the “normal” $T_{\nu_{\mu,\tau}}$ model. The light element synthesis in an $\sim 20 M_{\odot}$ Type II supernova with the normal temperature model well reproduces the supernova contribution of the ^{11}B production during Galactic chemical evolution (Yoshida et al. 2005, 2008). The third peak of r-process elements is also achieved in neutrino-driven wind models with this temperature model. In the second model, the temperature of $\nu_{\mu,\tau}$ and $\bar{\nu}_{\mu,\tau}$ is set to be $T_{\nu_{\mu,\tau}} = 8$ MeV. The same values as the normal model are adopted for T_{ν_e} and $T_{\bar{\nu}_e}$. This temperature model is referred to as the high $T_{\nu_{\mu,\tau}}$ model. A newly forming proto-neutron star in an SN Ic should be more compact than that of an SN II. Therefore, the neutrino temperature of the collapsing proto-neutron star is larger than that of SNe II (e.g. Sumiyoshi et al. 2006).

The mass fraction distributions of ^{11}B , ^{11}C , ^{10}B , ^7Li , and ^7Be in the SN Ic are shown in Figure 1. The mass fractions are of the order of $\sim 10^{-8}$ for ^{11}B and ^{11}C and $\sim 10^{-11} - 10^{-10}$ for ^{10}B , ^7Li , and ^7Be . The yield of each species strongly depends on the corresponding branching ratio of the reactions. The light elements are mainly produced in the O/Ne layer ($M_r > 7.4 M_{\odot}$). The mass fractions in the O/Si layer ($4.6 M_{\odot} < M_r < 7.4 M_{\odot}$) are smaller than in the outer layer. The Si/S layer ($3.7 M_{\odot} < M_r < 4.6 M_{\odot}$) where carbon burned out indicates no light elements. The mass fractions of some light elements are also large in the innermost region where α -rich freeze out is achieved ($M_r < 2.6 M_{\odot}$) and complete Si-burning occurs ($2.6 M_{\odot} < M_r < 3.5 M_{\odot}$). There are no qualitative differences in the mass fraction distributions between the normal and high $T_{\nu_{\mu,\tau}}$ models.

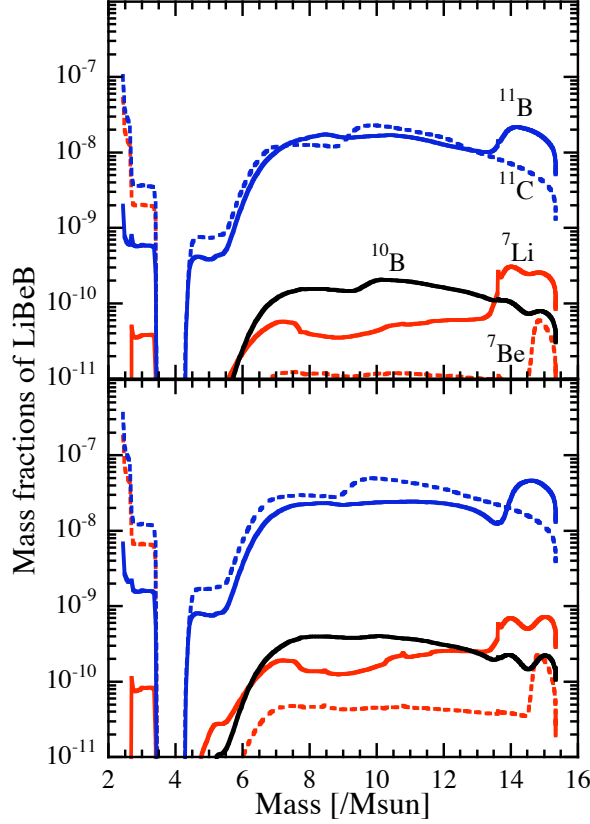


Figure 1. The mass fraction distributions of light elements produced via the ν -process as functions of the mass coordinate. Shown are the cases of the SN 1998bw model ($M_{\text{CO}} = 15M_{\odot}$, $E_{\text{ex}} = 3 \times 10^{52}$ ergs) with $T_{\nu_e} = 3.2$ MeV, $T_{\bar{\nu}_e} = 5$ MeV, and $T_{\nu_{\mu\tau}} = 6$ MeV (*top*) and 8 MeV (*bottom*) at 75 seconds after the energy release.

The mass fraction of each species in the high $T_{\nu_{\mu,\tau}}$ model at a given mass coordinate is roughly twice as the corresponding one in the normal $T_{\nu_{\mu,\tau}}$ model.

Some of light elements produced through ^{12}C -neutrino reactions are decomposed by explosive nucleosynthesis occurring immediately after the shock arrival. ^{11}B , ^{11}C , and ^{10}B are decomposed by collisions with protons and α -particles. ^7Li and ^7Be are photo-disintegrated to ^3H and ^3He , respectively. After the shock passage, the exploding and cooling materials are still irradiated by neutrinos, so that light elements are produced through the ν -process again. We note that the mass fractions of ^{11}B , ^7Li , and ^7Be in the outermost region ($M_r > 13.5M_{\odot}$) are larger than the corresponding ones in the inner region because they are not decomposed in explosive nucleosynthesis.

In the innermost region, light elements are produced after the termination of the nuclear statistical equilibrium. The main product in α -rich freeze out is ^4He . About 20% of ^4He by mass fraction is also produced in complete Si-burning. The ν -process of ^4He produces ^3H and ^3He in cooling materials. The α -capture reactions followed by the ν -process produce ^7Li and ^7Be . Furthermore, ^{11}B and ^{11}C are produced by α -captures and ^{10}B is produced through $^7\text{Be}(\alpha, p)^{10}\text{B}$.

In both cases of $T_{\nu_{\mu,\tau}}$ a significant amount of ^{11}B is synthesized ($2.69 \times 10^{-7} M_{\odot}$ for the normal $T_{\nu_{\mu,\tau}}$ model and $5.46 \times 10^{-7} M_{\odot}$ for the high $T_{\nu_{\mu,\tau}}$ model). It should be noted that the amounts of ^{11}B produced through the ν -process include those of ^{11}C which decays to ^{11}B with a half life of 20 minutes. The yield of ^7Li is on the order of $10^{-9} - 10^{-8} M_{\odot}$ in the SN Ic model. This yield is much smaller than that produced in SNe II (e.g. Yoshida et al. 2008). Most of ^7Li in SNe II is produced through the ν -process of ^4He and the following α -capture reactions in the He-rich layer. On the other hand, almost all H and He layers of SN Ic progenitors have been stripped via stellar wind and/or binary effect before explosion. The yields of ^6Li , ^9Be , and ^{10}B are on the order of or below $10^{-9} M_{\odot}$. They are also much smaller than the ^{11}B yield. This is due to smaller branching ratios of neutrino- ^{12}C reactions (Yoshida et al. 2008).

2.3. Spallation reactions

Supernova explosions accelerate and expel the stellar materials into the interstellar space, polluting the universe with newly synthesized elements. The progenitors of SNe Ic are so compact that a very small fraction of ejecta can be accelerated nearly to the speed of light, interact with the interstellar matter (Nakamura & Shigeyama 2004) or the circumstellar matter (Nakamura et al. 2006), and produce the light element isotopes via spallation reactions of CNO with protons or α -particles. The surface layers of SNe Ic, which are composed of C and O, impinge on the H or He nuclei in the ambient medium and spall into LiBeB. Here we use the result for a SN 1998bw model constructed by Nakamura & Shigeyama (2004). 0.3% ($0.04 M_{\odot}$) of the ejecta attain enough energy ($\gtrsim 10 \text{ MeV/A}$) to undergo spallations (see eq. 2.2). They solved the transfer equation for each element i expressed as

$$\frac{\partial F_i(\epsilon, t)}{\partial t} = \frac{\partial[\omega_i(\epsilon)F_i(\epsilon, t)]}{\partial \epsilon} - \frac{F_i(\epsilon, t)}{\Lambda} \rho v_i(\epsilon), \quad (2.1)$$

where Λ is the loss lengths in g cm^{-2} , ρ denotes the mass density of the ISM, $v_i(\epsilon)$ the velocity of the element i with an energy per nucleon of ϵ . The initial condition for the mass of element i with an energy per nucleon ϵ at time $t = 0$, $F_i(\epsilon, t = 0)$, is derived from the numerical calculations of explosions or an empirical formula

$$\frac{M(> \epsilon)}{M_{\text{ej}}} = A \left(\frac{E_{\text{ex}}/10^{51} \text{ ergs}}{M_{\text{ej}}/1 M_{\odot}} \right)^{3.4} \times \left(\frac{\epsilon}{10 \text{ MeV}} \right)^{-3.6}, \quad (2.2)$$

where M_{ej} is the mass of the ejecta and the constant A is equal to 1.9×10^{-4} for the current model. Then the yield of a light element l via the $i + j \rightarrow l + \dots$ reaction is estimated from

$$\frac{dN_l}{dt} = n_j \int \sigma_{i,j}^l(\epsilon) \frac{F_i(\epsilon, t)}{A_i m_p} v_i(\epsilon) d\epsilon, \quad (2.3)$$

where N_l is the number of the produced light element l , n_j is the number density of an element j in the interstellar matter, $\sigma_{i,j}^l$ the cross section of $i + j \rightarrow l + \dots$ reaction given by Read & Viola (1984), A_i the mass number of the element i . The interstellar matter is assumed to be composed of neutral H and He with the number densities of $n_{\text{H}} = 1 \text{ cm}^{-3}$ and $n_{\text{He}} = 0.1 \text{ cm}^{-3}$.

Their results show that the mass of ^{11}B produced via spallation reactions is $1.34 \times 10^{-6} M_{\odot}$, which is larger than that synthesized via the ν -process even in the high $T_{\nu_{\mu,\tau}}$ model. The resultant isotopic ratio of $^{10}\text{B}/^{11}\text{B}$ ($\sim 1/3$) in this model is predominantly determined by the ratio of cross sections of the reaction $\text{p}, \alpha + \text{O} \rightarrow ^{10}\text{B}$ to that of $\text{p}, \alpha + \text{O} \rightarrow ^{11}\text{B}$.

3. Conclusions

Nakamura & Shigeyama (2004) concluded that SNe Ic may not play an important role in B isotope productions because of the low isotope ratios $^{11}\text{B}/^{10}\text{B} \sim 2.8$ compared with observations in meteorites (4.05 ± 0.05), and other ^{11}B sources like the ν -process in SNe II are necessary. We estimate the production of light elements including boron isotopes via the ν -process in an SN Ic and find that SNe Ic can be as powerful ^{11}B producers as SNe II. The resulting number ratios of B isotopes from both the ν -process and spallations $^{11}\text{B}(+^{11}\text{C})/^{10}\text{B} = 3.66 - 4.28$ well match with observations. It is reasonable to assume the small radii of neutrino spheres because of the compactness of SN Ic progenitors, leading to the high temperatures of emitted neutrinos and anti-neutrinos. High $T_{\nu_{\mu\tau}}$ results in high LiBeB yields through neutral current reactions in the ν -process, which raises the potential role of SNe Ic in the light element production.

The combined mechanism of light element production described here, the ν -process and spallations, may also be effective in the case of Type Ib supernovae where progenitor stars without H-rich envelope explode. In such a case, the outermost layers consist of He and the α -particle fusion reaction producing lithium isotopes become important. Furthermore, Meynet & Maeder (2002) suggested that the He layers of very metal-poor stars contain primary nitrogen produced during the He-burning phase by the CNO cycle in the H-burning shell stimulated by rotationally-induced diffusion of carbon into the H-burning shell. This nitrogen may enhance the light element production via spallations because the cross sections of spallation reactions involving nitrogen tend to have relatively low energy thresholds and high peak values. Observationally some low-metallicity halo stars have been found to have high abundances of ^6Li or ^9Be beyond the theoretical predictions, which engages our interest in SNe Ib even if they might not accelerate their envelopes effectively because their progenitors are not so compact as those of SNe Ic.

References

- Cameron, A. G. W. 1955, *ApJ*, 121, 144
 Fields, B. D., Daigne, F., Cassé, M., & Vangioni-Flam, E. 2002, *ApJ*, 581, 389
 Heger, A., Kolbe, E., Haxton, W. C., Langanke, K., Martínez-Pinedo, G., & Woosley, S. E. 2005, *Phys. Lett. B*, 606, 258
 Higdon, J. C., Lingenfelter, R. E., & Ramaty, R. 1998, *ApJ*, 509, L33
 Kohri, K., Narayan, R., & Piran, T. 2005, *ApJ*, 629, 341
 Maceroni, C., Testa, V., Plez, B., García Lario, P., & D'Antona, F. 2002, *A&A*, 395, 179
 Meneguzzi, M., Audouze, J., & Reeves, H. 1971, *A&A*, 15, 337
 Meynet, G., & Maeder, A. 2002, *A&A*, 390, 561
 Nakamura, K., & Shigeyama, T. 2004, *ApJ*, 610, 888
 Nakamura, K., Inoue, S., Wanajo, S., & Shigeyama, T. 2006, *ApJ*, 643, L115
 Nakamura, T., Mazzali, P. A., Nomoto, K., & Iwamoto, K. 2001, *ApJ*, 550, 991
 Read, S. M., & Viola, V. E. 1984, *Atomic Data and Nuclear Data Tables*, 31, 359
 Rollinde, E., Maurin, D., Vangioni, E., Olive, K. A., & Inoue, S. 2008, *ApJ*, 673, 676
 Romano, D., Matteucci, F., Ventura, P., & D'Antona, F. 2001, *A&A*, 374, 646
 Spite, F., & Spite, M. 1982, *A&A*, 115, 357
 Sumiyoshi, K., Yamada, S., Suzuki, H., & Chiba, S. 2006, *Phys. Rev. Lett.*, 97, 091101
 Surman, R., & McLaughlin, G. C. 2005, *ApJ*, 618, 397
 Suzuki, T. K., & Inoue, S. 2002, *ApJ*, 573, 168
 Ventura, P., D'Antona, F., & Mazzitelli, I. 2002, *A&A*, 393, 215
 Woosley, S. E., Hartmann, D. H., Hoffman, R. D., & Haxton, W. C. 1990, *ApJ*, 356, 272
 Yoshida, T., Kajino, T., & Hartmann, D. H. 2005, *Phys. Rev. Lett.*, 94, 231101
 Yoshida, T., Suzuki, T., Chiba, S., Kajino, T., Yokomakura, H., Kimura, K., Takamura, A., & Hartmann, D. H. 2008, *ApJ*, 686, 448

The search for the origin of the light nuclei Li, Be, B

Hubert Reeves¹

CNRS, France

Abstract. My aim is to show how the abundance ratios of the light elements (6 to 11) are related to the properties of the strong nuclear interaction and, in particular, to the major influence of closed shells of neutrons and protons, (the magic numbers : 2, 8, etc) on the binding energies of the nuclei.

Keywords. Nuclear reactions, nucleosynthesis, abundances – ISM: cosmic rays

1. Introduction

The α -particle has a very high binding energy, resulting from its doubly magic structure : two protons and two neutrons. This fact results, on the one hand, on the relatively high binding energies of the nuclei containing the equivalent of an integer number of α -particles (C-12, O-16, Ne-20, Mg-24, Si-28 : the so-called α -nuclei) but also on the very low binding energy of the light nuclei : lithium, beryllium, and boron, the most extreme case being the instability of the mass-5 and of the mass-8. Immediately after their formation these nuclei rapidly decay in an α -mix (a group of nuclei containing the maximum number of α -particles.)

As shown in Table 1, Be-9 is hardly bound, and B-11 is more bound than B-10. Lithium -6 and Lithium-7 are quite comparable to the Bs. These low binding energies with respect to the α -mix are the reasons why these elements can not withstand the high temperatures of the stellar interiors.

2. Where were they made ?

There are several hints for the identification the formation mechanisms of lithium, beryllium, and boron.

Hint no 1: The amplitude of the nuclear cross sections for their formation by high energy protons on heavy nuclei (spallation) are closely related to their cosmic abundances.

We consider high energy processes in a cold region. For instance cosmic ray protons on C-12 or O-16 on interstellar gas. The physics of these reactions is best described by the Enrico Fermi hot ball model. The target nucleus is first heated to very high temperatures by the energy of the incident bolid. It thermalizes and cools by evaporation of part of its

Table 1. Table of binding energies of the light nuclei with respect to an α -mix. The number in MeV gives the energy release by the break up of the nucleus in a group of light particles containing the maximum amount of α -particles (dubbed an α -mix)

Li-6	2.45 MeV
Li-7	1.24 MeV
Be-9	88 KeV
B-10	5.97 MeV
B-11	11.2 MeV

nuclear constituents (neutrons, protons, alphas). The residual nucleus can be Li, Be, or B.

One of the tenets of quantum physics is that the probability of a reaction leading to a specific result is proportional to the number of equivalent ways of producing this result. This, in turn, is a measure of the volume of phase space available for the reactions, hence of the amount of kinetic energy released by the reactions. The products with low binding energies release a larger volume of space phase and have hence a larger formation probability. This is well illustrated when one considers the cross-sections for the formation of the light nuclei by high energy protons on C-12. As expected, Be has the smallest value, followed by Li and B. The cross-section for B-11 is larger than for B-10. The case of Li will be considered later.

Hint no 2: These nuclei are much more abundant in galactic cosmic rays than in nature. Note that boron is more abundant than nitrogen!

3. Nuclear physics data

In the 1960 when this model was presented, practically no data on the nuclear cross sections were available. In the following years I visited a number of nuclear laboratories (Los Alamos, CERN, Darmstadt, Berkeley, Moscow, Leningrad, Orsay) to present this proposal. The reactions of the nuclear physicists was typically “Yes, this is interesting but because of the need of obtaining highly purified targets, it would take many years to complete this project. We can not get involved for such a long period of time.”

Fortunately, in 1965, I met a group of physicists of Orsay, France led by René Bernas, who were already pursuing such experiments. We joined forces to interpret the results in the nucleosynthesis context.

Taking into account the fact that each accelerator works at a given energy, and that the cosmic ray particles span a large range of energies, from MeV to GeV and more, it became necessary for the nuclear physicists to bring their isotope separators to different accelerators in France, Germany, USSR, and Switzerland (CERN) in order to patiently build the full cross sections of the various reactions involved.

I want here to give credit to these scientists by giving their names : Marcelle Epherre, Elie Gradstajn, François Yiou, Robert Klapisch.

4. Comparison of abundances with the calculated values

Calculations were then performed of the abundances and isotopic ratios, taking into account the spectrum of energy in galactic cosmic rays and the nuclear cross sections obtained in the laboratories. The results and their astrophysical implications are discussed in the following.

The beryllium abundance can be taken as a measure of the integral activity of the bombardment of the cosmic rays throughout the life of our Galaxy. Indeed the product of the present formation rate of Be times the life of the Galaxy yields an abundance quite comparable to the observed abundance.

The relative probabilities of formation of the various isotopes can be used to evaluate the contribution of GCR to the other light isotopes. We define a term $F(obs/calc)(x/y)$ as the ratio of the observed abundances of two nuclei x and y over the calculated ratio of their formation rates in GCR.

Boron over beryllium

The observed ratio in the solar system SS (sun and meteorites) is 23. The calculated

GCR ratio is 15. We have also observations of this ratio in the metal poor stars of ~ 20 , constant with metallicities down to (-3) (one thousand solar).

The observed isotopic ratio in the solar system is $11/10 = 4.0$, while the formation ratio is 2.5. We probably need an extra source of B-11, which could come from stellar processes. One possibility is the C-12 desintegration by neutrino collisions in supernovae which would generate B-11 but no B-10. However the uncertainties involved in the calculations of the yields are so large that no meaningful comparison can be made.

We consider the case of B-10.

$$F = (10/9)_{obs}/(10/9)_{calc} = (116/22)/5 = 1.04$$

showing that this isotope is a pure GCR product.

Lithium 7/lithium-6

The GCR ratio is ~ 2 while the SS is 12.5. This was the first indication of a possible other source of Lithium-7. Thanks to the observations of François and Monique Spite, we associate this source to the Big Bang Nucleosynthesis. Studies of the fossil radiation (CMB) by the satellite WMAP have confirmed this association.

However, since the contribution of BBN to the formation of Li-6 is negligible, we may ask if this element is a pure product of GCR. Computing the ratio of its abundance to the Be-9 abundance we find :

$$F(6/9)_{(obs)/calc} = 6.5/5 = 1.3$$

confirming the value of the hypothesis.

Some observations of lithium in interstellar gas, in particular around the star Rho Ophiucus, have locally given values much smaller than the solar system values. One possibility is the collision of fast alphas on Helium-4 which generates Li-6 and Li-7 with ratios around 2. We note that the respective cross-sections involve alphas of energies around ten to one hundred Mev per nucleon, appreciably smaller than the mean particle energy in the GCR (hundreds of Mev). This may involve special astrophysical contexts such as the activity of high energy emitting particles stars in these area.

To complete this operation we compute the ratio of B-10 to Li-6

$$F(10/6)_{obs/calc} = (116/144)/1 = 0.8$$

confirming that the nuclei of Li-6, Be-9, and B-10 are pure products of the GCR.

5. Conclusions

It is of interest to note that the three nucleosynthetic processes : Big Bang, Galactic cosmic rays, and stellar nucleosynthesis cover suitably well the light elements abundances ($A < 12$).

The Big Bang is responsible for the atoms with mass number 2, 3, most of 4, and 7 (mostly in old stars).

The GCR is responsible for 6, 9, 10, and also a part of 7 and most of 11.

Stellar nucleosynthesis is responsible for most of 7, some 4, and perhaps some 3 and 11. And also of the elements from carbon to the heaviest elements : thorium and uranium.

References

The references are given in the paper of Nicolas Prantzos.



Hubert Reeves with some of his students and grand-students:
Thibaut Decressin, Ana Palacios, Nikos Prantzios, Sylvie Vauclair
Nadège Lagarde, Thierry Montmerle, Corinne Charbonnel



André Maeder & Sylvie Vauclair

Origin of cosmic rays and evolution of spallogenic nuclides Li, Be and B

Nikos Prantzos

Institut d' Astrophysique de Paris
 98bis, Bd. Arago, 75014 Paris
 email: prantzos@iap.fr

Abstract. A short overview is presented of current issues concerning the production and evolution of Li, Be and B in the Milky Way. In particular, the observed “primary-like” evolution of Be is re-assessed in the light of a novel idea: it is argued that Galactic Cosmic Rays are accelerated from the wind material of *rotating* massive stars, hit by the forward shock of the subsequent supernova explosions. The pre-galactic levels of both Li isotopes remain controversial at present, making it difficult to predict their Galactic evolution. A quantitative estimate is provided of the contributions of various candidate sources to the solar abundance of Li.

1. Introduction

The idea that the light and fragile elements Li, Be and B are produced by the interaction of the energetic nuclei of galactic cosmic rays (GCR) with the nuclei of the interstellar medium (ISM) was introduced 40 years ago (Reeves et al. 1970, Meneguzzi et al. 1971, hereafter MAR). In those early works it was shown that, taking into account the relevant cross-sections and with plausible assumptions about the GCR properties - source composition, intensity and spectrum - one may reproduce reasonably well the abundances of those light elements observed in GCR and in meteorites (pre-solar).

Among the required ingredients for such a calculation, the relevant spallation cross sections of CNO nuclei are accurately measured in the laboratory. The source composition and the equilibrium energy spectrum of GCR are inferred from a combination of observations and models of GCR propagation in the Milky Way (e.g. in the framework of the so-called “leaky box” model). Once the equilibrium spectra of GCR in the ISM are established, the calculation of the resulting abundances of LiBeB is straightforward, at least to first order[†]. The production rate (s^{-1}) of the abundance $Y_L = N_L/N_H$ (by number) of LiBeB nuclei is given by

$$\frac{dY_L}{dt} = F_{p,a}^{GCR} \sigma_{pa+CNO} Y_{CNO}^{ISM} + F_{CNO}^{GCR} \sigma_{pa+CNO} Y_{p,a}^{ISM} P_L + F_a^{GCR} \sigma_{a+a} Y_a^{ISM} P_L \quad (1.1)$$

where: F ($\text{cm}^{-2} \text{s}^{-1}$) is the average GCR flux of protons, alphas or CNO, Y the abundances by number of those nuclei in the ISM, and σ (cm^2) is the average (over the equilibrium energy spectrum of GCR) cross-section for the corresponding spallation reactions producing LiBeB. The first term in the right hand member of this equation (fast protons and alphas hitting CNO nuclei of the ISM) is known as the “direct” term, the second one (fast CNO nuclei being fragmented on ISM protons and alphas) is the “reverse” term and the last one involves “spallation-fusion” reactions, concerning only the Li isotopes. P_L is the probability that nuclide L (produced at high energy) will be

[†] The full calculation should include production by spallation of other primary and secondary nuclides, such as ^{13}C ; however, this has only second order effects.

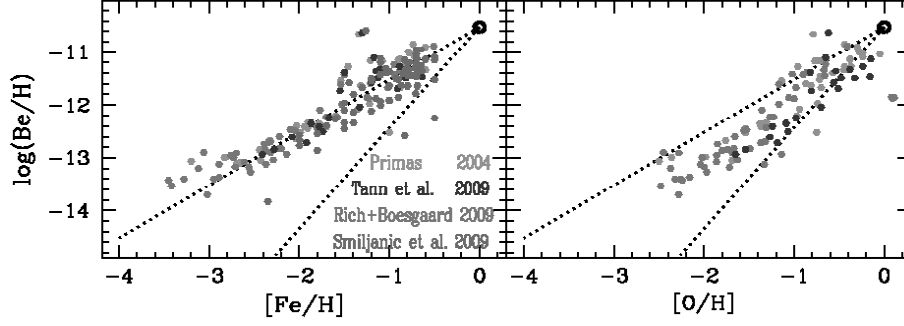


Figure 1. Observations of Be vs. Fe (*left*) and vs. O (*right*). In both panels, dotted lines indicate slopes of 1 (primary) and 2 (secondary). Be clearly behaves as a primary vs. Fe, whereas there is more scatter in the data vs. O.

thermalized and remain in the ISM (see, e.g. Prantzos 2006). Obviously, the GCR flux term $F_{CNO}^{GCR} \propto Y_{CNO}^{GCR}$ is proportional to the abundances of CNO nuclei in GCR, a fact of paramount importance for the evolution of Be and B (see next sections).

Substituting appropriate values for GCR fluxes ($F_p^{GCR} \sim 10 \text{ p cm}^{-2} \text{ s}^{-1}$ for protons and scaled values for other GCR nuclei), for the corresponding cross sections (averaged over the GCR equilibrium spectrum $\sigma_{p,a+CNO \rightarrow Be} \sim 10^{-26} \text{ cm}^2$) and for ISM abundances $Y_{CNO} \sim 10^{-3}$, and integrating for $\Delta t \sim 10^{10} \text{ yr}$, one finds $Y_{Be} \sim 2 \cdot 10^{-11}$, i.e. approximately the meteoritic Be value. Satisfactory results are also obtained for ${}^6\text{Li}$ and ${}^{10}\text{B}$.

Two problems were identified with the GCR production, compared to meteoritic composition: the ${}^7\text{Li}/{}^6\text{Li}$ ratio (~ 2 in GCR, but ~ 12 in meteorites) and the ${}^{11}\text{B}/{}^{10}\text{B}$ ratio (~ 2.5 in GCR, but ~ 4 in meteorites). It was then suggested in MAR that supplementary sources are needed for ${}^7\text{Li}$ and ${}^{11}\text{B}$. Modern solutions to those problems involve *stellar* production of $\sim 60\%$ of ${}^7\text{Li}$ (in the hot envelopes of AGB stars and/or novae, see Sec. 7) and of $\sim 40\%$ of ${}^{11}\text{B}$ (through ν -induced spallation of ${}^{12}\text{C}$ in SN, see Sec. 5). In both cases, however, uncertainties in the yields are such that observations are used to constrain the yields of the candidate sources rather than to confirm the validity of the scenario.

2. Primary Be: the problem

Observations of halo stars in the 90s revealed a linear relationship between Be/H and Fe/H (Gilmore et al. 1991, Ryan et al. 1992) as well as between B/H and Fe/H (Duncan et al. 1992). That was unexpected, since Be and B were thought to be produced as *secondaries*, by spallation of the increasingly abundant CNO nuclei. Indeed, the first two terms in Eq. 1.1 were thought to evolve in the same way with time (or metallicity), since the composition of GCR Y_{CNO}^{GCR} was supposed to evolve in step with the one of the ISM Y_{CNO}^{ISM} . Only the Li isotopes, produced at low metallicities mostly by $\alpha + \alpha$ reactions were thought to be produced as primaries (Steigman and Walker 1992). The only way to produce primary Be is by assuming that GCR have always the same CNO content, as suggested in Duncan et al. (1992). Other efforts to enhance the early production of Be, by e.g. invoking a better confinement - and thus, higher fluxes - of GCR in the early Galaxy (Prantzos et al. 1993) failed. The reason for that failure was clearly revealed by the “energetics argument” put forward by Ramaty et al. (1997): if SN are the main source of GCR energy, there is a limit to the amount of light elements produced per SN, which depends on GCR and ISM composition. If the metal content of *both* ISM and GCR is

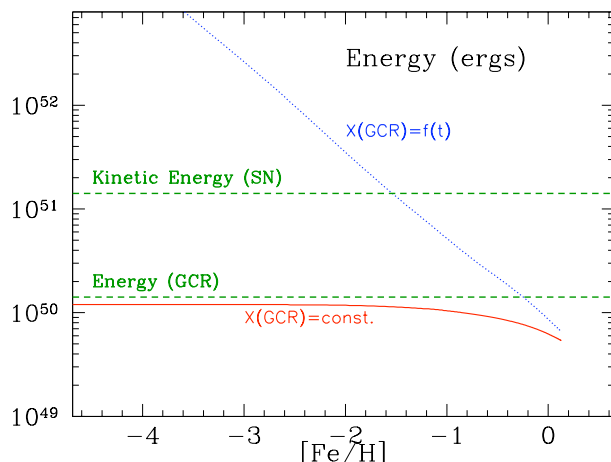


Figure 2. Energy input required from energetic particles accelerated by one CCSN in order to produce a given mass of Be, such as to have $[\text{Be}/\text{Fe}]=0$ (solar), assuming that a core collapse SN produces, on average, $0.1 M_{\odot}$ of Fe. *Solid* curve corresponds to the case of a constant composition for GCR, *dotted* curve corresponds to a time variable composition, following the one of the ISM. In the former case, the required energy is approximately equal to the energy imparted to energetic particles by supernovae, namely ~ 0.1 of their kinetic energy of $\sim 1.5 \cdot 10^{51}$ ergs; in the latter case, the energy required to keep $[\text{Be}/\text{Fe}]=0$ becomes much larger than the total kinetic energy of a CCSN for metallicities $[\text{Fe}/\text{H}] \leq -1.6$.

low, there is simply not enough energy in GCR to keep the Be yields constant (Fig. 2)[†]. Since the ISM metallicity certainly increases with time, the “direct” component in Eq. 1.1 produces only secondary LiBeB. The only possibility to have \sim constant LiBeB yields is by assuming that the “reverse” component is primary, i.e. that GCR have a \sim constant metallicity. This has profound implications for our understanding of the GCR origin. It should be noted that before those Be and B observations, no one would have the idea to ask “what was the GCR composition in the early Galaxy?”.

3. Origin of cosmic rays

For quite some time it was thought that GCR originate from the average ISM, where they are accelerated by the *forward shocks* of SN explosions (Fig. 3.A). However, this can only produce secondary Be.

A \sim constant abundance of C and O in GCR can “naturally” be understood if SN accelerate their own ejecta, through their *reverse shock* (Ramaty et al. 1997, see Fig. 3.B). However, the absence of unstable ^{59}Ni (decaying through e^- capture within 10^5 yr) from observed GCR suggests that acceleration occurs $>10^5$ yr after the explosion (Wiedenbeck et al. 1999) when SN ejecta are presumably already diluted in the ISM. Furthermore, the reverse shock has only a small fraction of the SN kinetic energy, while observed GCR require a large fraction of it[‡].

[†] For reasons unknown to the author, the energetics argument was obviously not understood by many prolific researchers in the field in the late 90ies.

[‡] The power of GCR is estimated to $\sim 10^{41}$ erg s^{-1} galaxywide, i.e. about 10% of the kinetic energy of SN, which is $\sim 10^{42}$ erg s^{-1} (assuming 3 SN/century for the Milky Way, each one endowed with an average kinetic energy of $1.5 \cdot 10^{51}$ ergs).

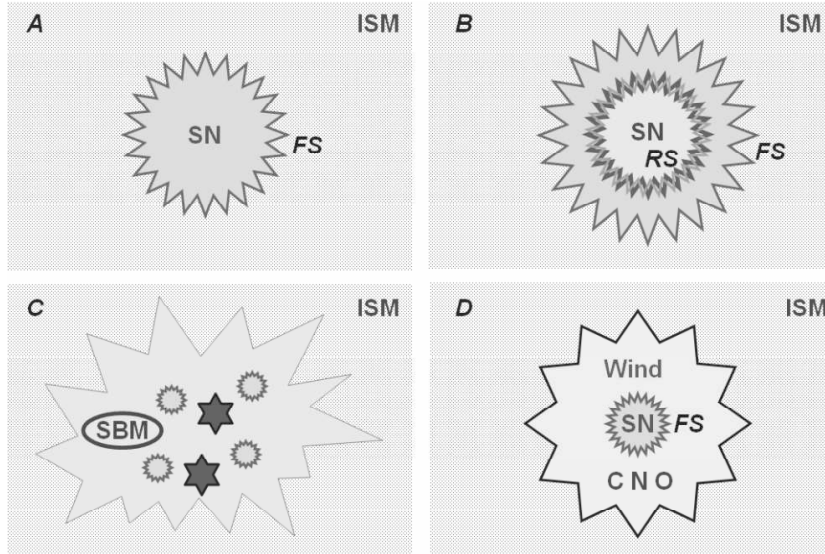


Figure 3. Scenarios for the origin of Galactic cosmic rays (GCR). *A:* GCR originate from the interstellar medium (ISM) and are accelerated from the forward shock (FS) of supernovae (SN). *B:* GCR originate from the interior of supernovae and are accelerated by the reverse shock (RS), propagating inwards. *C:* GCR originate from superbubble material (SBM), enriched by the metals ejected by supernovae and massive star winds; they are accelerated by the forward shocks of supernovae and stellar winds. *D:* GCR originate from the wind material of massive *rotating* stars, *always rich in CNO* (but not in heavier nuclei); they are accelerated by the forward shock of the SN explosion.

Higdon et al. (1998) suggested that GCR are accelerated out of *superbubbles* (SB) material (Fig. 3.C), enriched by the ejecta of many SN as to have a large and \sim constant metallicity. In this scenario, it is the forward shocks of SN that accelerate material ejected from other, previously exploded SN. Furthermore, it has been argued that in such an environment GCR could be accelerated to higher energies than in a single SN remnant (Parizot et al. 2004). That scenario has also been invoked in order to explain the present day source isotopic composition of GCR (Binns et al. 2005, Rauch et al. 2009). Notice that the main feature of that composition, namely a large $^{22}\text{Ne}/^{20}\text{Ne}$ ratio, is explained as due to the contribution of winds from Wolf-Rayet (WR) stars (e.g. Prantzos et al. 1987), and the SB scenario offers a plausible (but not unique) framework in bringing together contributions from both SN and WR stars.

However, the SB scenario suffers from (at least) two problems. First, core collapse SN are observationally associated to HII regions (van Dyk et al. 1996) and it is well known that the metallicity of HII regions reflects the one of the *ambient ISM* (i.e. it can be very low, as in IZw18) rather than the one of SN. Moreover, Higdon et al. (1998) evaluated the time interval Δt between SN explosions in a SB to a comfortable $\Delta t \sim 3 \times 10^5$ yr, leaving enough time to ^{59}Ni to decay before the next SN explosion and subsequent acceleration. However, Prantzos (2005) noticed that SB are constantly powered not only by SN but also by the strong winds of massive stars (with integrated energy and acceleration efficiency similar to the SN one, e.g. Parizot et al. 2004), which should continuously accelerate ^{59}Ni , as soon as it is ejected from SN explosions. Binns et al. (2008) argued that the problem may be alleviated from the fact that only the most massive (and thus, short-

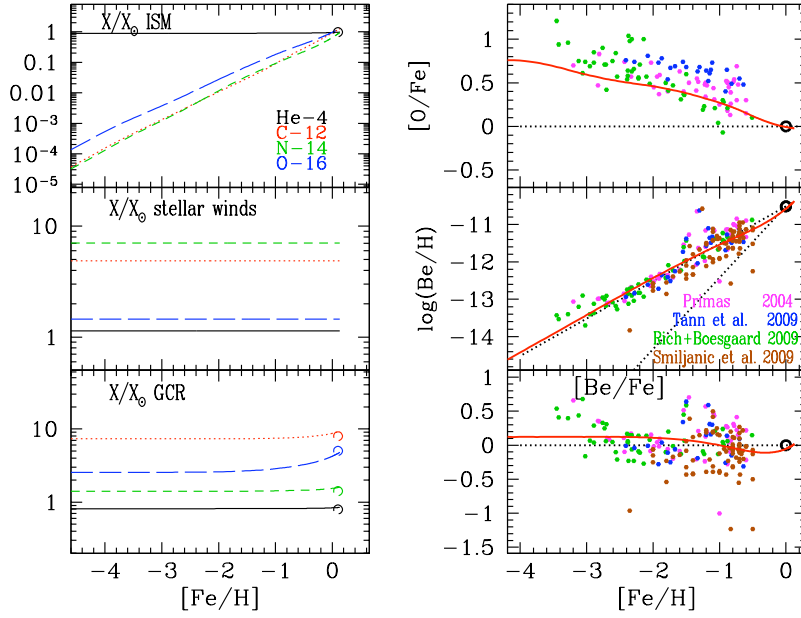


Figure 4. *Left:* Evolution of the chemical composition (in corresponding solar abundances) of He-4 (solid), C-12 (dotted), N (short dashed) and O (long dashed) in: ISM (top), massive star winds (middle) and GCR (bottom). Dots in lower panel indicate estimated GCR source composition (from Ellison et al. 1997). *Right:* Evolution (solid curves) of O/Fe (top), Be/H (middle) and Be/Fe (bottom); dotted lines indicate solar values in top and bottom panels, primary and secondary Be in middle panel.

lived) stars of an OB association emit strong winds; during the late (and longest) fraction of the lifetime of the SB (a few 10^7 years) particles are accelerated episodically (by SN explosions only) and no more continuously. Still, it is hard to imagine that superbubbles have always the same average metallicity, especially during the early Galaxy evolution, where metals were easily expelled out of the shallow potential wells of the small sub-units forming the Galactic halo (e.g. Prantzos 2008).

4. Cosmic rays from stellar winds and primary Be

In this work we propose a different explanation for the origin of GCR, which can also provide a satisfactory explanation for the primary nature of Be evolution. We first notice that there is now substantial evidence that GCR are indeed accelerated in SN remnants (e.g. Berezhko et al. 2009 and references therein). We then notice that, contrary to the case of non-rotating massive stars, which lose mass only at high metallicity, *rotating* massive stars display substantial mass loss down at very low (or even zero) metallicities (e.g. Meynet, this volume). The winds of those stars are enriched in CNO (products of H and He burning *within* the star itself) at all metallicities and at about the same level; it is precisely this enrichment of the WR winds at all metallicities that allows us to understand the observed primary behaviour of N down to the lowest metallicity halo stars (Chiappini et al. 2006). This gives some confidence in using the same model results to predict the composition of GCR over the history of the Milky Way.

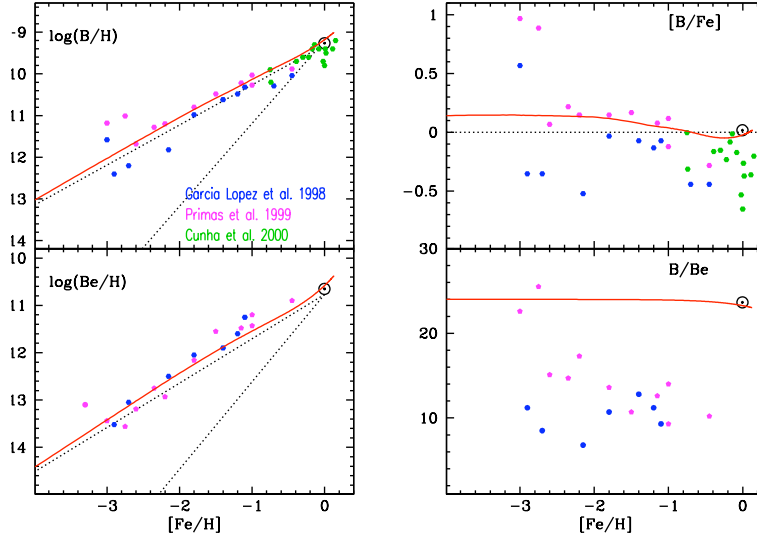


Figure 5. *Left:* Evolution of B (*top*) and Be (*bottom*); in both panels, *dotted lines* indicate primary and secondary evolution and *solid curves* indicate model evolution, including appropriately normalised ν -yields for ^{11}B . *Right:* Evolution of B/Fe (*top*) and B/Be (*bottom*). In the latter case, data indicate a subsolar mean value of $B/Be \sim 14$, compatible with exclusively GCR production of both elements, but the uncertainties (not shown here) are too large to allow conclusions.

We assume then that GCR are accelerated when the forward shocks of SN propagate into the previously ejected envelopes of rotating massive stars, which have been partially mixed with the surrounding ISM. The calculation of the resulting GCR composition $Y^{GCR}(M)$ is far from trivial: it will be mostly $Y^{Wind}(M)$ in the case of SN with initial mass $M > 20 M_{\odot}$ (having lost a large fraction of their mass in the wind) and mostly Y^{ISM} in the case of $M = 10\text{--}20 M_{\odot}$ stars, having suffered low mass losses. For illustration purposes we adopt here, as a function of metallicity Z , $Y_{paCNO}^{GCR}(Z) = 0.5 [Y_{paCNO}^{Wind}(Z) + Y_{paCNO}^{ISM}(Z)]$, where $Y^{Wind}(Z)$ is provided by the Geneva models (G. Meynet, private communication) and is integrated over a stellar IMF, whereas $Y^{ISM}(Z)$ is provided by the chemical evolution model (left panels in Fig. 4).

The calculation of the Be evolution is then straightforward and nicely fits the data (right panels in Fig. 4); it is the first time that such a calculation is performed *not by assuming* a given $Y_{paCNO}^{GCR}(Z)$ but by *calculating* it in a (hopefully) realistic way.

5. Boron-11 from ν -nucleosynthesis ?

As mentioned in Sec. 2, a supplementary source of ^{11}B is required in order to obtain the meteoritic $^{11}\text{B}/^{10}\text{B} = 4$ ratio. That source may be the ν -process in SN, extensively studied in Woosley et al. (1990): a fraction of the most energetic among the $\sim 10^{59}$ neutrinos of a SN explosion spallate ^{12}C nuclei in the C-shell of the stellar envelope to provide ^{11}B (but no other light nuclide). Soon after the HST observations of the primary behaviour of B (Duncan et al. 1992) it was realised that the ν -process can provide just such a primary B (Olive et al. 1994). But, if Be is produced as primary by GCR (Sec. 5), then more than $\sim 50\%$ of B is also produced as primary, leaving a rather small role to the ν -process. In

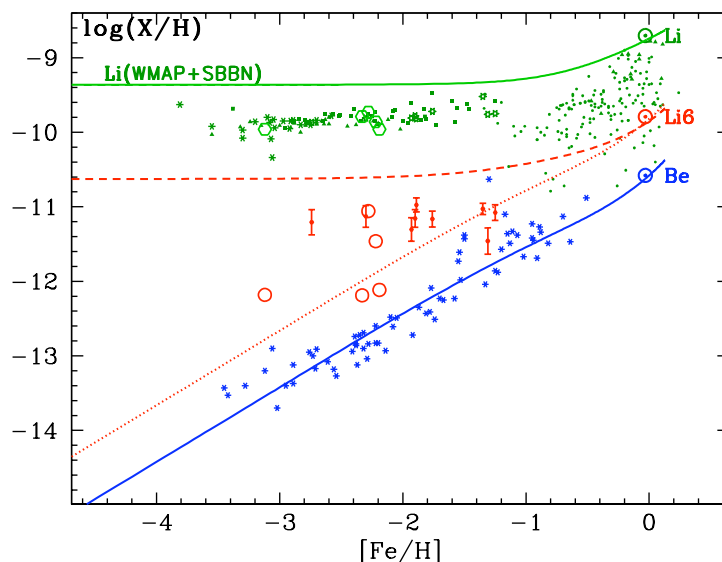


Figure 6. Evolution of total Li (*upper* set of data points and *solid* curve for model assuming high primordial ${}^7\text{Li}$), Be (*lower* set of points and *solid* curve) and ${}^6\text{Li}$ (*intermediate* set of points and curves). ${}^6\text{Li}$ data are from Asplund et al. (2006, small filled circles with error bars) and Garcia-Perez et al. (2009, large open circles with - large - error bars not displayed), while model curves are for a canonical (“low”) pre-galactic ${}^6\text{Li}$ (*dotted*) and a “high” pre-galactic ${}^6\text{Li}$ (*dashed*). In the latter case, a minimum amount of depletion within stars (equal to that of ${}^7\text{Li}$) has been conservatively assumed.

fact, the large uncertainties in the ν yields of ${}^{11}\text{B}$ do not allow an accurate evaluation of the B evolution: rather the B evolution (resulting from both GCR and ν -process) has to be used in order to constrain the B yields of SN.

The results of such an “exercise” appear in Fig. 5. In order to fit the observations, the ν yields of Woosley and Weaver (1995) had to be divided by a factor of ~ 6 , otherwise B/H and B/Fe would be overproduced. Notice the model B/Be ratio is always ~ 24 (i.e. solar), substantially higher than the observed, but *highly uncertain*, B/Be ~ 14 ratio in halo stars (which is consistent with pure GCR production of both elements!). Clearly, future observations with HST are required to clarify that important issue.

6. Early ${}^7\text{Li}$ and ${}^6\text{Li}$: “high” or “low” ?

For a long time, the Li “plateau” in low metallicity halo stars (discovered by Spite and Spite 1982) was considered to reflect the primordial abundance of ${}^7\text{Li}$. However, the precise determination of baryonic density through observations of the cosmic microwave background, combined to results of standard Big bang nucleosynthesis (SBBN), suggests that the true value of primordial ${}^7\text{Li}$ should be 2-3 times higher. It is not yet clear whether this discrepancy is due to some problems with SBBN, whether non-standard particle physics might cure it, or whether primordial ${}^7\text{Li}$ is depleted in the surface convective zones of low metallicity stars with such an astonishing uniformity (see many contributions in this volume). Other suggestions, like e.g. astration by a pre-galactic Pop. III population of massive stars (Piau et al. 2006) face severe problems of metal overproduction (Prantzos

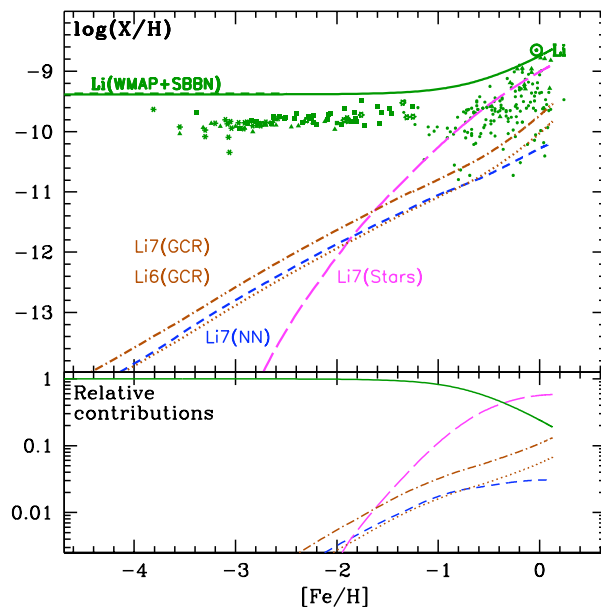


Figure 7. Evolution of total Li (*top*) and percentages of its various components (*bottom*): Li-7 from GCR (*dot-dashed*), Li-6 from GCR (*dotted*), Li-7 from ν -nucleosynthesis (NN, *dashed*) and Li-7 from a delayed stellar source (novae and/or AGB stars, *long dashed*). *Solid* curves indicate total Li (*upper panel*) and primordial ${}^7\text{Li}$ (*lower panel*).

2006). This issue, one of the most important ones for our understanding of mixing in stellar interiors, has also important implications for the chemical evolution of Li, as we shall see below.

The report of an “upper envelope” for ${}^6\text{Li}/\text{H}$ in low metallicity halo stars (Asplund et al. 2006) gave a new twist to the LiBeB saga. The reported ${}^6\text{Li}/\text{H}$ value at $[Fe/H] = -2.7$ is much larger (by a factor of 20-30) than expected if GCR are the only source of the observed ${}^6\text{Li}/\text{H}$ in that star, assuming that GCR can account for the observed evolution of Be (see Fig. 6). But, if it turns out that the true primordial Li is the one corresponding to the WMAP+SBBN value, then the initial ${}^6\text{Li}$ values in halo stars should be at least a factor of 3 higher than evaluated by Asplund et al. (2006, see Fig. 6). It should be noticed, however, that such high ${}^6\text{Li}$ values are not obtained in other investigations (Cayrel et al. 2008, Steffen et al. 2009).

In the past few years, the possibility of important pre-galactic production of ${}^6\text{Li}$ by non-standard GCR has drawn considerable attention from theoreticians, who proposed several scenarios:

- 1) Primordial, non-standard, production during Big Bang Nucleosynthesis: the decay/annihilation of some massive particle (e.g. neutralino) releases energetic nucleons/photons which produce ${}^3\text{He}$ or ${}^3\text{H}$ by spallation/photodisintegration of ${}^4\text{He}$, while subsequent fusion reactions between ${}^4\text{He}$ and ${}^3\text{He}$ or ${}^3\text{H}$ create ${}^6\text{Li}$ (e.g. Jedamzik 2004, and this meeting). Observations of ${}^6\text{Li}/\text{H}$ constrain then the masses/cross-sections/densities of the massive particle.

- 2) Pre-galactic, by fusion reactions of ${}^4\text{He}$ nuclei, accelerated by the energy released

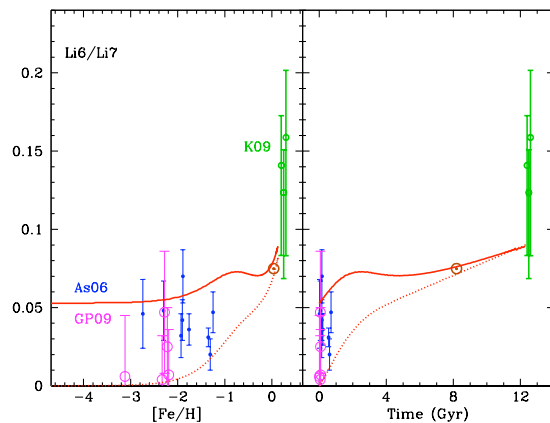


Figure 8. *Left:* Evolution of Li6/Li7 ratio as a function of $[\text{Fe/H}]$ (*left*) and of time (*right*). Data are from Asplund et al. (2006, As06), Garcia-Perez et al. (2009, GP09) and Kawanomoto et al. (2009, K09). *Solid curves* correspond to a “high” pre-galactic Li-6 and *dotted curves* to standard (low) pre-galactic Li-6.

by massive stars (Reeves 2005) or by shocks induced during structure formation (Suzuki and Inoue 2002).

3) In situ production by stellar flares, through $^3\text{He}+^4\text{He}$ reactions involving large amounts of accelerated ^3He (Tatischeff and Thibaud, 2007).

Prantzos (2006) showed that the energetics of ^6Li production by accelerated particles constrain severely any scenario proposed in category (2) above, including jets accelerated by massive black holes [this holds also for the “stellar flare” scenario, the parameters of which have to be pushed to their extreme values in order to obtain the “upper envelope” of the Asplund et al. (2006) observations]. This difficulty is confirmed by Evoli et al. (2008), who calculated pre-galactic ^6Li production by $\alpha + \alpha$ reactions with a semi-analytical model for the evolution of the early Milky Way; they found maximum values shorter by factors >10 (and plausible values shorter by 3 orders of magnitude) than the values reported by Asplund et al. (2006).

7. Evolution of Li and $^6\text{Li}/^7\text{Li}$

Since GCR can only produce a $^7\text{Li}/^6\text{Li}$ ratio of ~ 2 , instead of the meteoritic (pre-solar) value of ~ 12 , another source of ^7Li had to be found. In the two decades following the original MAR paper, four such sources were identified: three possible stellar sources and the hot early Universe of the Big Bang. The latter has certainly operated, as testified by the observed Li “plateau” in low metallicity halo stars; depending on the true primordial value (see Fig. 7), it may contribute from 8 to 20% of the solar ^7Li . Among the stellar sources, observational evidence exists only for AGB stars, where high Li abundances have been detected in some cases. But the corresponding model yields (from $^3\text{He}+^4\text{He}$ in the bottom of the convective envelope) are highly uncertain, and this is also the case for the other two candidate sources of novae (from explosive H-burning) and core collapse SN (from ν -induced nucleosynthesis); notice that both novae and AGBs enter the Galactic scene with some time delay (“slow” ^7Li component), contrary to SN and GCR.

^7Li is thus the only isotope having three distinctively different types of sources:

stellar, BBN and GCR. *Assuming* that the ν -yields of ${}^7\text{Li}$ are well established (through the corresponding ${}^{11}\text{B}$ yields, see Sec. 6), one may try to estimate the evolution of the remaining “slow” stellar contribution to ${}^7\text{Li}$, from the combined action of novae and AGB stars, i.e. by removing from the observed evolutionary curve of Li/H vs Fe/H the BBN, GCR and ν contributions. The result of such an exercise is displayed in Fig. 7. The “slow” stellar component contributes from 50-65% of the solar ${}^7\text{Li}$ (depending on whether high or low primordial ${}^7\text{Li}$ is adopted); similar numbers are found in the analysis of Matteucci (this volume).

Finally, Fig. 8 displays the evolution of ${}^6\text{Li}/{}^7\text{Li}$ ratio, compared to data for the early halo (highly uncertain, see previous section) and in the nearby Galactic disk (along three different lines of sight). Theoretical predictions depend on the adopted pre-galactic ${}^6\text{Li}/{}^7\text{Li}$ ratio, but a generic feature is a late rise of ${}^6\text{Li}/{}^7\text{Li}$, due to the late secondary production of ${}^6\text{Li}$ from GCR.

References

- Asplund M., Lambert D., Nissen P., Primas F., Smith V., 2006, *ApJ* 644, 229
 Berezhko E., Ksenofontov, L., Völk H. J., 2009, *AA* 505, 169
 Binns W., Wiedenbeck M., Arnould M., et al., 2005, *ApJ* 634, 351
 Binns W., Wiedenbeck M., Arnould M., et al., 2008, *New Astronomy Reviews* 52, 427
 Cayrel R., Steffen M., Bonifacio P., Ludwig H.-G., Caffau E., 2008, arXiv:0810.4290
 Chiappini C., Hirschi R., Meynet G. et al., 2006, *AA* 449, L27
 Duncan D., Lambert D., Lemke M., 1992, *ApJ* 584, 595
 Ellison D., Drury L., Meyer J.-P., 1997, *ApJ* 487, 197
 Evoli C., Salvadori S., Ferrara A., 2008, *MNRAS* 390, L14
 Garca Prez A. E., Aoki W., Inoue S., et al. 2009, *AA* 504, 213
 Gilmore G., Gustafsson B., Edvardsson B., Nissen P., 1992, *Nature* 375, 379
 Higdon J., Lingenfelter R., Ramaty R., 1998, *ApJ* 509, L33
 Jedamzik K., 2004, *PhysRevD* 70, 0603524
 Kawanomoto S., Kajino T., Aoki, W., et al., 2009, *ApJ* 701, 1506
 Meneguzzi M., Audouze J., Reeves H., 1971, *AA* 15, 337
 Olive K., Prantzos N., Scully S., Vangioni-Flam E., 1994, *ApJ* 424, 66
 Parizot E., Marcowith A., van der Swaluw E., Bykov A., Tatischeff V., 2004, *AA* 424, 747
 Piau L., Beers T., Balsara D., et al., 2006, *ApJ* 653, 300
 Prantzos N., 2005, *NuPhA* 758, 249
 Prantzos N., 2006, *AA* 448, 665
 Prantzos N., 2008, *AA* 489, 525
 Prantzos N., Arnould M., Arcoragi J. P., 1987, *ApJ* 315, 209
 Prantzos N., Casse M., Vangioni-Flam E., 1993, *ApJ* 403, 630
 Ramaty R., Kozlovsky B., Lingenfelter R., Reeves H., 1997, *ApJ* 488, 730
 Rauch B. F., Link J. T., Lodders K., et al., 2009, *ApJ* 697, 2083
 Reeves H., 2005, *EAS Publications Series*, Vol. 17, p. 15
 Reeves H., Fowler W., Hoyle F., 1970, *Nature* 226, 727
 Ryan S. Norris J., Bessell M., Deliyannis C., 1992, *ApJ* 388, 184
 Spite F., Spite M., 1982, *AA* 115, 357
 Steffen M., Cayrel R., Bonifacio P., Ludwig H.-G., Caffau E., 2009, arXiv:0910.5917
 Steigman G., Walker T., 1992, *ApJ* 385, L13
 Suzuki T., Inoue S., 2002, *ApJ* 573, 168
 Tatischeff V., Thibaud J.-P., 2007, *AA* 467, 265
 van Dyk S., Hamuy M., Filippenko A., 1996, *AJ* 111, 2017
 Wiedenbeck M. et al., 1999, *ApJ* 523, L61
 Woosley S., Hartmann D., Hoffman R., Haxton W., 1990,, *ApJ* 356, 272
 Woosley S., Weaver T., 1995, *ApJS*, 101, 181

Beryllium abundances and the formation of the halo and the thick disk

Rodolfo Smiljanic^{1,2}, L. Pasquini², P. Bonifacio^{3,4,5}, D. Galli⁶,
B. Barbuy¹, R. Gratton⁷, and S. Randich⁶

¹IAG, University of São Paulo, São Paulo, Brazil, ²ESO, Garching bei München, Germany,
email: rsmiljan@eso.org

³GEPI Observatoire de Paris - Meudon, France, ⁴INAF, Osservatorio di Trieste, Trieste, Italy,

⁵CIFIST Marie Curie Excellence Team, ⁶INAF- Osservatorio di Arcetri, Firenze, Italy

⁷INAF-Osservatorio di Padova, Padova, Italy,

Abstract. The single stable isotope of beryllium is a pure product of cosmic-ray spallation in the ISM. Assuming that the cosmic-rays are globally transported across the Galaxy, the beryllium production should be a widespread process and its abundance should be roughly homogeneous in the early-Galaxy at a given time. Thus, it could be useful as a tracer of time. In an investigation of the use of Be as a cosmochronometer and of its evolution in the Galaxy, we found evidence that in a $\log(\text{Be}/\text{H})$ vs. $[\alpha/\text{Fe}]$ diagram the halo stars separate into two components. One is consistent with predictions of evolutionary models while the other is chemically indistinguishable from the thick-disk stars. This is interpreted as a difference in the star formation history of the two components and suggests that the local halo is not a single uniform population where a clear age-metallicity relation can be defined. We also found evidence that the star formation rate was lower in the outer regions of the thick disk, pointing towards an inside-out formation.

Keywords. Stars: abundances, late-type – Galaxy: halo, thick disk

1. Introduction

The single stable isotope of beryllium, ^9Be , is a pure product of cosmic-ray spallation of heavy nuclei (mostly CNO) in the interstellar medium (Reeves et al. 1970). In this sense, the production of Be can occur in two ways. In the so-called direct process the cosmic rays are composed of protons and α -particles and these collide with CNO nuclei of the medium. In the so-called inverse process the cosmic rays are composed of accelerated CNO nuclei that collide with protons and α -particles of the medium.

Observational works on Be abundances in metal-poor stars (Rebolo et al. 1988; Gilmore et al. 1992; Molaro et al. 1997; Boesgaard et al. 1999; Smiljanic et al. 2009) find that $\log(\text{Be}/\text{H})$ and $[\text{Fe}/\text{H}]$ (or $[\text{O}/\text{H}]$) show a linear relation with slope close to one. Such slope argues that Be behaves as a primary element in the early Galaxy and its production mechanism is independent of the ISM metallicity. This means that the dominant production mechanism of Be is the inverse process (Duncan et al. 1992).

If one assumes that the cosmic-rays are globally transported across the Galaxy, than it follows that the Be production should be a widespread process. Beryllium can be produced anywhere in the Galaxy. One may thus expect that the Be abundances are rather homogeneous at a given time in the early Galaxy. It should have a smaller scatter than the products of stellar nucleosynthesis (Suzuki et al. 1999; Suzuki & Yoshii 2001) and could thus be employed as a cosmochronometer for the early stages of the Galaxy (Beers et al. 2000; Suzuki & Yoshii 2001).

This was tested by Pasquini et al. (2004, 2007) who calculated Be abundances in turn-off stars of two globular clusters, NGC 6397 and NGC 6752. These Be abundances

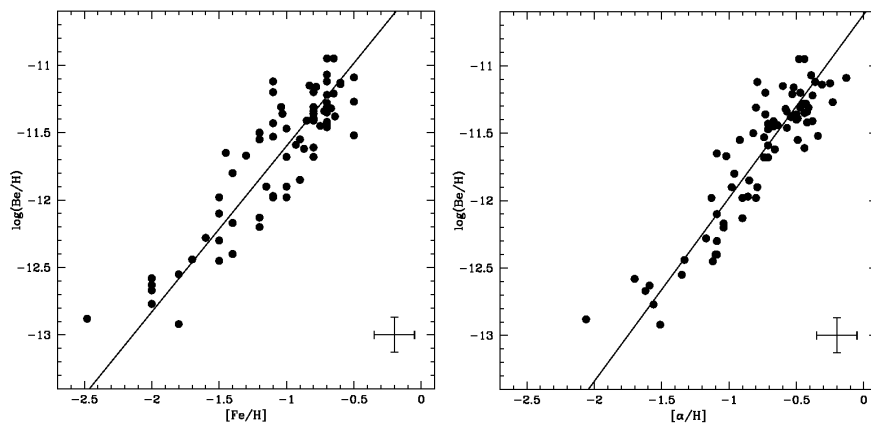


Figure 1. Abundances of Be as a function of $[\text{Fe}/\text{H}]$ (left panel) and of $[\alpha/\text{Fe}]$ (right panel). This figure is adapted from Smiljanic et al. (2009).

were used to derive ages by means of a comparison with a model of the evolution of Be with time (Valle et al. 2002). These ages agree well with those derived from theoretical isochrones, supporting the use of Be as a cosmochronometer.

Pasquini et al. (2005) then used a sample of 20 halo and thick-disk stars, previously analyzed by Boesgaard et al. (1999), to investigate the evolution of star formation rate in these two Galactic components. The idea is to use a diagram of $[\text{O}/\text{Fe}]$ vs. $\log(\text{Be}/\text{H})$ where the abscissa can be considered as increasing time and the ordinate as the star formation rate. A possible separation between stars of the two components was found and interpreted as a difference in the time scales of star formation.

Smiljanic et al. (2009) analyzed the largest sample of halo and thick-disk stars to date, extending the investigation of Be as cosmochronometer and its role as a discriminator of the different stellar populations in the Galaxy. These results are discussed in more detail in the following sections.

More details about Be can also be found in the references cited above and in many contributions in this volume, e.g., A. Boesgaard, D. Lambert, F. Primas, and H. Reeves.

2. The relation of Be with $[\text{Fe}/\text{H}]$ and $[\alpha/\text{H}]$

The beryllium abundances calculated by Smiljanic et al. (2009) are shown in Fig. 1 as a function of both $[\text{Fe}/\text{H}]$ and $[\alpha/\text{H}]$. Linear relations with slopes close to one, as found in previous works, are seen in these plots (the slope is 1.23 for $[\text{Fe}/\text{H}]$ and 1.37 for $[\alpha/\text{H}]$).

The scatter of the abundances seen in these plots is larger than that found by previous works in the literature. Statistically, because of the size of the error bars, it is not possible to say whether the observed scatter is real. However, it was possible to find among the sample stars, stars that have similar atmospheric parameters, same metallicity, normal unaltered Li abundances, but different Be abundances. The direct comparison of the spectra of these stars is shown in Fig. 14 of Smiljanic et al. (2009). This comparison strongly argues that at least part of the observed scatter is real.

Two different explanations can be put forward to understand the scatter. One is that it is caused by local effects, such as the proximity to supernovae (or as suggested by Smiljanic et al. (2008) to explain the case of the Be-rich star HD 106038 the proximity to

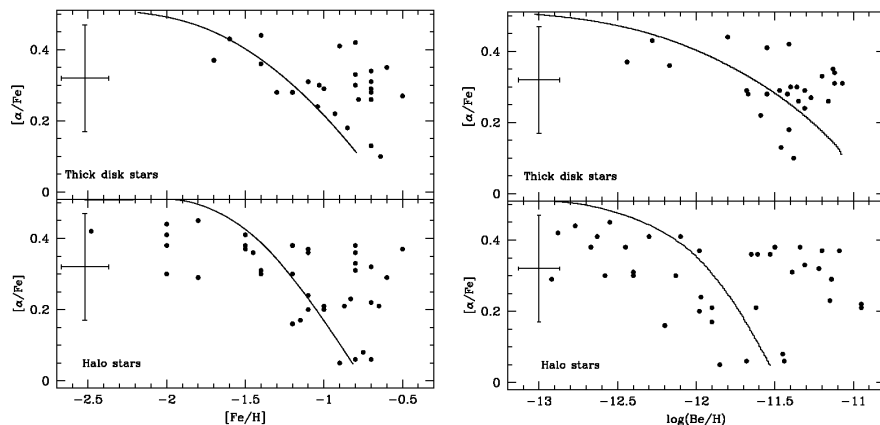


Figure 2. Diagram of $[\alpha/\text{Fe}]$ as a function of $[\text{Fe}/\text{H}]$ (left panel) and of $\log(\text{Be}/\text{H})$ (right panel). The thick-disk stars are shown in the upper panels and the halo stars in the lower ones. The thick-disk stars behave in the same way in both plots. The halo stars, however, clearly divide into two sequences when $[\alpha/\text{Fe}]$ is plotted against $\log(\text{Be}/\text{H})$. The curves are the predictions of the models by Valle et al. (2002). This figure is adapted from Smiljanic et al. (2009).

a hypernova). The other is related to the stars belonging to different stellar populations. As we discuss below, this second explanation is the preferred one.

A figure similar to Fig. 1 with the stars divided according to its membership to the halo or the thick disk star does not show a obvious division. This may be caused in part by the narrow metallicity range of the thick-disk stars (metal-poor thick-disk stars are rare). However, if such a plot is made it becomes clear that the scatter of the abundances for the halo stars is larger than that for the thick-disk stars.

3. Stellar Populations

We further investigate the different stellar populations in Fig. 2, using a diagram of $[\alpha/\text{Fe}]$ vs. $\log(\text{Be}/\text{H})$. In Smiljanic et al. (2009) oxygen abundances were not available, so mean abundances of α -elements were used instead. Again, the abscissa can be considered as increasing time and the ordinate as the star formation rate. Here we also present some new preliminary oxygen abundances determined from the infrared triplet at 777nm for a subsample of the halo stars (Fig. 3). The oxygen abundances were calculated using spectrum synthesis and the same codes and line lists used in Smiljanic et al. (2008, 2009). The oxygen abundances are corrected for NLTE effects following Fabbian et al. (2009). To calculate the oxygen abundances a new reduction of the red-arm UVES spectra, where the OI lines are located, was necessary. The red UVES spectra is usually strongly affected by fringing. This can, however, be corrected with a new reduction using the latest UVES pipeline.

When using the Be abundances instead of Fe, it becomes clear that, with either α or oxygen abundances, the halo stars define two clear distinct sequences (Figs. 2 and 3). One sequence is chemically similar to the thick disk, the other agrees with the behavior expected for the halo stars in the models of Valle et al. (2002). The thick disk stars behave the same no matter if using Be or Fe (Fig. 2).

Checking the kinematics of the stars, however, it is possible to notice that the group

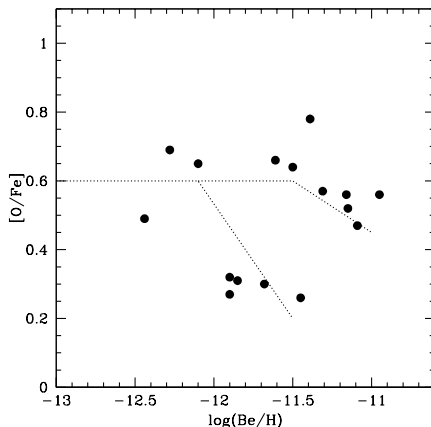


Figure 3. The $[O/Fe]$ ratio as a function of beryllium abundances for a subsample of the halo stars analyzed in Smiljanic et al. (2009). These preliminary oxygen abundances were calculated using the OI triplet at 777nm. The abundances are corrected for NLTE (Fabbian et al. 2009). The lines are only traced to guide the eye.

of low- α halo stars, that follows the expected behavior of the models, have similar kinematics. We define this group from the diagram of Fig. 2 as the stars with $[\alpha/Fe] \leq 0.25$ and $\log(Be/H) \leq -11.4$. In Fig. 4 we show diagrams of both $[\alpha/Fe]$ and $\log(Be/H)$ as a function of V , the component of the space velocity of the star in the direction of the disk rotation, and of R_{min} , the perigalactic distance of the stellar orbit. The low- α group (open symbols) have mostly $V \sim 0$ and $R_{min} \leq 1$ kpc. They seem to be a group of non-rotating stars going very close to the Galactic center, a behavior that might be expected to be shown by accreted stars that sink to the Galactic center by dynamical friction. They also form a very tight and well-defined sub-sequence in a diagram of $[Fe/H]$ vs. $\log(Be/H)$ (Fig. 5). This fact helps to explain why the halo stars show a larger scatter in this kind of diagram.

The splitting into two components may be related to the accretion of external systems or to variations of star formation in different and initially independent regions of the early halo. The interpretation is still open, it is however clear that the halo is not a single uniform population with a single age-metallicity relation. A similar division was found by Nissen & Schuster (1997, 2009) but using Fe as a tracer of time. The division seems clearer when Be is used as a time scale.

For the thick disk, it is possible to see in the lower-right panel of Fig. 4 a significant anticorrelation of $[\alpha/Fe]$ with perigalactic distance. This anticorrelation might be interpreted as evidence that the SFR was lower in the outer regions of the thick disk. A similar correlation however is not seen for Be. This lack of anticorrelation seems to indicate that Be is not affected by the local details of star formation, confirming that it can be used as a time scale. Although the range in Be abundances covered by the thick disk is very small, it is possible to see in Fig. 4 that the thick disk stars with smallest Be concentrate in the inner regions of the disk. As these are expected to be old stars, this result seems to point towards an inside-out formation of the thick disk.

One remaining question is how does this possible division of the halo stars compare to our current understanding of the formation of the Galactic halo? Given that we are analyzing a sample of local halo stars this division is likely not a consequence of the

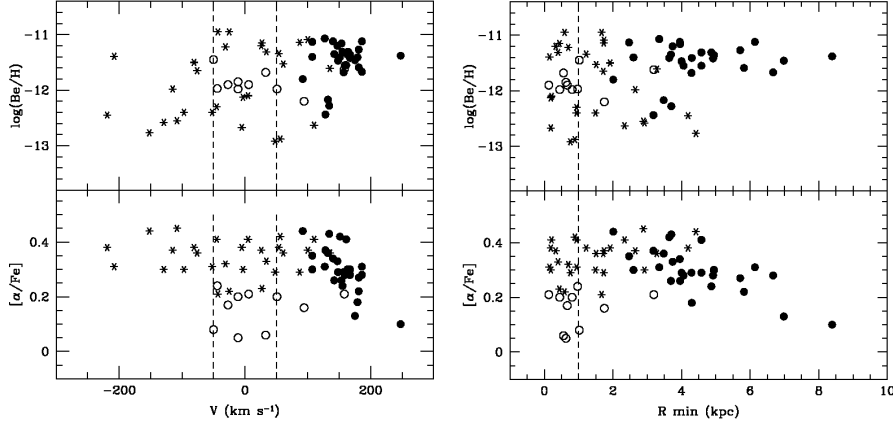


Figure 4. The $[\alpha/\text{Fe}]$ ratio and the Be abundances as a function of V , the component of the space velocity of the star in the direction of the disk rotation (left panel), and of R_{min} , the perigalactic distance of the stellar orbit (right panel). Thick disk stars are shown as filled circles, the low- α halo stars as open symbols, and the remaining halo stars as starred symbols. The low- α stars tend to have V close to zero and $R_{\text{min}} \leq 1$ kpc. This figure is adapted from Smiljanic et al. (2009).

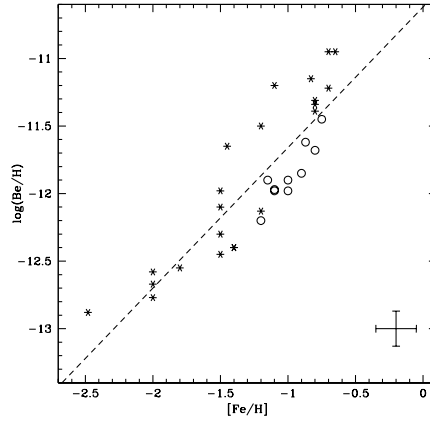


Figure 5. The beryllium abundances as a function of $[\text{Fe}/\text{H}]$ only for the halo stars. The low- α stars seem to form a tight and well defined sub-sequence. This figure is adapted from Smiljanic et al. (2009).

inner vs. outer halo dichotomy, as discussed for example by Carollo et al. (2007, 2009). According to Carollo et al. (2007), the outer halo has a metallicity distribution that peaks at $[\text{Fe}/\text{H}] \sim -2.20$ and dominates the stellar population in distances beyond 15–20 Kpc from the Galactic center. The inner halo, on the other hand, has a metallicity distribution that peaks at $[\text{Fe}/\text{H}] \sim -1.60$ and dominates the stellar population in distances up to 10–15 Kpc. Although we did not check in detail to which of these halo components our sample stars belong, we note that they have metallicities between $[\text{Fe}/\text{H}] = -2.00$ and -0.50 . The low- α stars in particular have $-1.20 \leq [\text{Fe}/\text{H}] \leq -0.70$. We thus believe most

of our sample stars are definitely inner halo stars. This implies that our results suggest a dichotomy of the inner halo.

There are other literature results that seem to indicate a possible division of the inner halo, from both the observational and the theoretical point of view. On the observational side, Morrison et al. (2009), based on the kinematics of a sample of metal-poor stars, conclude that the local inner halo seems to divide into two components. One is moderately flattened, has no rotation, has a clumpy distribution in energy and angular momentum, and $[\text{Fe}/\text{H}] < -1.50$. The second is highly flattened, has a small prograde rotation, and $-1.50 < [\text{Fe}/\text{H}] < -1.00$. This last component is distinct from the metal-weak thick disk.

On the theoretical side, Zolotov et al. (2009) present new simulations of the formation of disk galaxies in a Λ CDM universe. They allow for star formation both in the primary potential well of the galaxy being modelled and in dark matter subhalos that are later accreted. They show that the final stellar population in the inner halo of a galaxy formed like this has a dual nature. It is composed both by ‘in situ stars’, formed in the inner Galaxy and later displaced to the halo, and by accreted stars, formed in the subhalos.

Acknowledgements

This work has been supported by studentships and fellowships to R.S. by FAPESP (04/13667-4 and 08/55923-8) and CAPES (1521/06-3), and by financial support from the ESO DGDF. R.S. also acknowledges financial support from the organizers for his participation in this meeting.

References

- Beers, T. C., Suzuki, T. K., & Yoshii, Y. 2000, in: Proc. IAU Symp. No. 198, p. 425
- Boesgaard, A. M., Deliyannis, C. P., King, J. R., et al. 1999, *AJ*, 117, 1549
- Carollo, D., Beers, T. C., Lee, Y.-S., et al. 2007, *Nature*, 450, 1020
- Carollo, D., Beers, T. C., Chiba, M. et al. 2009, arXiv:0909.3019
- Duncan, D. K., Lambert, D. L., & Lemke, M. 1992, *ApJ*, 401, 584
- Fabbian, D., Asplund, M., Barklem, P. S., et al. 2009, *A&A*, 500, 1221
- Gilmore, G., Gustafsson, B., Edvardsson, B., & Nissen, P. E. 1992, *Nature*, 357, 379
- Molaro, P., Bonifacio, P., Castelli, F., & Pasquini, L. 1997, *A&A*, 319, 593
- Morrison, H. L., Helmi, A., Sun, J., et al. 2009, *ApJ*, 694, 130
- Nissen, P. E. & Schuster, W. J. 1997, *A&A*, 326, 751
- Nissen, P. E. & Schuster, W. J. 2009, in: Proc. IAU Symp. No. 254, p. 103
- Pasquini, L., Bonifacio, P., Randich, S., Galli, D., & Gratton, R. G. 2004, *A&A*, 426, 651
- Pasquini, L., Bonifacio, P., Randich, S., et al. 2007, *A&A*, 464, 601
- Pasquini, L., Galli, D., Gratton, R. G., et al. 2005, *A&A*, 436, L57
- Rebolo, R., Abia, C., Beckman, J. E., & Molaro, P. 1988, *A&A*, 193, 193
- Reeves, H., Fowler, W. A., & Hoyle, F. 1970, *Nature*, 226, 727
- Smiljanic, R., Pasquini, L., Bonifacio, P. et al. 2009, *A&A*, 499, 103
- Smiljanic, R., Pasquini, L., Primas, F. et al. 2008, *MNRAS*, 385, L93
- Suzuki, T. K. & Yoshii, Y. 2001, *ApJ*, 549, 303
- Suzuki, T. K., Yoshii, Y., & Kajino, T. 1999, *ApJ*, 522, L125
- Valle, G., Ferrini, F., Galli, D., & Shore, S. N. 2002, *ApJ*, 566, 252
- Zolotov, A., Willman, B., Brooks, A. M. et al. 2009, *ApJ*, 702, 1058

DICUSSION C. The stellar yields in He-3, He-4 and Li-7: main sources, observational constraints, and problems

André Maeder

Geneva Observatory, University of Geneva, CH-1290 Versoix, Switzerland

email: andre.maeder@unige.ch

Keywords. Nucleosynthesis, abundances

I am pleased to recall that the first determination of the Li-abundance in the Sun was made at the Geneva Observatory in 1975 by Edith Müller, Eric Peytremann and Ramiro de la Reza on the basis of spectra taken at Kitt Peak. The first Be determination was also made in Geneva the same year by Y. Chmielewski, J. Brault (Kitt Peak National Observatory) and E. Müller. These two outstanding works opened the door for all further investigations on these light elements.

The yields of light elements are a matter where the shock of ideas frequently occurs, with new facts arising and different interpretations. This is particularly the case at present concerning the He abundance in globular clusters and the relation between the ^7Li abundances and planets. This made the discussions at IAU Symposium very lively and interesting. I will try my best to summarize the main points, restore the essence of the discussions and give a proper credit to the various contributors.

Normally, stellar evolution provides the chemical yields which are used as an input for the models of the chemical evolution of galaxies. The inverse path, i.e. using the observations of galactic trends in chemistry to infer the stellar properties is like trying to derive the properties of an egg from an omelette, as stated by Jean Audouze long time ago. Nevertheless, in the case of the very early stellar generations, the only direct infos we often have on the stellar properties come from the observed trends in the chemical evolution of galaxies. In this case, we can even say that we use a “fossil omelette” to reconstruct the original stellar properties of the very early stellar generations.

1. The yields in He-4, the globular clusters, and related questions

The relative helium to oxygen enrichment $\Delta Y/\Delta O$ obtained by Manuel Peimbert is 3.3 ± 0.7 , a ratio which typically applies to stars with solar abundances. We notice that the yields in He and O do not come from the same mass range, and that the above ratio depends heavily on mass loss, mixing, mass limit for black hole formation, cutoff mass in supernovae, etc... The question of the slope of the $\Delta Y/\Delta Z$ according to the metallicity Z is raised by Francesca Matteucci. Manuel Peimbert points out that $\Delta Y/\Delta Z$ may reach a value of about 4 at Z higher than solar.

The big question concerns the multiple sequences found in globular clusters, following the VLT study of ω Cen by Piotto and colleagues. The globular clusters have experienced successive starburst episodes, the recent one bearing the signature of strong He-enrichments. The red sequence corresponds to $Z = 10^{-3}$, $Y = 0.246$, while the blue sequence has $Z = 2 \cdot 10^{-3}$, $Y = 0.38$. Formally, this corresponds to a large He-enrichment for a minute one in heavy elements, i.e. $\Delta Y/\Delta Z \sim 10^2$. The discussions bear, not on the reality of the high He-content, but rather on its origin. Some authors in literature support the idea that the galactic winds driven by supernovae have removed the contributions in heavy elements, because they are ejected at high speed. Manuel Peimbert notes the C/O ratios in the gas may provide information on the

importance of the ejecta of heavy elements in the galactic winds. The observations show low C/O ratios, which indicates that there is no important losses of O-rich material by the galactic winds. The material forming the ejected galactic winds is likely rather well mixed. Francesca Matteucci notes that the same remark seems to also apply to dwarf galaxies. Donatella Romano nevertheless mentions there are observations in a dwarf galaxy of galactic winds showing typical SN II ejecta.

One may wonder whether the galactic infall could not counterbalance the effects of selective ejecta. Monica Tosi emphasizes that all galaxies experience infalls, while only a few show galactic winds. She points out that dwarfs galaxies tend to develop galactic winds. She mentions that the above mentioned C observations are made in nearby galaxies, where there is likely no galactic winds.

Georges Meynet supports a different idea, i.e. that fast rotating massive stars at low Z lose a lot of mass as a result of rotational mixing and mass loss, thus making the He yields very large. He also relates these excesses to the anomalies of the CEMP (Carbon rich extremely metal poor stars). Some authors support losses from AGB stars or contributions from binaries. He emphasizes that massive and AGB stars do not produce exactly the same chemical anomalies and that this may be a way to disentangle the two types of contributions.

Why do these large He abundances do not affect the general $\Delta Y/\Delta Z$ ratio? Is it because the fraction of stars which form under the above peculiar conditions is too small? This seems likely, however this could be the source of some scatter in the Y vs. Z relation at low Z . Francesca Matteucci remarks that the peculiar solutions for the globular clusters do not necessarily apply to the Galaxy and she emphasizes the interest to perform some tests in the Galactic bulge.

Among other points, Marc Pinsonneault emphasizes the interest to get He abundances from asteroseismology in all possible objects. Nikos Prantzos remarks that the Sun places very good constraint on the $\Delta Y/\Delta Z$ ratio. This gives a value within the error bars of that given by Manuel Peimbert.

2. The surprising flat behaviors of the He-3/He ratio

In solar-type stars, a bump of ${}^3\text{He}$ forms at mass fraction 0.55 and the standard models predict that this ${}^3\text{He}$ should be ejected in the more advanced stages. The massive stars on the contrary destroy ${}^3\text{He}$ over most of their interior, both the initial cosmological one and the new amounts they may have synthesized, thus their yields are negative. The net result of the standard models integrated over the mass spectrum, as shown by models of the chemical evolution of galaxies made by Monica Tosi, is that the ${}^3\text{He}/\text{He}$ ratio should increase with the $[\text{O}/\text{H}]$ abundance ratio. In the Galaxy, this ratio should decrease with the galactocentric distance.

However, the problem is that more than 90% of the solar-type stars show no ${}^3\text{He}$ enrichment or at least much less than predicted. Among the planetary nebulae, only a few (7 as discussed by Tom Bania) show ${}^3\text{He}$ enhancements in agreement with the current expectations. Also contrary to the model expectations, the ${}^3\text{He}/\text{He}$ ratio is flat with respect to $[\text{O}/\text{H}]$ as discussed by Gary Steigmann and Tom Bania. The ${}^3\text{He}/\text{He}$ ratio is similar to that given by the standard Big Bang nucleosynthesis. Also, this ratio does not show the expected variations with the galactocentric radius or with the oxygen abundance. This is the so-called He-3 problem, the reality of which is not disputed.

Gary Steigman emphasizes that ${}^3\text{He}$ is both produced and destroyed, but in a way that the net production is zero, so that it keeps to the level of the standard Big-Bang synthesis. Corinne Charbonnel supports these views. She emphasizes that the low-mass stars have small positive yields (even with the thermohaline mixing), thus they do not destroy the cosmological ${}^3\text{He}$. The planetary nebulae with the predicted ${}^3\text{He}$ abundances also have the classically predicted ${}^{12}\text{C}/{}^{13}\text{C}$ isotopic ratios. In relation with her models, Corinne Charbonnel mentions that it would be interesting to know the magnetic fields in RGB stars with the classical ${}^{12}\text{C}/{}^{13}\text{C}$ isotopic ratios.

Monica Tosi mentions that the present HII regions exhibit no ${}^3\text{He}/\text{He}$ gradient in the Milky Way, she emphasizes this confirms that there is no net overall production of ${}^3\text{He}$ at the present

epoch. Manuel Peimbert questions whether there are biases in the studies of the planetary nebulae showing nitrogen enrichments. Tom Bania confirms that the sample of observed planetary nebulae is currently biased in favor of those showing nitrogen enrichments.

A possible solution for the ^3He problem is that proposed by Nadège Lagarde, Corinne Charbonnel, and Jean-Paul Zahn, it implies an instability due to thermohaline mixing. This instability, like salt fingers, occurs when matter with an higher mean molecular weight μ lies above matter with a lower μ . The reaction $^3\text{He} + ^3\text{He} \rightarrow ^4\text{He} + 2\text{p}$ results in the conversion of two particles into three ones at the basis of the ^3He bump. Thus, there it reduces the μ -value making a local inversion which creates an instability. One may note that this solution is reminiscent of the so-called “solar spoon” proposed decades ago by D. Gough.

However, the question arises why do some planetary nebulae still have the expected ^3He enrichments. The answer by Corinne Charbonnel is that this may be due to a magnetic field inhibiting the thermohaline instability. She proposes that these planetary nebulae are the descendants of the magnetic Ap stars. In both cases, the proportions of these objects are about 5%. Further investigations are needed to test these possibilities.

3. Questions regarding lithium: the Li plateau, Li in RGB and AGB stars, relation with planets

It is remarkable that thanks to the efforts of many people we now seem to have a consistent interpretation of the various physical effects shaping the Li abundance in the T_{eff} region surrounding the Li dip (see Fig. 1).

When one refers to the (in principle) unmodified Li abundance, it means the abundance on the left side of the Li dip as shown in the Figure. These Li abundances for stars covering a large range of $[\text{Fe}/\text{H}]$ show an essentially flat distribution over the whole range of metallicities except their increase for the higher $[\text{Fe}/\text{H}]$ corresponding to Pop. I stars. The almost flat part is the so-called “Spite plateau”. The big problem is that this abundance plateau lies a factor of about 3 below the predictions of standard Big-Bang nucleosynthesis. In this respect, there is an interesting poster by Sbordone et al. on the low-metallicity end of the Spite plateau. Below $[\text{Fe}/\text{H}] = -3$, he notes that there is no plateau anymore, but a growth of $A(\text{Li})$ with $[\text{Fe}/\text{H}]$ and a large scatter.

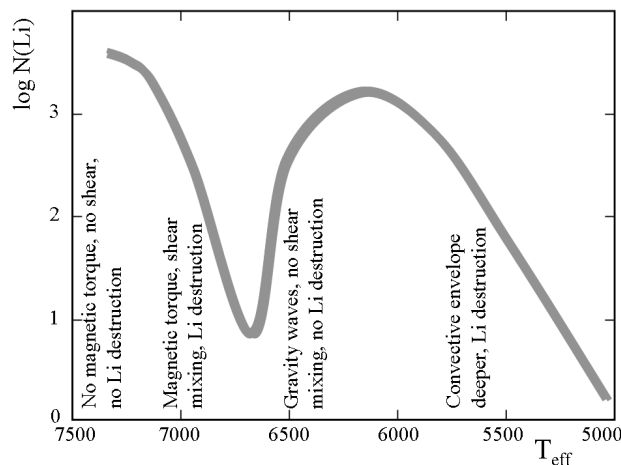


Figure 1. The physical effects shaping the Li dip as a function of the effective temperature. Adapted from S. Talon et C. Charbonnel.

The main lesson concerning the Li abundance $A(\text{Li})$ on the hot side of the dip is that it appears to be a multivariate function of the form

$$A(\text{Li}) = f(\text{mass}, Z, \text{age}, \text{rotation}, \text{pre-MS}, \text{disk lifetime}, \dots), \quad (3.1)$$

some effects being still disputed. The evolutionary effects along the tracks in the HR diagram are clearly predicted by the stellar models and they are also observed along the sequences of globular clusters. The T_{eff} scale is of particular importance along the subgiant branch, as emphasized in several interventions in the discussion.

There are clear differences of views on the age effect on the Li-abundances. For Sofia Randich, each cluster behaves in a different way and the relation with age is uncertain. Jorge Melendez however shows that the Li abundances for the available solar twins of the Hipparcos catalogue present a strong correlation with age in agreement with the Charbonnel & Talon (2005, Science, 309, 2189) models.

Andreas Korn wonders whether the Li dip is also observed in PopII stars as in Pop I stars. Suzanne Talon answers that Pop II stars are so old that the Pop II stars with masses at the level of the Li dip already occupy the subgiant branch, thus it may not be easy to see the it. Corinne Charbonnel further comments that the dip has nevertheless been found in halo stars (Charbonnel & Primas, 2005, A&A, 442, 961) and in NGC 6397 by Lind et al. (2009, A&A, 503, L545).

There are theoretical and observational evidences of some additional lithium depletion near the bump of the red giant branch (RGB) and various mechanisms are proposed to account for this depletion, in particular the hot-bottom burning and the thermohaline mixing. There is a variety of Li abundances in RGB and AGB stars. 1% of the GK giants are Li-rich, there are also Li rich AGB stars, which may be related to the Cameron-Fowler mechanism. To a question concerning the origin of the Li-depleted stars, Marc Pinsonneault suggests they are mergers.

Francesca Matteucci then makes some comments regarding ω Cen and the related problems. One may recall here that in his presentation Piercarlo Bonifacio has suggested, from the similarity of the Li content in ω Cen and in the Galactic halo field stars (which have experienced different evolutionary histories), that there is no evidence of a pre-galactic Li depletion by a generation of very massive stars as was suggested by Laurent Piau. Bonafacio has also noted the absence of difference in the Li content of stars in ω Cen over a range of 5 Gyr in ages, he has claimed that this is contradiction with the current explanations of the Li plateau based on diffusion processes. Francesca Matteucci wonders about the assumed 5 Gyr scatter and also on the sampling of data.

The last topic approached in this discussion concerns the relation between the enhanced Li-depletion and the occurrence of planets in solar-type stars. This interesting result was shown by Garik Israelian and also presented by Nuno Santos in his review. The point is however challenged in a poster by Jorge Melendez.

There are several possible interpretations of the above fact. The merging of a giant planet may bring additional angular momentum in the outer layers, thus driving mixing and Li-depletion, also the pollution resulting from the merging may give rise to thermohaline mixing as was suggested by Sylvie Theado and Sylvie Vauclair. Marc Pinsonneault makes comments on the importance of the disk and of rotation in the pre-Main Sequence evolution. He emphasizes the need to measure rotation rates. The key parameter (as firstly emphasized by Jerome Bouvier) is the disk lifetime. A longer disk lifetime means more disk locking in the pre-MS phase and thus a lower mean rotation on the ZAMS. The longer disk lifetime also leads to higher mixing due to more differential rotation in *slowly* rotating stars. Another consequence of the longer disk lifetime is that there is more possibilities for the formation of planets. This may establish a relation between the Li-depletion and the occurrence of planets via the longer disk lifetime.

This discussion was a beautiful illustration of the major open questions remaining in our understanding of the abundances of the light elements. I thank Patrick Eggenberger for his help in taking notes of the session. I apologize for any deviation from the exact meaning of the contributors, I hope nobody will bring me to the court for that.

Discussion D: Observational problems with Li, Be and B

Poul Erik Nissen¹

¹Department of Physics and Astronomy, University of Aarhus, DK-8000 Aarhus C, Denmark
email: pen@phys.au.dk

Abstract. In Discussion D the following problems were addressed: Has ${}^6\text{Li}$ really been detected in the atmospheres of metal-poor halo stars? Is there a downward trend or increased scatter of Li abundances in stars on the ‘Li-plateau’ at metallicities $[\text{Fe}/\text{H}] \lesssim -2.5$? Are there significant differences of Li abundances in main-sequence, turn-off, and sub-giant stars in globular clusters? Is the Li abundance in solar-type stars related to the presence of planets? How does the Be abundance in dwarf stars increase with the heavy-element abundance, and is there a cosmic scatter in Be at a given $[\text{Fe}/\text{H}]$? The discussion of these problems is summarized and some suggestions for future observational and theoretical studies are mentioned.

Keywords. stars: abundances, atmospheres, interiors – planetary systems – ISM: abundances – early universe

1. Introduction

Observational problems with lithium and beryllium, which have attracted much attention in recent years, were taken up during Discussion D. Boron, on the other hand, was not included in the discussion, because observational progress for this element has been slow in recent years due to the 5-year hiatus in the UV high-resolution instrumentation at the HST. In the following, I briefly report on the main subjects of the discussion.

2. ${}^6\text{Li}$ in the atmospheres of metal-poor halo stars

The discussion focused on the claimed 1D LTE (> 2 -sigma) detections of ${}^6\text{Li}$ in warm, metal-poor halo dwarf stars by Asplund et al. (2006) and Asplund & Meléndez (2008) including the very metal-poor stars G 64-12 with ${}^6\text{Li}/{}^7\text{Li} = 0.059 \pm 0.021$ and G 64-37 with ${}^6\text{Li}/{}^7\text{Li} = 0.111 \pm 0.032$. As emphasized by Martin Asplund, one may question a detection of ${}^6\text{Li}$ for a given star, but the collective distribution of ${}^6\text{Li}/{}^7\text{Li}$ can only be explained if ${}^6\text{Li}$ is present in the atmospheres of some of these metal-poor stars.

According to Martin Asplund (this volume), the ${}^6\text{Li}/{}^7\text{Li}$ ratio derived from the profile of the Li I 6708 Å resonance line does not change significantly if a 3D non-LTE analysis is applied instead of a 1D LTE analysis. Matthias Steffen (this volume), on the other hand, finds that the derived ${}^6\text{Li}/{}^7\text{Li}$ ratio is 0.01 to 0.02 smaller when using 3D non-LTE instead of 1D LTE. If such a zero-point shift in the derived ${}^6\text{Li}/{}^7\text{Li}$ values is included, then the distribution of ${}^6\text{Li}/{}^7\text{Li}$ is more compatible with the absence of ${}^6\text{Li}$ in the stellar atmospheres, although a few stars, such as HD 84937, still seem to have ${}^6\text{Li}$ detected at the 2-sigma level.

The difference in the estimation of the 3D (convective) effects on the derived value of ${}^6\text{Li}/{}^7\text{Li}$ may be connected to the way the analysis of the spectra is performed. Asplund et al. use other lines than Li I 6708 Å to determine the line broadening arising from the projected stellar rotation velocity, $V_{\text{rot}} \sin i$, whereas Steffen et al. assume a value

$V_{rot} \sin i = 0$ or 2 km s^{-1} and use only the Li line itself. Clearly, further 3D non-LTE studies are needed, and checks of line asymmetries induced by 3D convective motions should be performed for spectral lines that are formed in the same way and at the same atmospheric depth as the Li I 7698 Å line in the spectrum of HD 84937 (Smith et al. 2001) and the Na I D lines in the very metal-poor stars G 64-12 and G 64-37.

As emphasized by several participants, a clear detection of the ^6Li isotope at a level of $^6\text{Li}/^7\text{Li} \sim 0.05$ in metal-poor halo stars with metallicities $[\text{Fe}/\text{H}] \lesssim -3$ would have profound effects on our understanding of the formation of Li. As shown by Nikos Prantzos (this volume) cosmic ray processes cannot explain the corresponding high $^6\text{Li}/\text{Be}$ ratio at $[\text{Fe}/\text{H}] \sim -3$. Pre-galactic production of ^6Li or non-standard Big-Bang nucleosynthesis have to be invoked (Karsten Jedamzik, this volume).

Concern was raised about the quality of the high-resolution spectra that have been used to determine $^6\text{Li}/^7\text{Li}$. High resolution ($R \gtrsim 10^5$), and high signal-to-noise ($S/N \gtrsim 500$) are needed. In addition, one has to be very careful with the flat-fielding and rectification of the spectra to ensure that the continuum near the Li I 6708 Å line is accurate to better than 0.2%. In this connection, it was mentioned that the non-detection of ^6Li in G 64-37 ($^6\text{Li}/^7\text{Li} = 0.01 \pm 0.04$) by García Pérez et al. (2009) (in contrast to the 3-sigma detection by Asplund & Meléndez quoted above) may be due to problems with residual fringes after flat-fielding of the Subaru/HDS spectra, as also discussed by García Pérez et al. themselves.

When discussing the Li isotope ratio, it should not be forgotten that ^6Li has been clearly detected in nearby interstellar clouds. As a new development in this field, Christopher Howk (this volume) presented the first measurements of the Li I 6708 Å line associated with gas in the Small Magellanic Cloud, which is known to be about a factor of four more metal-poor than the Sun. The high-resolution spectrum, which was taken with UVES and has a S/N of 250, suggests that ^6Li is present corresponding to $^6\text{Li}/^7\text{Li} \sim 0.12$. A still higher S/N spectrum is needed to confirm this interesting detection of ^6Li in a metal-poor galaxy.

3. The ‘Spite plateau’ at the lowest metallicities

Sbordone et al. (this volume) presented evidence that halo stars with $T_{\text{eff}} \gtrsim 5900 \text{ K}$ and $[\text{Fe}/\text{H}] < -2.5$ show a decline and increasing scatter of Li abundances as a function of decreasing metallicity. At $[\text{Fe}/\text{H}] \sim -3.5$, the average Li abundance, $A(\text{Li}) = \log(N_{\text{Li}}/N_{\text{H}}) + 12$, is 1.9 dex and the scatter is around 0.2 dex. In contrast, the Li abundance for halo stars with metallicities in the range $-2.5 < [\text{Fe}/\text{H}] < -1.5$ is nearly constant at a level of $A(\text{Li}) = 2.2$ with a scatter of 0.05 dex only. It was emphasized that this result does not depend on the effective temperature scale applied.

Meléndez et al. (this volume) find, however, that the increased scatter in Li abundance below $[\text{Fe}/\text{H}] = -2.5$ goes away if one selects the ‘plateau’ stars according to the condition $T_{\text{eff}} > 5850 - 180 [\text{Fe}/\text{H}] \text{ K}$, i.e. with a strong metallicity dependence in the temperature limit; at $[\text{Fe}/\text{H}] = -3.0$ only stars with $T_{\text{eff}} > 6390 \text{ K}$ are included. Still, there is a tendency that stars with $[\text{Fe}/\text{H}] < -2.5$ have a 0.1 dex lower Li abundance than stars with $[\text{Fe}/\text{H}] > -2.5$.

Meléndez et al. (this volume) suggest that the turbulent diffusion models of Richard et al. (2005) can explain the large difference between the Li abundance predicted from WMAP + SBBN ($A(\text{Li}) \sim 2.7$) and the abundance of the plateau stars ($A(\text{Li}) \sim 2.2$), if models with a high parameter of turbulent mixing ($T6.25$) are adopted. The same models introduce a rather strong dependence of Li depletion on stellar mass, which may explain the scatter in $A(\text{Li})$ at the lowest metallicities, but turbulent diffusion models with

metallicities below $[\text{Fe}/\text{H}] = -2.0$ are still to be calculated. It would also be important to obtain a better understanding of the free parameter in the turbulent diffusion models from physical principles.

The derived stellar Li abundances depend critically on the adopted effective temperatures; if T_{eff} is increased by 100 K, $A(\text{Li})$ increases by 0.07 dex. Over the years, there has been much discussion of the effective temperature scale for late-type stars especially for the metal-poor halo stars. Recent calibrations based on the IRFM method (González Hernández & Bonifacio 2009; Casagrande et al. 2009) agree, however, very well, and point to a fairly high temperature scale, i.e. $T_{\text{eff}} \sim 6500$ K for a very metal-poor star at the turn-off point. It is interesting that new 3D calculations of the profiles of Balmer lines (Ludwig et al. 2009) support such high temperatures. Further work on 3D non-LTE modelling of Balmer lines and comparison with observed profiles is, however, needed.

4. Lithium in globular clusters

Recent studies of Li abundance differences along the evolutionary sequence of stars in NGC 6397 were reviewed by Andreas Korn (this volume) and further discussed by Karin Lind (this volume) and Jonay González Hernández (this volume). Both high-resolution VLT/UVES spectra of 18 stars analyzed by Korn et al. (2007) and medium-resolution GIRAFFE spectra for 349 stars analyzed by Lind et al. (2009) suggest that the turn-off stars in NGC 6397 are more Li-poor, by about 0.1 dex, than subgiants which have not yet undergone dredge-up. Based on VLT/GIRAFFE spectra González Hernández et al. (2009) also find a difference of about 0.1 dex between 84 subgiants and 79 main-sequence stars in NGC 6397 selected in a narrow color range $0.57 < B - V < 0.63$. This suggests that Li sinks by diffusion during the MS/TO phase but to a depth low enough to prevent Li destruction such that some Li can be restored into the atmosphere, when a star evolves to the SG stage and the convection zone deepens.

It was noted that the two Li studies of NGC 6397 by Lind et al. and González Hernández et al. do not agree concerning the details of the trend of $A(\text{Li})$ as a function of T_{eff} . The Lind et al. results suggest that $A(\text{Li})$ decreases with increasing T_{eff} along the subgiant branch, whereas González Hernández et al. find the opposite trend. Karin Lind warned that these trends are somewhat uncertain, because of correlated errors in T_{eff} and $A(\text{Li})$. Jonay González Hernández stressed that the turbulent diffusion model by Richard et al. (2005), which explains the difference between the WMAP based Li abundance, $A(\text{Li}) \sim 2.7$, and the overall level of $A(\text{Li}) \sim 2.3$ in the globular cluster stars, i.e. the $T6.25$ model, does not explain the observed difference between $A(\text{Li})$ in SG and MS stars. Clearly, more work is needed. Li data for other globular clusters than NGC 6397 would be very important.

Piercarlo Bonifacio (this volume) presented a study of Li abundances in turnoff and subgiant stars belonging to ω Cen based on high-resolution spectra obtained with the ESO VLT. He considered ω Cen as the nucleus of an external galaxy that has been accreted by the Milky Way. According to Villanova et al. (2007), the stars observed span an age range of five Gyr. The preliminary results show that 30 stars with metallicities in the range $-1.9 < [\text{Fe}/\text{H}] < -1.5$ are distributed along a Li ‘plateau’ with $A(\text{Li}) \sim 2.1$ and a scatter of the order of 0.1 dex. Given the five Gyr age-spread and the constancy of $A(\text{Li})$ at 2.1 dex, Piercarlo Bonifacio pointed out that it is difficult to explain the difference in $A(\text{Li})$ with respect to a primordial Li abundance of 2.7 dex by intrinsic stellar depletion. Li depletion in an early generation of massive stars, as suggested by Piau et al. (2006), was also considered an unlikely explanation by Piercarlo Bonifacio, because it seems surprising if this scenario would lead to the same depletion in the Milky

Way and in an external galaxy. Nikos Prantzos remarked that the suggestion of Piau et al. is excluded because Li astration in massive Pop III stars would be accompanied by heavy element production to a level much higher than we are observing in the very metal-poor halo stars.

5. Lithium in solar-type stars

Garik Israelian (this volume) described a new investigation of the Li abundance in Sun-like stars with and without detected planets based on spectra obtained with the HARPS spectrograph at the ESO 3.6 m telescope. For a limited range of ± 80 K around the solar effective temperature, only two out of 24 stars with detected planets have $A(\text{Li}) > 1.5$, whereas 29 out of 60 stars without detected planets have $A(\text{Li}) > 1.5$ (Israelian et al. 2009). Furthermore, there are no systematic differences in metallicity and age (as estimated from chromospheric activity) between stars with and without detected planets that could explain the difference in $A(\text{Li})$. Hence, there seems to be evidence for enhanced Li depletion in Sun-like stars with orbiting planets. Israelian et al. suggest that the presence of a planetary system affects the angular momentum evolution of a star in a way that leads to a higher degree of rotational mixing of Li to interior regions, where it can be destroyed.

Meléndez et al. (this volume), on the other hand, find that solar-analogue stars with and without detected giant planets follow the same relation between atmospheric Li abundance and stellar age (determined from isochrones). This relation agrees well with that predicted by Charbonnel & Talon (2005) from models including the influence of gravity waves on the internal rotation of the Sun. Meléndez et al. also find that solar-twin stars (mass $M = (1.00 \pm 0.04) M_{\text{Sun}}$ and metallicity $[\text{Fe}/\text{H}] = 0.0 \pm 0.1$) having the same *chemical* terrestrial planet signature as the Sun (Meléndez et al. 2009) follow the same Li vs. age relation as solar twins without the signature of terrestrial planets. These investigations suggest that one has to select stars with and without planets in narrow mass, age and metallicity ranges before comparing their Li abundances. More work on larger samples of solar-twin stars is needed before final conclusions on Li differences between stars with and without planets can be made.

6. The Galactic evolution of beryllium

The formation and evolution of beryllium were discussed in talks by Ann Boesgaard, Francesca Primas and Rodolfo Smiljanic (this volume).

Beryllium abundances derived from Keck/HIRES spectra by Rich & Boesgaard (2009) for 49 stars ranging in metallicity from $[\text{Fe}/\text{H}] = -3.5$ to -0.5 and with oxygen abundances derived from OH lines in the UV suggest that the slope of $\log(\text{Be})$ vs. $\log(\text{O})$ may change from ~ 0.75 for stars with $[\text{O}/\text{H}] < -1.6$ to ~ 1.6 for stars with $[\text{O}/\text{H}] > -1.6$. As suggested by Ann Boesgaard, this could be due to a change in the dominant production mechanisms for Be. In the early Galaxy, Be formed by a primary process, i.e. high energy CNO atoms from supernovae hitting interstellar protons, whereas at later times the dominant (secondary) reaction is high energy protons from SNe hitting interstellar CNO.

Smiljanic et al. (2009) have used VLT/UVES spectra to determine Be abundances in a sample of 90 stars with metallicities mostly in the range $-2.0 < [\text{Fe}/\text{H}] < -0.5$. Atmospheric parameters and abundances of the α -capture elements (Mg, Si, Ca, Ti) were adopted from literature. Li abundances are used to eliminate stars, possibly affected by depletion, from the sample. Interestingly, there is a significant scatter of Be at a given

[Fe/H]: the halo stars tend to split into two populations one with low Be and α/Fe , and another one with high Be and α/Fe like in the thick disk stars.

Francesca Primas (this volume) presented new Be data based on UVES spectra, which show that the two distinct populations of low- α and high- α halo stars discovered by Nissen & Schuster (2009) define different trends in the $\log(\text{Be})$ - [Fe/H] diagram, thus confirming the results of Smiljanic et al. (2009). Furthermore, a hint of a flattening of the beryllium evolutionary trend at the lowest metallicities, $[\text{Fe}/\text{H}] \lesssim -2.5$, is found. As noted by Nikos Prantzos, this may be a signature of Be production by hypernovae.

From these works, it is clear that the evolution of Be in the Milky Way is more complicated than thought before, and that further studies of Be abundances in a larger sample of halo and disk stars may reveal interesting information about cosmic-ray processes and Galactic evolution. Investigations of non-LTE and 3D effects are, however, important in order to obtain accurate abundances of Be as well as Fe, O and the α -capture elements.

References

- Asplund, M., Lambert, D.L., Nissen, P.E., Primas, F., & Smith, V.V. 2006, *ApJ*, 644, 229
- Asplund, M., & Meléndez, J. 2008, in *First Stars III*, eds. B.W. O'Shea, A. Heger, and T. Abel, *AIP Conf. Proc.*, vol. 990, 342
- Casagrande, L., Ramírez, I., Meléndez, J., Bessell, M., & Asplund, M. 2009, *A&A*, (submitted)
- Charbonnel, C., & Talon, S. 2005, *Science*, 309, 2189
- García Pérez, A.E., Aoki, W., Inoue, S., et al. 2009, *A&A*, 504, 213
- González Hernández, J.I., & Bonifacio, P. 2009, *A&A*, 497, 497
- González Hernández, J.I., Bonifacio, P., Caffau, E., et al. 2009, *A&A*, 505, L13
- Israelian, G., Mena, E.D., Santos, N.C., et al. 2009, *Nature*, 462, 189
- Korn, A.J., Grundahl, F., Richard, O., et al. 2007, *ApJ*, 671, 402
- Lind, K., Primas, F., Charbonnel, C., Grundahl, F., & Asplund, M. 2009, *A&A*, 503, 545
- Ludwig, H.-G., Behara, N.T., Steffen, M., & Bonifacio, P. 2009, *A&A*, 502, L1
- Meléndez, J., Asplund, M., Gustafsson, B., & Yong, D. 2009, *ApJ*, 704, L66
- Nissen, P.E., & Schuster, W.J. 2009, in *The Galaxy Disk in Cosmological Context (IAU Symp. 254)*, eds. J. Andersen, J. Bland-Hawthorn, and B. Nordström, (Cambridge Univ. Press), p. 103
- Piau, L., Beers, T.C., Balsara, D.S., et al. 2006, *ApJ*, 653, 300
- Rich, J.A., & Boesgaard, A.M. 2009, *ApJ*, 701, 1519
- Richard, O., Michaud, G., & Richer, J. 2005, *ApJ*, 619, 538
- Smiljanic, R., Pasquini, L., Bonifacio, P., Galli, D., Gratton, R.G., Randich, S., & Wolff, B. 2009, *A&A*, 499, 103
- Smith, V.V., Vargas-Ferro, O., Lambert, D.L., & Olgin, J.G. 2001, *AJ*, 121, 453
- Villanova, S., Piotto, G., King, I.R., et al. 2007, *ApJ*, 663, 296



Cristina Chiappini



Beatriz Barbuy

Chemical evolution of D in the Local Disk

Takuji Tsujimoto¹ and Joss-Bland-Hawthorn²

¹National Astronomical Observatory, Mitaka-shi, Tokyo 181-8588, Japan

email: taku.tsujimoto@nao.ac.jp

²Institute of Astronomy, School of Physics, University of Sydney, NSW 2006, Australia

Abstract. Chemical features of the local disk have firmly established the picture for the formation of the Galactic disk that the star formation has proceeded under the continuous accretion of low-metallicity gas from the halo. It sets two determinant processes for the evolution of deuterium (D), that is, the destruction of D in the interior of stars and the supply of new (nearly) primordial D associated with the gas infall. Conventional Galactic chemical evolution (GCE) models predict that this scheme leads to a monotonic decrease in D/H with time and ends up in the present-day D/H abundance $(D/H)_0$ which is severely lower than the recently observed estimates. These predicted features are the natural results of a construction of the metal-rich (\sim solar abundance) local star+gas system. Here we propose that the new GCE models, that incorporate large-scale winds from the Galactic bulge which entrain heavy elements and drop them on the disk with the recent tendency of star formation in tune with the observed implications, make the system rich in both metals and D. In addition, our finding of a gradual increase in D/H with time during the last several Gyr is observationally supported by the D/H abundance for the protosolar cloud lower than $(D/H)_0$.

Keywords. Galaxy: disk, evolution — Stars: abundances

Recent *Far-Ultraviolet Spectroscopic Explorer* (FUSE) observations reveal that the present-day D/H abundance $(D/H)_0$ for interstellar matter (ISM) in the Galactic disk is surprisingly as high as $\geq 2.31 \pm 0.24 \times 10^{-5}$ close to the primordial $(D/H)_p$ after correcting for dust depletion (Linsky *et al.* 2006). The high D/H abundance of $2.2^{+0.8}_{-0.6} \times 10^{-5}$ in the warm neutral medium of the lower Galactic halo, which originates in the disk and is elevated into the halo (Savage *et al.* 2007), strongly supports the claim by Linsky *et al.*

The difference between $(D/H)_p$ and $(D/H)_0$ is defined as a deuterium astration factor $f_d = (D/H)_p / (D/H)_0$. The value of f_d should absolutely be > 1 , because it is believed that all D are produced during Big Bang nucleosynthesis, and only the destruction process of D occurs in the interior of stars in the post-Big Bang evolution. Thus, the value of f_d is determined by the fraction of matter which has never been cycled through stars in the present ISM. Accordingly, f_d is closely related to the enrichment degree by heavy elements in the Galaxy evolution through star formation that destroys D while fresh heavy elements are released into the ISM when the stars die. In the end, due to the fact that the D abundance in the ISM is anti-correlated with the metallicity in the system, the well-enriched (\sim solar metallicity) local disk demands a high f_d . Indeed, the standard GCE models predict $f_d = 1.39 - 1.83$ for the local disk (Romano *et al.* 2006). In other words, the local abundances of heavy elements such as Fe or α -elements in the ISM and long-lived stars imply $f_d \approx 1.4$ at the least, that is equivalent to $(D/H)_0 < 2.0 \times 10^{-5}$. On the other hand, the high $(D/H)_0$ implied by the recent observations means a smaller f_d . For the estimates of $(D/H)_p = 2.75 \times 10^{-5}$ (Cyburt *et al.* 2003) and $(D/H)_0 = 2.31 \times 10^{-5}$, we obtain $f_d = 1.19$, which is incompatible with the theoretical prediction.

The D/H abundances which bridge between the primordial $(D/H)_p$ and the present-day $(D/H)_0$ give a crucial information on the evolution of D. Viewing from this angle the

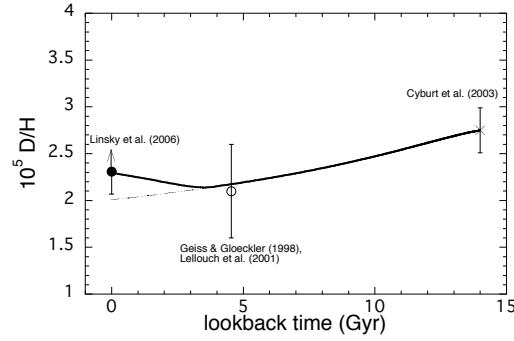


Figure 1. The evolution of D/H abundance in the local disk predicted by the wind+decreasing SFR model (solid line). For reference, the model case with a constant SFR coefficient is shown by the dashed line. Three observed points are for the primordial value (Cyburt *et al.* 2003), the value for the protosolar cloud (Geiss & Gloeckler 1998, Lellouch *et al.* 2001), and the local ISM value (Linsky *et al.* 2006).

D/H in the protosolar cloud, which represents the abundance at the age of ~ 4.6 Gyr in the Galaxy, the obtained results are quite intriguing. The D/H abundances deduced from the atmosphere of jupiter (Lellouch *et al.* 2001) or from the solar wind (Geiss & Gloeckler 1998) are 2.1 ± 0.4 (0.5) $\times 10^{-5}$. If these estimates are correct, does it imply that D in the local disk has gradually increased during the last several Gyr?

Recent several works reveal the star formation history in the local disk, claiming that the star formation rate (SFR) has been clearly declining for the last several Gyr (Fuchs *et al.* 2009). In addition, recent new view on chemical evolution of the Galactic disk has suggested that large-scale winds from the Galactic bulge, which entrain a large amount of heavy elements, enrich the disk (Tsujimoto 2007). Theoretical framework that the Galaxy disk has evolved through an ongoing infall and the winds, together with the renewed constraint from the star formation history in the local disk, will open a new channel for the interpretation of the D evolution in the local disk.

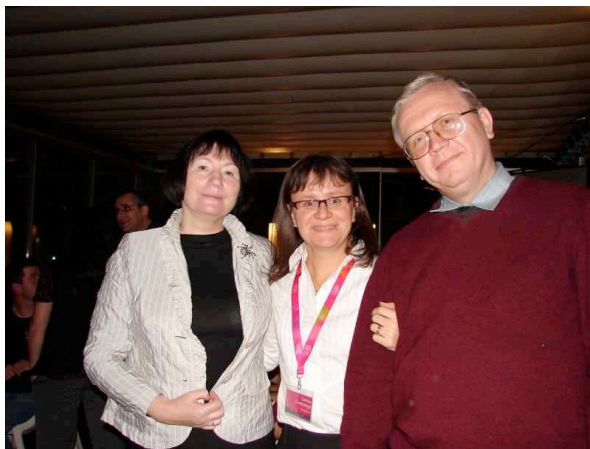
The predicted time-evolution of D/H in this scheme is shown in Figure 1. Here the primordial $(D/H)_0$ is set to be 2.75×10^{-5} . From its initial value, the D/H abundance starts to decrease with time, and subsequently its change turns to a gradual increase around 4 Gyr ago. This turnover results from the supply of primordial D by an infall that overwhelms the destruction of D through the star formation owing to its low rate. Then, it finally enables to achieve a present-day high D/H abundance of 2.3×10^{-5} , fully consistent with the observed value, after passing $D/H \sim 2.1 \times 10^{-5}$ equivalent to the protosolar value around 4.6 Gyr ago. For reference, the case with a constant SFR over the full age is indicated by dashed line.

References

- Cyburt, R. H., Fields, B. D., & Olive, K. A. 2003, *Phys. Lett. B*, 567, 227
 Fuchs, B., Jahreiß, H., & Flynn, C. 2009, *AJ*, 137, 266
 Geiss, J., & Gloeckler, G. 1998, *Space Sci. Rev.*, 84, 239
 Lellouch, E. et al. 2001, *A&A*, 670, 610
 Linsky, J. L. et al. 2006, *ApJ*, 647, 1106
 Romano, D., Tosi, M., Chiappini, C., & Matteucci, F. 2006, *MNRAS*, 369, 295
 Savage, B. D., Lehner, N., Fox, A., Wakker, B., & Sembach, K. 2007, *ApJ*, 659, 1222
 Tsujimoto, T. 2007, *ApJ*, 665, L115



IAU 268 women in front of the Museum of Natural History



Tamara Mishenina, Corinne Charbonnel, Yuri Izotov



Anna Faviola Marino, Oscar Gonzalez,
Antonino Milone, Marcella di Criscienzo



Jean-Paul Zahn

Author Index

- Angelou, G. C. – 405
 Aoki , W. – 337
 Asplund, M. – **191**, 211, 263, 341
 Aurière , M. – 347

 Balachandran , S. C. – 339
 Balser, D. S. – 81, **101**
 Bania, T. M. – **81**, 101
 Barbuy, B. – **325**, 483
 Barzdis , A. – 361
 Baumann, P. – 341
 Bedin, L. R. – 183
 Beers, T. C. – 337, 355
 Behara, N. – 257, 355
 Belik , S. I. – 343
 Bellazzini , M. – 187
 Bellini, A. – 183
 Bharat Kumar, Y. – **327**
 Bland-Hawthorn, J. – 499
 Boesgaard, A. M. – **231**
 Bohuon, E. – 427
 Bonifacio, P. – 215, 257, **269**, 329, 355, 483
 Bowler, B. P. – 231
 Bragaglia , A. – **119**, **169**, 177
 Brott , I. – 411
 Busso, M. – 311, 425

 Caffau, E. – 215, 257, **329**, 355
 Cantiello, M. – 411
 Carigi, L. – 91
 Carretta, E. – 169, 177
 Casagrande, L. – **129**, 211
 Cassisi, S. – 169
 Cavichia, O. – **171**
 Cayrel, R. – 215, 257, 355
 Charbonnel, C. – 135, 263, 357, 365, 423, **441**
 Chatterjee, S. K. – **39**
 Chiappini , C. – 141, 447
 Christlieb , N. – 355
 Cignoni, M. – 187
 Costa, R. D. D. – 171, **173**, 181
 Cunha, K. – **243**

 D’Antona , F. – **395**
 de Laverny, P. – 347
 de Medeiros, J. R. – 347
 de Mink, S. E. – 411
 Decressin , T. – **135**
 Delgado Mena , E. – 291
 Di Criscienzo, M. – **175**

 do Nascimento Jr, J. D. – 347
 D’Orazi, V. – 169, **177**
 Drake, N. A. – 351
 Dunkley, J. – **17**

 Eggenberger, P. – 141, **381**
 Ekström , S. – 141, 421, **447**
 Elliott, L. – **331**
 Eriksson, K. – 325

 Federman , S. R. – 237
 Ferland, G. – **163**
 Fields , B. D. – 65
 Flynn, C. – 129
 François , P. – 355
 Freytag , B. – 355
 Frischknecht, U. – **421**

 Galli , D. – 483
 Galvez-Ortiz, C. – 291
 Geiss, J. – **71**
 Georgy, C. – 141, 421, 447
 Gloeckler , G. – 71
 Gonzalez , O. A. – **333**
 Gonzalez Hernandez, J. I. – **257**, 291, 355
 Gratton , R. – 169, 177, 183, 483
 Grenon, M. – 325
 Grundahl, F. – 263
 Guandalini, R. – **311**, 425
 Gustafsson , B. – 325

 Hébrard , G. – **59**
 Hill , V. – 355
 Hirschi, R. – 141, 421, 447
 Holleck, S. – 423
 Honda, S. – 337
 Howk, J. C. – **335**

 Idiart , T. E. P. – 173, 181
 Israelian, G. – **285**, 291
 Ito, H. – **337**
 Izotov, Y. I. – **107**, 163
 Izzard, R. G. – 411

 Jasiewicz, G. – 423
 Jedamzik, K. – **27**

 Kajino, T. – 33, 463
 Kaufer, A. – **317**
 Kolev, D. – 347
 Konstantinova-Antova, R. – 347

- Korn , A. J. – **249**
 Kovtyukh , V. V. – 343
 Kudryavtsev, D. O. – 351
 Kusakabe , M. – **33**

 Lagarde, N. – 357, **423**, 441
 Lambert , D. L. – **3**, 237, 339
 Langer, N. – **411**
 Lattanzio, J. C. – 405
 Lèbre, A. – 347
 Levesque, E. M. – 231
 Lind , K. – 191, **263**
 Linsky, J. L. – **53**
 Lubowich, D. – **179**
 Lucatello, S. – 169, 177
 Ludwig, H.-G. – 215, 257, 329, 355
 Luridiana, V. – 91

 Maciel, W. J. – 171, 173, **181**
 Maeder, A. – 141, 381, 447, **489**
 Mayor, M. – 291
 Maiorca, E. – 311, 425
 Mallik, S. V. – **339**
 Marino, A. F. – **183**
 Mathews, G. J. – 33
 Matteucci, F. – 187, **454**
 Melendez , J. – **211**, **341**, 345
 Meynet, G. – 135, **141**, 381, 421, 447
 Milone, A. P. – 183
 Mishenina, T. V. – **343**
 Molaro, P. – 355
 Monaco, L. – 269

 Nakamura, K. – **463**
 Nissen, P. E. – **493**
 North , P. – 423

 Pace , G. – **345**
 Palacios, A. – **347**
 Palmerini, S. – 311, **425**
 Pancino, E. – 187, 269
 Pasachoff , J. M. – 179
 Pasquini, L. – 357, 483
 Peimbert, M. – **91**, 163, 185
 Peimbert, A. – 91, 163, **185**
 Peterson , R. C. – **349**
 Pinsonneault, M. H. – **375**
 Piotto, G. – 183
 Plez, B. – 355
 Polosukhina-Chuvaeva , N. S. – **351**
 Pompéia , L. – 325
 Porter, R. L. – 163
 Portinari, L. – 129
 Prantzos, N. – **473**
 Primas, F. – **221**, 263,
 Prodanovic, T. – **65**

 Ramirez, I. – 211, 341
 Randich, S. – **275**, 291, 483
 Rauscher, T. – 421
 Rebolo, R. – 291
 Reddy, B. E. – 327
 Reeves, H. – **469**
 Rich, J. A. – 231
 Ritchey, A. M. – **237**
 Romano, D. – **187**, **431**
 Rood, R. T. – 81, 101
 Ryan, S. G. – 331

 Santos, N. C. – **291**
 Sbordone , L. – 257, 269, **355**
 Schuster, W. J. – 211
 Sembach, K. – **43**
 Shavrina, A. V. – 351
 Sheffer, Y. – 237
 Shetrone, M. – 423
 Shigeyama, T. – 463
 Sivarani, T. – 355
 Skillman, E. D. – **113**, 163
 Smiljanic, R. – **357**, **483**
 Smirnova, A. – 351
 Smith, V. V. – **301**, 423
 Soderblom, D. – **359**
 Soubiran, C. – 343
 Sousa, S. – 291
 Spite , F. – 201, 355
 Spite , M. – **201**, 355
 Stancliffe, R. J. – **405**
 Steffen, M. – **215**, 257, 329, 355
 Steigman, G. – **19**, 65, 163

 Talon, S. – **365**
 Théado, S. – **427**
 Thielemann, F.-K. – 421
 Tominaga , N. – 337
 Tosi, M. – **153**, 187
 Trevisan , M. – 325
 Tsujimoto, T. – **499**

 Udry , S. – 291
 Uttenthaler, S. – 311

 Van't Veer , C. – 355
 Vauclair, S. – **387**, 427
 Ventura, P. – **147**, 395
 Villanova, S. – 183, 269

 Winteler , C. – 421

 Yoon, S.-C. – 411
 Yoshida, T. – 33, 463

 Zacs , L. – **361**
 Zaggia, S. – 257
 Zoccali, M. – 183